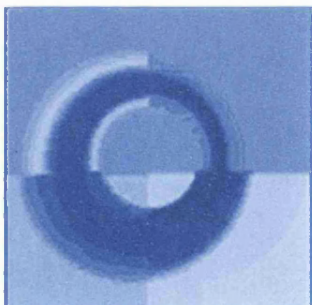


**CONE AND CENTRAL RECEPTOR
DYSTROPHIES - A CLINICAL AND
MOLECULAR GENETIC
INVESTIGATION**

Michel Michaelides BSc, MB BS, MRCOphth

Thesis submitted for the degree of Doctor of Medicine

February 2004



Institute of Ophthalmology



Moorfields Eye Hospital

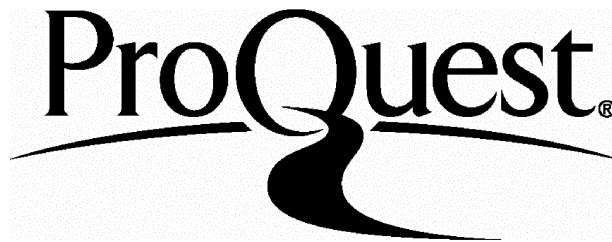
ProQuest Number: U643875

All rights reserved

INFORMATION TO ALL USERS

The quality of this reproduction is dependent upon the quality of the copy submitted.

In the unlikely event that the author did not send a complete manuscript and there are missing pages, these will be noted. Also, if material had to be removed, a note will indicate the deletion.



ProQuest U643875

Published by ProQuest LLC(2016). Copyright of the Dissertation is held by the Author.

All rights reserved.

This work is protected against unauthorized copying under Title 17, United States Code.
Microform Edition © ProQuest LLC.

ProQuest LLC
789 East Eisenhower Parkway
P.O. Box 1346
Ann Arbor, MI 48106-1346

DECLARATION

I declare that this thesis submitted for the degree of
Doctor of Medicine is composed by me and the work herein is my own.

Any work done in collaboration is clearly stated.

Michel Michaelides BSc, MB BS, MRCOphth

ABSTRACT

The cone, cone-rod and central receptor dystrophies form part of a heterogeneous group of retinal dystrophies that are a major cause of childhood blindness.

Detailed phenotyping has been performed in several patient groups, including the stationary cone dysfunction syndromes (achromatopsia, blue cone monochromatism, oligocone trichromacy and an X-linked cone dysfunction syndrome associated with myopia and dichromacy); progressive cone dystrophies (cone dystrophy with supernormal rod responses and a cone dystrophy associated with mutation in *CNGB3*); cone-rod dystrophies (CORDs) (an autosomal dominant cone-rod dystrophy (CORD7), a syndrome of CORD with amelogenesis imperfecta and enhanced S-cone syndrome); central receptor dystrophies (two large autosomal dominant macular dystrophy pedigrees). Detailed phenotyping has included clinical examination, colour fundus photography, autofluorescence imaging, electrophysiological assessment, visual field testing, colour vision testing, and dark-adapted perimetry.

This study identifies further mutations in known genes causing achromatopsia and describes the first report of progressive cone dystrophy caused by mutations in *CNGB3*. Mutation screening of the candidate gene, *PROM1*, in one of the pedigrees with autosomal dominant macular dystrophy has revealed a novel mutation. Mutation screening of *NR2E3*, the gene associated with enhanced S-cone syndrome has been performed and several novel mutations identified. The CORD syndrome associated with abnormalities in teeth enamel formation, amelogenesis imperfecta, has been recently mapped to a region encompassing the gene *CNGA3*. Consequently extraction of mRNA from mouse teeth has been undertaken, from which cDNA has been synthesised and used to assess whether *CNGA3* or *CNGB3* is expressed in developing teeth. Neither appeared to be expressed in the mouse tooth at the studied developmental stages.

TABLE OF CONTENTS

DECLARATION	2
ABSTRACT	3
LIST OF TABLES	14
LIST OF FIGURES	16
PUBLICATIONS	20
ABBREVIATIONS	23
1.0 INTRODUCTION	25
1.1 THE CONE AND CONE-ROD DYSTROPHIES	26
1.1.1 <i>The retinal anatomical substrate of vision</i>	27
1.1.1.1 Photoreception	27
1.1.1.2 Bipolar cells	32
1.1.1.3 Ganglion cells	33
1.1.2 <i>The cone dysfunction syndromes</i>	33
1.1.2.1 Complete achromatopsia	35
1.1.2.1.1 Clinical findings	35
1.1.2.1.2 Molecular genetics	35
1.1.2.1.2.1 <i>CNGA3 & CNGB3</i>	35
1.1.2.1.2.2 <i>GNAT2</i>	39
1.1.2.2 Incomplete achromatopsia	40
1.1.2.2.1 Clinical findings	40
1.1.2.2.2 Molecular genetics	41
1.1.2.3 Blue cone (S-cone) monochromatism	42
1.1.2.3.1 Clinical findings	42
1.1.2.3.2 Molecular genetics	44
1.1.2.4 Oligocone trichromacy	46
1.1.2.4.1 Clinical findings	46
1.1.2.4.2 Molecular genetics	46
1.1.2.5 Bornholm eye disease	47
1.1.2.5.1 Clinical findings	47
1.1.2.5.2 Molecular genetics	47

1.1.2.6 Cone-monochromatism	47
1.1.3 <i>Progressive cone and cone-rod dystrophies</i>	48
1.1.3.1 Clinical findings	49
1.1.3.2 Molecular genetics	52
1.1.4 <i>Goldmann-Favre & Enhanced S-cone syndrome</i>	57
1.1.4.1 Clinical findings	57
1.1.4.2 Molecular genetics	58
1.1.5 <i>Management of the cone and cone-rod dystrophies</i>	59
1.2 THE INHERITED MACULAR DYSTROPHIES	60
1.2.1 <i>Autosomal recessive inheritance</i>	62
1.2.1.1 Stargardt disease and Fundus Flavimaculatus	62
1.2.1.1.1 Clinical findings	62
1.2.1.1.2 Molecular genetics	64
1.2.2 <i>Autosomal dominant inheritance</i>	67
1.2.2.1 Autosomal dominant Stargardt-like macular dystrophy	67
1.2.2.1.1 Clinical findings	67
1.2.2.1.2 Molecular genetics	67
1.2.2.2 Best Disease (vitelliform macular dystrophy)	68
1.2.2.2.1 Clinical findings	68
1.2.2.2.2 Molecular genetics	69
1.2.2.3 Adult vitelliform macular dystrophy	70
1.2.2.3.1 Clinical findings	70
1.2.2.3.2 Molecular genetics	71
1.2.2.4 Pattern dystrophy	71
1.2.2.4.1 Clinical findings	71
1.2.2.4.2 Molecular genetics	72
1.2.2.5 Doyme honeycomb retinal dystrophy	74
1.2.2.5.1 Clinical findings	74
1.2.2.5.2 Molecular genetics	75
1.2.2.6 Autosomal dominant drusen and macular degeneration	75
1.2.2.6.1 Clinical findings	75
1.2.2.6.2 Molecular genetics	76

1.2.2.7 North Carolina macular dystrophy	76
1.2.2.7.1 Clinical findings	76
1.2.2.7.2 Molecular genetics	76
1.2.2.8 Progressive bifocal chorioretinal atrophy	77
1.2.2.8.1 Clinical findings	77
1.2.2.8.2 Molecular genetics	78
1.2.2.9 Sorsby fundus dystrophy	78
1.2.2.9.1 Clinical findings	78
1.2.2.9.2 Molecular genetics	79
1.2.2.10 Central areolar choroidal dystrophy	80
1.2.2.10.1 Clinical findings	80
1.2.2.10.2 Molecular genetics	80
1.2.2.11 Dominant cystoid macular dystrophy	80
1.2.2.11.1 Clinical findings	80
1.2.2.11.2 Molecular genetics	81
1.2.3 <i>X-linked inheritance</i>	81
1.2.3.1 X-linked juvenile retinoschisis	81
1.2.3.1.1 Clinical findings	81
1.2.3.1.2 Molecular genetics	81
1.2.4 <i>Mitochondrial inheritance</i>	82
1.2.4.1 Maternally inherited diabetes and deafness	82
1.2.5 <i>Conclusions</i>	83
1.3 PHENOTYPING TECHNIQUES	84
1.3.1 <i>History and examination</i>	84
1.3.2 <i>Imaging</i>	85
1.3.2.1 Fundus photography	85
1.3.2.2 Autofluorescence imaging	85
1.3.3 <i>Electrophysiological testing</i>	86
1.3.4 <i>Psychophysical testing</i>	88
1.3.4.1 Colour vision assessment	88
1.3.4.1.1 Plate tests	88
1.3.4.1.2 Cap tests	89
1.3.4.1.3 Anomaloscopy	91

1.3.4.1.4 Computerised tests	92
1.3.4.2 Perimetry and dark adaptometry	92
1.4 MOLECULAR GENETIC TECHNIQUES	94
1.4.1 <i>Functional candidate gene approach</i>	94
1.4.2 <i>Positional candidate gene approach</i>	94
1.4.3 <i>Linkage analysis</i>	95
1.4.3.1 Genetic markers	96
1.4.4 <i>Mutation analysis</i>	96
2.0 MATERIALS AND METHODS	98
2.1 PATIENT ASCERTAINMENT	99
2.2 PATIENT ASSESSMENT	99
2.2.1 <i>Clinical history and examination</i>	100
2.2.2 <i>Further examination techniques</i>	100
2.3 SAMPLE COLLECTION	101
2.4 MATERIALS	101
2.4.1 <i>Buffers and reagents</i>	101
2.4.2 <i>Gel electrophoresis</i>	101
2.4.3 <i>Kits utilised</i>	102
2.5 METHODS	102
2.5.1 <i>Human genomic DNA extraction from whole blood</i>	102
2.5.2 <i>Human genomic DNA extraction from buccal swabs</i>	103
2.5.3 <i>Spectrophotometry</i>	104
2.5.4 <i>Size fractionation of DNA by gel electrophoresis</i>	104
2.5.5 <i>The Polymerase chain reaction (PCR)</i>	105
2.5.5.1 Reaction principles	105
2.5.5.2 Standard PCR parameters	107
2.5.6 <i>Primer design and PCR optimisation</i>	108
2.5.7 <i>Elution of target PCR fragments</i>	109
2.5.8 <i>Automated DNA sequencing and ethanol precipitation</i>	109
2.5.9 <i>Operation of automated sequencer</i>	111
2.5.10 <i>In silico genetic analysis</i>	111
2.5.11 <i>Nucleic acid extraction</i>	112
2.5.11.1 mRNA isolation	112

2.5.11.2 Quantification of mRNA	112
2.5.11.3 Precipitation of mRNA	112
2.5.12 Reverse transcription PCR (RT-PCR)	113
2.5.13 Bioinformatics	113

PART 1 CONE DYSFUNCTION SYNDROMES

3.0 ACHROMATOPSIA	114
3.1 INTRODUCTION	115
3.2 AIMS	118
3.3 PHENOTYPE	118
3.3.1 <i>Methods</i>	119
3.3.2 <i>Results</i>	119
3.4 <i>CNGB3</i> MUTATION SCREENING	126
3.4.1 <i>Methods</i>	126
3.4.2 <i>Results</i>	126
3.5 DISCUSSION	133
3.6 CONCLUSIONS	137
3.7 <i>GNAT2</i> PHENOTYPE	138
3.7.1 <i>Patients and methods</i>	139
3.7.2 <i>Results</i>	140
3.7.3 <i>Discussion</i>	145
3.7.4 <i>Conclusions</i>	147
4.0 BLUE CONE MONOCHROMATISM	148
4.1 INTRODUCTION	149
4.2 AIMS	152
4.3 METHODS	152
4.3.1 <i>Patients and clinical assessment</i>	152
4.4 RESULTS	155
4.4.1 <i>Phenotype</i>	155
4.4.2 <i>Genotype</i>	162
4.5 DISCUSSION	165
4.6 CONCLUSIONS	168

5.0 OLIGOCONE TRICHROMACY	170
5.1 INTRODUCTION	171
5.2 AIMS	171
5.3 METHODS	172
5.3.1 <i>Patients and methods</i>	172
5.3.2 <i>CNGB3 mutation screening</i>	172
5.4 RESULTS	173
5.4.1 <i>Phenotype</i>	173
5.4.2 <i>CNGB3 mutation screening</i>	176
5.5 DISCUSSION	178
5.6 CONCLUSIONS	181

6.0 X-LINKED CONE DYSFUNCTION SYNDROME WITH MYOPIA AND DICHROMACY **182**

6.1 INTRODUCTION	183
6.2 AIMS	183
6.3 METHODS	184
6.3.1 <i>Patients and methods</i>	184
6.3.2 <i>Molecular genetic analysis</i>	185
6.4 RESULTS	185
6.4.1 <i>Phenotype</i>	185
6.4.2 <i>Genotype</i>	194
6.5 DISCUSSION	196
6.6 CONCLUSIONS	200

PART 2 PROGRESSIVE CONE & CONE-ROD DYSTROPHIES

7.0 PROGRESSIVE CONE DYSTROPHY ASSOCIATED WITH CNGB3	201
7.1 INTRODUCTION	202
7.2 AIMS	203
7.3 METHODS	204
7.3.1 <i>Patients and methods</i>	204
7.3.2 <i>CNGB3 mutation screening</i>	205

7.4 RESULTS	206
7.4.1 <i>Phenotype</i>	206
7.4.2 <i>Genotype</i>	209
7.5 DISCUSSION	211
7.6 CONCLUSIONS	214
8.0 CONE DYSTROPHY WITH SUPERNORMAL ROD RESPONSES	215
8.1 INTRODUCTION	216
8.2 AIMS	217
8.3 METHODS	217
8.3.1 <i>Patients and methods</i>	218
8.3.2 <i>NR2E3 mutation screening</i>	219
8.4 RESULTS	220
8.4.1 <i>Phenotype</i>	220
8.4.2 <i>NR2E3 mutation screening</i>	229
8.5 DISCUSSION	229
8.6 CONCLUSIONS	232
9.0 AN AUTOSOMAL DOMINANT CONE-ROD DYSTROPHY (CORD7)	233
9.1 INTRODUCTION	234
9.2 AIMS	235
9.3 PATIENTS AND METHODS	235
9.3.1 <i>Patients</i>	235
9.3.2 <i>Methods</i>	236
9.4 RESULTS	237
9.5 DISCUSSION	249
9.6 CONCLUSIONS	253
10.0 CONE-ROD DYSTROPHY ASSOCIATED WITH AMELOGENESIS IMPERFECTA	254
10.1 INTRODUCTION	255
10.2 AIMS	257
10.3 METHODS	257

10.3.1 <i>Clinical assessment</i>	257
10.3.1.1. Ocular	257
10.3.1.2 Dental	258
10.3.2 <i>Molecular genetics</i>	259
10.3.2.1 <i>CNGA3</i> mutation screening	259
10.3.2.2 Genotyping	259
10.3.2.3 RNA extraction and precipitation	260
10.3.2.4 RT-PCR	260
10.3.2.5 <i>CNGA3</i> and <i>CNGB3</i> expression studies	261
10.4 RESULTS	261
10.4.1 <i>Phenotype</i>	261
10.4.1.1 Ocular	261
10.4.1.2 Dental	264
10.4.2 <i>Molecular genetics</i>	266
10.4.2.1 <i>CNGA3</i> mutation screening and segregation of the 2q11 region	266
10.4.2.2 <i>CNGA3</i> and <i>CNGB3</i> expression in developing mouse teeth	266
10.5 DISCUSSION	268
10.6 CONCLUSIONS	270
11.0 ENHANCED S-CONE SYNDROME	271
11.1 INTRODUCTION	272
11.2 AIMS	273
11.3 METHODS	273
11.3.1 <i>Patients and methods</i>	273
11.3.2 <i>NR2E3</i> mutation screening	274
11.4 RESULTS	275
11.4.1 <i>Patients</i>	275
11.4.2 <i>NR2E3</i> mutation screening	285
11.5 DISCUSSION	291
11.6 CONCLUSIONS	296

PART 3 INHERITED MACULAR DYSTROPHIES

12.0 AN AUTOSOMAL DOMINANT BULL’S-EYE MACULAR DYSTROPHY (MCDR2)	297
12.1 INTRODUCTION	298
12.2 AIMS	298
12.3 METHODS	298
12.3.1 <i>Patients and clinical assessment</i>	299
12.3.2 <i>Linkage analysis</i>	300
12.3.3 <i>PROM1 mutation screening</i>	301
12.4 RESULTS	303
12.4.1 <i>Phenotype</i>	303
12.4.2 <i>Molecular genetics</i>	309
12.4.2.1 Linkage analysis	309
12.4.2.2 <i>PROM1</i> mutation screening	310
12.5 DISCUSSION	312
12.6 CONCLUSIONS	316
13.0 AN AUTOSOMAL DOMINANT MACULAR DYSTROPHY (MCDR3) RESEMBLING NORTH CAROLINA MACULAR DYSTROPHY	318
13.1 INTRODUCTION	319
13.2 AIMS	319
13.3 METHODS	320
13.3.1 <i>Patients and clinical assessment</i>	320
13.3.2 <i>Linkage analysis</i>	320
13.4 RESULTS	322
13.4.1 <i>Phenotype</i>	322
13.4.2 <i>Linkage analysis</i>	330
13.5 DISCUSSION	330
13.6 CONCLUSIONS	333

14.0 CONCLUDING REMARKS AND FUTURE PERSPECTIVES	335
15.0 ACKNOWLEDGEMENTS	338
16.0 REFERENCES	339
17.0 PUBLICATIONS	370

LIST OF TABLES

Table	Title	Page
<i>INTRODUCTION</i>		
Table 1.1	Summary of the cone dysfunction syndromes	34
Table 1.2	Cone-rod dystrophies (CORDs) with identified genes and known chromosomal loci	56
Table 1.3	Syndromic CORDs with identified genes and known chromosomal loci	57
Table 1.4	Chromosomal loci and causative genes in inherited macular dystrophies	61
<i>ACHROMATOPSIA</i>		
Table 3.1	Summary of clinical findings in achromatopsia	122 & 123
Table 3.2	Summary of psychophysical data in achromatopsia	124 & 125
Table 3.3	<i>CNGB3</i> disease-causing mutations	127
Table 3.4	Amino acid conservation in cone and rod β -subunits of CNG channel proteins at sites of missense mutations in <i>CNGB3</i>	128
Table 3.5	<i>CNGA3</i> disease-causing mutations	133
Table 3.6	Summary of clinical findings in <i>GNAT2</i> pedigree	143
<i>BLUE CONE MONOCHROMATISM</i>		
Table 4.1	Primers for amplification of the LCR and exons 1 to 6 of the L- and M-opsin genes	163
Table 4.2	Nucleotide differences between L and M exons used for opsin gene identification	164
<i>OLIGOCONE TRICHROMACY</i>		
Table 5.1	Summary of clinical findings in oligocone trichromacy	176
Table 5.2	Summary of psychophysical findings in oligocone trichromacy	177

PROGRESSIVE CONE DYSTROPHY ASSOCIATED WITH CNGB3

Table 7.1	Summary of clinical findings	208
------------------	------------------------------	-----

CONE DYSTROPHY WITH SUPERNORMAL ROD RESPONSES

Table 8.1	Summary of clinical findings in COD/SuperROD	223
Table 8.2	Refraction, VA progression, nyctalopia and photopic visual fields	224

AN AUTOSOMAL DOMINANT CONE-ROD DYSTROPHY (CORD7)

Table 9.1	Summary of clinical findings in CORD7	240
------------------	---------------------------------------	-----

CONE-ROD DYSTROPHY ASSOCIATED WITH AMELOGENESIS IMPERFECTA

Table 10.1	Syndromes with associated cone-rod dystrophy (CORD)	256
Table 10.2	D2S2187 primers	260
Table 10.3	Primers for amplification of murine <i>CNGA3</i> and <i>CNGB3</i>	261

ENHANCED S-CONE SYNDROME

Table 11.1	Primers for amplification of <i>NR2E3</i>	275
Table 11.2	Summary of clinical findings in ESCS	283 & 284
Table 11.3	<i>NR2E3</i> disease-causing mutations	286
Table 11.4	Amino acid conservation in <i>NR2E3</i> receptors at sites of identified missense mutations	287

AN AUTOSOMAL DOMINANT BULL'S-EYE MACULAR DYSTROPHY (MCDR2)

Table 12.1	<i>PROM1</i> 5'-3' primer sequences	303
Table 12.2	Lack of amino acid conservation across species at site of missense mutation in prominin-1	310

AN AUTOSOMAL DOMINANT MACULAR DYSTROPHY (MCDR3)

RESEMBLING NORTH CAROLINA MACULAR DYSTROPHY

Table 13.1	Summary of clinical findings in MCDR3	329
-------------------	---------------------------------------	-----

LIST OF FIGURES

Figure	Title	Page
<i>INTRODUCTION</i>		
Figure 1.1	Phototransduction cascade	32
Figure 1.2	Location of CNGA3 mutations	37
Figure 1.3	Location of CNGB3 mutations	38
Figure 1.4	Bull's-eye maculopathy	50
Figure 1.5	Cone-rod dystrophy (early and end-stage)	51
Figure 1.6	Enhanced S-cone syndrome	58
Figure 1.7	Stargardt disease	63
Figure 1.8	Best disease	69
Figure 1.9	Pattern dystrophy	72
Figure 1.10	Doyme honeycomb retinal dystrophy	74
Figure 1.11	North Carolina macular dystrophy	77
Figure 1.12	Sorsby fundus dystrophy	78
Figure 1.13	MIDD associated maculopathy	82
Figure 1.14	HRR plates and the M-R minimal test	91
<i>MATERIALS AND METHODS</i>		
Figure 2.1	Schematic diagram of the polymerase chain reaction	106
<i>ACHROMATOPSIA</i>		
Figure 3.1	CNGA3 and CNGB3 polypeptide structure	116
Figure 3.2	Fundi in achromatopsia	120
Figure 3.3	CNGB3 Exon 5 mutation	128
Figure 3.4	CNGB3 Exon 13 mutation	129
Figure 3.5	Segregation of F525N in family 17	129
Figure 3.6	Location of novel CNGB3 and CNGA3 mutations	130
Figure 3.7	CNGB3 5'UTR and Exon 1 variants	132
Figure 3.8	GNAT2 pedigree	140
Figure 3.9	Typical fundi of GNAT2 family	141
Figure 3.10	Electrophysiological data from two GNAT2 patients	142

Figure 3.11	Enlarged Farnsworth D-15 (PV-16)	144
 <i>BLUE CONE MONOCHROMATISM</i>		
Figure 4.1	Achromatopsia and BCM ERGs	151
Figure 4.2	BCM families	154
Figure 4.3	Fundi in BCM	158
Figure 4.4	Opsin array of BCM individuals	165
 <i>OLIGOCONE TRICHROMACY</i>		
Figure 5.1	Full-field ERGs in four oligocone trichromacy patients	174
 <i>X-LINKED CONE DYSFUNCTION SYNDROME WITH MYOPIA AND DICHROMACY</i>		
Figure 6.1	ERGs of affected males from Family A	186
Figure 6.2	Family A pedigree	187
Figure 6.3	Subject A1 D15 Test	188
Figure 6.4	Myopic fundi with tilted optic discs of patient C1	190
Figure 6.5	Myopic fundi with tilted optic discs of patient D1	191
Figure 6.6	Family E pedigree	192
 <i>PROGRESSIVE CONE DYSTROPHY ASSOCIATED WITH CNGB3</i>		
Figure 7.1	Progressive cone dystrophy pedigree	204
Figure 7.2	Fundi	207
Figure 7.3	The Farnsworth Munsell 100-hue colour vision test	207
Figure 7.4	Sequence electropherograms of exon 11 and exon 10 of <i>CNGB3</i>	210
Figure 7.5	Sequence alignment of the pore region of human cone and rod α - and β -subunits of the CNG channels	211
 <i>CONE DYSTROPHY WITH SUPERNORMAL ROD RESPONSES</i>		
Figure 8.1	Colour fundus photographs and AF images in COD/SuperROD	225 & 226
Figure 8.2	ERGs of cases 6 and 7	227
Figure 8.3	Scotopic red and blue 30° static threshold perimetry of case 1 and case 5	228

AN AUTOSOMAL DOMINANT CONE-ROD DYSTROPHY (CORD7)

Figure 9.1	Four-generation pedigree of a British family with autosomal dominant cone-rod dystrophy (CORD7)	236
Figures 9.2	Colour fundus photographs and AF images in CORD7	241 & 242
Figure 9.3	Peripheral retinal atrophy in CORD7	243
Figure 9.4	Fundus photographs and FFA of II:5	244
Figure 9.5	Fundus autofluorescence imaging of IV:2	245
Figure 9.6	Patient IV:3 ERG data showing progressive deterioration of retinal function	245
Figure 9.7	Electrophysiological traces from the patients examined	246
Figure 9.8	Scotopic red and blue 30° static threshold perimetry of IV:3 and III:2	248

CONE-ROD DYSTROPHY ASSOCIATED WITH AMELOGENESIS IMPERFECTA

Figure 10.1	Two-generation pedigree of a Kosovan family with autosomal recessive CORD and amelogenesis imperfecta	258
Figure 10.2	Fundus photographs showing bilateral macular RPE mottling and atrophy	262
Figure 10.3	Electrophysiological testing	263
Figure 10.4	Amelogenesis imperfecta phenotype	265
Figure 10.5	Expression of <i>CNGA3</i> and <i>CNGB3</i>	267
Figure 10.6	Murine <i>CNGA3</i> & <i>CNGB3</i> primer validation	267

ENHANCED S-CONE SYNDROME

Figure 11.1	Typical pigment clumping seen in ESCS (Patient 7)	276
Figure 11.2	Typical pigment clumping seen in ESCS (Patient 11)	277
Figure 11.3	Fundus findings in ESCS	277
Figure 11.4	AF and FFA findings in ESCS	278
Figure 11.5	AF images showing a spoke-like area of AF centred on the macula (Patient 16)	279
Figure 11.6	AF images showing a ring of increased AF (Patient 8)	279
Figure 11.7	OCT images showing bilateral macular cystic spaces	280
Figure 11.8	Typical ERG data seen in ESCS	282
Figure 11.9	<i>NR2E3</i> V49M mutation	287

Figure 11.10	<i>NR2E3</i> Y81C mutation	287
Figure 11.11	<i>NR2E3</i> splice acceptor intron 1 mutation (C→G)	288
Figure 11.12	<i>NR2E3</i> splice acceptor intron 1 mutation (A→C)	288
Figure 11.13	Consensus sequences for 5' and 3' splice sites in nuclear protein-coding genes and location of splice site mutations identified in <i>NR2E3</i>	289
Figure 11.14	<i>NR2E3</i> splice acceptor intron 8 mutation (G→A)	290
Figure 11.15	<i>NR2E3</i> R311Q mutation	290

AN AUTOSOMAL DOMINANT BULL'S-EYE MACULAR DYSTROPHY (MCDR2)

Figure 12.1	<i>MCDR2</i> pedigree	300
Figure 12.2	Proposed structural model of prominin-1	302
Figure 12.3	AF images of <i>MCDR2</i> patient V:1	304
Figures 12.4	Fundi, FFA, & AF images of <i>MCDR2</i> patients IV:2 & III:6	307 & 308
Figure 12.5	The full-field ERG of patient III:2	309
Figure 12.6	Sequence electropherograms of exon 10 of <i>PROM1</i>	311
Figure 12.7	Segregation of Arg373Cys mutation	311
Figure 12.8	Positions of Arg373Cys and the stop codon described by Maw <i>et al.</i> (2000)	312
Figure 12.9	Expression studies in 293T cells of EGFP-tagged wild-type and Arg373Cys mutant prominin-1 protein	316

AN AUTOSOMAL DOMINANT MACULAR DYSTROPHY (MCDR3)

RESEMBLING NORTH CAROLINA MACULAR DYSTROPHY

Figure 13.1	<i>MCDR3</i> pedigree	321
Figures 13.2	Fundi & AF images of <i>MCDR3</i> patients	323 - 327

PUBLICATIONS

Aligianis IA, ForsheW T, Johnson S, **Michaelides M**, Johnson CA, Trembath RC, Hunt DM, Moore AT, Maher ER. Mapping of a novel locus for achromatopsia (*ACHM4*) to 1p and identification of a germ line mutation in the α subunit of cone transducin (*GNAT2*). *J Med Genet.* 2002;39:656-660.

Michaelides M, Johnson S, Poulson A, Bradshaw K, Bellmann C, Hunt DM, Moore AT. An Autosomal Dominant Bull's Eye Macular Dystrophy (MCDR2) that maps to the short arm of chromosome 4. *Invest Ophthalmol Vis Sci.* 2003;44:1657-1662.

Michaelides M, Johnson S, Tekriwal AK, Holder GE, Bellmann C, Kinning E, Woodruff G, Trembath RC, Hunt DM, Moore AT. An early-onset autosomal dominant macular dystrophy (MCDR3) resembling North Carolina macular dystrophy maps to chromosome 5. *Invest Ophthalmol Vis Sci.* 2003;44:2178-2183.

Michaelides M, Hunt DM, Moore AT. The genetics of inherited macular dystrophies. *J Med Genet.* 2003;40:641-650.

Michaelides M, Aligianis IA, Holder GE, Simuovic MP, Mollon JD, Maher ER, Hunt DM, Moore AT. Cone dystrophy phenotype associated with a frameshift mutation (M280fsX291) in the α -subunit of cone specific transducin (*GNAT2*). *Br J Ophthalmol.* 2003;87:1317-1320.

Michaelides M, Hunt DM, Moore AT. The cone dysfunction syndromes. *Br J Ophthalmol.* 2004;88:291-297

Michaelides M[†], Johnson S[†], Aligianis IA, Ainsworth JR, Mollon JD, Maher ER, Moore AT, Hunt DM. Achromatopsia caused by novel mutations in both *CNGA3* and *CNGB3*. *J Med Genet.* 2004 (in press).

[†] Joint first authors

Michaelides M, Aligianis IA, Ainsworth JR, Good P, Mollon JD, Maher ER, Moore AT, Hunt DM. Progressive cone dystrophy associated with mutation in *CNGB3*. *Invest Ophthalmol Vis Sci*. 2004 (in press).

Michaelides M, Holder GE, Bradshaw K, Hunt DM, Mollon JD, Moore AT. Oligocone trichromacy - a rare and unusual cone dysfunction syndrome. *Br J Ophthalmol*. 2004 (in press).

Michaelides M, Johnson S, Simunovic MP, Bradshaw K, Holder GE, Mollon JD, Moore AT, Hunt DM. Blue cone monochromatism: a phenotype and genotype assessment with evidence of progressive loss of cone function in older individuals. *Eye* 2004 (in press).

Michaelides M, Bloch-Zupan A, Holder GE, Hunt DM, Moore AT. An autosomal recessive cone-rod dystrophy associated with amelogenesis imperfecta. *J Med Genet*. 2004 (in press).

Michaelides M, Johnson S, Simunovic MP, Bradshaw K, Holder GE, Mollon JD, Moore AT, Hunt DM. X-linked cone dysfunction syndrome with myopia and protanopia. (submitted for publication).

Michaelides M, Mollon JD, Holder GE, Webster A, Bird AC, Hunt DM, Moore AT. A detailed study of the phenotype of an unusual progressive cone dystrophy with supernormal rod responses. (submitted for publication).

Michaelides M, Holder GE, Fitzke FW, Webster A, Hunt DM, Bird AC, Moore AT. A detailed study of the phenotype of an autosomal dominant cone-rod dystrophy (CORD7) associated with mutation in the gene for RIM1. (submitted for publication).

ARVO Poster Presentations

Good PA, Banerjee S, Aligianis I, Siddiqi R, Johnson S, Ainsworth JR, **Michaelides M**, Hunt D, and Moore T. Electroretinography in the definition of phenotypes of rod monochromatism. *Invest Ophthalmol Vis Sci*. 2003;44: E-Abstract 1488.

Michaelides M, Johnson S, Poulson A, Bradshaw K, Bellmann C, Hunt DM, and Moore AT. An autosomal dominant bull's-eye macular dystrophy (MCDR2) that maps to chromosome 4p. *Invest Ophthalmol Vis Sci.* 2003;44: E-Abstract 1495.

Johnson S, **Michaelides M**, Aligianis IA, Trembath RC, Ainsworth J, Maher ER, Moore AT, and Hunt DM. Achromatopsia associated with mutations in *CNGA3* and *CNGB3*. *Invest Ophthalmol Vis Sci.* 2003;44: E-Abstract 2300.

Oxford Congress Poster Presentation

Michaelides M, Johnson S, Simunovic MP, Bradshaw K, Holder GE, Mollon JD, Hunt DM, and Moore AT. X-linked cone dysfunction syndromes. 2003.

Oral Presentations

The Royal College of Ophthalmologists Annual Congress, 2003.

Michaelides M, Johnson S, Holder GE, Woodruff G, Hunt DM, Moore AT. An early-onset autosomal dominant macular dystrophy (MCDR3) resembling North Carolina macular dystrophy (NCMD) maps to chromosome 5.

The European Paediatric Ophthalmology Society, 2002.

Michaelides M, Holder GE, Bradshaw K, Hunt DM, Mollon JD, Moore AT. Oligocone trichromacy.

The European Paediatric Ophthalmology Society, 2003.

Michaelides M, Francis PJ, Johnson S, Woodruff G, Hunt DM, Bird AC, Moore AT. Genetic heterogeneity in the North Carolina macular dystrophy phenotype.

ABBREVIATIONS

AD	Autosomal dominant
AF	Autofluorescence
AR	Autosomal recessive
ARMD	Age-related macular degeneration
ATP	Adenosine triphosphate
BCM	Blue cone monochromatism
BED	Bornholm eye disease
BEM	'Bull's-eye' maculopathy
bp	Base pair
Ca²⁺	Calcium ion
CACD	Central areolar choroidal dystrophy
CaM	Calmodulin
cDNA	Complementary deoxyribonucleic acid
CNG	cyclic nucleotide-gated
COD	Cone dystrophy
CORD	Cone-rod dystrophy
DNA	Deoxyribonucleic acid
dNTPs	Deoxyribonucleic acid triphosphates
EDTA	Ethylene diamine tetra-acetic acid
EOG	Electro-oculogram/electro-oculography
ERG	Electroretinogram/electroretinography
FFM	Fundus flavimaculatus
FM	Farnsworth-Munsell
GCAP	Guanylate cyclase activating protein
gDNA	Genomic DNA
Hm	Homozygous
HRR	Hardy, Rand, Rittler plates
Ht	Heterozygous
ISCEV	International society for clinical electrophysiology of vision
LCR	Locus control region
MCDR1	North Carolina macular dystrophy
MIDD	Maternally inherited diabetes and deafness

M-R	Mollon-Reffin minimal test
mRNA	Messenger RNA
PBCRA	Progressive bifocal chorioretinal atrophy
PBS	Phosphate buffer solution
PCD	Progressive cone dystrophy
PCR	Polymerase chain reaction
PDE	Phosphodiesterase
PERG	Pattern ERG
RetGC	Retinal guanylate cyclase
RM	Rod monochromatism
RNA	Ribonucleic acid
RNase	Ribonuclease
RP	Retinitis pigmentosa
RPE	Retinal pigment epithelium
RT-PCR	Reverse-transcription polymerase chain reaction
SFD	Sorsby fundus dystrophy
SNP	Single nucleotide polymorphism
SRNVM	Subretinal neovascular membrane
STGD	Stargardt disease
T_a°C	Annealing temperature
TAE	Tris/acetate/EDTA buffer
tRNA	Transfer RNA
UV	Ultra violet
v/v	Volume/volume
wt	Wild-type
w/v	Weight/volume
XL	X-linked
XLRS	X-linked juvenile retinoschisis

CHAPTER 1

INTRODUCTION

The cone and central receptor dystrophies are an extremely heterogeneous group of disorders, both in terms of clinical features and underlying molecular genetic basis. There have been considerable advances made in recent years of our understanding of the pathogenesis of these retinal dystrophies. This improved knowledge of disease mechanisms has raised the possibility of potential future treatments for these disorders, for which there are no specific therapies available at the present time.

The cone and central receptor dystrophies will be discussed separately in the ensuing introduction.

1.1 THE CONE AND CONE-ROD DYSTROPHIES

The cone and cone-rod dystrophies comprise a heterogeneous group of disorders characterised by visual loss, abnormalities of colour vision, visual field loss, and a variable degree of nystagmus and photophobia. There is absent or severely impaired cone function on electroretinography (ERG). Patients with cone-rod disorders develop additional rod system abnormalities that lead to night-blindness later in the disease process.

The cone dystrophies can be usefully divided into stationary (cone dysfunction syndromes) and progressive disorders. Progressive cone dystrophies usually present in childhood or early adult life, with many patients developing rod photoreceptor involvement in later life, thereby leading to considerable overlap between the 'cone' and 'cone-rod' dystrophies.

A brief discussion of retinal photoreceptors and phototransduction will follow prior to the description of the various cone dysfunction syndromes and progressive cone and cone-rod disorders.

1.1.1 *The retinal anatomical substrate of vision*

1.1.1.1 Photoreception

Cone and rod photoreceptors differ in their photopigment content, physiology and morphology. Rods have long, thin, cylindrical outer segments, whereas cones have shorter conical outer segments. The rod outer segment contains a stack of discs, formed from invaginations of the cell's plasma membrane, and it is within these discs that rod photopigment, rod opsin, is located. There is a constant process of disc renewal that takes place, with the retinal pigment epithelium (RPE) playing a central role in the removal of shed stacks of discs by a process of phagocytosis and subsequent degradation. Lipofuscin pigments are generated in the RPE as a by-product of this degradation pathway and abnormal lipofuscin accumulation has been identified in several inherited retinal disorders.

In contrast to rod photoreceptors, cone cells do not have discrete discs, rather their outer segment's plasma membrane is highly invaginated, thereby creating the membranes upon which the phototransduction cascade proteins can be inserted. This also results in a greater cone outer segment surface area than the rod outer segment, even though it is smaller in volume (Yau, 1994).

The rods have one form of photopigment, whilst there are three cone photopigments. The different photopigments use the same light-sensitive chromophore, 11-*cis*-retinal, but differ in their protein (opsin) content. The peak sensitivity of the rod pigment is approximately 496nm, whilst the cone photopigment peaks are at about 420nm, 530nm

and 560 nm, for S-(short), M-(middle) and L-(long) cone photopigments respectively. In terms of the amino acid sequences of these photopigments, the M- and L-cone opsins are around 96% identical, whereas these two photopigments share an identity of approximately 42% with the S-cone opsin and rod opsin (Nathans *et al.*, 1986b). The L- and M- pigment genes are located on the X chromosome, the S cone pigment, is encoded by a gene located on chromosome 7 (Nathans *et al.*, 1986a; Nathans *et al.*, 1986b), and the gene for rod opsin is on chromosome 3q (Nathans & Hogness, 1984). The wild-type arrangement of the L- and M-opsin genes consists of a head-to-tail array of two or more repeat units of 39kb on chromosome Xq28. Transcriptional regulation of the L- and M-visual pigment genes is controlled by an upstream locus control region (LCR) (Nathans *et al.*, 1989). Stochastic pairing is believed to occur between the LCR and either the L- or M- pigment gene promoter to activate transcription (Wang *et al.*, 1992, 1999; Smallwood *et al.*, 2002).

The chromophore is synthesised and renewed within the RPE; the all-*trans* form of retinol (obtained from either photoreceptor or choriocapillaris) is isomerised into 11-*cis*-retinol upon entering the RPE. This in turn undergoes esterification to give 11-*cis*-retinal. However cone cells also have access to a second pathway of retinoid metabolism via their close anatomical association with Müller cells (Mata *et al.*, 2002). The chromophore, 11-*cis*-retinal, is connected by a covalent Schiff-base linkage with a lysine residue in the seventh helix of the opsin molecule. The seven opsin membrane helices form a pocket within which the chromophore is situated, with 11-*cis*-retinal being the only form that can bind to the opsin. The absorption of light causes photoisomerisation of 11-*cis*-retinal to all-*trans*-retinal with subsequent protein conformational change and exposure of opsin residues necessary for binding and activation of transducin, the next intermediate in the phototransduction cascade.

Physiologically, the rods and cones also differ. Rods are sensitive to smaller amounts of light, and their physiology reflects the fact that they are designed to operate optimally at low illumination levels. Rods show a slower electrical response to light and are coupled electrically to adjacent rods (Lamb, 1996), thereby allowing rods to summate their response over time and space. In total darkness, there is a constant inflow of cations into the photoreceptor outer segment ('dark current'). When light is absorbed by the photopigment, it becomes activated, and in turn interacts with transducin, a three subunit guanine nucleotide binding protein, stimulating the exchange of bound GDP for GTP. The α -transducin subunit, which is bound to GTP, is then released from its β - and γ -subunits and activates cGMP-phosphodiesterase by removing the inhibitory γ -subunits from the active site of this enzyme. cGMP-phosphodiesterase lowers the concentration of cGMP in the photoreceptor which results in closure of cGMP-gated (CNG) cation channels, with consequent membrane hyperpolarization and decreased release of neurotransmitter at the synapse (Stryer, 1991). The activated photopigment is phosphorylated into the inactive form by an enzyme known as arrestin or retinal S-antigen. CNG cation channels in cone photoreceptors are believed to be composed of two α - and two β -subunits. Closure of these cation channels results in a reduction of intracellular calcium ion (Ca^{2+}) concentration since there is continued active transport of ions out of the cell. Ca^{2+} concentrations change dramatically during phototransduction and the change in Ca^{2+} concentration is important for the recovery of the dark state of photoreceptors. One important mechanism is via the regulation of retinal guanylate cyclase (RetGC1). RetGC1 is a retina-specific membrane bound guanylate cyclase located in photoreceptor outer segments (Dizhoor *et al.*, 1994). As Ca^{2+} concentration falls, RetGC1 is activated by the Ca^{2+} -sensitive guanylate cyclase activating proteins (GCAPs) to regenerate cGMP (Palczewski *et al.*, 1994; Dizhoor *et al.*, 1995). The CNG

cation channel's affinity for cGMP is itself responsive to intracellular Ca^{2+} concentration and this is thought to be modulated by calmodulin (Hsu and Molday, 1993). The CNG channels have a higher affinity for cGMP under conditions of low intracellular Ca^{2+} concentration, thereby resulting in more channels adopting an open conformation and an increased influx of cations, eventually leading to membrane depolarisation and release of neurotransmitter. Calcium ions can also inhibit the phosphorylation of rhodopsin via the protein recoverin or S-modulin (Klenchin *et al.*, 1995). A schematic representation of the phototransduction cascade is shown in **Figure 1.1**.

There are a number of further differences between rods and cones including their opsins, proteins in the phototransduction cascade, and their intra-retinal connections. Several differences are seen in the proteins of the phototransduction process of rods and cones. The rod-specific cGMP-gated channel subunits (CNGA1 & CNGB1) are encoded by *CNGA1* and *CNGB1* (Dhallan *et al.*, 1992; Ardell *et al.*, 1996), whereas the cone-specific subunits (CNGA3 & CNGB3) are encoded by *CNGA3* and *CNGB3* (Biel *et al.*, 1994; Sundin *et al.*, 2000). In addition, cones have a specific transducin and cGMP-phosphodiesterase (PDE) (Gillespie and Beavo, 1988); indeed it remains a possibility that the different cone types may each have their own transducins, or at least α -transducin subunits (Lerea *et al.*, 1989). Rod transducin α - and γ -subunits are encoded by *GNAT1* (Ngo *et al.*, 1993) and *GNGT1* (Scherer *et al.*, 1996) respectively, while *GNAT2* (Morris & Fong, 1993) and *GNGT2* (Ong *et al.*, 1995; Ong *et al.*, 1997) encode the cone specific α - and γ -transducin subunits respectively. There is also evidence that rods and cones have distinct β -transducin subunits (Peng *et al.*, 1992). Rod PDE comprises an α -subunit, a β -subunit and two identical γ -subunits encoded by *PDE6A* (Pittler *et al.*, 1990), *PDE6B* (Bateman *et al.*, 1992; Collins *et al.*, 1992) and *PDE6G* (Dollfus *et al.*, 1993) respectively. Whilst in cones, PDE occurs as a homodimer of two α' -subunits (*PDEA2*;

Piriev *et al.*, 1995; Feshchenko *et al.*, 1996) associated with a γ -subunit (*PDE6H*; Shimizu-Matsumoto *et al.*, 1996) and three proteins of 11-, 13-, and 15-kD. The 11- and 13-kD proteins are similar to the rod γ -subunits, while the 15-kD δ -subunit binds to both rod and cone PDE (Beavo, 1995). Arrestin also differs in retinal photoreceptors, S-arrestin (Ngo *et al.*, 1990) being present in rods, and X-arrestin in cones (Murakami *et al.*, 1993). A Ca^{2+} -binding protein called visinin, believed to be the cone equivalent of recoverin, has also been identified (Polymeropoulos *et al.*, 1995).

Cones are typically 100 times less sensitive than rods and their response kinetics are several times faster, but the underlying mechanisms remain largely unknown. Several factors are likely to be involved in the difference in transduction gain and kinetics between the rods and cones, including differences in the biochemistry of the cGMP cascade, the quicker decline of Ca^{2+} concentration in cone outer segments, and differences in the rate of spontaneous isomerisation of the visual pigments. L-cone pigment has been shown to isomerise spontaneously 10,000 times more frequently than rod pigment (Kefalov *et al.*, 2003). The high spontaneous activity adapts the cones even in darkness, thereby making them less sensitive and contributes to faster kinetics than rods.

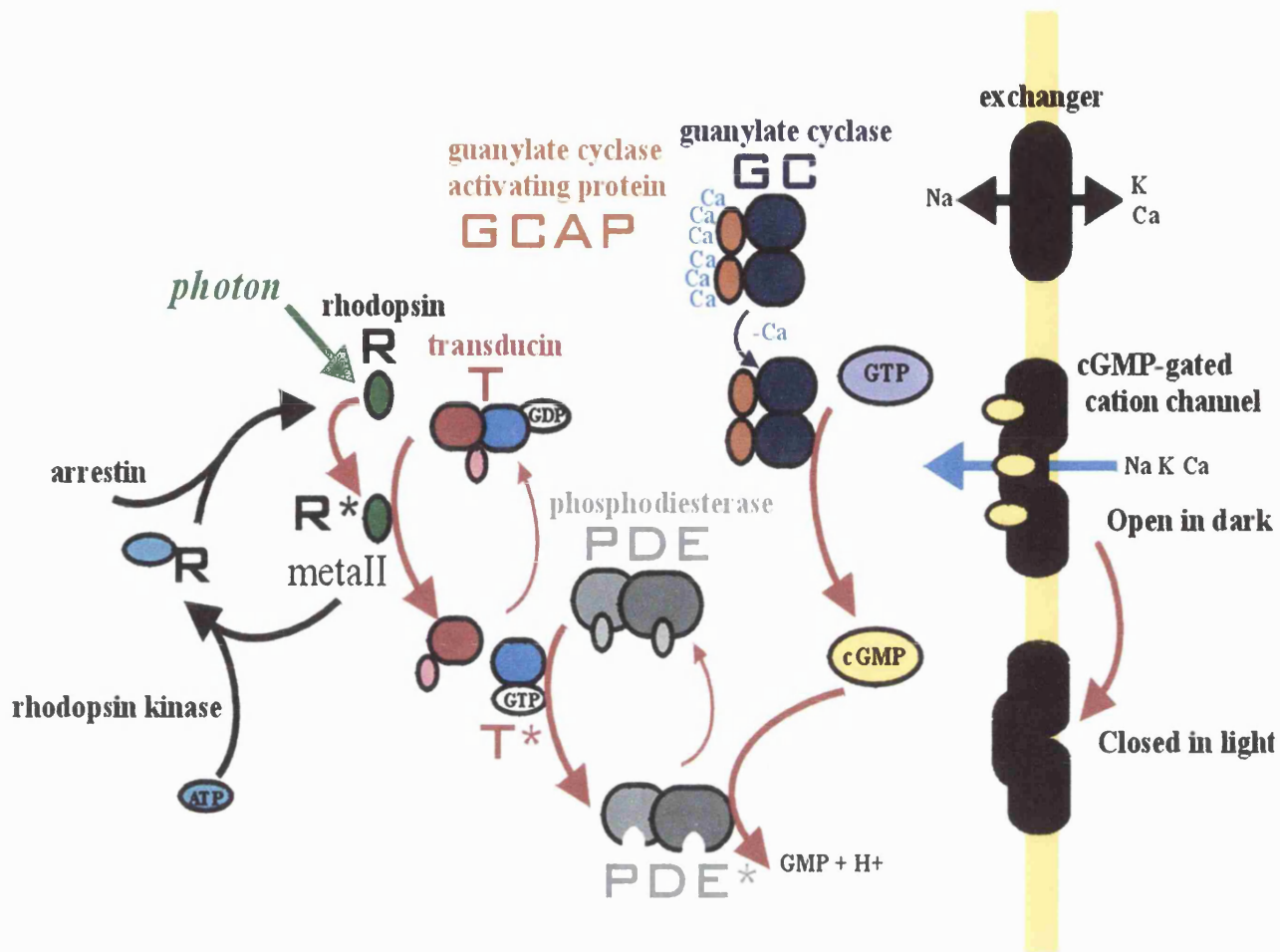


Figure 1.1
Phototransduction cascade

1.1.1.2 Bipolar cells

At the fovea individual cone cells synapse with bipolar cells in a one to one ratio, as opposed to the peripheral retina where numerous cone cells connect to a single bipolar cell. Cones make connections with two distinctly different types of bipolar cell: one type is called the ON-bipolar cell because it is depolarised after exposure to light, and the other is called the OFF-bipolar because it is hyperpolarized in response to light. There are further sub-divisions amongst bipolar cells, for example S-cones appear to synapse with different bipolars than the L-/M- cones (Kolb *et al.*, 1997). Rods are subserved by their own bipolar cells which form connections with as many as 50 rod photoreceptors.

1.1.1.3 Ganglion cells

The ganglion cells can be sub-divided into two major classes, the tonic and the phasic ganglion cells. The tonic cells have smaller receptive fields than phasic cells found at the same retinal eccentricity, and in addition, they have smaller axon diameters; reflected in a slower conduction speed. Phasic cells produce transient responses to unchanging stimuli presented in their receptive fields, whereas tonic cells produce sustained responses. Phasic cells appear to convey information about motion, low contrast and low spatial frequency, whilst tonic cells convey information about colour and higher contrast and spatial frequency (Mollon, 1990). Phasic cells transmit their signals to the magno-cellular layers (1 and 2) of the lateral geniculate nucleus, whereas tonic cells transmit to the parvo-cellular layers (3,4,5 and 6).

1.1.2 *The cone dysfunction syndromes*

The stationary cone dystrophies are better described as cone dysfunction syndromes since the term ‘dystrophy’ is usually used to describe a progressive process. These different syndromes encompass a wide range of clinical, electrophysiological and psychophysical findings (Michaelides *et al.*, 2004d). These stationary subtypes are congenital with normal rod function, whereas in progressive cone dystrophies, onset is usually in childhood or early adult life and patients usually develop rod photoreceptor dysfunction in later life.

The cone dysfunction syndromes that will be discussed are complete and incomplete achromatopsia, oligocone trichromacy, blue cone monochromatism, Bornholm eye disease and cone-monochromatism. These syndromes are summarised in **Table 1.1**.

Cone Dysfunction Syndrome	Alternative names	Mode of Inheritance	Visual acuity	Refractive error	Nystagmus	Colour vision	Fundi	Mutated Gene(s) or Chromosome locus
Complete achromatopsia	Rod monochromatism Typical achromatopsia	Autosomal recessive	6/36 - 6/60	Often hypermetropia	Present	Absent	Usually normal	<i>CNGA3</i> <i>CNGB3</i> <i>GNAT2</i> Chromosome 14
Incomplete achromatopsia	Atypical achromatopsia	Autosomal recessive	6/24-6/60	Often hypermetropia	Present	Residual	Usually normal	<i>CNGA3</i>
Oligocone trichromacy	Oligocone syndrome	Autosomal recessive	6/12 - 6/24	Equal incidence of myopia and hypermetropia	Usually Absent	Normal	Normal	-
Cone monochromatism	-	Uncertain	6/6	-	Absent	Absent or markedly reduced	Normal	-
Blue cone monochromatism	X-linked atypical achromatopsia X-linked incomplete achromatopsia	X-linked	6/24 - 6/60	Often myopia	Present	Residual tritan discrimination	Usually normal or myopic changes	i) Deletion of the LCR ii) Single inactivated L/M hybrid gene
Bornholm eye disease	-	X-linked	6/9 – 6/18	Moderate to high myopia with astigmatism	Absent	Deuteranopia	Myopic	Xq28

Table 1.1 Summary of the cone dysfunction syndromes

LCR = Locus control region

1.1.2.1 Complete achromatopsia

1.1.2.1.1 Clinical findings

Complete achromatopsia, typical achromatopsia or rod monochromatism (RM), is a stationary disorder, characterised by an absence of functioning cone photoreceptors in the retina. RM has an incidence of about 1 in 30,000 (Sharpe and Nordby, 1990; Sharpe *et al.*, 1999). Affected individuals usually present in infancy with poor visual acuity, pendular nystagmus and photophobia. A hypermetropic refractive error is common and it is often found that the nystagmus wanes with time. Affected individuals usually achieve a visual acuity of 6/60, have absent colour vision and have normal rod function but absent cone function on psychophysical testing (Hess and Nordby, 1986). Fundus examination is usually normal, however infrequently central or mid-peripheral retinal pigment epithelial abnormalities are present. Electroretinography (ERG) reveals absent cone responses and normal rod function (Andreasson and Tornqvist, 1991).

1.1.2.1.2 Molecular genetics

Achromatopsia is recessively inherited and genetically heterogeneous. To date, three achromatopsia genes have been identified, *CNGA3*, *CNGB3*, and *GNAT2*. The first molecular genetic report of achromatopsia was a cytogenetic analysis of a 20-year-old woman with achromatopsia and multiple developmental abnormalities (Pentao *et al.*, 1992). Maternal isodisomy of chromosome 14 was demonstrated. However, there has been no subsequent confirmation of a locus on chromosome 14.

1.1.2.1.2.1 *CNGA3* & *CNGB3*

In 1997 a genome-wide search for linkage was performed in a consanguineous Jewish kindred, establishing linkage to a 14cM region on 2q11 (Arbour *et al.*, 1997). This

disease interval was further refined to a 3cM region in a study of eight families of different ethnic and racial origins, and *CNGA3* was identified as a candidate gene within this interval (Wissinger *et al.*, 1998).

CNGA3 encodes the α -subunit of the cGMP-gated (CNG) cation channel in human cone photoreceptors, the final critical effector in the phototransduction cascade. In the dark, cGMP levels are high in cone cells, therefore enabling cGMP to bind to the α - and β -subunits of CNG channels, resulting in them adopting an open conformation and permitting an influx of cations, with consequent cone depolarisation. In light conditions, activated photopigment initiates a cascade culminating in increased cGMP-phosphodiesterase activity, thereby lowering the concentration of cGMP in the photoreceptor which results in closure of CNG cation channels and consequent cone hyperpolarization (Stryer, 1991).

Missense mutations in highly conserved residues of *CNGA3* were initially described in five families with complete achromatopsia from Germany, Norway and the United States (Kohl *et al.*, 1998). Recent studies have revealed more than 50 disease-causing mutations in *CNGA3* (Wissinger *et al.*, 2001; Eksandh *et al.*, 2002; Johnson *et al.*, 2003b). Mutations have been identified throughout the *CNGA3* protein, including the five-transmembrane domains, the pore region and cGMP-binding site (Figure 1.2). However, four mutations in particular (Arg277Cys, Arg283Trp, Arg436Trp and Phe547Leu) are found most commonly, accounting for approximately 40% of all mutant *CNGA3* alleles (Wissinger *et al.*, 2001) (Figure 1.2).

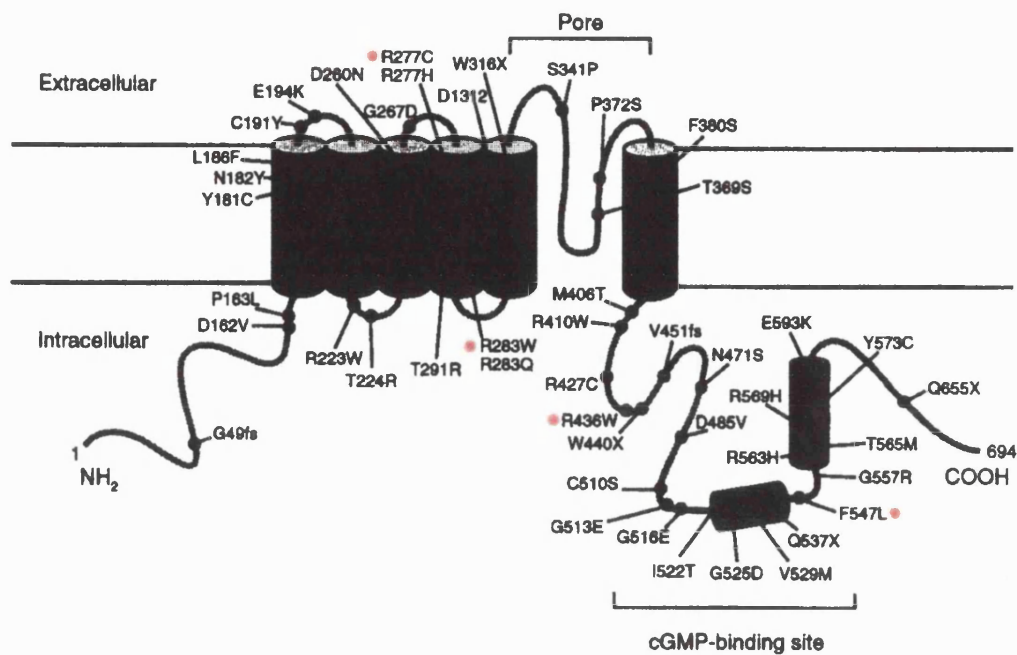


Figure 1.2

Location of CNGA3 mutations

The four most common mutations are highlighted

(adapted from Wissinger *et al.*, 2001)

Analysis of the homologous *CNGA3* knockout-mouse model showed complete absence of physiologically measurable cone function, a decrease in the number of cones in the retina, and morphological abnormalities of the remaining cones (Biel *et al.*, 1999).

The second gene identified in patients with achromatopsia was aided by the study of a population with an unusually high incidence of the disease. 5% to 10% of the Pingelapese people of the Eastern Caroline Islands in Micronesia in the western pacific have achromatopsia (Brody *et al.*, 1970). This is most probably related to the sharp reduction of the island's population to approximately 20 individuals following a typhoon in 1775, with the island being subsequently repopulated during two centuries of isolation. Linkage analysis in this population excluded the *CNGA3* locus on 2q but demonstrated linkage to

8q21-q22 (Winick *et al.*, 1999). Sundin *et al.* (2000) narrowed the region to 1.4cM and identified a missense mutation, Ser435Phe, in the Pingelapese achromats, at a highly conserved site in *CNGB3*, the gene coding for the β -subunit of cone photoreceptor CNG-cation channel. They also identified two independent frameshift deletions in a different population, Pro273fs and Thr383fs, thereby establishing that achromatopsia is the null phenotype of *CNGB3*. A similar study by Kohl *et al.* (2000) identified six mutations in *CNGB3*; three were novel: Arg203stop, Glu366stop, and a putative splice-site defect. Rojas *et al.* (2002) have since identified Asp149fs in a consanguineous Chilean family (**Figure 1.3**). The most frequent mutation of *CNGB3* identified to date is the one base-pair frameshift deletion, 1148delC (Thr383fs), which accounts for up to 84% of *CNGB3* mutant disease chromosomes (Kohl *et al.*, 2000; Kohl *et al.*, 2001).

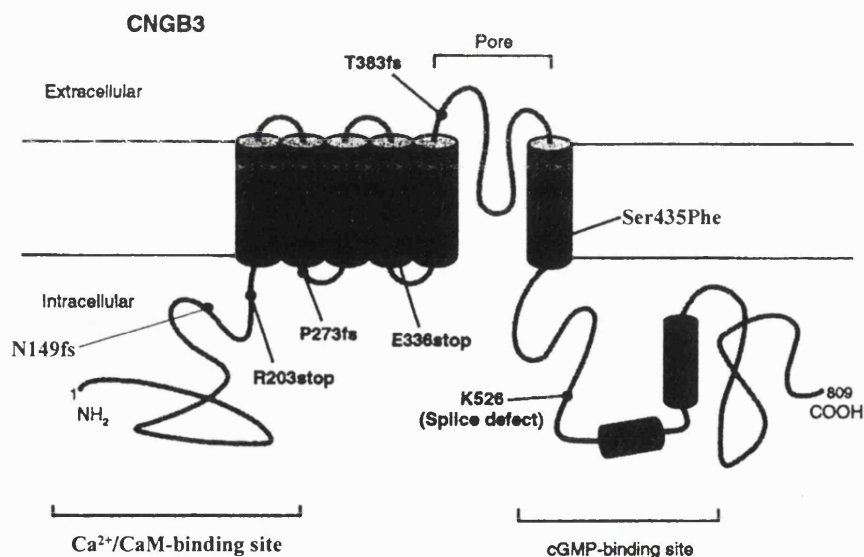


Figure 1.3

Location of CNGB3 mutations

(adapted from Weleber, 2002) CaM = Calmodulin

Currently there is far greater allelic heterogeneity of *CNGA3* mutants (over 50 mutations described) when compared to *CNGB3* (~7). It is known that *CNGA3* subunits can form functional homomeric channels when expressed alone, whereas *CNGB3* subunits alone do not appear to form functional channels (Finn *et al.*, 1998). It is therefore plausible that some *CNGB3* null mutations are not detected since sufficient channel function may be possible solely with normal *CNGA3* subunits, leading to a relatively normal phenotype ; whilst this may appear biologically plausible, it remains unlikely.

The majority of *CNGA3* mutations identified to date are missense mutations, indicating that there is little tolerance for substitutions with respect to functional and structural integrity of the channel polypeptide. This notion is supported by the high degree of evolutionary conservation among CNG channel α -subunits. In contrast, the majority of *CNGB3* alterations are nonsense mutations. It is currently proposed that approximately 25% of achromatopsia results from mutations of *CNGA3* (Wissinger *et al.*, 2001) and 40-50% from mutations of *CNGB3* (Kohl *et al.*, 2000; Kohl *et al.*, 2001). Therefore, whilst mutations in the cone channel subunit genes, *CNGA3* and *CNGB3*, account for the majority of achromats, there is a significant proportion of patients for whom neither *CNGA3* nor *CNGB3* mutations can be found (~30%). The phenotype associated with mutations in these two channel protein genes appears to be in keeping with previous clinical descriptions of achromatopsia (Kohl *et al.*, 1998; Kohl *et al.*, 2000; Sundin *et al.*, 2000; Wissinger *et al.*, 2001; Eksandh *et al.*, 2002).

1.1.2.1.2.2 *GNAT2*

GNAT2, located at 1p13, is the third gene to be recently implicated in achromatopsia (Aligianis *et al.*, 2002; Kohl *et al.*, 2002). *GNAT2* codes for the α -subunit of cone-specific transducin. In cone cells, light activated photopigment interacts with transducin,

a three subunit guanine nucleotide binding protein, stimulating the exchange of bound GDP for GTP. The cone α -transducin subunit, which is bound to GTP, is then released from its β - and γ - subunits and activates cGMP-phosphodiesterase by removing the inhibitory γ -subunits from the active site of this enzyme.

All the *GNAT2* mutations identified to date result in premature translation termination and in protein-truncation at the carboxy-terminus (Aligianis *et al.*, 2002; Kohl *et al.*, 2002). However, mutations in this gene are thought to be responsible for less than 2% of patients affected with this disorder (Kohl *et al.*, 2002), suggesting the presence of further genetic heterogeneity in achromatopsia.

The three genes described to date associated with achromatopsia, *CNGA3*, *CNGB3* and *GNAT2*, encode proteins in the cone phototransduction cascade. It is therefore reasonable to propose that further cone-specific intermediates involved in phototransduction represent good candidates. These include the genes encoding the cone specific β - and γ -transducin subunits and cone phosphodiesterase.

1.1.2.2 Incomplete achromatopsia

1.1.2.2.1 Clinical findings

Prior to the identification of the underlying molecular basis of blue cone monochromatism (BCM), BCM was known as X-linked incomplete or atypical achromatopsia. However, the term incomplete or atypical achromatopsia is best reserved for the description of individuals with autosomal recessive disease where the phenotype is a variant of complete achromatopsia. Individuals with incomplete achromatopsia (atypical achromatopsia) retain residual colour vision and have mildly better visual acuity (6/24-6/60) than those with complete achromatopsia (Pokorny *et al.*, 1982; Simunovic

and Moore, 1998). In all other respects, the phenotype of these two conditions is indistinguishable.

Three subtypes of incomplete achromatopsia have been demonstrated via colour matching experiments (Pokorny *et al.*, 1982):

- i) Colour matches are governed by rods and M-cones (incomplete achromatopsia with protan luminosity) (Smith *et al.*, 1978);
- ii) Colour matches are governed by L- and M-cones;
- iii) Colour matches mediated by rods, L-cones and S-cones (incomplete achromatopsia with deutan luminosity) (Smith *et al.*, 1979; van Norren and de Vries-de Mol, 1981).

1.1.2.2.2 Molecular genetics

As in complete achromatopsia, mutations in *CNGA3*, the gene encoding the α -subunit of the cGMP-gated cation channel in cones, have been identified in individuals with incomplete achromatopsia (Wissinger *et al.*, 2001). Insufficient psychophysical data is provided in the study by Wissinger *et al.* (2001) to be able to classify these individuals into the three colour-matching subtypes described above.

The nineteen mutations identified were all missense mutations, located throughout the channel polypeptide including the transmembrane domains, ion pore and cGMP-binding region. However, only three of these missense mutations, Arg427Cys, Arg563His, and Thr565Met, were found exclusively in patients with incomplete achromatopsia (Wissinger *et al.*, 2001). Therefore in the majority of cases of incomplete achromatopsia, factors other than the specific causative mutation, such as modifier genes or environmental influences, may dictate the phenotype. The missense variants identified in

incomplete achromatopsia must be compatible with residual channel function since the phenotype is milder than in complete achromatopsia.

Mutations in *CNGB3* or *GNAT2* have not been reported in association with incomplete achromatopsia, despite mutant *CNGB3* alleles being identified twice as commonly as *CNGA3* variants as the cause of complete achromatopsia. However, all *GNAT2* mutations to date, and the vast majority of *CNGB3* mutants, result in premature termination of translation, and thereby truncated and most probably non-functional phototransduction proteins. Therefore, an incomplete achromatopsia phenotype is unlikely to be compatible with these genotypes which are predicted to encode mutant products lacking any residual function.

1.1.2.3 Blue cone (S-cone) monochromatism

1.1.2.3.1 Clinical findings

Blue cone monochromatism (BCM), previously also known as X-linked incomplete achromatopsia, affects less than 1 in 100,000 individuals, and is characterised by absence of L- and M- cone function (Pokorny *et al.*, 1979). Thus, the blue cone monochromat possesses rod vision and a normal short wavelength sensitive cone mechanism.

As in rod monochromacy, BCM typically presents in infancy with reduced visual acuity, pendular nystagmus, photophobia and normal fundi. The nystagmus often wanes with time. Visual acuity is in the order of 6/24 to 6/60. Eccentric fixation may be present and myopia is a common finding (Weleber, 1988). BCM is distinguished from rod monochromatism (RM) by the results of psychophysical and electrophysiological testing. The photopic ERG is profoundly reduced in both, although the S-cone ERG is well preserved in BCM (Gouras and MacKay, 1990). Classification can also be aided by

family history, because BCM is inherited as an X-linked recessive trait, whereas both subtypes of rod monochromacy show autosomal recessive inheritance.

Rod monochromats cannot make colour judgements, but rather will use brightness cues to differentiate between colours. This contrasts with blue cone monochromats who do have access to colour discrimination, though this does depend upon the luminance of the task: at mesopic levels, they have rudimentary dichromatic colour discrimination based upon a comparison of the quantum catches obtained by the rods and the S-cones (blue cones) (Alpern *et al.*, 1971; Reitner *et al.*, 1991). Colour discrimination is reported to deteriorate with increasing luminance (Young and Price, 1985). Therefore, blue cone monochromats may be distinguished from rod monochromats by means of colour vision testing: blue cone monochromats are reported to display fewer errors along the vertical axis in the Farnsworth 100-Hue test (fewer tritan errors), and they may also display protan-like ordering patterns on the Farnsworth D-15 (Weis and Biersdorf, 1989). In addition, the Berson plates have been claimed to provide a good separation of blue cone monochromats from rod monochromats (Berson *et al.*, 1983; Haegerstrom-Portnoy *et al.*, 1996). Therefore, in order to clinically distinguish RM and BCM, colour vision tests that probe the tritan axis of colour as well as the deutan and protan need to be employed, since the presence of residual tritan discrimination suggests BCM.

BCM is generally accepted to be a stationary disorder; although Fleischman and O'Donnell (1981) reported one BCM family with macular atrophy and noted a slight deterioration of visual acuity and colour vision during a twelve year follow-up period, as well as foveal pigmentary changes. There are two further reports of individuals with BCM displaying a progressive retinal degeneration (Nathans *et al.*, 1989; Ayyagari *et al.*, 1999).

1.1.2.3.2 Molecular genetics

In order to derive colour vision, the normal human visual system compares the rate of quantum catches in the three classes of cone, S-, M- and L-cones. The L- and M- pigment genes are located on the X chromosome and the S-cone pigment is encoded by a gene located on chromosome 7 (Nathans *et al.*, 1986a; Nathans *et al.*, 1986b). The wild-type arrangement of the L- and M-opsin genes consists of a head-to-tail array of two or more repeat units of 39kb on chromosome Xq28 that are 98% identical at the DNA level (Nathans *et al.*, 1986a; Nathans *et al.*, 1986b). The highly homologous L- and M-opsin genes are thereby predisposed to unequal inter- and intragenic recombination. Transcriptional regulation of the L- and M- visual pigment genes is controlled by an upstream locus control region (LCR) (Nathans *et al.*, 1989; Wang *et al.*, 1992). Mutations that result in the lack of functional L- and M- pigments, and thus inactivate the corresponding cones, have been identified in the majority of BCM cases studied (Nathans *et al.*, 1989; Nathans *et al.*, 1993).

Mutation analyses introduced by Nathans and colleagues have proved highly efficient at establishing the molecular basis for BCM (Nathans *et al.*, 1989; Nathans *et al.*, 1993).

The mutations in the L- and M- pigment gene array causing BCM fall into two classes:

1. In the first class, a normal L- and M- pigment gene array is inactivated by a deletion in the LCR, located upstream of the L- pigment gene. A deletion in this region abolishes transcription of all genes in the pigment gene array and therefore inactivates both L- and M- cones.

2. In the second class of mutations, the LCR is preserved but changes within the L- and M- pigment gene array lead to loss of functional pigment production. The most common genotype in this class consists of a single inactivated L/M hybrid gene. The first step in this second mechanism is unequal crossing over reducing the number of

genes in the array to one, followed in the second step by a mutation that inactivates the remaining gene. The most frequent inactivating mutation that has been described is a thymine-to-cytosine transition at nucleotide 648, which results in a cysteine-to-arginine substitution at codon 203 (Cys203Arg), a mutation known to disrupt the folding of cone opsin molecules (Kazmi *et al.*, 1997). Reyniers *et al.* (1995) have also described a family where BCM is due to Cys203Arg mutations in both L- and M- pigment genes in the array. A third molecular genetic mechanism has been described in a single family of BCM where exon 4 of an isolated red pigment gene had been deleted (Ladekjaer-Mikkelsen *et al.*, 1996).

Combined results of previous studies (Nathans *et al.*, 1989; Nathans *et al.*, 1993; Ayyagari *et al.*, 1999; Ayyagari *et al.*, 2000) provide evidence for the general conclusion, first put forward by Nathans *et al.* (1989), that there are different mutational pathways to BCM. The data suggest that 40% of blue cone monochromat genotypes are a result of a one-step mutational pathway that leads to deletion of the LCR. The remaining 60% of blue cone monochromat genotypes comprise a heterogeneous group of multi-step pathways. The evidence thus far shows that many of these multi-step pathways produce visual pigment genes that carry the inactivating Cys203Arg mutation, which eliminates a highly conserved disulphide bond (Karnik and Khorana, 1990). This cysteine residue is located in the second extracellular loop of the opsin and, together with a conserved cysteine residue at position 126 in the first extracellular loop, forms a disulphide bond necessary for stabilisation of the tertiary structure of the protein (Kazmi *et al.*, 1997).

These studies have however failed to detect the genetic alteration that would explain the BCM phenotype in all assessed individuals (Nathans *et al.*, 1993; Ayyagari *et al.*, 2000). Indeed Nathans *et al.* (1993) found that in nine subjects out of thirty-five individuals with BCM (25%), the structure of the opsin array did not reveal the genetic

mechanism for the disorder. This failure to identify disease-causing variants in the opsin array may suggest that there is genetic heterogeneity yet to be identified in BCM; or that further upstream regulators of opsin array expression remain to be revealed.

1.1.2.4 Oligocone trichromacy

1.1.2.4.1 Clinical findings

Oligocone trichromacy is a rare cone dysfunction syndrome, which is characterised by reduced visual acuity, mild photophobia, normal fundi, reduced amplitude of the cone ERG, but with colour vision within normal limits. The disorder was first described by Van Lith (1973). Since then Keunen *et al.* (1995) have described a further four patients, whilst Neuhann *et al.* (1978) and more recently Ehlich *et al.* (1997) have each reported a single case. The two cases reported by Van Lith and Ehlich both had pendular nystagmus.

It has been proposed that these patients might have a reduced number of normal functioning cones (oligocone syndrome) with preservation of the three cone types in the normal proportions, thereby permitting trichromacy (Van Lith, 1973). Keunen *et al.* (1995) tested this hypothesis by screening foveal cone photopigment density. A reduced density difference of the foveal cone photopigment with a normal time constant of photopigment regeneration was found in all patients. Colour matching and increment threshold spectral sensitivity were normal. This provided evidence for the hypothesis of a reduced number of foveal cones (decreased density differences) with otherwise normal functioning residual cones.

1.1.2.4.2 Molecular genetics

Oligocone trichromacy is likely to be inherited as an autosomal recessive trait. The molecular genetic basis of the disorder is currently unknown. Genes involved in retinal

photoreceptor differentiation, at a stage when cone numbers are being determined, may represent good candidate genes.

1.1.2.5 Bornholm eye disease

1.1.2.5.1 Clinical findings

Syndromic X-linked myopia has been reported in a large five-generation Danish family that had its origins on the Danish island of Bornholm, and has therefore been named Bornholm Eye Disease (BED) (Haim *et al.*, 1988; Schwartz *et al.*, 1990). The syndrome manifests as moderate to high myopia combined with astigmatism, and impaired visual acuity. Additional signs are moderate optic nerve head hypoplasia, thinning of the RPE in the posterior pole with visible choroidal vasculature, and abnormal cone ERGs (Haim *et al.*, 1988). Affected family members are all deuteranopes, with a stationary natural history. This disorder is therefore best characterised as an X-linked cone dysfunction syndrome with myopia and deuteranopia.

1.1.2.5.2 Molecular genetics

Linkage analysis performed in the original BED family has mapped the locus to Xq28, in the same chromosomal region therefore as the L/M opsin gene array (Schwartz *et al.*, 1990).

1.1.2.6 Cone-monochromatism

Monochromatic vision is diagnosed by a patient's ability to match any two colours merely by adjusting their radiance, when all other cues are absent. In rod monochromatism there is an absence of functioning cone photoreceptors with visual

perception depending almost exclusively on rods. The rod monochromat therefore has markedly reduced visual acuity and total colour-blindness.

Cone-monochromatism is another rare form of congenital colour-blindness, in which visual acuity is normal (Weale, 1953; Weale, 1959). The incidence of cone-monochromatism is estimated at one in a 100 million (Pitt, 1944). Unlike rod monochromatism, cone-monochromatism has never been noted in more than one family member (Weale, 1953). The colour vision defect may be incomplete for certain colours and may vary both with the size of the field viewed and the level of luminance (Weale, 1953; Crone, 1956; Weale, 1959). A normal ERG is present in this disorder thereby supporting the notion of abnormal processing central to the retinal photoreceptors and bipolar cells (Ikeda and Ripps, 1966; Krill and Schneidman, 1966). This notion was first proposed following the demonstration of red- and green-sensitive pigments at the fovea in cone-monochromats (Weale, 1959) and the ability of such patients to use ocular chromatic aberration as a cue for altering accommodation (Fincham, 1953). In addition, Gibson (1962) has been able to demonstrate the presence of three mechanism-sensitivity curves for the cone-monochromat that are similar to those found in normal individuals, representing evidence of colour mediating mechanisms in the cone-monochromat, and thereby providing further evidence for a possible post-receptoral defect in this disorder.

1.1.3 Progressive cone and cone-rod dystrophies

The inherited cone dystrophies are a heterogeneous group of disorders, with autosomal recessive, autosomal dominant and X-linked recessive inheritance all having been reported. The functional deficit is confined to the photopic system in some forms of cone dystrophy but in others, perhaps the majority, there is later evidence of rod dysfunction (cone-rod dystrophy). The distinction between cone and cone-rod dystrophies may be

difficult, particularly during childhood, and is dependent upon adequate electrophysiological testing.

In this thesis cone-rod dystrophy (CORD) will be used for those retinal disorders in which subjects have significant secondary involvement of the rod system at an early stage, leading to difficulties with night vision. This contrasts with progressive cone dystrophies in which rod involvement, if present, occurs in older individuals, with a more variable deterioration of night vision.

1.1.3.1 Clinical findings

In contrast to the cone dysfunction syndromes which present in early infancy, the progressive cone dystrophies are not usually symptomatic until later childhood or early adult life. The age of onset of visual loss and the rate of progression show wide variability in the different families reported but visual acuity usually deteriorates over time to 6/60 or counting fingers. Photophobia is a prominent early symptom.

Individuals with CORD develop the typical findings of a cone dystrophy in early life but later there is evidence of rod involvement with associated night-blindness. The retinal dystrophy is either isolated or associated with systemic abnormalities. Autosomal dominant, autosomal recessive and X-linked recessive inheritance have all been reported. When an inheritance pattern can be reliably established, it is most commonly autosomal dominant (Krill *et al.*, 1973; Moore *et al.*, 1992).

Since all three classes of cone photoreceptor are usually affected, the colour vision defects seen are along all three colour axes, often progressing to complete loss of colour vision over time. Exceptions to this are cases where there is a predominant involvement of L-cones leading to a protan colour vision phenotype (Reichel *et al.*, 1989; Kellner *et al.*, 1995). Autosomal dominant cone dystrophy pedigrees with early tritan colour vision

defects have also been reported (Bresnick *et al.*, 1989; Went *et al.*, 1992). Fundus examination may show a typical bull's eye maculopathy (**Figure 1.4**). However, in some cases there may only be minor macular RPE atrophy. The optic discs show a variable degree of temporal pallor. The retinal periphery is usually normal in pure cone dystrophies although rarely white flecks similar to those seen in fundus flavimaculatus may be seen.

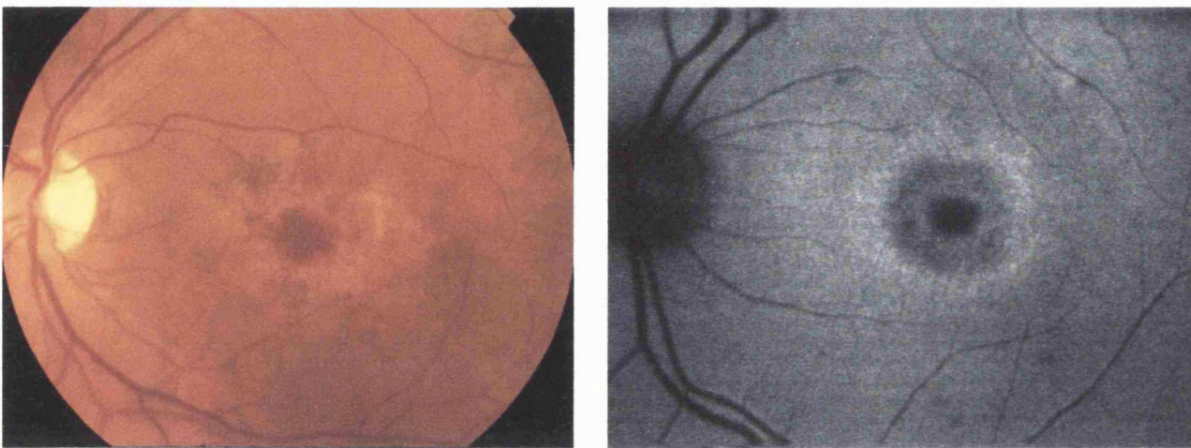


Figure 1.4

Bull's-eye maculopathy

(Colour fundus photograph and autofluorescence (AF) image)

In patients with CORD, fundus examination shows macular atrophy or a bull's-eye maculopathy in the early stages. Peripheral RPE atrophy, retinal pigmentation, arteriolar attenuation and optic disc pallor are often seen in the late stages of the disease process (**Figure 1.5**).

The 'dark choroid' sign may be seen on fluorescein angiography (Uliss *et al.*, 1987). A tapetal-like sheen which may change in appearance on dark adaptation (Mizuo-Nakamura phenomenon) has been described in association with X-linked (XL) CORD (Jacobson *et al.*, 1989).

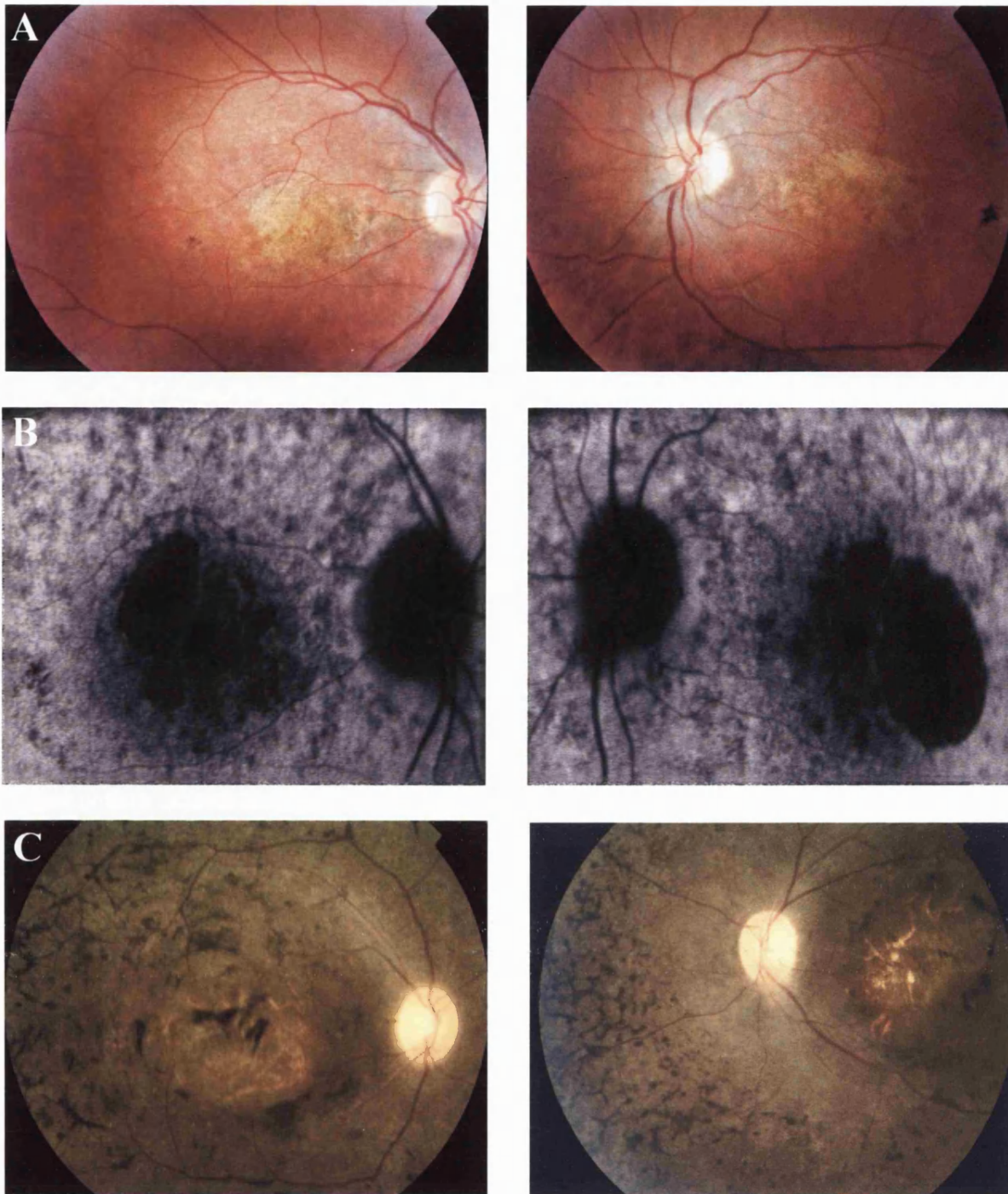


Figure 1.5

Cone-rod dystrophy (early and end-stage)

A & B Colour fundus photographs and AF images of early-stage CORD

C Colour fundus photographs of end-stage CORD

In pure cone dystrophies or in the early stages of CORDs electroretinography shows normal rod responses but substantially abnormal cone responses. The 30Hz flicker ERG is usually of increased implicit time but rarely, such as in the cone dystrophy related to guanylate cyclase activating protein-1 (GCAP1) mutation (Payne *et al.*, 1998; Downes *et al.*, 2001), the implicit time is normal and amplitude reduction is the only abnormality. In CORDs both rod and cone thresholds are elevated on psychophysical testing and the ERG shows reduced rod and cone amplitudes. Generalised abnormalities of rod and cone responses are seen, with the cone ERGs being more abnormal than the rod ERGs. The 30Hz cone flicker ERG implicit time is usually delayed. An unusual CORD has been reported which is characterised by abnormal cone function and supernormal rod responses (Gouras *et al.*, 1983; Alexander and Fishman, 1984a). Obligate carriers of X-linked cone dystrophy may show evidence of cone dysfunction on electrophysiological or psychophysical testing (Jacobson *et al.*, 1989; Reichel *et al.*, 1989).

1.1.3.2 Molecular genetics of progressive cone and cone-rod dystrophies

Most cases of progressive cone and cone-rod dystrophy are sporadic but when familial cases are seen the most common mode of inheritance is autosomal dominant (AD). Most of the sporadic cases probably represent autosomal recessive inheritance, but some may represent new AD mutations and in severely affected males X-linked disease.

Several loci and causative genes have been identified in the progressive cone and cone-rod dystrophies (**Table 1.2**). Currently six genes have been associated with AD disease; *CRX* (Evans *et al.*, 1994; Freund *et al.*, 1997), *GUCY2D* (Kelsell *et al.*, 1998b; Udar *et al.*, 2003), *RIMI* (Johnson *et al.*, 2003), *peripherin/RDS* (Nakazawa *et al.*, 1996), *GUCA1A* (Payne *et al.*, 1998; Downes *et al.*, 2001), and *AIPL1* (Sohocki *et al.*, 2000), with more yet to be discovered.

Three mutations in *GUCA1A*, the gene encoding GCAP1, have been reported in autosomal dominant pedigrees (COD3); Tyr99Cys (Payne *et al.*, 1998), Pro50Leu (Downes *et al.*, 2001) and Glu155Gly (Wilkie *et al.*, 2001). The main functional consequence of both Tyr99Cys and Glu155Gly has been shown to be a loss of Ca²⁺ sensitivity (Dizhoor *et al.*, 1998; Wilkie *et al.*, 2001). Mutant GCAP1 protein activates RetGC1 at low Ca²⁺ concentrations but fails to inactivate at high Ca²⁺ concentrations, thereby leading to the constitutive activation of RetGC1 in photoreceptors, even at the high Ca²⁺ concentrations of the dark-adapted state. The consequent dysregulation of intracellular Ca²⁺ and cGMP levels is believed to lead to cell death, with cone cells being predominantly affected due to the higher concentrations of RetGC1 and GCAP1 in cone photoreceptors (Dizhoor *et al.*, 1998; Wilkie *et al.*, 2001). In contrast to the Tyr99Cys and Glu155Gly associated families, the phenotype seen in the pedigree with the Pro50Leu mutation is highly variable, with some subjects having a cone-rod dystrophy rather than isolated cone dysfunction. The mechanism of disease of the Pro50Leu mutation is less clear, but may be due to haplo-insufficiency, secondary to increased GCAP1 susceptibility to protease activity and increased thermal instability (Newbold *et al.*, 2001).

Three mutations in *GUCY2D*, the gene encoding RetGC1, have also been reported in AD pedigrees (CORD5 and CORD6); Glu837Asp (Kelsell *et al.*, 1998b), Arg838Cys (Kelsell *et al.*, 1998b; Udar *et al.*, 2003) and Arg838His (Udar *et al.*, 2003). Codons 837 and 838 encode part of the highly conserved dimerisation domain of the RetGC1 protein. Functional studies have shown that the identified base changes at codon 838 result in altered GCAP1-stimulated cyclase activity. Arg838Cys and Arg838His mutants have been shown to have activity equal or superior to wild-type at low Ca²⁺ concentrations (Wilkie *et al.*, 2000). However, these mutants showed a higher apparent affinity for

GCAP1 than did wild-type RetGC1, and altered Ca^{2+} sensitivity of the GCAP1 activation, with marked residual activity at high Ca^{2+} concentrations (Wilkie *et al.*, 2000). Within the photoreceptor, this would result in a failure to inactivate cyclase activity at high physiological Ca^{2+} concentrations and an abnormal phototransduction recovery phase. The consequent dysregulation of intracellular Ca^{2+} and cGMP levels may lead to cell death.

The detailed phenotypic study that has been performed of the AD CORD, CORD7, will be discussed subsequently. CORD7 was originally mapped in a four-generation, non-consanguineous British family to a 7cM region of chromosome 6q14, flanked by the markers D6S430 and D6S1625 (Kelsell *et al.*, 1998a). A candidate gene screening approach identified a mutation in the Rab3A-interacting molecule (*RIMI*) gene in CORD7 (Johnson *et al.*, 2003). The G to A point mutation results in an Arg844His substitution in the highly conserved C₂A domain of the RIM1 protein and was found to segregate with disease. *RIMI* is expressed in brain and retinal photoreceptors where it is localised to the pre-synaptic ribbons in ribbon synapses, with the protein product believed to play an important role in synaptic transmission and plasticity (Wang *et al.*, 1997; Lonart, 2002; Sun *et al.*, 2003).

To date three genes have been associated with autosomal recessive disease; *ABCA4* (Cremers *et al.*, 1998), *CNGA3* (Wissinger *et al.*, 2001) and *RPGRIP1* (Hameed *et al.*, 2003).

Missense mutations in *CNGA3* have been identified in autosomal recessive cone dystrophies, having been reported in a single individual with a progressive cone dystrophy phenotype and in two individuals with cone-rod dystrophy (Wissinger *et al.*, 2001). As described before, *CNGA3* mutations are a common cause of the stationary

disorder achromatopsia; the possible reasons for a progressive phenotype in other individuals may include the particular combination of missense mutations present in these subjects; some amino-acid substitutions may be more deleterious to channel function than others. Further potential phenotypic influences include the presence of modifier genes or environmental effects.

Mutations in *ABCA4* have been shown to date to be the commonest cause of autosomal recessive cone-rod dystrophy (Cremers *et al.*, 1998; Maugeri *et al.*, 2000; Fishman *et al.*, 2003). *RPGRIP1* mutations have also been identified in autosomal recessive pedigrees (Hameed *et al.*, 2003), whilst mutations in *RPGR*, the gene encoding the protein that interacts with RPGRIP1, have been associated with X-linked (XL) families (Mears *et al.*, 2000; Demirci *et al.*, 2002). XL disease has also been mapped to COD1 (Xp21-p11.1) (Meire *et al.*, 1994), COD2 (Xq27) (Bergen *et al.*, 1997) and COD4 (Xp11.4-q13.1) (Jalkanen *et al.*, 2003).

The loci and genes identified in the cone-rod dystrophies are summarised in **Table 1.2**; with those associated with syndromic disorders shown in **Table 1.3**.

CORD; OMIM Number	Mode of Inheritance	Chromosome Locus	Mutated Gene	References
CORD1; 600624	Autosomal recessive	18q21.1-q21.3	Not identified	Warburg <i>et al.</i> , 1991
CORD2; 120970	Autosomal dominant	19q13.1-q13.2	<i>CRX</i>	Evans <i>et al.</i> , 1994 Freund <i>et al.</i> , 1997
CORD3; 604116	Autosomal recessive	1p21-p13	<i>ABCA4</i>	Cremers <i>et al.</i> , 1998
CORD5 & CORD6; 600977 & 601777	Autosomal dominant	17p13-p12	<i>GUCY2D</i>	Kellsell <i>et al.</i> , 1998b Udar <i>et al.</i> , 2003
CORD7; 603649	Autosomal dominant	6q14	<i>RIMI</i>	Johnson <i>et al.</i> , 2003
CORD8; 605549	Autosomal recessive	1q12-q24	Not identified	Khaliq <i>et al.</i> , 2000
CORD9;	Autosomal recessive	8p11	Not identified	Danciger <i>et al.</i> , 2001
CORD; 304020	X-linked	Xp21.1-p11.3 (COD1)	<i>RPGR</i>	Mears <i>et al.</i> , 2000 Demirci <i>et al.</i> , 2002
CORD	X-linked	Xp11.4-q13.1 (COD4)	Not identified	Jalkanen <i>et al.</i> , 2003
CORD 179605	Autosomal dominant	6p21.2-cen	<i>Peripherin/RDS</i>	Nakazawa <i>et al.</i> , 1996
CORD 601691	Autosomal recessive	1p21-p13	<i>ABCA4</i>	Maugeri <i>et al.</i> , 2000 Fishman <i>et al.</i> , 2003
CORD 605446	Autosomal recessive	14q11	<i>RPGRIP1</i>	Hameed <i>et al.</i> , 2003
CORD 600053	Autosomal recessive	2q11	<i>CNGA3</i>	Wissinger <i>et al.</i> , 2001
CORD 600364	Autosomal dominant	6p21.1	<i>GUCA1A</i>	Downes <i>et al.</i> , 2001
CORD 604011	-	17q11.2	<i>UNC119</i>	Kobayashi <i>et al.</i> , 2000
CORD 604392	Autosomal dominant	17p13.1	<i>AIPL1</i>	Sohocki <i>et al.</i> , 2000

Table 1.2

**Cone-rod dystrophies (CORDs) with identified genes and
known chromosomal loci.**

Syndromic CORD; OMIM Number	Mode of Inheritance	Chromosome Locus	Mutated Gene	References
CORD & Amelogenesis imperfecta; 217080	Autosomal recessive	2q11	Not identified	Downey <i>et al.</i> , 2002
CORD & Spinocerebellar ataxia type 7; 164500	Autosomal dominant	3p12-13	<i>SCA7</i>	Aleman <i>et al.</i> , 2002
CORD & NF1; 136550	Autosomal dominant	17q	<i>NF1</i>	Kylstra and Aylsworth, 1993
CORD & Bardet-Biedl syndrome; 209900, 606151, 600151 600374, 603650, 607590	Autosomal recessive	11q13 16q21 3p13-p12 15q22.3-q23 2q31 20p12 4q27	<i>BBS1</i> <i>BBS2</i> Not identified <i>BBS4</i> Not identified <i>BBS6</i> <i>BBS7</i>	Mykytyn <i>et al.</i> , 2002 Nishimura <i>et al.</i> , 2001 Sheffield <i>et al.</i> , 1994 Mykytyn <i>et al.</i> , 2001 Young <i>et al.</i> , 1999 Katsanis <i>et al.</i> , 2000 Badano <i>et al.</i> , 2003
CORD & Alström syndrome; 203800	Autosomal recessive	2p13	<i>ALMS1</i>	Collin <i>et al.</i> , 2002

Table 1.3

**Syndromic CORDs with identified genes and
known chromosomal loci.**

1.1.4 Goldmann-Favre & Enhanced S-cone syndrome

1.1.4.1 Clinical findings

Goldmann-Favre is a rare autosomal recessive disorder characterised by gradual visual loss or night-blindness with ocular findings that include liquefaction of the vitreous, macular retinoschisis and peripheral RPE atrophy and pigmentation. The retinal dystrophy is progressive resulting in extensive visual field loss and variable central visual loss. ERG is markedly abnormal or undetectable. Studies of patients with the Goldmann-Favre syndrome using spectral ERG have demonstrated that S-cones are less affected than the mid-spectral cones (Jacobson *et al.*, 1991). This finding suggests that there is

overlap between Goldmann-Favre syndrome and the more recently described Enhanced S-cone syndrome (ESCS), where there are increased numbers of cones responsive to short wavelength light, nyctalopia and foveal schisis/cysts (Jacobson *et al.*, 1990; Marmor *et al.*, 1990) (**Figure 1.6**). Goldmann-Favre syndrome may represent a severe form of ESCS.

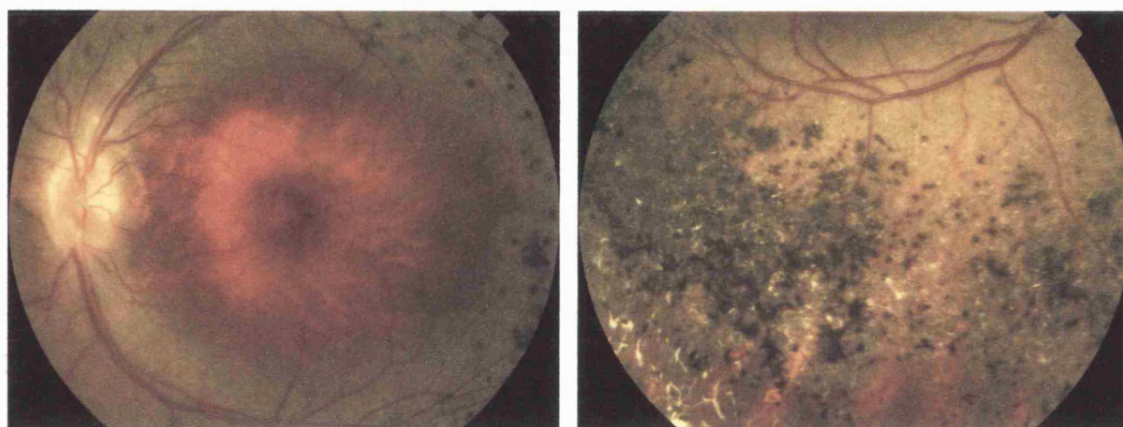


Figure 1.6

Enhanced S-cone syndrome

These disorders are unique in that they are the only examples of inherited retinal dystrophies where a gain in retinal function is seen. This gain is associated with improved tritan discrimination.

1.1.4.2 Molecular genetics

Mutations in *NR2E3* (encoding a transcription factor), a gene believed to play a role in determining cone cell fate (Haider *et al.*, 2000; Milam *et al.*, 2002), have been identified in ESCS and Goldmann-Favre. In ESCS there is evidence of an increase in S-cone numbers, with mutations in *NR2E3* thought to cause disordered cone cell differentiation, possibly by encouraging default to the S-cone pathway and thereby altering the relative

ratio of cone subtypes. A minority of cones are found to co-express L-/M- and S-opsins (Milam *et al.*, 2002).

1.1.5 Management of the cone and cone-rod dystrophies

There is currently no specific treatment for any of the cone dysfunction syndromes or cone and cone-rod dystrophies. Nevertheless, it is important that the correct diagnosis is made at an early stage, in order to be able to provide accurate information on prognosis and to be able to offer informed genetic counselling. Prenatal diagnosis is possible when the mutation(s) causing disease in the family is known.

Although there is no specific treatment available for this group of disorders, the provision of appropriate spectacle correction, low vision aids and educational support is very important. Photophobia is often a prominent symptom in the cone disorders and therefore tinted spectacles or contact lenses may be beneficial to patients, in terms of both improved comfort and vision. For example, in achromatopsia, spectacle or contact lens tint aims to prevent rod saturation while maintaining residual cone function. In complete achromatopsia a deep red tint is most effective, allowing wavelengths of low luminous efficiency for rod photoreceptors to be transmitted to the retina, whilst those of a higher luminous efficiency (short-wavelength light) are absorbed by the filter (Haegerstrom-Portnoy *et al.*, 1996). Incomplete achromats are thought to benefit more from reddish brown lenses rather than deep red lenses, which on account of their narrow spectral transmission, would eliminate their residual colour discrimination. In contrast, magenta tints which prevent rod saturation whilst allowing transmission of blue light are indicated in BCM (Haegerstrom-Portnoy *et al.*, 1996).

1.2 THE INHERITED MACULAR DYSTROPHIES

The inherited macular dystrophies (central receptor dystrophies) comprise a heterogeneous group of disorders characterised by central visual loss and atrophy of the macula and underlying RPE (Michaelides *et al.*, 2003b). The different forms of macular degeneration encompass a wide range of clinical, psychophysical and histological findings. The complexity of the molecular basis of monogenic macular disease is now beginning to be elucidated with the identification of many of the disease-causing genes. Nine disease-causing genes have been identified to date (Table 1.4), which have provided new insights into the pathogenesis of macular degeneration.

Age-related macular degeneration (ARMD), the leading cause of blind registration in the developed world, may also have a significant genetic component to its aetiology. Genes implicated in monogenic macular dystrophies are strong candidate susceptibility genes for ARMD, although to date, with the possible exception of *ABCA4*, none of these genes have been shown to confer increased risk of ARMD.

A description of the well-described inherited macular dystrophies follows. Systemic disorders with a macular dystrophy component will not be discussed.

Macular Dystrophy; OMIM Number	Mode of Inheritance	Chromosome Locus	Mutated Gene	References
Stargardt disease/Fundus Flavimaculatus; 248200	Autosomal recessive	1p21-p22 (STGD1)	<i>ABCA4</i>	Kaplan <i>et al.</i> , 1993 Allikmets <i>et al.</i> , 1997b
Stargardt-like macular dystrophy; 600110	Autosomal dominant	6q14 (STGD3)	<i>ELOVL4</i>	Stone <i>et al.</i> , 1994 Zhang <i>et al.</i> , 2001
Stargardt-like macular dystrophy; 603786	Autosomal dominant	4p (STGD4)	<i>PROM1</i>	Kniazeva <i>et al.</i> , 1999
Autosomal dominant 'bull's-eye' macular dystrophy	Autosomal dominant	4p (MCDR2)	<i>PROM1</i>	Michaelides <i>et al.</i> , 2003c
Best macular dystrophy; 153700	Autosomal dominant	11q13	<i>VMD2</i>	Petrukhin <i>et al.</i> , 1998 Caldwell <i>et al.</i> , 1999
Adult vitelliform dystrophy; 179605	Autosomal dominant	6p21.2-cen	<i>Peripherin/RDS</i>	Felbor <i>et al.</i> , 1997
Pattern dystrophy; 169150	Autosomal dominant	6p21.2-cen	<i>Peripherin/RDS</i>	Nichols <i>et al.</i> , 1993 Weleber <i>et al.</i> , 1993
Doyme honeycomb retinal dystrophy; 126600	Autosomal dominant	2p16	<i>EFEMP1</i>	Stone <i>et al.</i> , 1999
North Carolina macular dystrophy; 136550	Autosomal dominant	6q14-q16.2 (MCDR1)	Not identified	Small <i>et al.</i> , 1999 Reichel <i>et al.</i> , 1998 Rabb <i>et al.</i> , 1998
Autosomal dominant macular dystrophy resembling MCDR1	Autosomal dominant	5p15.33-p13.1 (MCDR3)	Not identified	Michaelides <i>et al.</i> , 2003d
NCMD-like associated with deafness	Autosomal dominant	14q (MCDR4)	Not identified	Francis <i>et al.</i> , 2003
Progressive bifocal chorioretinal atrophy; 600790	Autosomal dominant	6q14-q16.2	Not identified	Kelsell <i>et al.</i> , 1995
Sorsby fundus dystrophy; 136900	Autosomal dominant	22q12.1-q13.2	<i>TIMP3</i>	Weber <i>et al.</i> , 1994a Felbor <i>et al.</i> , 1995
Central areolar choroidal dystrophy; 215500	Autosomal dominant	6p21.2-cen 17p13	<i>Peripherin/RDS</i> Not identified	Hoyng <i>et al.</i> , 1996 Lotery <i>et al.</i> , 1996
Dominant cystoid macular dystrophy; 153880	Autosomal dominant	7p15-p21	Not identified	Kremer <i>et al.</i> , 1994
Juvenile retinoschisis; 312700	X-linked	Xp22.2	<i>XLRS1</i>	Sauer <i>et al.</i> , 1997
Maternally inherited diabetes and deafness 520000	Mitochondrial	mtDNA	<i>tRNA^{Leu}</i> <i>encoding region</i>	van den Ouweland <i>et al.</i> , 1992

Table 1.4

Chromosomal loci and causative genes in inherited macular dystrophies

1.2.1 Autosomal recessive inheritance

1.2.1.1 Stargardt disease and Fundus Flavimaculatus

1.2.1.1.1 Clinical findings

Stargardt macular dystrophy (STGD) is the most common inherited macular dystrophy with a prevalence of 1 in 10,000 and an autosomal recessive mode of inheritance. It shows a very variable phenotype with a variable age of onset and severity. Most cases present with central visual loss in early teens and typically there is macular atrophy with white flecks at the level of the RPE at the posterior pole on ophthalmoscopy (**Figure 1.7**). Fluorescein angiography classically reveals a dark or masked choroid. The reduced visualisation of the choroidal circulation in the early phase of fundus fluorescein angiography (FFA) is believed to be secondary to excess lipofuscin accumulation in the RPE, thereby obscuring fluorescence emanating from choroidal capillaries (Fish *et al.*, 1981). The retinal flecks appear hypofluorescent on FFA early in their evolution but at a later stage they appear hyperfluorescent due to RPE atrophy.

The abnormal accumulation of lipofuscin, the presence of active and resorbed flecks, and RPE atrophy leads to a characteristic appearance on fundus autofluorescence imaging in STGD (Lois *et al.*, 2001) (**Figure 1.7**).

Histopathology of donated eyes has revealed that changes in the RPE begin near the equatorial peripheral retina and include increasingly excessive lipofuscin content and cell loss towards the macula. The changes in the retina parallel those in the RPE, including accumulation of lipofuscin in photoreceptor inner segments, loss of photoreceptors, and reactive Müller cell hypertrophy (Eagle *et al.*, 1980; Birnbach *et al.*, 1994).

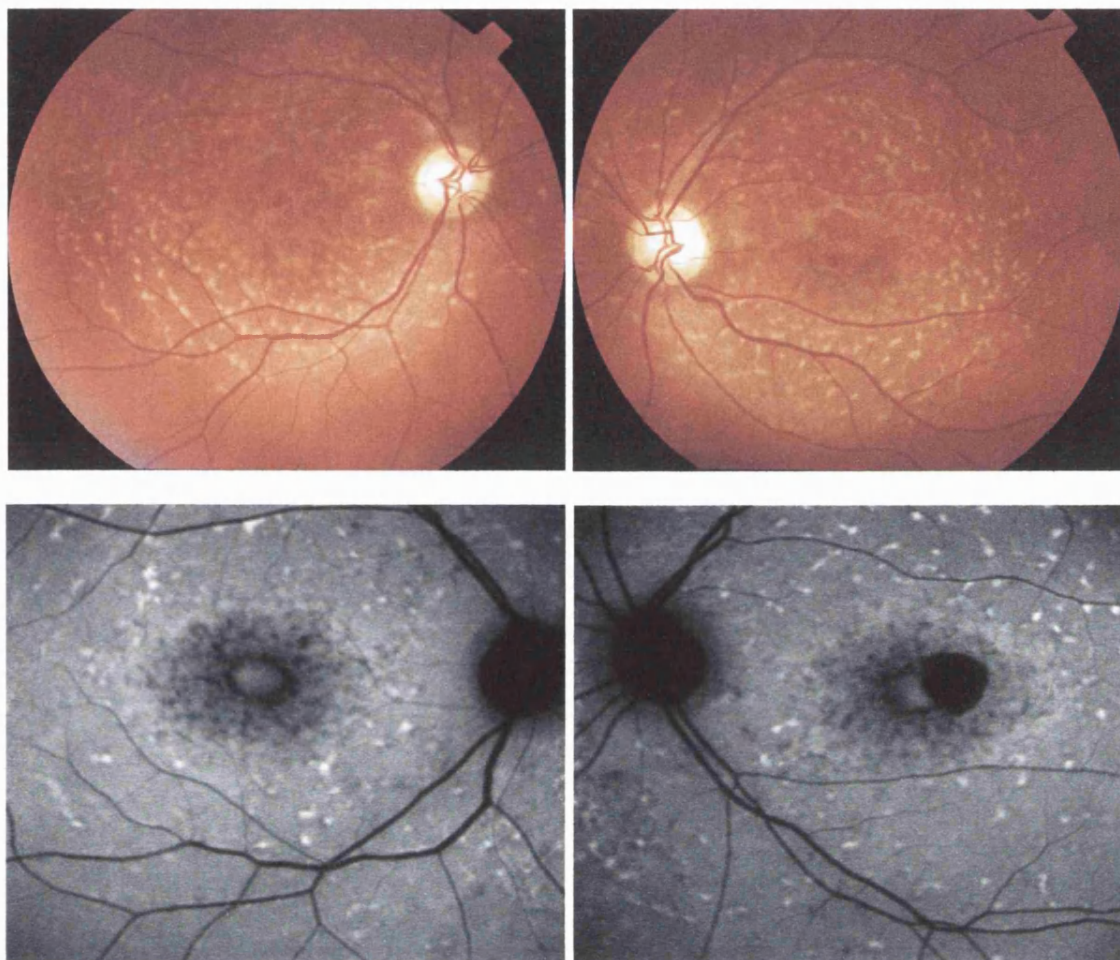


Figure 1.7

Stargardt disease

(Colour fundus photographs and AF images)

Stargardt disease may also present in adult life when the visual loss may be milder. When the retinal flecks are seen without atrophy the term fundus flavimaculatus (FFM) is often used to describe the phenotype but it appears that Stargardt disease and FFM are caused by mutations in the same gene and both patterns may be seen within the same family. In a recent detailed phenotypic study, based on ERG findings, patients with STGD/FFM could be classified into 3 groups (Lois *et al.*, 2001). In group 1, there was severe pattern ERG abnormality with normal scotopic and full-field ERGs. In group 2,

there was additional loss of photopic function, and in group 3, there was loss of both photopic and scotopic function. Differences among groups were not explained on the basis of differences in age of onset or duration of disease, suggesting that these electrophysiological groups may represent different phenotypic subtypes, and thereby may be useful in helping to provide an accurate prognosis. Patients in group 1 generally had better visual acuity, more restricted distribution of flecks and macular atrophy, whereas those in group 3 had the worst visual acuity, more widespread flecks and macular atrophy was universal.

1.2.1.1.2 Molecular genetics

The locus for STGD/FFM was mapped to chromosome 1p using homozygosity mapping in inbred families (Kaplan *et al.*, 1993), and the causative gene characterised, *ABCA4* (previously denoted *ABCR*) (Allikmets *et al.*, 1997b).

ABCA4 encodes a transmembrane rim protein located in the discs of rod and foveal cone outer segments, that is involved in ATP-dependent transport of retinoids from photoreceptor to RPE (Sun and Nathans, 1997; Weng *et al.*, 1999; Molday *et al.*, 2000). Failure of this transport results in deposition of a major lipofuscin fluorophore, A2E (N-retinylidene-N-retinylethanolamine), in the RPE (Weng *et al.*, 1999). It is proposed that this accumulation may be deleterious to the RPE, with consequent secondary photoreceptor degeneration.

The high allelic heterogeneity of *ABCA4* is clearly demonstrated by the fact that approximately 400 sequence variations in this gene have been reported. This highlights the potential difficulties in confidently assigning disease-causing status to sequence variants detected when screening such a large (50 exons) and polymorphic gene. Nonsense mutations that can be predicted to have a major effect on the encoded protein

can be confidently predicted to be disease-causing. However, a major problem occurs with missense mutations since sequence variants are common in controls and therefore establishing pathogenicity may be problematic. Therefore large studies assessing whether particular sequence variants are statistically more frequently seen in STGD patients than controls are likely to be helpful (Webster *et al.*, 2001). Direct evidence of pathogenicity can be established by functional analysis of the encoded mutant protein (Sun *et al.*, 2000), although such studies are very time consuming and labour-intensive. The availability of multiple independent families with the same mutation may also provide evidence in support of disease causation.

It is currently believed that: i) homozygous null mutations cause the most severe phenotype of autosomal recessive retinitis pigmentosa (RP), ii) combinations of a null mutation with a moderate missense mutation result in autosomal recessive CODR, and iii) combinations of null/mild missense or two moderate missense mutations cause STGD/FFM (van Driel *et al.*, 1998).

Assessment of functional activity of mutant ABCA4 transporter has been performed by Sun *et al.* (2000). For example, the missense mutations, Leu541Pro and Gly1961Glu, are associated with severely reduced but not abolished ATPase activity, whereas nonsense mutations would be predicted to have a more severe effect on protein function. Such predictions and functional assay results have been used to establish whether genotype-phenotype correlations can be reliably made. Gerth *et al.* (2002) have reported a detailed assessment of the phenotype of sixteen patients with STGD/FFM with known ABCA4 mutations. Correlation between the type and combination of ABCA4 mutations with the severity of the phenotype in terms of age of onset and level of photoreceptor dysfunction was possible in many cases. However, in some siblings there were unexplained differences in phenotype. It has been proposed that in these instances other

genes may have a modifying effect or environmental factors may have a role to play (Lois *et al.*, 1999). This is a recurring theme in the inherited macular dystrophies, in that the underlying ‘genetic context’ within which disease-associated mutations are expressed can influence the eventual phenotype observed. In addition, variable retinal phenotype within families may be explained by different combinations of *ABCA4* mutations segregating within a single family (Paloma *et al.*, 2002).

Knockout mice (*abca4*^{-/-}) show a striking deposition of the major lipofuscin fluorophore, A2E, in the RPE (Weng *et al.*, 1999). Heterozygous loss of the ABCA4 protein has also been shown to be sufficient to cause a phenotype in mice similar to STGD and ARMD in humans (Mata *et al.*, 2001), suggesting that the STGD carrier-state may predispose to the development of ARMD.

Light-exposed A2E-laden RPE exhibits a propensity for apoptosis especially with light in the blue part of the spectrum (Sparrow *et al.*, 2000). During RPE irradiation (430nm), A2E self-generates singlet oxygen with the latter in turn reacting with A2E to generate DNA-damaging epoxides (Sparrow *et al.*, 2002; Sparrow *et al.*, 2003). The antioxidants vitamins E and C have been shown to reduce A2E-epoxidation, with a corresponding reduction in the incidence of DNA damage and cell death, by quenching singlet oxygen (Sparrow *et al.*, 2003). This raises the exciting possibility of a simple therapy.

A different strategy of reducing A2E-related toxicity by inhibiting the formation of such lipofuscin pigments has also been reported (Mata *et al.*, 2000; Radu *et al.*, 2003). It has been shown that A2E synthesis can be virtually blocked by raising *abca4*^{-/-} mice in total darkness (Mata *et al.*, 2000). Recently it has also been demonstrated in the *abca4*^{-/-} mouse model that isotretinoin blocks the formation of A2E and the accumulation of lipofuscin pigments in the RPE (Radu *et al.*, 2003). Isotretinoin (13-*cis*-retinoic acid) is

known to slow the synthesis of 11-*cis*-retinaldehyde and regeneration of rhodopsin by inhibiting 11-*cis*-retinol dehydrogenase in the visual cycle. Light activation of rhodopsin results in the release of all-*trans*-retinaldehyde, which constitutes the first reactant in A2E biosynthesis. It remains to be assessed whether isotretinoin is a potential treatment for other forms of macular degeneration associated with lipofuscin accumulation.

1.2.2 Autosomal dominant inheritance

1.2.2.1 Autosomal dominant Stargardt-like macular dystrophy

1.2.2.1.1 Clinical findings

The clinical appearance of autosomal dominant (AD) Stargardt-like macular dystrophy is so similar to the common autosomal recessive form of the disorder that it is difficult to differentiate between them by fundus examination alone (Donoso *et al.*, 2001). However, individuals reported with features of AD STGD-like dystrophy have a milder phenotype with relatively good functional vision, minimal colour vision defects and no significant electro-oculography (EOG) or ERG abnormalities (Donoso *et al.*, 2001). The ‘dark choroid’ sign on fluorescein angiography which is typical in the recessive form, but not diagnostic, is uncommon in the dominant form of the disorder.

1.2.2.1.2 Molecular genetics

Two chromosomal loci have been identified, 6q14 (STGD3) (Stone *et al.*, 1994) and 4p (STGD4) (Kniazeva *et al.*, 1999). Two mutations, a 5-bp deletion and two 1-bp deletions separated by four nucleotides, in the gene *ELOVL4* have been associated with STGD3 and other macular dystrophy phenotypes including pattern dystrophy (Bernstein *et al.*, 2001; Zhang *et al.*, 2001).

ELOVL4 is expressed in the rod and cone photoreceptor inner segments. The protein product is believed to be involved in retinal fatty acid metabolism since it has significant homology to a family of proteins involved in fatty acid elongation.

1.2.2.2 Best Disease (vitelliform macular dystrophy)

1.2.2.2.1 Clinical findings

Best disease is a dominantly inherited macular dystrophy which is characterised clinically by the classical feature of a round or oval yellow subretinal macular deposit (**Figure 1.8**). The yellow material is gradually resorbed over time, leaving an area of RPE atrophy and often subretinal fibrosis. Full-field ERG is normal but the EOG shows a very reduced or absent light rise indicating that there is widespread dysfunction of the RPE. The visual prognosis in Best disease is surprisingly good, with most patients retaining reading vision into the fifth decade of life or beyond.

Mohler and Fine (1981) have classified the phenotype into five stages. Stage 0 (pre-vitelliform) is characterised by a normal fundus appearance in an asymptomatic gene carrier with an abnormal EOG. In stage I minor RPE changes are seen. The classical vitelliform lesion (stage II) is characterised by the ‘egg-yolk’ macular lesion. This appearance is usually seen during the first or second decades, often associated with normal, or slightly reduced visual acuity. The ‘egg-yolk’ begins to break up secondary to resorption of the yellow material lying between the RPE and sensory retina (stage IIa), with visual impairment usually being noticeable at this stage. Stage III (pseudohypopyon) is seen when part of the lesion is resorbed leaving the appearance of a ‘fluid level’ at the macula. The yellow material is completely resorbed over time, leaving an area of RPE atrophy (stage IVa) and often subretinal fibrosis (IVb). Choroidal neovascularisation is an established complication leading to severe visual loss (IVc).

In common with STGD, histopathology of donated eyes from patients with Best disease has shown accumulation of lipofuscin throughout the RPE (Frangieh *et al.*, 1982; Weingeist *et al.*, 1982). Although the ophthalmoscopic abnormality is usually confined to the macular region, this evidence of more widespread retinal involvement is in common with the majority of inherited macular dystrophies described to date.

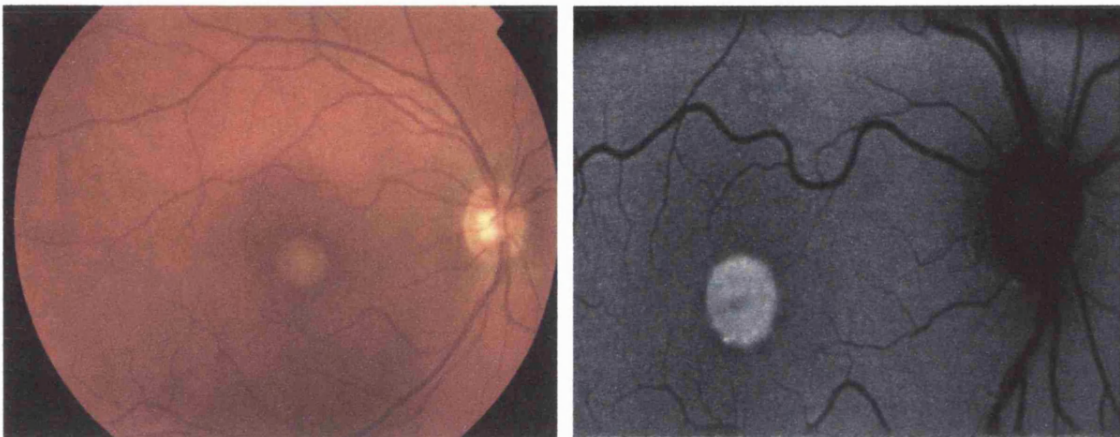


Figure 1.8

Best disease

(Colour fundus photograph and AF image)

1.2.2.2.2 Molecular genetics

Best disease shows very variable expressivity. Most individuals carrying mutations in the *VMD2* gene on chromosome 11q13 (Forsman *et al.*, 1992; Petrukhin *et al.*, 1998; Caldwell *et al.*, 1999), have an abnormal EOG, but the macular appearance may be normal in some (Mohler and Fine, 1981). There is only one individual reported with evidence of non-penetrance, in that he is a mutant *VMD2* gene carrier with a normal fundus examination and normal EOG (Weber *et al.*, 1994b). Family members who carry a mutation in the *VMD2* gene and who have minimal macular abnormality or a normal

fundus appearance (but abnormal EOG) in early adult life, usually retain near normal visual acuity long term.

The protein product of *VMD2*, bestrophin, has been localised to the basolateral plasma membrane of the RPE where it forms a component of a chloride channel responsible for maintaining chloride conductance across the basolateral membrane of the RPE (Marmorstein *et al.*, 2000; Sun *et al.*, 2002). This chloride current regulates fluid transport across the RPE. It has been suggested following optical coherence tomography of patients with Best disease, that impaired fluid transport in the RPE secondary to abnormal chloride conductance, may lead to accumulation of fluid and/or debris between RPE and photoreceptors and between RPE and Bruch's membrane, leading to detachment and secondary photoreceptor degeneration (Fisher *et al.*, 2001; Pianta *et al.*, 2003).

The variable expression of Best disease remains unexplained; although again, other genes in addition to *VMD2*, and/or environmental influences may play a role in the wide range of clinical expression seen.

1.2.2.3 Adult vitelliform macular dystrophy

1.2.2.3.1 Clinical findings

Adult vitelliform macular dystrophy (AVMD) is often confused with Best disease, although as the name suggests it has a later onset, lacks the typical course through different stages of macular disease seen in classical Best disease, and the EOG is usually normal (Brecher and Bird, 1990). The typical clinical appearance is of bilateral, round or oval, yellow, symmetrical, sub-retinal lesions, typically one-third to one-half optic disc diameter in size.

1.2.2.3.2 Molecular genetics

Mutations in the *peripherin/RDS* gene on chromosome 6p have been identified in AVMD (Felbor *et al.*, 1997). It has been proposed that mutations in *peripherin/RDS* are present in approximately 20% of patients with AVMD (Felbor *et al.*, 1997), which implies further genetic heterogeneity.

1.2.2.4 Pattern dystrophy

1.2.2.4.1 Clinical findings

The pattern dystrophies are a group of inherited disorders of the RPE which are characterised by bilateral symmetrical yellow-orange deposits at the macula in various distributions, including butterfly or reticular-like patterns (**Figure 1.9**). These deposits most likely represent lipofuscin accumulation.

These dystrophies are often associated with a relatively good visual prognosis, although in some cases a slowly progressive loss of central vision can occur. There is usually psychophysical or electrophysiological evidence of widespread photoreceptor dysfunction (Kemp *et al.*, 1994). Electrophysiological findings usually reveal abnormal pattern ERG, normal full-field ERG, but abnormal EOG.

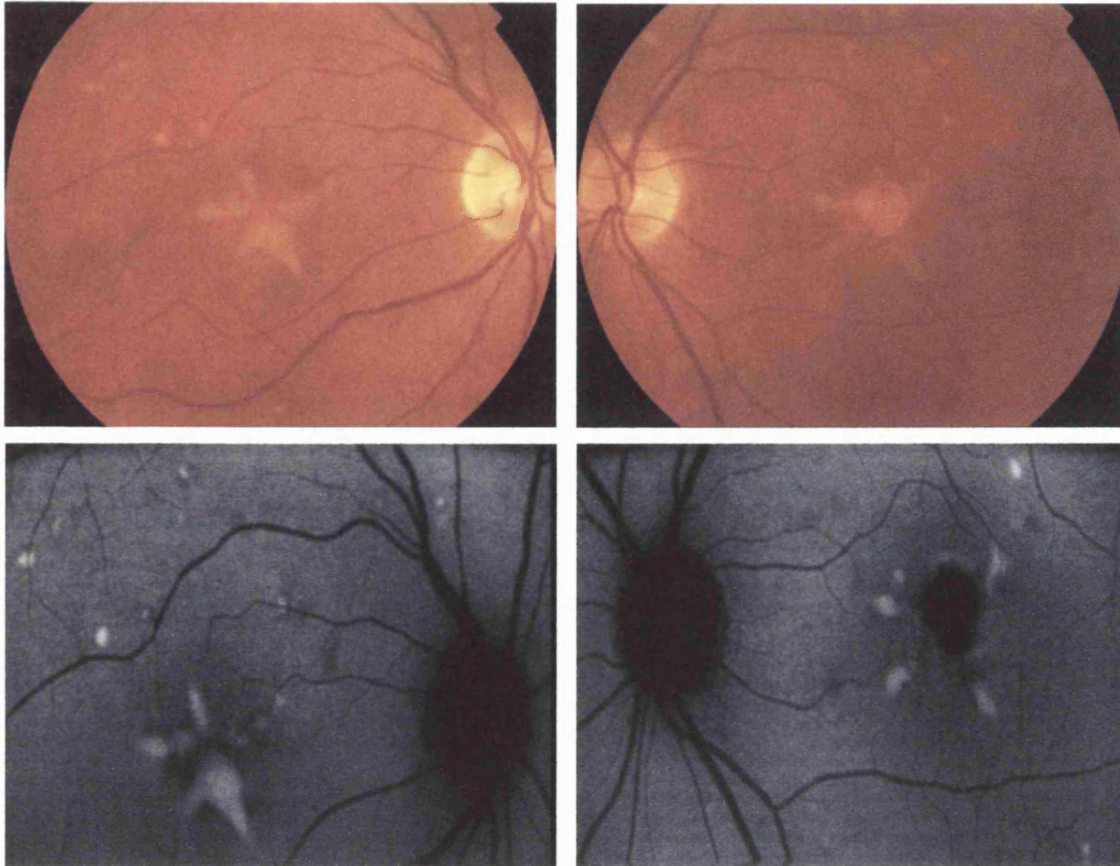


Figure 1.9

Pattern dystrophy

(Colour fundus photographs and AF images)

1.2.2.4.2 Molecular genetics

Mutations in the *peripherin/RDS* gene on chromosome 6p have been identified in patients with pattern dystrophies (Nichols *et al.*, 1993; Weleber *et al.*, 1993), and have also been implicated in autosomal dominant RP (Kajiwara *et al.*, 1991). The *RDS* gene was originally identified in a strain of mice with a photoreceptor degeneration known as 'retinal degeneration, slow' (*rds*). Subsequently, the orthologous human *peripherin/RDS* gene was shown to cause autosomal dominant RP. Mutation in codon 172 of *peripherin/RDS* has also been implicated in autosomal dominant macular dystrophy

(Downes *et al.*, 1999). Weleber *et al.* (1993) described a single family in which a 3-bp deletion in *peripherin/RDS* resulted in RP, pattern dystrophy and FFM in different individuals. This represents a further example of the likely modifying effects of genetic background or environment.

The peripherin/RDS protein is a membrane-associated glycoprotein restricted to photoreceptor outer segment discs in a complex with ROM1. It may function as an adhesion molecule involved in the stabilisation and maintenance of a compact arrangement of outer segment discs (Travis *et al.*, 1991). Peripherin has also been shown to interact with the GARP domain (glutamic acid- and proline-rich region) of the beta-subunit of rod cGMP-gated channels, in a complex that includes the Na/Ca-K exchanger (Poetsch *et al.*, 2001). This interaction may have a role in anchoring the channel-exchanger complex in the plasma membrane of rod outer segments.

The *rds* mouse, which is homozygous for a null mutation in *peripherin/RDS*, is characterised by a complete failure to develop photoreceptor discs and outer segments, downregulation of rhodopsin expression, and apoptotic loss of photoreceptor cells. Ali *et al.* (2000) have demonstrated that subretinal injection in these mice of recombinant adeno-associated virus encoding a *peripherin/RDS* transgene, resulted in the generation of outer segment structures and formation of new stacks of discs containing both peripherin/RDS and rhodopsin. Moreover, electrophysiological function was also preserved. This study demonstrates in an animal model the efficacy of *in vivo* gene transfer to restore structure and more importantly function. Further assessment of this model has shown that the potential for ultrastructural improvement is dependent upon the age at treatment, but the effect of a single injection on photoreceptor ultrastructure may be long-lasting (Sarra *et al.*, 2001). These findings suggest that successful gene therapy in

patients with photoreceptor defects may ultimately depend upon intervention in early stages of disease and upon accurate control of transgene expression.

1.2.2.5 Doyne honeycomb retinal dystrophy

(malattia leventinese; autosomal dominant drusen)

1.2.2.5.1 Clinical findings

In this disorder small round yellow-white deposits under the RPE are characteristically distributed at the macula and around the optic disc, and begin to appear in early adult life. Visual acuity is maintained through the fifth decade, but patients usually become legally blind by the seventh decade. Visual loss is usually due to macular atrophy, but less commonly may follow a subretinal neovascular membrane (SRNVM) (**Figure 1.10**). The presence of drusen-like deposits makes this dystrophy potentially very relevant to ARMD.



Figure 1.10

Doyne honeycomb retinal dystrophy

(A macular SRNVM is also present)

1.2.2.5.2 Molecular genetics

A single mutation, Arg-345-to-Trp (R345W) in the gene *EFEMP1* on chromosome 2p has been identified in the majority of patients with dominant drusen (Stone *et al.*, 1999). *EFEMP1* is a widely expressed gene of unknown function. Based on its sequence homology to the fibulin and fibrillin gene families, *EFEMP1* is predicted to be an extracellular matrix glycoprotein, but otherwise remains uncharacterised. However, it has been recently proposed that misfolding and aberrant accumulation of *EFEMP1* within RPE cells and between the RPE and Bruch's membrane may underlie drusen formation in Doyme Honeycomb retinal dystrophy and ARMD. *EFEMP1* itself does not appear to be a major component of the drusen (Marmorstein *et al.*, 2002).

Genetic heterogeneity in autosomal dominant drusen has been suggested by Tarttelin *et al.* (2001), since they found that only seven of the 10 families (70%) and one of the 17 sporadic patients (6%) investigated had the R345W mutation. No other *EFEMP1* mutation was detected in these patients. Other families showing linkage to chromosome 2p16 raise the possibility of an upstream *EFEMP1* promoter mutation or a second dominant drusen gene at this locus.

1.2.2.6 Autosomal dominant drusen and macular degeneration (DD)

1.2.2.6.1 Clinical findings

Stefko *et al.* (2000) have described a highly variable clinical phenotype in a North American family with an autosomal dominant drusen disorder with macular degeneration (DD). Most young adults had fine macular drusen and good vision. Affected infants and children may have congenital atrophic maculopathy and drusen. There was also evidence of progression in late adulthood with moderate visual loss.

1.2.2.6.2 Molecular genetics

The gene for the disease has been mapped to chromosome 6q14 and appears to be adjacent to but distinct from the locus for North Carolina macular dystrophy (MCDR1) (Kniazeva *et al.*, 2000). The disease interval overlaps with that of STGD3 and an autosomal dominant atrophic macular degeneration (adMD) (Griesinger *et al.*, 2000), raising the possibility that they may be allelic disorders. However, the phenotype of DD differs from that of STGD3 and adMD. Macular drusen are a hallmark of DD, whilst RPE atrophy and subretinal flecks are prominent features of STGD3 and adMD. The true situation will only be resolved by the identification of the underlying genetic mutations.

1.2.2.7 North Carolina macular dystrophy

1.2.2.7.1 Clinical findings

North Carolina macular dystrophy (MCDR1) is an autosomal dominant disorder which is characterised by a variable macular phenotype and a non-progressive natural history. Bilaterally symmetrical fundus appearances in MCDR1 range from a few small (less than 50µm) yellow drusen-like lesions in the central macula (grade 1) to larger confluent lesions (grade 2) and macular colobomatous lesions (grade 3) (**Figure 1.11**). Occasionally MCDR1 is complicated by SRNVM formation at the macula. EOG and ERG are normal indicating that there is no generalised retinal dysfunction.

1.2.2.7.2 Molecular genetics

Linkage studies have mapped MCDR1 to a locus on chromosome 6q16. To date, MCDR1 has been described in various countries and no evidence of genetic heterogeneity has been reported (Rabb *et al.*, 1998; Reichel *et al.*, 1998; Small *et al.*, 1999). The

identification of the gene responsible for this disorder is keenly awaited as it will help to improve our understanding of the pathogenesis of drusen and SRNVM.



Figure 1.11

North Carolina macular dystrophy

1.2.2.8 Progressive bifocal chorioretinal atrophy (PBCRA)

1.2.2.8.1 Clinical findings

PBCRA is an autosomal dominant disorder characterised by nystagmus, myopia and progressive macular and nasal retinal atrophic lesions (Douglas *et al.*, 1968). Marked photopsia in early or middle age and retinal detachment extending from the posterior pole are recognised complications (Godley *et al.*, 1996). Both ERG and EOG are abnormal, reflecting widespread abnormality of photoreceptors and RPE.

1.2.2.8.2 Molecular genetics

PBCRA has been linked to 6q14-q16.2 (Kelsell *et al.*, 1995). The PBCRA disease interval overlaps with the established MCDR1 interval. These two autosomal dominant macular dystrophies have many phenotypic similarities. However, PBCRA differs significantly from MCDR1 in several important ways, including slow progression, abnormal colour vision, extensive nasal as well as macular atrophy and abnormal ERG and EOG. Therefore, if allelic, it is likely that different mutations are involved in their aetiology. An alternative explanation is that PBCRA and MCDR1 are caused by mutations in two different adjacent genes.

1.2.2.9 Sorsby fundus dystrophy

1.2.2.9.1 Clinical findings

Sorsby fundus dystrophy (SFD) is a rare, autosomal dominant macular dystrophy, with onset of night blindness in the third decade and loss of central vision from macular atrophy or SRNVM by the fifth decade (**Figure 1.12**). A tritan colour defect has been previously suggested as an early sign in SFD (Berninger *et al.*, 1993).



Figure 1.12

Sorsby fundus dystrophy
(A macular SRNVM is also present)

1.2.2.9.2 Molecular genetics

The tissue inhibitor of metalloproteinase-3 (*TIMP3* gene on chromosome 22q) is implicated in SFD (Weber *et al.*, 1994a; Felbor *et al.*, 1995; Jacobson *et al.*, 2002). Most of the known mutations in *TIMP3*, including Ser181Cys (Weber *et al.*, 1994a), Ser156Cys (Felbor *et al.*, 1995) and Tyr172Cys (Jacobson *et al.*, 2002), introduce potentially unpaired cysteine residues in the C-terminus of the protein. An abnormal tertiary protein structure may arise therefore from inappropriate disulfide bond formation. This may alter *TIMP3* mediated extracellular matrix turnover leading to the thickening of Bruch's membrane and the widespread accumulation of abnormal material beneath the RPE that is seen histologically (Chong *et al.*, 2000).

The finding that treatment with high doses of oral vitamin A reverses night blindness in this disorder (Jacobson *et al.*, 1995), suggests that retinal dysfunction may be due to a reduction in the permeability of Bruch's membrane, resulting in the hindrance of transport of vitamin A from the choriocapillaris to the photoreceptors by accumulated extracellular debris beneath the RPE. *TIMP3* has been recently shown to be a potent inhibitor of angiogenesis, which may account for the recognised complication of choroidal neovascularisation seen in SFD (Qi *et al.*, 2003). *TIMP3* inhibits vascular endothelial growth factor (VEGF)-mediated angiogenesis, most probably by blockade of VEGF-2 receptors (Qi *et al.*, 2003).

Further insights into the pathophysiology of SFD may follow the development of a knock-in mouse carrying a disease-related Ser156Cys mutation in the orthologous murine *TIMP3* gene (Weber *et al.*, 2002). Immunolabeling studies and biochemical data from these mice indicate that site-specific excess rather than absence or deficiency of functional *TIMP3* may be the primary consequence of the known *TIMP3* mutations. Furthermore, a recent human pathological study has provided supportive evidence that

this excess is secondary to decreased breakdown of TIMP3 rather than an increase in its expression (Chong *et al.*, 2003).

1.2.2.10 Central areolar choroidal dystrophy (CACD)

1.2.2.10.1 Clinical findings

CACD is characterised by bilateral, symmetrical, subtle mottling of the RPE at the macula in the early stages. The mottling then progresses to atrophy of the RPE and choriocapillaris.

1.2.2.10.2 Molecular genetics

An Arg142Trp mutation in *peripherin/RDS* has been implicated as one cause of this rare autosomal dominant macular dystrophy (Hoyng *et al.*, 1996). Sporadic cases of CACD have also been described but no mutations were found in *peripherin/RDS* (Hoyng *et al.*, 1996). A second locus at chromosome 17p13 has also been identified by a genome wide linkage search in a large Northern Irish family (Lotery *et al.*, 1996).

1.2.2.11 Dominant cystoid macular dystrophy

(Dominant cystoid macular oedema)

1.2.2.11.1 Clinical findings

Cystoid macular oedema with leaking perifoveal capillaries on fluorescein angiography is seen in all affected patients. Other features include onset usually in the fourth decade, typically a moderate to high hypermetropic refractive error, and a normal ERG (Deutman *et al.*, 1976).

1.2.2.11.2 Molecular genetics

Genetic linkage has been established to 7p15-p21 (Kremer *et al.*, 1994). The causative gene remains to be identified.

1.2.3 X-linked inheritance

1.2.3.1 X-linked juvenile retinoschisis (XLRS)

1.2.3.1.1 Clinical findings

XLRS is a vitreoretinal degeneration which presents either in an infant with nystagmus, or more commonly in childhood with mild loss of central vision. The characteristic fundus abnormality is a cystic spokewheel-like maculopathy (foveal schisis) in virtually all affected males. Peripheral retinal abnormalities including bilateral schisis cavities, vascular closure, inner retinal sheen and pigmentary retinopathy are seen in approximately 50% of cases (George *et al.*, 1995). Full-field ERG typically reveals a negative waveform, in that the a-wave is larger in amplitude than the b-wave. Prognosis is good in most affected males as long as retinal detachment or vitreous haemorrhage does not occur.

1.2.3.1.2 Molecular genetics

XLRS has been linked to Xp22.2 and mutations in the gene *XLRS1* (also recently referred to as *RS1*) have been identified (Sauer *et al.*, 1997). Juvenile retinoschisis shows a wide variability in the phenotype between, as well as within, families with different genotypes (Eksandh *et al.*, 2000). *XLRS1* encodes a 224 amino acid protein, retinoschisin (RS1), which contains a highly conserved discoidin domain implicated in cell-cell adhesion and cell-matrix interactions, functions which correlate well with the observed splitting of the

retina in XLRS. Many missense and protein-truncating mutations of *XLRSl* have now been identified and are thought to be inactivating (The Retinoschisis Consortium, 1998).

1.2.4 Mitochondrial inheritance

1.2.4.1 Maternally inherited diabetes and deafness (MIDD)

MIDD is a recently described subtype of diabetes mellitus that co-segregates with an adenine-to-guanine transition at position 3243 of mitochondrial DNA (A3243G), in a transfer RNA leucine (tRNA^{Leu} [UUR]) encoding region (Reardon *et al.*, 1992; van den Ouweland *et al.*, 1992).

Macular pattern dystrophy (MPD) has been found in association with MIDD (Massin *et al.*, 1995). In a multi-centre study, 86% of MIDD patients were found to have bilateral MPD, characterised by RPE hyperpigmentation that can surround the macula, or be more extensive and also encompass the optic disc (Massin *et al.*, 1999). In advanced cases areas of RPE atrophy encircling the macula can be seen, which may coalesce and involve the fovea at a late stage (**Figure 1.13**).

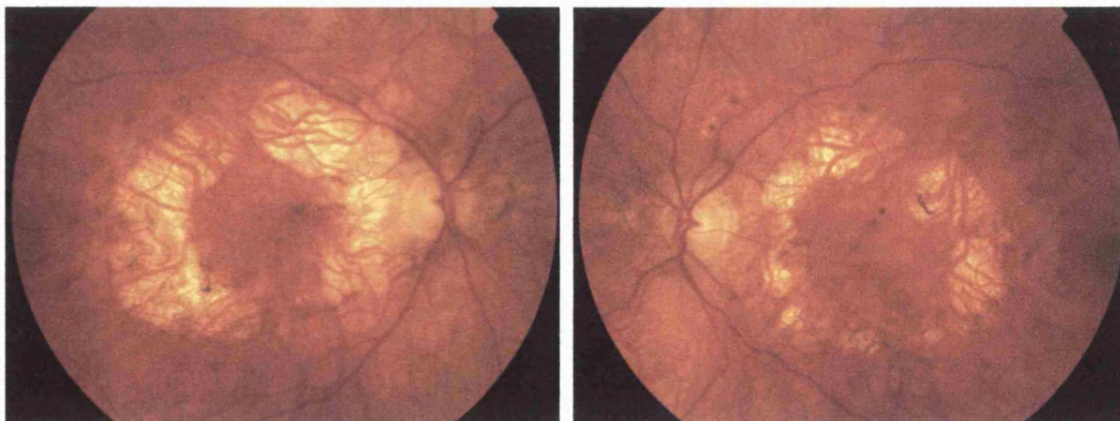


Figure 1.13
MIDD associated maculopathy

Prognosis however is generally good, with 80% of patients in the multi-centre study having visual acuity of 6/7.5 or better in both eyes (Massin *et al.*, 1999). Since the prevalence of MPD in MIDD is high, the association of a MPD with diabetes should raise the possibility of screening for a mutation of mitochondrial DNA.

1.2.5 Conclusions

ARMD is by far the most common form of macular degeneration. ARMD is the leading cause of blindness in patients over the age of 65 years in the western world. Despite its prevalence, its aetiology and pathogenesis are still poorly understood, and currently effective treatment options are limited for the majority of patients.

ARMD has a genetic contribution to its aetiology. Putative susceptibility loci have been identified on chromosome 1q25-q31 (Klein *et al.*, 1998; Weeks *et al.*, 2001; Majewski *et al.*, 2003), chromosome 17q25 (Weeks *et al.*, 2001) and on chromosomes 3, 5, 9 and 10 (Weeks *et al.*, 2000; Majewski *et al.*, 2003); whereas it has been suggested that the e4 allele of the apolipoprotein E gene and an Alu polymorphism in the angiotensin-converting enzyme gene may have a protective effect on ARMD risk (Klaver *et al.*, 1998; Hamdi *et al.*, 2002).

Inherited monogenic macular dystrophies share many important features with ARMD and have the advantage that they are more readily studied. One of the major difficulties in studies of ARMD is its late onset. Parents of affected individuals are often deceased and their children have yet to manifest the disease. In contrast, there are several forms of macular dystrophy, such as STGD/FFM, Best disease and MCDR1, which manifest signs and symptoms at an early age. These dystrophies and others have been characterised in large numbers of family members, spanning several generations, thereby making them far more amenable to genetic analysis. Furthermore, several of these macular dystrophies

share many important clinical and histopathological similarities with ARMD, including an abnormal accumulation of lipofuscin in the RPE and a concomitant loss of function of overlying photoreceptors and central vision.

Nevertheless to date, with the possible exception of *ABCA4*, none of these genes have been shown to confer increased risk of ARMD (Allikmets *et al.*, 1997a; Stone *et al.*, 1998; De La Paz *et al.*, 1999; Stone *et al.*, 1999; Lotery *et al.*, 2000; Weeks *et al.*, 2000; Stone *et al.*, 2001; Zhang *et al.*, 2001). However, all new macular dystrophy genes represent good candidates for ARMD.

1.3 PHENOTYPING TECHNIQUES

A detailed study of the phenotype is an essential prerequisite to molecular genetic studies aimed at the identification of the causative genes. It is important that the status of family members is clearly established and the detailed phenotype may suggest possible candidate genes. Once the causative mutations have been identified, detailed phenotypic studies may help to understand disease mechanisms and suggest novel therapeutic approaches.

The study of phenotype over time will allow more accurate advice on prognosis and will also provide information on natural history that will be important prior to the commencement of future treatment trials.

1.3.1 *History and examination*

The cornerstone of characterising the clinical features of any retinal dystrophy is a full general and ophthalmological history, followed by a careful ophthalmological examination, including the use of the most appropriate measure of visual acuity. The symptoms that are established may suggest central or peripheral retinal involvement, or

may implicate possible cone or rod dysfunction. For example, photophobia and colour vision loss is consistent with cone dysfunction, whilst night vision difficulties suggest abnormality of the rod system. A careful family history is important to help ascertain the mode of inheritance.

1.3.2 Imaging

1.3.2.1 Fundus photography

High resolution digital colour fundus photography is important both in recording and monitoring progression of retinal degeneration. Such photographs are also useful when comparisons are made with images obtained with other retinal imaging techniques such as fundus fluorescein angiography (FFA) or autofluorescence (AF) imaging.

1.3.2.2 Autofluorescence imaging

AF imaging is a relatively new method that allows the visualisation of the RPE by taking advantage of its intrinsic fluorescence derived from lipofuscin (von Rückmann *et al.*, 1995; 1997a; 1999). AF imaging with a confocal scanning laser ophthalmoscope can therefore provide useful information about the distribution of lipofuscin in the RPE, and give indirect information on the level of metabolic activity of the RPE which is largely determined by the rate of turnover of photoreceptor outer segments (von Rückmann *et al.*, 1999).

There is evidence of continuous degradation of autofluorescent material in the RPE (von Rückmann *et al.*, 1999). Progressive loss of lipofuscin occurs when there is reduced metabolic demand due to photoreceptor cell loss, which appears as areas of decreased AF. Areas of increased AF correspond to a group of RPE cells containing higher quantities of lipofuscin than their neighbours and may represent areas at high risk for

photoreceptor cell loss (von Rückmann *et al.*, 1997b). It has been demonstrated histologically that the number of photoreceptor cells is reduced in the presence of increased quantities of lipofuscin in the RPE, leading to the proposal that autofluorescent material may accumulate prior to cell death (Dorey *et al.*, 1989).

1.3.3 Electrophysiological testing

Electrophysiological assessment is useful in helping to establish both the site of retinal abnormality, in terms of the retinal level (e.g. photoreceptor/RPE as opposed to inner retinal), and the location, in terms of macular and/or peripheral retinal dysfunction.

The standard electrophysiological tests that are performed include an electro-oculogram (EOG), a full-field electroretinogram (ERG) and pattern ERG (PERG); the protocols for these are detailed by the International Society for Clinical Electrophysiology of Vision (Marmor and Zrenner, 1993; Marmor and Zrenner, 1998; Bach *et al.*, 2000). More sophisticated testing can include S-cone-specific ERGs (Gouras and McKay, 1990; Arden *et al.*, 1999), multifocal ERG (Hood, 2000) and the recording of ON- and OFF- responses. S-cone ERGs represent a response to a short-wavelength stimulus recorded in the presence of longer wavelength adaptation, thereby selectively probing S-cone function.

The ERG is the massed electrical response of the retina, and allows assessment of generalised retinal function under photopic and scotopic conditions using a Ganzfeld bowl flash stimulus. Standard ERG traces include the rod-specific response, the maximal (mixed rod-cone) response, the 30Hz flicker response and the (single flash) photopic response. Individual ERG components have origins in different retinal layers and may localise the site of dysfunction (Fishman *et al.*, 2001). The rod-specific ERG b-wave reflects rod-system sensitivity, and is generated at the level of the inner nuclear layer. The

first 10-12 ms of the a-wave of the maximal response relates to photoreceptor hyperpolarisation, and is the best measure of photoreceptor function. The slope of the linear portion of the a-wave can be related to the kinetics of phototransduction. The b-wave of the maximal ERG response arises in the mid-retina, principally the rod ON-bipolar cells and thus defines function that is post-phototransduction or post-receptoral. 30Hz flicker and photopic (single flash) ERGs allow assessment of cone-system function. There are mid-retinal contributions to both the a- and b-waves of the photopic (single flash) response, but also a photoreceptor contribution to the photopic a-wave. More detail of inner retinal photopic function can be revealed using long duration photopic stimulation to elicit separate ON- and OFF- responses relating to depolarising and hyperpolarising cone bipolar cell systems.

The PERG, usually elicited using high contrast checkerboard reversal, mainly reflects central retinal function. There are two major components; the positive P50 and negative N95. Evidence to date suggests that the N95 component arises in the spiking activity of the retinal ganglion cells. The PERG P50, driven by the macular photoreceptors, can be used as an objective index of macular function.

The EOG utilises the standing potential difference between the back of the eye and the electro-positive cornea. It is a mass response of the whole of the retina and is generated across the RPE. The EOG thus allows assessment of the photoreceptor/RPE interface and its generation depends on the integrity of the photoreceptors; a reduced EOG is generally accompanied by a reduction in the full-field ERG unless dysfunction is confined to the RPE. The EOG is assessed by measuring constant eye movements under conditions of progressive dark then light adaptation, performed according to international recommendations. There is a “dark trough” after 12-15 minutes dark adaptation and a

“light peak” after 7-10 minutes light adaptation. The ratio between the light peak and dark trough, expressed as a percentage, is the commonly used parameter.

Classification of retinal dystrophies is in part determined by the nature of the electrophysiological abnormalities. Generalised retinal function is revealed by full-field ERG, and central retinal function with PERG. Patients with generalised retinal dysfunction and severe ERG abnormalities can have normal PERGs if the macula is spared. Conversely, patients with disease confined to the macula have normal ERGs, but the PERG P50 may be profoundly abnormal.

1.3.4 *Psychophysical testing*

1.3.4.1 Colour vision assessment

Effective colour vision testing employs a battery of tests including the use of Ishihara pseudoisochromatic plates, the Hardy, Rand and Rittler (HRR) plates (American Optical Company, NY), SPP2 plates for acquired colour deficiency, Farnsworth Munsell (FM) 100-hue test, Farnsworth D-15, the Mollon-Reffin (M-R) Minimal test, computerised colour vision testing and anomaloscopy. Salient features of these colour vision tests will be briefly discussed.

1.3.4.1.1 Plate tests

Plate tests rely upon known characteristics of colour vision deficiencies in order to detect and diagnose patients with colour abnormalities. The Ishihara pseudoisochromatic plate test is the most widely used test of colour vision in clinical practice; whilst it is quick and easy to use, it has certain limitations. Unlike the Ishihara plates, the advantages of the HRR test are that it contains designs for tritan screening and also has a series of plates

having different colour difference steps enabling the grading of the severity of protan, deutan and tritan defects (**Figure 1.14**). The SPP tests differ from the Ishihara plates in that they use uniformly sized and spaced circles in their arrays.

1.3.4.1.2 Cap tests

These tests can be divided into two categories. The first type of cap test (FM 100-hue and Farnsworth D-15) relies upon colour ordering; the subject is given a randomly arranged series of colours which must be rearranged in a progressive manner. Typically such tests employ colour series whose chromaticity co-ordinates lie in a circle or ellipse around neutral. The second type of cap test (M-R minimal test) requires the subject to discriminate coloured objects from non-coloured (i.e. grey) objects; this type of test gives an estimation of saturation discrimination. The FM 100-hue, Farnsworth D-15 and the M-R test are all performed under CIE Standard Illuminant C from a MacBeth Easel lamp.

In the Farnsworth D-15 test the subject constructs a colour order beginning with a single reference colour and the results are plotted on a circular diagram representing the hue circle. Major errors give rise to lines that cross the diagram and indicate that colours from the opposite side of the hue circle have been placed together. The enlarged Farnsworth D-15 (PV-16), which utilises larger diameter caps, is employed in order to detect any residual colour discrimination that might be present in patients with low vision.

The FM 100-hue test was designed to examine hue-discrimination ability in normal observers and to evaluate hue-discrimination losses in colour-deficient individuals. The degree of colour deficiency can be estimated from the error score and the type of deficiency is analysed from the graphical presentation of the results. The FM 100-hue test consists of 85 Munsell colours representing a complete hue circle. Characteristic plots for

observers with congenital protan, deutan and tritan deficiency show concentrations of errors in two well-defined positions that are nearly diametrically opposite in the polar diagram. The conspicuity of the axis of confusion in the error plot and the total error score indicate the severity of colour deficiency. For example, blue cone monochromats have high FM 100-hue error scores, but when compared to rod monochromats, they make fewer errors along the vertical axis (fewer tritan errors).

The Mollon-Reffin (M-R) Minimal test is a saturation discrimination type test (Mollon *et al.*, 1991) (Figure 1.14). The caps used in this test are of a similar design to those in the D-15 and FM 100-hue tests. The test features series of caps that lie along protan, deutan and tritan lines respectively. In addition, there is one demonstration cap, which does not lie along a dichromatic confusion axis. The remainder of the caps are all neutral, but have a varying lightness (there are a total of 9 grey caps). The examiner places one coloured cap amongst a group of neutral caps and asks the subject to tap the side of the cap that is coloured. The coloured caps vary in their saturation, so the severity of the defect can be assessed. It can be performed by children as young as 5. Blue cone monochromats discriminate reasonably well along the tritan line, whereas rod monochromats do poorly on all lines.

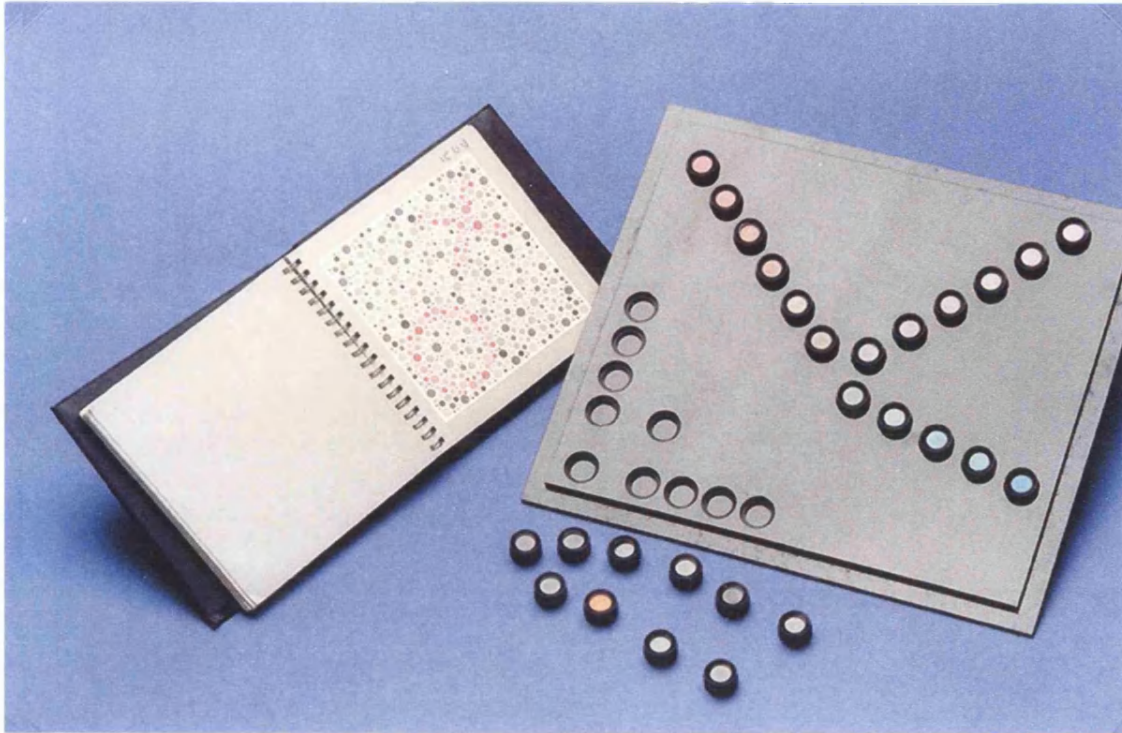


Figure 1.14

HRR plates and the M-R minimal test

1.3.4.1.3 Anomaloscopy

The Nagel anomaloscope presents the Rayleigh match, whereby two halves of a circular 2° field are illuminated respectively by monochromatic yellow (589nm) and a mixture of monochromatic red (670nm) and green (546nm). The subject makes at least three matches by adjusting both the colour mixture and the yellow luminance controls until identity of the two halves of the fields is achieved. The limits of the matching range are then established by the examiner setting values for the red-green ratio and the subject adjusting only the yellow luminance control to determine whether an exact match can be obtained. Since S-cones do not contribute to the Rayleigh match, BCM males and complete achromats generally match over the entire range of test intensities, indicating no contribution of L- or M- cones in the macula.

1.3.4.1.4 Computerised tests

The Cambridge Colour Test (Mollon *et al.*, 1989) is a computerised colour vision test, consisting of a circular array within which there are discs of varying sizes; a certain subset of discs are coloured so that they may form the letter C. Like the Landolt C acuity chart, this test measures a subject's threshold by having him/her determine the orientation of the gap in the C, only in this case threshold is determined for the minimum saturation required to correctly identify the position of the gap. The original version of the test determined threshold along protan, deutan and tritan confusion lines. In an extension of this original test, colour discrimination ellipses are derived by testing along twenty different axes in colour space (Regan *et al.*, 1994). This alteration makes the test particularly suitable for assessing acquired deficiencies.

In order to detect any residual colour discrimination that might be present in patients with low vision, a modification of the Cambridge Colour Test has been devised (P4 test) (Simunovic *et al.*, 1998). In the modified test, the stimulus array consists of only four large discs, organised in a diamond pattern. Each disc subtends 4 deg of visual angle at the viewing distance of 1 m. On any presentation, one of the discs differs in chromaticity from the remaining three, and the patient's task is to identify this disc by pressing one of four buttons within 4 seconds. To ensure that the discrimination is on the basis of chromaticity, the luminance of each disc is given a random value chosen from six levels between 4 and 24 cd/m².

1.3.4.2 Perimetry and dark adaptometry

Perimetry can be divided into static and kinetic visual field testing. Kinetic perimetry involves the detection of a moving target, the brightness of which is held constant, whilst

static perimetry involves the detection of a stationary target, the brightness of which is varied. Testing may be performed as a threshold or suprathreshold analysis.

Automated visual field assessment is an objective measure of retinal function that can be performed quickly and in a repeatable manner. Dark-adapted perimetry and dark adaptometry have in the past helped to define subtypes of retinal disorders, for example in RP. Automated static threshold perimetry can be performed in both dark- and light-adapted states, with a Humphrey field analyser often being employed (Allergan Humphrey, Hertford, UK).

Following dark-adaptation, static threshold perimetry is performed with a red (dominant wavelength, 650nm) and then a blue (dominant wavelength, 450nm) filter in the stimulus beam. Dark-adapted perimetry thereby provides an assessment of cone and rod sensitivities at different retinal eccentricities (Jacobson *et al.*, 1986; Steinmetz *et al.*, 1993).

Dark adaptometry allows the investigation of both rod and cone kinetics and the measurement of absolute photoreceptor thresholds (Alexander and Fishman, 1984b; Chen *et al.*, 1992). The Humphrey field analyser can be used and is usually controlled by a computerised program. Fully dark-adapted rod thresholds are measured before exposure to the adapting light and the assessment of recovery from full bleach. The normal dark adaptation curve is biphasic, where the first curve represents the cone threshold and is reached in 5-10 minutes, and the second curve represents the rod threshold and is reached after approximately 30 minutes. The rod-cone break is a well-defined point between these two curves.

1.4 MOLECULAR GENETIC TECHNIQUES

The resources generated from the Human Genome Project have accelerated the discovery of human genes responsible for disease. The Human Genome Project was launched in October 1990 with the publication of a research plan to establish the sequence of the entire human genome. The working draft of the human genome was accomplished on June 26th 2000.

In essence two different strategies are employed to identify genes responsible for inherited retinal disorders; functional or positional candidate gene approaches:

1.4.1 Functional candidate gene approach

The first approach is to screen genes known to play a role in retinal development, structure and physiology, in a panel of diverse affected individuals with inherited retinal dystrophies. The chromosomal region(s) where the families may map is unknown at the time of mutation screening.

1.4.2 Positional candidate gene approach

The second approach however, is dependent upon knowledge of the position of the gene in the human genome. The chromosomal locus is usually identified by linkage analysis (section 1.4.3), but translocation breakpoints may also identify a chromosomal locus. Ideally once the disease interval has been refined, plausible candidate genes within this established region can be identified with the aid of bioinformatics. Database information on tissue-specific expression patterns, protein structure and known orthologues is helpful in identifying suitable candidate genes for mutation screening.

1.4.3 Linkage analysis

Linkage analysis is the method used in families in order to ascertain the location of the disease gene in the human genome. Genetic linkage analysis is based upon the observation that alleles of two genes located very close to each other on the same chromosome tend to be inherited together, or co-segregate. As the distance between two genes increases, the creation of new combinations of alleles by homologous recombination during meiosis becomes more likely. Recombination events are known to occur with increased frequency on the shorter arms compared to the longer arms of chromosomes and at the telomeric ends compared to the centromeres. The frequency of this crossover event is called the recombination fraction (θ) which ranges in value from 0.00 to 0.5. Linkage analysis is fundamentally a calculation of probability based on an observed association between the inheritance of a known chromosomal marker allele and the presence of the disease phenotype. A comparison is made between the probability that the observed distribution of alleles would arise under the hypothesis of linkage ($\theta < 0.5$) and the probability that this distribution would occur randomly ($\theta = 0.5$). The ratio of these two probabilities is the odds ratio (L). The odds ratio, L, is usually converted to a LOD score (Z), which is the decimal logarithm of L. By convention, a LOD score of ≥ 3.0 is regarded as significant evidence that two loci are linked. This is equivalent to a 1:1000 or less likelihood that the observed linkage has occurred by chance. The presence of a negative LOD score suggests that the two loci are unlinked and, by convention, a LOD score of ≤ -2.0 is required to disprove linkage at the stated recombination fraction.

LOD scores can be calculated with a variety of computer packages including MLINK program within Cyrillic 2.1.1 and web based programmes such as Genetic Linkage User Environment (GLUE).

Having identified a chromosomal region by linkage analysis, two methods are used to identify the disease gene; either positional cloning, or the candidate gene approach (section 1.4.2). Positional cloning is both laborious and time-consuming. Whereas, the candidate gene approach has the potential to reveal the correct disease gene without the need for exhaustive cloning in the region defined by genetic or physical mapping.

1.4.3.1 Genetic markers

A marker defines a particular chromosomal locus and helps in differentiating homologous chromosomes. Markers should ideally be both informative and polymorphic. Informativeness refers to the difference in DNA between individuals in a population whereas polymorphism is defined as the number of differences in DNA (alleles) in the population. An allele of a marker that co-segregates with disease identifies the portion of the chromosome that is inherited from affected parent to affected child in autosomal dominant disease.

The markers used to establish genetic linkage are currently usually microsatellite markers with a variable number of tandem repeats (VNTR). The informativeness and polymorphic nature of a marker can be quantified by its polymorphic information content (PIC), which is determined by the number of alleles and their frequency in the population. The PIC value is the probability that a marker in the offspring will enable one to establish from which parent the marker was inherited. A PIC value of greater than 70% signifies an extremely polymorphic gene.

1.4.4 Mutation analysis

Once a sequence change in a candidate gene is identified in an affected individual, it becomes necessary to demonstrate that it is responsible for the disease phenotype. In the

first instance in order to exclude the possibility of a common polymorphism, the sequence change must co-segregate in the pedigree with the disease phenotype and must not be present in a panel of at least a 100 ethnically matched control chromosomes.

A coding sequence change in association with the disruption of an evolutionary conserved region of the polypeptide structure is highly suggestive that the sequence variant is associated with disease. In addition, the amino acid substitution per se, that results from the sequence change, can provide evidence in support of potential pathogenicity; for example a substitution that results in a change in charge or size. Furthermore, the identification of the same mutation in a different unrelated family with the same phenotype is evidence in favour of the variant causing the disease.

However, the only definitive evidence of pathogenicity that can be obtained is from detailed functional studies *in vitro* or in animal models, assessing the effects, if any, of the identified mutation.

CHAPTER 2

MATERIALS AND METHODS

2.1 PATIENT ASCERTAINMENT

Patients were primarily recruited from Professor A. T. Moore's clinics at Moorfields Eye Hospital and Addenbrooke's Hospital, Cambridge. A minority of patients/families were referred by other consultant ophthalmologists within the United Kingdom. Patients were then contacted by telephone in order to explain the nature of the study, with a written information sheet being forwarded if they were willing to participate.

Informed consent was obtained from all participants - in the case of children (younger than 16-years-old), consent was provided by their parents. The ethics committee of Moorfields Eye Hospital approved the study (protocol number MOOA1001). All research adhered to the tenets of the declaration of Helsinki.

2.2 PATIENT ASSESSMENT

Detailed phenotyping was carried out in patients with: **(i)** various stationary cone disorders including rod monochromatism, S-cone monochromatism, oligocone trichromacy and a novel X-linked cone dysfunction syndrome associated with myopia and dichromacy; **(ii)** a progressive cone dystrophy phenotype; **(iii)** a number of unusual cone-rod dystrophy phenotypes including cone dystrophy with supernormal rod responses, a progressive cone-rod dystrophy (CORD7), and a rare recessive syndrome of cone-rod dystrophy with amelogenesis imperfecta; and **(iv)** autosomal dominant macular dystrophy phenotypes.

The phenotyping was primarily performed at Moorfields Eye Hospital in London and in Professor J. D. Mollon's Psychophysics Laboratory at the Department of Experimental Psychology at the University of Cambridge.

2.2.1 Clinical history and examination

A detailed medical, ophthalmological and family history was taken from all participating subjects (including unaffected relatives where appropriate). This was followed by a full ophthalmological examination, including distance and near visual acuity assessment, colour vision testing with HRR plates, and careful dilated fundus slit-lamp examination.

2.2.2 Further examination techniques

These techniques include colour fundus photography, fundus autofluorescence imaging, electrophysiological testing, and psychophysical testing including colour vision assessment and perimetry/dark adaptometry. These techniques are all discussed in sections 1.3.2, 1.3.3 and 1.3.4.

Electrophysiological assessment included an International Society for Clinical Electrophysiology of Vision (ISCEV)-standard electro-oculogram (EOG), full-field electroretinogram (ERG) and pattern ERG (PERG) (Marmor and Zrenner, 1993; Marmor and Zrenner, 1998; Bach *et al.*, 2000). Testing was performed in the electrophysiology laboratories at Moorfields Eye Hospital (Dr. G. E. Holder) or Addenbrooke's Hospital (Dr. K. Bradshaw).

Detailed colour vision assessment was performed in the majority of subjects. The colour vision tests used included the Ishihara pseudoisochromatic plates, the Hardy, Rand and Rittler (HRR) plates (American Optical Company, NY), SPP2 plates for acquired colour deficiency, Farnsworth Munsell (FM) 100-hue test, Farnsworth D-15 and PV-16, the enlarged and standard Mollon-Reffin (M-R) Minimal test, computerised colour vision testing (Cambridge colour vision test and P4 test) and anomaloscopy.

2.3 SAMPLE COLLECTION

Following informed consent blood samples or buccal swabs were obtained from patients and unaffected relatives where indicated. In certain instances when samples were not obtained after clinical examination, blood samples or buccal swabs were collected by the local general practitioner and forwarded to the laboratory.

Two 10ml EDTA impregnated vials of venous blood were collected from each adult (10mls or less from each child) and immediately taken to the laboratory at the Department of Molecular Genetics, Institute of Ophthalmology. One of these two vials of blood from each patient underwent DNA extraction, with the other vial being stored at -20°C. When blood samples could not be collected, Cytobrushes (Medscand MD) were used to collect buccal cells. To obtain a sample, the brush was swept along the buccal mucosa for 30 seconds (3 cytobrushes per patient), with the sample ideally being collected at least three hours after the last meal. Samples were then transferred to 2.5mls of sterile phosphate buffer solution (PBS), followed by subsequent DNA extraction or storage at -20°C.

2.4 MATERIALS

2.4.1 *Buffers and reagents*

All reagents used were supplied by Sigma (UK), BDH Laboratory Supplies, GibcoBRL, Promega and Pharmacia unless otherwise stated.

2.4.2 *Gel electrophoresis*

- **50x TAE** Electrophoresis buffer (per litre): 24.2% (w/v) Tris base, 57.1ml glacial acetic acid, 0.05M EDTA (pH 8.0).

- **Ficoll Loading dyes (10x):** 25% (w/v) Ficoll, 0.25M EDTA, 0.25% (w/v) Orange G or Bromophenol blue in 1xTAE.

2.4.3 Kits utilised

- Nucleon® DNA Extraction Kit - Nucleon®Biosciences, Scotlab, Manchester
- Wizard™ Minicolumn Kit - (Promega)
- ABI Prism™ Big Dye™ Terminator Cycle Sequencing Kit with AmpliTaq® DNA Polymerase, FS - v.3.0 and v.4.0 (Applied Biosystems)
- QuickPrep® *Micro* mRNA Purification Kit (Pharmacia Biotech)
- SuperScript™ First-Strand Synthesis System for RT-PCR (GibcoBRL Ltd, Life Technologies)

2.5 METHODS

2.5.1 Human genomic DNA extraction from whole blood

The Nucleon® DNA Extraction Kit (Nucleon®Biosciences) was used for extraction of DNA from human whole blood samples. The recommended protocol was followed and is briefly described below.

Human blood samples (approximately 10mls) were allowed to thaw at room temperature. The whole sample was transferred into a 50ml Falcon tube and prepared for DNA extraction by addition of 40ml of Reagent A (10mM Tris-HCl pH 8.0, 320mM sucrose, 5mM MgCl₂, 1% triton-X-100). The tube was briefly mixed by inversion before centrifugation for 10 minutes at 2000xg. The supernatant was removed and the cell pellet resuspended in 2ml Reagent B (as supplied) which mediates cell lysis. De-proteinisation of the sample was achieved by addition of 500µl of sodium perchlorate (5M; as supplied), followed by mixing by inversion for 1 minute. 2ml of chloroform and 300µl Nucleon ®

Silica suspension (as supplied) were added to extract the DNA from the sample and again inverted to mix. Following a further 10 minute centrifugation at 2000xg the upper phase containing DNA was carefully aspirated into a fresh 50ml Falcon tube to which two volumes of ethanol were added for DNA precipitation. DNA was precipitated by gentle inversion of the tubes, and removed using a surgical needle. The genomic DNA (gDNA) was redissolved in 250µl of sterile distilled water. Integrity of DNA and yields were determined by gel electrophoresis and spectrophotometry.

2.5.2 Human genomic DNA extraction from buccal swabs

Three buccal swabs (Medscand MD) were taken from each patient and stored in 2.5mls of PBS. DNA extraction was performed using QIAamp® DNA Mini kit (Quiagen Ltd, UK).

Briefly, according to the protocol, a combination of inversion, vortexing and pipetting was used to suspend the buccal cells in 0.9% (w/v) saline, which was then removed to a fresh tube and centrifuged at 1000xg for 2 minutes. The pellet was transferred to an eppendorf tube containing 600µl PBS. 20µl of QIAGEN protease solution and 600µl of buffer AL were added and mixed by vortexing for 15 seconds. Samples were then incubated at 56°C following which 600µl of absolute ethanol was added; this mixture, in 700µl aliquots, was transferred to a QIAamp spin column and centrifuged at 6000xg for 1 minute. 500µl of buffer AW2 was then added to the spin column and centrifuged at 13000xg for 3 minutes. The spin column was then transferred to a fresh collection tube, 150µl of distilled sterile water was added to the spin column and the filtrate containing extracted gDNA collected by centrifugation at 6000xg for 1 minute.

2.5.3 Spectrophotometry

To determine the integrity and yield of DNA, samples were diluted by a factor of 100 with dH₂O and the absorption measured at 260nm and 280nm using a UV500 visible spectrometer (Unicam).

Purity of DNA was determined by the ratio of absorbance at 260nm to that at 280nm. High quality, pure DNA has a 260nm:280nm ratio of ≥ 1.8 . The following equation was applied to determine yield:

$$\text{DNA concentration } \mu\text{g/ml} = \text{Abs}_{260\text{nm}} \times \text{dilution factor} \times 50 \text{ (for DNA) or } 40 \text{ (for RNA)}$$

2.5.4 Size fractionation of DNA by gel electrophoresis

DNA preparations and PCR products were size separated by agarose gel electrophoresis. In order to optimise the resolution, the percentage (w/v) agarose used was varied according to the size of DNA fragments to be separated. In general, the larger the expected fragment size of DNA the lower the gel percentage of agarose used. Agarose (ordinary agarose or low melting temperature (LMT) agarose; BioRad) was dissolved in 1x TAE buffer by heating in a microwave oven. Once the agarose solution had cooled to below 60°C, ethidium bromide (Fluka BioChemika) was added to a final concentration of 5µg/ml and the solution was poured into a sealed gel casting tray.

Before loading into the agarose gel, 1/10 volume of 10x Orange G loading dye was added to each sample. A commercial 1kb DNA ladder or ϕ X174 DNA/*Hae* III ladder marker was loaded alongside samples as a molecular size standard. Unless otherwise stated, agarose gels were run in 1x TAE electrophoresis buffer. The ethidium bromide in the gel becomes intercalated with the DNA, which following electrophoresis, allows the DNA fragments to be visualised on a UV transilluminator (302nm) and photographed.

2.5.5 Polymerase chain reaction

2.5.5.1 Reaction principles

Polymerase chain reaction (PCR) allows the amplification of specific DNA sequences using two oligonucleotide primers which are designed to hybridise to opposite strands of the DNA and flank the target DNA region. The target DNA is denatured in the presence of a large excess of the two primers and then returned to a temperature which will allow the primers to anneal to the DNA. A heat-stable DNA polymerase (isolated from the thermophilic bacterium *Thermus aquaticus* and therefore called *Taq* polymerase) which synthesises DNA in the 5' to 3' direction, and all four nucleoside triphosphates are included in the reaction mix, with the sample incubated at a temperature optimal for elongation (extension).

In the first cycle two copies of the target sequence with indeterminate 3' termini are produced. The three steps of denaturing, annealing and extension are repeated, producing another four copies of the target sequence. Two of the new copies will have indeterminate 3' termini but two will now have termini dictated by the 5' terminus of the other primer. In subsequent cycles of reactions there will be further exponential amplification of DNA flanked by each primer (n cycles of PCR amplify the target 2^n -fold; **Figure 2.1**).

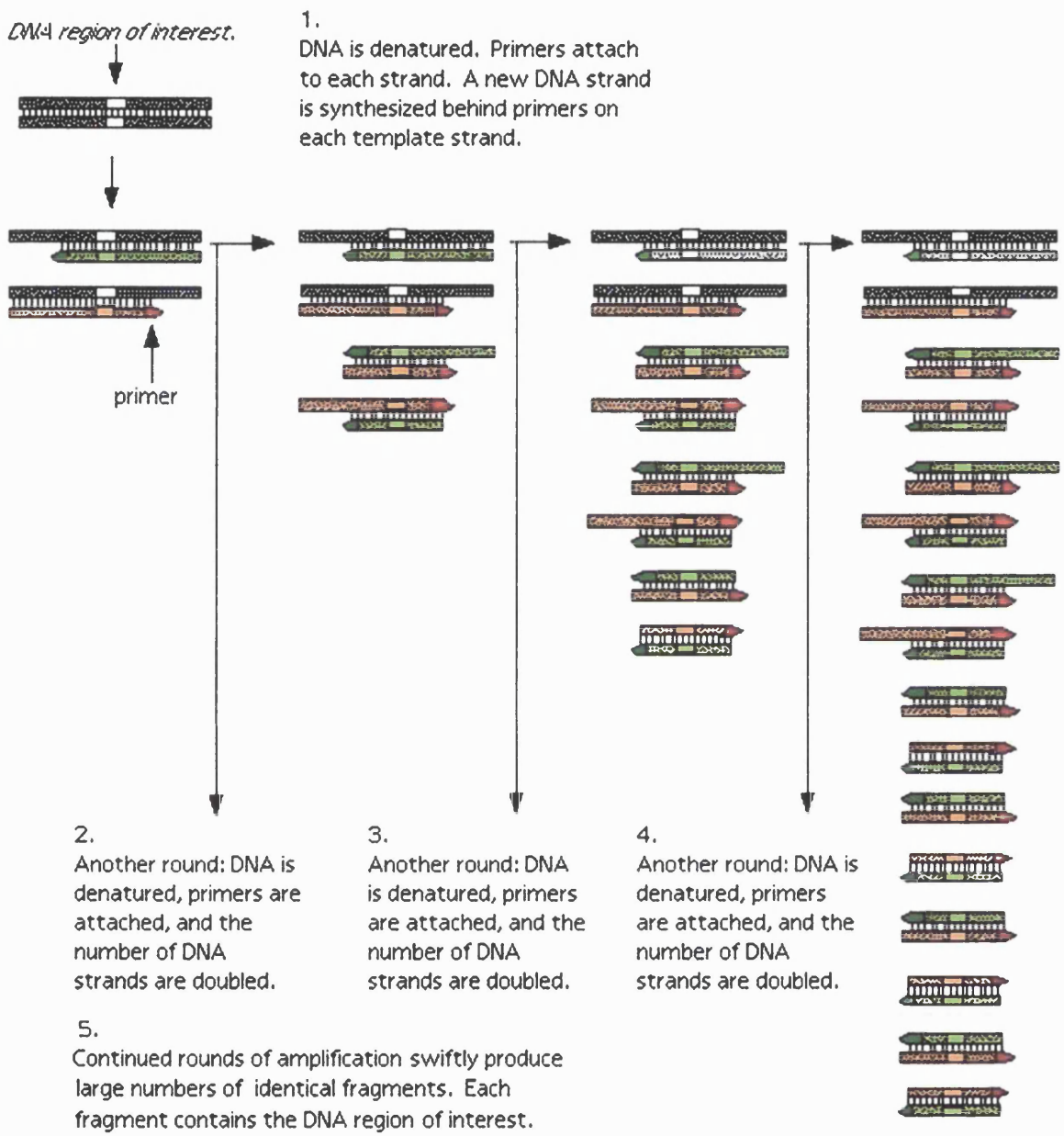


Figure 2.1
Schematic diagram of the polymerase chain reaction

2.5.5.2 Standard PCR parameters

All primers for standard PCR were supplied by Sigma-Genosys Ltd, UK. Fluorescent-labelled oligonucleotides for automated genotyping were from Applied Biosystems.

Standard PCR reactions were performed in a final volume of 50 μ l containing the following:

- 1 x concentration NH₄ buffer (Bioline)
- 1.5 mM MgCl₂
- 200 μ M each dNTP
- 10pmols each of sense and antisense primers
- 200ng-1 μ g DNA
- 1U Bio*Taq* (Bioline)
- X μ l dH₂O (volume made up to 50 μ l)

The DNA underwent an initial denaturation stage at 95°C for 4 minutes. Standard thermal cycling conditions were 35 cycles of:

Denaturation:	95°C for 30 seconds
Annealing:	T _a °C for 30 seconds
Extension:	72°C for 1 minute

The cycling was followed by a final extension at 72°C for 4 minutes and cooling to 4°C.

PCR products were either immediately run on an agarose gel or stored at -20°C.

2.5.6 *Primer design and PCR optimisation*

When designing primer pairs for PCR amplification of known sequences, several guidelines are followed as far as possible to ensure optimal priming:

- random base distribution and similar GC content for both primers (preferably below 50% of the total)
- an anchoring single or double C and/or G at either end (but not complementary)
- minimal secondary structure (i.e. no self-complementarity)
- low complementarity to each other (to reduce the incidence of ‘primer dimer’ formation)
- no greater than 4°C difference between the T_m values of both primers; given the above constraints
- primer length of at least 20 nucleotides to increase the sequence specificity.

The optimal annealing temperature for specific primer pairs was approximated by first calculating the melting temperature (T_m) of each primer, which is dependent on the nucleotide sequence, and was derived using the following formula:

$$4(G+C) + 2(A+T) = T_m$$

and then by assigning an annealing temperature 4 to 6°C lower than the lowest primer T_m value obtained.

Primer pairs were then tested by PCR of several samples of human genomic DNA, including a ‘no DNA’ negative control, followed by electrophoresis on agarose gels to assess the adequacy of the PCR conditions for subsequent experiments. Additional bands to the authentic PCR product suggested cross-hybridisation of the primers to sequences within the genomic DNA that bear some degree of homology to the intended target

sequence. These extra products could usually be eradicated or significantly reduced, by increasing the annealing temperature by 1 to 2°C, or by decreasing the magnesium concentration.

2.5.7 Elution of target PCR fragments

Following electrophoresis, PCR product bands of interest were visualised and excised from the gel under long-wavelength UV light, with the aid of scalpel blades.

For purification of DNA, the agarose slices were placed in a Wizard™ Minicolumn which was then placed in a 1.5ml eppendorf tube and centrifuged at 13000xg for 20 minutes at 4°C. The resin within the column retains contaminants including primer dimers and amplification primers which may interfere with subsequent analysis of the DNA. Collected DNA was then stored at -20°C.

2.5.8 Automated DNA sequencing and ethanol precipitation

The ABI 3100 Genetic Analyser was used routinely in this research. Sequencing reactions were carried out using ABI PRISM™ Big Dye™ Terminator Cycle Sequencing Kit with AmpliTaq® DNA Polymerase, FS versions 3.0 and 4.0 (Applied Biosystems).

Essentially, the protocol used followed that provided by the manufacturer. 3-10ng of purified template DNA was cycle sequenced using the Big Dye™ AmpliTaq® dideoxy kit and the appropriate sequencing primer. The Big Dye™ reaction mix contains all of the required reagents: dye terminators; deoxynucleoside triphosphates; AmpliTaq® DNA Polymerase, FS; *rTth* pyrophosphate; magnesium chloride and buffer. 4µl of Big Dye™ version 3.0 or 2µl of Big Dye™ version 4.0 reaction mix was used in a total reaction

volume of 10 μ l, the remainder of which was made up with 3-10ng template DNA, 1.6 μ M sequencing primer, and made up to volume with dH₂O. The combined reaction volume of 10 μ l was then cycled on the Perkin Elmer 9600 PCR machine with the following cycling profile for 25 cycles:

Rapid thermal ramp to 96°C

96°C for 10 seconds

Rapid thermal ramp to 50°C

50°C for 5 seconds

Rapid thermal ramp to 60°C

60°C for 4 minutes

The cycle sequenced samples then underwent DNA precipitation involving:

- addition of 64 μ l of 96% (v/v) ethanol and 26 μ l of dH₂O to each sample, then left to stand for 20 minutes
- pelleting of precipitate by centrifugation for 20 minutes at 13000xg
- the supernatant was carefully removed and washing of the pellet was performed with 200 μ l of 70% (v/v) ethanol
- sample was then centrifuged at 13000xg for 15 minutes
- the supernatant was again carefully removed and the sample was left to air dry in order to remove remaining ethanol.

For analysis on the ABI 3100 automated sequencer, the resultant pellets were resuspended in 12 μ l formamide (Applied Biosystems), vortexed and the entire 12 μ l loaded on to a microtitre plate.

2.5.9 Operation of automated sequencer

Sequenced samples to be analysed by the ABI 3100 Genetic Analyser were loaded into 96-well microtitre plates, two of which could be run on the sequencer at a time, and run as per the manufacturer's instructions. This automated process involves samples being electrophoretically injected into fused-silica capillaries that are filled with polymer. DNA fragments migrate towards the other end of the capillaries, with the shorter fragments moving faster than the longer fragments. Fragments enter a detection cell and move through a laser beam in turn. The laser light causes excitation of the fluorescent dye on the fragments which is captured by a CCD camera and converted into electronic information. This information is transferred to the computer workstation for processing by the 3100 Data Collection software. The software for final analysis of the data, *Sequence Analysis*[™], presents the data in two formats: a text file and a sequence analysis file. The latter type of file incorporates the electropherogram data, and constitutes the original sequence data.

2.5.10 In silico genetic analysis

Raw data containing DNA sequence were generated by the ABI PRISM[™] *Sequence Analysis*[™] software for Apple Macintosh computers. GeneWorks[™] (version 2.5.1) was used to collate, store and align sequences of different PCR products to highlight mismatches or nucleotide deletions/insertions and also to align sequences of interest derived from different species in order to assess evolutionary conservation.

2.5.11 Nucleic acid extraction

2.5.11.1 mRNA isolation

In order to extract a sufficient amount of mRNA from limited mouse dental tissue the QuickPrep® *Micro* mRNA Purification Kit (Pharmacia Biotech) was utilised. This method provides mRNA without first needing total RNA. The protocol was carried out in accordance with manufacturer's instructions. Briefly, up to 0.1 g of tissue was homogenised in an extraction buffer containing a high concentration of guanidium thiocyanate (GTC), thereby ensuring the rapid inactivation of any endogenous RNases. The extract was then diluted three-fold with an elution buffer (10mM Tris-HCL (pH 7.5), 1mM EDTA) to reduce the GTC concentration. The suspension was centrifuged to produce a clear homogenate.

The mRNA isolation was achieved by passing the homogenate through an Oligo(dT)-Cellulose pellet, with poly(A)+ RNA binding to the Oligo(dT)-Cellulose. This pellet was washed several times in high and low salt buffers before eluting the mRNA at 65°C in 0.4 ml of elution buffer.

2.5.11.2 Quantification of mRNA

mRNA concentration was determined at this stage by spectrophotometry using the formula:

$$[\text{mRNA}] = A_{260} \times \text{dilution factor} \times 40 \mu\text{g/ml}$$

2.5.11.3 Precipitation of mRNA

To precipitate the mRNA, a 1/10 volume of potassium acetate solution (2.5 M), 10µl of a glycogen solution (5-10 mg/ml), and 1ml of 95% (v/v) ethanol were added. The sample

was placed at -20°C overnight. Precipitated mRNA was collected the following day by centrifugation and eluted in 50µl of elution buffer.

2.5.12 Reverse transcription PCR (RT-PCR)

cDNA synthesis from an mRNA template was achieved by RT-PCR with the Superscript First-Strand Synthesis System (GibcoBRL). This procedure is able to convert 1-5µg of total RNA or 50-500ng of mRNA into first-strand cDNA. The manufacturer's protocol was followed. The mRNA was targeted with an oligo (dT)₁₂₋₁₈ primer (0.5µg) and cDNA synthesis was performed by the Superscript II RT enzyme (50U). RNase H was then added to remove the RNA, leaving only cDNA viable as a template for subsequent PCR reactions.

2.5.13 Bioinformatics

URLs used for bioinformatics analysis throughout this research are as follows:

The National Center for Biotechnology Information (NCBI), <http://www.ncbi.nlm.nih.gov>

Unigene, <http://www.ncbi.nlm.nih.gov/UniGene/>

BLAST, <http://www.ncbi.nlm.nih.gov/BLAST>

Ensembl, <http://www.ensembl.org/>

UCSC Human Genome Browser, <http://genome.ucsc.edu/index.html>

RetNet, <http://www.sph.uth.tmc.edu/Retnet/home.htm>

Online Mendelian Inheritance in Man, <http://www3.ncbi.nlm.nih.gov/Omim/>

CHAPTER 3

ACHROMATOPSIA

3.1 INTRODUCTION

Achromatopsia is a stationary disorder of cone function presenting in infancy with pendular nystagmus, photophobia and reduced central vision (sections 1.1.2.1 and 1.1.2.2). It can be usefully subdivided into the *complete* and *incomplete* subtypes. Subjects with incomplete achromatopsia have residual colour vision on detailed testing and slightly better visual acuity.

Mutations in three phototransduction-related genes have been identified to date in patients with achromatopsia: *CNGA3*, *CNGB3* and *GNAT2* (sections 1.1.2.1.2 and 1.1.2.2.2). *CNGA3* and *CNGB3* respectively encode the α - and β - subunits of the cGMP-gated (CNG) cation channel expressed in cone photoreceptors. *GNAT2* encodes the α -subunit of cone-specific transducin. Most of the mutations identified in *CNGA3* are missense mutations, whilst nonsense mutations predominate in *CNGB3*, and exclusively truncating variants having been shown in *GNAT2*. Current estimates suggest that about 25% of achromats have mutations in *CNGA3*, 40-50% in *CNGB3* and $\leq 1\%$ in *GNAT2*.

Both the *CNGA3* and *CNGB3* polypeptides have six transmembrane domains with a loop between domains 5 and 6 that forms the pore of the channel (**Figure 3.1**). Both the N- and C-terminal loops are intracellular, with a cGMP-binding site near the C-terminus. A similar cyclic nucleotide-gated channel is involved in olfaction, but in this case cAMP is the nucleotide involved. The β -subunit differs in also having a calcium-calmodulin binding domain near the N-terminus; although it has recently been suggested that calmodulin (CaM) regulation involves functionally important CaM-binding sites in both the N- and C-terminal cytoplasmic domains (Peng *et al.*, 2003a). The β -subunits of ion channels often modulate ionic conductance and selectivity of the channel (Kaupp and Seifert, 2002; Matulef and Zagotta, 2003).

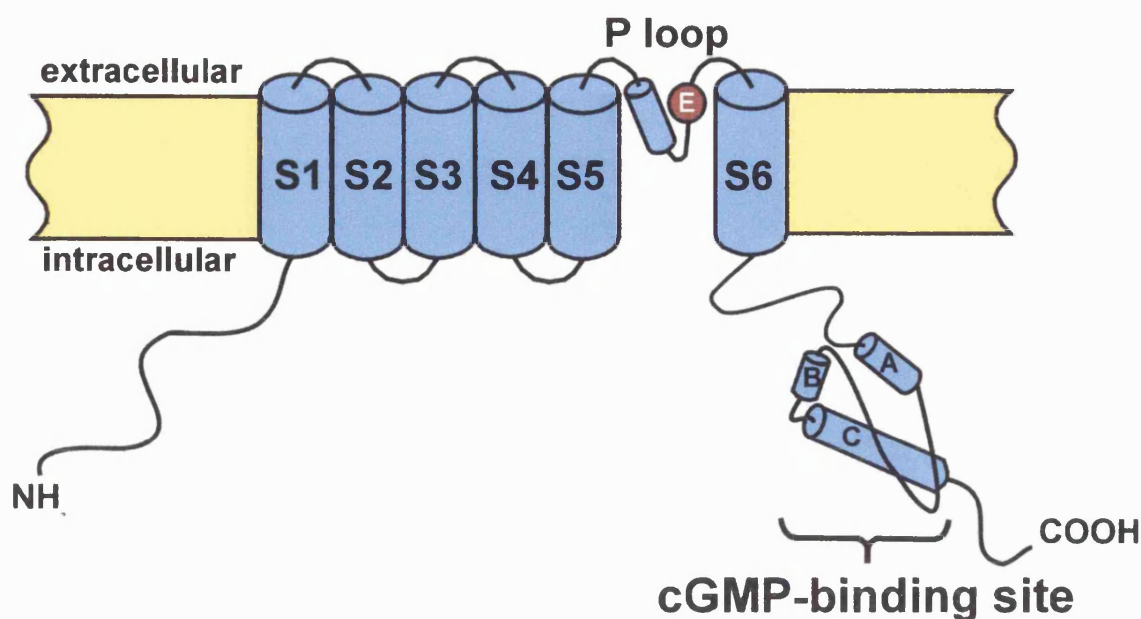


Figure 3.1

CNGA3 and CNGB3 polypeptide structure

(CNGB3 also has a calcium-calmodulin binding domain near the N-terminus)

Most reported studies have been conducted on the rod cGMP-gated channels. The stoichiometry of both the rod and cone channels remains uncertain. Currently it is thought that an individual rod channel consists of three α -subunits and a single β -subunit (Zheng *et al.*, 2002). It is however known that CNGA3 subunits can form functional homomeric channels when expressed alone, whereas CNGB3 subunits do not appear to form functional channels when expressed alone (Finn *et al.*, 1998). Relatively little detail is presently known about the contribution of different portions of the CNGA3 and CNGB3 polypeptides to cone photoreceptor CNG channel function, with the majority of work to date involving the CNGA1 and CNGB1 subunits of the corresponding rod cation channel. From this work it has been shown that binding of Ca^{2+} , via calmodulin to the N-terminus of the β -subunit disrupts the interaction between this region and the C-terminal region of the α -subunit, reducing sensitivity of the channel to cyclic nucleotides and

thereby leading to inhibition of function (Trudeau and Zagotta, 2002a). Furthermore, it has been shown that failure of this interaction leads to lack of functional channels at the membrane surface (Trudeau and Zagotta, 2002a; Trudeau and Zagotta, 2002b).

The CNG ion channels serve as final targets of signal transduction in vertebrate photoreceptors (section 1.1.1.1). In the dark, CNG channels are kept open by the binding of cGMP thereby allowing a steady influx of $\text{Ca}^{2+}/\text{Na}^+/\text{k}^+$ ions into the photoreceptor outer segment with consequent membrane depolarisation and release of glutamate neurotransmitter. Following activation of the phototransduction cascade by light, cGMP bound to CNG channels is hydrolysed thus enabling the closure of these channels, shutting off the inward cation current, and thereby leading to membrane hyperpolarization and decreased synaptic release of glutamate.

CNGA3 was the first of the human cone CNG-channel subunit genes to be cloned (Wissinger *et al.*, 1997). The human gene is composed of seven exons and spans approximately 30kb of genomic sequence. A more recent study identified two additional exons designated '0' and '2b' (Wissinger *et al.*, 2001), increasing the total number of *CNGA3* exons to nine; with exon 0 thought to have a role in transcription regulation and exon 2b extending the amino-terminal part by 55 amino acids. However, these extra 55 residues are not always taken into account when mutations have been described in the literature. The gene encodes a 749 amino acid polypeptide. All functionally relevant domains of the gene, except for the first two membrane spanning segments, are located on a large terminal exon.

CNGB3 was cloned simultaneously by two groups (Kohl *et al.*, 2000; Sundin *et al.*, 2000). The human gene has 18 exons and spans ~200kb of genomic DNA. Intron/exon boundaries obey the GT-AG splice rule except for exon 13 which is GC instead of GT. The gene encodes an 810 amino acid polypeptide. There is a calmodulin-binding domain,

six α -helical transmembrane segments, a hydrophilic pore structure and a cyclic-nucleotide binding site.

3.2 AIMS

The purpose of this study included a clinical and psychophysical phenotypic assessment of patients with achromatopsia. Having ascertained a panel of UK patients, screening of *CNGB3* was to be performed. By combining the *CNGB3* findings with the results of a parallel study of *CNGA3*, an estimate of the relative frequency of mutations in each gene would be established and a subset of individuals without mutations in these genes would be identified. A genotype-phenotype comparison could also be attempted.

In a large consanguineous family which was part of the panel ascertained, in whom neither *CNGA3* nor *CNGB3* mutations were identified, a homozygous *GNAT2* nonsense mutation was found (Aligianis *et al.*, 2002). The phenotype associated with this mutation was re-evaluated in a detailed fashion (section 3.7).

3.3 PHENOTYPE

A panel of patients (35 patients from 23 families) ascertained from two British centres, Moorfields Eye Hospital and Birmingham Children's Hospital, were examined clinically and also underwent electrophysiological testing and psychophysical assessment. Individuals were diagnosed with achromatopsia on the basis of the presence of characteristic clinical and psychophysical findings, and electrophysiological evidence of absent or severely reduced cone ERG, with normal rod responses.

3.3.1 Methods

A full medical and ophthalmic history was obtained and an ophthalmological examination performed. Patients with clinical findings consistent with a diagnosis of achromatopsia underwent electrophysiological assessment which included full-field electroretinogram (ERG) and pattern ERG, according to the protocols recommended by the International Society for Clinical Electrophysiology of Vision (Marmor *et al.*, 1998; Bach *et al.*, 2000). The ERG testing was performed in the electrophysiology departments of Drs Holder, Bradshaw and Good, respectively.

Detailed psychophysical testing (section 1.3.4.1) included the use of Hardy, Rand and Rittler (HRR) plates (American Optical Company, NY), Farnsworth-Munsell (FM) 100-hue test, Farnsworth D-15 and PV-16, the Mollon-Reffin (M-R) Minimal test (Mollon *et al.*, 1991), a computerised colour vision test (Mollon and Reffin, 1989; Regan *et al.*, 1994), and anomaloscopy. The FM 100-hue, Farnsworth D-15 and the M-R test were all performed under CIE Standard Illuminant C from a MacBeth Easel lamp. This detailed colour vision assessment was performed predominantly in order to identify those individuals with incomplete achromatopsia, in order to investigate whether their genotypes differed from those ascertained to have the complete subtype. All colour vision testing was performed at Professor J. D. Mollon's laboratory at the Department of Experimental Psychology, University of Cambridge.

3.3.2 Results

The clinical, electrophysiological and psychophysical findings are summarised in **Tables 3.1 and 3.2**. All affected subjects had photophobia and nystagmus of variable severity. The nystagmus was commonly found to wane with time. Visual acuity ranged between 6/36 and CF. An equal incidence of myopia and hypermetropia was seen in the panel. In

the majority of cases fundus examination was normal (**Figure 3.2**). In 7 families (12 individuals) macular RPE changes were detected, with mild mid-peripheral RPE atrophy in one subject (**Figure 3.2**). All affected individuals had absent cone ERG responses with normal rod function.

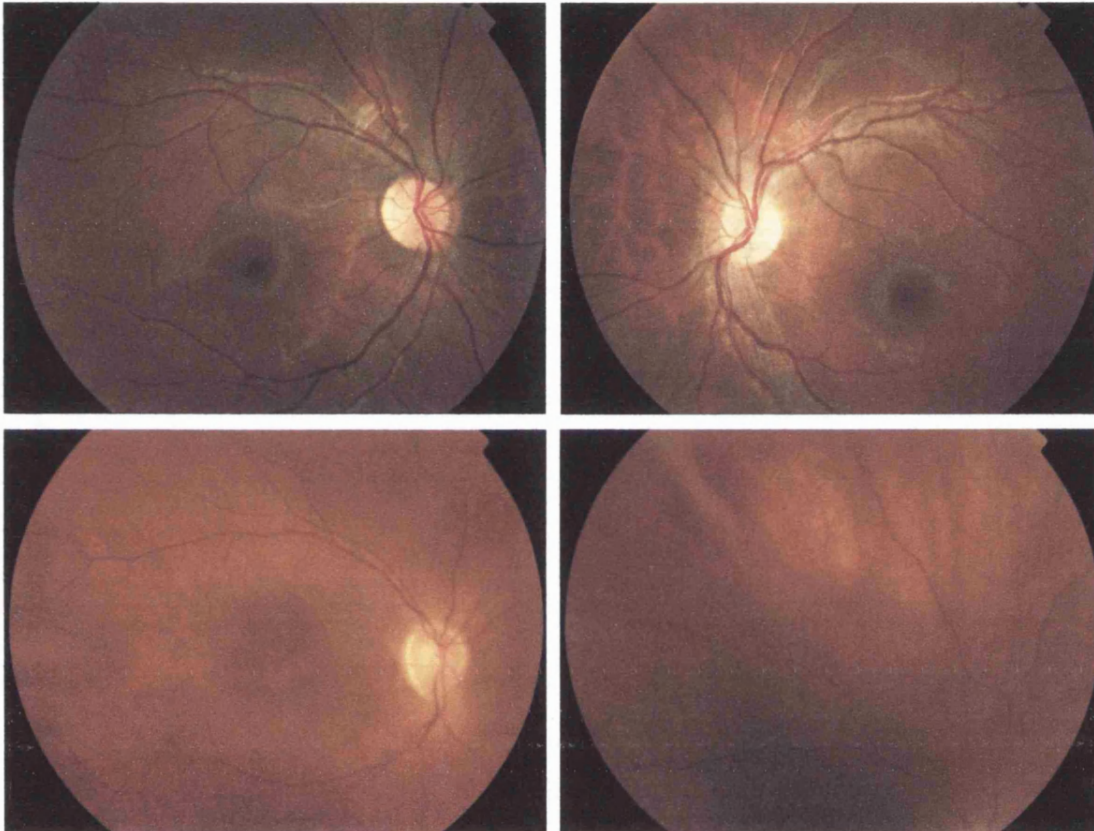


Figure 3.2

Fundi in achromatopsia

Above: normal fundi usually seen in achromatopsia

Below: macular & mid-peripheral RPE atrophy

On detailed colour vision testing none of the affected subjects in the first 22 families were found to have residual colour vision, thereby placing all these individuals in the complete subtype of achromatopsia. Tests designed for use in patients with low vision

were also employed in an attempt to detect any residual discrimination; including the use of the enlarged M-R minimal test, the PV-16 (enlarged Farnsworth D-15), and a computerised colour vision test (P4) (Simunovic *et al.*, 1998; section 1.3.4.1.4). However these tests also failed to detect any residual colour vision.

Therefore a complete achromatopsia phenotype, on the basis of lack of colour vision, was detected in all subjects of our panel, thereby precluding any evaluation of potential phenotype-genotype relationships. Visual acuity assessment was also in keeping with the diagnosis of complete achromatopsia since in the majority of cases vision was 6/60, with better acuity expected in an incomplete phenotype.

Only in family 23 was significant residual colour vision detected. They were found to have a *GNAT2* mutation and their detailed phenotype will be discussed below in section 3.7.

Family	Patient	Status	Age (yrs)	VA	Refraction	Macula	Cone	Colour
				OD - OS	OD : OS		ERG	Vision
1	RM1	A	32	6/60 - 6/60	-0.5/-3.0 x180 : -1.0/-3.0 x180	Slight atrophy	Absent	Absent
	RM2	A	34	6/60 - 6/60	-1.0/-1.5 x120 : -2.0/-2.0 x105	Slight atrophy	Absent	Absent
	RM3	N	60	-	-	NAD	-	-
2	RM4	N	39	6/6 - 6/6	-	NAD	-	Normal
	RM5	A	9	6/60 - 6/60	+3.0/+1.5 x15 : +3.0/+1.5 x75	Slight atrophy	Absent	Absent
	RM6	A	7	6/60 - 6/60	+6.5/-2.0 x10 : +6.0/-2.0 x180	-	Absent	Absent
3	RM7	A	10	6/60 - 6/60	+0.75/+1.0 x90 : +1.0/+1.0x90	NAD	Absent	Absent
	RM8	N	28	-	-	-	-	-
	RM9	A	8	3/60 - 3/60	+4.5/+2.5 x80 : +4.0/+2.5 x 95	NAD	Absent	Absent
	RM10	N	26	6/6 - 6/6	-	NAD	-	Normal
4	RM11	A	38	6/60 - 6/60	-2.5/-1.5 x180 : -2.5/-1.5 x170	Slight atrophy	Absent	Absent
5	RM12	A	10	6/60 - 6/60	+3.0/-0.5 x90 : +3.5/-0.75x100	NAD	Absent	Absent
	RM13	N	30	-	-	-	-	Normal
6	RM14	A	39	6/60 - 3/60	-0.5/-0.5 x180 : -1.0/-1.0 x10	NAD	Absent	-
	RM15	A	28	6/60 - 6/60	-1.0/-0.5 x120 : -1.5/-0.25 x10	NAD	Absent	-
7	RM16	N	43	6/6 - 6/6	-	-	-	Normal
	RM17	A	16	6/60 - 6/60	-	NAD	Absent	Absent
8	RM18	A	44	3/60 - 3/60	+2.0/-0.5 x110 : +3.0/-1.0 x 90	Slight RPE Δ	Absent	Absent
	RM19	N	77	6/9 - 6/9	-	-	-	Normal
9	RM20	A	15	6/36 - 6/36	-1.5/-1.5 x15 : -2.25/-2.0 x 180	NAD	Absent	Absent
10	RM21	A	9	3/60 - 3/60	+0.5/+3.0 x120 : +0.5/+2.5x85	NAD	Absent	Absent
	RM22	N	37	6/6 - 6/6	-	NAD	-	Normal
	RM23	N	52	6/6 - 6/6	-	NAD	-	Normal
11	RM24	A	19	6/60 - 6/60	+4.5/-2.0 x180 : +4.0/-2.5x180	NAD	Absent	Absent*
	RM25	N	40	-	-	-	-	Normal
12	RM26	A	26	6/36 - 6/36	-	NAD	Absent	Absent*
13	RM27	A	25	6/60 - 6/60	-	NAD	-	-
14	RM28	A	19	6/36 - 6/36	-8.5/-3.5 x10 : -8.5/-3.0 x170	NAD	Absent	Absent

Table 3.1 (Part 1) Summary of clinical findings in achromatopsia

Family	Patient	Status	Age (yrs)	VA OD - OS	Refraction OD : OS	Macula	Cone ERG	Colour
								Vision
15	RM29	N	50	-	-	-	-	-
	RM30	N	55	-	-	-	-	-
	RM31	A	20	6/60 - 6/60	-1.5/-2.5 x120 : -1.25/-2.0 x85	NAD	Absent	Absent
	RM32	A	14	6/60 - 6/60	-1.5/-2.25 x180 : -2.5/-2.25 x5	NAD	Absent	Absent
16	RM33	N	40	6/6 - 6/6	-	-	-	-
	RM34	A	12	3/36 - 3/36	+1.0/+0.5 x 90 : +1.5/+0.5x110	NAD	Absent	Absent
	RM35	N	43	6/6 - 6/6	-	-	-	Normal
	RM36	A	5	2/60 - 3/60	+3.0/+2.5 x90 : +3.0/+2.0 x90	NAD	Absent	-
17	RM37	A	34	6/36 - 6/36	-8.0/-2.0 x90 : -7.5/-2.5 x105	NAD	Absent	Absent
	RM38	A	32	6/60 - 6/60	-6.0/-1.0 x90 : -6.5/-1.5 x180	NAD	Absent	Absent
	RM39	A	28	6/60 - 6/60	-	NAD	Absent	Absent
18	RM40	A	5	6/60 - 6/60	-	NAD	Absent	-
19	RM41	A	6	6/60 - 6/60	-	NAD	Absent	Absent
	RM42	N	43	6/6 - 6/6	-	NAD	-	Normal
20	RM43	A	24	6/60 - 6/60	+3.0/-1.0 x 90 : +2.5/-0.5 x 85	RPE Δ	Absent	Absent
21	RM44	A	5	6/60 - 6/60	-3.5/+3.0 x90 : -3.0/+4.5 x105	NAD	Absent	-
22	RM45	A	9	6/36 - 6/36	-	RPE Δ	Absent	-
23	RM46	A	41	6/60 - 6/60	-2.0/+2.0 x110 : -2.5/+1.5 x70	Mild	Absent	Absent
	RM47	N	33	6/6 - 6/6	-	RPE Δ	30Hz Cone	Normal
	RM48	A	20	6/60 - 6/60	+1.5/+1.5 x110 : +1.0/+2.0x80	in affected	ERG	Residual
	RM49	A	19	CF - 6/60	Balance : -2.0/+3.0 x 75	subjects	Residual	Residual
	RM50	A	35	CF - CF	-3.5/+3.0 x30 : -4.0/+3.0 x160		S-cone	Absent
	RM51	A	44	CF - CF	-2.0/+2.0 x135 : -1.5/+1.5 x45		ERG	Residual

Table 3.1 (Part 2) Summary of clinical findings in achromatopsia

Family 23 has a GNAT2 mutation; their phenotype is described in detail in section 3.7

(*Absent with HRR and Ishihara plates. Detailed assessment not performed due to lack of patient co-operation; Δ = Changes)

Family	Patient	ISH	HRR	PV-16	M-R	Sloan	Anomaloscopy	Colour
		OD	OD		OD	Matches	Matching	Vision
		OS	OS		OS		Range	
1	RM1	1/17	Nil	Scotopic	P(no)D(no)T(no)	Achromatic	0-73	Nil
		1/17	Nil	Scotopic	P(no)D(no)T(no)	Achromatic	0-73	Residual
	RM2	1/17	Nil	Scotopic	P(no)D(no)T(no)	Achromatic	0-73	Nil
		1/17	Nil	Scotopic	P(5)D(no)T(no)	Achromatic	0-73	Residual
2	RM5	1/17	Nil	Scotopic	P(no)D(no)T(no)	Achromatic	0-73	Nil
		1/17	Nil	Scotopic	P(no)D(no)T(no)	Achromatic	0-73	Residual
	RM6	1/17	Nil	Scotopic	P(no)D(no)T(no)	Achromatic	0-73	Nil
		1/17	Nil	Scotopic	P(no)D(no)T(no)	Achromatic	0-73	Residual
3	RM7	1/17	Nil	Scotopic	P(no)D(no)T(no)	Achromatic	0-73	Nil
		1/17	Nil	Scotopic	P(no)D(no)T(no)	Achromatic	0-73	Residual
	RM9	1/17	Nil	Scotopic	P(no)D(6)T(no)	Achromatic	-	Nil
		1/17	Nil	Scotopic	P(no)D(no)T(no)	Achromatic	-	Residual
4	RM11	-	Nil	Scotopic	P(no)D(no)T(no)	Achromatic	0-73	Nil
			Nil	Scotopic	P(no)D(no)T(no)	Achromatic	0-73	Residual
5	RM12	1/17	Nil	Scotopic	P(no)D(no)T(no)	Achromatic	0-73	Nil
		1/17	Nil	Scotopic	P(no)D(no)T(no)	Achromatic	0-73	Residual
7	RM17	-	Nil	Scotopic	P(no)D(no)T(no)	Achromatic	0-73	Nil
			Nil	Scotopic	P(no)D(no)T(no)	Achromatic	0-73	Residual
8	RM18	2/17	Nil	Scotopic	P(no)D(no)T(no)	Achromatic	0-73	Nil
		2/17	Nil	Scotopic	P(no)D(no)T(no)	Achromatic	0-73	Residual
9	RM20	-	-	Scotopic	P(no)D(no)T(no)	Achromatic	0-73	Nil
				Scotopic	P(no)D(no)T(no)	Achromatic	0-73	Residual
10	RM21	2/17	Nil	Chaotic	P(no)D(6)T(no)	Achromatic	0-73	Nil
		2/17	Nil	Scotopic	P(no)D(5)T(no)	Achromatic	0-73	Residual
11	RM24	1/17	Nil	-	-	-	-	-
		1/17	Nil					
12	RM26	1/17	Nil	-	-	-	-	-
		1/17	Nil					

Table 3.2 (Part 1) Summary of psychophysical data in achromatopsia

(ISH = Ishihara plates; HRR = Hardy, Rand, Rittler plates;

M-R = Mollon-Reffin minimal test; PV-16 = enlarged Farnsworth D-15)

Family	Patient	ISH	HRR	PV-16	M-R	Sloan	Anomaloscopy	Colour
		OD	OD		OD	Matches	Matching	Vision
		OS	OS		OS		Range	
14	RM28	1/17	Nil	Scotopic	P(no)D(no)T(no)	-	0-73	Nil
		1/17	Nil	Scotopic	P(no)D(no)T(no)		0-73	Residual
15	RM31	1/17	Nil	Chaotic	P(no)D(no)T(no)	-	0-73	Nil
		1/17	Nil	Scotopic	P(no)D(no)T(no)		0-73	Residual
	RM32	1/17	Nil	Scotopic	P(no)D(no)T(no)	-	-	Nil
		1/17	Nil	Scotopic	P(no)D(no)T(no)			Residual
16	RM34	1/17	Nil	Scotopic	P(no)D(no)T(5)	Achromatic	0-73	Nil
		1/17	Nil	Scotopic	P(no)D(no)T(no)	Achromatic	0-73	Residual
17	RM37	2/17	Nil	Scotopic	P(5)D(no)T(no)	Achromatic	0-73	Nil
		2/17	Nil	Scotopic	P(no)D(no)T(no)	Achromatic	0-73	Residual
	RM38	1/17	Nil	Chaotic	P(no)D(no)T(no)	Achromatic	-	Nil
		1/17	Nil	Scotopic	P(no)D(no)T(no)	Achromatic		Residual
	RM39	1/17	Nil	Scotopic	P(no)D(no)T(no)	Achromatic	-	Nil
		1/17	Nil	Scotopic	P(no)D(no)T(no)	Achromatic		Residual
19	RM41	1/17	Nil	Scotopic	P(no)D(no)T(no)	Achromatic	0-73	Nil
		1/17	Nil	Scotopic	P(no)D(6)T(no)	Achromatic	0-73	Residual
20	RM43	1/17	Nil	Chaotic	P(no)D(no)T(no)	Achromatic	0-73	Nil
		1/17	Nil	Scotopic	P(no)D(no)T(no)	Achromatic	0-73	Residual
23	RM46	2/17	Nil	Scotopic	P(no)D(no)T(no)	Achromatic	0-73	Nil
		2/17	Nil	Scotopic	P(no)D(no)T(no)	Achromatic	0-73	Residual
	RM48	-	-	Chaotic	P(no)D(7)T(4)	-	0-73	Residual
		-	-	Chaotic	P(no)D(no)T(5)		0-73	(inc P4)
	RM49	-	-	-	-	-	-	Residual
		-	-	Scotopic	P(no)D(6)T(5)		0-73	(inc P4)
	RM50	1/17	Nil	Scotopic	P(no)D(no)T(no)	Achromatic	0-73	Nil
		1/17	Nil	Scotopic	P(no)D(no)T(no)	Achromatic	0-73	Residual
	RM51	-	-	Minor errors	P(no)D(7)T(5)	-	0-73	Residual
		-	-		P(no)D(6)T(5)		0-73	(inc P4)

Table 3.2 (Part 2) Summary of psychophysical data in achromatopsia

Family 23 has a GNAT2 mutation; their phenotype is described in detail in section 3.7

(P4 = computerised colour vision test for subjects with low vision; section 1.3.4.1.4)

3.4 *CNGB3* MUTATION SCREENING

Blood samples were collected from patients and family members after informed consent was obtained. Total genomic DNA was extracted from the blood samples using a Nucleon®Biosciences kit.

3.4.1 *Methods*

The coding sequences of *CNGB3* were amplified by PCR in each individual using primer sequences and conditions as published by Kohl *et al.* (2000). *CNGA3* was screened by a colleague in a parallel study. Standard 50µl PCR reactions were performed as described previously. After resolution on a 1% (w/v) LMT agarose gel, products were excised and eluted.

Direct sequencing of PCR products was carried out on an ABI 3100 Genetic Analyser using the original PCR primers in the sequencing reactions. The sequence was examined for alterations utilising *Sequencing Analysis* (ABI Prism™) and *GeneWorks*™ software. GenBank sequences were used to construct an alignment of channel protein sequences and to analyse the evolutionary conservation of the corresponding amino acid positions. The sequences used were the CNG channel cone β-subunits of human (accession number AF272900), mouse (NM013927) and dog (AF490511), and the rod β-subunits of human (AF042498) and rat (NM031809). Sequences were aligned using *GeneWorks*™ software.

3.4.2 *Results*

The 18 coding exons of *CNGB3* were screened for mutations in the panel of small families/probands with achromatopsia. The 8 coding exons of *CNGA3* were screened by a colleague in a parallel study.

Three sequence variants in the coding region of *CNGB3* were found in the panel of patients that most likely represent disease-causing mutations (Table 3.3). Of these, two are novel as follows. A 595delG frameshift mutation in exon 5 (Glu199fs) that results in a truncated polypeptide of 200 amino acids was found as a compound heterozygote change in family 3 (Figure 3.3), and a Phe525Asn substitution (1573/4TT→AA; exon 13) as a homozygous change in family 17 (Figure 3.4). The Phe525Asn (F525N) substitution co-segregated with disease (Figure 3.5). Phe525 is conserved across other CNG receptor subunits (Table 3.4) and the Phe525Asn missense mutation was not found in a screen of 100 control chromosomes.

Family/affected individuals	<i>CNGB3</i> Mutation	Amino acid substitution
3 / RM7, RM9	Ht 1148delC	Thr383fs
	Ht 595delG	Glu199fs
11 / RM24	Hm 1148delC	Thr383fs
14 / RM28	Ht 1148delC	Thr383fs
15 / RM31, RM32	Hm 1148delC	Thr383fs
17 / RM37, RM38, RM39	Hm 1573/4TT→AA	Phe525Asn
19 / RM41	Hm 1148delC	Thr383fs
20 / RM43	Hm 1148delC	Thr383fs
21 / RM44	Hm 1148delC	Thr383fs
22 / RM45	Hm 1148delC	Thr383fs
1 / RM1, RM2	Ht 919A→G	Ile307Val*

Table 3.3

***CNGB3* disease-causing mutations**

(Ht = heterozygous, Hm = homozygous. Mutations in **bold** represent novel alterations. *Substitution at non-conserved residue that is unlikely to be disease-associated (see text))

Residue	Human cone β	Murine cone β	Canine cone β	Human rod β	Rat rod β
27	Asn	Lys	Asn	Lys	Lys
307	Ile	Leu	Val	Leu	Leu
525	Phe	Phe	Phe	Phe	Phe

Table 3.4

Amino acid conservation in cone and rod β -subunits of CNG channel proteins at sites of missense mutations in CNGB3.

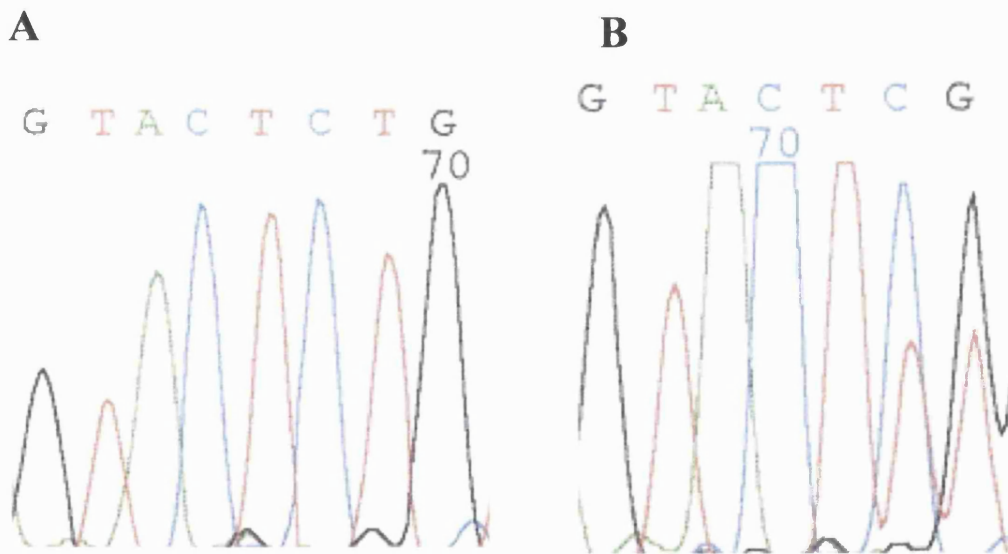


Figure 3.3

CNGB3 Exon 5 mutation

A - Wild-type (wt) Exon 5

B - Ht Glu199fs

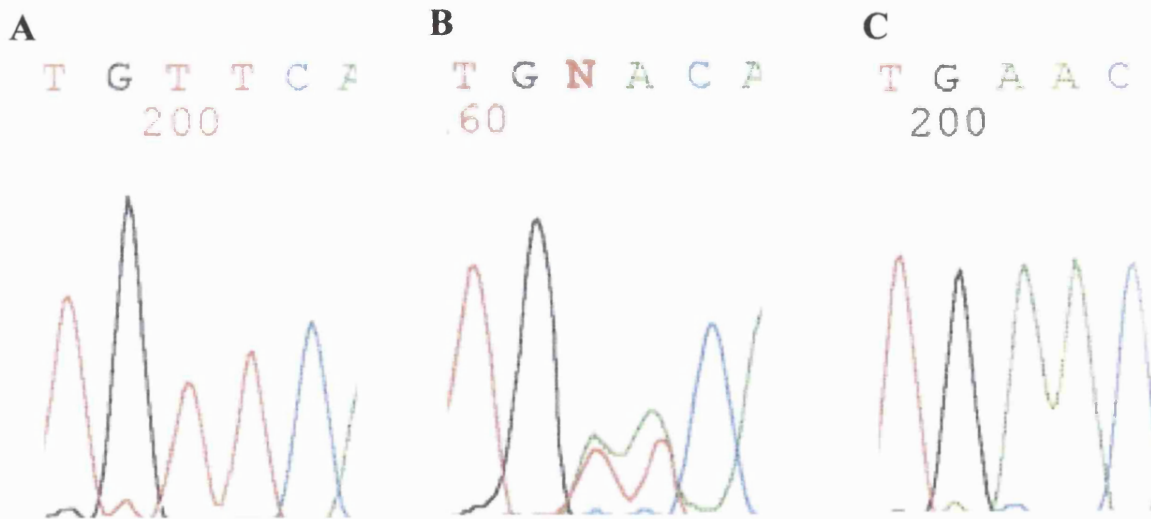


Figure 3.4

CNGB3 Exon 13 mutation

A - wt Exon 13 **B** - Ht F525N

C - Hm F525N

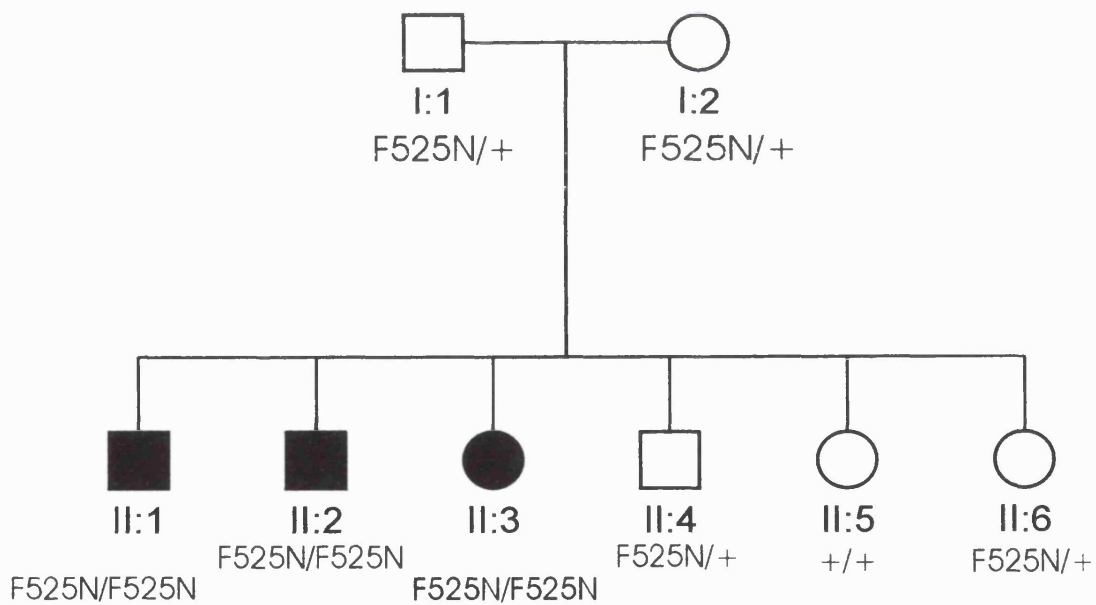


Figure 3.5

Segregation of F525N in family 17

The third mutation identified, Thr383fs (1148delC), located in exon 10, has been previously reported as the most common disease-causing mutation in achromatopsia (Kohl *et al.*, 2000; Kohl *et al.*, 2001). In the present study, this 1-bp deletion, 1148delC, was found to segregate in 8 of the 9 families with *CNGB3* mutations. The locations of the novel Glu199fs and Phe525Asn mutations (and novel *CNGA3* mutations) in the channel protein are shown in **Figure 3.6**.

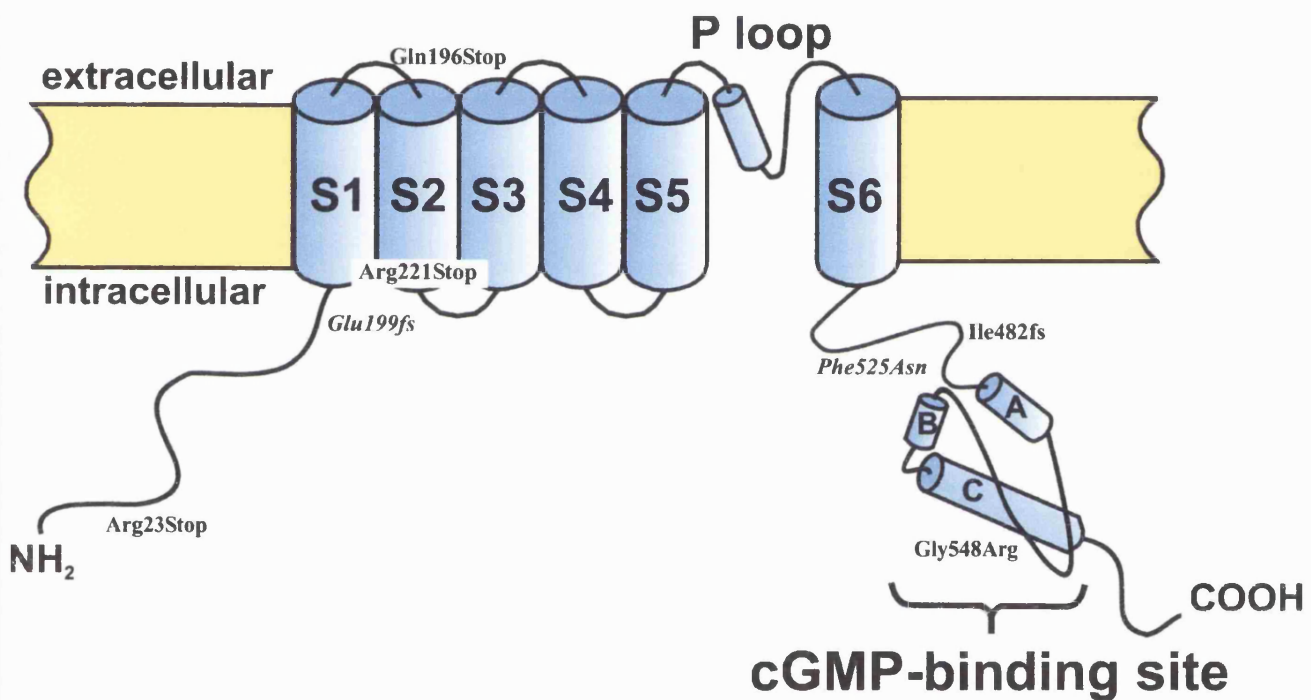


Figure 3.6

Location of novel CNGB3 and CNGA3 mutations

(Novel *CNGB3* mutations: Glu199fs & Phe525Asn; and the five novel *CNGA3* mutants)

An Ile307Val substitution was detected in affected and unaffected individuals in family 1. This is unlikely however to represent a disease-causing mutation since it is a very conservative substitution at a site that is not conserved across species (**Table 3.4**). In

fact, Val307 is encoded by the normal canine gene. Therefore Ile307Val is likely to represent a polymorphism.

In addition, five SNPs were identified. The common 892A→C (Thr298Pro) and 2264A→G (Glu755Gly) polymorphisms have been previously reported (Kohl *et al.*, 2000). Silent polymorphisms are C→T at nucleotide 487 (Gln163Gln), G→A at nucleotide 1752 (Leu584Leu), and A→G at nucleotide 2214 (Glu738Glu).

In family 16 with a heterozygous *CNGA3* mutation (Arg436Trp) (**Table 3.5**), a single T→G nucleotide change was also found in the 5'UTR of the *CNGB3* gene, 36bp upstream of the ATG start codon (**Figure 3.7 A & B**). This is present in the heterozygous state in affected male subjects RM34 and RM36, inherited from their mother RM33, together with a second β -subunit variant (80A→G) that encodes an Asn27Ser substitution inherited from their father, RM35 (**Table 3.4; Figure 3.7 C & D**). Since a heterozygous *CNGA3* mutation had been already detected in this family, it is probable that both the 5'UTR variant and the Asn27Ser substitution are polymorphisms. However, in the absence of a second *CNGA3* mutation in this family, the possibility remains that the achromatopsia may originate from an interaction between the *CNGA3* and *CNGB3* mutations.

All control chromosomes were screened by direct sequencing.

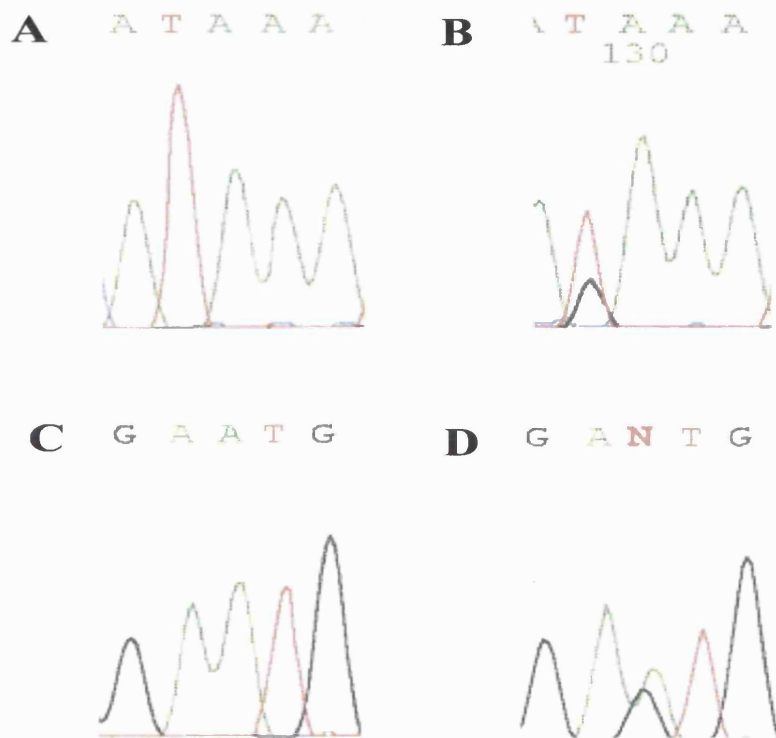


Figure 3.7

***CNGB3* 5'UTR and Exon 1 variants**

A - wt 5'UTR **B** - Ht 5'UTR variant

C - wt Exon 1 **D** - Ht Asn27Ser

The results of *CNGA3* screening performed by a colleague are shown in **Table 3.5**.

Following the exclusion of a mutation in both *CNGA3* and *CNGB3* in family 23, a novel homozygous frameshift mutation in *GNAT2* (c842_843insTCAG; M280fsX291) was identified (Aligianis *et al.*, 2002). This was undertaken in collaboration with Professor E. R. Maher and Dr. I. A. Aligianis of the University of Birmingham. The detailed phenotype in this family is described below in section 3.7.

Family/affected individuals		Mutation	Amino acid substitution
2 / RM5, RM6	Ht	667C→T	Arg223Trp
4 / RM11	Ht	734C→T	Thr245Met*
5 / RM12	Hm	1642G→A	Gly548Arg
7 / RM17	Hm	67C→T	Arg23Stop
8 / RM18	Hm	586C→T	Gln196Stop
9 / RM20	Ht	1482insC	Ile482fs
	Ht	1706G→A	Arg569His
10 / RM21	Hm	700C→T	Arg221Ser
13 / RM27	Hm	1641C→A	Phe547Leu
16 / RM34, RM36	Ht	1306C→T	Arg436Trp
18 / RM40	Hm	1641C→A	Phe547Leu

Table 3.5

***CNGA3* disease-causing mutations**

(*Substitution at non-conserved residue that is unlikely to be disease-associated)

3.5 DISCUSSION

Mutations in the genes *CNGA3* and *CNGB3* encoding the α - and β -subunits of cone photoreceptor CNG channels have been described in subjects with achromatopsia. These proteins are functionally important therefore in all three classes of human cones. Moreover, analysis of the homologous *CNGA3* knockout-mouse model shows complete absence of physiologically measurable cone function, a decrease in the number of cones in the retina, and morphological abnormalities of the remaining cones (Biel *et al.*, 1999).

Unlike previous studies which indicated that approximately 25% of patients with achromatopsia have alterations in *CNGA3* (Wissinger *et al.*, 2001) and 40-50% in *CNGB3* (Kohl *et al.*, 2000; Kohl *et al.*, 2001); an equal distribution of mutations across the two genes has been observed in this study, with 39% families with mutations in

CNGA3 (9 of 23 families) and 39% in *CNGB3* (9 of 23 families). In family 23 a homozygous frameshift mutation was subsequently identified in *GNAT2*.

No CNG-channel mutations were identified in four families (excluding family 23), although two of these had heterozygous substitutions (Thr245Met in *CNGA3* and Ile307Val in *CNGB3*) that are most likely not disease-associated since neither residue is conserved in other CNG receptors. However, final confirmation of the lack of disease-association will require a functional assay of the altered protein. Therefore, only 18% (4/22) of families were without a clear disease-causing mutation. This contrasts with the ~30% reported in previous studies. Patient ascertainment in our study has been very rigorous, and this may be the explanation for the higher percentage of mutation identification in one or other of the CNG channel protein genes in our study. The majority of families (16 of 23) are from one British clinical centre, Moorfields Eye Hospital, whereas previous studies have ascertained patients via multiple centres in the USA and Europe. Inclusion criteria may have been therefore less uniform such that other forms of cone dystrophy may have been included. Another possibility is that the population of our study is less heterogeneous. This seems less likely however as the two UK centres are in large multicultural cities and this is reflected by the fact that many subjects are not from a European background.

This study has identified two previously unreported *CNGB3* mutations, Phe525Asn (F525N) and Glu199fs. These two mutations add to the seven *CNGB3* mutations previously reported: 5 nonsense variants: Pro273fs, Thr383fs, Arg203stop, Glu366stop, Asp149fs; a single missense mutation, Ser435Phe (S435F); and a solitary putative splice-site defect (Kohl *et al.*, 2000; Sundin *et al.*, 2000; Rojas *et al.*, 2002). The third *CNGB3* mutation identified in our study, Thr383fs, was the most frequent mutation detected, being present in 8 of 23 families (35%), and represented ~80% of *CNGB3* mutant alleles;

a proportion that is in agreement with previous reports of Thr383fs constituting up to 84% of *CNGB3* mutant disease chromosomes (Kohl *et al.*, 2000; Kohl *et al.*, 2001).

The novel frameshift mutation, Glu199fs, is likely to be subject to nonsense mediated mRNA decay. However if translated, it would result in premature termination of translation and therefore severely truncated polypeptides lacking the following critical functional elements: the six transmembrane domains, the pore and cGMP-binding site (**Figure 3.6**). Therefore, Glu199fs is likely to represent a null allele.

The missense mutation, F525N, results in the substitution of a highly conserved amino acid (**Table 3.4**), and is located 19 amino acid residues upstream from the proposed cGMP-binding site. There are several plausible modes of pathogenicity for F525N. One possibility is that the region of the polypeptide within which F525N resides has a role in interacting with α -subunit C- or N-terminal intracellular domains in order to form stable channel complexes and that this contact is disrupted by the mutation. This type of interaction has been demonstrated in rod CNG-subunits, whereby the failure of interaction between the N-terminus of the β -subunit and the C-terminal region of the α -subunit, leads to lack of functional channels at the membrane surface (Trudeau and Zagotta, 2002a; Trudeau and Zagotta, 2002b). A second mechanism of action of F525N might involve reducing channel sensitivity to cGMP, thereby leading to inhibition of function. There is also a rod CNG-channel precedent for this mechanism; it has been shown that disruption of interaction between the N-terminus of the β -subunit and the C-terminus of the α -subunit (secondary to binding of Ca^{2+} , via calmodulin to the N-terminus), results in a reduction in sensitivity of the channel to cyclic nucleotides with consequent inhibition of function (Trudeau and Zagotta, 2002a).

To date, F525N is only the second missense mutation identified in *CNGB3*. The first being the missense mutation, Ser435Phe (S435F), believed to be the underlying cause of

the unique high incidence (5-10%) of achromatopsia in the Pingelapese people of the Eastern Caroline Islands in Micronesia (Brody *et al.*, 1970; Kohl *et al.*, 2000; Sundin *et al.*, 2000). S435F is located in the sixth transmembrane domain of the CNGB3 polypeptide (Figure 1.3). It has been recently reported that the S435F mutation, when co-expressed with human wild-type CNGA3 subunits in *Xenopus* oocytes, results in an increased affinity for cGMP, a decreased single channel conductance, and a decreased sensitivity to blockage by L-cis-diltiazem (Peng *et al.*, 2003b). In contrast, co-expression of mutant Thr383fs β -subunits with wild-type CNGA3 subunits produced channels with properties indistinguishable from homomeric CNGA3 channels, consistent therefore with the complete non-functioning of the truncated protein (Peng *et al.*, 2003b). This expression study suggests that achromatopsia may arise from either disturbance of cone cGMP-channel gating and permeation, or from the absence of functional CNGB3 subunits.

Homozygous *CNGB3* mutations were present in 7 families, whilst compound heterozygous mutations were found in one family. Only a single heterozygous mutation, Thr383fs, could be found in *CNGB3* in one family (family 14); the second mutation is either in an intron or promoter region that is outside the regions sequenced or in an as yet unidentified exon. It is also possible that a larger deletion might be present in the other allele that would not have been detected by our screening strategy; this later possibility could be assessed with Southern blot analysis.

An autosomal recessive canine cone degeneration (cd) that occurs naturally in the Alaskan Malamute and German Shorthaired Pointer breeds is phenotypically similar to human achromatopsia. Canine *CNGB3* mutations have been identified in both of these breeds, thereby establishing these cd-affected dogs as the only naturally-occurring large animal model of human achromatopsia (Sidjanin *et al.*, 2002). Such models provide a

valuable system for exploring disease mechanisms and evaluating the potential for gene therapy.

3.6 CONCLUSIONS

In a panel of carefully ascertained patients, mutations in *CNGA3* and *CNGB3* are found to be causative in ~80% of families (Johnson[†], Michaelides[†] *et al.*, 2004). Unlike previous studies, a similar incidence of mutations was identified in both genes. Genotype-phenotype correlations on the basis of detailed colour vision testing could not be probed. This was due to the fact that none of the panel of patients with *CNGA3/CNGB3* mutations had significant residual colour vision. Therefore, their colour vision phenotype was effectively identical, thereby precluding any correlation assessment.

The three genes described to date associated with achromatopsia, *CNGA3*, *CNGB3*, and *GNAT2* encode proteins in the cone phototransduction cascade. It is therefore reasonable to propose that further cone-specific intermediates involved in phototransduction represent good candidates, although these will represent uncommon causes of achromatopsia, since only 4 families (17%) in our study did not have mutations in the three currently identified genes. The candidates include the genes encoding the cone specific β - and γ -transducin subunits (Peng *et al.*, 1992; Ong *et al.*, 1995; Ong *et al.*, 1997) and cone phosphodiesterase α' - and γ -subunits (Piriev *et al.*, 1995; Feshchenko *et al.*, 1996; Shimizu-Matsumoto *et al.*, 1996). It is of interest that immunological studies of the canine *cd*-affected retina have demonstrated a specific absence or delocalisation of β - and γ - cone-specific transducin subunits from the outer segments of pre-degenerate cone photoreceptors. However, genes for both subunit proteins have been excluded as canine *cd* genes (Akhmedov *et al.*, 1997; Akhmedov *et al.*, 1998). Nevertheless, these

phototransduction proteins remain reasonable candidates to be screened in individuals not found to have mutations in the three genes already described.

Mutations in rod-specific *CNGA1* and *CNGB1* result in moderate to severe retinitis pigmentosa, a progressive retinal dystrophy (Dryja *et al.*, 1995; Bareil *et al.*, 2001); whilst to date neither *CNGA1* nor *CNGB1* mutants have been described in association with stationary disorders. Missense mutations in *CNGA3* have been described in two individuals with cone-rod dystrophy and in a single individual with a progressive cone dystrophy phenotype (Wissinger *et al.*, 2001). We have now also demonstrated mutations in *CNGB3* in a consanguineous family with progressive cone dystrophy (Michaelides *et al.*, 2004a).

3.7 GNAT2 PHENOTYPE

In Family 23 of our panel, no mutations were identified in either *CNGA3* or *CNGB3*. This family was a large consanguineous Pakistani family and was therefore suitable for a genome-wide linkage screen of microsatellite markers to identify regions of homozygosity/autozygosity. This study was undertaken in collaboration with Professor E. R. Maher and Dr. I. A. Aligianis of the University of Birmingham. Significant linkage to a 16cM autozygous region between markers D1S485 and D1S534 on chromosome 1p13 was established. *GNAT2*, the gene encoding cone-specific α -transducin, was identified as a positional candidate in this interval. Screening of this gene by direct sequence analysis demonstrated a frameshift mutation (c842_843insTCAG; M280fsX291) that segregated with disease (Aligianis *et al.*, 2002). Kohl *et al.* (2002) have published similar findings, of other nonsense mutations in *GNAT2*, in five independent families with achromatopsia.

A detailed description of the phenotype associated with *GNAT2* inactivation has not been previously reported. Therefore, the phenotype of our large consanguineous Pakistani family (panel family 23), with a novel frameshift mutation in *GNAT2*, has been reviewed (Michaelides *et al.*, 2003a).

3.7.1 Patients and methods

Five affected members of a three-generation, consanguineous Pakistani family were assessed (**Figure 3.8**).

A full medical history was taken and an ophthalmological examination performed. Examined subjects also underwent colour fundus photography, fundus autofluorescence imaging and a full electrophysiological assessment which included S-cone ERGs using a previously described protocol (Arden *et al.*, 1999).

Detailed colour vision testing (section 1.3.4.1) included the use of HRR and Sloan achromatopsia plates, PV-16, the enlarged M-R Minimal test and a computerised colour vision test (P4) designed for subjects with low vision (section 1.3.4.1.4). The PV-16 and the enlarged M-R test were used in order to detect any residual colour discrimination that might be present in patients with low vision: the coloured discs of the PV-16 were 33 mm in diameter and those of the enlarged M-R test were 26 mm in diameter (corresponding to visual angles of 3.8 and 3.3 deg at a viewing distance of 500 mm).

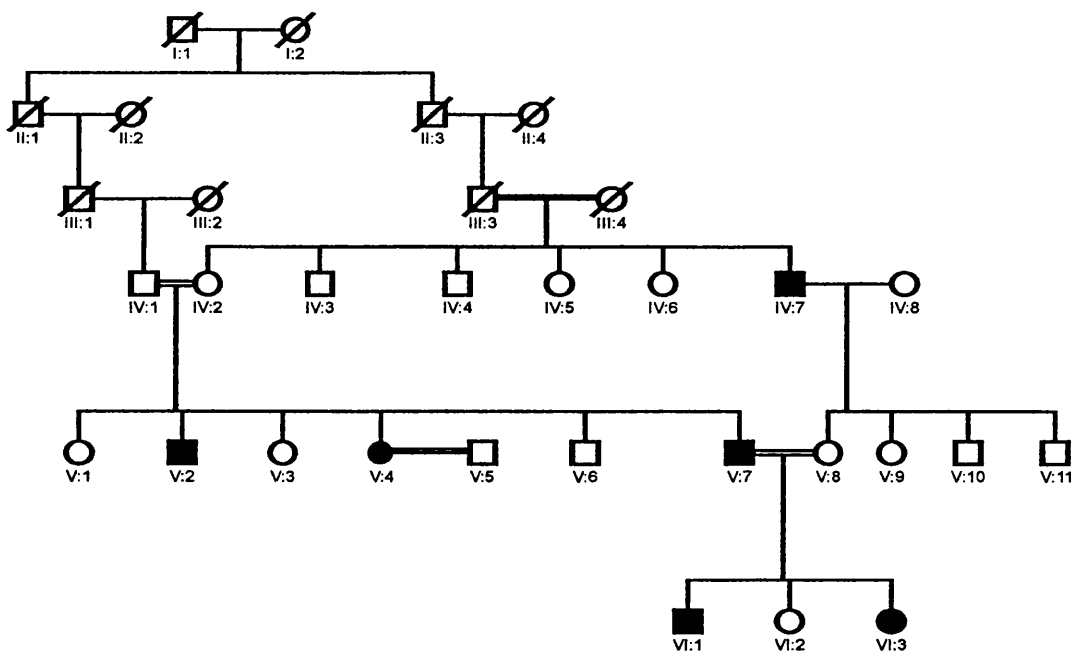


Figure 3.8
GNAT2 pedigree

3.7.2 Results

All five patients had a history of nystagmus from infancy, mild photophobia, defective colour vision, and poor visual acuity (6/60 to CF). They all described improved vision in mesopic conditions. Examination of the anterior segment was unremarkable, except for one individual (VI:3) who had a unilateral congenital cataract. Fundus examination revealed a mildly abnormal foveal appearance but without frank atrophy or pigmentation (Figure 3.9). Peripheral retinal examination was normal in all subjects.

ERG testing showed absent cone responses to 30Hz flicker, small responses to short wavelength stimulation, and normal rod-specific ERGs, but mildly subnormal maximal

response a-wave amplitudes (**Figure 3.10**). Autofluorescence imaging was normal in all individuals. Clinical findings are summarised in **Table 3.6**.

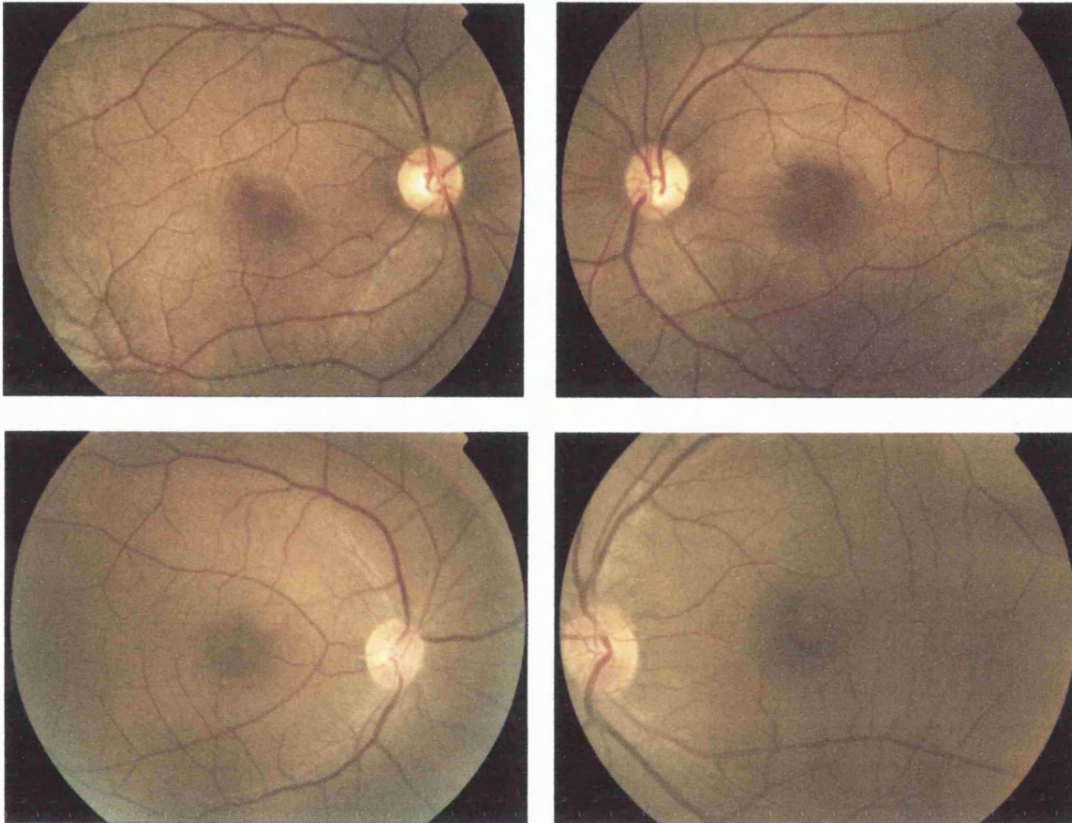


Figure 3.9
Typical fundi of GNAT2 family

Two older individuals (**V:2** and **V:7**) described a gradual deterioration of vision. Visual acuity in **V:7** was 6/36 in both eyes when he first presented thirty years ago, whilst his current best corrected acuity was CF. His brother **V:2**, also showed evidence of deterioration of visual acuity from 6/60 in both eyes documented 10 years ago, to CF at present. Both subjects have more prominent horizontal pendular nystagmus than other affected family members.

All five patients had abnormal colour vision. At the Nagel anomaloscope all five patients exhibited a scotopic spectral sensitivity. Four patients displayed a scotopic

pattern of arrangement on PV-16. One patient, **V:7**, unlike a typical patient with complete achromatopsia, produced only one major transposition on the PV-16 (**Figure 3.11**). Rudimentary colour discrimination was also detected in three individuals on testing with the M-R minimal test, with variable ability to identify the most saturated chip along the deutan and/or tritan axes. Further evidence of residual colour vision was provided by the colour discrimination ellipses produced on computerised colour vision testing. The other two individuals, **V:2** and **V:4**, displayed no residual colour vision and displayed typical achromatic matches on Sloan plates.

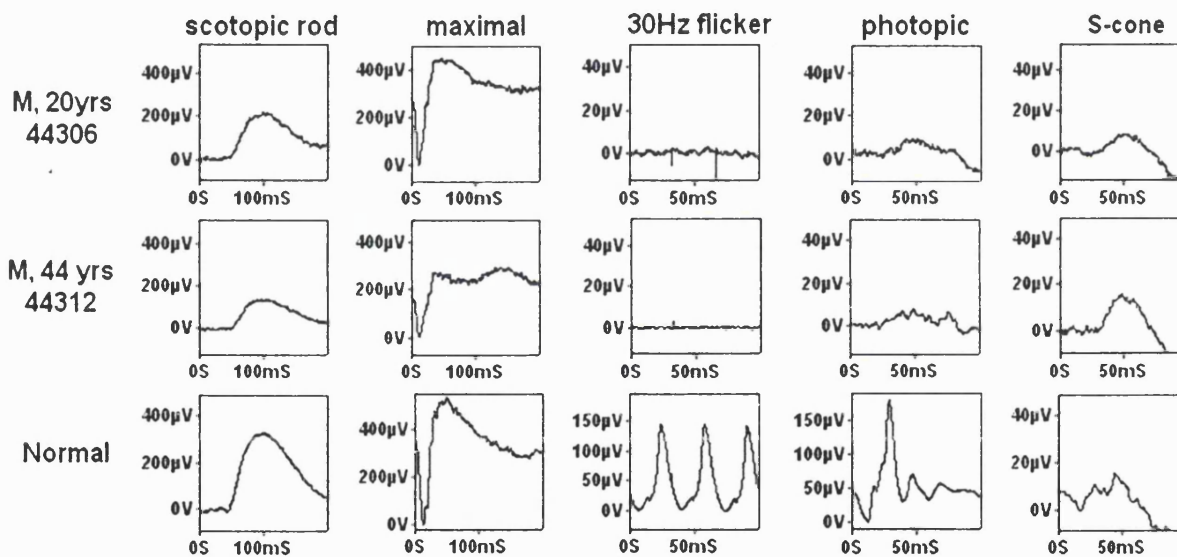


Figure 3.10

Electrophysiological data from a father (V:7) and son (VI:1).

Both patients have normal rod-specific ERGs. Flicker ERG is undetectable in both patients, but there is some very low amplitude activity with single flash stimulation. S-cone specific stimulation, using a blue light superimposed on an orange background (Arden et al., 1999), suggests some preservation of mechanisms sensitive to short wavelengths. Note the presence of an earlier peak at ~30ms in the normal, absent in the two patients, which reflects activity from L- /M- cone systems.

Patient	Age	VA OD OS	Refraction	Horizontal pendular nystagmus	ERG	Fundus	M-R Colour Vision Test
V:2	35	OD: CF OS: CF	-3.5/+3.0 x 30 -4.0/+3.0 x 160	Prominent	Absent 30Hz cone responses; Normal rod- specific responses	Abnormal foveal appearance	P(no)D(no)T(no) P(no)D(no)T(no)
V:4	41	OD: 6/60 OS: 6/60	-2.0/+2.0x110 -2.5/+1.5 x 70	Absent	Absent 30Hz cone responses; Normal rod- specific responses	Abnormal foveal appearance	P(no)D(no)T(no) P(no)D(no)T(no)
V:7	44	OD: CF OS: CF	-2.0/+2.0 x135 -1.5/+1.5 x 45	Prominent	Absent 30Hz cone responses; Normal rod- specific responses	Abnormal foveal appearance	P(no)D(7)T(5) P(no)D(6)T(5)
VI:1	20	OD: 6/60 OS: 6/60	+1.5/+1.5x110 +1.0/+2.0 x 80	Absent	Absent 30Hz cone responses; Normal rod- specific responses	Abnormal foveal appearance	P(no)D(7)T(4) P(no)D(no)T(5)
VI:3	19	OD: CF OS: 6/60	Balance -2.0/+3.0 x 75	Minimal	Absent 30Hz cone responses; Normal rod- specific responses	Abnormal foveal appearance	NA P(no)D(6)T(5)

Table 3.6

Summary of clinical findings in *GNAT2* pedigree

M-R = Mollon-Reffin test. The letters give the axis P-protan, D-deutan, and T-tritan.

The number enclosed in brackets gives the least saturated chip that could be discriminated

from the greys. VI:3 has a right-sided congenital cataract.

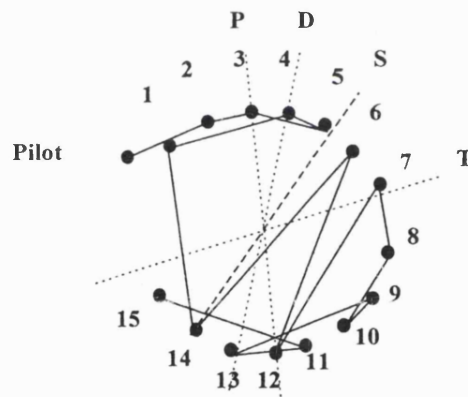
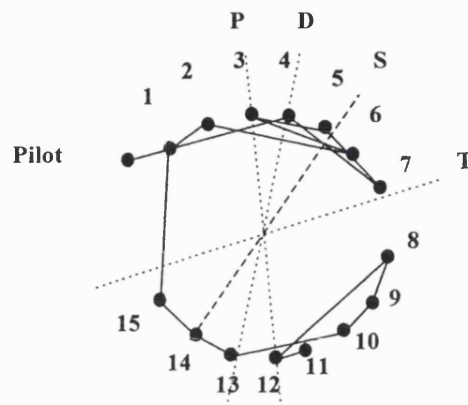
Figure 3.11

Enlarged Farnsworth D-15 (PV-16)

Above: PV-16 plot of patient **V:7** in our family. Only one major transposition is seen; providing further evidence of residual colour vision.

Below: PV-16 plot with a more typical scotopic arrangement made by a patient with complete achromatopsia for comparison.

P = Protan; **D** = Deutan; **T** = Tritan;
S = Scotopic



3.7.3 Discussion

The phenotype is characterised by mild photophobia, nystagmus, abnormal colour vision and poor visual acuity (6/36 to CF). On detailed colour vision testing, residual colour discrimination was detected in three individuals. ERGs revealed absent cone responses, with normal rod-specific ERGs. We were able to record S-cone ERG responses in all patients. In two older subjects, a worsening of visual acuity with age has been documented, although we have no definitive evidence of progressive deterioration in retinal function.

The residual S-cone function detected in this *GNAT2*-associated phenotype is intriguing. The evidence that *GNAT2* is expressed in all three cone types comes from the immunohistochemical demonstration that an antibody raised against cone α -transducin peptides cross-reacts with all three classes of cone photoreceptor in the human retina (Lerea *et al.*, 1989). This does not however definitively rule out the possibility that S-cones may express an alternative form of α -transducin, since identical epitopes may be present on both forms. It may also be significant that Southern blot analysis of human genomic DNA indicated that there may be more than one cone α -transducin gene (Lerea *et al.*, 1989). Therefore, it remains a possibility that *GNAT2* is not expressed in S-cones, and that the residual S-cone function detected in our family arises from the use of another distinct form of α -transducin. The residual tritan colour discrimination detected may be accounted for by a comparison between quantum catches in the remaining functional S-cones and rod photoreceptors, in the manner proposed to underlie colour discrimination detected in blue cone monochromatism (Reitner *et al.*, 1991). This phenotype is similar therefore to the incomplete form of achromatopsia in terms of residual colour vision.

However, unlike either incomplete or complete achromatopsia, we have been able to record S-cone ERG responses in our patients and, in two older subjects, a worsening of

visual acuity with age has been documented. There appears to be only one case report of achromatopsia associated with progressive retinal degeneration, in the form of mid-peripheral retinal pigmentation and concentric constriction of peripheral visual fields (Eksandh *et al.*, 2002). It was also reported that a few of the younger subjects in that achromatopsia series had small residual cone responses on ERG (Eksandh *et al.*, 2002). Taken together therefore, these findings may represent evidence that progression in retinal dysfunction may be present in at least some individuals with achromatopsia, but no natural history studies are available to corroborate this.

Transducin, a three subunit guanine nucleotide binding protein, acts as a link between light-activated photopigment and the activation of cGMP-phosphodiesterase (section 1.1.1.1). cGMP-phosphodiesterase lowers the concentration of cGMP in the photoreceptor which results in closure of cGMP-gated cation channels and consequent photoreceptor hyperpolarization. Thus, the finding of a germline *GNAT2* mutation in a family with cone dystrophy is consistent with the known function of the *GNAT2* product. Furthermore, a missense mutation, Gly38Asp, in human rod-specific α -transducin, which is 83% homologous to cone α -transducin (Fong, 1992; Morris and Fong, 1993), has been shown to be associated with the Nougaret form of congenital stationary night blindness (Dryja *et al.*, 1996).

The frameshift mutation identified in our family results in a truncated protein that lacks 63 amino acids from the C-terminus. All the *GNAT2* mutations identified by Kohl *et al.* (2002) would also result in premature termination of translation and in protein-truncation at the C-terminus. This region contains important functional domains of α -transducin which have been shown to interact with rhodopsin (Cai *et al.*, 2001) and phosphodiesterase γ -subunit (Liu *et al.*, 1996). However, if this mutation were to lead to a complete lack of α -transducin function, it is difficult to explain the residual colour vision

along deutan and tritan axes and the S-cone ERGs recorded in these individuals, if these are entirely cone-mediated mechanisms. In addition to the possibility already discussed of an alternate S-cone α -transducin, it is also possible that the mutation results in a protein which although severely reduced in efficacy, may still show some residual α -transducin function. Alternatively, there may be some redundancy within the cone phototransduction pathway that allows a level of continued function despite sub-optimal or absent function of one of the components of the cascade.

3.7.4 Conclusions

The phenotype associated with mutation in the α -subunit of cone-specific transducin is characterised by a cone dystrophy with an infantile onset, a deterioration of visual acuity with time in older individuals, and evidence of residual colour discrimination and S-cone function. In this family the disorder may be better described as an early-onset progressive cone dystrophy; although electrophysiological or psychophysical evidence would be required prior to being able to definitively describe this disorder as progressive.

Further detailed assessment of other families with *GNAT2* mutations will help to establish the phenotypic variability associated with *GNAT2* variants.

CHAPTER 4

BLUE CONE MONOCHROMATISM

4.1 INTRODUCTION

In order to derive colour vision, the normal human visual system compares the rate of quantum catches in three classes of cone; the short (S or blue) wavelength sensitive, middle (M or green) wavelength sensitive and long (L or red) wavelength sensitive cones, which are maximally sensitive to light at 430 nm, 535 nm, and 565 nm respectively. This triad of cone types provides the physiological substrate for trichromacy.

Each cone class contains its own visual pigment composed of an opsin protein linked by a Schiff base to the chromophore retinal. In humans, the L- and M-opsins are encoded by genes on the X chromosome, and the S-opsin by a gene located on chromosome 7 (Nathans *et al.*, 1986a; Nathans *et al.*, 1986b). There are three types of inherited colour vision deficiency in which vision is dichromatic; each type corresponds to a selective defect in one of the three receptor mechanisms. Protanopia and deuteranopia are characterised by defects of the red- and green-sensitive mechanisms respectively. They are among the common X-linked disorders of colour vision whose association with alterations in the visual pigment gene cluster at Xq28 identified those genes as encoding the red- and green-sensitive visual pigments (Nathans *et al.*, 1986a; Nathans *et al.*, 1986b). The wild-type arrangement of the L- and M-opsin genes consists of a head-to-tail array of two or more repeat units of 39kb on chromosome Xq28 that are 98% identical at the DNA level (Nathans *et al.*, 1986a). This high level of identity would appear to predispose the L- and M-opsin genes to unequal inter- and intragenic recombination. Transcriptional regulation of the L and M genes is controlled by an upstream locus control region (LCR) (Nathans *et al.*, 1989). In contrast, tritanopia is an autosomal dominant disorder that is characterised by a selective defect of the blue-sensitive mechanism and is due to dominant mutations in the S-cone opsin gene.

Blue cone (S-cone) monochromatism (BCM), or X-linked incomplete achromatopsia, is a rare congenital stationary cone dysfunction syndrome, affecting less than 1 in 100,000 individuals, characterised by absence of L- and M-cone function (section 1.1.2.3.1). As in achromatopsia (Chapter 3), BCM typically presents with reduced visual acuity, pendular nystagmus and photophobia. Visual acuity is of the order of 6/24 to 6/60. BCM is distinguished from achromatopsia via psychophysical or electrophysiological testing. The 30Hz cone ERG is undetectable in both disorders. However in contrast to achromatopsia, in BCM the single flash photopic ERG is often recordable, albeit small and late, and the S-cone ERG is well preserved (Gouras and MacKay, 1990) (**Figure 4.1**). BCM patients have high Farnsworth-Munsell 100-Hue scores, but have fewer errors in the vertical (tritan) axis when compared with achromats. S-cone monochromats also have better tritan discrimination when assessed with plate tests such as the Berson colour plates (Berson *et al.*, 1983; Haegerstrom-Portnoy *et al.*, 1996).

Mutations in the L- and M-opsin gene array that result in the lack of functional L- and M- pigments, and thus inactivate the corresponding cones, have been identified in the majority of BCM cases studied (Nathans *et al.*, 1989; Nathans *et al.*, 1993) (section 1.1.2.3.2). The mutations identified in the L- and M-opsin gene array fall into two classes. In the first class, a normal L- and M-opsin gene array is inactivated by a deletion in the LCR, located upstream of the L-opsin gene (Wang *et al.*, 1992). In the second class of mutations, the LCR is preserved but changes within the L- and M- pigment gene array lead to loss of functional pigment production. The most common genotype in this class consists of a single inactivated L/M hybrid gene. The first step in this second mechanism is thought to be unequal crossing over that reduces the number of genes in the array to one, followed by a mutation that inactivates the remaining gene. A frequent inactivating mutation that has been described is the thymine-to-cytosine transition at nucleotide

position 648, which results in a cysteine-to-arginine substitution at codon 203 (Nathans *et al.*, 1989; Nathans *et al.*, 1993).

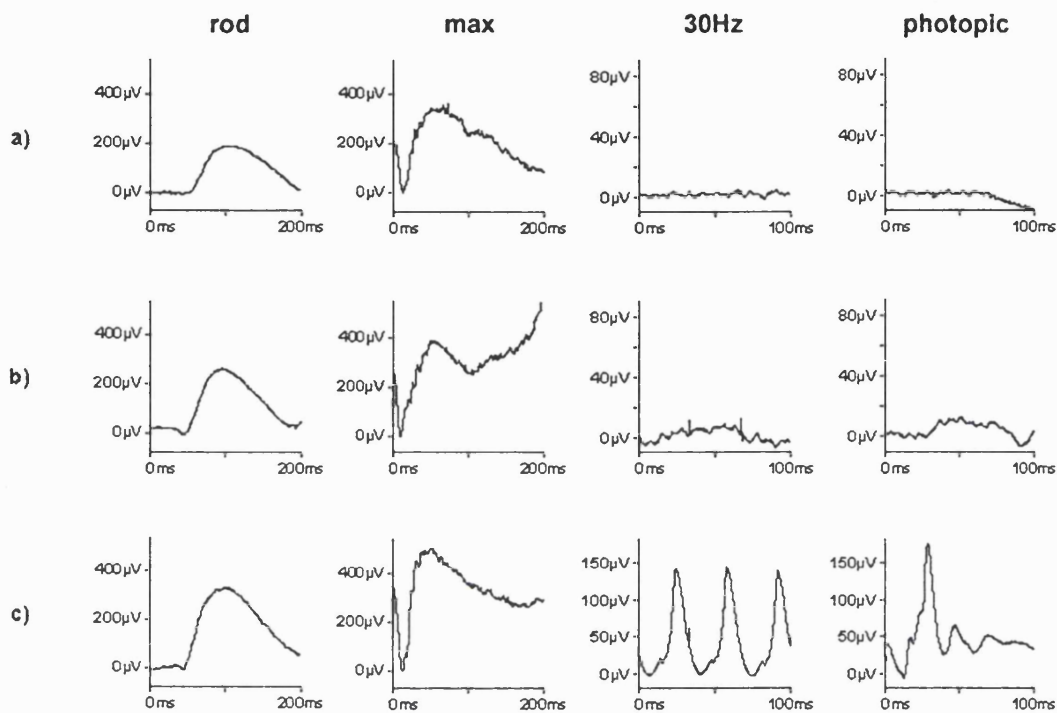


Figure 4.1

Achromatopsia and BCM ERGs

ERGs from a patient with complete achromatopsia (a), a patient with BCM (S-cone monochromatism) (b) and a representative normal (c).

The rod-specific and maximal ERGs show no definite abnormality in both cone dysfunction syndromes. The 30Hz flicker ERG is undetectable in both, but the single flash photopic (cone) ERG is small and late, typical of S-cone origins. The scale for the photopic ERGs in the two patients differs from that in the normal subject better to illustrate the low amplitude photopic single flash response in the S-cone monochromat.

4.2 AIMS

To perform a detailed clinical and psychophysical assessment of members of four British families affected with BCM. The molecular basis of BCM in three of these families was investigated in a parallel study by a colleague; with the aim of determining whether a genotype-phenotype correlation might be feasible.

4.3 METHODS

Affected and unaffected members of four families (Families A to D) with presumed BCM were examined clinically and underwent electrophysiological and detailed psychophysical testing.

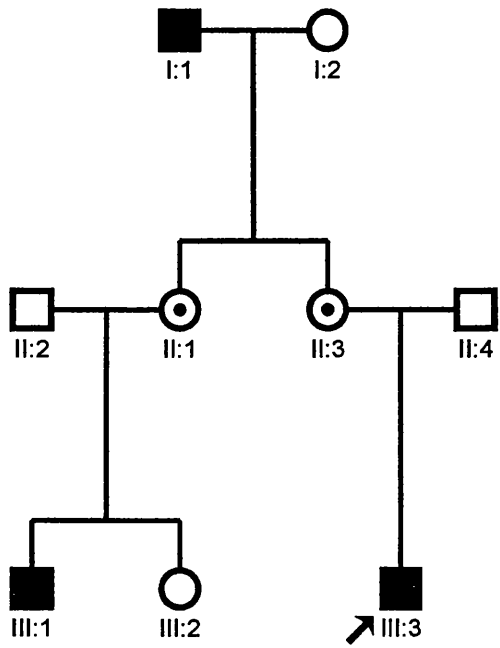
Subsequently blood samples were taken for DNA extraction (Families A, B & C). The strategy for molecular analysis was to amplify the coding regions of the L- and M-cone opsin genes and the upstream LCR by polymerase chain reaction and to examine these fragments for mutations by direct sequencing. The molecular genetic investigation was undertaken in a parallel study by a colleague.

4.3.1 *Patients and clinical assessment*

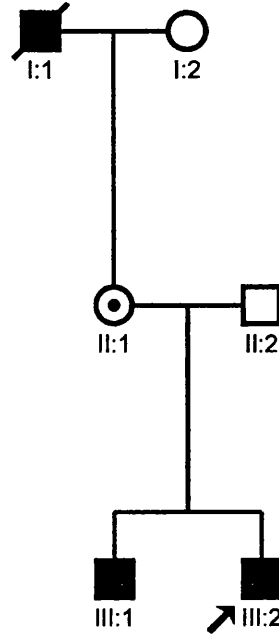
Affected and unaffected members of four families with presumed BCM were assessed (**Figure 4.2**).

A full medical and ophthalmic history was taken and an ophthalmological examination performed in all assessed family members. Affected individuals had an ERG performed and colour fundus photography. Adults had an ERG that conformed to the ISCEV standard (Marmor *et al.*, 1998), but the children had a modified protocol using skin electrodes.

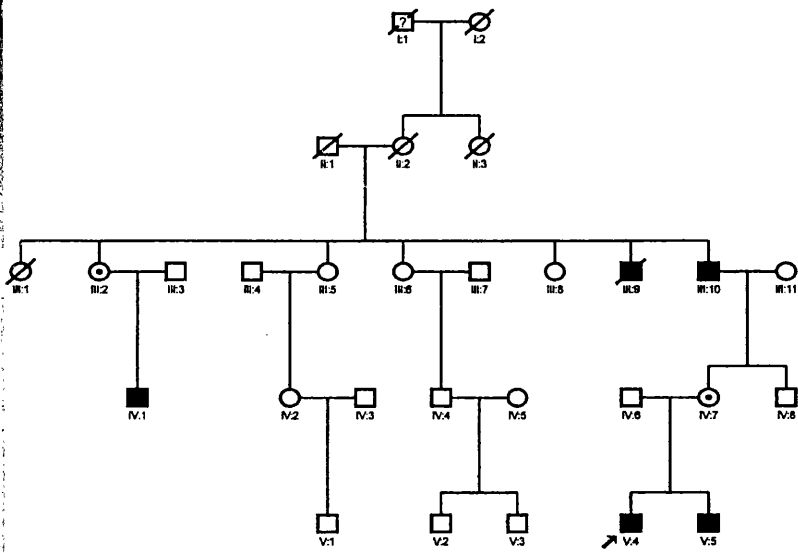
Detailed colour vision testing (section 1.3.4.1) included the use of HRR plates and SPP2 plates for acquired colour deficiency, Farnsworth D-15 and PV-16, the standard and enlarged Mollon-Reffin (M-R) Minimal test (Mollon *et al.*, 1991), a computerised colour vision test (Mollon *et al.*, 1989; Regan *et al.*, 1994) and anomaloscopy. All colour vision testing was performed at Professor J. D. Mollon's laboratory at the Department of Experimental Psychology, University of Cambridge.



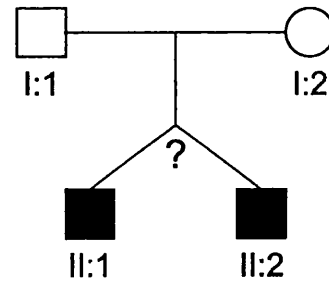
Family A



Family B



Family C



Family D

Figure 4.2
BCM families

4.4 RESULTS

4.4.1 *Phenotype*

Affected males were found to have had pendular nystagmus, photophobia and reduced vision from soon after birth. Visual acuity ranged from 6/24 to 6/60. Nystagmus was reported to become less prominent with age; indeed on examination it was absent in the older affected patients. Affected subjects had absent 30Hz cone responses with normal rod function.

Protan-like D-15 arrangements were detected in our group of patients; a finding previously reported in patients with BCM (Weis and Biersdorf, 1989). In addition, we were able to demonstrate that the M-R minimal test is a useful colour discrimination test to aid in the diagnosis of BCM. Importantly, the M-R test was also found to be both quick and easy to perform. Affected males were shown to fail on the protan and deutan axes, but retained good discrimination on the tritan axis of the M-R test. This is compelling evidence for residual colour vision in BCM. This residual tritan discrimination was also readily detected with HRR plates. In two families psychophysical testing demonstrated evidence for progression of disease (Michaelides *et al.*, 2004e).

FAMILY A

An X-linked mode of inheritance appears most likely (**Figure 4.2**).

III:3 This 7-year-old boy (proband) was originally seen at one year of age. He was found to have horizontal pendular nystagmus, normal fundi and clear media. A family history of nystagmus, photophobia and 'colour-blindness' affecting males of the family, including his grandfather (**I:1**) and male cousin (**III:1**), was established. ERG testing revealed absent cone responses but normal rod responses.

He had a visual acuity of 3/36 in each eye with his myopic correction. Psychophysical testing on the M-R test and HRR plates revealed reasonable discrimination only along the tritan axis. On computerised testing his colour discrimination ellipses were oriented along the angle expected of someone making colour discriminations based on a comparison of quantum catches in the rods and S-cones (Mollon *et al.*, 1989; Regan *et al.*, 1994; Simunovic, 1999).

I:1 This 60-year-old man was found to have a visual acuity of 6/36 in the right eye and 6/60 in the left. He was found to have clear lenses and mild macular RPE changes. As a child he had obvious nystagmus, but this had improved throughout life, to the point that it was not at all noticeable. He felt that his vision had continued to slowly deteriorate throughout life. Cone ERG responses was absent but rod responses were normal. On the basis of his results on the HRR plates, the D-15/PV-16, the M-R minimal test and anomaloscopy, it was concluded that he had no residual colour vision.

III:1 His 12-year-old grandson had a visual acuity of 6/60 in the right eye and 6/36 in the left. He had clear media and normal fundi. He displayed evidence of residual colour discrimination; demonstrating reasonable discrimination along the tritan line of M-R test and also on the SPP2 tritan plates. He displayed a protan ordering of the D-15. On computerised testing his ellipses were oriented along the angle that is expected for colour discriminations based solely upon a comparison of quantum catches in the rods and the S-cones.

Patients **II:2**, **II:3** and **II:4** were asymptomatic and on detailed psychophysical testing were found to have normal colour vision. The father of patients **III:1** and **III:2** was not available for psychophysical testing.

A consistent psychophysical hypothesis from these observations would be that the proband **III:3**, and **III:1** have inherited from their maternal grandfather, **I:1**, via their mothers, an X-chromosome with an altered opsin array that has led to BCM. Since **III:3** and **III:1** both have some residual colour discrimination and their grandfather has none, it would appear that their condition is not stationary. **III:3** and **III:1** can be labelled blue cone monochromats, whereas their grandfather behaves as a rod monochromat, presumably as a result of continued S-cone loss. The lack of colour vision seen in the grandfather is highly unlikely to be due to lenticular changes since his lenses were found to be clear.

FAMILY B

An X-linked inheritance pattern appears most likely (**Figure 4.2**).

III:2 This 12-year-old boy (proband) had pendular nystagmus, poor visual acuity (6/24 in both eyes) and myopia. Ocular media were clear with mild myopic fundus changes (**Figure 4.3**). ERG revealed absent cone but normal rod responses.

On psychophysical testing, anomaloscopy and Sloan's test for achromatopsia suggested a rod dominated spectral sensitivity function. On the D-15, he showed the protan-like pattern reported for BCM by Weis and Biersdorf (1989). On the computer test, he failed completely on the protan and deutan lines, but scored nearly normally along the tritan line, which modulates the blue cones. In addition, his ellipses were well aligned to the theoretical S-cone/rod confusion axis, consistent with the mechanism

whereby colour discriminations are based upon a comparison between rod and S-cone quantum catches. Exactly the same pattern was exhibited on the M-R test: he could not find saturated protan and deutan probes amongst the grey distractors but could find the least saturated tritan cap. On the SPP2 plates for acquired colour deficiencies he passed the plates that are failed by those with purely scotopic vision (rod monochromats; RM).



Figure 4.3
Fundi in BCM

Tilted pale optic discs and myopic fundus changes in patient **III:2** of family B

III:1 This 14-year-old brother of the proband also presented with pendular nystagmus, poor visual acuity (6/24 in the right eye and 6/36 in the left), myopia and photophobia. Ocular media were clear with myopic fundus changes. ERG revealed absent cone responses but normal rod function. He showed reasonable discrimination only along the tritan axis on HRR testing. He declined further psychophysical testing.

II:1 The 50-year-old mother of **III:1** and **III:2** was asymptomatic. ERG and colour vision testing was normal.

I:1 Maternal grandfather of the propositus was said to have had poor eyesight since birth and to have always had great problems with colour vision. The grandfather had an elder brother who had also worn glasses and had suffered with poor vision since infancy. Both were deceased at the time of investigation.

FAMILY C

An X-linked mode of inheritance appears most likely (**Figure 4.2**).

V:4 This 7-year-old boy (proband) originally presented as an infant with nystagmus and photophobia. His current visual acuity was recorded at 6/24 in both eyes. He had clear ocular media with normal fundi. He had a family history of nystagmus, poor visual acuity and colour vision affecting males of the family including his grandfather (**III:10**) and uncle (**IV:1**). ERG revealed absent cone responses but normal rod function.

On the D-15 he showed confusions characteristic of congenital red-green deficiency or BCM rather than a scotopic axis (RM). On the M-R minimal test he failed the protan and deutan axes but discriminated on the tritan axis. On the HRR plates he passed all the tritan plates and failed all the protan/deutan plates.

V:5 This 6-year-old boy had nystagmus and a visual acuity of 6/36 in the right eye and 6/24 in the left. He had clear ocular media with normal fundi. On the M-R test he failed the protan and deutan axes but discriminated well on the tritan axis. Computerised testing corroborated these findings; he failed completely on the deutan line and discriminated very poorly on the protan line, which hold almost constant the blue cone signal, but scored almost normally along the tritan line, which modulates the blue cones.

III:10 This 70-year-old grandfather of **V:4 & V:5** has had poor vision and nystagmus since childhood. The nystagmus had become less prominent over time. He felt that his vision had gradually deteriorated since childhood. He had early lens opacities with minimal yellowing of the lens and mild macular RPE changes. ERG revealed absent cone responses and normal rod function.

On detailed psychophysical testing there was little evidence of any residual colour vision. On anomaloscopy he displayed the classical brightness matching function of an achromat. On the D-15 his responses were anarchic. He failed all plates on the SPP2 series. On the M-R test he failed the protan and deutan axes completely but did show some residual discrimination on the tritan axis, detecting the most saturated cap.

IV:1 This 50-year-old man was found to have a visual acuity of 6/36 in both eyes, with no nystagmus. He complained of poor vision since childhood and that he had always had trouble with colour vision. He had clear lenses and normal fundi. Little residual colour vision could be detected. On the M-R test he failed completely on all three axes with both eyes. On anomaloscopy he behaved like an achromat.

IV:6 & IV:7 were both asymptomatic and had entirely full colour vision on detailed testing.

Since the grandfather (**III:10**), uncle (**IV:1**), and two grandchildren (**V:4 & V:5**) share the same genotype (section 4.4.2), the condition therefore appears to be progressive. The children show a residual colour discrimination that is lacking in both older men. There is convincing psychophysical evidence to suggest that the children have functional S-cones. The loss of residual colour vision seen in the two older men in this family is highly

unlikely to be due to lenticular changes alone, since the lenses were found to be either clear (IV:1) or only minimally yellow (III:10). A markedly yellow lens would be required to result in any significant loss of colour vision and such yellowing would be unlikely to result in the degree of loss of tritan function seen in this family.

FAMILY D

The inheritance pattern cannot be established; it was not possible to extend the pedigree since the brothers were adopted (Figure 4.2).

II:1 This 11-year-old boy had horizontal pendular nystagmus, poor visual acuity (6/36 in both eyes) and myopia. Ocular media were clear with normal fundi. ERG revealed absent 30Hz cone responses but normal rod responses. However, a significant S-cone ERG response could be recorded.

He identified all the tritan plates on the HRR correctly whilst failing all the protan/deutan plates. The M-R test revealed excellent tritan function, being able to identify the least saturated chip with either eye, with variable ability to identify the most saturated protan or deutan chip. On the D-15 (PV-16), he showed a protan-like arrangement with either eye. On the computer test, his ellipses were well aligned to the theoretical S-cone/rod confusion axis, consistent with the mechanism whereby colour discriminations are based upon a comparison between rod and S-cone quantum catches.

II:2 This 11-year-old twin brother of the proband also presented with pendular nystagmus, poor visual acuity (6/24 in both eyes), myopia and photophobia. Ocular media were clear with normal fundi. ERG revealed absent 30Hz cone responses but normal rod responses. However, a significant S-cone ERG response could be recorded.

He showed good discrimination only along the tritan axis on HRR testing. The M-R test also revealed excellent tritan function, being able to identify the least saturated chip

with his left eye and second least with his right eye. Discrimination along the protan and deutan axes of the M-R test was markedly reduced being unable to recognize the most saturated protan chip, with variable ability to identify the more saturated deutan chips. On the D-15 (PV-16), he showed a protan-like arrangement when tested with either eye. On the computer test, his ellipses were also well aligned to the theoretical S-cone/rod confusion axis.

4.4.2 Genotype

A set of PCR primer pairs was used to amplify the X-linked L- and M-opsin genes that underlie the L and M pigments and the LCR that controls the opsin gene array (**Table 4.1**). The identification of L- or M-opsin gene depends on a number of sequence differences that are confined to exons 2-5 (**Table 4.2**). Sequence analysis was carried out by a colleague in a parallel study.

Family A Sequence analysis demonstrated the presence of a single M-opsin gene in the array of the affected subjects. However, no further alterations of this gene were identified. Examination of the entire LCR revealed an unaltered sequence. The mutational basis of disease in this family remains uncertain.

Family B Sequence representing only the L gene was present for exons 2 to 4, while for exon 5 only sequence of the M gene was observed. This is consistent with the presence in affected members of family B of only a single 5'-L/M-3' hybrid gene in their opsin array. Moreover, alignment of exon 4 of the hybrid gene in these individuals with wild-type exon 4 sequence showed that this opsin gene carried the previously reported T→C nucleotide alteration which encodes the Cys203Arg substitution (**Figure 4.4**).

Sequence analysis of obligate carriers demonstrated that both L- and M-opsin genes are present in the opsin gene array and that the T→C transition in exon 4 is also carried in an L opsin gene in these individuals.

Family C Affected individuals of family C also carry the Cys203Arg mutation within a single 5'-L/M-3' hybrid gene in the array. In this case, the cross-over between the L and M genes which is required for generation of the hybrid gene, occurred within exon 3 (Figure 4.4).

Primer Name	5'-3' Sequence	T _a ⁰ C
LCR1+	ggcaaatggccaaatggt	49
LCR1-	ccatgctatttgaagcc	
L/M.Ex1F	ggtgggaggaggaggtctaa	64
L/M.Ex1R	ggtggccccagtcagcc	
L/M.Ex2F	ggtatagacaggcggtgctg	60
L/M.Ex2R	gtgaatgagtgtttccgcc	
L/M.Ex3F	gtctaagcaggacagtgggaagcttgct	60
L/M.Ex3R	taaggtcacagagtctgacc	
L/M.Ex4F	aaaacccccacccagttgg	58
L/M.Ex4R	aggagtctcagtggactcat	
L/M.Ex5F	cctctctctctccccacaac	62
L/M.Ex5R	caggtggggccatcactgca	
L/M.Ex6F	agggaaggctcgggcacgta	60
L/M.Ex6R	gataaattacattattttacaggg	

Table 4.1

Primers for amplification of the LCR and exons 1 to 6 of the L- and M-opsin genes

Primers designed and used by a colleague for mutation screening.

L/M opsin exon	Nucleotide	L sequence	M sequence
2	194	C	T
	331	A	G
	347	C	A
3	457	C	A
	538	T	G
4	691	T	C
	699	G	A
	700	C	G
	701	T	C
	708	A	G
5	822	A	G
	825	T	C
	827	T	G
	830	G	A
	832	A	T
	837	G	T
	855	A	G
	890	T	C
	894	G	C
	928	A	T

Table 4.2

Nucleotide differences between L and M exons used for opsin gene

identification

Figure 4.4

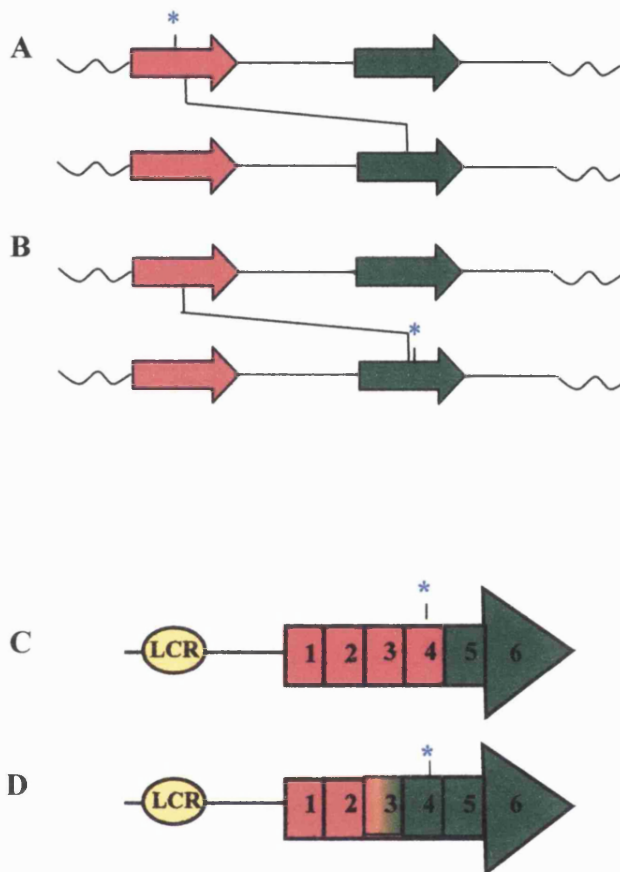
Opsin array of BCM individuals

A – The molecular events required for generation of the genotype of affected individuals in family B.

B – The molecular events required for generation of the genotype of affected individuals in family C.

C – **Family B** in which affected individuals possess a single hybrid gene, which is a result of recombination within intron 4, and T→C mutation in exon 4 (*).

D – **Family C** in which affected individuals possess a single hybrid gene, which is a result of recombination within exon 3, and T→C mutation in exon 4 (*).



4.5 DISCUSSION

Clinically, individuals with achromatopsia/rod monochromacy (complete or incomplete) and BCM share many features. They have poor visual acuity, pendular nystagmus, photophobia, and in the majority of cases funduscopy is unremarkable. However, individuals with BCM may have slightly better visual acuity and are more likely to be myopic. Classification can also be aided by family history, since BCM is inherited as an X-linked recessive trait, whereas both types of achromatopsia are autosomal recessive.

Blue cone monochromats can be distinguished from both types of rod monochromats by psychophysical threshold testing or electroretinographic studies at different wavelengths. Regardless of category, rod monochromats classically have very poor or no colour discrimination. Complete rod monochromats cannot make colour judgements, but rather will use brightness cues to differentiate between colours. When confronted with tasks where luminance cues cannot be used, these patients perform very poorly indeed (e.g. FM 100 hue scores are very high, D-15 arrangement patterns are characteristic and ordered along a scotopic axis).

In agreement with previous studies we have found that this contrasts with blue cone monochromats who do have access to colour discrimination. Their access to colour vision is believed to be based upon a comparison of the quantum catches obtained by the rods and the S-cones (Reitner *et al.*, 1991; Alpern and Lee, 1971). We have corroborated the finding of protan-like ordering patterns on the D-15 in BCM, and also found that the same is true of the enlarged version of the test, the PV-16. Our patient series has also demonstrated that the residual tritan discrimination that is characteristic of BCM can be readily and consistently detected with HRR plates and the M-R minimal test.

The protan-like patterns on D-15 testing of patients with BCM, is not necessarily indicative of colour discrimination, since it is possible that BCM individuals order the chips of this test according to their relative lightness to the S-cone mechanism (Hess *et al.*, 1989). Relevant to this is our demonstration that affected males also retain reasonable discrimination on the tritan axis of the M-R test. Since this test utilises lightness randomisation, it should not be possible for those with BCM to discriminate the target chips by lightness cues. Furthermore, those patients who were examined with a computer-controlled saturation discrimination task displayed discrimination ellipses with major axes well aligned to the theoretical S-cone/rod confusion axis. This provides

additional evidence that it is possible to derive colour discrimination at low photopic levels via a comparison of quantum catches in the S-cones and rods, as has been previously suggested.

BCM is generally accepted to be a stationary disorder but deterioration and the development of foveal pigmentary changes has been reported in a family with macular atrophy over a 12 year period (Fleischman and O'Donnell, 1981). There are two further reports of individuals with BCM displaying a progressive retinal degeneration (Nathans *et al.*, 1989; Ayyagari *et al.*, 1999); in both cases the genotype consisted of deletion of the LCR. In two of our families (A & C) there has also been progression in the severity of the condition. Since, in family A, the children have normal tritan function, and their grandfather has none, it would appear that the condition is not stationary. The two children can be labelled blue cone monochromats, whereas their grandfather behaves as a rod monochromat, presumably secondary to loss of S-cones. In family C, the grandfather, uncle, and two grandchildren share the same genotype. Since these children show convincing psychophysical evidence that S-cones are still surviving, whereas both older men in this family lack residual colour discrimination, the condition also appears to be progressive in this family. Moreover, the genotype identified in this family of a single 5'-L/M-3' hybrid gene with an inactivating mutation differs from previous reports of progression, where an LCR deletion was present. There is therefore no consistent genotype associated with progression of BCM.

Combined results of previous studies provide evidence for the general conclusion, first put forward by Nathans *et al.* (1989), that there are different mutational pathways to BCM. The data suggest that 40% of blue cone monochromat genotypes are a result of a one-step mutational pathway that leads to deletion of the LCR. The remaining 60% of blue cone monochromat genotypes comprise a heterogeneous group of multi-step

pathways. The evidence thus far shows that many of these multi-step pathways produce visual pigment genes that carry the inactivating Cys203Arg mutation. In our study, the genetic mechanism identified was unequal recombination resulting in an array comprising a single 5'-L/M-3' hybrid gene carrying a Cys203Arg mutation.

The affected subjects assessed in family A, would appear to possess only an M-opsin gene in the visual pigment array, which would be expected to produce dichromacy rather than monochromacy. Sequence analysis failed to reveal a mutation in any of the six opsin gene exons or the LCR. The diagnosis of BCM on clinical and psychophysical grounds is clear in this family, as is the X-linked inheritance, so it would seem most likely that the inactivating mutation in this case has not been identified. Other studies have also failed to detect the genetic alteration that would explain the BCM phenotype in all assessed individuals (Nathans *et al.*, 1993; Ayyagari *et al.*, 2000). Indeed Nathans *et al.* (1993) found that the structure of the opsin array did not reveal the genetic mechanism for the disorder in 9 of 35 affected patients. This failure to identify disease-causing variants in the opsin array may suggest genetic heterogeneity yet to be identified in BCM.

4.6 CONCLUSIONS

Although BCM is usually a stationary disorder, we have identified two families in which there is good psychophysical evidence suggestive of progression. The genotype identified in one of these families of a single inactivated 5'-L/M-3' hybrid gene differs from previous reports of progression, where an LCR deletion was present. Our finding that nystagmus associated with BCM may become less prominent over time, is not generally well recognised.

The M-R Minimal test and HRR plates have been demonstrated to be useful colour discrimination tests to aid in the diagnosis of BCM across a wide range of age groups. Affected males repeatedly failed the protan and deutan axes, but retained good discrimination on the tritan axis of the M-R test, whereas patients with RM perform poorly along all three axes.

CHAPTER 5

OLIGOCONONE TRICHRMACY

5.1 INTRODUCTION

In cone dysfunctions one or more of the three cone types are deficient or absent. Patients generally have a congenital colour vision defect, which remains stationary during life. Several alterations of cone vision have been defined by the phenotypic changes in colour matches and colour discrimination: anomalous trichromacy, dichromacy, monochromatism and achromatism. Complete achromats have no functioning cone photoreceptors, whilst incomplete achromats have residual colour vision.

Oligocone trichromacy is a rare cone dysfunction syndrome, which is characterised by reduced visual acuity, photophobia, normal fundi, and abnormal cone ERGs, but normal colour vision. The disorder was first described by Van Lith in 1973. Since then Keunen *et al.* (1995) have described a further four patients, whilst Neuhann *et al.* (1978) and more recently Ehlich *et al.* (1997), have each reported a single case.

It has been proposed that these patients have a reduced number of normal functioning cones (oligocone syndrome) with preservation of the three cone types in the normal proportions, thereby permitting trichromatic colour vision (van Lith, 1973). It would therefore appear to be best described as a stationary cone dysfunction syndrome with trichromacy; making it an unusual disorder of cone function.

5.2 AIMS

To investigate the detailed phenotype of a case series of six patients with presumed oligocone trichromacy, representing the largest case series to date.

CNGB3 was chosen as a candidate gene to screen since oligocone trichromacy is considered by some to be an incomplete form of achromatopsia; with *CNGB3* mutations representing the most common cause of the cone dysfunction syndrome, achromatopsia (Chapter 3).

5.3 METHODS

The six affected individuals underwent an ophthalmological examination, electrophysiological testing and detailed psychophysical testing.

5.3.1 *Patients and methods*

Six affected individuals from four different families were assessed. Families **A** and **C** respectively contained two affected brothers and two affected sisters; family **B** contained a single male patient, and family **D** a single female patient. One or both parents from each family were also assessed. In addition the grandmother of the two brothers in family **A** was also examined.

A full medical history was taken and ophthalmological examination performed. ISCEV standard electrophysiological assessment included an EOG and ERG. A broad range of colour vision tests were performed (section 1.3.4.1), including the use of HRR plates, Farnsworth Munsell (FM) 100-hue test, Farnsworth D-15 & PV-16, the M-R test, a computerised colour vision test and anomaloscopy. The computerised test, allows measurement of colour discrimination along tritan, deutan and protan axes (Mollon *et al.*, 1989; Regan *et al.*, 1994). The FM 100-hue, Farnsworth D-15/PV-16 and the M-R test were all performed under CIE Standard Illuminant C from a MacBeth Easel lamp.

5.3.2 *CNGB3 mutation screening*

The 18 coding exons of *CNGB3* were amplified by PCR in four affected individuals using primer sequences and conditions as published by Kohl *et al.* (2000). Standard 50µl PCR reactions were performed as described previously. After resolution on a 1% (w/v) LMT agarose gel, products were excised and eluted. Direct sequencing of PCR products

was carried out on an ABI 3100 Genetic Analyser using the original PCR primers in the sequencing reactions. The sequence was examined for alterations utilising *Sequencing Analysis* (ABI Prism™) and *GeneWorks*™ software.

5.4 RESULTS

5.4.1 Phenotype

All six affected patients had a history of reduced visual acuity from infancy (6/12 to 6/24), not improved by full spectacle correction. They complained of mild photophobia, but were not aware of any colour vision deficiency. They had no nystagmus and fundi were normal.

In the two sisters (Cases 4 & 5) the cone flicker ERGs were severely reduced and there was a shorter latency than normal of the cone single flash ERG b-wave. One patient (Case 6) showed delayed and mildly reduced cone flicker ERGs with minimal photopic single flash ERG changes and a normal waveform maximal response. One patient (Case 3) showed a delayed cone flicker ERG with a “double peak”, a single flash cone ERG with the b-wave more affected than the a-wave and a mildly electronegative maximal response. Representative traces appear in **Figure 5.1**. Clinical findings are summarised in **Table 5.1**.

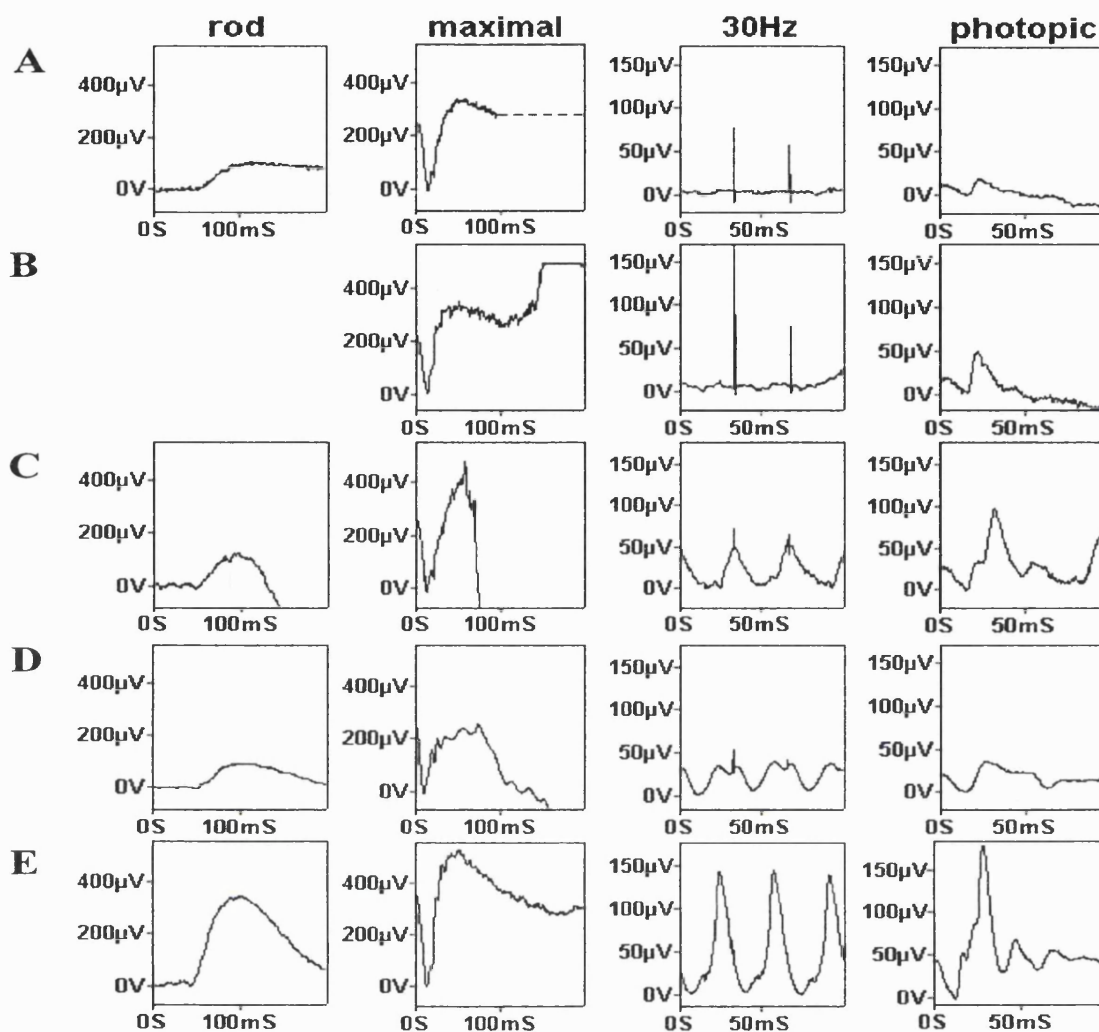


Figure 5.1 *Full-field ERGs in four oligocone trichromacy patients*

Data from a normal subject are shown for comparison (E).

Case 4 (A) shows no definite rod-specific abnormality; maximal response a-wave is mildly subnormal but of normal implicit time; cone single flash and flicker ERGs are severely reduced. Of interest, the b-wave implicit time is shorter than normal.

Case 5 (B) shows similar features; data for a rod specific response are unavailable.

Case 6 (C) has rod-specific and maximal responses quantitatively similar to cases 4 and 5. Cone ERGs however are much better preserved; the flicker ERG is subnormal and also delayed with single flash cone photopic ERG showing only borderline abnormal b-wave implicit time.

Case 3 (D) has a rod-specific response of abnormally low amplitude, but the maximal response shows a reduced b:a ratio suggesting dysfunction post-phototransduction. There is a delayed "double-peaked" flicker ERG, and the short latency photopic b-wave seen in cases 4 and 5 is not present.

Both the father and 80-year-old grandmother of the two brothers in family A were also examined. The father was found to have a visual acuity of 6/5 in both eyes, with normal colour vision, fundi and electrophysiological testing. The grandmother complained of reduced visual acuity, which she had been aware of since the age of 50. Despite bilateral cataract extractions in the past, her visual acuity was counting fingers in the right eye and 1/36 in the left eye. Fundoscopy revealed early 'bull's-eye' maculopathy in both eyes, whereas fundus examination of her grandsons was normal. ERG revealed absent cone responses, with normal rod function, suggesting that she also has a cone dystrophy. She has been unavailable for further psychophysical testing.

The six affected patients reported good colour vision and neither they nor their parents were aware of any colour vision abnormality. On examination, all had good colour vision. The psychophysical findings are summarised in **Table 5.2**. The various colour vision tests either revealed completely normal colour vision or slightly elevated discrimination thresholds. Anomaloscopy revealed matching ranges within normal limits, indicating the presence of long- and middle-wave cones of normal spectral sensitivity at the macula, whilst the absence of pseudoprotonomaly suggests that photopigment is present at normal optical densities in individual cone photoreceptors. One or both parents of all cases were tested and all had normal colour vision.

Family	Case	Age Yrs	VA	Refractive Error	Cone ERG
A	1	8	6/12 OD 6/18 OS	+2.0/+1.50 x 90 +2.5/+1.75 x 90	Absent cone ERG
A	2	6	6/18 OD 6/18 OS	+3.0/+1.00 x 90 +3.5/+1.25 x 90	Absent cone ERG
B	3	8	6/12 OD 6/12 OS	+1.25/+1.5 x 90 +1.25/+2.0 x 90	Reduced cone b:a wave ratio
C	4	14	6/24 OD 6/12 OS	-11.0/-2.00 x 30 -8.5/-3.00 x 155	Markedly reduced cone ERG
C	5	6	6/24 OD 6/24 OS	-8.0/-1.50 x 20 -9.5/-2.00 x 110	Markedly reduced cone ERG
D	6	8	6/24 OD 6/36 OS	-13.0/-1.5 x 170 -13.0/-1.25 x 10	Delayed and mildly reduced cone ERG

Table 5.1

Summary of clinical findings in oligocone trichromacy

Cases 1 and 2 are brothers

Cases 4 and 5 are sisters

5.4.2 *CNGB3* mutation screening

All 18 coding exons were successfully sequenced. However, no *CNGB3* mutations were detected in the four affected individuals who were screened.

Case	Age yrs	HRR	D-15	Mollon-Reffin (M-R) Minimal Test	Anomaloscopy	Cambridge Computerised Colour Test
1A	8	All correct	Normal	Slight elevation of discrimination threshold along deutan axis	Normal range	Slight elevation of discrimination thresholds along all three colour axes
2A	6	All correct	Normal	Slight elevation of discrimination threshold along deutan axis	Normal range	Slight elevation of discrimination thresholds along all three colour axes
3B	8	All correct	-	Slight elevation of discrimination thresholds -protan and deutan axes	Normal range	Slight elevation of discrimination thresholds along all three colour axes
4C	14	All correct	Normal	Normal	Normal range	Within the normal range along all three axes
5C	6	2 plates incorrect	2 minor transpositions	Normal	Normal range	Slight elevation of discrimination thresholds along all three colour axes
6D	8	1 plate incorrect	2 minor transpositions	Normal	Normal range	Slight elevation of discrimination thresholds along all three colour axes

Table 5.2 Summary of psychophysical findings in oligocone trichromacy

5.5 DISCUSSION

The largest case series to date of patients with Oligocone trichromacy has been established (Michaelides *et al.*, 2004c). The six patients in our series had moderately reduced visual acuity (6/12 to 6/24) and mild photophobia, with normal visual fields and fundi. There was no nystagmus which contrasts to the two cases reported by Van Lith (1973) and Ehlich *et al.* (1997) who both had pendular nystagmus. Electrophysiological testing provided evidence of retinal dysfunction predominantly confined to the cone system.

The cone ERG findings in our patients were poorly concordant. Cone flicker ERG responses were markedly reduced in two siblings, who additionally showed a photopic b-wave of shortened implicit time. This may suggest some preservation of the cone OFF-pathway, as the implicit time of the OFF- response in normal subjects is similar to that in the two patients. Other patients showed clearly present but delayed and reduced cone flicker ERGs, with one showing a mildly electronegative maximal response. The cone system implicit time changes are not expected in restricted disease, and are more usually associated with generalised dysfunction rather than loss of function. A post-receptoral processing abnormality may be present in some individuals, as suggested by the b:a ratio reductions. This phenotypic heterogeneity suggests that there may be more than one mechanism for disease pathogenesis, and thus that there may also be genetic heterogeneity associated with the oligocone phenotype.

Some patients in the present series had a mild reduction of colour discrimination, but no patient had markedly abnormal colour vision. Anomaloscopy revealed normal matching ranges, which indicates the presence of long- and middle-wave cones of normal spectral sensitivity and of normal optical density. The slightly elevated discrimination thresholds that were detected are compatible with a reduction in cone numbers.

It has been proposed that patients with oligocone trichromacy might have a reduced number of normal functioning cones with preservation of the three cone types in normal proportion, thereby enabling trichromacy (van Lith, 1973). Keunen *et al.* (1995) tested this hypothesis by screening foveal cone photopigment density in four patients with oligocone trichromacy. A reduced density difference of the foveal cone photopigment with a normal time constant of photopigment regeneration was found in all patients. Colour matching and increment threshold spectral sensitivity were normal. This provided supportive evidence for the hypothesis of a reduced number of foveal cones (decreased density differences) with otherwise normal functioning residual cones. Dysfunction of foveal cones alone will not affect the full-field ERG (Holder, 2001). Peripheral retinal cones are also affected, as shown by the full-field cone ERG abnormalities, profound in some patients, and our data do not support the hypothesis that the remaining cones function normally. Peripheral retinal colour vision in these patients would be of interest, as it may help establish whether peripheral colour discrimination is indeed reduced. Multifocal ERG may help determine whether central cone loss is 'patchy' or 'uniform' (Hood, 2000).

It has been thought likely that the mode of inheritance is autosomal recessive. However, both brothers and their paternal grandmother are affected in family A, more suggestive of autosomal dominant inheritance. As their father is unaffected there would need to be incomplete penetrance. Equally, previous reports have suggested this disorder to be stationary, but there is clinical evidence of progression in family A of this study, with worsening visual acuity and the development of 'bull's-eye' maculopathy in the older affected individual. However, until molecular genetic data become available it can not be proven that the grandmother's cone dysfunction is the same disorder as that of the two brothers.

It has previously been suggested that oligocone trichromacy may represent a form of incomplete achromatopsia. It is therefore feasible that mutation within the three currently identified genes associated with achromatopsia, *CNGA3*, *CNGB3* and *GNAT2*, may underlie the molecular basis for this disorder; thereby leading to the screening of *CNGB3* in our series. However, since oligocone trichromacy may have a developmental component, it is equally tempting to propose that genes involved in retinal photoreceptor differentiation, when cone numbers are being determined, also represent good candidate genes, rather than mutation within the three genes that encode cone-specific intermediates within the phototransduction cascade. It is therefore possible that molecular genetic analysis of this disorder may help to shed light on cone photoreceptor development. Furthermore, since electrophysiological testing suggests that the site of abnormality may not be exclusively at the level of the photoreceptor, genes expressed preferentially in the inner retina may represent alternative candidates. Interestingly, retinal ON- bipolar cells have also now been shown to express cone-specific cyclic nucleotide-gated channels (encoded by *CNGA3* & *CNGB3*) (Henry *et al.*, 2003).

Oligocone trichromacy is perceived to be a rare disorder, and it has previously been proposed that patients have a reduced number of retinal cones that function normally. That may apply to central cones, but our data suggest that remaining peripheral cones do not function normally. Equally, as our six patients have been ascertained over a relatively short period of time (three years), the disorder may be more common than previously recognised.

5.6 CONCLUSIONS

The phenotype associated with oligocone trichromacy has been detailed, with the electrophysiological findings suggesting that there may be more than one disease mechanism. The relatively good visual acuity, minimal photophobia, lack of nystagmus and good colour vision are findings consistent with significant remaining central cone function.

The mode of inheritance in most cases is likely to be autosomal recessive, and whilst previous reports have suggested that this disorder is stationary, in one of our families there is clinical evidence suggestive of progression. The possibility that this cone dysfunction syndrome may be progressive in some individuals is in keeping with findings that also imply continued degeneration in the minority of patients with other cone dysfunction syndromes, including achromatopsia and BCM; this may be secondary to other genetic modifiers or environmental influences.

CHAPTER 6

X-LINKED CONE DYSFUNCTION SYNDROME WITH MYOPIA AND DICHROMACY

6.1 INTRODUCTION

Disorders of cone function have been described with autosomal dominant, autosomal recessive, or X-linked (XL) patterns of inheritance. They may be progressive or stationary; the latter group include the well characterised dysfunction syndromes of rod monochromatism, a recessive dystrophy in which there are no functioning cones, and blue cone monochromatism, an XL disorder in which there are only two functional classes of photoreceptor (rods and S-cones).

We have ascertained four families with XL inheritance of a stationary cone disorder, characterised by myopia, moderate visual loss and a protan colour vision abnormality; and a further single family with cone dysfunction associated with deuteranopia. The involvement of a protan colour vision abnormality with progressive cone dystrophy has been reported previously (Reichel *et al.*, 1989; Kellner *et al.*, 1995). However, it is unusual since dichromacy which arises either from the loss of L- or M-opsin gene sequences (Deeb *et al.*, 1992), or from the presence of a missense mutation in the opsin gene with consequent loss of function (Winderickx *et al.*, 1992; Ueyama *et al.*, 2002), has not been associated with cone dystrophy in extensive studies of dichromats (Deeb *et al.*, 1992; Neitz *et al.*, 1995; Jagla *et al.*, 2002). Nevertheless, opsin mutations are seen in the stationary cone dysfunction syndrome, blue cone monochromatism (Nathans *et al.*, 1989).

6.2 AIMS

Five families were ascertained with features compatible with a cone dystrophy, dichromacy and myopia. The phenotype in the five families has been examined in detail.

In a parallel study conducted by a colleague, the XL L- and M- opsin genes in affected members of four of these families have been examined to determine whether mutations in these genes may underlie the disorder.

6.3 METHODS

The pedigrees of all 5 families showed only males affected, with no evidence of male to male transmission, consistent with XL inheritance. Affected and unaffected members of five families with a presumed XL cone dystrophy were examined clinically and also underwent extensive psychophysical testing.

Blood samples were taken for DNA extraction and molecular genetic analysis was performed by a colleague in a parallel study.

6.3.1 Patients and methods

A full medical history was taken and ophthalmological examination performed in all affected subjects. Electrophysiological testing included ISCEV standard ERG and EOG. Colour fundus photography was also undertaken.

Detailed colour vision testing (section 1.3.4.1) included the use of HRR plates, SPP2 plates for acquired colour deficiency, Farnsworth Munsell (FM) 100-hue test, Farnsworth D-15 and PV-16, the Mollon-Reffin (M-R) Minimal test, a computerised colour vision test and anomaloscopy. The computerised test allows measurement of colour discrimination along tritan, deutan and protan axes (Mollon and Reffin, 1989; Regan *et al.*, 1994). The FM 100-hue, Farnsworth D-15/PV-16 and the M-R test were all performed under CIE Standard Illuminant C from a MacBeth Easel lamp.

6.3.2 Molecular genetic analysis

In the four families found to have protanopia, affected males and female carriers were analysed in a parallel study. Independent reactions were set up to amplify the locus control region (LCR) and all exons of the L- and M-opsin genes from genomic DNA by PCR. Primer pairs which would co-amplify both L- and M-opsin exonic sequence were designed within each intron approximately 50bp from the intron-exon junction in order that the whole of each exon, some flanking DNA and the splice sites were amplified. Mutation analysis was carried out by directly sequencing PCR products using PCR primers, with the L- and M- genes being distinguished by using known nucleotide differences between the two highly homologous genes (**Table 4.2**).

6.4 RESULTS

6.4.1 Phenotype

All affected subjects displayed myopia (moderate to high), astigmatism, reduced visual acuity (6/12 - 6/36), and normal fundi (myopic changes and tilted optic discs were seen in some individuals). In four families (A to D) a predominantly protan colour vision phenotype was established. A deutan colour vision phenotype was present in family E. No nystagmus was observed. The ERGs of affected males demonstrated normal rod function but a marked attenuation of cone responses (**Figure 6.1**).

There has been no clinical evidence of progression in any subjects to date. In family A, an older affected member of the family was available for testing; his clinical findings were entirely comparable to those of his grandchildren's, thereby suggesting that this XL cone disorder with myopia and dichromacy is stationary.

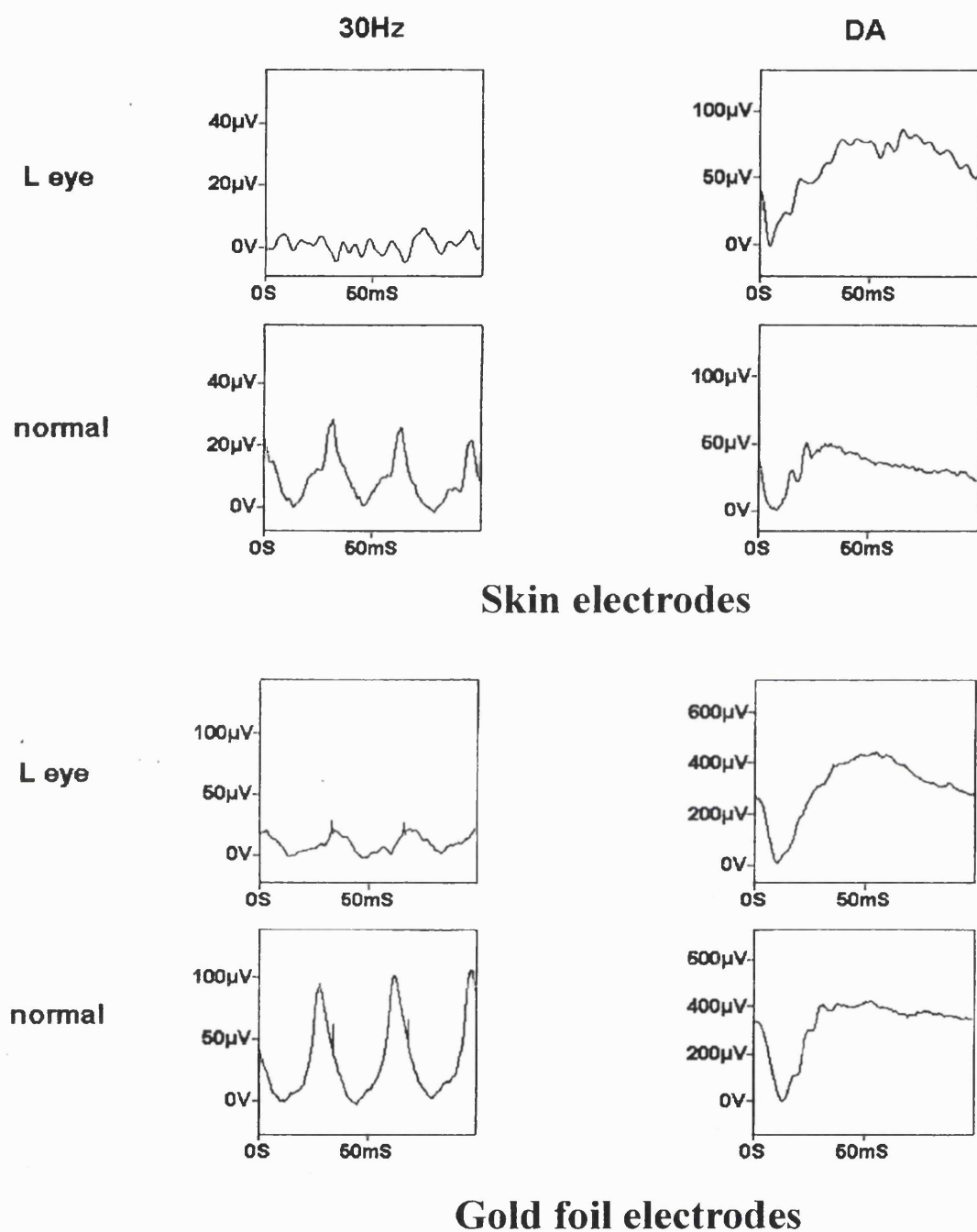


Figure 6.1

ERGs of affected males from Family A recorded using both skin (above) and gold foil (below) electrodes.

The **left-hand column** shows cone responses for recordings at 30Hz flicker stimulation; the **right-hand column** shows dark-adapted mixed rod-cone (maximal) responses. Cone responses are markedly reduced, whilst rod responses are within normal limits (maximal response a-wave amplitude being a measure of rod photoreceptor function).

Family A has two affected brothers who originally presented in the first decade of life with poor visual acuity (**Figure 6.2**).

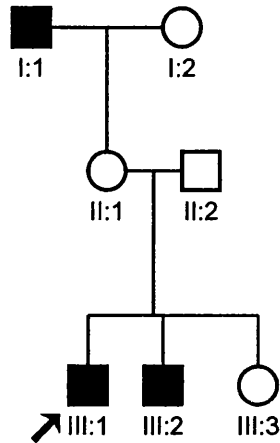


Figure 6.2
Family A pedigree

Patient **A1** was a 15-year-old boy (proband) with reduced visual acuity (6/12 both eyes), a colour vision defect, high myopia and astigmatism (OD: -9.50/-3.50 x 5, OS: -10.00/-2.50 x 5), and a divergent squint. Fundus examination was normal. Electrophysiological testing revealed abnormal cone responses but normal rod function.

Patient **A2** was his 8-year-old brother who presented with reduced visual acuity (6/18 both eyes), and was also found to have a colour vision defect, and myopia with an astigmatic error (OD: -3.50/-3.50 x 5, OS: -3.00/-4.00 x 180). Fundus examination revealed a myopic fundus but was otherwise unremarkable. ERG showed evidence of generalised cone dysfunction with normal rod responses.

Patient **A3** was their 67-year-old maternal grandfather who had suffered with poor vision since childhood and had a visual acuity of 6/12 in both eyes with a myopic correction (OD: -2.00/-3.00 x 10, OS: -2.50/-2.50 x 120). Testing with the HRR revealed a protan colour vision defect; further detailed testing was not possible.

On psychophysical testing, **A1** displayed a protanopic Rayleigh match with both eyes. D-15 (**Figure 6.3**) and computerised testing also revealed protan colour deficiency. The M-R minimal test revealed normal tritan colour discrimination and a red-green defect in each eye. Testing of **A2** with HRR plates revealed red-green colour deficiency with predominantly protan errors; whilst M-R testing showed normal tritan colour discrimination and a red-green defect in both eyes. Both parents of the two brothers were also tested and had normal colour vision.

There has been no deterioration in vision of either brother since presentation 8 years ago, and since grandfather's vision has remained stable throughout life, it suggests that the cone dysfunction is stationary.

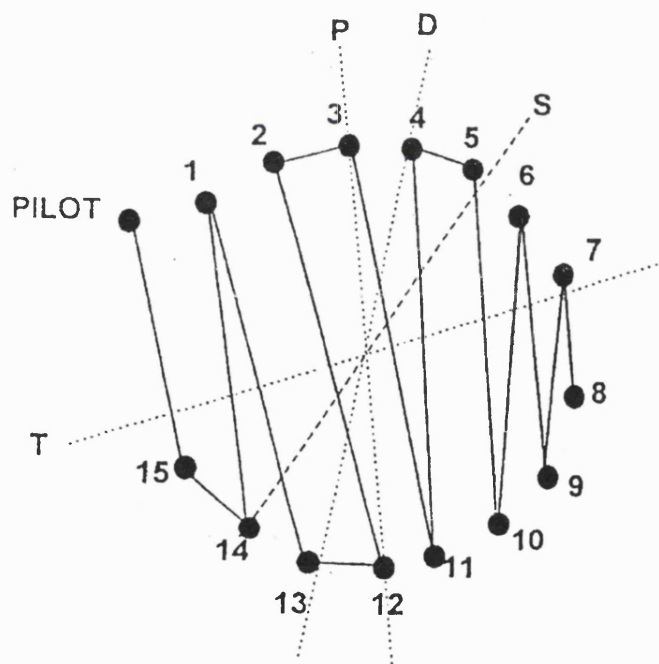


Figure 6.3

Subject A1 D15 Test

The 15 filled circles each represent a coloured chip which, when ordered by an individual with normal colour vision, form a colour circle of pastel hues. Red/green colour vision deficient subjects make characteristic crossings from one side of the colour circle to the other. Here, individual **A1** makes crossings along the confusion pattern for a protanopic dichromat (P).

Family B comprises two affected brothers, **B1** and **B2**, who both first presented in the first decade of life with poor visual acuity.

Patient **B1** was an 18-year-old man with visual acuity of 6/18 in each eye with his myopic correction (OD: -6.00/-2.00 x 15, OS: -6.00/-2.50 x 160). Fundus examination was normal. ERG showed evidence of generalised cone dysfunction with normal rod responses.

Patient **B2** was his 22-year-old brother, with 6/12 visual acuity in each eye, a colour vision defect, and myopia with astigmatism (OD: -3.00/-3.00 x 25, OS: -2.50/-2.50 x 130). Fundoscopy revealed normal fundi, other than tilted discs. ERG showed evidence of generalised cone dysfunction with normal rod function.

At the anomaloscope, both brothers made colour matches consistent with a diagnosis of protanopia. Similarly, both of the brothers displayed protan ordering on the D-15 test. On computerised colour vision testing, both brothers displayed discrimination ellipses that were oriented tightly along a protan axis. To date, there has been no deterioration in visual acuity since presentation 9 years ago. Both parents of the two brothers were also tested and showed normal colour vision.

Family C has three affected brothers, **C1**, **C2** and **C3**, who all presented in the first decade of life with poor visual acuity and mild photophobia.

Patient **C1**, a 7-year-old boy with poor visual acuity (6/36 in the right eye, 6/24 in the left eye), was found to have a colour vision defect, myopia and astigmatism (OD: -3.00/-2.50 x 30, OS: -3.25/-1.25 x 165). Fundoscopy revealed myopic fundi with tilted optic discs

(Figure 6.4). ERG showed evidence of generalised cone dysfunction with normal rod function.

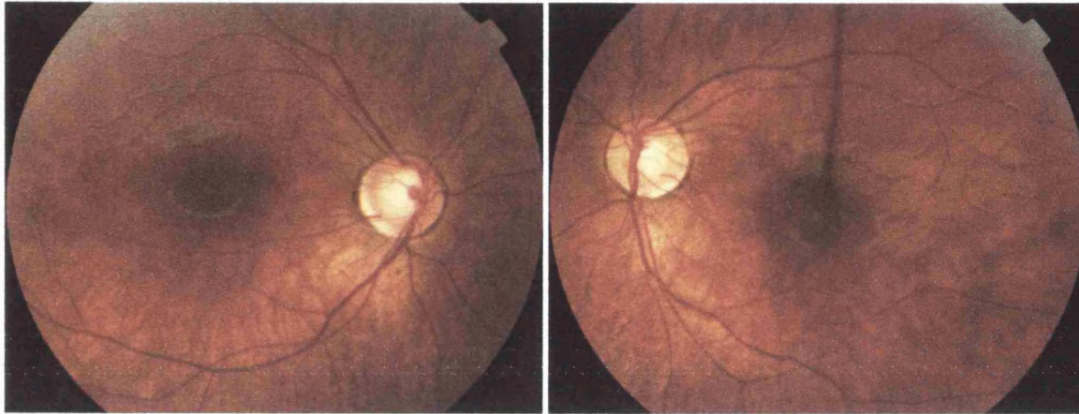


Figure 6.4

Myopic fundi with tilted optic discs of patient C1

Patient **C2**, a 5-year-old boy with 6/12 visual acuity in both eyes, was found to have a colour vision defect, myopia and astigmatism (OD: -2.00/-1.50 x 180, OS: -2.00/-1.00 x 180). Fundoscopy revealed normal fundi. ERG showed evidence of significant loss of cone function with normal rod responses.

Patient **C3**, a 4-year-old boy with poor visual acuity (6/18 in both eyes), was found to have a colour vision defect, myopia and astigmatism (OD: -2.50/-2.25 x 180, OS: -2.50/-2.25 x 180). Fundoscopy revealed normal fundi. ERG showed abnormal cone function with normal rod responses.

The young age of the three affected male brothers in this pedigree limited the range of psychophysical testing. The two tested males, **C1** and **C2**, both displayed good discrimination along the tritan axis of the M-R test. However, both showed significantly elevated thresholds for red-green discriminations and HRR testing also provided evidence

of a protan colour deficit. Their sister and mother were found to have normal visual acuity and normal colour vision. To date, there has been no deterioration in visual acuity since presentation 4 years ago.

Family D The assessed affected individual had a maternal family history of his mother's male cousin and grandfather both being colour blind and suffering from reduced visual acuity from a young age, not fully corrected by spectacles. Neither was willing to undergo clinical or psychophysical testing.

Patient **D1** was a 7-year-old boy who presented with a visual acuity of 6/24 in the right eye, 6/18 in the left eye. He was found to have a colour vision defect, myopia and astigmatism (OD: -4.75/-1.00 x 80, OS: -4.75/-1.00 x 120). Fundoscopy revealed myopic fundi with tilted optic discs (**Figure 6.5**). ERG showed evidence of generalised cone dysfunction with normal rod responses.

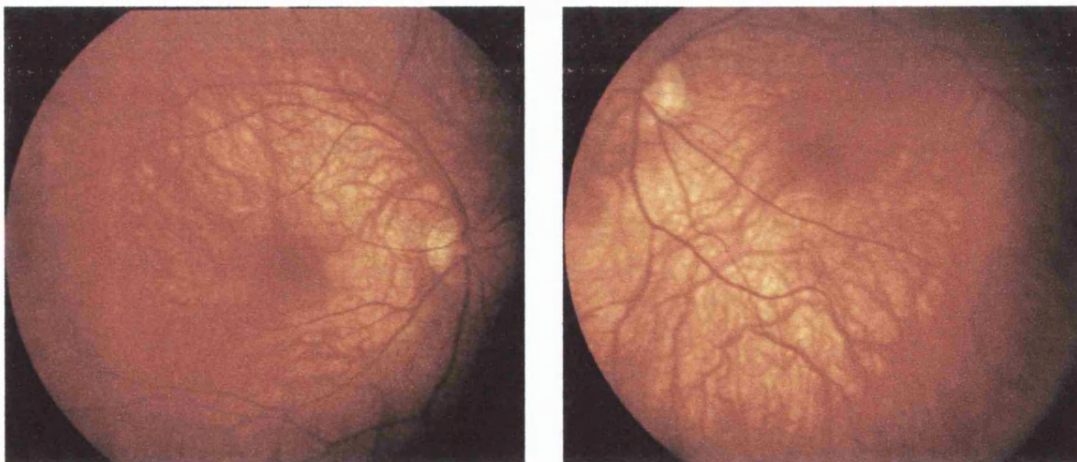


Figure 6.5

Myopic fundi with tilted optic discs of patient D1

On the City University colour vision test and HRR, a red-green deficiency was detected, with mainly a protan defect. On the D-15, he showed a predominantly protan sequence of errors with each eye. At the anomaloscope he showed a protan spectral sensitivity and on computerised colour testing his discrimination ellipse was oriented in a protan direction. His mother was found to have entirely normal colour vision.

Family E has three affected brothers, **E1**, **E2** and **E3**, who all presented in the first decade of life with poor visual acuity and mild photophobia. The family are originally from Morocco (**Figure 6.6**).

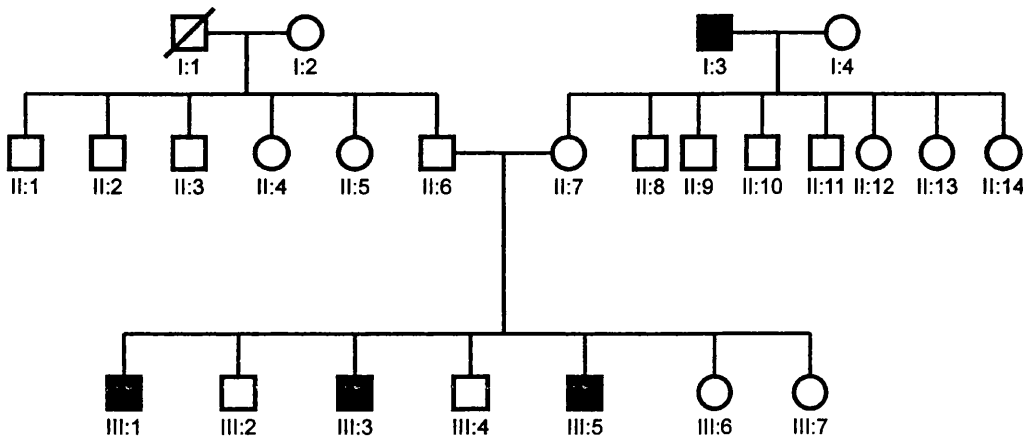


Figure 6.6

Family E pedigree

Patient **E1**, a 23-year-old man with poor visual acuity (6/24 in both eyes), was found to have a colour vision defect, high myopia and astigmatism (OD: -8.00/-1.50 x 30, OS: -9.25/-1.25 x 180). Fundoscopy revealed myopic fundi. ERG showed evidence of generalised cone dysfunction with normal rod function.

Patient **E2**, his 26-year-old brother had a visual acuity of 6/24 in both eyes and a red-green colour vision defect. He also had a myopic refractive error with astigmatism (OD: -7.00/-1.50 x 60, OS: -6.00/-1.00 x 180). Fundoscopy revealed myopic fundi.

Patient **E3**, a 14-year-old boy with poor visual acuity (6/36 in both eyes), was found to have a colour vision defect, high myopia with astigmatism (OD: -10.0/-2.50 x 70, OS: -10.0/-2.50 x 115) and a divergent squint. Fundoscopy revealed tilted optic discs but otherwise normal fundi. ERG showed abnormal cone function with normal rod responses.

Patients **E1** and **E3** were available for detailed psychophysical testing. **E1** on HRR testing was found to have a red-green deficiency, with more deutan than protan errors. On the D-15, he showed a predominantly deutan sequence of errors with his right eye; making only one major transposition with his left eye. At the anomaloscope he showed a deutan spectral sensitivity with both eyes, and on computerised colour testing his discrimination ellipse was oriented in a predominantly deutan direction. On the D-15, **E2** showed a deutan ordering with both eyes and on computerised testing his discrimination ellipses generated with both eyes were oriented along a deutan axis. On anomaloscopy protanomalous matches were made with both eyes. Smith *et al.*, (1979) have previously reported deuteranopia in association with protanomalous anomaloscopy matches. Their mother was found to have normal colour vision.

Therefore, in contrast to Families A to D, family E has a deutan colour vision phenotype rather than protan; otherwise in keeping with the other four families they also have cone dysfunction, myopia with astigmatism, lack nystagmus, and display an XL inheritance pattern.

6.4.2 Genotype

Since patients from families A to D showed clear evidence of protanopia, experiments were undertaken in a parallel study to establish whether novel mutations in the L- and M-opsin gene array on the X chromosome were responsible for the colour vision defect and cone dysfunction.

The activity of the opsin gene array is controlled by the LCR which is approximately 3.5 kb upstream of the L gene, with the M gene a further 24 kb downstream (Nathans *et al.*, 1986a; Dulai *et al.*, 1999). This tandem array may however be extended by additional M or hybrid L/M genes in normal subjects; or may be contracted to a single L or M gene in the case of deuteranopia or protanopia respectively (Nathans *et al.*, 1986a; Deeb *et al.*, 1992; Neitz and Neitz, 2000), or to a single hybrid gene where the nature of the colour vision defect will depend on the particular combination of L and M gene exons (Neitz and Neitz, 2000).

The L and M genes are highly homologous. Nevertheless, there are several sequence differences that differentiate exons 2 to 5 of the L and M opsin genes (exons 1 and 6 of the two genes are identical). A number of studies have demonstrated that the spectral differences that distinguish the L and M pigments are almost entirely the result of amino acid differences at only three sites, 180 encoded by exon 3, and 277 and 285, encoded by exon 5 (Merbs and Nathans, 1993; Asenjo *et al.*, 1994).

Family A Direct sequencing of the PCR products generated using PCR primers that amplify both genes demonstrated the presence of the LCR and both L and M opsin genes in subjects A1, A2 and A3. Sequence data for exon 4 showed the presence of a T→C nucleotide transition at position 648 in all affected family members. This change results in a Cys203Arg substitution in the opsin protein molecule, a change that is known to disrupt opsin folding (Kazmi *et al.*, 1997) and is responsible for the loss of gene function

in certain molecular classes of blue cone monochromatism (Nathans *et al.*, 1989). Further experiments suggested the presence of both wild type and mutant variants of exon 4 in both the L and M opsin genes. This would imply that affected members of family A had at least two L and two M opsin genes, and in both cases, at least one was normal and one mutant. The presence of protanopia in this family would indicate that only the normal copy of the M gene is expressed, with the first L gene in the array inactivated by the Cys203Arg mutation.

Family B Sequence data for **B1** and **B2** demonstrated the presence of an intact LCR and the full complement of L-opsin gene exons. There was, however, no evidence of an M-opsin gene exon 2, indicating that a hybrid gene is present that is composed of exons 1-2 from the L gene and exons 3-6 from the M gene. This gene would be expected to encode a pigment that is spectrally identical to a standard M gene. It is the presence of an L gene that is inconsistent with the protanopia seen in the affected family members. What cannot be established from this data however is whether the L gene is expressed and the colour vision defect would suggest that it is not. No other sequence change was identified within the opsin gene array that would account for the cone dysfunction.

Family C Sequence data from family C indicated that the LCR and all the L and M gene exons were present except for L gene exon 5. This would indicate that at least two opsin genes are present in the array in this family, a normal M and a hybrid L/M gene. The protanopia is consistent with the expression of one or more of these genes since both would give a pigment with a λ_{\max} around 535 nm. There was no evidence however for a mutation to account for the cone dysfunction.

Family D Sequence analysis demonstrated that exons 3 and 5 of the L gene are absent from the gene array of the affected proband in family D. This is again consistent with protanopia if the gene(s) in the array lack both of the key exons 3 and 5 for spectral tuning. There is however again no mutation to account for the cone dystrophy.

The alterations in the L and M genes described for the four families were present in all affected members and shown to be carried by obligate carrier females in each family but not in unaffected members. Since the cone dysfunction is only seen in male members of the families with protanopia, this would indicate that the cone dysfunction shares the same XL inheritance pattern.

6.5 DISCUSSION

The affected members of the different families described in this study have a very similar stationary cone dysfunction syndrome that is characterised by moderate to high myopia, astigmatism, moderately reduced visual acuity, mild photophobia, normal or myopic fundi, and evidence of a selective impairment of the L cones (Families A to D) or M cones (Family E) on psychophysical testing. There is also evidence for X-linked inheritance. Nystagmus was not present in affected subjects.

The association therefore of protanopia/deutanopia with cone dysfunction indicates a potential role for opsin gene mutations in the aetiology of the disorder. However, although the molecular analysis of the opsin gene array on the X-chromosome revealed changes that are clearly consistent with the protanopia in three of the families (A, C & D), in each case the changes are different. The only opsin gene mutation that could potentially account for the cone dysfunction, is the Cys203Arg substitution in family A; this mutation has been shown to impair the folding and stability of opsin photopigment

(Kazmi *et al.*, 1997). Similar point mutations have previously been reported to cause retinitis pigmentosa (Hwa *et al.*, 2001). The Cys203Arg substitution has also been identified in blue cone monochromatism (Nathans *et al.*, 1989) and deutan (deuteranopia and deuteranomaly) congenital colour vision deficiency (Neitz and Neitz, 2000). Whether cone dysfunction or congenital colour vision deficiency is associated with this mutation appears to be determined by the remaining functional cone pigment genes that an individual possesses. In addition, other genetic modifying factors may play a role in determining the phenotype, such as the variable L:M cone ratio that has been reported, ranging from 2:1 to 10:1 (Hagstrom *et al.*, 2000; Kremers *et al.*, 2000; Carroll *et al.*, 2002). It is conceivable that individuals with a heavily skewed ratio in favour of L-cones may thereby have the majority of their cones inactivated by the Cys203Arg mutation and therefore have a cone dysfunction rather than solely a colour vision anomaly. However, the presence of normal M and L opsin genes in an expanded opsin gene array in family A makes it uncertain whether this change is responsible for the dysfunction. Although to date, to the best of our knowledge, the Cys203Arg mutation has not been described in association with congenital protanopia. This suggests that since the L:M ratio is usually skewed in favour of L cones, this deleterious mutation when present in the L gene results in cone dysfunction rather than an isolated colour vision defect. In the other three families, there were no changes in the opsin gene array that could in isolation account for the cone dysfunction.

There has been no visual deterioration in any of our patients, suggesting that the disorder in these families is stationary. Progressive cone dystrophies (PCDs) are not usually symptomatic until late childhood or early adult life whereas in our families, presentation was within the first decade of life, with patients often symptomatic in the first few years of life. In the PCDs, photophobia is a prominent early symptom, often

associated with nystagmus. In contrast, our patients did not have nystagmus, and photophobia was mild. PCDs usually show evidence of retinal degeneration, although in some cases there may be only minor macular RPE atrophy and pigmentation. Fundus appearance was normal in our affected family members (other than myopic changes in some individuals).

A constant feature of the disorder in our families was myopia. Myopia can be inherited either as an autosomal recessive or as an XL trait and in the latter case, it is well known as a component of congenital stationary night blindness (Musarella *et al.*, 1989) and retinitis pigmentosa (Kaplan *et al.*, 1992). One example of XL myopia is Åland Eye Disease, but this is associated with nystagmus, hypopigmentation of the fundus and abnormal dark adaptation (Forsius and Eriksson, 1964). Another example has been reported in a large five-generation Danish family that had its origins on the Danish island of Bornholm. The syndrome has therefore been named Bornholm Eye Disease (BED) (Haim *et al.*, 1988; Schwartz *et al.*, 1990). In that family, the syndrome manifests as myopia combined with astigmatism, and impaired visual acuity. Additional signs are moderate optic nerve head hypoplasia, thinning of the RPE in the posterior pole with visible choroidal vasculature, and reduced cone ERG responses as the most constant finding. Importantly all affected members in this family have deuteranopia and a stationary natural history. Linkage analysis mapped the BED locus to Xq28 (Schwartz *et al.*, 1990), in the same chromosomal region therefore as the L/M opsin gene array.

Our five families share many characteristics with the original BED pedigree, namely XL inheritance, cone ERG dysfunction, myopia with astigmatism, poor visual acuity, dichromacy, and absence of nystagmus. Family E had deuteranopia in keeping with the BED pedigree, whereas families A to D had protanopia. It therefore appears likely that the disorder described in our families represents the same stationary cone dysfunction

syndrome as reported in the Danish kindred. If so, since BED was mapped to Xq28, the failure to find mutations in the opsin gene array to clearly account for the cone dysfunction in our families raises the possibility that the cone dysfunction component of the disorder may be ascribed to an adjacent, but separate locus. However, the cone dystrophy that has been mapped to Xq27 (COD2), displays a different and progressive phenotype (Bergen and Pinckers, 1997). This does not however exclude the COD2 locus; for example, it has been demonstrated previously and also in this thesis, that mutation in both *CNGA3* and *CNGB3*, can be associated with both stationary and progressive cone disorders, with contrasting phenotypes (Wissinger *et al.*, 2001; Michaelides *et al.*, 2004a).

We have not been able to identify any patients with a similar XL cone dysfunction syndrome without dichromacy. It appears that this form of cone dysfunction is only seen in association with dichromacy. The different molecular explanations for the dichromacy in the four families preclude a founder effect as the basis for this association. Indeed, linkage disequilibrium in this chromosomal region is unlikely, given the high frequency of crossing over within the opsin gene array in the generation of numerical variants of M and L genes (Drummond-Borg *et al.*, 1989) and gene hybrids (Deeb *et al.*, 1992). One possible explanation remains that important opsin array alterations, such as deletions, have not been identified using the genetic strategy employed in this study, or that there are as yet unidentified opsin promoter regions within which the causative mutations reside. Equally, the effects of a cone pigment modifying gene at the Xq28 locus may underlie this stationary cone dysfunction syndrome. An alternative explanation is that the cone dysfunction arises from a mutation in a gene that only causes cone dysfunction when expressed in dichromats. If the cone dysfunction we describe is identical to BED, then the dysfunction gene is likely to be adjacent to the opsin gene array and causes

dysfunction in both protanopes and deuteranopes. Thus, normal trichromats with the mutation are entirely asymptomatic. In other words it is plausible that BED may be a digenic disorder that depends on the presence of two changes, a mutation in a “cone dysfunction” gene and dichromacy arising from changes in the L/M opsin gene array on the X chromosome.

6.6 CONCLUSIONS

The five families described here represent a novel stationary cone dysfunction syndrome characterised by myopia with astigmatism, dichromacy and XL inheritance.

The molecular genetic basis for this cone dysfunction disorder remains uncertain, although the strong phenotypic similarities between these families and the BED kindred, suggests that this disorder is also likely to map to the Xq28 region. The opsin array alterations detected in our families, whilst largely explaining the colour vision phenotype (protanopia), are unlikely in isolation to cause the cone dysfunction. The only possible exception to this is the Cys203Arg mutation identified in family A. It remains possible that the dichromacy and the cone dysfunction have different genetic origins. Further detailed molecular genetic analysis of these families should help to resolve the current uncertainty.

CHAPTER 7

PROGRESSIVE CONE DYSTROPHY ASSOCIATED WITH *CNGB3*

7.1 INTRODUCTION

Progressive cone dystrophies (PCDs) are a clinically heterogeneous group of disorders. In contrast to the stationary cone dysfunction syndromes, which present in early infancy and childhood, the PCDs are not usually symptomatic until late childhood or early adult life.

In the PCDs, photophobia is a prominent early symptom and there is progressive loss of central vision and colour vision, with nystagmus also being a common feature (Simunovic and Moore, 1998). Fundus examination often reveals a typical ‘bull’s-eye’ maculopathy, although in some cases there may be only minor atrophy and pigmentation of the macular retinal pigment epithelium. The optic nerve head may show a variable degree of temporal pallor.

PCDs are usually characterised by a progressive loss of colour vision, with all three classes of cone photoreceptor affected, thereby producing colour vision defects along all three colour axes; often progressing to complete loss of colour vision over time (Goodman *et al.*, 1963; Simunovic and Moore, 1998). Exceptions to this are cases where there is a predominant involvement of L-cones leading to a protan colour vision phenotype (Reichel *et al.*, 1989; van Everdingen *et al.*, 1992; Kellner *et al.*, 1995). Autosomal dominant cone dystrophy pedigrees with early tritan colour vision defects have also been reported (Bresnick *et al.*, 1989; Marré *et al.*, 1989; Went *et al.*, 1992).

The PCDs are also genetically heterogeneous, with autosomal dominant (AD), autosomal recessive (AR) and X-linked (XL) inheritance all having been described. Several loci and causative genes have been identified in the PCDs. XL cone dystrophies have been mapped to COD1 (Xp21-p11.1) (Meire *et al.*, 1994) and COD2 (Xq27) (Bergen and Pinckers, 1997). Mutations in *CNGA3* (Wissinger *et al.*, 2001) have been identified in AR cone dystrophies, *GUCA1A* (encoding GCAP1) mutations have been

reported in an AD pedigree (Payne *et al.*, 1998), and *RPGR* mutations in XL pedigrees (Yang *et al.*, 2002).

However with time, the majority of PCDs appear to develop rod system involvement (Moore, 1992; Simunovic and Moore, 1998), at which point they are better described as cone-rod dystrophies; in which case several other genes may be implicated, including *ABCA4* (Maugeri *et al.*, 2000), *CRX* (Freund *et al.*, 1997), *GUCY2D* (Kelsell *et al.*, 1998b), *RIMI* (Johnson *et al.*, 2003), *Peripherin/RDS* (Nakazawa *et al.*, 1996), *AIPL1* (Sohocki *et al.*, 2000), *RPGRIP1* (Hameed *et al.*, 2003) and *RPGR* (Mears *et al.*, 2000).

In contrast, achromatopsia is a stationary cone disorder which presents at an earlier age. To date, three genes associated with achromatopsia have been characterised (section 1.1.2.1.2), *CNGA3* and *CNGB3*, located at chromosome 2q11 and 8q21 respectively, which encode the α - and β -subunits of the cGMP-gated cation channel in cone cells, and *GNAT2*, located at 1p13, encoding the cone α -transducin subunit.

Missense mutations in *CNGA3* have been previously reported in two individuals with cone-rod dystrophy and in a single individual with a progressive cone dystrophy phenotype (Wissinger *et al.*, 2001). However, mutations in *CNGB3* have not been previously associated with PCD.

7.2 AIMS

To determine the molecular basis for phenotypic variability in a three-generation consanguineous family containing a single individual with complete achromatopsia and three individuals with progressive cone dystrophy.

7.3 METHODS

A three-generation family with autosomal recessive cone dystrophy was ascertained. Four affected individuals underwent ophthalmological examination, electrophysiological assessment, colour fundus photography, and psychophysical testing. Blood samples were taken from affected and unaffected family members for DNA extraction and subsequently mutation screening of *CNGB3* was undertaken.

7.3.1 Patients and methods

Four affected members of a consanguineous Pakistani family with cone dystrophy were assessed (Figure 7.1).

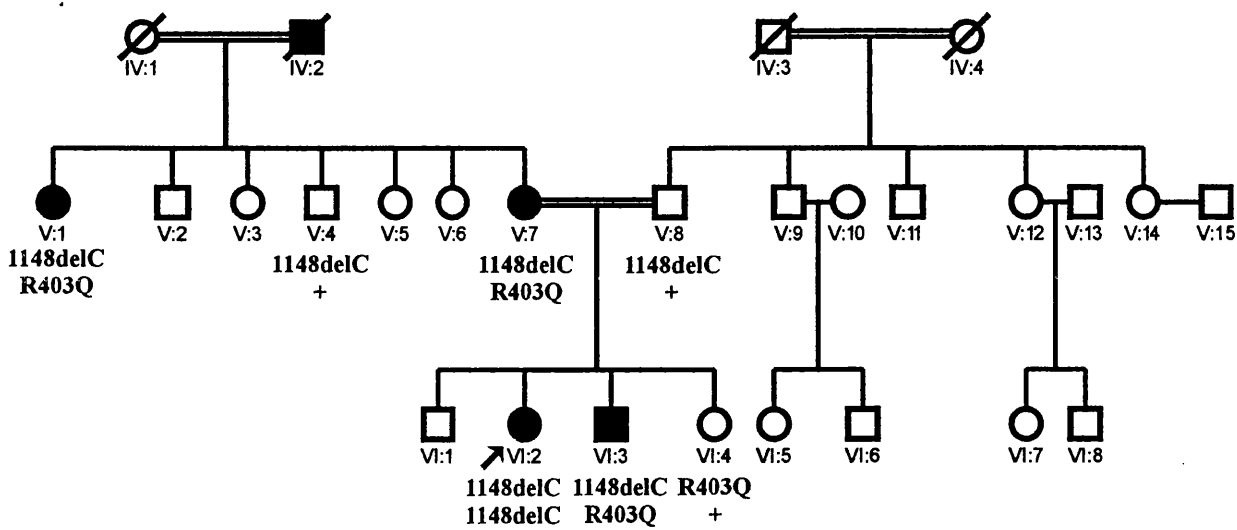


Figure 7.1

Progressive cone dystrophy pedigree

(The segregation of the *CNGB3* sequence variants, Thr383fs and R403Q, is shown.)

A full medical history was taken and ophthalmological examination performed. Subjects also underwent colour fundus photography and ISCEV standard EOG and full-field ERG. Colour vision testing using the enlarged Farnsworth D-15 (PV-16) and/or the Farnsworth Munsell (FM) 100-hue test was performed in all four affected individuals. In two affected subjects (V:7 and VI:2) further colour vision testing was possible including the use of HRR plates, Sloan achromatopsia plates, the M-R minimal test and anomaloscopy. The PV-16, FM 100-hue test, Sloan achromatopsia plates, and the M-R test were all performed under CIE Standard Illuminant C from a MacBeth Easel lamp.

7.3.2 *CNGB3* mutation screening

The 18 coding exons of *CNGB3* were amplified by PCR in each individual using primer sequences and conditions as previously published (Kohl *et al.*, 2000). Standard 50 μ l PCR reactions were performed as previously described. After resolution on a 1% (w/v) LMT agarose gel, products were excised and eluted. Direct sequencing of PCR products was carried out on an ABI 3100 Genetic Analyser using the original PCR primers in the sequencing reactions. The sequence was examined for alterations utilising *Sequencing Analysis* (ABI PrismTM) and *GeneWorks*TM software.

GenBank sequences were used to construct an alignment of channel protein sequences and to analyse the evolutionary conservation of the corresponding amino acid positions. The sequences used were the cGMP-gated (CNG) channel cone β -subunits of human (accession number AF272900), mouse (AJ243572) and dog (AF490511), and the rod β -subunits of human (AF042498) and rat (NM031809).

7.4 RESULTS

7.4.1 *Phenotype*

The index case (VI:2) had a phenotype indistinguishable from complete achromatopsia, in that she had complete absence of colour vision on detailed testing, prominent pendular nystagmus from early infancy, photophobia and visual acuity of 3/60. Her fundi were found to be normal (Figures 7.2a & b), and on ERG testing she had absent cone responses, with normal rod function.

In contrast, the three other individuals in the family (V:1, V:7 and VI:3) presented with findings consistent with a progressive cone dystrophy phenotype. Their visual problems started later in childhood, ranging from 3 to 14 years-of-age, and a variable deterioration in visual acuity over time has been documented (Table 7.1). On examination, all three subjects were found to have residual colour vision and bilateral well-demarcated pigmented macular atrophy (Figures 7.2c & d). Psychophysical testing revealed a generalised dyschromatopsia affecting all three axes, with the colour vision defect being much worse along the tritan than red-green axis.

In individual V:7 colour vision testing at two time points demonstrated progressive deterioration of cone function. At age 37 her FM 100-hue test total error score was 248, whilst twelve years later it had increased to 400 (normal age-matched total error score is less than 100), with more tritan than red-green errors on both occasions (Figure 7.3). Colour vision testing of V:7 with HRR plates and the M-R minimal test confirmed the generalised dyschromatopsia, with the colour vision defect being worst along the tritan axis. ERG testing performed at two time points, in two individuals (V:7 and VI:3) demonstrated a progressive deterioration in cone function.

Clinical findings are summarised in Table 7.1.

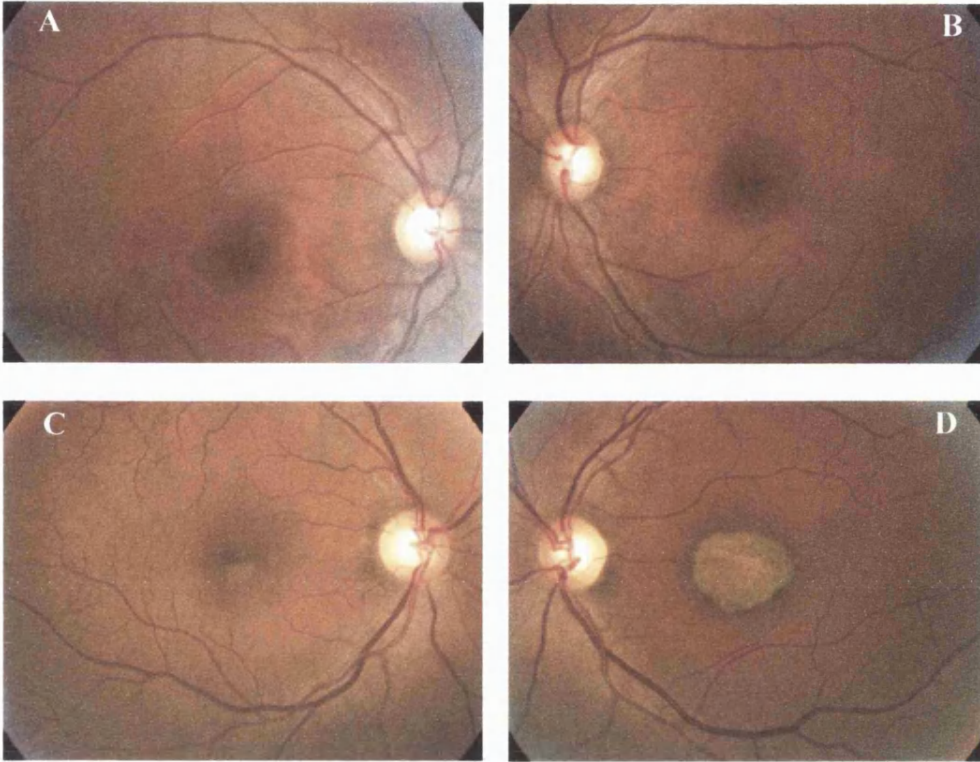


Figure 7.2

Above: normal fundi seen in VI:2

Below: typical fundus appearance seen in V:1, V:7 and VI:3

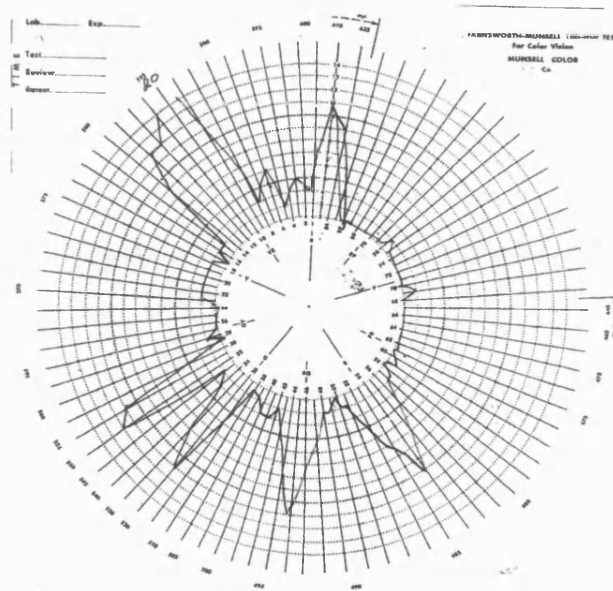


Figure 7.3

The Farnsworth Munsell 100-hue colour vision test

performed by V:7, demonstrating a tritan axis of confusion with an error score of 400.

Patient	Age Yrs	Visual acuity OD OS	Refractive Error OD OS	Nystagmus	ERG	Macula	Colour Vision
VI:2	8	3/60 3/60	+4.50/-1.0 x 90 +3.00/-1.0 x 90	Pendular	Absent cone responses Normal rod function	Normal	Absent
	24	3/60 3/60	+4.75 DS +3.25 DS	Pendular	Absent cone responses Normal rod function	Normal (Figure 2a & 2b)	Absent
VI:3	6	6/24 6/24	+2.50 DS +2.00 DS	Manifest latent	Reduced cone responses Normal rod function	Bilateral pigmented macular atrophy OS>OD	Residual D15 tritan axis
	22	1/60 2/60	+1.0 DS +1.0 DS	Manifest latent	Markedly reduced cone responses Normal rod function	Bilateral pigmented macular atrophy OS>OD	Residual
V:7	37	6/24 6/24	Plano/+2.0 x 90 Plano/+1.0 x 90	Latent	Reduced cone responses Normal rod function	Bilateral pigmented macular atrophy OS>OD	Residual D15 tritan axis
	43	6/36 6/36	Plano/+2.0 x 90 Plano/+1.0 x 90	Latent	Reduced cone responses Normal rod function	Bilateral pigmented macular atrophy OS>OD	FM 100-hue: tritan axis with error score of 268
	49	6/36 6/36	-	Latent	Markedly reduced cone responses Normal rod function	Increased bilateral pigmented macular atrophy OS>OD (Figure 2c & 2d)	FM 100-hue: tritan axis with error score of 400 (Figure 4)
V:1	42	6/24 6/24	-1.25 DS -0.75 DS	Absent	-	Bilateral pigmented macular atrophy	-
	56	6/36 6/36	-	Absent	Reduced cone responses Normal rod function	Increased bilateral pigmented macular atrophy	Residual FM 100-hue: tritan axis with error score of 584

Table 7.1 Summary of clinical findings

7.4.2 Genotype

The 18 coding exons of *CNGB3* were screened for mutations in affected and unaffected family members. As shown in **Figure 7.1**, the index case with complete achromatopsia was found to be homozygous for the one base-pair frameshift deletion, 1148delC (Thr383fs). The other three affected individuals were found to be compound heterozygotes, carrying the Thr383fs mutation and a novel missense mutation, Arg403Gln (G→A change at nucleotide 1208) (**Figure 7.4**). Unaffected relatives were either homozygous wild-type (wt), Thr383fs/wt heterozygotes, or Arg403Gln/wt heterozygotes. The segregation of these *CNGB3* mutations can be seen in **Figure 7.1**.

The Arg403Gln (R403Q) mutation was not detected in one hundred ethnically matched control chromosomes, indicating that it is not a common polymorphism. The position and nature of this substitution is fully consistent with disease association. Arg403 is located in the middle of the pore domain of the CNG channel subunit. It is conserved in other mammalian (dog and mouse) cone β -subunits but replaced in rod β -subunits by Lys, another positively charged residue. Alignment of the pore region of cone and rod α - and β -subunits (**Figure 7.5**) demonstrates the high degree of sequence conservation in this region, particularly within each subunit class. The two classes differ however in the number of charged residues, with only one (Glu) in the α -subunits but three in the β -subunits. The Glu in the α -subunit is known to be responsible for Ca^{2+} binding in homotetrameric CNGA channels (Root and MacKinnon, 1993; Eismann *et al.*, 1994; Park and MacKinnon, 1995; Gavazzo *et al.*, 2000), and the loss of charge arising from the Arg403Gln substitution in the β -subunit is likely to be significant therefore for the functioning of the pore region.

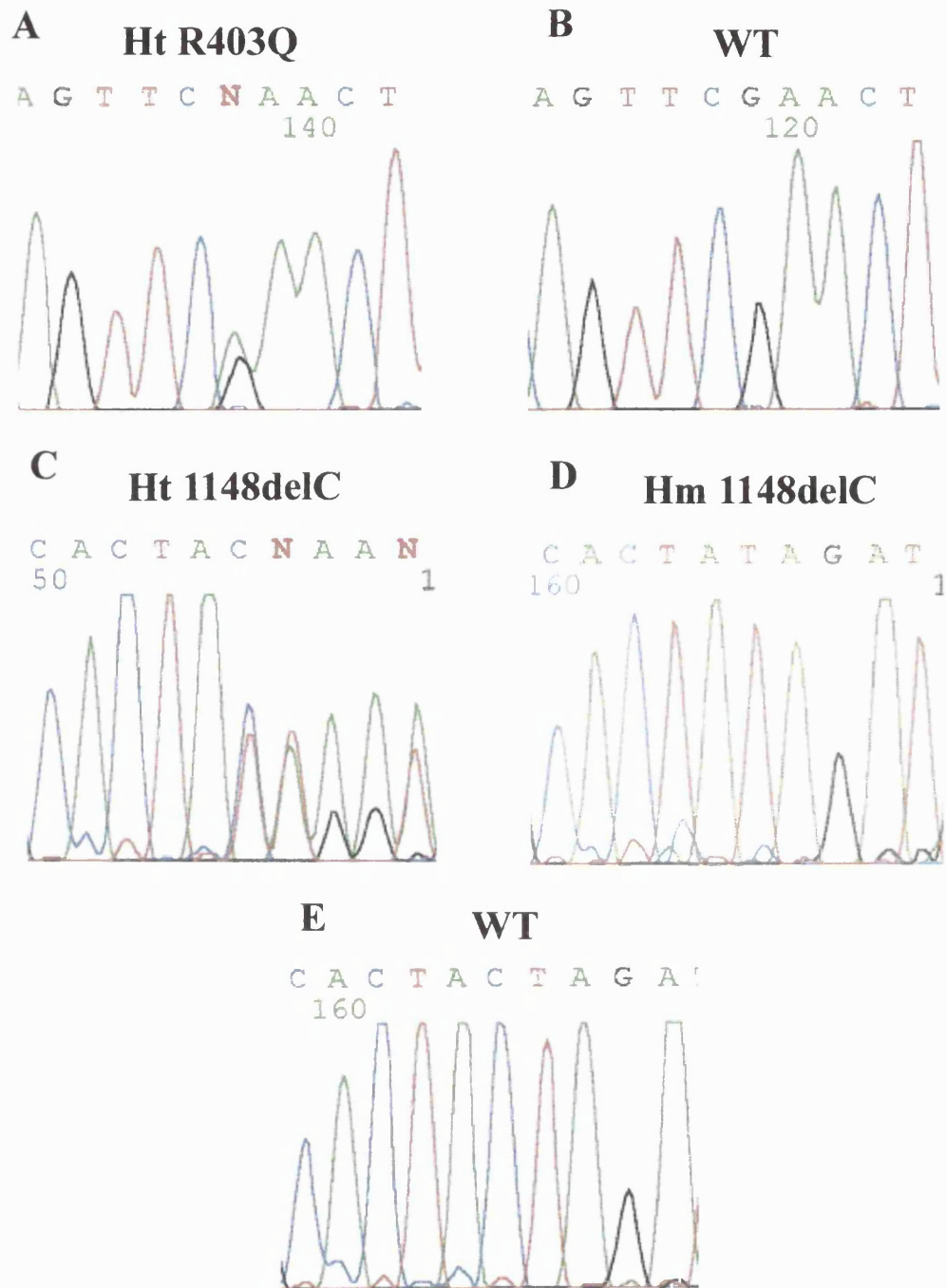


Figure 7.4

Sequence electropherograms of exon 11 (A-B) and exon 10 (C-E) of CNGB3

A: Affected compound heterozygote showing the G→A change at nucleotide 1208 which results in the novel missense mutation, Arg403Gln. **B:** Unaffected subject.

C: Heterozygous 1148delC mutation. **D:** Homozygous 1148delC mutation.

E: Unaffected subject.

Rod α (CNGA1) VYSLYWSTLTLTTIG**E**TPP
Cone α (CNGA3) VYSLYWSTLTLTTIG**E**TPP
** ** *** *

Rod β (CNGB1) I**R**CYYWAV**K**TLITIGGLPD
Cone β (CNGB3) L**R**CYYWAV**R**TLITIGGLP**E**

↑

Figure 7.5

Sequence alignment of the pore region of human cone and rod α - and β -subunits of the CNG channels

The position of the Arg403Gln substitution is shown (arrow). Charged residues are highlighted and identity of residues across both rod and cone subunits is indicated by an asterisk.

7.5 DISCUSSION

Mutations in *CNGB3* are a common cause of the stationary cone dysfunction syndrome, achromatopsia (Chapter 3). The novel Arg403Gln mutation reported here, when associated with the frameshift mutation Thr383fs, results in PCD; to the best of our knowledge, this is the first demonstration of PCD caused by mutation in *CNGB3* (Michaelides *et al.*, 2004a).

Two sequence variants have been identified in this pedigree, Thr383fs and Arg403Gln. Thr383fs, the most common disease mutation identified in *CNGB3* (Kohl *et al.*, 2000; Kohl *et al.*, 2001; Johnson *et al.*, 2004), would generate, if translated, a truncated channel subunit that lacks three important regions, the pore domain, the sixth α -helical transmembrane region, and the cGMP-binding site. The index case with

complete achromatopsia is homozygous for this null mutation, Thr383fs, whereas the three other affected individuals with PCD are compound Thr383fs/Arg403Gln heterozygotes. The novel missense alteration we have identified, Arg403Gln (R403Q), is located in the middle of the pore domain of the CNG channel subunit at a site conserved in other cone β -subunits and occupied by another positively charged residue, Lys, in rod β -subunits. The mutation places neutral Gln into this site. This change in charge from a positively charged Arg to an uncharged Gln may affect cation transfer through the channel pore, and thereby adversely affect channel function.

Negatively charged residues are known to be important for the binding of Ca^{2+} to the pore (Root and MacKinnon, 1993; Eismann *et al.*, 1994; Park and MacKinnon, 1995; Gavazzo *et al.*, 2000); replacement of the single charged Glu residue in the α -subunit pore region (**Figure 7.5**) with various neutral residues abolishes high-affinity Ca^{2+} -binding (Park and MacKinnon, 1995; Seifert *et al.*, 1999; Gavazzo *et al.*, 2000). Similar experiments have not been carried out with the β -subunit so the precise role of Arg403 has yet to be established. However, the markedly reduced colour vision and visual acuity present in compound heterozygotes would indicate that the mutant Gln403 subunit supports only limited cation movement through the channel to account for the residual cone function seen in these patients. Nevertheless, this contrasts with the total loss of function and complete colour-blindness associated with homozygosity for the Thr383fs frameshift mutation, noted in this study and elsewhere (Kohl *et al.*, 2000; Sundin *et al.*, 2000; Eksandh *et al.*, 2002; Johnson *et al.*, 2004).

The progressive nature of the disorder in the compound heterozygous patients is currently more difficult to explain. One possibility is that truncated mutant protein arising from the Thr383fs mutant allele accumulates over time, leading to progressive cone cell loss; however it is most likely that the frameshift mutation will be subject to nonsense

mediated mRNA decay and therefore not be translated. Alternatively, it seems more probable that the progressive nature of the disorder arises from effects of the R403Q missense mutation. The abnormal functioning of the mutant protein may alter the intracellular levels of Ca^{2+} and/or cGMP; such changes in cGMP are known to result in photoreceptor loss in the *rd* mouse (Bowes *et al.*, 1990), and may also underlie the cone-rod and cone dystrophies associated with dominant mutations in *GUCY2D*, the retinal form of guanylyl cyclase type 1 (Kelsell *et al.*, 1998; Wilkie *et al.*, 2000), and its activating protein, GCAP1 (encoded by *GUCA1A*) (Payne *et al.*, 1998; Wilkie *et al.*, 2001).

The *CNGB3* missense mutation, Ser435Phe (S435F), is located in the sixth transmembrane domain of the *CNGB3* polypeptide. Although causing complete achromatopsia (Kohl *et al.*, 2000; Sundin *et al.*, 2000), the recent report that the Ser435Phe mutation, when co-expressed with human wild-type *CNGA3* subunits in *Xenopus* oocytes (Peng *et al.*, 2003b), results in an increased affinity for cGMP, a decreased single channel conductance, and a decreased sensitivity to blockage by L-cis-diltiazem, demonstrates that mutant effects on β -subunit function have the potential to alter the balance between cGMP and Ca^{2+} within the photoreceptor. Indeed, since S435F, located in a transmembrane domain, has been demonstrated to affect channel properties it is certainly plausible that R403Q, a mutation actually located within the pore region itself, may also affect channel conductance and thereby lead to a cone dystrophy phenotype. In contrast, co-expression of mutant Thr383fs β -subunits with wild-type *CNGA3* subunits produced channels with properties indistinguishable from homomeric *CNGA3* channels, consistent therefore with the complete non-functioning of the truncated protein (Peng *et al.*, 2003b).

7.6 CONCLUSIONS

Mutations in *CNGB3*, which have previously been shown to cause achromatopsia, are also associated with autosomal recessive progressive cone dystrophy. This is the first report of *CNGB3* mutations as a cause of progressive cone dystrophy.

A novel Arg403Gln mutation has been identified. This missense mutation is located in the middle of the pore domain of the cone CNG cation channel β -subunit, which when associated with the nonsense mutation Thr383fs, results in a progressive cone dystrophy.

It has been possible to establish a genotype-phenotype correlation in this pedigree. The homozygous Thr383fs genotype is associated with complete achromatopsia, in which there is absent cone function. This contrasts with the compound heterozygote genotype, Thr383fs/Arg403Gln, where it is likely there is residual mutant protein function, and results in a PCD phenotype.

CHAPTER 8

CONE DYSTROPHY WITH SUPERNORMAL ROD RESPONSES

8.1 INTRODUCTION

An unusual cone disorder associated with abnormal rod responses has been described, characterised by supernormal and delayed rod ERG b-waves (Gouras *et al.*, 1983; Alexander and Fishman, 1984a; Sandberg *et al.*, 1990; Kato *et al.*, 1993; Rosenberg and Simonsen, 1993; Hood *et al.*, 1996). This retinal dystrophy was first described by Gouras *et al.* (1983) in two siblings with generalised loss of cone vision, clinical evidence of progression, and nyctalopia. Cone ERGs were markedly reduced whilst the rod b-wave was supernormal in amplitude in response to intense flashes, but smaller than normal and delayed over the lower intensity series. Alexander and Fishman (1984) reported two similar cases with supernormal rod ERGs without nyctalopia, suggestive of good rod function despite an abnormal scotopic ERG.

In only one other inherited retinal disease, enhanced S-cone syndrome (ESCS), is a supranormal photoreceptor response seen, namely a supernormal S-cone ERG associated with enhanced S-cone function (improved tritan discrimination) (Jacobson *et al.*, 1990; Marmor *et al.*, 1990). In contrast, whilst there are supernormal rod ERGs recorded in the cone dystrophy with supernormal rod responses phenotype (COD/SuperROD), there is no reported augmentation of rod function. In ESCS there is evidence of an increase in S-cone numbers and mutations within *NR2E3* have been identified, a gene believed to play a role in determining cone cell fate (Haider *et al.*, 2000; Milam *et al.*, 2002). Mutations in *NR2E3* are thought to cause disordered cone cell differentiation, possibly by encouraging default to the S-cone pathway and thereby altering the relative ratio of cone subtypes. However the mechanism of disease in COD/SuperROD is currently unknown. It remains controversial whether defects in phototransduction secondary to dysregulation of intracellular cGMP levels are involved (Nicol and Miller, 1978; Lipton, 1983; Gouras *et al.*, 1983;

Pawlyk *et al.*, 1991). A more recent investigation has suggested that phototransduction in this phenotype is within normal limits and that the site of disease is beyond the outer segment, involving a delay in the activation of inner nuclear layer activity (Hood *et al.*, 1996). The identification of the underlying molecular genetic basis of this rare cone dystrophy will help to clarify the pathogenesis of this phenotype.

The largest case series to date of patients with this unusual phenotype of cone dystrophy with supernormal rod responses is described herein. In view of the supernormal electrophysiological responses characteristic of this disorder and the fact that rod photoreceptors share more properties in common with S-cones than mid-spectral cones (Zrenner and Gouras, 1979; Reitner *et al.*, 1991), mutation screening of *NR2E3* has also been performed in a subset of our affected subjects.

8.2 AIMS

To characterise the disorder in detail with the aim of improving knowledge of the natural history of the disorder and to help shed light upon disease mechanisms. In a subset of affected subjects *NR2E3* was screened for disease-causing mutations.

8.3 METHODS

Nine subjects with the phenotype of cone dystrophy with supernormal rod responses (COD/SuperROD) were ascertained. After informed consent, a detailed medical and ophthalmic history was obtained and a full ophthalmological examination performed. All patients underwent colour fundus photography and electrophysiological testing. Five subjects underwent fundus autofluorescence (AF) imaging, automated photopic and dark-

adapted perimetry, and dark adaptometry. Six individuals had a detailed colour vision assessment. In four individuals *NR2E3* was screened for mutations.

8.3.1 Patients and methods

Nine subjects (five simplex cases and two sibling pairs), of variable ethnic origin, with the phenotype of COD/SuperROD underwent ophthalmological assessment.

Fundus AF imaging was undertaken using the confocal scanning laser ophthalmoscope (cSLO) (Zeiss Prototype; Carl Zeiss Inc, Oberkochen, Germany). Electrophysiological assessment included an electro-oculogram (EOG), full-field electroretinogram (ERG) and pattern ERG (PERG), incorporating the protocols recommended by the International Society for Clinical Electrophysiology of Vision. S-cone ERGs were also recorded (Arden *et al.*, 1999).

Colour vision testing included the use of Hardy, Rand, Rittler (HRR) plates (American Optical Company, New York), Farnsworth Munsell (FM) 100-hue test, enlarged Farnsworth D-15 (PV-16), the standard and enlarged Mollon-Reffin (M-R) Minimal test, a computerised colour vision test and anomaloscopy. The FM 100-hue, PV-16 and the M-R test were all performed under CIE Standard Illuminant C from a MacBeth Easel lamp.

Five affected subjects underwent detailed perimetry and dark adaptation. Static threshold perimetry in the dark- and light-adapted states was performed using a Humphrey field analyser (Allergan Humphrey, Hertford, UK). For dark-adapted visual fields, the pupil was dilated with 2.5% (w/v) phenylephrine hydrochloride and 1% (w/v) tropicamide, and the patient was dark adapted for 45 minutes. The Humphrey field analyser was modified for use in dark-adapted conditions; an infrared source illuminated the bowl, and an infrared monitor was used to detect eye movements. Fields were recorded using the central 30-2,

peripheral 30/60-2, and macular programs. The target size corresponded to Goldmann size V for peripheral testing and to Goldmann size III for macular programs. Each was performed with a red (dominant wavelength, 650nm) and then blue (dominant wavelength, 450nm) filter in the stimulus beam.

For dark adaptometry, two test locations were chosen at 3° and 9°. The Humphrey field analyser was used controlled by a custom computerised program (PS/2 model 50; International Business Machines, Armonk, NY) (Alexander and Fishman, 1984b; Chen *et al.*, 1992). Fully dark-adapted thresholds were measured at the two coordinates with the blue filter in the stimulus beam before exposure to the adapting light.

8.3.2 *NR2E3* mutation screening

Blood samples were taken from four individuals for DNA extraction and mutation screening of *NR2E3*. Total genomic DNA was extracted from blood samples using a Nucleon®Biosciences kit. The coding sequences of *NR2E3* were amplified by PCR in each individual using primer sequences and conditions as described in Chapter 11. Standard 50µl PCR reactions were performed as described previously. After resolution on a 1% (w/v) LMT agarose gel, products were excised and eluted. Direct sequencing of PCR products was carried out on an ABI 3100 Genetic Analyser using the original PCR primers in the sequencing reactions. The sequence was examined for alterations utilising *Sequencing Analysis* (ABI Prism™) and *GeneWorks*™ software.

8.4 RESULTS

8.4.1 *Phenotype*

The ethnicity of our nine subjects was diverse, with geographical origin from Britain, Somalia, Pakistan, Iran and the United Arab Emirates. The age of onset of symptoms was in the first and second decades of life with subjects presenting with reduced central vision and marked photophobia. Visual acuity (VA) ranged from 6/12 to 6/60. Three individuals had mild nystagmus. The photophobia was a very significant source of discomfort and difficulty. All subjects were moderately to highly myopic, with variable degrees of astigmatism. Four individuals were aware of a progressive deterioration in VA and colour vision. Examination of clinical notes revealed that there had been progressive reduction in recorded VA in two other patients who had not reported such deterioration.

The three oldest patients in the case series complained of nyctalopia, whereas the younger subjects denied difficulties with night vision, suggesting that poor night vision may be a later feature of the disorder. Detailed colour vision testing revealed that all individuals had severely reduced colour discrimination predominantly along the protan-deutan axes, and possessed far better residual tritan colour vision. In two subjects it was possible to establish a predominantly protan colour vision phenotype, and in three other individuals a deutan phenotype was present. Clinical findings are summarised in **Tables 8.1 and 8.2**.

Fundoscopy revealed a range of macular appearances including normal fundi (two subjects), mild retinal pigment epithelial (RPE) disturbance, and 'bull's-eye' maculopathy (BEM) (**Table 8.1, Figure 8.1**). Mild temporal optic nerve pallor was present in five subjects. The peripheral retina was normal. In three individuals AF imaging revealed a perifoveal ring of increased AF (**Table 8.1, Figure 8.1**). In two older subjects an area of

increased AF was seen at the central macula; in one of these subjects a perifoveal ring of increased AF was still evident, whilst in the other the central highly fluorescent zone was encircled by an area of relative decreased AF (**Table 8.1, Figure 8.1**).

The PERG was absent in the seven subjects in whom testing was performed. ERG testing revealed reduced and delayed cone responses in all subjects (**Figure 8.2**). In seven individuals rod specific ERGs demonstrated supernormal and delayed rod responses. In the remaining two subjects rod responses were delayed and a profound and rapid b-wave amplitude increase with minimal increase in stimulus intensity was seen. In all subjects, at low light intensities rod ERG amplitudes were found to be sub-normal and undetectable at the lowest flash energies (which would elicit a response in normals), but as the light intensity was increased an abrupt increase in amplitude was seen, which at the higher flash energies may be at the upper limit of normal or exceed it (supernormal). These two patterns of final rod ERG amplitude at high flash energies have also been previously reported (Hood *et al.*, 1996). The marked delay of the rod ERG b-wave was most clearly seen at the lower flash intensities (**Figure 8.2**).

The slope of the ERG a-wave in both cone and rod systems was within normal limits in all patients. Delayed recovery from the peak of the photopic b-wave, with no evidence of an i-wave, was seen in all individuals. In the seven subjects tested, all had delayed OFF-responses. Previous evidence of disease progression has been based purely on clinical grounds. We have obtained electrophysiological data establishing definite progressive deterioration of retinal function in the one subject in whom repeat testing has been performed (Case 4). Representative electrophysiological traces of patients in this case series are shown in **Figure 8.2**.

Five affected individuals underwent more detailed psychophysical investigation. Photopic testing demonstrated decreased central visual field sensitivity, in the order of 10 to 20dB, with additional peripheral sensitivity loss, most marked in the superior visual field. Dark-adapted perimetry revealed central and peripheral sensitivity loss in the order of 15 to 30dB, with similar rod and cone threshold elevations. The superior visual field was more affected than the inferior (**Figure 8.3**). Dark adaptometry showed no clear delay in adaptation; however there were several patients in whom the rod-cone break was poorly defined.

There was a history of consanguinity in four families (three simplex cases and the two affected sisters). In the remaining cases there was no family history of retinal disorders, with cases either being isolated or a sibling pair, thereby making the most likely mode of inheritance autosomal recessive.

Case	Sex	Age	Visual Acuity OD - OS	Fundus	Autofluorescence (AF) Imaging	ERG	OFF- responses	PERG	Colour Vision
1	F	21	6/60 - 6/60	Bilateral mild macular atrophy with temporal optic nerve pallor Figure 8.1D	Bilateral perifoveal rings of relative increased AF Figure 8.1E	Reduced and delayed cone responses. Supernormal and delayed rod responses.	Reduced with delay	ND	Bilateral protan phenotype with reasonable tritan discrimination
2	M	16	6/12 - 6/18	Bilateral mild macular atrophy with temporal optic nerve pallor	Early bilateral perifoveal rings of relative increased AF	Reduced and delayed cone responses. Supernormal and delayed rod responses.	Delayed	ND	Bilateral protan phenotype with reasonable tritan discrimination
3	F	37	6/24 - 6/24	Bilateral macular RPE changes with areas of atrophy & pigmentation	Bilateral central macular area of increased AF with a subtle surrounding ring of increased AF	Reduced and delayed cone responses. Supernormal and delayed rod responses.	Reduced with delay	Absent	Bilateral deutan phenotype with good tritan discrimination
4	M	27	6/36 - 6/60	Bilateral mild macular RPE disturbance with temporal optic nerve pallor	Bilateral decreased AF centrally with a surrounding ring of relative increased AF	Reduced and delayed cone responses. Supernormal and delayed rod responses.	Reduced with delay	Absent	Bilateral greater reduction in protan than deutan discrimination with good tritan function
5	M	36	6/36 - 6/60	Bilateral 'Bull's- eye maculopathy (BEM)-like' RPE changes Figure 8.1B	Bilateral central macular area of markedly increased AF surrounded by a ring of relative decreased AF Figure 8.1C	Reduced and delayed cone responses. Supernormal-like and delayed rod responses.	Reduced with delay	Absent	Bilateral deutan phenotype with reasonable tritan discrimination
6	F	26	6/24 - 6/24	Bilateral mild macular atrophy with temporal optic nerve pallor	ND	Reduced and delayed cone responses. Supernormal and delayed rod responses.	ND	Absent	Bilateral markedly reduced red/green discrimination with reasonable tritan function
7	F	25	6/36 - 6/60	Bilateral macular atrophy with mild temporal optic nerve pallor Figure 8.1A	ND	Reduced and delayed cone responses. Supernormal-like and delayed rod responses.	Delayed	Absent	Bilateral markedly reduced red/green discrimination with reasonable tritan function
8	F	18	6/60 - 6/60	Normal appearance	ND	Reduced and delayed cone responses. Supernormal and delayed rod responses.	ND	Absent	Bilateral deutan phenotype with good tritan discrimination
9	M	13	6/18 - 6/18	Normal appearance	ND	Reduced and delayed cone responses. Supernormal and delayed rod responses	Delayed	Absent	Bilateral markedly reduced red/green discrimination with reasonable tritan function

Table 8.1 Summary of clinical findings in COD/SuperROD

Patients 1 & 2 are brother and sister. Patients 6 and 7 are sisters.

RPE = retinal pigment epithelium

BEM = bull's-eye maculopathy

ND = not done

Case	Age	Refraction	Presenting	Current	Night blindness	Photopic and dark-adapted Perimetry
		OD OS	VA OD OS	VA OD OS		
1	21	-5.0/-0.50 x 90 -5.50 DS	6/24 6/24	6/60 6/60	No	Central and sup>inf widespread peripheral VF loss
2	16	-3.5/-0.75 x 50 -4.5/-0.50 x 130	6/12 6/12	6/12 6/18	No	Central and sup>inf widespread peripheral VF loss
3	37	-4.0/ -0.50 x 90 -4.50 DS	6/24 6/24	6/24 6/24	Yes	Central and sup>inf widespread peripheral VF loss
4	27	-4.0 /-1.5 x 180 -5.0/-2.0 x 180	6/36 6/36	6/36 6/60	Yes	Central and sup>inf widespread peripheral VF loss
5	36	-1.0/-1.5 x 65 -1.0/-2.25 x 120	6/12 6/18	6/36 6/60	Yes	Central and sup>inf widespread peripheral VF loss
6	26	-2.5/-1.0 x 160 -3.75/-0.5 x 45	-	6/24 6/24	No	ND
7	25	-2.0/-1.5 x 90 -2.50/-0.5 x 45	-	6/36 6/60	No	ND
8	18	-6.25/-3.25 x20 -7.0/-2.0 x 165	6/36 6/36	6/60 6/60	No	ND
9	13	-6.50/-0.25 x90 -6.50/-0.50 x10	6/12 6/12	6/18 6/18	No	ND

Table 8.2

Refraction, VA progression, nyctalopia and photopic visual fields

Sup = superior

Inf = inferior

ND = not done

> = greater than

VF = visual field

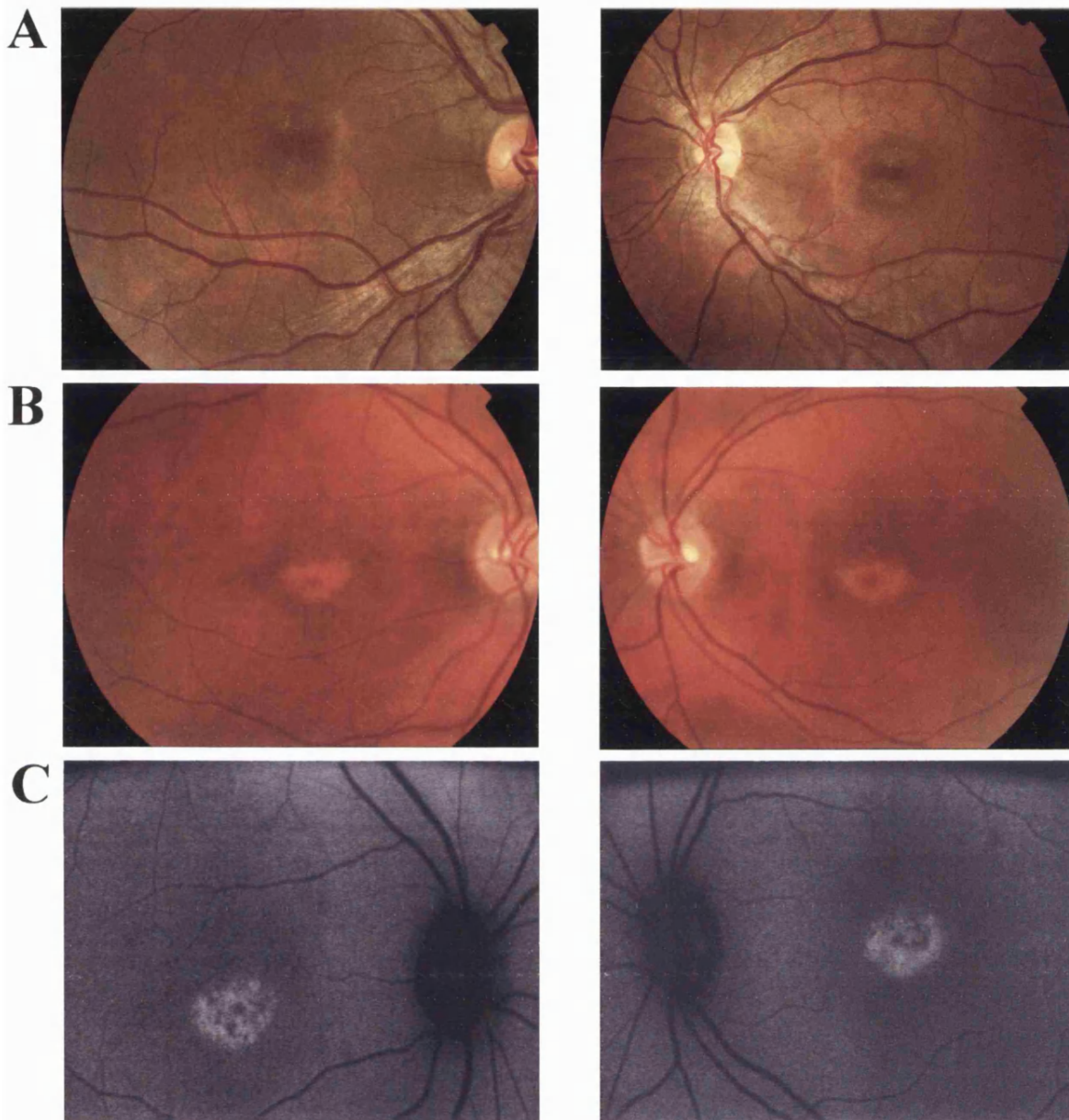


Figure 8.1

Colour fundus photographs and AF images in COD/SuperROD

Figure A Case 7 Fundus photographs showing bilateral macular atrophy, left worse than right.

Figure B Case 5 Fundus photographs showing bilateral 'Bull's-eye maculopathy (BEM)-like' RPE changes.

Figure C Case 5 AF imaging showing bilateral central macular areas of markedly increased AF surrounded by a ring of relative decreased AF.

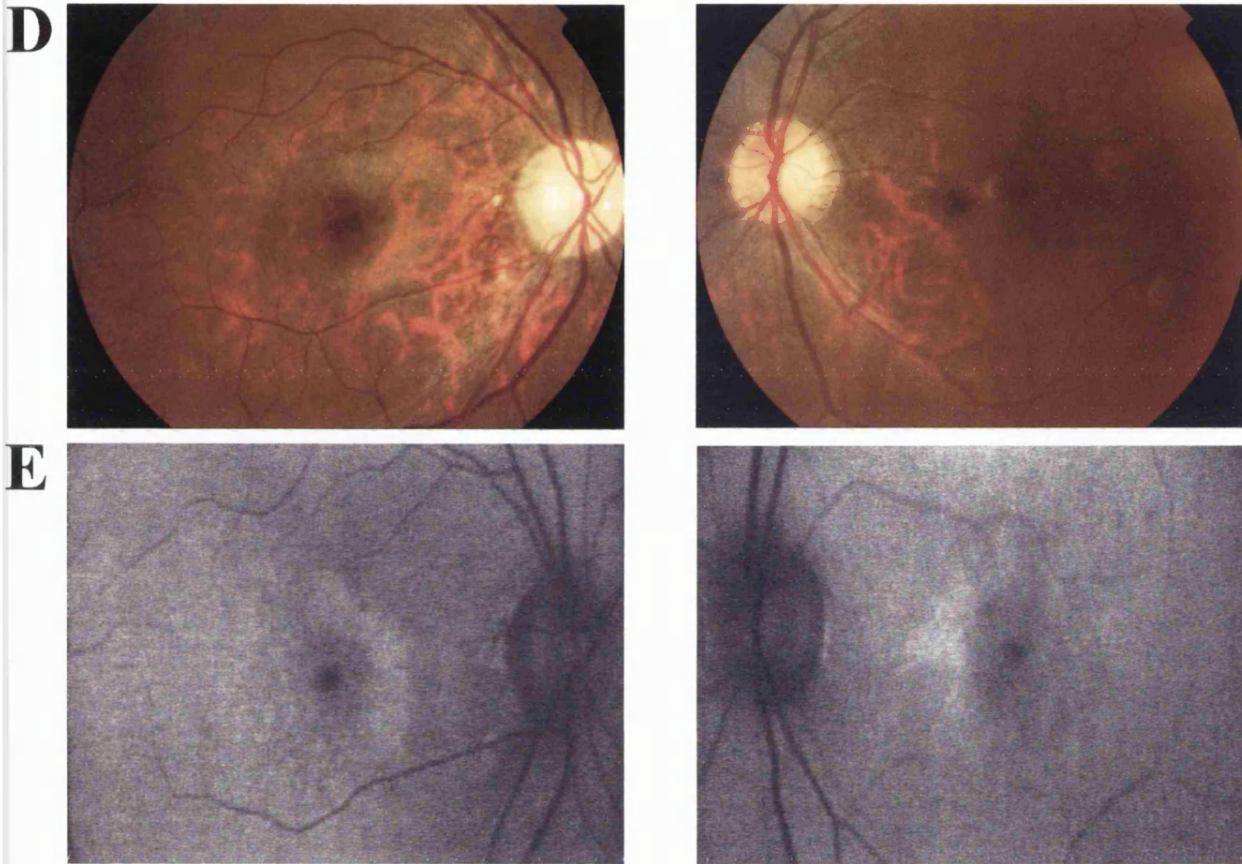


Figure 8.1

Figure D Case 1 Fundus photographs showing bilateral mild macular atrophy with mild temporal optic nerve pallor.

Figure E Case 1 Fundus autofluorescence imaging showing bilateral perifoveal rings of relative increased AF.

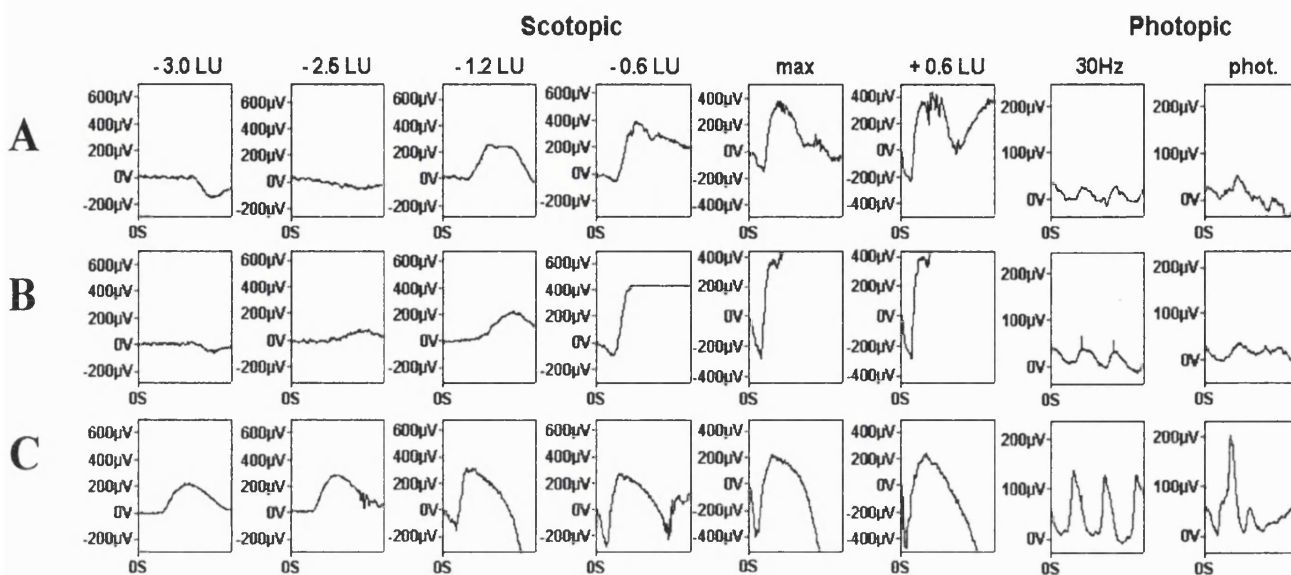


Figure 8.2 ERGs of cases 6 and 7

A = Case 6 B = Case 7

C = Data from a normal subject are shown for comparison.

Low intensity stimulation shows a waveform similar to a scotopic threshold response in the two patients. The ISCEV Standard rod response b-wave (-2.5LU) is not detectable in case 6, and although present in case 7, it is very delayed and subnormal. A relatively small increase in stimulus intensity then produced a disproportionately large b-wave increase in the patients compared with normal. At the highest intensity, there is a highly distinctive waveform with a reasonable a-wave amplitude, but the a-wave trough is broadened, and there is then a high amplitude b-wave. Cone single flash and flicker ERGs are delayed and reduced.

8.4.2 *NR2E3* mutation screening

Mutation screening of the nine exons and flanking splice-site regions of *NR2E3*, failed to identify any disease-causing sequence variants in four affected individuals (Cases 1 to 4).

8.5 DISCUSSION

The detailed phenotype of the cone dystrophy with supernormal rod responses (COD/SuperROD) has been described. Whilst ERG recordings are required to make a definitive diagnosis, we have found several consistent clinical features in our case series. The retinal dystrophy was characterised by onset in the first or second decades of life, with marked photophobia, myopia, reduced colour vision along the red-green axis with relatively preserved tritan discrimination, and central scotomata with peripheral widespread sensitivity loss predominating in the superior visual field. There was often RPE disturbance at the macula with a normal retinal periphery. AF imaging demonstrated either a perifoveal ring or a central macular area of relative increased AF. Nyctalopia is a later feature of the disorder. These clinical characteristics may be helpful in suggesting the presence of a COD/SuperROD phenotype.

AF imaging allows the visualisation of the RPE by taking advantage of its intrinsic fluorescence derived from its lipofuscin content. In three individuals AF imaging revealed a perifoveal ring of increased AF. In the two oldest subjects an area of increased AF was seen at the central macula. The presence of these two AF phenotypes suggests that over time there is a cumulative increase of autofluorescent material at the central macula. This increased lipofuscin is most likely to reflect the inability of the RPE to process outer segment debris, or alternatively increased outer segment turnover. It has been demonstrated histologically that the number of photoreceptor cells is reduced in the presence of increased

quantities of lipofuscin in the RPE, suggesting that autofluorescent material may accumulate prior to cell death (Dorey *et al.*, 1989; von Rückmann *et al.*, 1997).

The PERG was absent in all subjects in whom testing was performed, indicative of marked macular dysfunction. ERG testing revealed generalised dysfunction of rod and cone systems. In all subjects, at low light intensities rod-specific ERG amplitudes were found to be sub-normal, delayed, and undetectable at the lowest flash energies, but as the light intensity increased an abrupt increase in amplitude was seen, which at the higher flash energies may be at the upper limit of normal or exceed it (supernormal). The initial phase of both rod and cone a-waves was well formed suggesting that the kinetics of phototransduction are within normal limits and implying that this disorder is not a primary phototransduction abnormality. The ultimately high amplitude rod b-waves recorded suggest relatively normal inner nuclear layer function. Delayed recovery from the peak of the photopic b-wave, with no evidence of an i-wave, was seen in all individuals and is an unusual finding whose implication is unknown. The delayed OFF- responses recorded are an uncommon finding in retinal dystrophies and are again of uncertain significance. The electrophysiological data are consistent with a site of dysfunction that is likely to be post-phototransduction but pre-inner nuclear layer, most probably at the first synapse or alternatively at the horizontal cells. The putative synaptic abnormality would be in both rod and cone systems and may represent a 'gated mechanism,' whereby a threshold needs to be exceeded, following which transmission is restored. The period required to reach this threshold would correspond to the recorded delay in responses.

Evidence of disease progression has been suggested previously on clinical grounds alone (Gouras *et al.*, 1983). We have obtained electrophysiological data establishing definite progressive deterioration of retinal function, albeit in a single case. Four

individuals were aware of a progressive deterioration in VA and colour vision. Examination of clinical notes revealed that there had been a progressive reduction in recorded VA in two other patients who did not report such deterioration. In our case series there was a history of consanguinity in four families, namely first cousin marriages, and in the remaining cases there was no other family history of retinal disorders, indicative of an autosomal recessive mode of inheritance.

Cone and cone-rod dystrophies are usually characterised by a progressive loss of colour vision, with all three classes of cone photoreceptor affected, thereby producing colour vision defects along all three colour axes and often progressing to complete loss of colour vision over time. In our case series, detailed colour vision testing has revealed that all affected individuals had severely reduced colour discrimination predominantly along the red-green axes, and possessed far better residual tritan colour vision. In two subjects it was possible to establish a predominantly protan colour vision phenotype, whereas in three other individuals a deutan phenotype was present. Colour vision data reported previously is variable and sparse. Tritan function was well preserved in all subjects and may be a useful finding to suggest the diagnosis of COD/SuperROD. The explanation for this observation is however unclear but may relate either to a lower susceptibility of S-cones to the disease process than L-/M- cones; or given that the site of disease may be post-receptoral, to an alternate mode of post-receptoral process for S-cones that is not available to L-/M- cones. This latter process may be similar to that proposed for blue cone monochromatism, whereby colour discrimination is derived via a comparison of quantum catches in the S-cones and rods (Reitner *et al.*, 1991).

In view of the enhanced electrophysiological responses seen in the two cone dystrophies, ESCS and COD/SuperROD, and the fact that rod photoreceptors share more

properties in common with S-cones than with L-/M- cones, we performed mutation screening of *NR2E3* in a subset of our affected subjects but failed to identify any disease-causing sequence variants in these individuals. This has not been previously reported.

We have been able to characterise the COD/SuperROD phenotype in some detail and thereby gain an insight into disease progression, prognosis and pathogenesis. In the absence of any clear link between this unusual retinal disorder and a known retinal process, the identification of the gene mutated in this disorder would appear to be currently the only way to elucidate the disease mechanisms. The high prevalence of consanguinity identified in this case series suggests that there may be suitable families for homozygosity mapping to assist in isolating the molecular genetic basis of this condition.

8.6 CONCLUSIONS

This is the largest case series to date in which the clinical, psychophysical and electrophysiological characteristics of this unusual cone dystrophy with supernormal rod responses have been described.

Whilst the definitive diagnosis can only be made with electrophysiological testing, we have presented several characteristics that may increase suspicion of this diagnosis. We have identified a consistent colour vision phenotype of a relative sparing of tritan discrimination, we have presented novel AF data, and we can confidently identify an autosomal recessive mode of inheritance.

CHAPTER 9

AN AUTOSOMAL DOMINANT CONE-ROD DYSTROPHY (CORD7)

9.1 INTRODUCTION

The cone-rod dystrophies (CORDs) are a clinically heterogeneous group of retinal disorders which are characterised by reduced central vision, nystagmus, photophobia and poor night vision. The age of onset is variable, but many patients present in the first two decades of life.

CORDs are also genetically heterogeneous; autosomal dominant, autosomal recessive and X-linked recessive inheritance, have all been reported, and a number of causative genes and chromosomal loci have now been identified (section 1.1.3.2 and **Table 1.2**). When an inheritance pattern can be reliably established, it is most commonly autosomal dominant (ad) (Krill *et al.*, 1973; Moore, 1992). Currently six genes have been shown to be associated with adCORD; *CRX* (Freund *et al.*, 1997), *GUCY2D* (Kelsell *et al.*, 1998b; Udar *et al.*, 2003), *RIMI* (Johnson *et al.*, 2003), *Peripherin/RDS* (Nakazawa *et al.*, 1996), *GUCA1A* (Downes *et al.*, 2001), and *AIPL1* (Sohocki *et al.*, 2000), with more remaining to be discovered. Mutations in *ABCA4* are believed to be the commonest cause of autosomal recessive CORD (Maugeri *et al.*, 2000; Fishman *et al.*, 2003).

The adCORD, CORD7, was originally mapped in a four-generation, non-consanguineous British family to a 7cM region of chromosome 6q14, flanked by the markers D6S430 and D6S1625 (Kelsell *et al.*, 1998a). Recently, a candidate gene screening approach has identified a mutation in the Rab3A-interacting molecule (*RIMI*) gene in CORD7 (Johnson *et al.*, 2003). The G to A point mutation results in an Arg844His substitution in the highly conserved C₂A domain of the RIM1 protein and was found to segregate with disease. *RIMI* is expressed in brain and retinal photoreceptors where it is localised to the pre-synaptic ribbons in ribbon synapses, with the protein product believed

to play an important role in synaptic transmission and plasticity (Wang *et al.*, 1997; Lonart, 2002; Sun *et al.*, 2003).

9.2 AIMS

To perform a detailed study of the *CORD7* phenotype, in order to assist our understanding of the effects of the *RIMI* mutation on retinal function, and to gain insight into the disease mechanisms.

9.3 PATIENTS AND METHODS

9.3.1 Patients

A four-generation, non-consanguineous British family with an autosomal dominant cone-rod dystrophy (*CORD7*, OMIM 603649) was ascertained (**Figure 9.1**).

After informed consent, a detailed medical and ophthalmic history was obtained and a full ophthalmological examination performed. Affected subjects also underwent electrophysiological testing, automated photopic and dark-adapted perimetry, dark adaptometry, colour vision assessment, colour fundus photography and fundus autofluorescence imaging. Individuals were diagnosed as affected on the basis of the presence of retinal abnormality and in most cases associated decreased visual acuity.

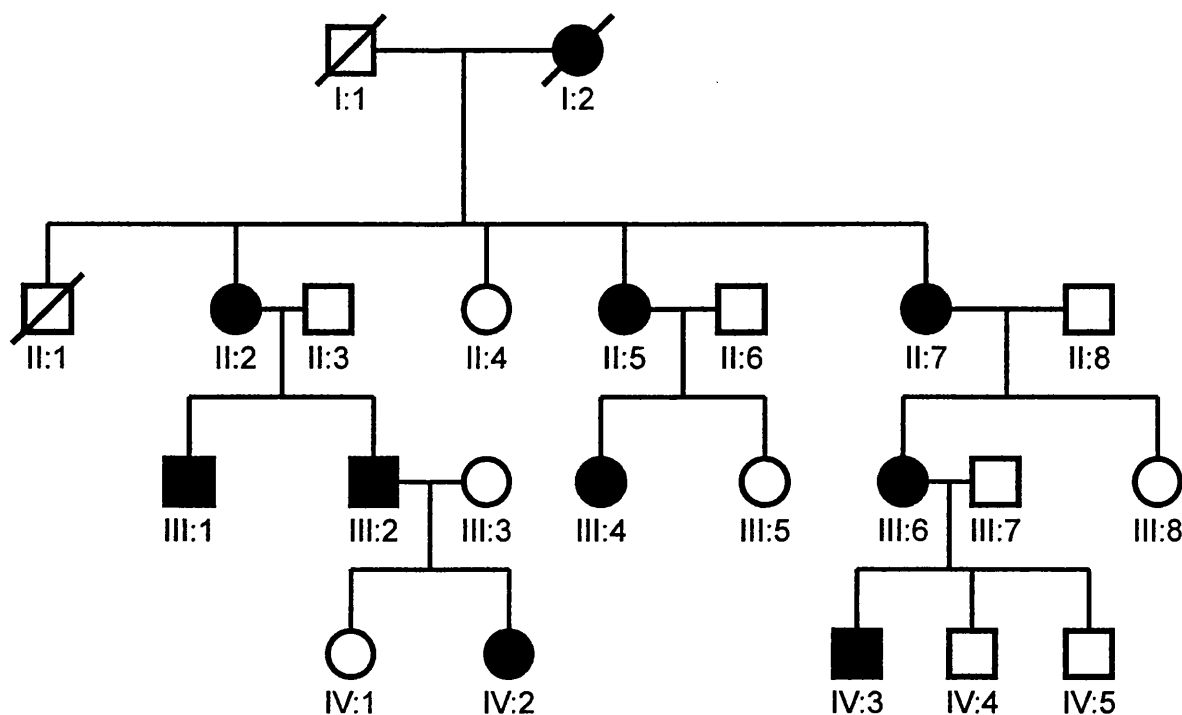


Figure 9.1

Four-generation pedigree of a British family with autosomal dominant cone-rod dystrophy (CORD7)

9.3.2 Methods

Fundus autofluorescence imaging was undertaken using the confocal scanning laser ophthalmoscope (cSLO) (Zeiss Prototype; Carl Zeiss Inc, Oberkochen, Germany). Electrophysiological assessment included an electro-oculogram (EOG), full-field electroretinogram (ERG) and pattern ERG (PERG), incorporating the protocols recommended by the International Society for Clinical Electrophysiology of Vision. Colour vision testing was performed using the Hardy, Rand, Rittler (HRR) plates (American Optical Company, New York).

Five affected subjects underwent detailed perimetry and dark adaptation. Static threshold perimetry in the dark- and light-adapted states was performed using a Humphrey

field analyser (Allergan Humphrey, Hertford, UK). For dark-adapted visual fields, the pupil was dilated with 2.5% (w/v) phenylephrine hydrochloride and 1% (w/v) tropicamide, and the patient was dark adapted for 45 minutes. The Humphrey field analyser was modified for use in dark-adapted conditions (Alexander and Fishman, 1984b; Jacobson *et al.*, 1986; Steinmetz *et al.*, 1993). An infrared source illuminated the bowl, and an infrared monitor (Phillips, Eindhoven, Holland) was used to detect eye movements. Fields were recorded using the central 30-2, peripheral 30/60-2, and macular programs. The target size corresponded to Goldmann size V for peripheral testing and to Goldmann size III for macular programs. Each was performed with a red (dominant wavelength, 650nm) and then blue (dominant wavelength, 450nm) filter in the stimulus beam.

For dark adaptometry, two test locations were chosen at 3° and 9°. The Humphrey field analyzer used was controlled by a custom computerised program (PS/2 model 50; International Business Machines, Armonk, NY) (Alexander and Fishman, 1984b; Chen *et al.*, 1992). Fully dark-adapted thresholds were measured at the two coordinates with the blue filter in the stimulus beam before exposure to the adapting light.

9.4 RESULTS

The autosomal dominantly inherited *CORD7* was present in a four-generation British family as shown in **Figure 9.1**. The age of onset of symptoms was variable and ranged from the second to the fifth decade of life. Most individuals described a progressive deterioration in central vision, night vision and peripheral visual field constriction especially during the third and fourth decades. Affected subjects experienced mild photophobia and had no evidence of nystagmus. The visual acuity ranged from 6/6 to 3/60. Mild to moderate dyschromatopsia was detected in the majority of individuals.

Fundoscopy revealed a range of macular appearances varying from mild retinal pigment epithelial (RPE) disturbance to extensive atrophy and pigmentation (**Table 9.1, Figure 9.2**). Retinal vessels were attenuated in four individuals and peripheral areas of retinal atrophy were present in two subjects (**Figure 9.3**). Subject **II:5**, had previously been noted to have a ‘Bull’s-eye maculopathy’ (BEM) appearance and a fluorescein angiogram performed at that time was consistent with this (**Figure 9.4**). On review her fundus appearance had progressed, with extensive macular atrophy now being present. The clinical findings are summarised in **Table 9.1**. Patients **II:3, II:8** and **IV:1**, were asymptomatic, had normal clinical examination, and did not carry the *RIMI* mutation; and were therefore designated as unaffected. All the affected individuals studied in detail carried the *RIMI* mutation.

Autofluorescence (AF) imaging in the majority of individuals revealed decreased macular AF centrally surrounded by a ring of increased AF (**Figures 9.2 & 9.5**). The decreased AF corresponded to the retinal atrophy seen ophthalmoscopically. ‘Bull’s-eye’ lesions were present in two individuals, consisting of a ring of decreased perifoveal autofluorescence bordered peripherally and centrally by increased autofluorescence (**Figure 9.2B**).

The pattern ERG was abnormal in all affected individuals, in keeping with macular dysfunction, and full-field ERG showed abnormal cone and rod responses. The ERG was variably affected and in three mildly affected individuals, full-field ERGs were only marginally abnormal. Cone amplitudes were reduced to a greater extent than rod. 30Hz cone flicker ERG implicit times were normal in all subjects except **IV:3**, in whom implicit time was delayed. Delayed recovery from the peak of the photopic b-wave, with no evidence of an i-wave, was seen in older individuals. There is electrophysiological

evidence of progressive deterioration in retinal function in subject **IV:3** (**Figure 9.6**).

Representative electrophysiological traces appear in **Figure 9.7**.

Five affected individuals underwent detailed perimetry and dark adaptometry. Photopic testing demonstrated decreased sensitivity, ranging from 2 to 3 log units, with central visual field loss and the upper peripheral field being more severely affected than the lower. Dark-adapted perimetry revealed a similar reduction in both rod and cone sensitivities, with well localised central loss, and peripheral loss being greater in the superior field than the inferior. Peripheral visual field sensitivity losses ranged from 6 to 10dB (**Figure 9.8**).

Dark adaptometry performed in mildly affected individuals showed rod final threshold elevation but no abnormality of kinetics. In more severely affected subjects both rod and cone threshold elevation was detected, and in one individual the rod-cone break was not detectable.

Patient	Age	Visual Acuity OD - OS	Fundus	Autofluorescence (AF) Imaging	EOG	ERG	PERG	Colour Vision
II:2	81	6/60 – 6/60	Bilateral symmetrical macular atrophy and attenuated retinal vessels Figure 9.2E	Bilateral decreased AF corresponding to atrophy seen on ophthalmoscopy with a surrounding ring of relative increased AF	-	Reduced cone and rod responses	Absent	Bilateral medium protan, deutan & tritan defects
II:5	68	3/36 – 3/60	Bilateral macular atrophy; attenuated retinal vessels and peripheral areas of atrophy Figure 9.3	Bilateral decreased AF corresponding to atrophy seen on ophthalmoscopy with a surrounding ring of relative increased AF	-	Markedly reduced cone and absent rod responses	Absent	Bilateral medium protan, deutan & tritan defects
II:7	75	6/9 – 6/9	Bilateral 'Bull's-eye maculopathy	Concentric rings of increased and decreased AF	N	Borderline reduced maximal responses	Reduced	Bilateral mild protan, deutan & tritan defects
III:1	52	6/36 - 6/36	Bilateral macular RPE changes with areas of atrophy & pigmentation; attenuated retinal vessels with peripheral areas of atrophy Figure 9.3	Bilateral decreased AF centrally with a surrounding ring of relative increased AF	-	Cone responses more markedly reduced than rod	Absent	Bilateral mild protan, deutan & tritan defects
III:2	48	6/9 – 6/9	OD : RPE changes OS: Well-defined area of macular atrophy Figure 9.2A	OD : Concentric rings of increased and decreased AF OS : Decreased AF corresponding to atrophy seen on ophthalmoscopy with surrounding ring of relative increased AF Figure 9.2B	N	Borderline reduction	Absent	Bilateral mild protan, deutan & tritan defects
III:6	53	3/60 – 6/60	Extensive RPE atrophy and areas of pigmentation OD > OS; and attenuated retinal vessels	Bilateral decreased AF centrally with a surrounding ring of relative increased AF	-	Cone responses more markedly reduced than rod	Absent	Bilateral medium protan, deutan & tritan defects
IV:2	18	6/6 – 6/6	Bilateral mild macular RPE changes	Bilateral perifoveal rings of relative increased AF Figure 9.5	N	Borderline reduction	Reduced	N
IV:3	31	6/18 – 3/60	Extensive RPE atrophy and areas of pigmentation OS > OD Figure 9.2C	Bilateral decreased AF centrally with a surrounding ring of relative increased AF Figure 9.2D	-	Markedly reduced cone and rod responses	Absent	Bilateral mild protan, deutan & tritan defects

Table 9.1 Summary of clinical findings in CORD7

N = Normal BEM = 'Bull's-eye' maculopathy

EOG = Electro-oculography ERG = Electro-retinography PERG = Pattern ERG

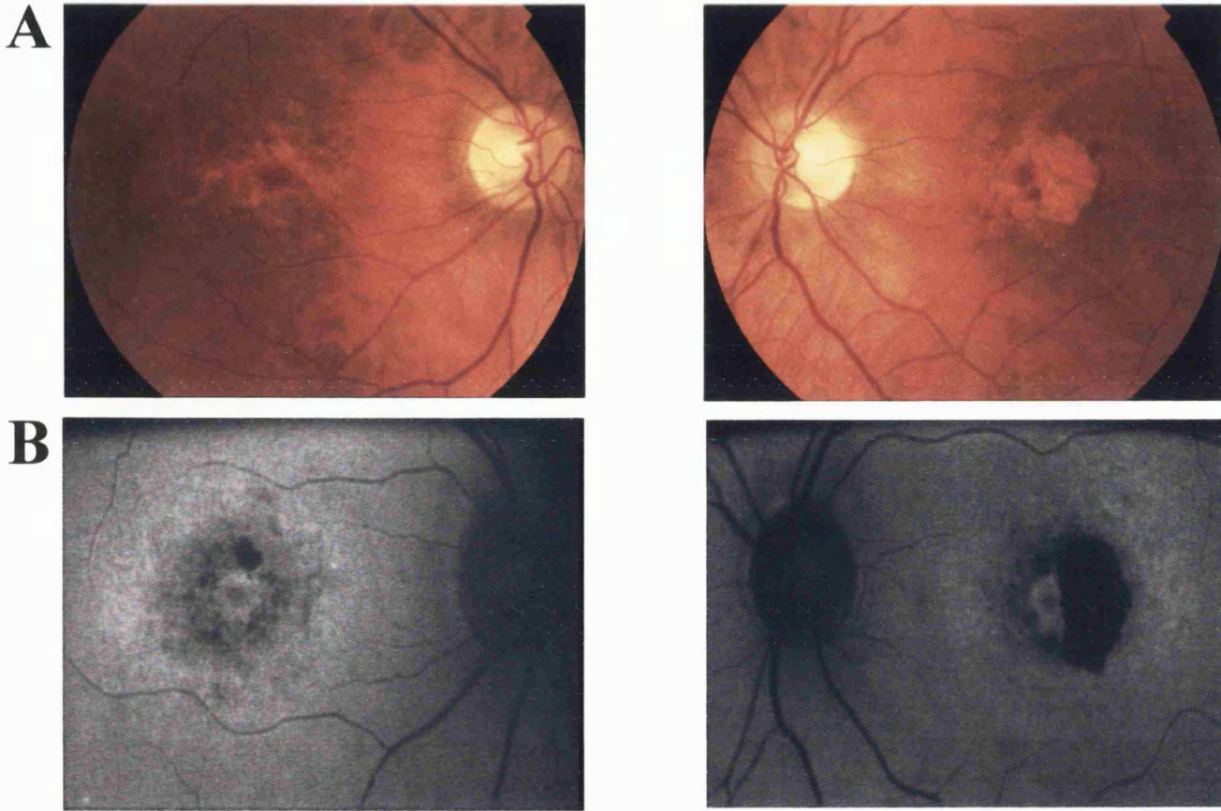


Figure 9.2A

Patient III:2 Fundus photographs showing bilateral macular RPE disturbance with a well-defined area of atrophy at the left macula.

Figure 9.2B

Patient III:2 Fundus AF imaging. **OD**: Concentric rings of increased and decreased AF in a BEM-like pattern. **OS**: Decreased AF corresponding to atrophy seen on ophthalmoscopy with a surrounding ring of relative increased AF.

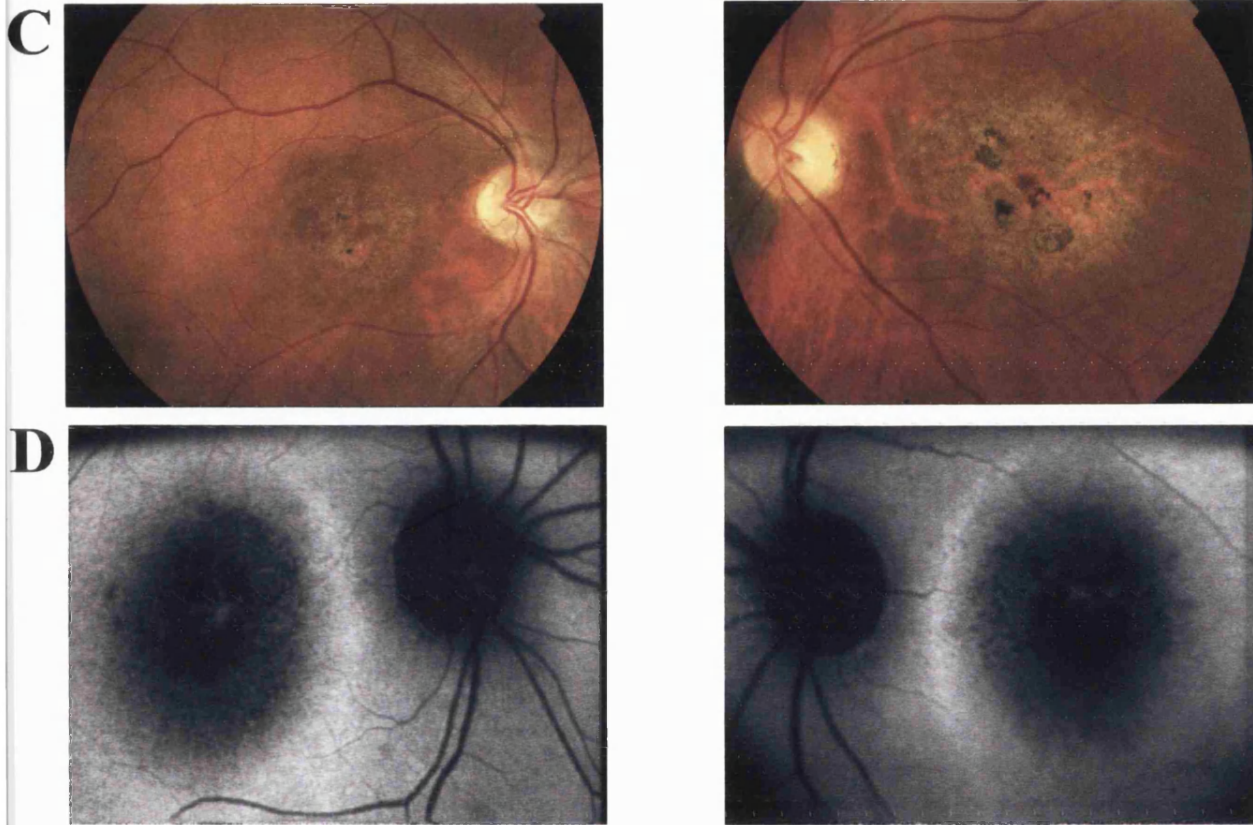


Figure 9.2C

Patient IV:3 Fundus photography showing extensive macular RPE atrophy and areas of pigmentation, worse in the left than right eye.

Figure 9.2D

Patient IV:3 Fundus AF imaging showing bilateral decreased AF centrally with a surrounding ring of relative increased AF.

E



Figure 9.2E

Patient II:2 Fundus photograph showing bilateral symmetrical well-circumscribed macular atrophy and attenuated retinal vessels.

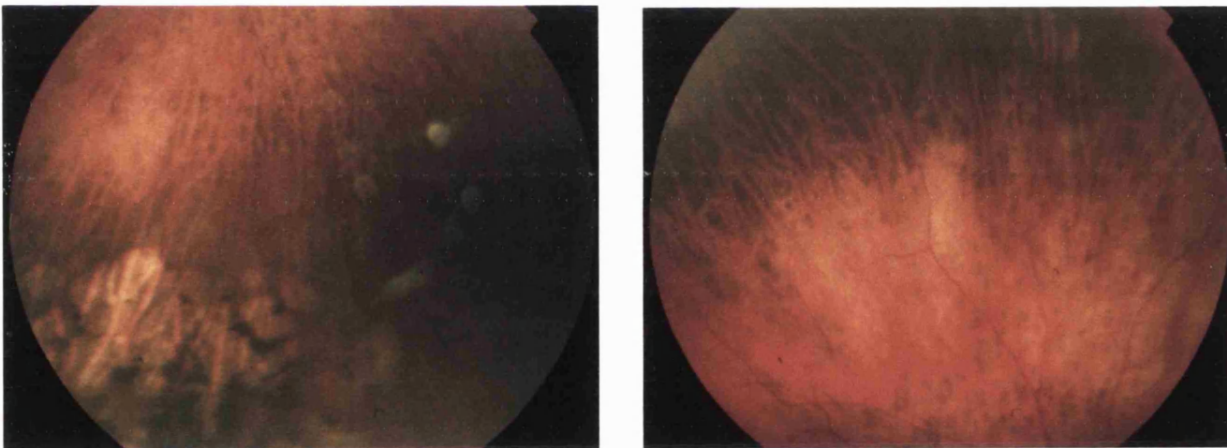


Figure 9.3

Peripheral retinal atrophy in CORD7

Fundus photographs of **II:5** & **III:1** showing areas of retinal atrophy.

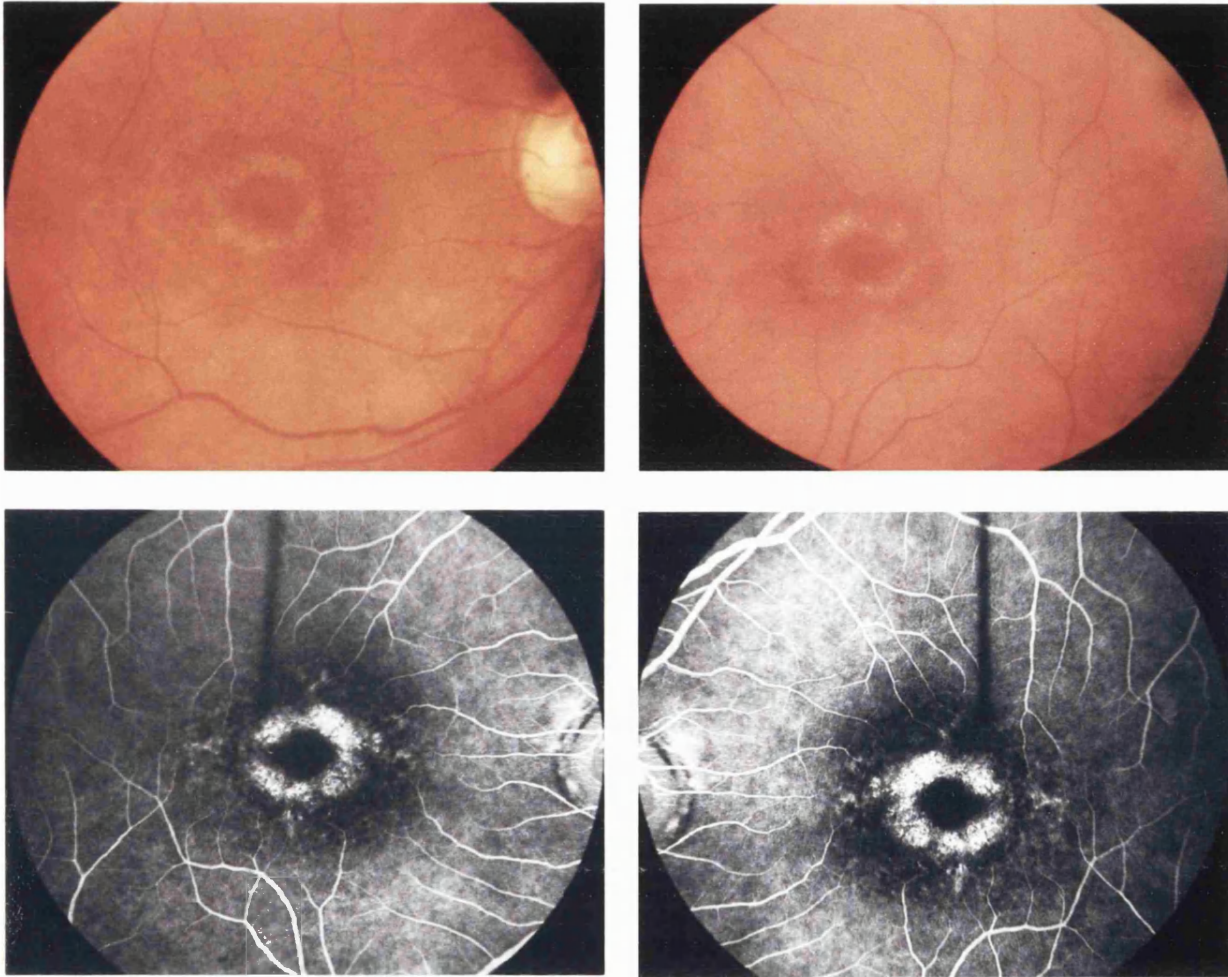


Figure 9.4

Fundus photographs and FFA of II:5,

showing a BEM appearance and a confirmatory fluorescein angiogram.

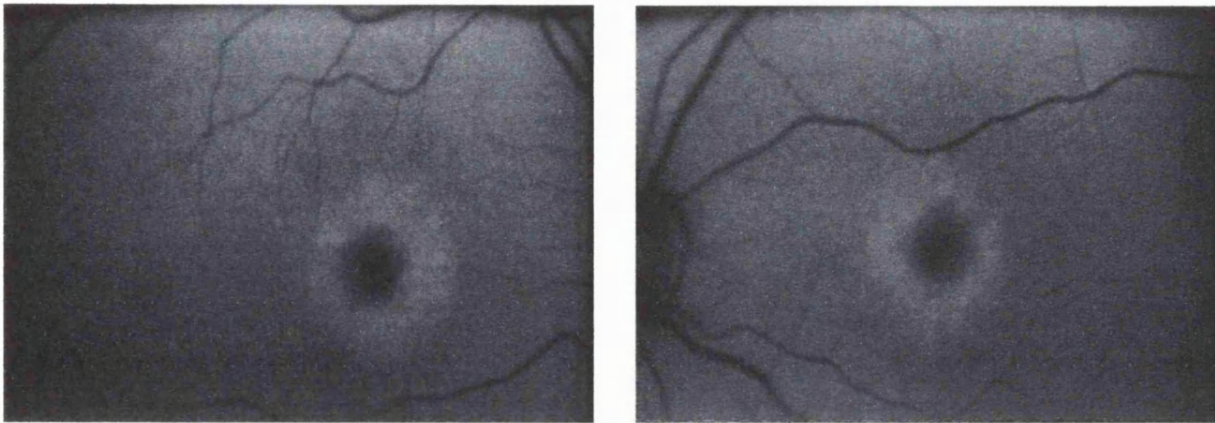


Figure 9.5

Fundus autofluorescence imaging of IV:2,
showing bilateral perifoveal rings of relative increased AF.

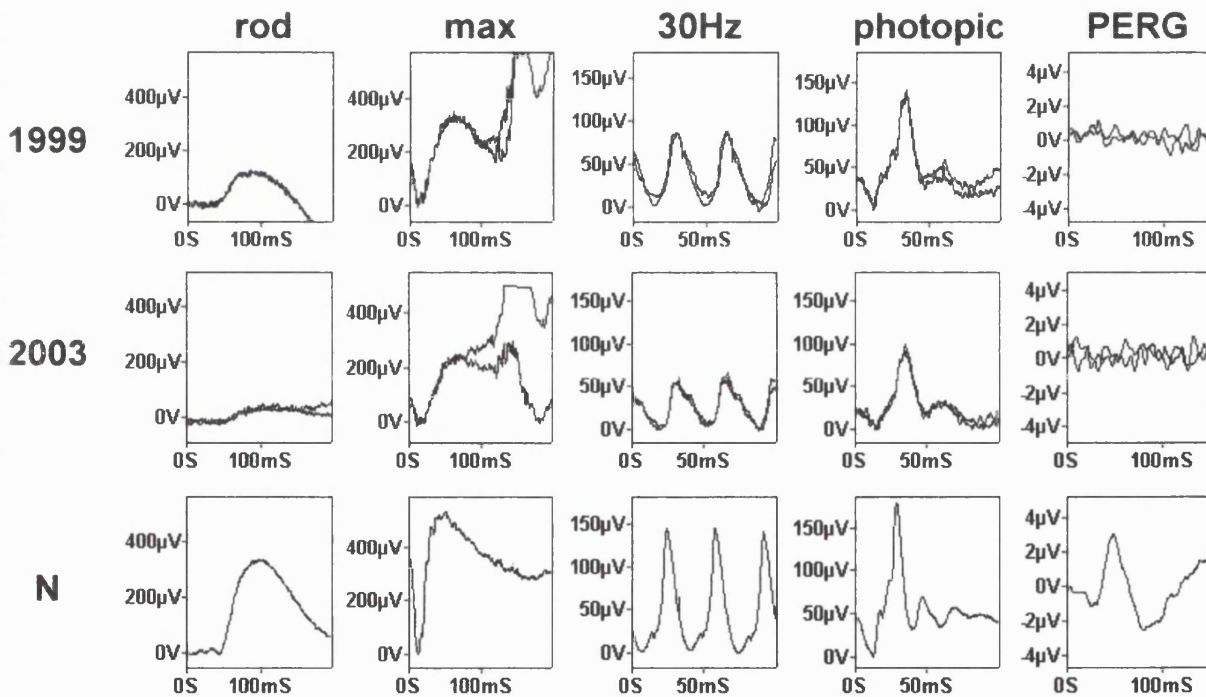


Figure 9.6

Patient IV:3 ERG data showing progressive deterioration of retinal function.

ERG findings demonstrate clear deterioration in rod specific ERG b-wave amplitude, and reduction in maximal response a-wave amplitude reflecting increasing loss of rod photoreceptor function. There are also changes in full-field cone derived ERGs. PERG was undetectable on both visits.

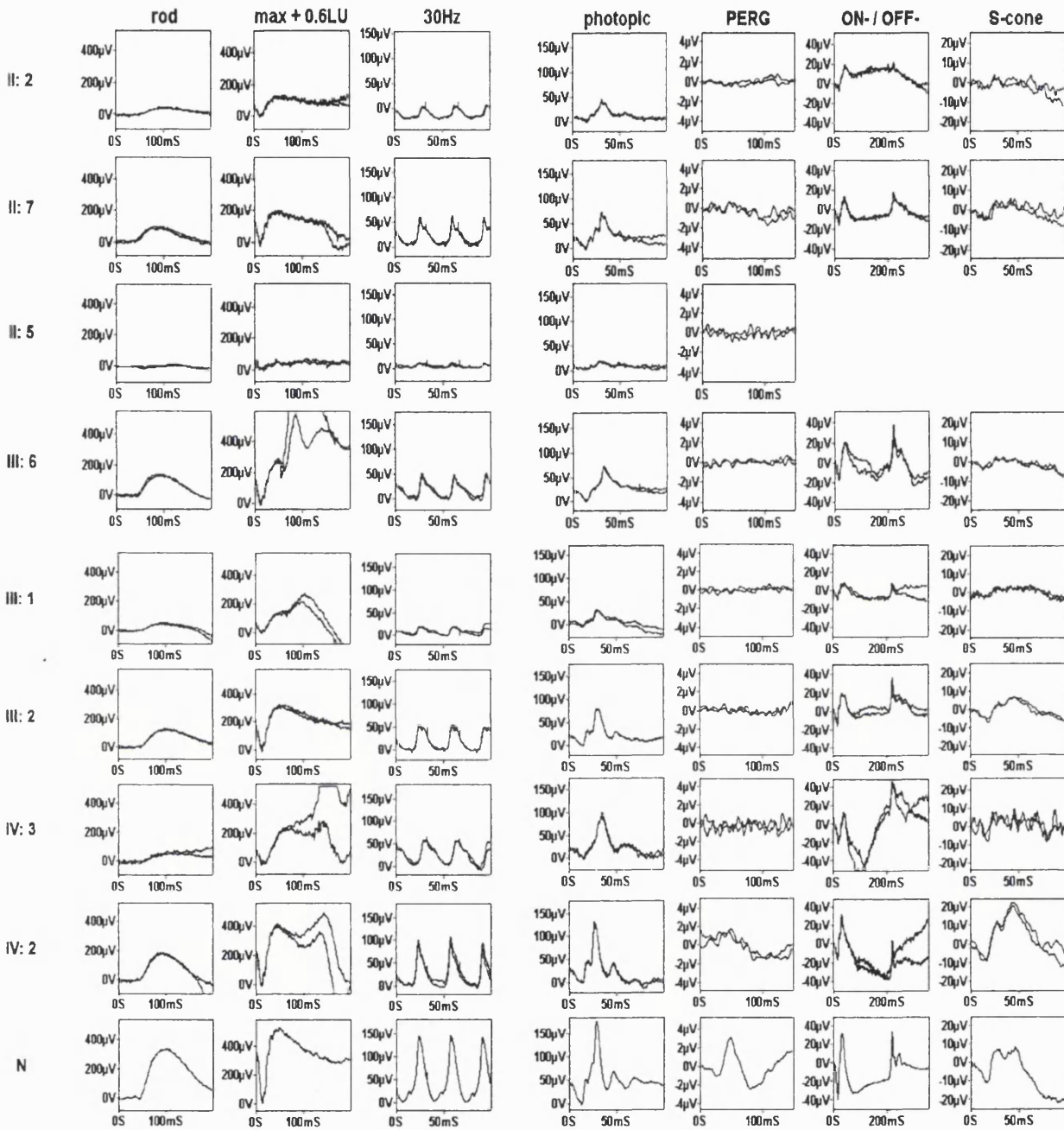


Figure 9.7

Electrophysiological traces from the patients examined,
with a normal (N) set of traces for comparison. (Legend on following page)

Figure 9.7 ERGs from the patients examined.

All show marked central cone dysfunction with pattern ERG being undetectable in most, and markedly reduced in the remaining patients.

Maximal response a-wave amplitude, a measure of rod photoreceptor function, is subnormal in all patients (Normal $> 250\mu\text{V}$ in young patients; $>200\mu\text{V}$ in older patients).

There is marked variation in severity within generations.

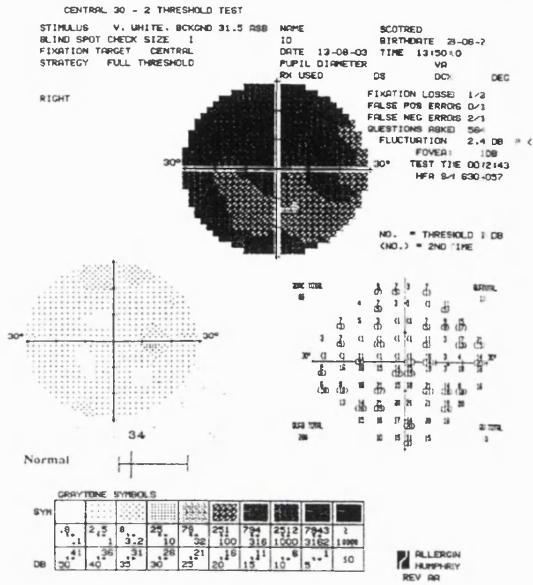
30Hz flicker ERG is abnormal in most patients (Normal $>70\mu\text{V}$ for younger patients; $>50\mu\text{V}$ in older patients), and is usually of normal implicit time, the only exceptions being **IV:3** where there is delay, and **III:6** where the values are borderline.

The absence of the i-wave, clearly seen in the normal and younger patients after the descent of the photopic b-wave, is of uncertain significance.

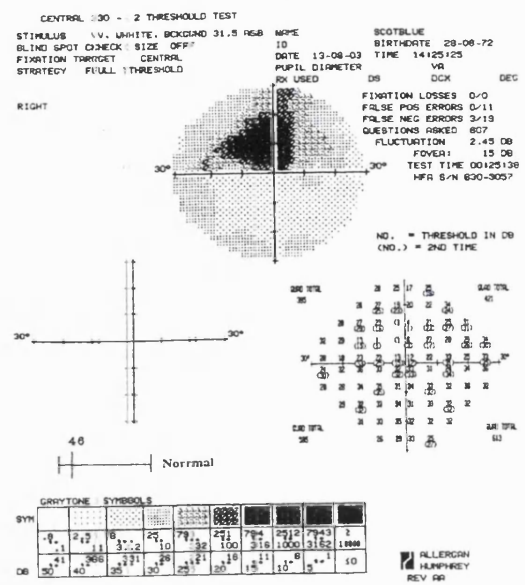
ÓN-/OFF- ERGs and short wavelength cone ERGs (S-cone) generally parallel the conventional cone ERGs, without specific preservation of any cone subsystem. The OFF-response is marginally delayed in patients **IV:3** and **III:6**.

IV:3

Scotopic Red

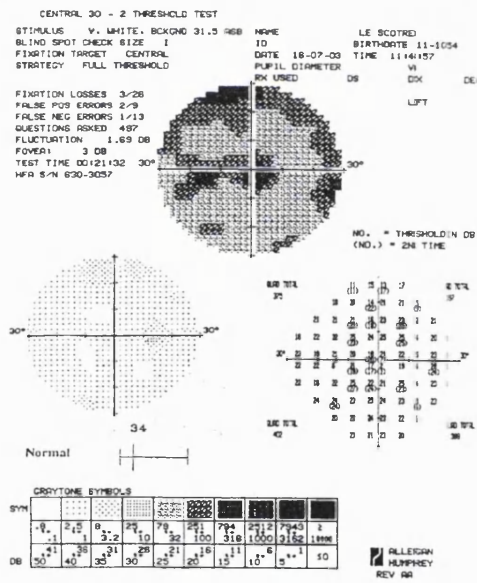


Scotopic Blue



III:2

Scotopic Red



Scotopic Blue

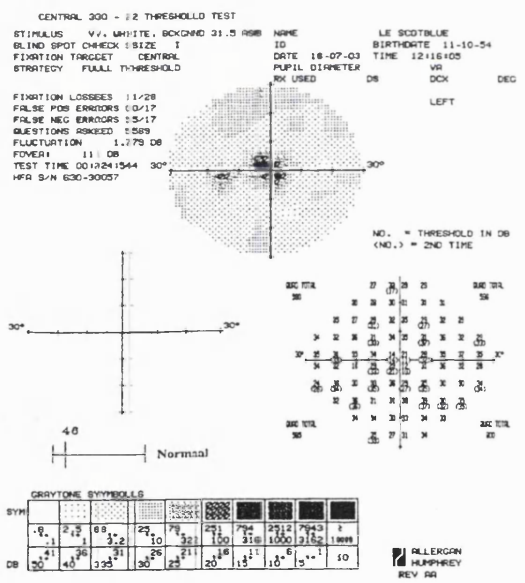


Figure 9.8

Scotopic red and blue 30° sati: threshold perimetry of IV:3 and III:2, showing central reduction of both central rod sensitivities, with peripheral loss being more marked in the inferior retina IV:3 more severely affected than III:2.

9.5 DISCUSSION

The detailed phenotype is described of the autosomal dominant cone-rod dystrophy, *CORD7*, associated with a point mutation in *RIMI*, a gene encoding a photoreceptor synaptic protein.

The phenotype is characterised by progressive deterioration in central vision, night vision and peripheral visual field, ophthalmoscopic abnormalities generally confined to the macula, and electrophysiological and psychophysical evidence of widespread cone and rod abnormalities; these findings are consistent with a *CORD*. The age of onset is variable, ranging from the second to fifth decades of life, with a worse visual prognosis generally associated with an earlier age of onset.

Subjects **II:7** and **III:2**, two of the least affected, first became symptomatic at the end of their fourth or early fifth decades and had a ‘bull’s-eye maculopathy-type’ phenotype, best demonstrated by AF imaging. Individuals with a more atrophic retinal phenotype described a steady progressive deterioration in their central vision throughout the third and fourth decades of life, with increasing night vision difficulties and awareness of constricted peripheral visual fields. One such individual, **II:5**, had previously been noted to have a BEM appearance and a fluorescein angiogram performed at the time was consistent with this diagnosis. The fundoscopic abnormalities were generally restricted to the macular region and ranged from mild RPE disturbance in the early stages to extensive chorioretinal atrophy and pigmentation.

Autofluorescence (AF) imaging allows the visualisation of the RPE by taking advantage of the fluorescent properties of lipofuscin (von Rückmann *et al.*, 1995; von Rückmann *et al.*, 1999). Affected subjects showed decreased AF corresponding to areas of atrophy seen ophthalmoscopically, which were encircled by a ring of increased AF. A perifoveal ring of

increased AF was also detected in the youngest individual (18-years-old), who had very mild RPE disturbance at the macula and was asymptomatic. The presence of a perifoveal ring may thus be an early indicator of affected status.

There is evidence of continuous degradation of autofluorescent material in the RPE (von Rückmann *et al.*, 1999). Progressive loss of lipofuscin occurs when there is reduced metabolic demand due to photoreceptor cell death, which results in areas of decreased AF in eyes with photoreceptor degeneration (von Rückmann *et al.*, 1999). It has been demonstrated histologically that the number of photoreceptors is reduced in the presence of increased quantities of lipofuscin in the RPE, in keeping with an accumulation of autofluorescent material prior to cell death (Dorey *et al.*, 1989; von Rückmann *et al.*, 1997b). It is therefore likely that in our family the ring of increased AF may represent the front of advancing concentric photoreceptor cell loss. It has been established that there is reduced sensitivity across the similar appearing ring of increased AF that can occur in retinitis pigmentosa, and a similar mechanism proposed (Robson *et al.*, 2003). This increase in lipofuscin may reflect either increased outer segment turnover or the inability of the RPE to process outer segment debris.

A bull's-eye maculopathy (BEM) was present in two family members, better seen on AF imaging than on direct ophthalmoscopy, in keeping with previous reports (Kurz-Levin *et al.*, 2002; Holder *et al.*, 2003). The pathogenesis of BEM is poorly understood. The characteristic appearance in which there is annular RPE atrophy and central sparing may correspond to the pattern of lipofuscin accumulation in the RPE, which in healthy individuals is highest at the posterior pole and shows a depression at the fovea (von Rückmann *et al.*, 1997b). BEM is a non-specific appearance that can occur in relation to a number of underlying disorders (Kearns and Hollenhorst, 1966; Krill *et al.*, 1973;

Deutman, 1974; Fishman *et al.*, 1977; O'Donnell and Welch, 1979; Kurz-Levin *et al.*, 2002).

The normal EOG suggests that there is no widespread dysfunction of the RPE, whilst the absent or markedly reduced PERG in all affected individuals demonstrates marked macular abnormality. ERG testing revealed no evidence of impaired synaptic transmission *per se*; there being no suggestion of electronegative ERG waveforms. Rod a-waves were profoundly abnormal suggesting that the primary site of dysfunction lies at the level of the photoreceptor. The unusual finding of a normal 30Hz flicker ERG implicit time suggests either that there is no significant abnormality of the phototransduction cascade, or that there is a rapid recovery from photoactivation, such as has been demonstrated in the cone dystrophy consequent upon mutation in retinal guanylate cyclase activating protein (GCAP1) (Downes *et al.*, 2001). A second unusual finding in older individuals was anomalous recovery from the peak of the photopic b-wave, with no evidence of an i-wave; the significance of which is unknown.

The Arg844His missense mutation located in the highly conserved C₂A domain of RIM1 was recently identified in the CORD7 family (Johnson *et al.*, 2003). The protein RIM1 localizes to the pre-synaptic active zone in conventional synapses and to pre-synaptic ribbons of ribbon synapses where it plays a critical role in the tethering of synaptic vesicles (Wang *et al.*, 1997; Betz *et al.*, 2001; Martin, 2002), although a post-docking role in regulating vesicle priming has also been suggested (Lloyd and Bellen, 2001; Koushika *et al.*, 2001). It is a large multi-domain protein with different regions responsible for the various interactions that it undertakes. Key domains are the N-terminal Rab3A-GTP binding site responsible for vesicle binding, and the two C-terminal C₂A domains that interact with other proteins in the synaptic complex, especially

synaptotagmin. The effect of the Arg844His mutation in the C₂A-domain may be to alter the affinity of RIM1 for either the α_{1D} -subunit of L-type Ca²⁺ channels or synaptotagmin (synaptic vesicle-associated Ca²⁺ sensor), and thereby the rate of synaptic vesicle docking and fusion in response to a Ca²⁺ signal (Johnson *et al.*, 2003). This may be expected to interfere with transmission at the photoreceptor synapse but electrophysiological testing of patients with *RIM1* mutations showed no evidence of inner retinal dysfunction, even in subjects with early disease. It thus remains likely that mutant RIM1 adversely affects function at the photoreceptor side of the synaptic complex, although abnormality of synaptic transmission itself has not been detected with current techniques.

This is the second example of a mutation in a protein with a potential role in synaptic function to give rise to a CORD phenotype; the first being a premature termination mutation in *UNC119*, a photoreceptor synaptic protein of undefined function that is also highly enriched in ribbon synapses (Kobayashi *et al.*, 2000). Histopathological assessment of a transgenic mouse model of this disorder showed synaptic degeneration (Kobayashi *et al.*, 2000). It is also of considerable interest that in a histopathological study of a patient with cone-rod dystrophy, the most prominent alteration seen in the retina was abnormal cone synapses, whereas such comparable synapse changes have not been reported in either rods or cones in other retinal dystrophies, including retinitis pigmentosa (Gregory-Evans *et al.*, 1998). This suggests that synaptic abnormalities may be a more common disease mechanism in CORD than other retinal disorders.

9.6 CONCLUSIONS

Although a number of different genetic mutations have been identified as causing cone-rod dystrophy, there have been few detailed phenotypic characterisation studies.

The detailed phenotype is described of the autosomal dominant cone-rod dystrophy, *CORD7*, which is associated with a point mutation in *RIMI*, a gene encoding a photoreceptor synaptic protein. The pattern of disease progression and long term visual outcome facilitates improved genetic counselling and advice on prognosis. Such phenotypic data will be invaluable in the event of future therapy.

CHAPTER 10

CONE-ROD DYSTROPHY ASSOCIATED WITH AMELOGENESIS IMPERFECTA

10.1 INTRODUCTION

The cone-rod dystrophies (CORDs) are a clinically and genetically heterogeneous group of progressive retinal disorders. They have similarities to the rod-cone or retinitis pigmentosa-type (RP) dystrophies, but can usually be distinguished on the basis of clinical findings and electrophysiology. The CORDs usually present with cone dysfunction-related symptoms, including photophobia, poor colour vision and reduced central visual function but with time poor night vision develops, reflecting rod photoreceptor involvement. CORD is usually an isolated finding; less commonly it may be associated with other systemic abnormalities, including dental anomalies. Syndromes with associated CORD are shown in **Table 10.1**.

The association of CORD with amelogenesis imperfecta (AI) has been reported only once previously in a large consanguineous Arabic family from the Gaza strip (Jalili and Smith, 1988). AI is an inherited group of disorders of tooth enamel deposition affecting enamel structure, composition, and thickness, and can be broadly divided into the primarily hypoplastic (quantitative defect with thin or missing areas of enamel but otherwise normal in structure) and hypomineralised/hypomature (qualitative defect of normal thickness enamel but poorly mineralised) variants. However, a new classification based on the molecular basis of the observed enamel phenotype will help to clarify the overlap in phenotypes that is commonly seen (Aldred *et al.*, 2003).

The disorder in the Arabic family mapped to a 2cM (5Mb) region on chromosome 2q11 that includes the *CNGA3* gene which encodes the α -subunit of the cGMP-gated cation channel in cone photoreceptors (Downey *et al.*, 2002). This represented a good candidate gene for this disorder since mutations in *CNGA3* are associated with the cone dysfunction syndrome achromatopsia and with cone dystrophy (Kohl *et al.*, 1998;

Wissinger *et al.*, 2001). However, no disease-causing sequence variants were identified in the family (Downey *et al.*, 2002).

We have ascertained a second family with the syndrome CORD associated with AI.

Syndromic CORD; OMIM Number	Mode of Inheritance	Locus	Mutated Gene	Systemic phenotype	References
CORD & Amelogenesis imperfecta; 217080	Autosomal recessive	2q11	Not identified	Defective tooth enamel	Downey <i>et al.</i> , 2002 Jalili and Smith, 1988
CORD & Spinocerebellar ataxia type 7; 164500	Autosomal dominant	3p12-13	<i>SCA7</i>	Cerebellar ataxia	Aleman <i>et al.</i> , 2002
CORD & Neurofibromatosis type 1; 136550	Autosomal dominant	17q	<i>NF1</i>	Neural tumours, skeletal defects, skin lesions, optic nerve glioma	Kylstra and Aylsworth, 1993
Bardet-Biedl syndrome; 209900, 606151, 600151, 600374, 603650, 607590	Autosomal recessive	11q13 16q21 3p13-p12 15q22.3-q23 2q31 20p12 4q27	<i>BBS1</i> <i>BBS2</i> Not identified <i>BBS4</i> Not identified <i>BBS6</i> <i>BBS7</i>	Polydactyly, obesity, variable mental retardation, hypogonadism	Mykytyn <i>et al.</i> , 2002 Nishimura <i>et al.</i> , 2001 Sheffield <i>et al.</i> , 1994 Mykytyn <i>et al.</i> , 2001 Young <i>et al.</i> , 1999 Katsanis <i>et al.</i> , 2000 Badano <i>et al.</i> , 2003
Alström syndrome; 203800	Autosomal recessive	2p13	<i>ALMS1</i>	Diabetes, obesity, deafness, other endocrine abnormalities	Collin <i>et al.</i> , 2002
CORD & Pierre-Marie ataxia; 212900	Autosomal dominant	Not identified	Not identified	Cerebellar ataxia	Bjork <i>et al.</i> , 1956
CORD & Trichomegaly; 204110	Autosomal recessive	Not identified	Not identified	Trichomegaly, synophrys, excessive facial and body hair	Jalili, 1989

Table 10.1
Syndromes with associated cone-rod dystrophy (CORD)

10.2 AIMS

To characterise in detail the ocular and dental phenotype of a rare autosomal recessive CORD associated with amelogenesis imperfecta, and to investigate aspects of the molecular genetic basis of the syndrome.

10.3 METHODS

Two affected siblings were identified in a two-generation, non-consanguineous Kosovan family. Subjects underwent detailed ophthalmological and dental examination.

Blood samples from affected and unaffected family members were taken for DNA extraction. Mutation screening of *CNGA3*, a previously identified candidate gene, was performed in addition to segregation analysis of the microsatellite marker, D2S2187, located 0.1Mb from *CNGA3*. mRNA extraction was performed from the first molars and lower incisors of E19 (birth)- and P2 (21 days post coïtum) -day CD1 mice, and following cDNA synthesis, transcripts of *CNGA3* and *CNGB3* were sought.

10.3.1 *Clinical assessment*

A two-generation Kosovan family with an autosomal recessive cone-rod dystrophy and amelogenesis imperfecta was examined (**Figure 10.1**).

10.3.1.1 Ocular

A full medical and ophthalmic history was obtained and an ophthalmological examination performed. The affected siblings also underwent colour fundus photography and electrophysiological assessment which included an ISCEV standard EOG, flash ERG and pattern ERG. Detailed colour vision testing (section 1.3.4.1) of the two affected brothers and their parents was performed. This included the use of the HRR plates, FM

100-hue test, Farnsworth D-15/PV-16, the M-R minimal test, a computerised colour vision test and anomaloscopy. The FM 100-hue, Farnsworth D-15/PV-16 and the M-R test were all performed under CIE Standard Illuminant C from a MacBeth Easel lamp.

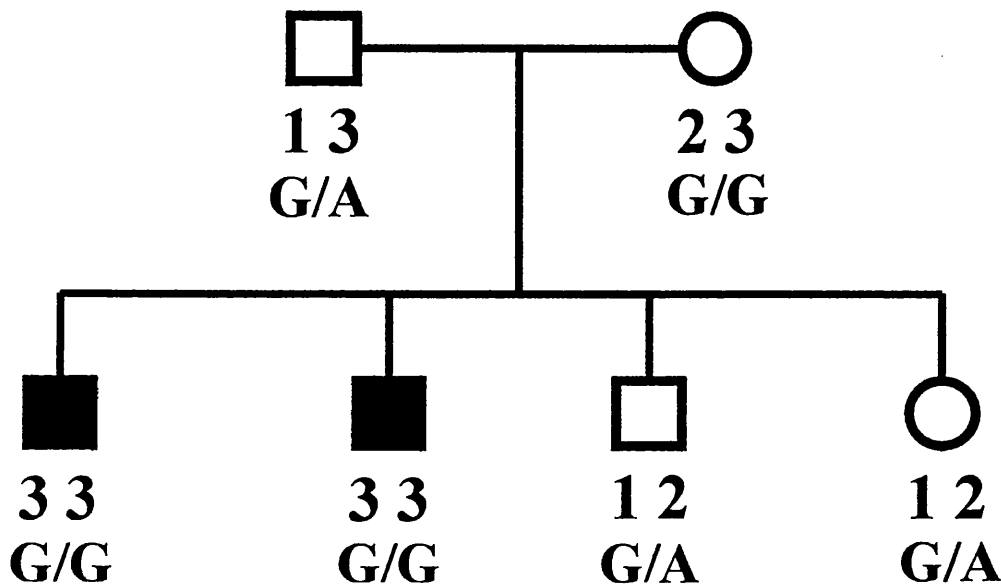


Figure 10.1

Two-generation pedigree of a Kosovan family with autosomal recessive cone-rod dystrophy and amelogenesis imperfecta

(The alleles present for the microsatellite marker, D2S2187, and the segregation of a SNP in *CNGA3*, are both shown)

10.3.1.2 Dental

The two affected brothers underwent a detailed dental assessment including radiographic examination (orthopantomograms). Primary teeth, extracted from both brothers for clinical reasons, were examined histologically. The dental assessment was undertaken by Dr Agnes Bloch-Zupan, Department of Paediatric Dentistry, Eastman Dental Institute for Oral Health Care Sciences, University College London.

10.3.2 Molecular genetics

10.3.2.1 *CNGA3* mutation screening

The coding sequences of *CNGA3* were amplified by PCR in each individual using primer sequences and conditions as previously published (Kohl *et al.*, 1998). Standard 50µl PCR reactions were performed as described previously. After resolution on a 1% (w/v) LMT agarose gel, products were excised and eluted. Direct sequencing of PCR products was carried out on an ABI 3100 Genetic Analyser using the original PCR primers in the sequencing reactions. The sequence was examined for alterations utilising *Sequencing Analysis* (ABI Prism™) and *GeneWorks*™ software.

10.3.2.2 Genotyping

Genotyping was carried out utilising the marker D2S2187, with the forward PCR primer being fluorescently labelled (**Table 10.2**). PCR reactions were carried in a 25µl reaction volume, containing 125ng DNA, 1 x NH₄ buffer (Bioline™), 1mM MgCl₂, 200µM each dNTP, 2.50pmols each of forward and reverse primer and 1U *BioTaq*. The thermocycling profile used consisted of an initial denaturation of 4 minutes at 95°C, immediately followed by 35 cycles of 95°C for 15 seconds, 61°C for 30 seconds and 72°C for 30 seconds, with a single final extension step of 72°C for 5 minutes.

PCR products were diluted and denatured in formamide and size-fractionated using an ABI 3100 Genetic Analyser. PCR products were automatically sized by the 3100 Data Collection Software version 1.0.1 program using ROX as the size standard and scored using the GeneMapper version 2.0 program.

Primer name	Sequence (5'-3')	T _a °C	Product size (bp)
D2S2187 F	gctccaaaccagcctc	61	133-159
D2S2187 R	gaagcctcacaatgcaac		

Table 10.2
D2S2187 primers

10.3.2.3 RNA extraction and precipitation

Messenger RNA (mRNA) was extracted from the first molars and lower incisors of 19- (E19=P0) and 21-day (P2) CD1 mice using the QuickPrep[®] *Micro* mRNA Purification Kit (Pharmacia Biotech). The dental tissue was homogenised in an extraction buffer containing a high concentration of guanidium thiocyanate. The extract was then diluted three-fold with an elution buffer (10mM Tris-HCL (pH 7.5), 1mM EDTA) and centrifuged to produce a clear homogenate. The mRNA isolation was achieved by passing the homogenate through an Oligo(dT)-Cellulose pellet. This pellet was then washed several times in high and low salt buffers before the mRNA was eluted at 65°C in 0.4 ml of elution buffer.

In order to precipitate the mRNA, a 1/10 volume of K Acetate solution (2.5 M), 10µl of a glycogen solution (5-10 mg/ml), and 1ml of 95% (v/v) ethanol were added, followed by overnight storage at -20°C. Precipitated mRNA was collected the following day by centrifugation, dried and dissolved in 50µl of elution buffer.

10.3.2.4 RT-PCR

cDNA synthesis from an mRNA template was achieved by using the Superscript First-Strand Synthesis System (GibcoBRL). The mRNA was targeted with an oligo(dT)₁₂₋₁₈ primer (0.5µg) and cDNA synthesis was performed by the Superscript II RT enzyme

(50U). RNase H was added to remove the RNA, leaving only cDNA viable as a template for subsequent PCR reactions.

10.3.2.5 *CNGA3* and *CNGB3* expression studies

cDNA synthesised from the E19- and P2-day murine dental tissue was used as a template in 50µl PCR reactions using primers designed against murine *CNGA3* and *CNGB3* sequences (Table 10.3). As a positive control, primers designed against the murine house-keeping gene, *GAPDH*, were used with both 19- and 21-day tooth cDNA. The efficacy of the designed *CNGA3* and *CNGB3* primers was tested on murine whole eye cDNA.

Primer name	Sequence (5'-3')	T _a °C	Product size (bp)
CNGA3 F	agtcttctataactggtgtc	54	480
CNGA3 R	cgggagagtcgtgcatac		
CNGB3 F	atgtcgagcagaactcac	52	480
CNGB3 R	agatgatatcacatacgatg		

Table 10.3
Primers for amplification of murine *CNGA3* and *CNGB3*

10.4 RESULTS

10.4.1 *Phenotype*

10.4.1.1 Ocular

The two affected brothers presented in the first few years of life with nystagmus, marked photophobia and reduced visual acuity. Both brothers complained of progressive deterioration of central vision with later development of difficulties with night vision. When examined at age 8 and 10-years-old respectively, both brothers had a visual acuity

of 3/60 in each eye and each had fine pendular nystagmus. There was no strabismus. Fundus examination revealed bilateral macular atrophy and pigmentation (**Figure 10.2**).



Figure 10.2

*Fundus photographs showing bilateral macular
RPE mottling and atrophy*

Both brothers were hypermetropic and astigmatic; OD +6.50/-2.0 x12, OS +6.0/-2.0 x170 and OD +4.50/-1.75 x10, OS +4.50/-1.5 x170. Full-field ERG testing revealed no detectable photopic cone responses. Rod function was markedly abnormal (**Figure 10.3**).

Two ERGs performed four years apart were suggestive of progressive deterioration of retinal function. Detailed colour vision testing failed to demonstrate any residual colour vision.

Their parents and unaffected siblings were also assessed. They were asymptomatic and had a normal ocular clinical examination.

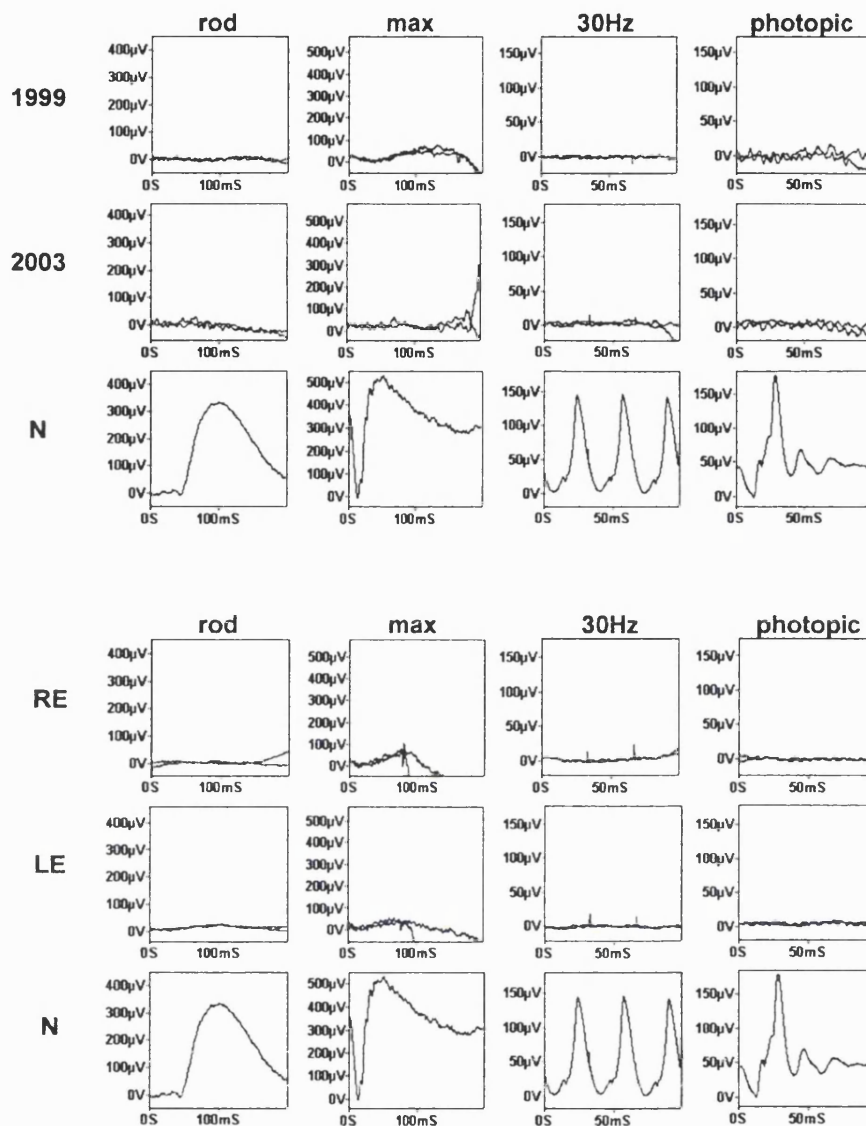


Figure 10.3
Electrophysiological testing

The upper set of traces, from the right eye of the 10-year-old patient in October 1999 and May 2003 compared with a normal subject. The cone derived 30Hz flicker and single flash photopic ERGs were undetectable on both occasions. The rod-specific ERG was undetectable on both occasions. The maximal response contained a detectable but delayed and profoundly subnormal amplitude a-wave with a delayed subnormal b-wave in 1999, but showed significant deterioration by 2003 with only residual detectable activity. The left eye findings (not shown) did not differ significantly.

The lower set of traces, from both right and left eyes of his 8-year-old brother compared with a normal subject, show undetectable photopic single flash and flicker ERGs, and severely reduced but detectable maximal responses.

The electrophysiological findings in both patients were in keeping with a severe cone-rod dystrophy.

10.4.1.2 Dental

Both brothers had the inherited enamel defect, amelogenesis imperfecta (**Figure 10.4**).

Primary teeth extracted for clinical reasons were examined histopathologically. Analysis of the lower second right primary incisor of the 8-year-old boy revealed a normal deciduous tooth appearance with enamel of relatively normal thickness and normal root structure. There was evidence of attrition. On decalcified sections the dentin was essentially normal with no evidence of residual enamel matrix. However, microscopic histology of the 10-year-old brother's primary canine revealed that the enamel showed areas of hypoplasia with thinning and irregular root structure. There was no evidence of hypomineralisation on decalcified sections.

These features when taken together are those of a hypoplastic/hypomineralised variant of AI, and also demonstrate that the defect might not be homogeneous in all sectors of the primary dentition. It is possible that the same would apply for the permanent dentition.

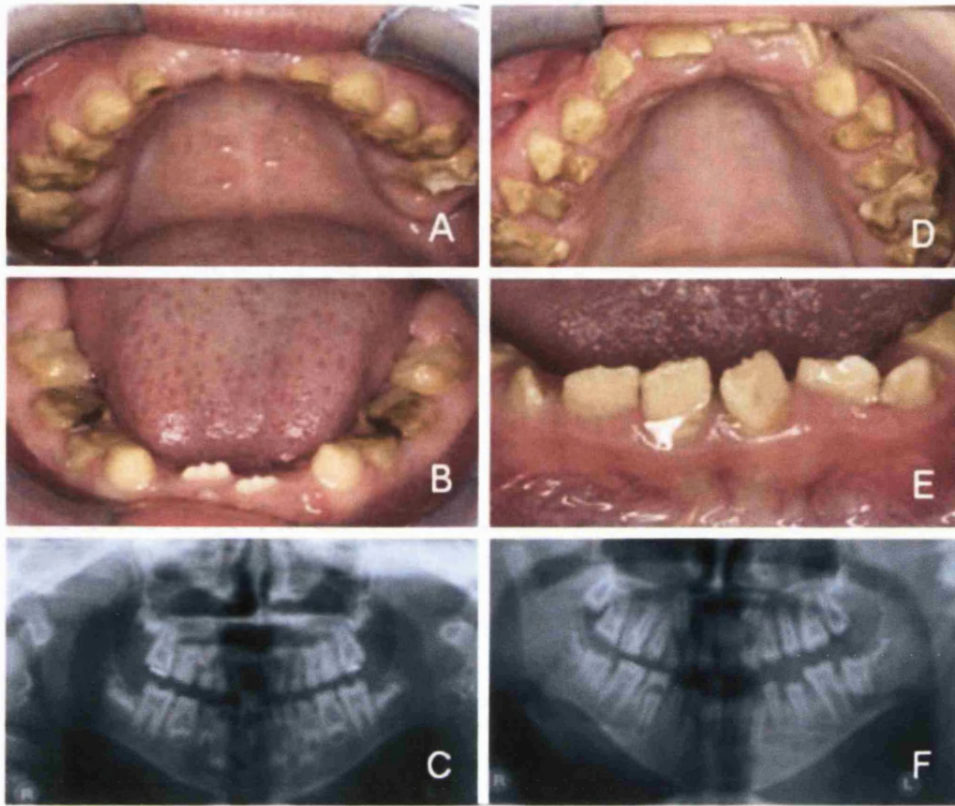


Figure 10.4
Amelogenesis imperfecta phenotype

A & B: 8-year-old boy in the mixed dentition phase. Severe signs of wear of the primary dentition are present, especially in the molar sector, with marked yellow-brown discolouration throughout. Dental caries are present. The first permanent molars are yellow, partially erupted and severely dysplastic with almost no enamel protective layer.

D & E: The 10-year-old proband was also in the mixed dentition stage. The teeth appear dysplastic and yellow/brown with almost no visible enamel. The tooth surface is rough and pitted.

C & F: Radiographic examination (orthopantomograms) showing teeth with no differential contrast between the putative enamel and dentin layers, suggesting an almost total lack of enamel, or the presence of a thin residual hypomineralised enamel layer.

10.4.2 Molecular genetics

10.4.2.1 *CNGA3* mutation screening and segregation of the 2q11 region

Screening of *CNGA3* failed to identify any disease-causing sequence variants. A SNP in exon 2b that encoded a Met112Ile substitution was identified, but was found to be only informative in determining one of the parental disease-associated alleles and not both (**Figure 10.1**). However, the pattern of segregation does rule out homozygosity for a large deletion that includes the *CNGA3* gene. The microsatellite marker D2S2187, which is located adjacent to the *CNGA3* gene, was therefore used to determine whether the region of chromosome 2q11 that contains *CNGA3* segregates with the CORD/AI phenotype. The three alleles present in this family provide evidence in support of an association between the disease and this chromosomal region (**Figure 10.1**).

10.4.2.2 *CNGA3* and *CNGB3* expression in developing mouse teeth

Study of *CNGA3* and *CNGB3* expression in developing teeth in CD1 mice of E19- and P2-day failed to identify transcripts from either gene (**Figure 10.5**). E19- and P2-day mice were chosen as enamel secretion/mineralisation would be expected to be occurring at these stages of development. If the cation channel genes had a role in dental mineralisation or enamel formation, it would seem likely that their transcripts should be detectable at these stages. The murine primers designed for *CNGA3* and *CNGB3* were validated by demonstrating that a PCR product of the correct size was generated using murine whole eye cDNA as the template (**Figure 10.6**); and a positive control in the form of the murine housekeeping gene, *GAPDH*, was used to check that cDNA had been successfully generated from these dental tissues. As shown in **Figure 10.5**, neither of the channel genes would appear to be expressed in teeth.

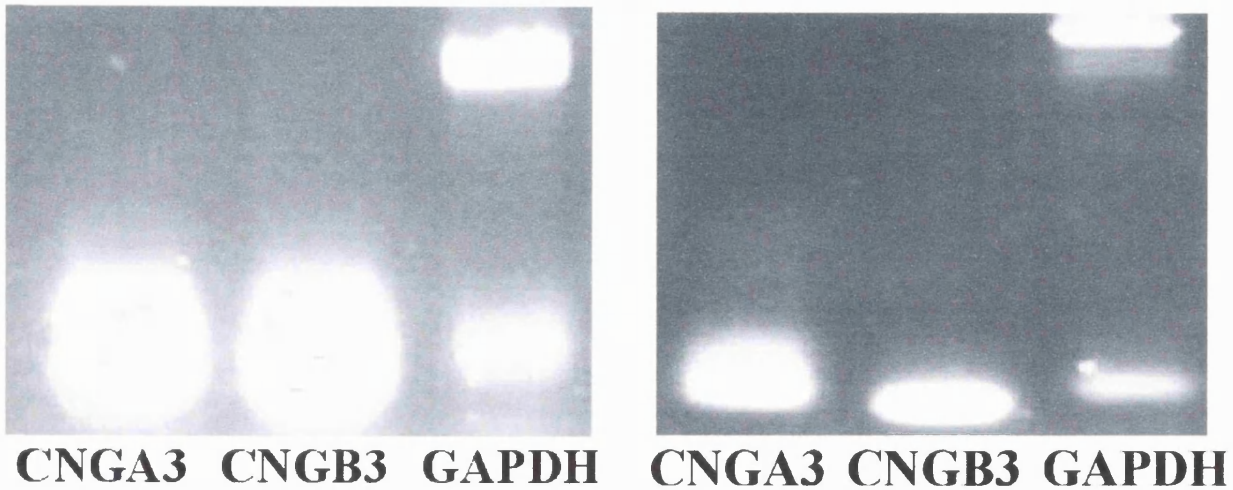


Figure 10.5

Expression of CNGA3 and CNGB3

Gel photographs [E19- (**Left**) & P2-day (**Right**)] showing that no PCR product was present for either *CNGA3* or *CNGB3* when using cDNA synthesised from developing mouse teeth as template; but that it was possible to obtain a PCR product with *GAPDH* primers.

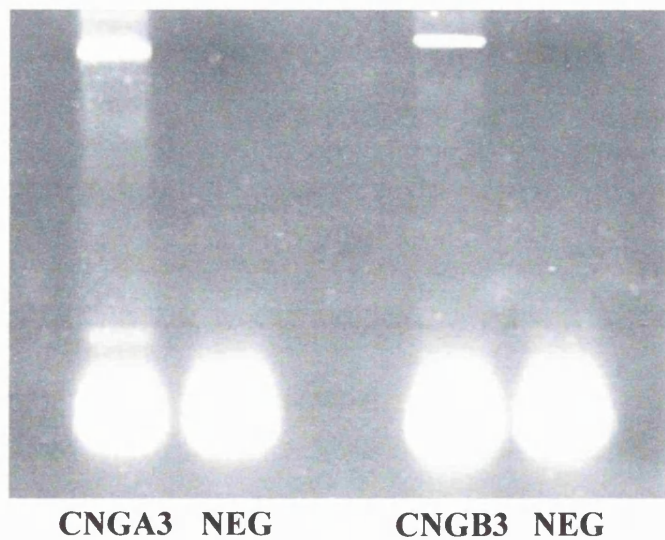


Figure 10.6

Murine CNGA3 and CNGB3 primer validation

The murine primers designed for *CNGA3* and *CNGB3* were validated by demonstrating that a PCR product of the correct size was generated using murine whole eye cDNA as the template.

10.5 DISCUSSION

The detailed phenotype has been described of a family with the autosomal recessive syndrome of cone-rod dystrophy (CORD) associated with amelogenesis imperfecta (AI). The retinal dystrophy was of early-onset, presenting in the first few years of life with photophobia and nystagmus. Visual acuity was severely reduced to 3/60 in childhood and there was complete absence of colour vision. Electrophysiological testing revealed undetectable cone ERGs and profoundly abnormal rod responses. The dental phenotype co-segregating with the CORD was that of hypoplastic/hypomineralised AI.

The only previous description of this syndrome is in a large Arabic family with 29 affected members across 7 generations (Jalili and Smith, 1988). The phenotype reported for that family was similar to that in the present study. The only significant ocular difference was that night blindness was not reported in the Arabic family and that scotopic ERGs were only mildly reduced in the youngest subject tested (12-years-old); whereas the two brothers in our family reported early onset of night blindness and the rod ERGs were profoundly abnormal.

The type of AI present was however different, with a hypomineralised variant identified in the Arabic family, and a hypoplastic/hypomineralised type in our family. AI is a collective term for a number of conditions with abnormal enamel formation and precise clinical diagnosis can be difficult. The differences in the findings in the two families may not therefore be significant. The precise delineation of the various forms of AI may need to await the identification of the causative genes (Aldred *et al.*, 2003).

Linkage analysis performed in the original Arabic family established a LOD score of 7.03 for the microsatellite marker D2S2187 on chromosome 2q11, with a disease interval encompassing the cation channel gene, *CNGA3* (Downey *et al.*, 2002). This is the first

report of AI associated with this region of chromosome 2. Subsequent mutation screening of *CNGA3* failed to identify a disease-causing sequence change (Downey *et al.*, 2002).

However *CNGA3* remained an attractive positional candidate gene since linkage data in the present study are consistent with a 2q11 chromosomal location for the disorder in our family. Also, with the molecular mechanisms underlying enamel formation currently being poorly understood, a gene involved in cation transfer may well be involved in the mineralisation process that underpins enamel deposition. However, we were also unable to find a disease-causing mutation in *CNGA3* and analysis of a SNP in *CNGA3* that segregates in our family also rules out the presence of a large deletion that includes the *CNGA3* gene. Finally, the absence of expression of *CNGA3* (and the related *CNGB3* gene) in developing teeth in CD1 mice of P0- and P2-day argues against the involvement of *CNGA3* in the disorder. It is thus unlikely that *CNGA3* is involved in either the AI or cone-rod dystrophy associated with this disease. An alternative explanation is that the CORD/AI phenotype is caused by a mutation in an adjacent gene.

Other candidate genes in the 2q11 region include *INPP4A* (Hs.32944) that encodes inositol polyphosphate-4-phosphatase, type I, a 107kDa protein, with a pattern of expression that includes the brain, retina, RPE and choroid. A null mutation in the mouse orthologue *inpp4a* in weeble mutant mice results in severe locomotor instability and significant neuronal loss in the cerebellum and in the hippocampus (Nystuen *et al.*, 2001). Neither the retinal nor the dental phenotypes of these mice have been described but it is of interest that the substrates of INPP4A are intermediates in a pathway affecting intracellular Ca^{2+} release (Berridge, 1993a; Berridge, 1993b), and are also involved in cell cycle regulation. The only gene in the region that is specifically expressed in the retina is *LYG2* (Hs.436468), which encodes a poorly characterised lysozyme. None are documented to be expressed in teeth. Identification of the gene(s) responsible for the

CORD/AI syndrome will help shed further light upon the mechanisms of enamel formation and retinal dystrophy.

10.6 CONCLUSIONS

A second family with the syndrome CORD associated with AI has been ascertained, and the ocular and dental phenotype has been further characterised (Michaelides *et al.*, 2004b).

Screening of *CNGA3* again failed to identify disease-causing mutations, and it has been demonstrated that *CNGA3* is not expressed at the developmental stages of the mouse teeth studied; providing further evidence to exclude *CNGA3* as the causative gene. However, segregation analysis of an adjacent microsatellite marker provides supportive evidence for the causative gene residing in the same chromosomal region (2q11) as identified for the Arabic family.

CHAPTER 11

ENHANCED S-CONE SYNDROME

11.1 INTRODUCTION

Enhanced S-cone syndrome (ESCS) is a rare autosomal recessive condition characterised by night blindness, a progressive natural history, maculopathy, restricted degenerative changes in the region of the vascular arcades, relatively mild visual field loss and an unusual, but diagnostic electroretinogram (ERG) (Marmor *et al.*, 1990).

Certain ERG features are characteristic of ESCS: the ERG responses to the same intensity flash under photopic and scotopic conditions are of similar waveform, being simplified and very delayed, and there is an increased response to short wavelength stimulation (Jacobson *et al.*, 1990; Marmor *et al.*, 1990; Hood *et al.*, 1995; Greenstein *et al.*, 1996). The latter observation has been suggested to relate to an increased number of S-cones replacing L- and M-cones rather than increased sensitivity of a normal density S-cone population (Hood *et al.*, 1995; Greenstein *et al.*, 1996; Haider *et al.*, 2000).

Goldmann-Favre is a rare autosomal recessive disorder with many similarities to ESCS. It is characterised by gradual visual loss or night-blindness with ocular findings that include liquefaction of the vitreous, macular retinoschisis and peripheral retinal pigment epithelial (RPE) atrophy and pigmentation. Peripheral retinoschisis and cataract may also occur. The retinal dystrophy is progressive resulting in extensive visual field loss and variable central visual loss. Fluorescein angiography may show evidence of peripheral capillary closure and vascular leakage (Fishman *et al.*, 1976). ERG is markedly abnormal or undetectable. Studies of patients with Goldmann-Favre syndrome using spectral ERG have demonstrated that S-cones are less affected than mid-spectral cones (Jacobson *et al.*, 1991); suggesting that there is overlap between Goldmann-Favre syndrome and ESCS. Indeed some authorities believe that the Goldmann-Favre syndrome represents severe ESCS.

The pigmentary deposition in ESCS is at the level of the RPE rather than intra-retinal, has a nummular (round) appearance, and tends to be mid-peripheral. Despite this characteristic appearance, patients can be mistakenly diagnosed with retinitis pigmentosa (RP). The ERG in ESCS is often diagnostic and can thus be helpful in making this distinction.

Mutations in *NR2E3* have been identified in ESCS and Goldmann-Favre (Haider *et al.*, 2000; Sharon *et al.*, 2003). *NR2E3* encodes a ligand-dependent transcription factor (Kobayashi *et al.*, 1999) that is believed to play a role in determining cone cell fate (Haider *et al.*, 2000; Milam *et al.*, 2002). In ESCS there is evidence of a greater than normal number of S-cones, with mutation in *NR2E3* thought to cause disordered cone cell differentiation, possibly by encouraging default to the S-cone pathway and thereby altering the relative ratio of cone subtypes (Szel *et al.*, 1994a; Szel *et al.*, 1994b; Milam *et al.*, 2002). In addition, a small number of cones have been shown to co-express L-/M- and S-opsins (Milam *et al.*, 2002).

11.2 AIMS

To review the phenotype of a panel of patients with ESCS and to subsequently screen *NR2E3* for mutations. Mutation screening was performed in order to determine the spectrum of sequence variants in ESCS patients ascertained in the UK and to establish the proportion of patients without causative mutations in *NR2E3*.

11.3 METHODS

11.3.1 *Patients and methods*

Sixteen patients, twelve individuals and two sibling pairs (two brothers and two sisters), with presumed ESCS were ascertained.

The clinical notes, colour fundus photographs and electrophysiological data (EOG, ERG, S-cone ERG and PERG) of all sixteen ESCS subjects were reviewed. Four of these patients presented for the first time during this study and were therefore seen in the clinic. Where possible optical coherence tomography (OCT) and fundus autofluorescence (AF) imaging was performed. In four subjects fundus fluorescein angiography (FFA) was undertaken.

11.3.2 *NR2E3* mutation screening

Blood samples were collected from patients after informed consent was obtained. Total genomic DNA was extracted from the blood samples using a Nucleon® Biosciences kit. In thirteen (13/16) patients *NR2E3* was screened for disease-causing mutations.

The gene *NR2E3* is located on chromosome 15q23, and has nine exons encoding a protein of 409 residues. The coding sequences and splice-junction sites of *NR2E3* were amplified by PCR in each individual using the primer sequences and annealing temperatures shown in **Table 11.1**. Standard 50µl PCR reactions were performed as described previously. After resolution on a 1% (w/v) LMT agarose gel, products were excised and eluted.

Direct sequencing of PCR products was carried out on an ABI 3100 Genetic Analyser using the original PCR primers in the sequencing reactions. The sequence was examined for alterations utilising *Sequencing Analysis* (ABI Prism™) and *GeneWorks*™ software. GenBank sequences were used to construct an alignment of nuclear receptor sequences and to analyse the evolutionary conservation of the corresponding amino acid positions. Sequences were aligned using *GeneWorks*™ software.

Primer	Sequence (5'-3')	T _a °C
Exon 1 F Exon 1 R	acaggggcacagagagacag aacctctggcccttacct	60°C for 1min
Exons 2 & 3 F Exons 2 & 3 R	tccagatggaagagtcacg tcaggacgacacgccagt	56°C
Exon 4 F Exon 4 R	actggcgtgtcgtcctga gaagccaagccctgctgt	54°C
Exon 5 F Exon 5 R	caagtactccctgccacctc gtaggtacctgatcccggaag	56°C
Exon 6 F Exon 6 R	tgagccagagaagctgtgtg ctggctgaagaggaccaag	55°C
Exon 7 F Exon 7 R	ggcgtggagtgaactcttc ggagagtgagaggcagatgg	55°C
Exon 8 F Exon 8 R	ctgtgctaagctcgactggtg gaggtcagggacaaatgagtg	60°C
Exon 9 F Exon 9 R	gtcgtaaaactgatggcgtcctc gcaaatgtttcgtttcagtagattg	60°C

Table 11.1

Primers for amplification of *NR2E3*

11.4 RESULTS

11.4.1 Patients

The panel of patients was of diverse ethnic and geographical origin, including Pakistan, Iran, the Philippines and UK/Europe. A clear history of consanguinity was present in two cases.

Clinical presentation was with long-standing night blindness and/or reduced central vision. The history of nyctalopia was from infancy in all subjects, with onset ranging from 2 to 6 years of age. Neither nystagmus, nor photophobia, was noted. Visual acuity

ranged from 6/9 to 2/60. Five patients were aware of a progressive deterioration; in one such subject there was a documented reduction in visual acuity from 6/6 to 6/24 over a 20 year follow-up period. The clinical findings are summarised in **Tables 11.2a** and **11.2b**.

A range of vitreous changes were noted in four subjects, including vitreous opacities, haze, and veils. In all individuals mid-peripheral retinal pigmentation, usually at the level of the RPE, and often associated with atrophy, was noted (**Figures 11.1 & 11.2**). These pigmented deposits were usually round lesions (**Figure 11.3**). In all subjects the location of the pigmentary changes included the region of the vascular arcades. In addition, white deposits were also often evident in areas of retinal abnormality (**Figure 11.3**). Macular retinoschisis-like changes were documented in six individuals. In two (2/6) of these subjects cysts were demonstrated with OCT. In the remaining four individuals (4/6), cystoid macular oedema was originally diagnosed on clinical examination. However, following a lack of demonstrable leakage on FFA, it was decided that the retinal appearance was more likely to be secondary to schisis.



Figure 11.1

Typical pigment clumping seen in ESCS (Patient 7)

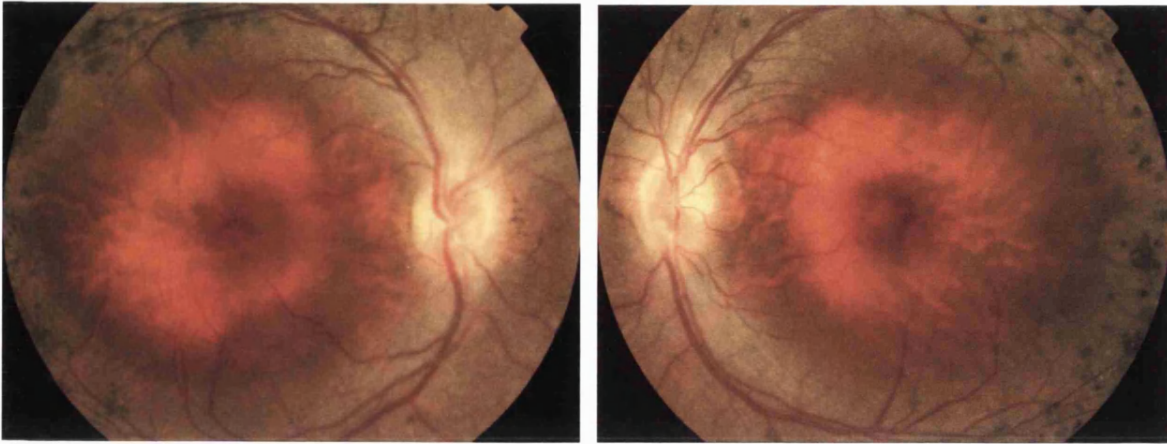


Figure 11.2

Typical pigment clumping seen in ESCS (Patient 11)

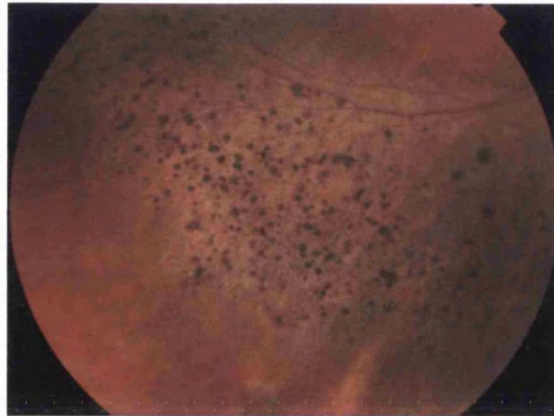


Figure 11.3

Fundus findings in ESCS

Typical nummular lesions of varying sizes (above)

Pigmented lesions interspersed with white deposits (below)

In patients 14, 15 and 16, detailed AF images were obtained showing a spoke-like area of relatively increased AF centred on the macula (**Figures 11.4 and 11.5**). The macula usually appears uniformly dark secondary to the presence of luteal pigment. A different AF phenotype was seen in patients 7 and 8 (sisters), with a ring of relative increased AF at the posterior pole (**Figure 11.6**), beyond which retinal AF is reduced or absent. In severely affected cases, AF imaging showed a complete lack of retinal autofluorescence.

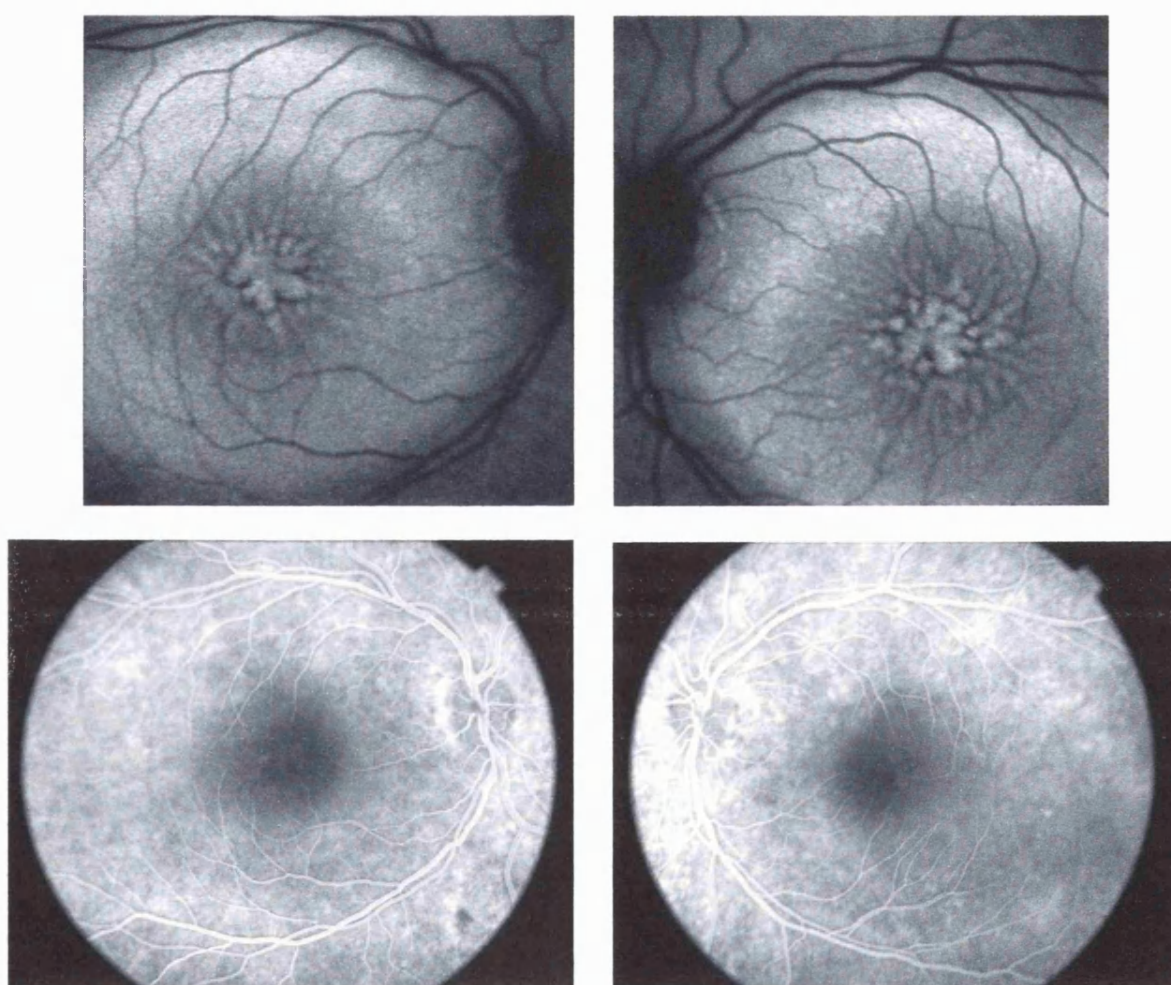


Figure 11.4

AF and FFA findings in ESCS

AF images showing a spoke-like area of AF centred on the macula (Patient 15)(above)

FFA showing absence of leakage at the macula (Patient 15) (below)(see text)

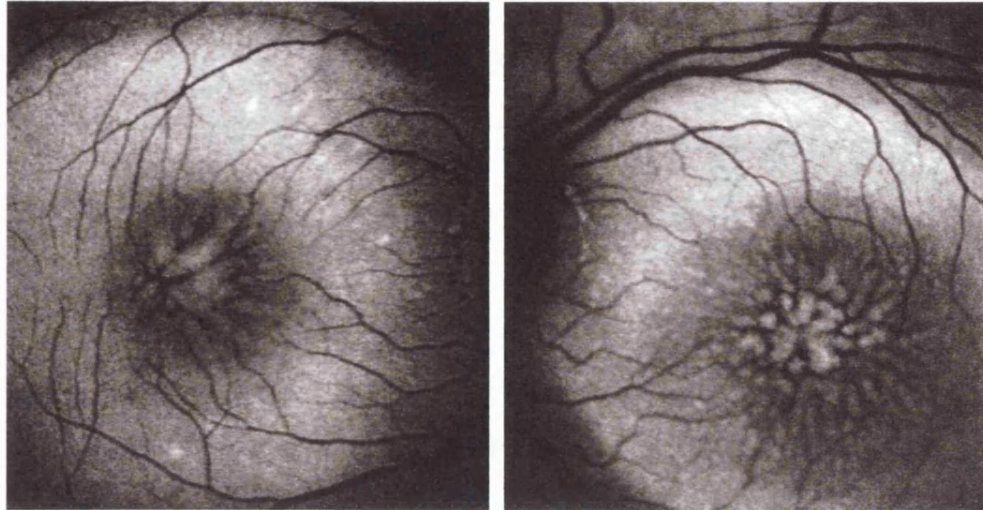


Figure 11.5

AF images showing a spoke-like area of AF centred on the macula (Patient 16)

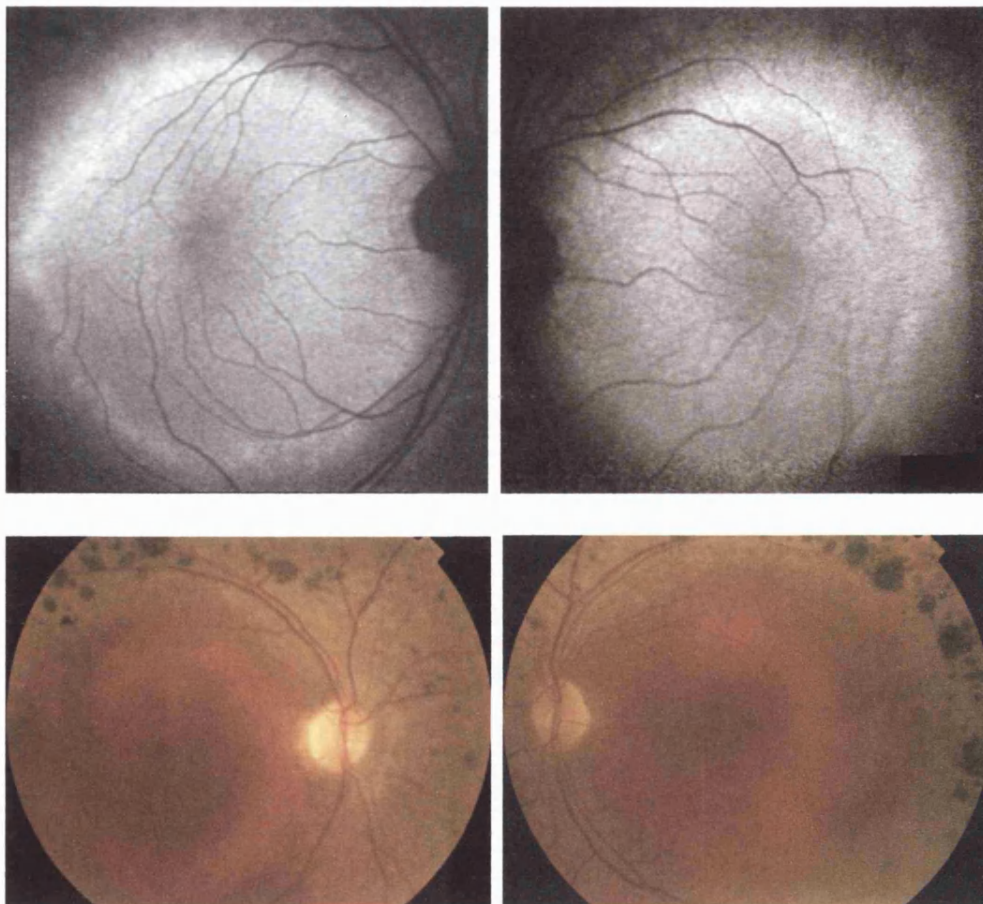


Figure 11.6

AF images showing a ring of increased AF (Patient 8)(above)

Colour fundus photographs for comparison (Patient 8)(below)

OCT clearly demonstrated macular cystic spaces in patients 11 and 14 (**Figure 11.7**). Interestingly, following the clinical suspicion of macular oedema in four other patients in whom a diagnosis of RP was originally proposed, OCT demonstrated cystic macular spaces. In three of these patients oral acetazolamide therapy was consequently undertaken, with no objective or subjective improvement noted. Subsequently, all four subjects had FFA performed, with no leakage being evident, thereby suggesting that these cystoid spaces at the macula were more likely to be due to retinoschisis than oedema.

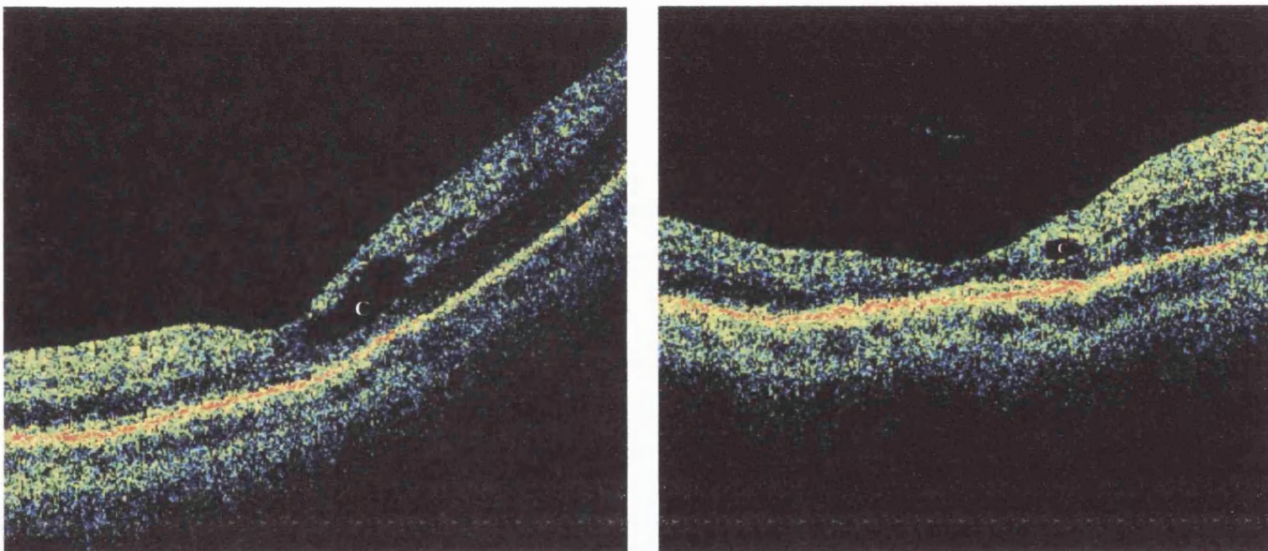


Figure 11.7

OCT images showing bilateral macular cystic spaces (c) (Patient 11)

A larger cyst is seen at the right macula than the left

Nine patients (9/16) had pathognomonic ERG changes of ESCS (**Figure 11.8**): the rod-specific ERG was undetectable, the ERGs to a standard single flash had a similar waveform under photopic and scotopic conditions, and the 30Hz flicker ERG was of lower amplitude than the single flash photopic ERG a-wave. ERG amplitudes showed high variability across patients related to the severity of degeneration. The older patients

tended to have the more severe abnormalities. Most patients showed abnormally large S-cone ERGs with minimal responses to L/M cone stimulation. EOG light rise was undetectable in the five patients in whom it was assessed. PERG, when present, was profoundly delayed. Sparing in the tritan axis on colour contrast sensitivity testing was found in 7 patients.

In the remaining seven patients (7/16) ERG changes were not pathognomonic of ESCS. In five of these subjects the ERG was undetectable and in the remaining two individuals it was profoundly reduced. The loss of retinal function in these seven subjects precluded the assessment of the presence or absence of the characteristic ERG features described in ESCS. Indeed, in the five patients with undetectable ERGs, this lack of retinal function found in association with pigmentary retinopathy and macular schisis/cysts, led to a clinical diagnosis of Goldmann-Favre syndrome.

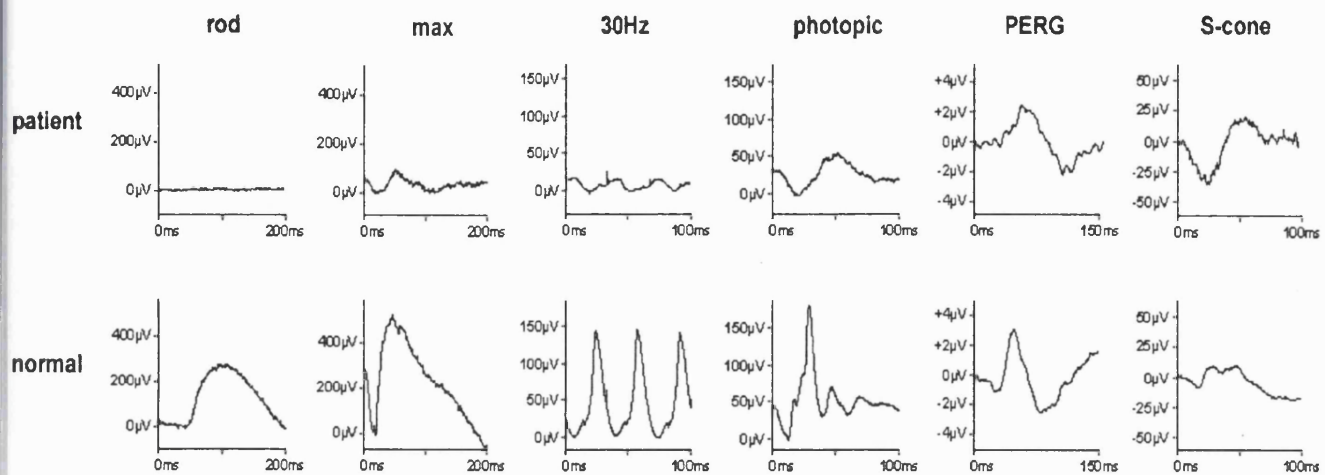


Figure 11.8

Typical ERG data seen in ESCS

The rod-specific ERG is undetectable in keeping with the known absence of rods in this disorder (Milam *et al.*, 2002). However, the two main diagnostic features are: **(i)** the similarity in waveform between the photopic and scotopic (max) ERG to the same stimulus, both of which show a simplified grossly delayed waveform, and **(ii)** the amplitude of the grossly delayed 30Hz flicker ERG being lower than that of the photopic a-wave. In a normal subject, the 30Hz flicker ERG amplitude always falls between that of the photopic a-wave and the photopic b-wave. The PERG is profoundly delayed in this case, although the PERG can be undetectable. Increased sensitivity to short wavelength stimulation is revealed by specific S-cone ERG recording (5ms blue stimulus on a bright orange background). In a normal subject, the S-cone ERG consists of two components: a late S-cone specific component at ~50ms and a L-/M- cone component at ~30ms. The earlier component is not present in the patient, and the later component is enhanced.

Patient	Sex	Age	VA OD OS	Refraction	Other findings	Fundus	ERG
1	F	13	OD: 6/9 OS: 6/24	+3.5/+1.25 x 90 +6.5/+1.5 x 90	Left convergent squint Left amblyopia	Schisis-like macular appearance White deposits at level of RPE in the region of the vascular arcades	Characteristic ESCS features
2	M	39	OD: 6/24 OS: 6/12	-0.5/-0.25 x50 -0.5/-0.25 x 180	Constricted visual fields	Schisis-like macular appearance Mid-peripheral pigmentation	Undetectable ERG
3	M	44	OD: 6/9 OS: 6/9	Low Hypermetropia	-	Mid-peripheral pigmentation and atrophy at level of RPE	Undetectable rod ERG Profoundly reduced cone ERG
4	F	21	OD: 6/9 OS: 6/9	Low myopia	Vitreous changes	Mid-peripheral pigmentation and atrophy at level of RPE	Characteristic ESCS features
5	F	25	OD: 2/60 OS: 6/36	Myopia	OD PCIOL OS Cataract Vitreous changes	Schisis-like macular appearance Retinal pigmentation and atrophy	Undetectable ERG
6	F	35	OD: 6/24 OS: 6/24	+4.0/+0.50 x 180 +5.0 DS	Vitreous changes	Mid-peripheral pigmentation and atrophy at level of RPE	Undetectable ERG
7	F	42	OD: 6/12 OS: 6/36	-	Constricted visual fields	Mid-peripheral pigmentation and atrophy at level of RPE	Characteristic ESCS features
8	F	43	OD: 6/60 OS: 6/36	Hypermetropia	Right convergent squint with amblyopia Constricted visual fields	Mid-peripheral pigmentation and atrophy at level of RPE	Characteristic ESCS features

Table 11.2a

Summary of clinical findings in ESCS

7 & 8 are sisters

Patient	Sex	Age	VA OD OS	Refraction	Other findings	Fundus	ERG
9	M	30	OD: 6/12 OS: 6/12	Myopia	Vitreous changes	Macular retinoschisis Minimal mid-peripheral pigmentation	Profoundly reduced rod and cone ERGs
10	M	12	OD: 6/36 OS: 6/36	-	Constricted visual fields Bilateral optic disc drusen	Mid-peripheral pigmentation and atrophy at level of RPE	Undetectable ERG
11	M	35	OD: 6/36 OS: 6/36	+4.50/-0.50 x145 +0.50/-1.0 x140	Constricted visual fields	Macular cysts on OCT Mid-peripheral pigmentation	Characteristic ESCS features
12	F	6	OD: 6/24 OS: 6/36	-	-	Mid-peripheral pigmentation and atrophy at level of RPE	Undetectable ERG
13	M	20	OD: 6/18 OS: 6/24	-	-	Mid-peripheral pigmentation and atrophy at level of RPE	Characteristic ESCS features
14	M	30	OD: 6/18 OS: 6/36	Hypermetropia	-	Macular cysts on OCT Mid-peripheral pigmentation and atrophy at level of RPE	Characteristic ESCS features
15	M	24	OD: 6/18 OS: 6/12	-	-	Mid-peripheral pigmentation and atrophy at level of RPE	Characteristic ESCS features
16	M	26	OD: 6/24 OS: 6/18	-	-	Mid-peripheral pigmentation and atrophy at level of RPE	Characteristic ESCS features

Table 11.2b
Summary of clinical findings in ESCS

15 & 16 are brothers

11.4.2 *NR2E3* mutation screening

The screening of the 9 coding exons of *NR2E3* for mutations, in thirteen members of the panel, yielded six sequence variants that most likely represent disease-causing mutations (**Table 11.3**). Two previously reported mutations were identified, a splice acceptor intron 1 mutation and the Arg311Gln substitution. The four novel mutations were two splice acceptor variants (intron 1 and intron 8) and two missense mutations (Val49Met and Tyr81Cys).

The Val49Met (V49M) substitution (145G→A; exon 2; **Figure 11.9**) was identified as a homozygous (Hm) change in patient 3; and the Tyr81Cys (Y81C) substitution (242A→G; exon 2; **Figure 11.10**) as a heterozygous (Ht) change in patients 7 and 8 (sisters). Both Val49 and Tyr81 are conserved across other *NR2E3* receptors (**Table 11.4**), and neither missense mutation was found in a screen of 100 control chromosomes. V49M and Y81C are both located in the conserved DNA binding domain of *NR2E3*.

The first novel splice acceptor (3' splice) mutation is a C→G nucleotide change at the intron 1 splice site (**Figure 11.11**; **Figure 11.13**), identified as a homozygous change in patient 13. One of the most common previously reported mutations in *NR2E3* is an A→C change at this same splice site (Haider *et al.*, 2000); a mutation that has also been frequently identified in our study in both heterozygous and homozygous states (5/8 patients) (**Figure 11.12**). The second novel splice acceptor mutation identified in our study is at intron 8 (G→A change; **Figure 11.13**; **Figure 11.14**), present as a homozygous change in patient 1. Neither novel splice acceptor mutation was found in a screen of 100 control chromosomes. The likely effect of the splice acceptor intron 1 and intron 8 mutations would be to cause aberrant splicing, resulting in either failure to remove these introns, or loss of exon 2 or exon 9 from the transcript as a result of splicing with the next intact splice acceptor site. A retained intron may lead to premature

termination of translation and a truncated protein which is either non-functional or has reduced efficacy. Loss of exons will result in the absence in the protein of amino acid residues encoded by these regions and since exons 2 and 9 encode residues involved in DNA-binding and ligand-binding respectively, a transcription factor of significantly reduced function would be predicted.

The final mutation identified is the most common previously reported mutation, R311Q (Arg311Gln) (923G→A; exon 6) (Haider *et al.*, 2000; ~45% of patients). In this study we have demonstrated this mutation as a heterozygous change in patient 4 (Figure 11.15). Clearly this mutation is far less prevalent in the population of our study than in the previous investigation by Haider *et al.* (2000).

No disease-causing sequence variants were identified in 5 patients (5/13). Two novel silent polymorphisms were demonstrated: A95A (285C→T; exon 3) and G288G (864T→A; exon 6).

Affected individuals	<i>NR2E3</i> Mutation	Predicted change
1	Hm splice acceptor intron 8 (G→A)	Aberrant splicing
3	Hm 145G→A	V49M
4	Ht splice acceptor intron 1 (A→C) Ht 923G→A	Aberrant splicing R311Q
6	Ht splice acceptor intron 1 (A→C)	Aberrant splicing
7	Ht splice acceptor intron 1 (A→C) Ht 242A→G	Aberrant splicing Y81C
8	Ht splice acceptor intron 1 (A→C) Ht 242A→G	Aberrant splicing Y81C
11	Hm splice acceptor intron 1 (A→C)	Aberrant splicing
13	Hm splice acceptor intron 1 (C→G)	Aberrant splicing

Table 11.3 *NR2E3* disease-causing mutations

Ht = heterozygous, Hm = homozygous. Mutations in bold represent novel alterations.

Residue	Human	Murine	Zebrafish	Fugu
49	Val	Val	Val	Val
81	Tyr	Tyr	Tyr	Tyr

Table 11.4

Amino acid conservation in NR2E3 receptors at sites of identified missense mutations

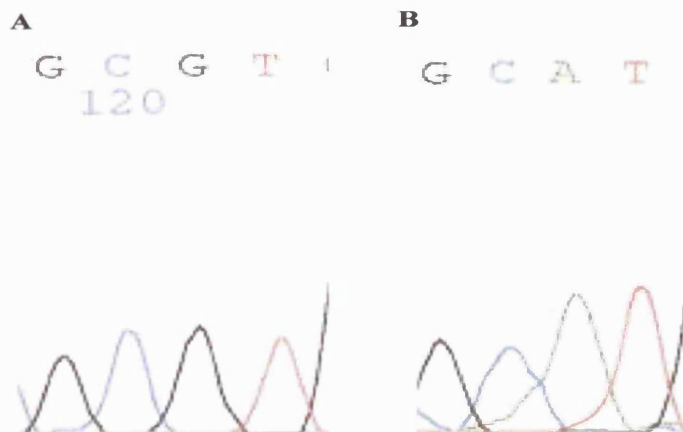


Figure 11.9

NR2E3 V49M mutation

A - Wild-type (wt) Exon 2 B - Hm V49M

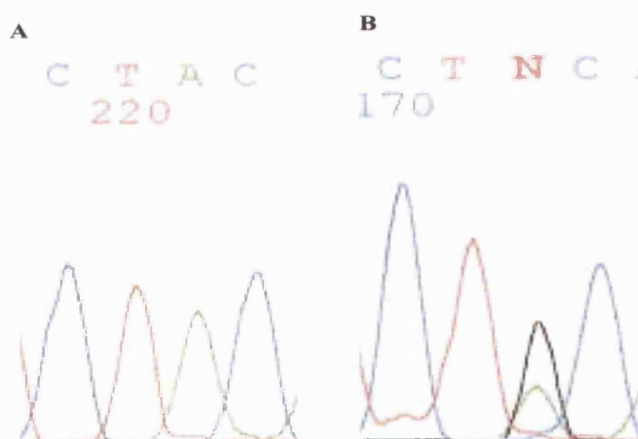


Figure 11.10

NR2E3 Y81C mutation

A - wt Exon 2 B - Ht Y81C

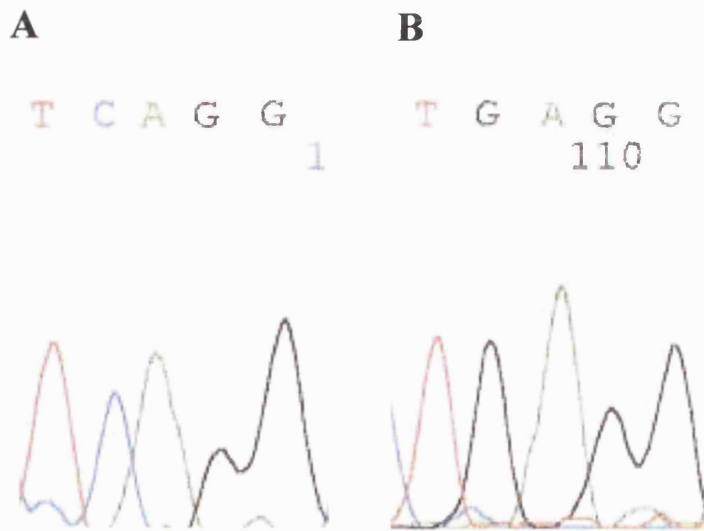


Figure 11.11

NR2E3 splice acceptor intron 1 mutation (C→G) (IVS1-3C>G)

A - wt Exon 2

B - Hm C→G splice variant

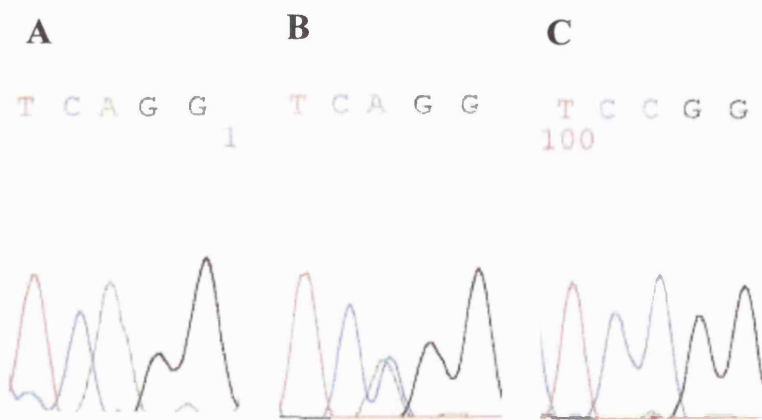


Figure 11.12

NR2E3 splice acceptor intron 1 mutation (A→C) (IVS1-2A>C)

A - wt Exon 2

B - Ht A→C splice variant

C - Hm A→C splice variant

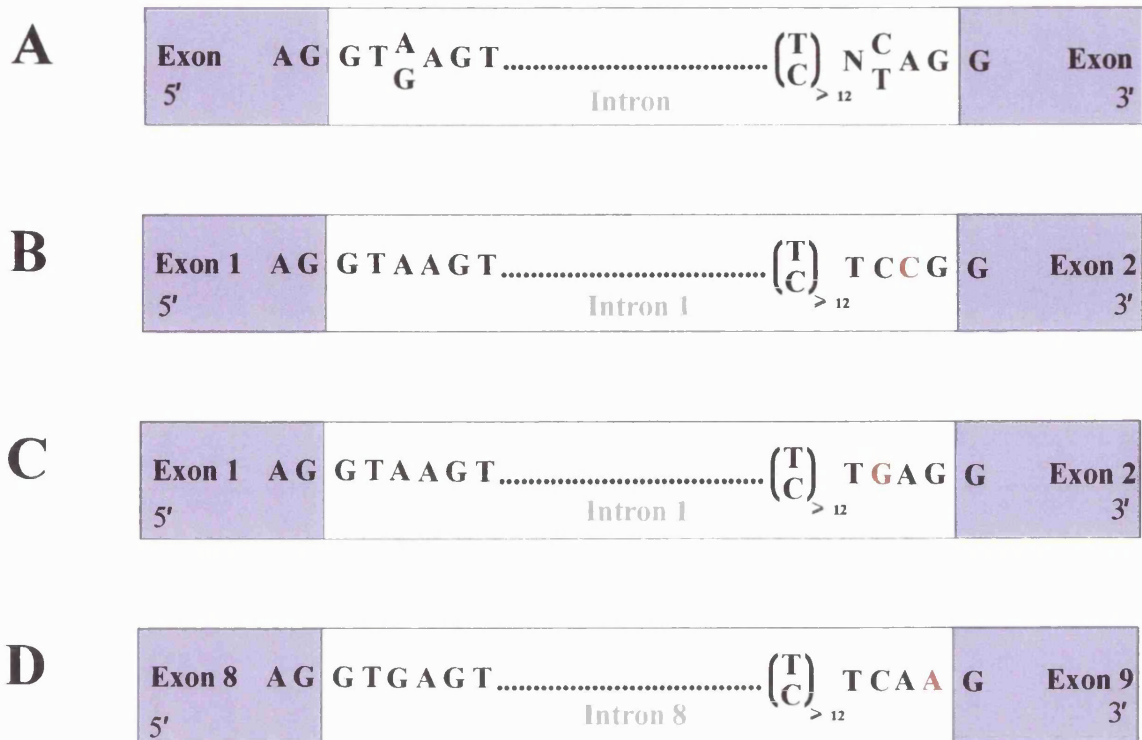


Figure 11.13 Consensus sequences for 5' and 3' splice sites in nuclear protein-coding genes and location of splice site mutations (shown in red) identified in *NR2E3*

- A** Consensus sequences for 5' and 3' splice sites. Exons are shaded in purple with the intervening intronic sequence in white.
- B** A/C splice acceptor mutation in intron 1 identified in our study and by Haider *et al.* (2000).
- C** Novel C/G splice acceptor mutation in intron 1
- D** Novel G/A splice acceptor mutation in intron 8

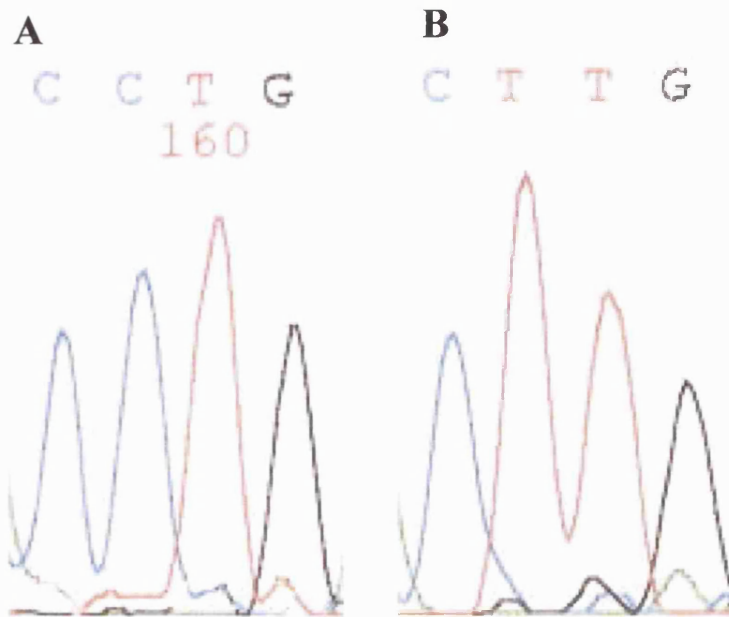


Figure 11.14

NR2E3 splice acceptor intron 8 mutation (*G*→*A*) (IVS8-1G>A)

A - wt Exon 9

B - Hm *G*→*A* (*C*→*T*) splice variant

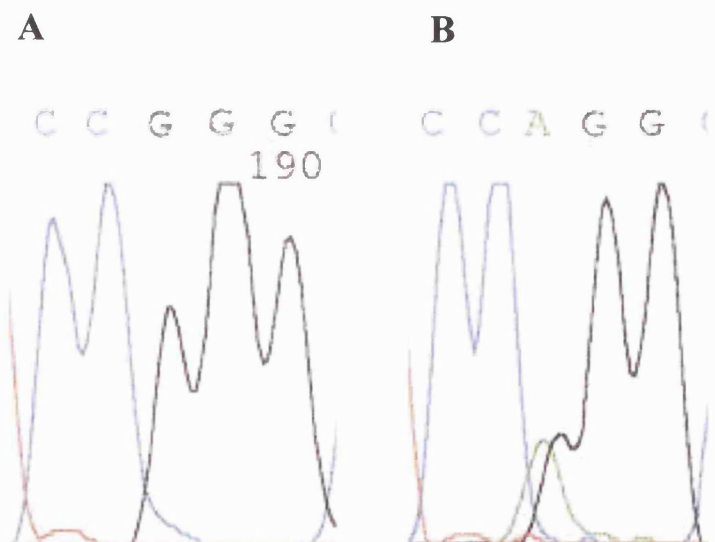


Figure 11.15

NR2E3 R311Q mutation

A - wt Exon 6

B - Ht R311Q

11.5 DISCUSSION

A panel of patients with a clinical diagnosis of either Enhanced S-cone Syndrome (ESCS) or Goldmann-Favre syndrome (GFS) has been ascertained and the phenotypes reviewed and further characterised in some instances. ESCS and GFS are both rare inherited causes of night blindness, with evidence that both are related to mutations in *NR2E3* (Haider *et al.*, 2000; Sharon *et al.*, 2003). A single histopathological report determined a retina devoid of rods, and a degenerate cone population principally containing short-wavelength sensitive pigment (Milam *et al.*, 2002).

All subjects in the panel had nyctalopia of early-onset. The severity of reduction in visual acuity was however variable; with some younger individuals being worse affected than older subjects. Nevertheless, in the main it appears that the retinal disorder in this panel is slowly progressive with a gradual deterioration of visual acuity and variable constriction of visual fields. Fundus findings were characteristic in all patients, with mid-peripheral nummular pigmentation, usually noted to be at the level of the RPE, and often associated with atrophy and white deposits. The discoid pattern, mid-peripheral distribution, and RPE level of the pigmentation are useful clinical findings in helping to distinguish ESCS/GFS from RP.

In a significant proportion of patients the ophthalmoscopic or OCT findings were consistent with macular schisis. The spoke-like distribution of relatively increased autofluorescence at the maculae, seen on AF imaging in three subjects, may be due to compression of the luteal pigment containing cellular elements by the cystic spaces giving rise to uneven absorption of short wavelength light. The ring of increased AF seen in some individuals represents areas of accumulation of lipofuscin at the level of the RPE.

It is of note that in four subjects determined to have cystoid macular oedema on the basis of ophthalmoscopy and OCT, subsequent FFA failed to demonstrate corroborative leakage. In the interim, three of these patients were treated with acetazolamide unnecessarily and without any notable benefit. These cystoid spaces, rather than indicating retinal oedema, are more likely to represent macular schisis, a feature known to be associated with the ESCS and GFS phenotypes. Macular schisis/cysts may well be a more common component of other retinal dystrophies than is currently recognised.

In nine subjects the standard Ganzfeld ERGs exhibited the characteristic features previously described in ESCS, namely absent rod-specific ERGs, delayed and similar waveforms of the scotopic and photopic responses, and abnormally large S-cone ERGs with minimal responses to L/M cone stimulation. These electrophysiological findings have been attributed to replacement of L- and M-cones, and possibly rods, by S-cones (Greenstein *et al.*, 1996). In the five patients in whom EOG testing was performed, the light rise was undetectable. A normal EOG light rise requires a normally functioning rod population in addition to a normally functioning RPE (Fishman *et al.*, 2001). The extinguished EOG light rise and absent rod-specific ERG are in keeping with an absence of rod function.

In the remaining seven patients the ERG responses were either undetectable or so profoundly reduced as to preclude the determination of the presence or absence of the aforementioned characteristic electrophysiological features of ESCS. This severe phenotype was labelled as GFS in five (5/7) of these subjects. Mutation screening of *NR2E3* established disease-causing mutations in this group of patients, in addition to the group of patients with typical ESCS ERG features. The commonly reported splice acceptor intron 1 mutation (A→C change; A/C) was identified in both groups. This is in keeping with previous suggestions that GFS represents the severe end of the spectrum of

the ESCS phenotype (Haider *et al.*, 2000). Sharon *et al.* (2003) have also recently described a single patient with GFS in whom *NR2E3* mutations were identified.

NR2E3 is a ligand-dependent transcription factor that has a role in determining the cone photoreceptor phenotype during embryogenesis and is required for the differentiation of L-/M-cones from S-cones (Szel *et al.*, 1994b; Haider *et al.*, 2000; Milam *et al.*, 2002). Mutation of *NR2E3* arrests cone differentiation at a stage when most cones are S-cones (or cones expressing multiple cone opsins), thereby resulting in a retina with an excess of S-cones (and a minority of cones co-expressing L-/M- and S-opsins) (Haider *et al.*, 2000; Milam *et al.*, 2002). The two most common mutations reported are the missense mutation R311Q (~45% of patients) and the A/C splice acceptor intron 1 mutation (~35%) (Haider *et al.*, 2000).

Cell fate is determined by both intrinsic (genetic) and extrinsic (including cellular interactions between cones) influences (Cepko, 1999). Evidence that S-cones represent the default pathway includes the excess of S-cones seen in foetal retinal grafts (Szel *et al.*, 1994a) and M-cone differentiation from S-cones in the rat (Szel *et al.*, 1994b). In ESCS, some L- and M-cones are likely to be present in the fovea to allow for good initial acuity and trichromatic vision. However, it is postulated that S-cones have usurped most of the L- and M- pathways centrally and virtually all of the rod pathways peripherally (Marmor *et al.*, 1999).

Six sequence variants in the coding region of *NR2E3* were found in our panel of patients that most likely represent disease-causing mutations. Four of these are novel: two missense mutations, Val49Met and Tyr81Cys, and two splice acceptor mutations, at intron 1 and intron 8 respectively. The first novel splice site mutation (C→G nucleotide change), is at the same intron 1 splice site previously identified as the second most common sequence variation in ESCS, that being an A→C change present in ~35% of

subjects (Haider *et al.*, 2000). In our study this A→C change was similarly frequently identified in ~38% of subjects screened. The second novel splice acceptor mutation is at intron 8 (G→A change); a region not previously identified as harbouring potentially disease-causing sequence variants. The splice acceptor intron 1 and intron 8 mutations would both be predicted to cause aberrant splicing, resulting in either a truncated non-functional protein, or one of significantly reduced efficacy; since exon 2 and exon 9 encode residues involved in DNA-binding and ligand-binding respectively. The subject homozygous for the splice acceptor mutation in intron 8 has a less severe phenotype, which may in part be a reflection of her young age and that her condition has yet to significantly progress, or that this splice site mutation has a less severe effect on receptor function, being located at the last coding exon, and thereby may be predicted to only affect the terminal portion of the ligand-binding domain.

The mutations, V49M and Y81C, are both located in the highly conserved DNA-binding domain of NR2E3. The subject homozygous for the V49M mutation has milder disease than other members of the panel. This mutation is located at the start of the proposed DNA-binding domain, whereas Y81C is in the central region of this domain. The individuals with the Y81C mutation were compound heterozygotes, thereby precluding a direct comparison; however they were found to be more severely affected, suggesting that the V49M may have a less adverse effect on DNA-binding.

No disease-causing sequence variants were identified in 5 patients (5/13); whereas in Haider *et al.* (2000) mutations were not identified in 2 subjects (2/29), with only heterozygous mutations detected in a further 8 patients. There are several possible explanations for the failure to identify mutations in the five individuals in our study. Disease-causing sequence variants may have been missed for several reasons, including that the mutations are intronic, in the promoter, or present in as yet unidentified exons. In

addition, heterozygous deletions might also have been missed by direct sequencing; Southern blotting or quantitative PCR may be useful techniques in identifying the individuals with such deletions. It also remains plausible that there is further genetic heterogeneity to be identified.

Nevertheless, it is of interest that there are a few differences between the subjects found to have *NR2E3* mutations and those in whom no sequence variants were identified. The five subjects without disease-causing mutations were found to have undetectable (4) or profoundly reduced (1) ERGs, thereby precluding assessment of S-cone function, and in the three subjects in whom refractive error data was available, a myopic error was recorded. Sharon *et al.* (2003) reported that all patients with *NR2E3* mutations in their study were hypermetropes, whereas hypermetropia was not a shared feature in the group of patients in whom they did not identify mutations (11/20 probands). In addition, in three of the patients without mutations in our study, the retinal pigmentation judged from the clinical notes or fundus photographs was not entirely typical of ESCS, being either sparse or not noted to be at the level of the RPE. A proportion of these five patients may be part of a collection of disorders termed clumped pigmentary retinal degeneration (CPRD) (To *et al.*, 1996). CPRD is believed to represent ~0.5% of patients with non-syndromic RP; with histopathological examination of a single case revealing that the clumps correspond to RPE cells packed with melanin granules (To *et al.*, 1996). Sharon *et al.* (2003) identified *NR2E3* mutations in subjects with CPRD (9/20), suggesting further genes implicated in this group of disorders. However, in these CPRD patients with *NR2E3* mutations, the ERG findings were in keeping with ESCS and therefore these subjects may represent patients with an incorrect clinical diagnosis of 'CPRD'.

Other candidate genes for ESCS/GFS include *NRL* and *THRB1*, since mutations in these genes in transgenic mice result in retinal disease similar to that found in *rd7* mice;

these *rd7* mice have been shown to lack any functional NR2E3 protein (Haider *et al.*, 2001). The *NRL* knockout mouse has a complete loss of rod function and super-normal S-cone responses (Mears *et al.*, 2001), and mice lacking the retina-specific exon of *THRBI* have an excess of S-cones (Ng *et al.*, 2001). However, Sharon *et al.* (2003) did not identify mutations in either of these candidate genes in the group of CPRD patients without *NR2E3* mutations. Acar *et al.* (2003) proposed that *NRL* mutants might modify clinical manifestations of ESCS patients carrying *NR2E3* mutations; however they did not find any disease-associated variants in *NRL*. Therefore, neither of these genes has been screened in a panel of patients with good evidence of ESCS in whom *NR2E3* has been excluded in the first instance.

Whilst the four novel mutations identified in this study, and other mutations described by Haider *et al.* (2000) and Sharon *et al.* (2003) appear likely to be disease-causing on the basis of either aberrant splicing or location at highly conserved domains critical to protein function, only direct functional studies assessing the effects of these sequence variants on NR2E3 stability, targeting and ability to interact effectively and reversibly with either DNA or ligand, can provide definitive evidence of pathogenicity.

11.6 CONCLUSIONS

The extent of visual loss due to retinal degeneration varies considerably within the ESCS phenotype, which may in part be related to age, but may also involve other genetic or environmental modifying factors.

Whilst mutations of *NR2E3* are likely to account for the majority of ESCS patients, there may be other genetic loci yet to be identified.

CHAPTER 12

AN AUTOSOMAL DOMINANT BULL'S-EYE MACULAR DYSTROPHY (MCDR2)

12.1 INTRODUCTION

The hereditary central receptor dystrophies are characterised by bilateral visual loss and the finding of generally symmetrical macular abnormalities on ophthalmoscopy. The age of onset is variable, but most present in the first two decades of life. There is considerable clinical and genetic heterogeneity. Macular dystrophies showing autosomal dominant (AD), autosomal recessive, X-linked recessive and mitochondrial inheritance have all been reported and there is considerable heterogeneity even within these subtypes. A number of causative genes have now been identified (**Table 1.4**), but more remain to be discovered.

Age-related macular degeneration (ARMD) may also have a significant genetic component in its aetiology. Genes implicated in monogenic macular dystrophies are potential candidates for genes conferring risk for ARMD, although to date, with the possible exception of *ABCA4*, none of these genes have been shown to confer increased risk of ARMD.

12.2 AIMS

To describe in detail the phenotype of an AD macular dystrophy. In a parallel study linkage analysis was performed to identify the chromosomal locus. Subsequently, a candidate gene was screened.

12.3 METHODS

A five-generation family with an AD macular dystrophy was ascertained. A full ophthalmological assessment was undertaken and blood samples were obtained for DNA extraction. Linkage analysis and subsequent mutation screening of the candidate gene *PROM1* was performed.

12.3.1 *Patients and clinical assessment*

Eleven members of a five-generation, non-consanguineous British family were examined (**Figure 12.1**). Although there was no male-to-male transmission, males and females were equally affected and AD inheritance is thought to be most likely.

A full medical and ophthalmic history was obtained and an ophthalmological examination performed. Colour vision testing was performed using the HRR plates. Affected subjects also underwent Humphrey automated photopic visual field perimetry, colour fundus photography and fundus autofluorescence imaging using the confocal scanning laser ophthalmoscope (cSLO) (Zeiss Prototype; Carl Zeiss Inc, Oberkochen, Germany). Electrophysiological assessment included ISCEV standard EOG, full-field ERG and pattern ERG. Patients **IV:2** and **V:1** underwent fundus fluorescein angiography (FFA).

Individuals were diagnosed as affected on the basis of the presence of macular abnormality and in most cases decreased visual acuity of variable magnitude.

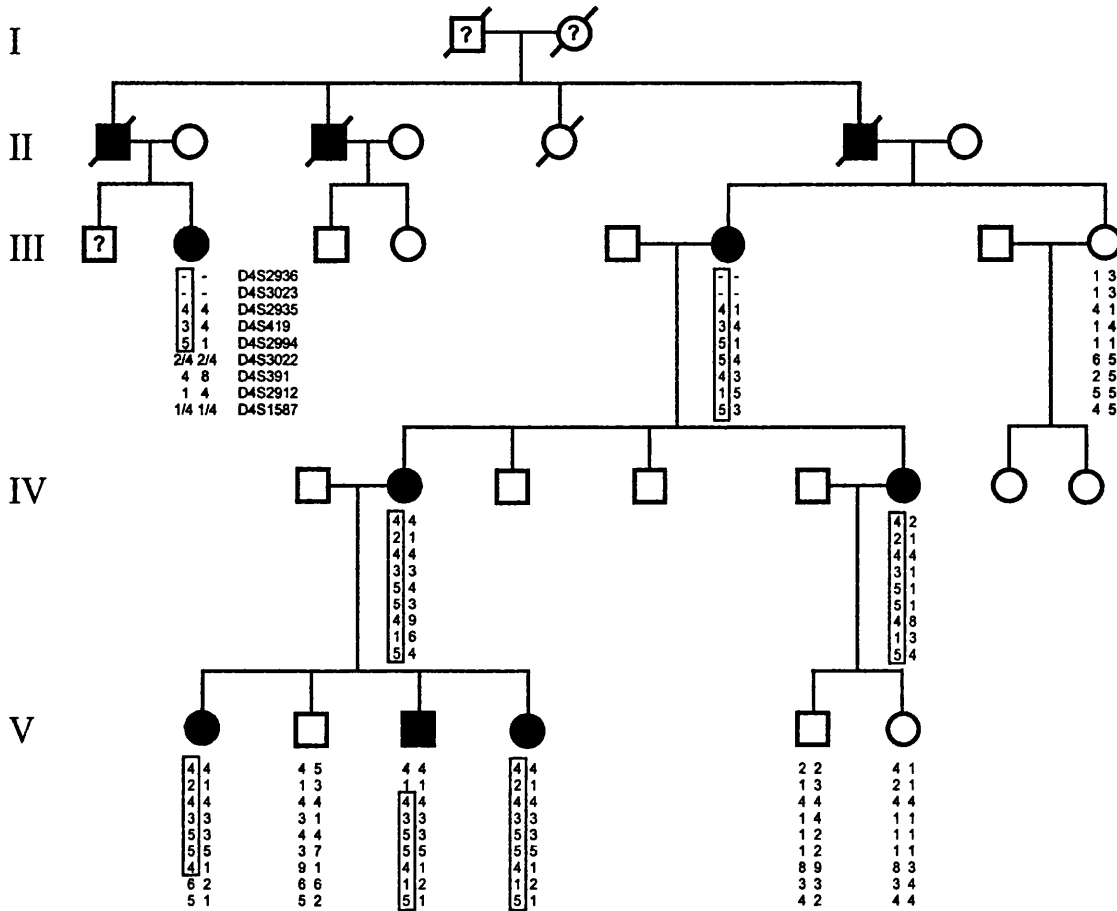


Figure 12.1

MCDR2 pedigree

Individuals are numbered according to their generation (indicated) and position in each generation numbering from left to right. The alleles present for each of the nine chromosome 4p microsatellite markers used are shown. The minimal disease region for each affected individual is boxed.

Linkage analysis performed by a colleague.

12.3.2 Linkage analysis

Linkage analysis was undertaken in a parallel study by a colleague. Genotyping was carried out utilizing markers from version 2.0 of the ABI MD-10 and HD-5 Linkage Mapping Sets (Applied Biosystems). These sets allow ~10cM and ~5cM resolution of the human genome respectively and consist of fluorescently labelled PCR primer pairs for

800 highly polymorphic dinucleotide-repeat microsatellite markers chosen from the Genethon human linkage map (Weissenbach *et al.*, 1992; Gyapay *et al.*, 1994; Dib *et al.*, 1996).

The strategy employed was that known macular and cone/cone-rod dystrophy loci were assessed in the first instance prior to a genome-wide screen.

12.3.3 *PROM1* mutation screening

Following identification of the disease interval on chromosome 4p, a positional candidate gene was determined by bioinformatics, *PROM1*. *PROM1* spans ~108kb of genomic DNA, consisting of 2580 base-pairs of cDNA and 25 exons. The encoded protein, prominin-1 has 860 amino acid residues.

Prominin-1 is a member of the prominin family of proteins, which are all characterised by five transmembrane segments and two large glycosylated extracellular loops (**Figure 12.2**). It has been suggested that prominin-1 may play a role in vertebrate photoreceptor disc morphogenesis (Corbeil *et al.*, 1999; Roper *et al.*, 2000; Corbeil *et al.*, 2001). A null mutation of *PROM1* has previously been reported to cause a recessive retinitis pigmentosa-like dystrophy (Maw *et al.*, 2000).

The 25 coding exons of *PROM1* were amplified by PCR in an affected and unaffected individual using primer sequences as shown in **Table 12.1**. Standard 50µl PCR reactions were performed as previously described. PCR conditions for all exons amplified were as follows: an initial denaturation of 3 minutes at 95°C, immediately followed by 35 cycles of 94°C for 45 seconds, 55°C for 45 seconds and 72°C for 1 minute, with a single final extension step of 72°C for 5 minutes. After resolution on a 1% (w/v) LMT agarose gel, products were excised and eluted. Direct sequencing of PCR products was carried out on

an ABI 3100 Genetic Analyser using the original PCR primers in the sequencing reactions. The sequence was examined for alterations utilising *Sequencing Analysis* (ABI Prism™) and *GeneWorks*™ software.

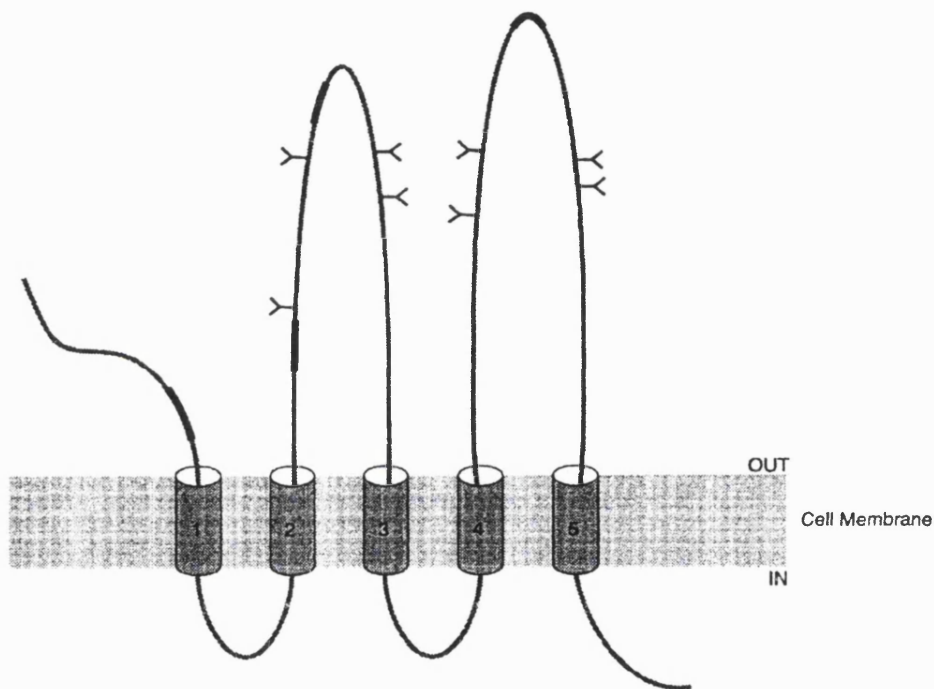


Figure 12.2

Proposed structural model of prominin-1

EXON1F	AAGGCTTCCAGAAGCTCTGAGGCA	EXON1R	GTGGGTGCGTTTGGAGATAAATCC
EXON2F	GATCTTTTCTAAAATATGCATT	EXON2R	CAGCCAAAATTTTCTCATACT
EXON3F	TCTGCCAAAATTCCTCACCTGCGT	EXON3R	GAAAGGCTTTCCAAGAGCAACTTG
EXON4F	TTGTGCTACAATATGTGCTGTTTC	EXON4R	CAGCCTAAAACACAATCAGTTGTT
EXON5F	GCTCTTCTCTCTCTGCCTTTTCCTG	EXON5R	GCTATCGCGGTACATAGAGATGATGG
EXON6F	GCCCTCTTATTGCCTTTGGACC	EXON6R	GTCTTCCCCCAACTTTCACG
EXON7F	CTTGAGGCAGTGTGGAGAGAATGAGG	EXON7R	GGGAACAAGAAAAGAGTGAGCAAGCC
EXON8F	GTAGATGAGGAGGGACTTGGC	EXON8R	CCCTGCCCGGCAATCCCCAGC
EXON9F	CTGCGATTGTACCCTGTAG	EXON9R	GCTATCACCTTCTTGGCAACC
EXON10F	GCCTCTCTACTCGTACTG	EXON10R	GCAATACTTGGCAACACATTTCTC
EXON11F	GGTGGTTCAGGCTTTTCTGTTTGG	EXON11R	CACCAGCTCCAAGGAGACAC
EXON12F	CTCCAGCCTTAGTCCAGCAGC	EXON12R	CACCAGAGTCAGCACCCAGTC
EXON13F	CACTGAAGACCCCAGGGC	EXON13R	GAAATCCAAGTTTCTGTTCAAG
EXON14F	GTATGTATGTTAGTGTAAAACCTG	EXON14R	CTCATTCCAGAAAAAGAACATC
EXON15F	CCTTCTCCTCATCTTCAGTGG	EXON15R	CCTAGATTTGGTGAAGGATGTG
EXON16F	GGCATGAGCCACCACATCCAGC	EXON16R	CCTAAAGGATCAAGCATGAACAC
EXON17F	GCCTACTAGATGTTGTGTTAAGGC	EXON17R	GGAACCTCTCCAGCAGC
EXON18F	GGATAGCGAGAGTGCTTTGAG	EXON18R	GCTGGGACCTATGAGAGATGAGC
EXON19F	GTGGGAAGGGAGGACACAAGG	EXON19R	GGTAGATAACTGAGGC
EXON20-21F	GGTCCAGGTCGTGGTGTTC	EXON20-21R	CCTCTGACCTGGTGGGAAGCC
EXON22F	GGAGATCCTTTTGTGACACC	EXON22R	GGTTTTGGATTCTCTCAAGCAG
EXON23F	CTTCACACAGTGCCTGGTCC	EXON23R	CTTTGAAGACAGCACCACC
EXON24F	GGGGGATGTAGTTGCTGAGC	EXON24R	CCTCCCCATCCCATCTAGG
EXON25F	GTAGTCCTTTGGTCTTTGAAG	EXON25R	CATACAGAGAGAAGTGAAGGC

Table 12.1

PROM1 5'-3' primer sequences

12.4 RESULTS

12.4.1 Phenotype

The disorder is present in a five-generation British family (**Figure 12.1**).

V:1 A 17-year-old woman (the proband) was first seen at age 13 having noticed blurred vision when reading and metamorphopsia. This difficulty with reading had gradually worsened. There were no reported problems with night vision. Visual acuity was 6/9 bilaterally. HRR revealed mild red-green defect and medium tritan defect bilaterally. Dilated funduscopy revealed bilateral macular retinal pigment epithelium (RPE) mottling and atrophy with fine perifoveal red granular patches. Visual fields

demonstrated mildly reduced central sensitivity. Fundus autofluorescence (AF) imaging revealed a ring of moderately increased perifoveal AF bilaterally (**Figure 12.3**). Fluorescein angiography showed localised masking of the choroidal fluorescence in the perifoveal area. The PERG P50 component was mildly sub-normal, consistent with macular dysfunction. EOG and full-field ERG were normal.

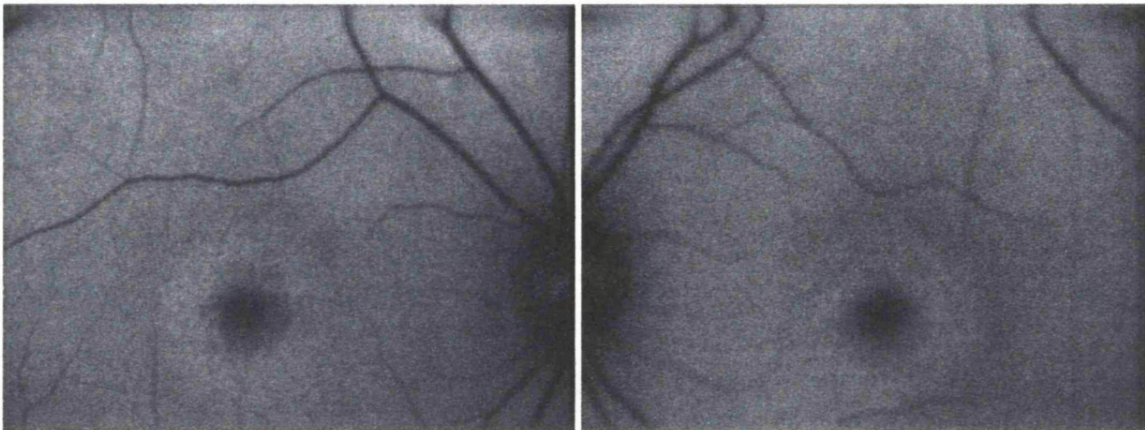


Figure 12.3

AF images of MCDR2 patient V:1

V:3 This 9-year-old boy complained of occasional difficulty with reading small print. Visual acuity was 6/6 bilaterally. HRR revealed mild red-green defect bilaterally. Fundoscopy revealed a bilaterally prominent foveal reflex and a red speckled appearance at the level of the RPE. Fundus AF revealed a mild perifoveal ring of increased autofluorescence. The ERG was normal. PERG and EOG were not performed due to poor co-operation.

V:4 This 14-year-old girl was asymptomatic, except for noticing some difficulty with colour vision, especially the colour blue. Visual acuity was found to be 6/5 bilaterally. Colour testing with HRR plates revealed a mild tritan and red-green defect in the left eye

and normal colour vision on the right. Fundus examination revealed a mild abnormality of the macula with bilateral red speckled appearance at the level of the RPE, more prominent in the left than the right eye. There was once again a prominent foveal reflex bilaterally. Fundus AF was unremarkable. PERG, ERG and EOG were normal.

IV:2 This 41-year-old woman complained of glare at night but was otherwise asymptomatic. Visual acuity was 6/5 bilaterally. Colour vision assessment with the HRR plates revealed generalised dyschromatopsia affecting protan, deutan and tritan axes. Fundoscopy revealed bilateral macular RPE mottling with a dark red perifoveal region (**Figure 12.4a**). Visual field testing revealed bilateral central scotomata. Fundus AF imaging revealed bilateral ‘bull’s-eye’ lesions, comprising of a ring of decreased perifoveal autofluorescence bordered peripherally and centrally (to a lesser extent) by increased autofluorescence (**Figure 12.4b**). Fluorescein angiography revealed masking of the choroidal fluorescence in the perifoveal area (**Figure 12.4c**). There was no recordable PERG; but EOG and ERG were normal.

IV:6 This 37-year-old woman complained of light sensitivity and glare at night. She had a visual acuity of 6/5 bilaterally and colour vision was normal. Fundoscopy revealed subtle bilateral foveal abnormalities, with central pallor and surrounding mottling of the RPE. Fundus AF showed an increased signal in the perifoveal region. Visual field testing was within normal limits. The PERG P50 component revealed low amplitude responses on the right and borderline abnormal on the left. EOG and full-field ERG were normal.

III:2 This 63-year-old woman was first seen at age 24 complaining of difficulty with reading and bilateral central visual field defects. Visual field testing at first presentation

with Bjerrum's tangent screen revealed bilateral central scotomata. Visual acuity at that time was 6/4 bilaterally. Granular pigmentation was noted at both maculae. Over a period of thirty-five years, visual acuity has gradually deteriorated to 6/24 in the right eye and 6/36 in the left. Fundoscopy now reveals a 'bull's-eye' maculopathy. The PERG was unrecordable from either eye. Rod and cone full-field ERG responses were sub-normal, suggesting a more widespread retinal dysfunction with disease progression (**Figure 12.5**). EOG was not possible due to lack of co-operation.

III:6 This 61-year-old woman was first seen at age 12 complaining of some difficulty with reading vision and light sensitivity. She felt that her vision was slow to adapt to dim illumination. Her visual acuity was 6/6 in her right eye and 6/9 in her left. Colour vision testing was normal. Dilated fundoscopy revealed bilateral RPE mottling, with a well-demarcated area of RPE atrophy at the right macula (**Figure 12.4d**). She had bilateral central scotomata on visual field testing. Fundus AF imaging revealed bilateral 'bull's-eye' lesions, which consisted of a ring of decreased perifoveal autofluorescence bordered peripherally (to a lesser extent) and centrally by increased autofluorescence (**Figure 12.4e**). The PERG was unrecordable. EOG was normal, but the rod and cone full-field ERG responses were sub-normal.

Patients V:2, V:5, V:6, IV:3 and III:8 were also assessed and were found to be asymptomatic with clinical examination being entirely normal.

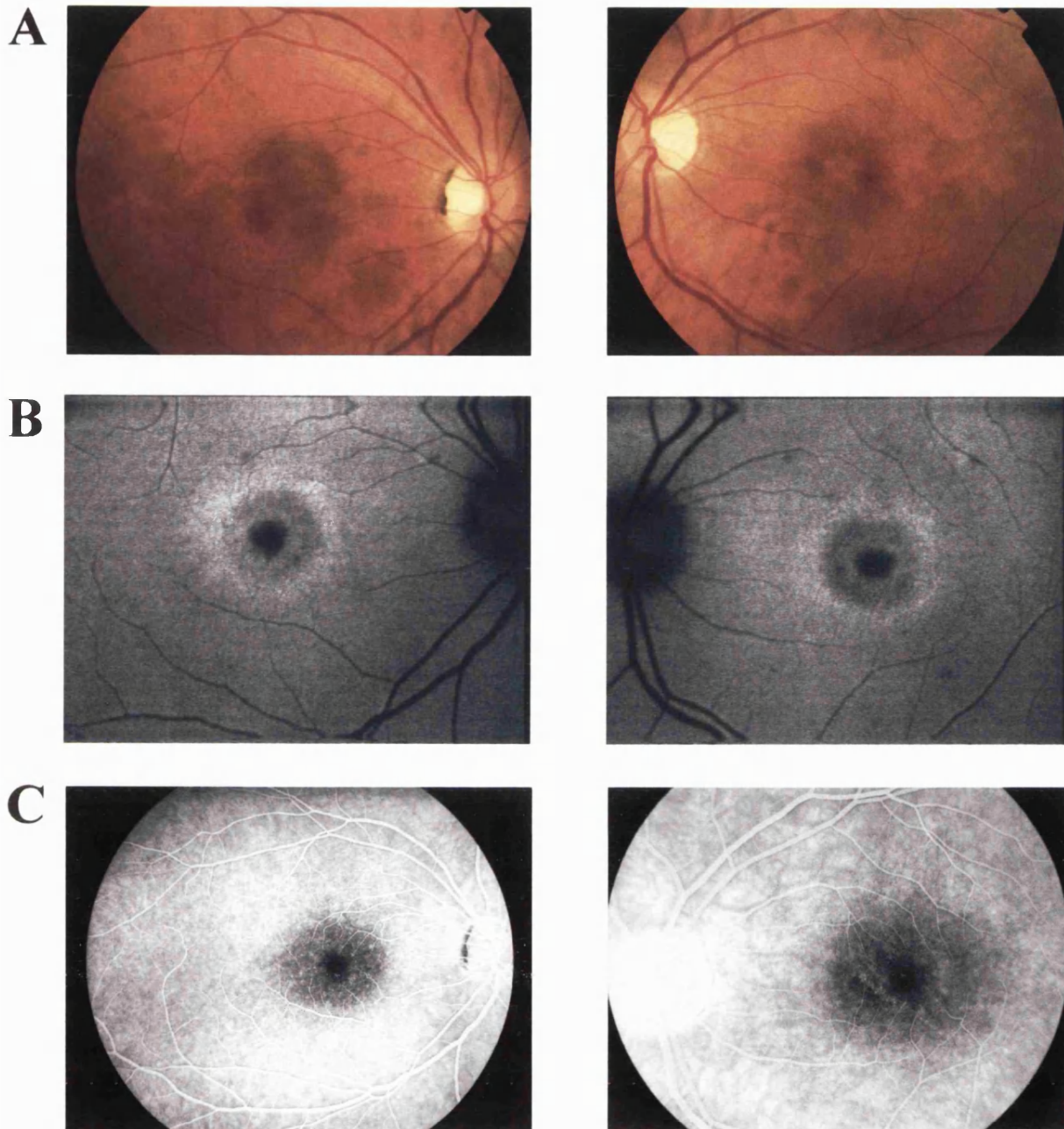


Figure 12.4

Fundi, FFA, & AF images of MCDR2 patient IV:2

A Fundus photograph showing bilateral RPE mottling and temporal optic disc pallor.

B Fundus AF imaging revealed bilateral 'bull's-eye' type lesions, comprising of a ring of decreased perifoveal autofluorescence bordered peripherally and centrally by increased autofluorescence.

C FFA showing bilateral localised masking of the choroidal fluorescence in the perifoveal area.

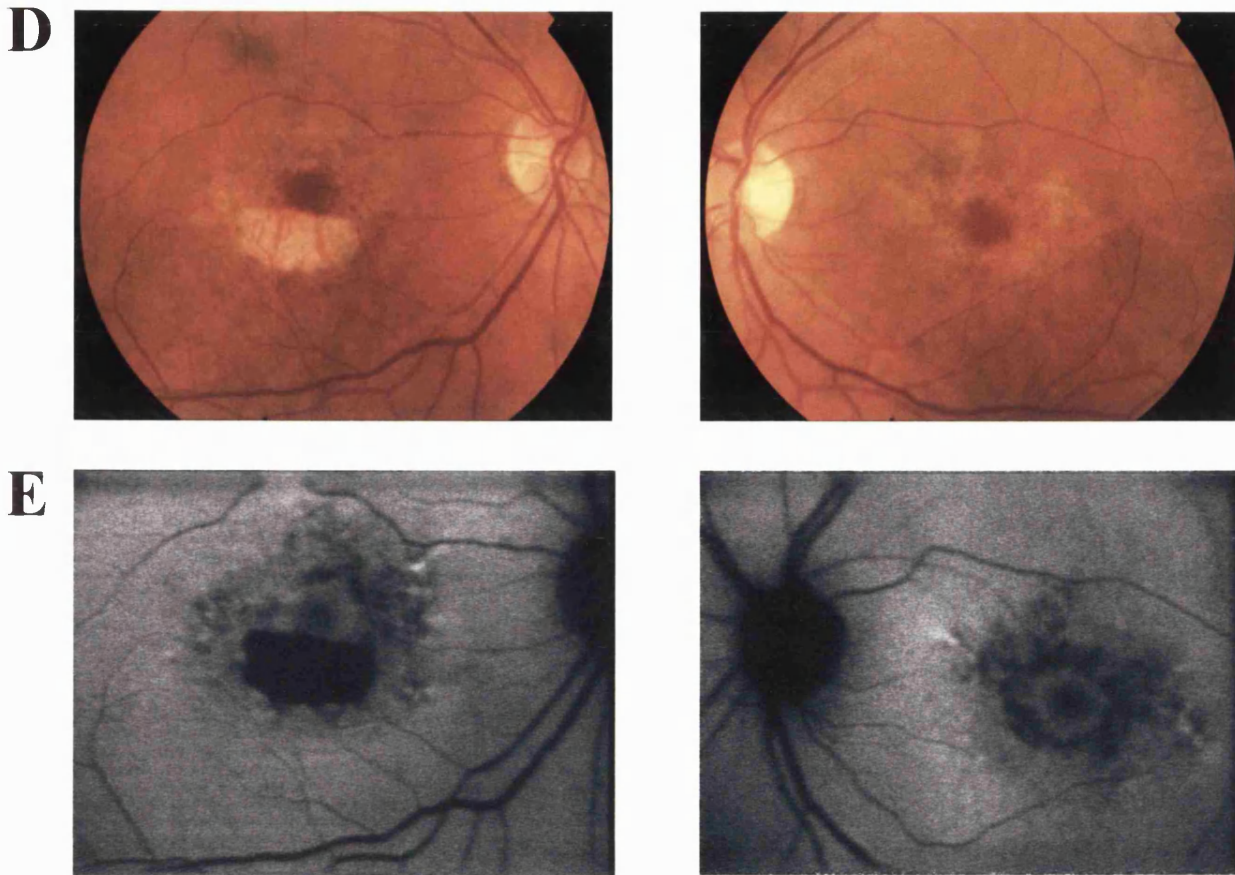


Figure 12.4

Fundi & AF images of MCDR2 patient III:6

D Fundus photograph showing bilateral ‘bull’s-eye’ maculopathy, with a well demarcated area of RPE atrophy at the right macula, and bilateral temporal optic disc pallor.

E Fundus AF imaging revealed bilateral ‘bull’s-eye’ type lesions, more prominent in the left than the right.

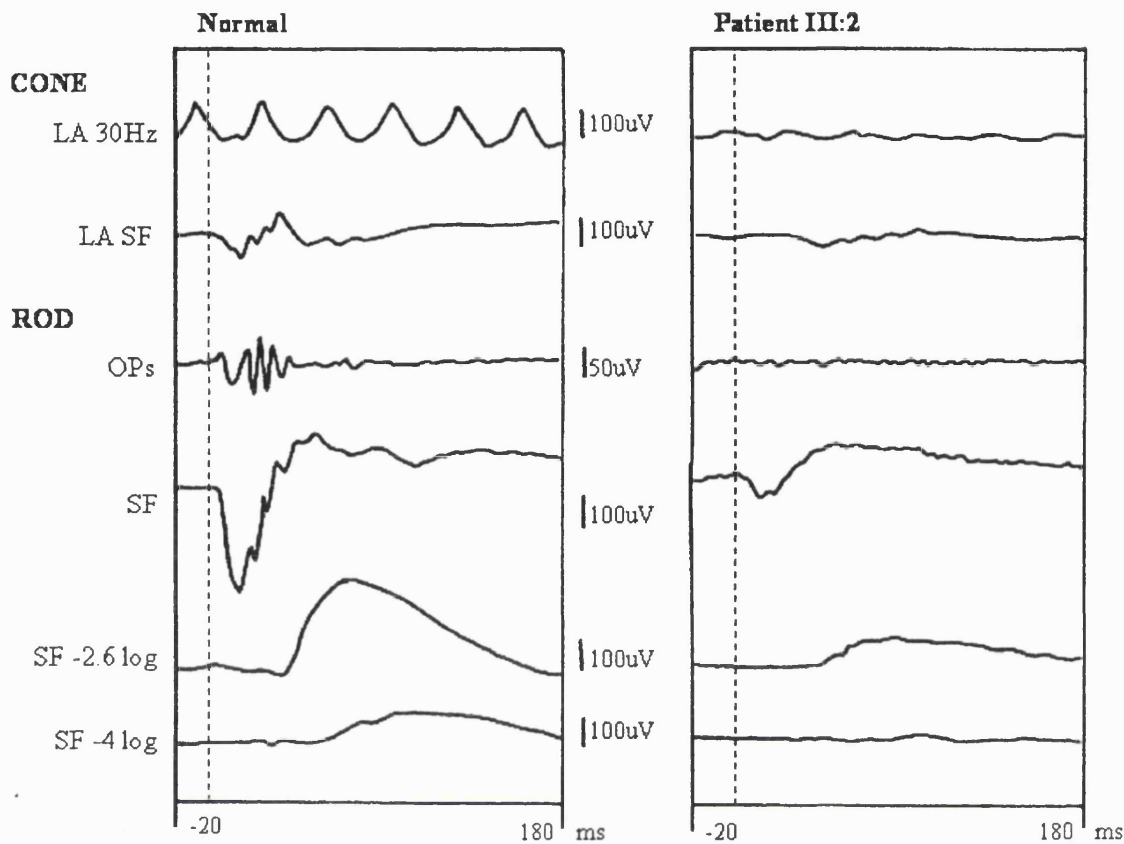


Figure 12.5

The full-field ERG of patient III:2

A normal control (on left) is shown for comparison. Patient III:2 has both reduced scotopic and photopic responses.

LA = Light Adapted; SF = Standard Flash (ISCEV Clinical ERG Standard);

OPs = Oscillatory Potentials; Broken line indicates time of stimulus flash.

12.4.2 Molecular genetics

12.4.2.1 Linkage analysis

In the first instance no significant linkage was found at known macular or cone/cone-rod dystrophy loci. In total ~50% of the genome was screened involving genotyping of 195 markers before significant linkage was established to chromosome 4p15.2-p16.3 with a maximum LOD score of 3.03 at a recombination fraction of 0.00 for marker D4S391.

Recombination in patients **III:2** and **V:3** (**Figure 12.1**) identified the flanking markers for this dominant macular dystrophy as D4S3022 and D4S3023, a genetic distance of 32cM.

12.4.2.2 *PROM1* mutation screening

The 25 coding exons of *PROM1* were screened for mutations in an affected and unaffected family member. An Arg373Cys missense mutation was identified in exon 10 (heterozygous C→T change at nucleotide 1117) of the affected subject (**Figure 12.6**). The Arg373Cys mutation was not detected in one hundred matched control chromosomes, indicating that it is not a common polymorphism. It was also found to segregate with disease; all unaffected relatives being homozygous for wild-type allele (CC), and affected subjects being heterozygotes, with nucleotides CT (**Figure 12.7**). However, Arg373 is not well conserved across species (**Table 12.2**).

Missense variant	Human	Murine	Rat	Zebrafish	Fugu
Arg373Cys	Arg	Asn	Asn	Glu	Glu

Table 12.2

Lack of amino acid conservation across species at site of missense mutation in prominin-1

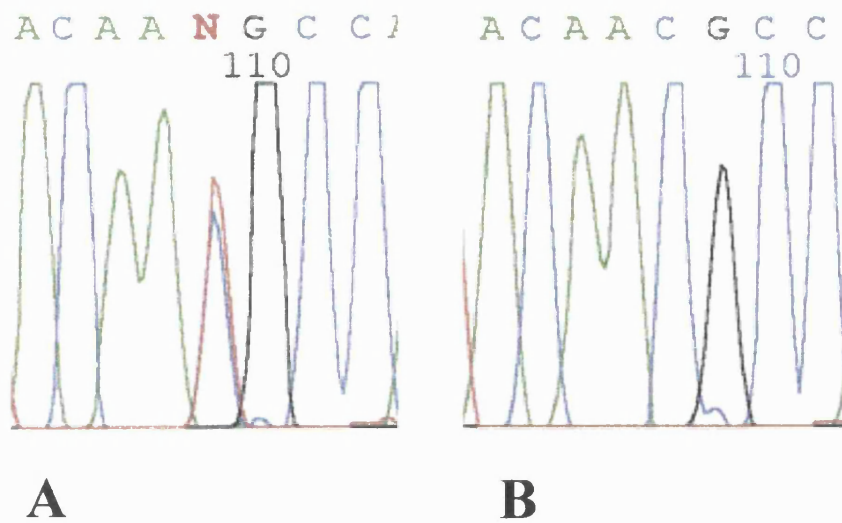


Figure 12.6

Sequence electropherograms of exon 10 of PROM1

A: Affected subject showing the C→T change at nucleotide 1117, which results in the missense mutation, Arg373Cys

B: Unaffected family member

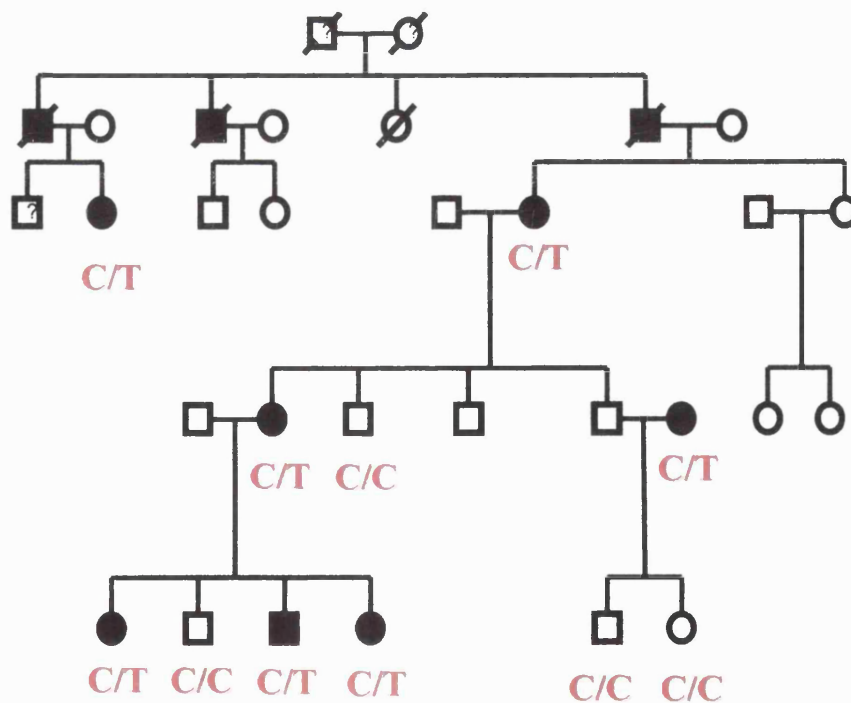


Figure 12.7

Segregation of Arg373Cys mutation

The position of the Arg373Cys mutation (red arrow) at the apical portion of the first extracellular domain of the proposed prominin-1 structure is illustrated in **Figure 12.8**. Also shown in **Figure 12.8** is the position of the premature stop codon (blue arrow) introduced in human prominin-1 by the deletion of nucleotide 1878 in *PROM1* in the retinal degeneration reported by Maw *et al.* (2000).

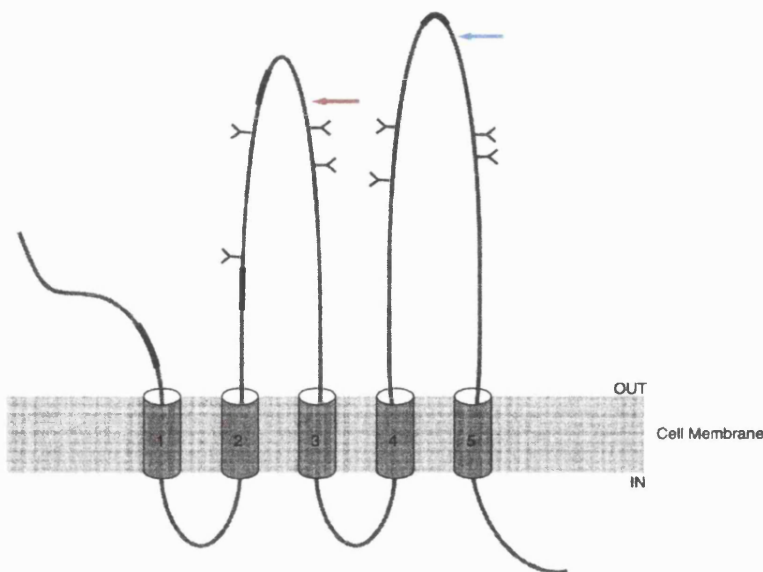


Figure 12.8
Positions of Arg373Cys (red arrow) and the stop codon (blue arrow) described by Maw et al. (2000)

12.5 DISCUSSION

An autosomal dominant macular dystrophy mapping to chromosome 4p15.2-p16.3 (Michaelides *et al.*, 2003c), with an Arg373Cys mutation in *PROM1* has been described. Following the convention established by the nomenclature used for North Carolina macular dystrophy phenotype (MCDR1), we have termed this disorder MCDR2 (MC = macular, D = dystrophy, R = retinal).

The macular dystrophy in this family is of early onset and in most affected individuals the disease is confined to the macular region. The early macular abnormalities include an increased foveal reflex and a red-speckled macular appearance, progressing to a more classical 'bull's-eye' maculopathy (BEM). Fluorescein angiography performed in two subjects with early disease showed hypofluorescence in the perifoveal area suggestive of accumulation in the RPE of an abnormal material which masks choroidal fluorescence. Older individuals have electrophysiological evidence of more widespread retinal dysfunction.

The pathogenesis of BEM is poorly understood. The characteristic appearance in which there is annular RPE atrophy and central sparing may correspond to the pattern of lipofuscin accumulation in the RPE, which in healthy individuals is highest at the posterior pole and shows a depression at the fovea (Wing *et al.*, 1978; von Rückmann *et al.*, 1997a). The initially spared centre usually becomes involved as the disease advances. It is evident that BEM is a non-specific appearance that can occur in relation to a number of underlying disorders at an early stage of their evolution (Kearns & Hollenhorst, 1966; Krill *et al.*, 1973; Deutman, 1974; Fishman *et al.*, 1977; O'Donnell & Welch, 1979).

AF imaging (section 1.3.2.2) with a cSLO can provide useful information about the distribution of lipofuscin in the RPE, and give indirect information on the level of metabolic activity of the RPE which is largely determined by the rate of turnover of photoreceptor outer segments. In our family concentric areas of increased AF at the macula were evident in some individuals before there was ophthalmoscopic evidence of retinal atrophy. This may suggest that the primary site of dysfunction is in the RPE, but the findings of a normal EOG indicate that there is no widespread RPE abnormality. Alternatively rather than due to an inability of the RPE to digest outer segment debris, the increased AF could occur as a result of primary pathology of the photoreceptors which in

the early stages of the disease is confined to the macular region but becomes more widespread in the late stages.

Linkage to chromosome 4p15.2-p16.3 was established. This region contains the candidate gene *PROM1*, encoding human prominin-1 which belongs to the prominin family of 5-transmembrane domain proteins. *PROM1* is expressed in retinoblastoma cell lines and adult retina, and the product of the mouse orthologue (*prom*) is concentrated in membrane evaginations at the base of the outer segments of rod photoreceptors (Maw *et al.*, 2000). A homozygous mutation in *PROM1* has been identified in an Indian pedigree with an autosomal recessive retinal dystrophy. The mutation results in the production of a truncated protein, and functional studies in transfected CHO cells have demonstrated that the truncated prominin protein fails to reach the cell surface, indicating that the loss of prominin may lead to retinal degeneration via the impaired generation of evaginations or conversion to outer segment discs (Maw *et al.*, 2000). Mutation screening of *PROM1* in our family identified an Arg373Cys mutation which was found to segregate with disease. This missense variant was not found to be present in 100 matched control chromosomes.

A locus for an autosomal dominant Stargardt-like disease has also been mapped to chromosome 4p (STGD4) in a Caribbean family (Kniazeva *et al.*, 1999). Analysis of extended haplotypes localised the disease gene to a 12cM interval between markers D4S1582 and D4S2397. This interval overlaps with our defined MCDR2 region. Interestingly, the phenotype detailed in our pedigree differs considerably from the Caribbean family in that neither of our patients who underwent FFA demonstrated the characteristic dark-choroid pattern that was seen in the Caribbean patients and our patients lacked the retinal flecks which were prominent in the Stargardt-like pedigree. Nevertheless, the same Arg373Cys missense mutation in *PROM1* has recently also been found to co-segregate with disease in the STGD4 pedigree (personal communication

Kang Zhang). This therefore represents a further example where the eventual macular dystrophy phenotype observed would appear to be dependent on environmental factors and/or the genetic context/background within which a mutation in a particular gene is expressed; in other words that modifying genes are likely to influence the final phenotype.

Extensive haplotype assessment (performed in Dr. Zhang's department, USA) of both the MCDR2 family and the STGD4 family has provided clear evidence that the two families are unrelated, thereby implying that the Arg373Cys mutation has arisen independently in two separate families. This is further supportive evidence of the likely pathogenicity of the identified mutation in *PROM1*. Furthermore, preliminary expression studies in 293T cells, of EGFP-tagged wild-type and Arg373Cys mutant prominin-1 protein, has demonstrated that the mutant fails to correctly target to the plasma membrane (performed in Dr. Zhang's department) (**Figure 12.9**).

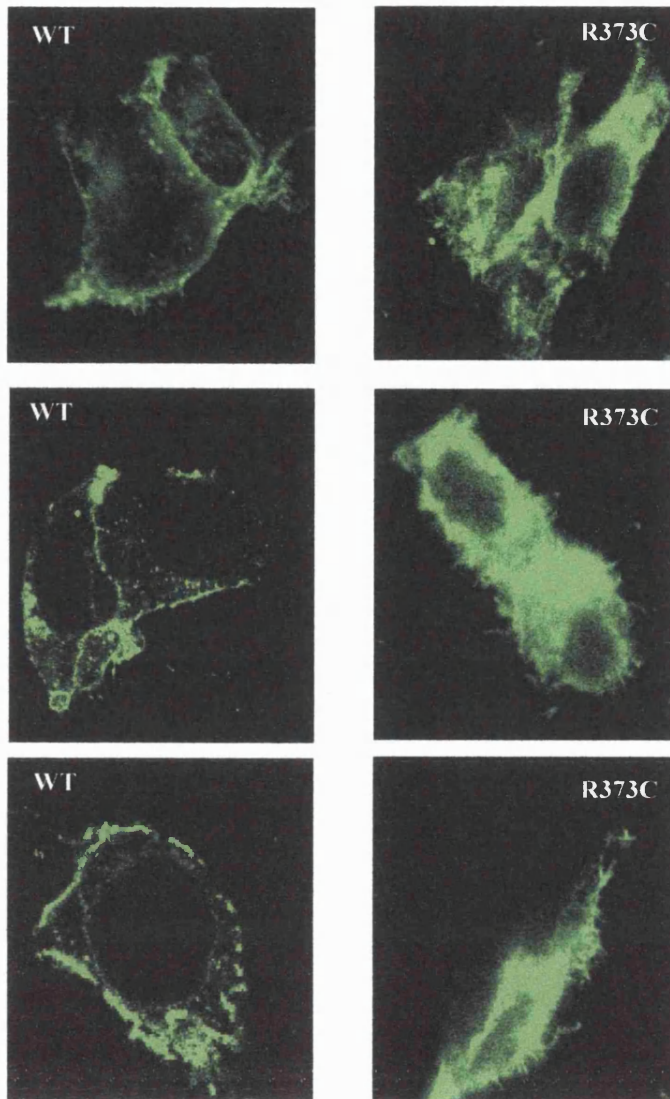


Figure 12.9

Expression studies in 293T cells of EGFP-tagged wild-type (WT)

and Arg373Cys (R373C) mutant prominin-1 protein

Performed by colleagues in Dr. Zhang's department, USA.

12.6 CONCLUSIONS

The MCDR2 phenotype is characterised by a 'bull's-eye' macular dystrophy first evident in the first or second decade of life. There is mild visual impairment, central scotomata and electrophysiological testing indicates that most affected individuals have disease

confined to the central retina but in older subjects the full-field ERG demonstrates more widespread rod and cone abnormalities.

MCDR2 maps to chromosome 4p15.2-p16.3. Mutation screening of *PROM1* identified an Arg373Cys mutation that segregated with disease. This *PROM1* mutation has also been found in the unrelated STGD4 macular dystrophy family providing further evidence in support of the proposed deleterious effects of this missense mutation. The absence of functional prominin-1 protein may impair either the generation of plasma membrane invaginations in the photoreceptor outer segment; and/or the subsequent membrane remodeling process leading to disc formation.

Two other important disc membrane proteins, peripherin/RDS and ROM1, when mutated, have been shown to cause a wide range of macular and retinal dystrophy phenotypes. The intra-familial phenotypic heterogeneity seen with mutations of either *RDS* (Weleber *et al.*, 1993; Apfelstedt-Sylla *et al.*, 1995) or *ROM1* (Sakuma *et al.*, 1995; Martinez-Mir *et al.*, 1997) provides genetic evidence suggestive of at least one other interacting protein. One potential candidate for these interactions may be prominin-1. Indeed conversely, it is a possibility that sequence variants in *RDS* or *ROM1*, play a role in leading to the distinct phenotypic differences seen in MCDR2 and STGD4.

CHAPTER 13

AN AUTOSOMAL DOMINANT MACULAR DYSTROPHY (MCDR3) RESEMBLING NORTH CAROLINA MACULAR DYSTROPHY

13.1 INTRODUCTION

The central receptor or macular dystrophies comprise a heterogeneous group of disorders in which there is variable visual loss associated with bilateral symmetrical macular abnormalities. A number of different genes causing macular dystrophy have been identified (Table 1.4), and the study of gene expression and function of the encoded proteins has improved our understanding of disease pathogenesis.

Although in most macular dystrophies the abnormal fundoscopic appearance is confined to the macular region, there is usually electrophysiological, psychophysical or histological evidence of widespread photoreceptor and retinal pigment epithelial dysfunction (Scullica and Falsini, 2001; Michaelides *et al.*, 2003b). This is consistent with the fact that most genes identified as causing macular dystrophy in man are expressed throughout the retina rather than solely the macular region (Musarella, 2001). There are however a few disorders where the disease does appear to be confined to the macular region. For example in North Carolina macular dystrophy (MCDR1), psychophysical and electrophysiological testing demonstrates that normal peripheral retinal function is retained (Small, 1998).

13.2 AIMS

To describe in detail the phenotype of an autosomal dominant (AD) macular dystrophy resembling North Carolina macular dystrophy. In a parallel study linkage analysis was performed by a colleague to identify the chromosomal locus.

13.3 METHODS

Thirteen members of a four-generation, non-consanguineous British family with an AD macular dystrophy were assessed (**Figure 13.1**). The clinical notes of three additional affected family members who were not available for examination were also reviewed. Blood samples were taken for DNA extraction and linkage analysis performed.

13.3.1 *Patients and clinical assessment*

A medical history was taken and a full ophthalmological examination performed. Colour vision testing was performed using the HRR plates. Affected subjects also underwent Humphrey automated photopic perimetry, colour fundus photography and fundus autofluorescence (AF) imaging using the confocal scanning laser ophthalmoscope (cSLO). Electrophysiological assessment included an ISCEV standard EOG and full-field ERG. Two subjects underwent fundus fluorescein angiography (FFA).

Individuals were diagnosed as affected on the basis of the presence of macular abnormality and in most cases associated decreased visual acuity.

13.3.2 *Linkage analysis*

Linkage analysis was undertaken in a parallel study by a colleague. Genotyping was carried out utilising markers from version 2.0 of the ABI MD-10 and HD-5 Linkage Mapping Sets (Applied Biosystems). These sets allow ~10cM and ~5cM resolution of the human genome respectively and consist of fluorescently labelled PCR primer pairs for 800 highly polymorphic dinucleotide-repeat microsatellite markers chosen from the Genethon human linkage map (Weissenbach *et al.*, 1992; Gyapay *et al.*, 1994; Dib *et al.*, 1996).

The strategy employed was that known macular and cone/cone-rod dystrophy loci were assessed in the first instance, prior to a genome-wide screen. Particular attention was paid to confirming the exclusion of the MCDR1 locus on chromosome 6q.

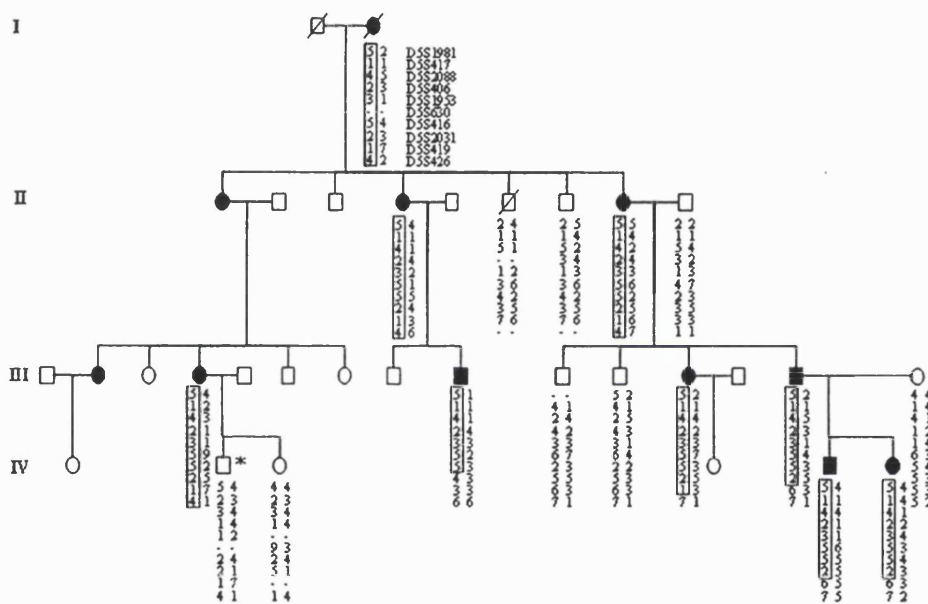


Figure 13.1

MCDR3 pedigree

Individuals are numbered according to their generation (indicated) and position in each generation numbering from left to right. The alleles present for each of the ten chromosome 5p microsatellite markers used are shown. The minimal disease region for each affected individual is boxed. Disease haplotype is defined by recombination events in individuals III:9 and IV:2.

Linkage analysis performed by a colleague.

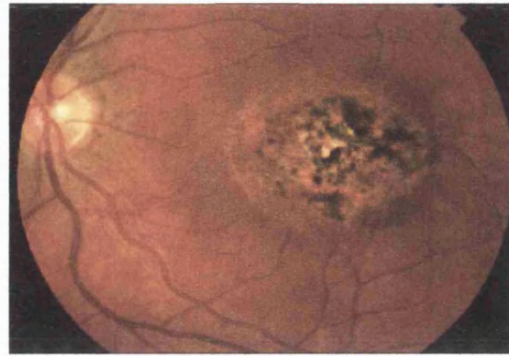
13.4 RESULTS

13.4.1 *Phenotype*

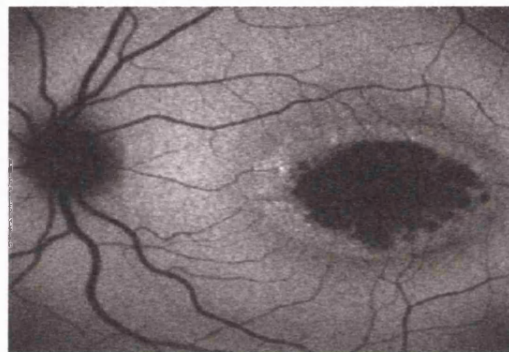
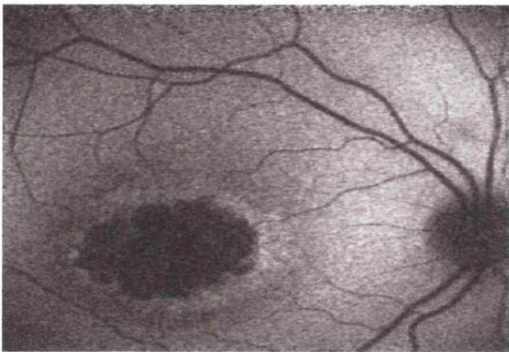
The disorder is present in a four-generation British family as shown in **Figure 13.1**. Patients **III:10**, **III:11**, **III:15**, **IV:2**, **IV:3** and **IV:4**, were asymptomatic with a normal clinical examination and were designated as unaffected. The affected individuals showed a range of macular appearances varying from multiple drusen-like deposits to focal atrophy and pigmentation (**Table 13.1**). EOG and full-field ERG was normal in all affected individuals.

IV:5 The proband, an 11-year-old boy, was first seen at age 4 having been referred from a pre-school screening clinic. His visual acuity was 6/9 in each eye with the Sheridan Gardiner test. Fundoscopy revealed sharply circumscribed bilateral central macular retinal pigment epithelial atrophy and pigment clumping with surrounding drusen-like deposits. Fluorescein angiography revealed mild macular window defects corresponding to the area of macular abnormality. At age 6 years, Snellen acuity was recorded at 6/18 in the right eye and 6/12 in the left eye. He has been reviewed recently and visual acuity has remained stable. His fundus appearance has become more marked, with slightly larger areas of atrophy and pigment clumping and more prominent fine drusen-like deposits (**Figure 13.2A**). Visual field testing was unreliable. Fundus autofluorescence imaging revealed bilateral central decreased autofluorescence (AF) with a surrounding ring of increased AF (**Figure 13.2B**). EOG and full-field ERG were normal. Colour vision testing was abnormal and involved protan, deutan and tritan axes.

2A



2B



Figures 13.2A & 13.2B

Fundi & AF images of MCDR3 patient IV:5

2A Fundus photographs showing bilateral macular RPE atrophy and pigment clumping, with surrounding drusen-like deposits.

2B Fundus AF imaging showing bilateral decreased AF centrally with a surrounding ring of relative increased AF.

IV:6 This 9-year-old girl was asymptomatic. Visual acuity was 6/4 in both eyes. Colour vision was normal. Fundoscopy revealed bilateral macular atrophy and pigmentation with fine drusen-like deposits (**Figure 13.2C**). Co-operation for fundus AF imaging was poor; however the images obtained were probably within normal limits. EOG and ERG were normal.

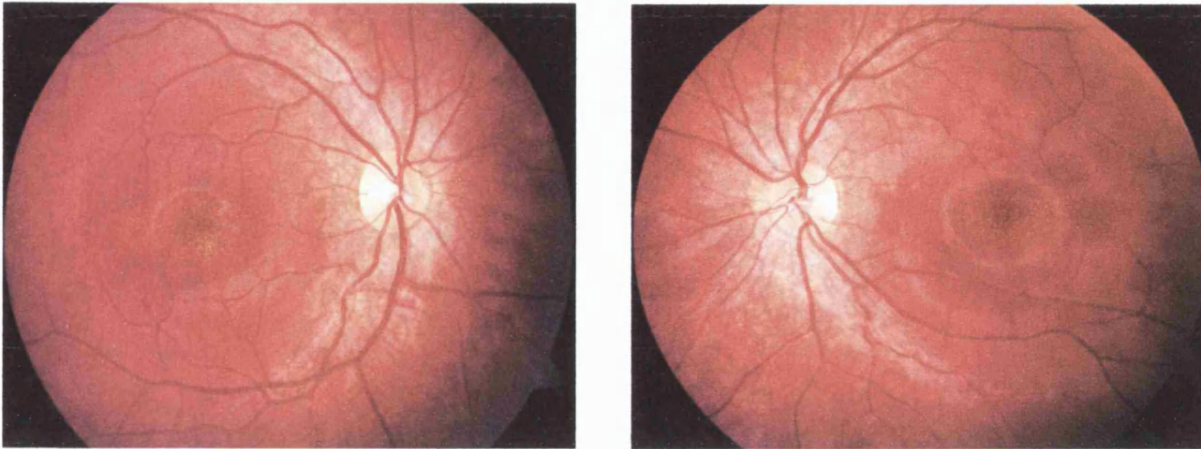


Figure 13.2C

Fundi of MCDR3 patient IV:6

Bilateral macular atrophy and pigmentation with fine drusen-like deposits

III:2 This subject was not available for study but examination of her clinical records, retinal photography and fluorescein angiography revealed that she had developed a sub-retinal neovascular membrane (SRNVM) prior to the age of 17 years in her right eye and had evidence of RPE atrophy with surrounding drusen-like deposits in the left eye (**Figure 13.2D**).

III:4 This 36-year-old woman complained of occasional blurred vision. Visual acuity was 6/5 bilaterally. Colour vision assessment revealed mild red-green defect in both eyes. Fundoscopy revealed extensive bilateral fine macular drusen-like deposits with areas of RPE atrophy. Fundus AF imaging revealed increased AF at both maculae, which appeared to correspond to the drusen-like deposits (**Figure 13.2E**). Visual field testing was normal. EOG and ERG were normal.

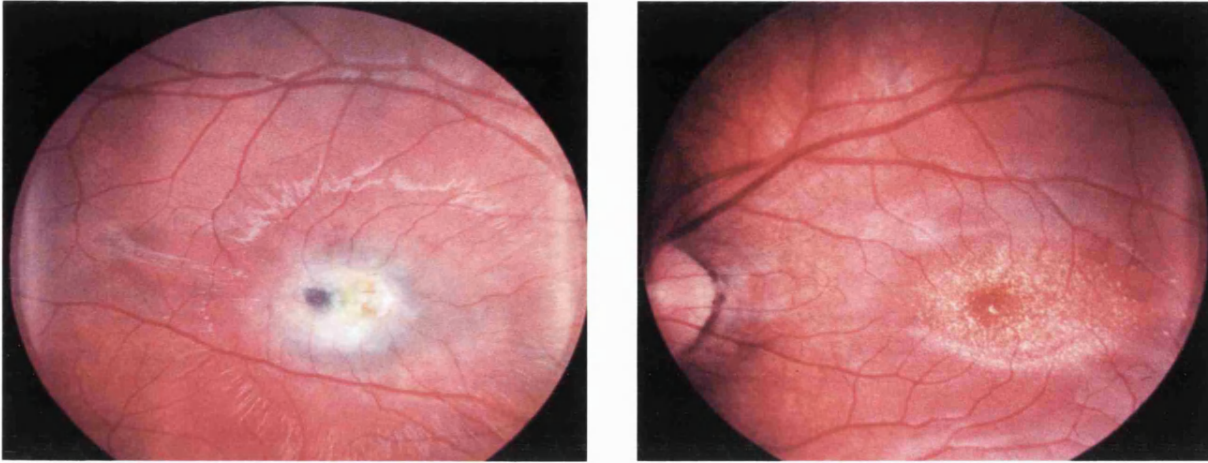


Figure 13.2D

Fundi of MCDR3 patient III:2

Acute SRNVM in the right eye and RPE atrophy with surrounding drusen-like deposits in the left eye

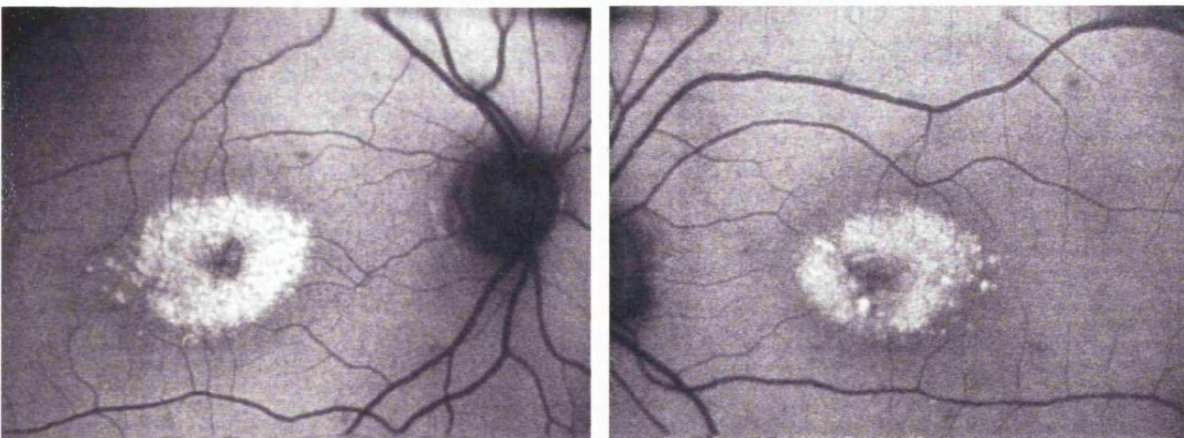


Figure 13.2E

AF images of MCDR3 patient III:4

Increased AF at both maculae, which corresponds to the drusen-like deposits seen ophthalmoscopically

III:9 This 16-year-old boy has had poor central vision and pendular nystagmus since infancy. His visual acuity was 6/60 in each eye and colour vision was normal. Fundoscopy revealed bilateral extensive macular atrophy and pigmentation. Visual field testing revealed bilateral central field defects. ERG was normal. Nystagmus precluded accurate EOG recordings.

III:12 This 27-year-old woman complained of occasional mild blurred vision. Her visual acuity was 6/6 in both eyes, with full colour vision. Fundoscopy revealed typical extensive fine macular drusen-like deposits with associated RPE atrophy and pigmentation. Visual field testing was normal. ERG and EOG were normal.

III:14 This 37-year-old man was asymptomatic. His visual acuity was 6/6 in each eye. Fundoscopy revealed typical extensive fine macular drusen-like deposits with associated RPE atrophy and pigmentation (**Figure 13.2F**). Visual field testing was normal. Fundus autofluorescence revealed increased AF at both maculae, which appeared to correspond to the drusen-like deposits. In addition, slight decreased AF was present centrally in both eyes (**Figure 13.2G**). EOG and full-field ERG were normal.

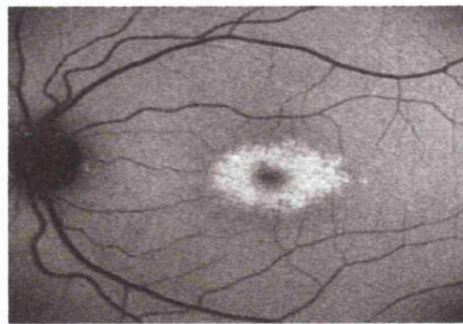
II:1 This 63-year-old woman was not available for study but examination of her clinical records revealed that she had developed bilateral disciform maculopathy prior to the age of 20.

II:4 This 50-year-old woman had poor vision and a left esotropia and amblyopia from childhood. Her visual acuity was 6/18 in her right eye, and 6/60 in her left. Colour vision testing revealed mild generalised dyschromatopsia. Fundoscopy revealed bilateral macular scarring associated with sub-retinal fibrosis and surrounding fine drusen-like deposits. The clinical appearance and FFA were consistent with previous SRNVM. She had bilateral central scotomata on visual field testing. EOG and full-field ERG were normal.

2F



2G



Figures 13.2F & 13.2G

Fundi & AF images of MCDR3 patient III:14

2F Fundus photograph showing bilateral typical fine macular drusen-like deposits with associated RPE atrophy and pigmentation.

2G Fundus AF imaging showing increased AF at both maculae, corresponding to the drusen-like deposits. In addition, slight decreased AF is seen centrally in both eyes.

II:8 This 60-year-old woman complained of occasional difficulties when reading. Her visual acuity was 6/9 in both eyes. Colour vision testing revealed mild generalised dyschromatopsia in the right eye and normal colour vision in the left. Fundoscopy revealed macular atrophy and surrounding fine drusen-like deposits. Visual field testing was unremarkable. Fundus autofluorescence revealed increased AF at both maculae, which appeared to correspond to the drusen-like deposits. In addition, slight decreased AF was present centrally in both eyes. EOG and full-field ERG were normal.

I:2 This 80-year-old woman was not available for study but examination of her clinical records revealed that she had evidence of bilateral macular atrophy and fibrosis consistent with previous SRNVM.

Patient	Age	Visual Acuity OD - OS	Fundus	AI Imaging	LOG	ERG	Visual Fields	Colour Vision
I:2*	80	-	Bilateral SRNVM	-	-	-	-	-
II:1*	63	-	Bilateral SRNVM	-	-	-	-	-
II:4	50	6/18 – 6/60	Bilateral macular scarring associated with sub-retinal fibrosis and surrounding fine drusen-like deposits. FFA was consistent with previous bilateral SRNVM	-	N	N	Bilateral central scotomata	Bilateral protan, deutan & tritan defects
II:8	60	6/9 - 6/9	Bilateral fine macular drusen-like deposits with areas of RPE atrophy & pigmentation	Increased AF at both maculae, corresponding to the drusen-like deposits	N	N	N	Bilateral protan, deutan & tritan defects
III:2*	37	6/60 – 6/12	OD : SRNVM OS: Macular drusen-like deposits with areas of RPE atrophy & pigmentation Figure 2D	-	-	-	-	-
III:4	36	6/5 – 6/5	Bilateral fine macular drusen-like deposits with areas of RPE atrophy & pigmentation	Increased AF at both maculae, corresponding to the drusen-like deposits Figure 2E	N	N	N	Bilateral protan & deutan defects
III:9	16	6/60 – 6/60	Bilateral extensive macular atrophy & pigmentation	-	N	N	Bilateral central scotomata	N
III:12	27	6/6 – 6/6	Bilateral fine macular drusen-like deposits with areas of RPE atrophy & pigmentation	-	N	N	N	N
III:14	37	6/6 – 6/6	Bilateral fine macular drusen-like deposits with associated RPE atrophy and pigmentation Figure 2F	Increased AF at both maculae, corresponding to the drusen-like deposits. Figure 2G	N	N	N	N
IV:5	11	6/18 - 6/12	Bilateral macular RPE atrophy and pigment clumping, with surrounding drusen-like deposits Figure 2A	Bilateral decreased AF centrally with a surrounding ring of relative increased AF Figure 2B	N	N	-	Bilateral protan, deutan & tritan defects
IV:6	9	6/4 – 6/4	Bilateral macular atrophy & pigmentation Figure 2C	-	N	N	N	N

Table 13.1 Summary of clinical findings in MCDR3

N = Normal; RPE = Retinal Pigment Epithelium; AF = Autofluorescence;

SRNVM = Sub-retinal neovascular membrane

* Patients I:2, II:1 and III:2 were not available for study but examination of clinical records, retinal photography and fluorescein angiography was performed. III:2 had developed SRNVM prior to the age of 17 years in her right eye. II:1 had developed bilateral disciform maculopathy prior to the age of 20.

13.4.2 Linkage analysis

In the first instance no significant linkage was found at known macular or cone/cone-rod dystrophy loci. In total ~50% of the genome was screened involving genotyping of 195 markers before significant linkage was established to chromosome 5p13.1-p15.33 with a maximum LOD score of 3.61 at a recombination fraction of 0.00, for marker D5S630 (Figure 13.1).

Unaffected individual IV:2 has two recombination events in the chromosome inherited from his affected mother which, along with the haplotype information for individual III:9 establishes D5S1981 and D5S2031 as the markers flanking the MCDR3 disease region. This represents a genetic distance of 35cM.

In view of the phenotypic similarity of this disorder to the North Carolina macular dystrophy (MCDR1) that maps to chromosome 6q16, this region has been examined in our family in greater detail. Linkage analysis has previously indicated that the MCDR1 gene is in the interval between D6S249 and D6S1671 (Small *et al.*, 1999). The LOD scores for these markers in our family were both $-\infty$ at $\theta=0.0$. In addition, haplotype analysis of these and additional markers adjacent to the MCDR1 region confirms that the disease in our family does not map to this region of the genome.

13.5 DISCUSSION

The autosomal dominant macular dystrophy in this family has an unusual phenotype. It is characterised by an early age of onset and is generally associated with relatively good vision despite significant macular abnormalities evident on ophthalmoscopy. Mild colour vision abnormalities are variably present in affected individuals. The macular appearance

varies from multiple drusen-like deposits to focal atrophy and pigmentation. With the exception of one young individual (IV:5) who showed an increase in retinal pigmentation and drusen-like deposits over a 6 year period, there was no evidence of change in macular appearance over time. Furthermore, although the retinal phenotype varied within the family, the severity of the changes is unrelated to age. Two individuals had angiographic evidence of SRNVM, and in an additional two, the macular appearances were consistent with this diagnosis. Following the convention established by the nomenclature used for North Carolina macular dystrophy phenotype (MCDR1), we have termed this disorder MCDR3 (Michaelides *et al.*, 2003d).

Visual field loss in family members was demonstrated only over the central macular lesions. The normal EOG and ERG in all affected individuals suggests that the dystrophy is localised to the macula and that there is no widespread involvement of retinal photoreceptors.

Affected subjects showed decreased AF corresponding to areas of atrophy seen ophthalmoscopically. In addition, concentric perifoveal areas of increased AF were evident and these were found to correspond to the drusen-like deposits. This finding is in direct contrast to drusen in age-related macular degeneration (ARMD), where there is generally little or no correspondence between the distribution of drusen and AF; although large soft foveal drusen may be associated with increased AF (von Rückmann *et al.*, 1997b; von Rückmann *et al.*, 1999; Lois *et al.*, 2002). However, the drusen-like deposits in the phenotype we describe, are small and fine, present from a young age, and are likely to have a different pathogenesis to hard drusen seen in the ageing eye. There is currently no published data on either the autofluorescence associated with MCDR1 drusen-like deposits,

or on their chemical composition. However, it has been recently proposed that misfolding and aberrant accumulation of EFEMP1 within RPE cells and between the RPE and Bruch's membrane may underlie drusen formation in Doyme Honeycomb retinal dystrophy and ARMD. Although EFEMP1 itself does not appear to be a major component of the drusen (Marmorstein *et al.*, 2002). Histopathology is available of the eye of one patient with MCDR1 which showed accumulation of lipofuscin in the RPE within the atrophic macular lesion (Small *et al.*, 2001). The mechanism of drusen formation in MCDR1 and MCDR3 is however uncertain but our understanding will be improved by identification of the causative genetic mutations.

MCDR3 has many phenotypic similarities to MCDR1, an autosomal dominant macular dystrophy which is characterised by a variable macular phenotype. Bilaterally symmetrical fundus appearances in MCDR1 range from a few small (less than 50µm) yellow drusen-like lesions in the central macula (grade 1) to larger confluent lesions (grade 2) and macular colobomatous lesions (grade 3) (Small, 1998). All three grades of lesion are seen in our pedigree. The electrophysiological changes seen in our family are also consistent with those reported in MCDR1 (Small, 1998). The only significant differences in the two phenotypes is that in our family colour vision testing was abnormal in the majority of affected individuals and there was evidence of disease progression, albeit in a single case.

Linkage studies have mapped MCDR1 to a locus on chromosome 6q16. To date, MCDR1 has been described in various countries and no evidence of genetic heterogeneity has been reported (Small *et al.*, 1997; Rabb *et al.*, 1998; Reichel *et al.*, 1998; Small *et al.*, 1999). In the family reported here we have excluded linkage to the MCDR1 locus and have obtained significant linkage to chromosome 5p. A further MCDR1-like macular dystrophy

associated with deafness (MCDR4), mapping to 14q, has been described recently; the MCDR1 locus was also excluded in that family (Francis *et al.*, 2003). Both MCDR3 and MCDR4 are highly similar to MCDR1 and thereby suggest the presence of genetic heterogeneity in the North Carolina macular dystrophy phenotype.

The MCDR3 disease interval contains three members of the cadherin gene family, cadherin-6, -10, -12, which are all highly expressed in the brain (Suzuki *et al.*, 1991; Kools *et al.*, 1999). Retinal expression has yet to be examined. These represent potential candidates, especially in light of the recent identification of mutations in both cadherin-23, in patients with Usher Syndrome type 1D, a condition that includes retinitis pigmentosa (von Brederlow *et al.*, 2002); and also in cadherin-3, in a syndrome of hypotrichosis with macular dystrophy (Sprecher *et al.*, 2001). However the region is large and many more potential candidate genes within the disease interval remain to be characterised.

Identification of the genes responsible for these disorders will help to improve our understanding of the mechanisms underlying macular development and may shed light on the pathogenesis of drusen and SRNVM.

13.6 CONCLUSIONS

In the present study the clinical and electrophysiological findings have been detailed of a family with a dominantly inherited macular dystrophy resembling MCDR1.

The MCDR1 locus on chromosome 6 has been excluded, and linkage in this family to a novel locus on chromosome 5 has been demonstrated; providing evidence for genetic heterogeneity in the North Carolina macular dystrophy phenotype.

The identification of the MCDR3 gene may have implications for ARMD, due to the prominence of drusen-like deposits and the complication of SRNVM in this early onset macular dystrophy.

CHAPTER 14

CONCLUDING REMARKS AND FUTURE PERSEPCTIVES

The purpose of this study has been to investigate in detail the phenotypes of several cone/cone-rod and central receptor dystrophies, and where possible probe the underlying molecular genetic basis of these disorders. The intention being to gain improved understanding of the characteristics, natural history and disease mechanisms of these conditions with resulting improved advice on prognosis and genetic counselling. The cone, cone-rod and central receptor dystrophies form part of a heterogeneous group of retinal dystrophies that are a major cause of childhood blindness.

The molecular characterisation of these disorders remains an important goal, so that in the event of future treatment options, it may thereby be possible to make a judgement as to whether particular patients are suitable. Clearly in the first instance the identification of the genetic defect will suggest potential mechanisms of disease and therapy. In addition, it is hoped that the study of the central receptor dystrophies will help us to gain insights into ARMD, the commonest cause of blindness in the developed world; both in terms of improved understanding of the recognised underlying genetic influences and also lead to a better grasp of the potential pathways of pathogenesis of this heterogeneous maculopathy.

Many genes have now been identified causing the various cone dysfunction syndromes, cone/cone-rod dystrophies and the inherited monogenic macular dystrophies. There is now an increasing need to address the functional implications of the encoded mutant proteins, in order to corroborate their proposed disease-causing status and also to better understand mechanisms of disease. Until such functional data is available for the multitude of mutations identified to date, it can not be assumed that all reported mutations are necessarily disease-causing. Indeed in direct contrast, it may also become

evident that certain 'polymorphisms', when associated with particular sequence variants, are in fact disease-causing. Achromatopsia associated with mutation of the cGMP-gated cation channel subunits is a good example of a cone disorder in which functional studies will be possible and informative; patch-clamp testing, expression studies to assess membrane targeting and the effects of pharmacological agents on channel conductance can be potentially determined.

There is currently no specific treatment for any of these retinal disorders. Nevertheless, it is important that the correct diagnosis is made, in order to be able to provide accurate information on prognosis and to be able to offer informed genetic counselling. Prenatal diagnosis is possible when the mutation(s) causing disease in the family is known. The provision of appropriate spectacle correction, low vision aids and educational support is also very important. Photophobia is often a prominent symptom in the cone/cone-rod disorders and therefore tinted spectacles or contact lenses may be beneficial to patients, in terms of both improved comfort and vision.

Although there is no specific treatment available for this group of disorders, it is hoped that further detailed investigation will improve our understanding of disease mechanisms and thereby assist in the development of effective therapies in the future.

15.0 ACKNOWLEDGEMENTS

I would first like to thank my principal supervisor, Professor A. T. Moore, for his constant support and encouragement. His enthusiasm, keen interest and insightfulness have been instrumental in making my time as a Research Fellow both enjoyable and productive. He has been very generous with his time and his advice has always been constructive and thoughtful.

I am also most indebted to Professor D. H. Hunt for his support and supervision of the molecular genetic investigations undertaken during my time at the Institute of Ophthalmology. Professor J. D. Mollon made me feel extremely welcome in his department and helped to make my time testing patients in Cambridge very pleasant.

Many individuals have been an excellent source of assistance both in the Department of Molecular Genetics and at Moorfields Eye Hospital, but moreover have been great fun to work with. At the Institute these include Suba, Neil, Simon, Sue, Marie, Sam, Phillippa, Jill, Ashwin, Zubin, Anita, Beverley, Zara, Quincy and Reshma. At MEH I am indebted to Dr G. E. Holder for his outstanding contributions and to his entire team for all their invaluable help; many others have been most generous with their assistance including Dr A. Webster, Sharon, Cindy, Sue, Lizzie, Jo and Irene.

I am also especially grateful to the many patients who kindly agreed to take part in this study and I have enjoyed the opportunity to meet so many interesting people and have the time to discuss their inherited conditions in detail.

This study would not have been possible without the support of a grant from the Guide Dogs for the Blind Association, for which I am most appreciative.

My parents, brother and sister continue to be a huge source of strength and love, for which I will always be truly thankful. My wonderful wife has been patient beyond the call of duty whilst I have been devoting so much of my time to this endeavour. Her support, love, humour and sandwiches have nourished me and made me a very happy man.

CHAPTER 16

REFERENCES

Acar C, Mears AJ, Yashar BM, Maheshwary AS, Andreasson S, Baldi A, Sieving PA, Iannaccone A, Musarella MA, Jacobson SG, Swaroop A. Mutation screening of patients with Leber Congenital Amaurosis or the enhanced S-Cone Syndrome reveals a lack of sequence variations in the *NRL* gene. *Mol Vis*. 2003;9:14-17.

Akhmedov NB, Piriev NI, Pearce-Kelling S, Acland GM, Aguirre GD, Farber DB. Canine cone transducin-gamma gene and cone degeneration in the cd dog. *Invest Ophthalmol Vis Sci*. 1998;39:1775-1781.

Akhmedov NB, Piriev NI, Ray K, Acland GM, Aguirre GD, Farber DB. Structure and analysis of the transducin beta3-subunit gene, a candidate for inherited cone degeneration (cd) in the dog. *Gene* 1997;194:47-56.

Aldred MJ, Savarirayan R, Crawford PJ. Amelogenesis imperfecta: a classification and catalogue for the 21st century. *Oral Dis*. 2003;9:19-23.

Aleman TS, Cideciyan AV, Volpe NJ, Stevanin G, Brice A, Jacobson SG. Spinocerebellar ataxia type 7 (SCA7) shows a cone-rod dystrophy phenotype. *Exp Eye Res*. 2002;74:737-745.

Alexander KR, Fishman GA. Supernormal scotopic ERG in cone dystrophy. *Br J Ophthalmol*. 1984a;68:69-78.

Alexander KR, Fishman GA. Prolonged rod dark adaptation in retinitis pigmentosa. *Br J Ophthalmol*. 1984b;68:561-569.

Ali RR, Sarra GM, Stephens C, Alwis MD, Bainbridge JW, Munro PM, Fauser S, Reichel MB, Kinnon C, Hunt DM, Bhattacharya SS, Thrasher AJ. Restoration of photoreceptor ultrastructure and function in retinal degeneration slow mice by gene therapy. *Nature Genet*. 2000;25:306-310.

Aligianis IA, Forshew T, Johnson S, Michaelides M, Johnson CA, Trembath RC, Hunt DM, Moore AT, Maher ER. Mapping of a novel locus for achromatopsia (*ACHM4*) to 1p and identification of a germline mutation in the α subunit of cone transducin (*GNAT2*). *J Med Genet*. 2002;39:656-660.

Allikmets R, Shroyer NF, Singh N, Seddon JM, Lewis RA, Bernstein PS, Peiffer A, Zabriskie NA, Li Y, Hutchinson A, Dean M, Lupski JR, Leppert M. Mutation of the Stargardt disease gene (*ABCR*) in age-related macular degeneration. *Science* 1997a;277:1805-1807.

Allikmets R, Singh N, Sun H, Shroyer NF, Hutchinson A, Chidambaram A, Gerrard B, Baird L, Stauffer D, Peiffer A, Rattner A, Smallwood P, Li Y, Anderson KL, Lewis RA, Nathans J, Leppert M, Dean M, Lupski JR. A photoreceptor cell-specific ATP-binding transporter gene (*ABCR*) is mutated in recessive Stargardt macular dystrophy. *Nat Genet*. 1997b;15:236-246.

Alpern M, Lee GB, Maaseidvaag F, Miller SS. Colour vision in blue cone 'monochromacy'. *J Physiol*. 1971;212:211-233.

Andreasson S, Tornqvist K. Electroretinograms in patients with achromatopsia. *Acta Ophthalmol (Copenh)*. 1991;69:711-716.

Apfelstedt-Sylla E, Theischen M, Ruther K, Wedemann H, Gal A, Zrenner E. Extensive intrafamilial and interfamilial phenotypic variation among patients with autosomal dominant retinal dystrophy and mutations in the human RDS/peripherin gene. *Br J Ophthalmol*. 1995;79:28-34.

Arbour NC, Zlotogora J, Knowlton RG, Merin S, Rosenmann A, Kanis AB, Rokhlina T, Stone EM, Sheffield VC. Homozygosity mapping of achromatopsia to chromosome 2 using DNA pooling. *Hum Mol Genet*. 1997;6:689-694.

Ardell MD, Aragon I, Oliveira L, Porche GE, Burke E, Pittler SJ. The beta subunit of human rod photoreceptor cGMP-gated cation channel is generated from a complex transcription unit. *FEBS Lett*. 1996;389:213-218.

Arden G, Wolf J, Berninger T, Hogg CR, Tzekov R, Holder GE. S-cone ERGs elicited by a simple technique in normals and in tritanopes. *Vis Res*. 1999;39:641-650.

Asenjo AB, Rim J, Oprian DD. Molecular determinants of human red/green color discrimination. *Neuron* 1994;12:1131-1138.

Ayyagari R, Kakuk LE, Bingham EL, Szczesny JJ, Kemp J, Toda Y, Feliuss J, Sieving PA. Spectrum of color gene deletions and phenotype in patients with blue cone monochromacy. *Hum Genet*. 2000;107:75-82.

Ayyagari R, Kakuk LE, Coats EL, Bingham EL, Toda Y, Feliuss J, Sieving PA. Bilateral macular atrophy in blue cone monochromacy (BCM) with loss of the locus control region (LCR) and part of the red pigment gene. *Mol Vis*. 1999;5:13-18.

Bach M, Hawlina M, Holder GE, Marmor MF, Meigen T, Vaegan, Miyake Y. Standard for pattern electroretinography. International Society for Clinical Electrophysiology of Vision. *Doc Ophthalmol*. 2000;101:11-18.

Badano JL, Ansley SJ, Leitch CC, Lewis RA, Lupski JR, Katsanis N. Identification of a novel Bardet-Biedl syndrome protein, BBS7, that shares structural features with BBS1 and BBS2. *Am J Hum Genet*. 2003;72:650-658.

Bareil C, Hamel CP, Delague V, Arnaud B, Demaille J, Claustres M. Segregation of a mutation in CNGB1 encoding the beta-subunit of the rod cGMP-gated channel in a family with autosomal recessive retinitis pigmentosa. *Hum Genet*. 2001;108:328-334.

Bateman JB, Klisak I, Kojis T, Mohandas T, Sparkes RS, Li TS, Applebury ML, Bowes C, Farber DB. Assignment of the beta-subunit of rod photoreceptor cGMP phosphodiesterase gene PDEB (homolog of the mouse rd gene) to human chromosome 4p16. *Genomics* 1992;12:601-603.

Beavo JA. Cyclic nucleotide phosphodiesterases: functional implications of multiple isoforms. *Physiol Rev*. 1995;75:725-748.

Bergen AAB, Pinckers AJLG. Localisation of a novel X-linked progressive cone dystrophy gene to Xq27: evidence for genetic heterogeneity. *Am J Hum Genet.* 1997;60:1468-1473.

Berninger TA, Polkinghorne PJ, Capon MR, Arden GB, Bird AC. Color vision defect. A early sign of Sorsby retinal dystrophy? *Ophthalmologie* 1993;90:515-518.

Bernstein PS, Tammur J, Singh N, Hutchinson A, Dixon M, Pappas CM, Zabriskie NA, Zhang K, Petrukhin K, Leppert M, Allikmets R. Diverse macular dystrophy phenotype caused by a novel complex mutation in the *ELOVL4* gene. *Invest Ophthalmol Vis Sci.* 2001;42:3331-3336.

Berridge MJ. Inositol trisphosphate and calcium signalling. *Nature* 1993a;361:315-325.

Berridge MJ. Cell signalling. A tale of two messengers. *Nature* 1993b;365:388-389.

Berson EL, Sandberg MA, Rosner B, Sullivan PL. Color plates to help identify patients with blue cone monochromatism. *Am J Ophthalmol.* 1983;95:741-747.

Betz A, Thakur P, Junge HJ, Ashery U, Rhee JS, Scheuss V, Rosenmund C, Rettig J, Brose N. Functional interaction of the active zone proteins Munc13-1 and RIM1 in synaptic vesicle priming. *Neuron* 2001;30:183-196.

Biel M, Seeliger M, Pfeifer A, Kohler K, Gerstner A, Ludwig A, Jaissle G, Fauser S, Zrenner E, Hofmann F. Selective loss of cone function in mice lacking the cyclic nucleotide-gated channel CNG3. *Proc Natl Acad Sci U S A.* 1999;96:7553-7557.

Biel M, Zong X, Distler M, Bosse E, Klugbauer N, Murakami M, Flockerzi V, Hofmann F. Another member of the cyclic nucleotide-gated channel family, expressed in testis, kidney, and heart. *Proc Natl Acad Sci U S A.* 1994;91:3505-3509.

Birnbach CD, Jarvelainen M, Possin DE, Milam AH. Histopathology and immunocytochemistry of the neurosensory retina in fundus flavimaculatus. *Ophthalmology* 1994;101:1211-1219.

Bjork A, Lindblom U, Wadensten L. Retinal degeneration in hereditary ataxia. *J Neurochem.* 1956;19:186-193.

Bowes C, Li T, Danciger M, Applebury ML, Farber DB. Retinal degeneration in the rd mouse is caused by a defect in the beta subunit of rod cGMP-phosphodiesterase. *Nature* 1990;347:677-680.

Brecher R, Bird AC. Adult vitelliform macular dystrophy. *Eye* 1990;4:210-215.

Bresnick GH, Smith VC, Pokorny J. Autosomal dominantly inherited macular dystrophy with preferential short-wavelength sensitive cone involvement. *Am J Ophthalmol.* 1989;108:265-276.

Brody JA, Hussels I, Brink E, Torres J. Hereditary blindness among Pingelapese people of Eastern Caroline Islands. *Lancet* 1970;1:1253-1257.

Cai K, Itoh Y, Khorana HG. Mapping of contact sites in complex formation between transducin and light-activated rhodopsin by covalent crosslinking: use of a photoactivatable reagent. *Proc Natl Acad Sci*. 2001;98:4877-4882.

Caldwell GM, Kakuk LE, Griesinger IB, Simpson SA, Nowak NJ, Small KW, Maumenee IH, Rosenfeld PJ, Sieving PA, Shows TB, Ayyagari R. Bestrophin gene mutations in patients with Best vitelliform macular dystrophy. *Genomics* 1999;58:98-101.

Carroll J, Neitz J, Neitz M. Estimates of L:M cone ratio from ERG flicker photometry and genetics. *J Vis*. 2002;2:531-542.

Cepko CL. The roles of intrinsic and extrinsic cues and bHLH genes in the determination of retinal cell fates. *Curr Opin Neurobiol*. 1999;9:37-46.

Chen JC, Fitzke FW, Pauleikhoff D, Bird AC. Functional loss in age-related Bruch's membrane change with choroidal perfusion defect. *Invest Ophthalmol Vis Sci*. 1992;33:334-340.

Chong NH, Alexander RA, Gin T, Bird AC, Luthert PJ. TIMP-3, collagen, and elastin immunohistochemistry and histopathology of Sorsby's fundus dystrophy. *Invest Ophthalmol Vis Sci*. 2000;41:898-902.

Chong NH, Kvanta A, Seregard S, Bird AC, Luthert PJ, Steen B. TIMP-3 mRNA is not overexpressed in Sorsby fundus dystrophy. *Am J Ophthalmol*. 2003;136:954-955.

Collin GB, Marshall JD, Ikeda A, So WV, Russell-Eggitt I, Maffei P, Beck S, Boerkoel CF, Siculo N, Martin M, Nishina PM, Naggert JK. Mutations in *ALMS1* cause obesity, type 2 diabetes and neurosensory degeneration in Alstrom syndrome. *Nat Genet*. 2002;31:74-78.

Collins C, Hutchinson G, Kowbel D, Riess O, Weber B, Hayden MR. The human beta-subunit of rod photoreceptor cGMP phosphodiesterase: complete retinal cDNA sequence and evidence for expression in brain. *Genomics* 1992;13:698-704.

Corbeil D, Roper K, Fargeas CA, Joester A, Huttner WB. Prominin: a story of cholesterol, plasma membrane protrusions and human pathology. *Traffic* 2001;2:82-91.

Corbeil D, Roper K, Hannah MJ, Hellwig A, Huttner WB. Selective localization of the polytopic membrane protein prominin in microvilli of epithelial cells - a combination of apical sorting and retention in plasma membrane protrusions. *J Cell Sci*. 1999;112:1023-1033.

Cremers FP, van de Pol DJ, van Driel M, den Hollander AI, van Haren FJ, Knoers NV, Tijmes N, Bergen AA, Rohrschneider K, Blankenagel A, Pinckers AJ, Deutman AF, Hoyng CB. Autosomal recessive retinitis pigmentosa and cone-rod dystrophy caused by splice site mutations in the Stargardt's disease gene *ABCR*. *Hum Mol Genet*. 1998;7:355-362.

Crone RA. Combined forms of congenital colour defects: a pedigree with atypical total colour blindness. *Br J Ophthalmol.* 1956;40:462-472.

Danciger M, Hendrickson J, Lyon J, Toomes C, McHale JC, Fishman GA, Inglehearn CF, Jacobson SG, Farber DB. CORD9 a new locus for arCRD: mapping to 8p11, estimation of frequency, evaluation of a candidate gene. *Invest Ophthalmol Vis Sci.* 2001;42:2458-2465.

De La Paz MA, Guy VK, Abou-Donia S, Heinis R, Bracken B, Vance JM, Gilbert JR, Gass JD, Haines JL, Pericak-Vance MA. Analysis of the Stargardt disease gene (*ABCR*) in age-related macular degeneration. *Ophthalmology* 1999;106:1531-1536.

Deeb SS, Lindsey DT, Hibiya Y, Sanocki E, Winderickx J, Teller DY, Motulsky AG. Genotype-phenotype relationships in human red/green color-vision defects: molecular and psychophysical studies. *Am J Hum Genet.* 1992;51:687-700.

Demirci FY, Rigatti BW, Wen G, Radak AL, Mah TS, Baic CL, Traboulsi EI, Alitalo T, Ramser J, Gorin MB. X-linked cone-rod dystrophy (locus COD1): identification of mutations in *RPGR* exon ORF15. *Am J Hum Genet.* 2002;70:1049-1053.

Deutman AF. Benign concentric annular macular dystrophy. *Am J Ophthalmol.* 1974;78:384-396.

Deutman AF, Pinckers AJL, Aan de Kerk AL. Dominantly inherited cystoid macular oedema. *Am J Ophthalmol.* 1976;82:540-548.

Dhallan RS, Macke JP, Eddy RL, Shows TB, Reed RR, Yau KW, Nathans J. Human rod photoreceptor cGMP-gated channel: amino acid sequence, gene structure, and functional expression. *J Neurosci.* 1992;12:3248-3256.

Dib C, Faure S, Fizames C, Samson D, Drouot N, Vignal A, Millasseau P, Marc S, Hazan J, Seboun E, Lathrop M, Gyapay G, Morissette J, Weissenbach J. A comprehensive genetic map of the human genome based on 5,264 microsatellites. *Nature* 1996;380:152-154.

Dizhoor AM, Boikov SG, Olshevskaya EV. Constitutive activation of photoreceptor guanylate cyclase by Y99C mutant of GCAP-1. Possible role in causing human autosomal dominant cone degeneration. *J Biol Chem.* 1998;273:17311-17314.

Dizhoor AM, Lowe DG, Olshevskaya EV, Laura RP, Hurley JB. The human photoreceptor membrane guanylyl cyclase, RetGC, is present in outer segments and is regulated by calcium and a soluble activator. *Neuron* 1994;12:1345-1352.

Dizhoor AM, Olshevskaya EV, Henzel WJ, Wong SC, Stults JT, Ankoudinova I, Hurley JB. Cloning, sequencing, and expression of a 24-kDa Ca²⁺-binding protein activating photoreceptor guanylyl cyclase. *J Biol Chem.* 1995;270:25200-25206.

Dollfus H, Mattei MG, Rozet JM, Delrieu O, Munnich A, Kaplan J. Physical and genetic localization of the gamma subunit of the cyclic GMP phosphodiesterase on the long arm of chromosome 17 (17q25). *Genomics* 1993;17:526-528.

Donoso LA, Edwards AO, Frost A, Vrabec T, Stone EM, Hageman GS, Perski T. Autosomal dominant Stargardt-like macular dystrophy. *Surv Ophthalmol.* 2001;46:149-163.

Dorey CK, Wu G, Ebenstein D, Garsd A, Weiter JJ. Cell loss in the ageing retina: relationship to lipofuscin accumulation and macular degeneration. *Invest Ophthalmol Vis Sci.* 1989;30:1691-1699.

Douglas AA, Waheed I, Wyse CT. Progressive bifocal chorio-retinal atrophy. A rare familial disease of the eyes. *Br J Ophthalmol.* 1968;52:742-751.

Downes SM, Fitzke FW, Holder GE, Payne AM, Bessant DA, Bhattacharya SS, Bird AC. Clinical features of codon 172 RDS macular dystrophy: similar phenotype in 12 families. *Arch Ophthalmol.* 1999;117:1373-1383.

Downes SM, Holder GE, Fitzke FW, Payne AM, Warren MJ, Bhattacharya SS, Bird AC. Autosomal dominant cone and cone-rod dystrophy with mutations in the guanylate cyclase activator 1A gene-encoding guanylate cyclase activating protein-1. *Arch Ophthalmol.* 2001;119:96-105.

Downey LM, Keen TJ, Jalili IK, McHale J, Aldred MJ, Robertson SP, Mighell A, Fayle S, Wissinger B, Inglehearn CF. Identification of a locus on chromosome 2q11 at which recessive amelogenesis imperfecta and cone-rod dystrophy cosegregate. *Eur J Hum Genet.* 2002;10:865-869.

Drummond-Borg M, Deeb SS, Motulsky AG. Molecular patterns of X chromosome-linked color vision genes among 134 men of European ancestry. *Proc Natl Acad Sci U S A.* 1989;86:983-987.

Dryja TP, Finn JT, Peng YW, McGee TL, Berson EL, Yau KW. Mutations in the gene encoding the alpha subunit of the rod cGMP-gated channel in autosomal recessive retinitis pigmentosa. *Proc Natl Acad Sci U S A.* 1995;92:10177-10181.

Dryja TP, Hahn LB, Reboul T, Arnaud B. Missense mutation in the gene encoding the alpha subunit of rod transducin in the Nougaret form of congenital stationary night blindness. *Nat Genet.* 1996;13:358-360.

Dulai KS, von Dornum M, Mollon JD, Hunt DM. The evolution of trichromatic color vision by opsin gene duplication in New World and Old World primates. *Genome Res.* 1999;9:629-638.

Eagle RC, Lucier AC, Bernardino VB, Yanoff M. Retinal pigment epithelial abnormalities in fundus flavimaculatus: a light and electron microscopic study. *Ophthalmology* 1980;87:1189-1200.

Ehlich P, Sadowski B, Zrenner E. Oligocone trichromasy, a rare form of incomplete achromatopsia. *Ophthalmologe* 1997;94:801-806.

Eismann E, Muller F, Heinemann SH, Kaupp UB. A single negative charge within the pore region of a cGMP-gated channel controls rectification, Ca²⁺ blockage, and ionic selectivity. *Proc Natl Acad Sci U S A*. 1994;91:1109-13.

Eksandh L, Kohl S, Wissinger B. Clinical features of achromatopsia in Swedish patients with defined genotypes. *Ophthalmic Genetics* 2002;23:109-120.

Eksandh LC, Ponjavic V, Ayyagari R, Bingham EL, Hiriyantha KT, Andreasson S, Ehinger B, Sieving PA. Phenotypic expression of juvenile X-linked retinoschisis in Swedish families with different mutations in the *XLRS1* gene. *Arch Ophthalmol*. 2000;118:1098-1104.

Evans K, Fryer A, Inglehearn C, Duvall-Young J, Whittaker JL, Gregory CY, Butler R, Ebenezer N, Hunt DM, Bhattacharya S. Genetic linkage of cone-rod retinal dystrophy to chromosome 19q and evidence for segregation distortion. *Nat Genet*. 1994;6:210-213.

Felbor U, Schilling H, Weber BHF. Adult vitelliform macular dystrophy is frequently associated with mutation in the *peripherin/RDS* gene. *Hum Mutat*. 1997;10:301-309.

Felbor U, Stohr H, Amann T, Schonherr U, Weber BH. A novel Ser156Cys mutation in the tissue inhibitor of metalloproteinases-3 (TIMP3) in Sorsby's fundus dystrophy with unusual clinical features. *Hum Mol Genet*. 1995;4:2415-2416.

Feshchenko EA, Andreeva SG, Suslova VA, Smirnova EV, Zagranichny VE, Lipkin VM. Human cone-specific cGMP phosphodiesterase alpha' subunit: complete cDNA sequence and gene arrangement. *FEBS Lett*. 1996;381:149-152.

Fincham E. Defects of the colour-sense mechanism as indicated by the accommodation reflex. *J Physiol*. 1953;121:570-580.

Finn JT, Krautwurst D, Schroeder JE, Chen TY, Reed RR, Yau KW. Functional co-assembly among subunits of cyclic-nucleotide-activated, nonselective cation channels, and across species from nematode to human. *Biophys J*. 1998;74:1333-1345.

Fish G, Grey R, Sehmi KS, Bird AC. The dark choroid in posterior retinal dystrophies. *Br J Ophthalmol*. 1981;65:359-363.

Fisher SK, Stone J, Rex TS, Linberg KA, Lewis GP. Experimental retinal detachment: a paradigm for understanding the effects of induced photoreceptor degeneration. *Prog Brain Res*. 2001;131:679-698.

Fishman GA, Birch DG, Holder GE, Brigell MG: *Electrophysiologic Testing in Disorders of the Retina, Optic Nerve, and Visual Pathway*, Second Edition. Ophthalmology Monograph 2. San Francisco: The Foundation of the American Academy of Ophthalmology; 2001

Fishman GA, Fishman M, Maggiano J. Macular lesions associated with retinitis pigmentosa. *Arch Ophthalmol*. 1977;95:798-803.

Fishman GA, Jampol LM, Goldberg MF. Diagnostic features of the Favre–Goldmann syndrome. *Br J Ophthalmol*. 1976;60:345–353.

Fishman GA, Stone EM, Eliason DA, Taylor CM, Lindeman M, Derlacki DJ. *ABCA4* gene sequence variations in patients with autosomal recessive cone-rod dystrophy. *Arch Ophthalmol*. 2003;121:851-855.

Fleischman JA, O'Donnell FE Jr. Congenital X-linked incomplete achromatopsia. Evidence for slow progression, carrier fundus findings, and possible genetic linkage with glucose-6-phosphate dehydrogenase locus. *Arch Ophthalmol*. 1981;99:468-472.

Fong SL. Characterisation of the human rod transducin alpha-subunit gene. *Nucleic Acids Res*. 1992;20:2865-2870.

Forsius H, Eriksson AW. Ein neues Augensyndrom mit X-chromosomaler Transmission. Eine Sippe mit Fundusalbinismus, Foveahypoplasie, Nystagmus, Myopie, Astigmatismus und Dyschromatopsie. *Klin Monatsbl Augenheilk*. 1964;144:447-457.

Forsman K, Graff C, Nordstrom S, Johansson K, Westermark E, Lundgren E, Gustavson KH, Wadelius C, Holmgren G. The gene for Best's macular dystrophy is located at 11q13 in a Swedish family. *Clin Genet*. 1992;42:156-159.

Francis PJ, Johnson S, Edmunds B, Kelsell RE, Sheridan E, Garrett C, Holder GE, Hunt DM, Moore AT. Genetic linkage analysis of a novel syndrome comprising North Carolina-like macular dystrophy and progressive sensorineural hearing loss. *Br J Ophthalmol*. 2003;87:893-898.

Frangieh GT, Green WR, Fine SL. A histopathologic study of Best's macular dystrophy. *Arch Ophthalmol*. 1982;100:1115-1121.

Freund CL, Gregory-Evans CY, Furukawa T, Papaioannou M, Looser J, Ploder L, Bellingham J, Ng D, Herbrick JA, Duncan A, Scherer SW, Tsui LC, Loutradis-Anagnostou A, Jacobson SG, Cepko CL, Bhattacharya SS, McInnes RR. Cone-rod dystrophy due to mutations in a novel photoreceptor-specific homeobox gene (*CRX*) essential for maintenance of the photoreceptor. *Cell* 1997;91:543-553.

Gavazzo P, Picco C, Eismann E, Kaupp UB, Menini A. A point mutation in the pore region alters gating, Ca⁽²⁺⁾ blockage, and permeation of olfactory cyclic nucleotide-gated channels. *J Gen Physiol*. 2000;116:311-26.

George ND, Yates JR, Moore AT. X linked retinoschisis. *Br J Ophthalmol*. 1995;79:697-702.

Gerth C, Andrassi-Darida M, Bock M, Preising MN, Weber BH, Lorenz B. Phenotypes of 16 Stargardt macular dystrophy/fundus flavimaculatus patients with known *ABCA4* mutations and evaluation of genotype-phenotype correlation. *Graefes Arch Clin Exp Ophthalmol*. 2002;240:628-638.

Gibson IM. Visual mechanisms in a cone-monochromat. *J Physiol*. 1962;161:P10-11.

Gillespie PG, Beavo JA. Characterization of a bovine cone photoreceptor phosphodiesterase purified by cyclic GMP-sepharose chromatography. *J Biol Chem.* 1988;263:8133-8141.

Godley BF, Tiffin PA, Evans K, Kelsell RE, Hunt DM, Bird AC. Clinical features of progressive bifocal chorioretinal atrophy: a retinal dystrophy linked to chromosome 6q. *Ophthalmology* 1996;103:893-898.

Goodman G, Ripps H, Siegel IM. Cone dysfunction syndromes. *Arch Ophthalmol.* 1963;70:214-231.

Gouras P, Eggers HM, Mackay C. Cone dystrophy, nyctalopia and supernormal rod responses. A new retinal degeneration. *Arch Ophthalmol.* 1983; 101: 718-24.

Gouras P, MacKay CJ. Electroretinographic responses of the short-wavelength-sensitive cones. *Invest Ophthalmol Vis Sci.* 1990;31:1203-1209.

Greenstein VC, Zaidi Q, Hood DC, Spehar B, Cideciyan AV, Jacobson SG. The enhanced S cone syndrome: an analysis of receptor and post-receptor changes. *Vision Res.* 1996;36:3711-3722.

Gregory-Evans K, Fariss RN, Possin DE, Gregory-Evans CY, Milam AH. Abnormal cone synapses in human cone-rod dystrophy. *Ophthalmology* 1998;105:2306-2312.

Griesinger IB, Sieving PA, Ayyagari R. Autosomal dominant macular atrophy at 6q14 excludes CORD7 and MCDR1/PBCRA loci. *Invest Ophthalmol Vis Sci.* 2000;41:248-255.

Gyapay G, Morissette J, Vignal A, Dib C, Fizames C, Millasseau P, Marc S, Bernardi G, Lathrop M, Weissenbach J. The 1993-94 Généthon human genetic linkage map. *Nat Genet.* 1994;7:246-339.

Haegerstrom-Portnoy G, Schneck ME, Verdon WA, Hewlett SE. Clinical vision characteristics of the congenital achromatopsias. II. Color vision. *Optom Vis Sci.* 1996;73:457-465.

Hagstrom SA, Neitz M, Neitz J. Cone pigment gene expression in individual photoreceptors and the chromatic topography of the retina. *J Opt Soc Am A Opt Image Sci Vis.* 2000;17:527-537.

Haider NB, Jacobson SG, Cideciyan AV, Swiderski R, Streb LM, Searby C, Beck G, Hockey R, Hanna DB, Gorman S, Duhl D, Carmi R, Bennett J, Weleber RG, Fishman GA, Wright AF, Stone EM, Sheffield VC. Mutation of a nuclear receptor gene, *NR2E3*, causes enhanced S cone syndrome, a disorder of retinal cell fate. *Nat Genet.* 2000;24:127-131.

Haider NB, Naggert JK, Nishina PM. Excess cone cell proliferation due to lack of a functional *NR2E3* causes retinal dysplasia and degeneration in *rd7/rd7* mice. *Hum Mol Genet.* 2001;10:1619-1626.

Haim M, Fledelius HC, Skarsholm D. X-linked myopia in a Danish family. *Acta Ophthalmol (Copenh)*. 1988;66:450-456.

Hamdi HK, Reznik J, Castellon R, Atilano SR, Ong JM, Udari N, Tavis JH, Aoki AM, Nesburn AB, Boyer DS, Small KW, Brown DJ, Kenney MC. Alu DNA polymorphism in ACE gene is protective for age-related macular degeneration. *Biochem Biophys Res Commun*. 2002;295:668-672.

Hameed A, Abid A, Aziz A, Ismail M, Mehdi SQ, Khaliq S. Evidence of *RPGRIP1* gene mutations associated with recessive cone-rod dystrophy. *J Med Genet*. 2003;40:616-619.

Henry D, Burke S, Shishido E, Matthews G. Retinal bipolar neurons express the cyclic nucleotide-gated channel of cone photoreceptors. *J Neurophysiol*. 2003;89:754-761.

Hess, RF, Mullen, KT, Sharpe, LT, & Zrenner, E. The photoreceptors in atypical achromatopsia. *Journal of Physiology* 1989;417:123-149.

Hess RF, Nordby K. Spatial and temporal limits of vision in the achromat. *J Physiol*. 1986;371:365-385.

Holder GE. Pattern electroretinography (PERG) and an integrated approach to visual pathway diagnosis. *Prog Retin Eye Res*. 2001;20:531-561.

Holder GE, Robson AG, Hogg CR, Kurz-Levin M, Lois N, Bird AC. Pattern ERG: clinical overview, and some observations on associated fundus autofluorescence imaging in inherited maculopathy. *Doc Ophthalmol*. 2003;106:17-23.

Hood DC. Assessing retinal function with the multifocal technique. *Prog Retin Eye Res*. 2000;19:607-646.

Hood DC, Cideciyan AV, Halevy DA, Jacobson SG. Sites of disease action in a retinal dystrophy with supernormal and delayed rod electroretinogram b-waves. *Vision Res*. 1996;36:889-901.

Hood DC, Cideciyan AV, Roman AJ, Jacobson SG. Enhanced S cone syndrome: evidence for an abnormally large number of S cones. *Vision Res*. 1995;35:1473-1481.

Hoyng CB, Heutink P, Testers L, Pinckers A, Deutman AF, Oostra BA. Autosomal dominant central areolar choroidal dystrophy caused by a mutation in codon 142 in the *peripherin/RDS* gene. *Am J Ophthalmol*. 1996;121:623-629.

Hsu YT, Molday RS. Modulation of the cGMP-gated channel of rod photoreceptor cells by calmodulin. *Nature* 1993;361:76-79.

Hwa J, Klein-Seetharaman J, Khorana HG. Structure and function in rhodopsin: Mass spectrometric identification of the abnormal intradiscal disulfide bond in misfolded retinitis pigmentosa mutants. *Proc Natl Acad Sci U S A*. 2001;98:4872-4876.

Ikeda H, Ripps H. The electroretinogram of a cone-monochromat. *Arch Ophthalmol*. 1966;75:513-517.

Jacobson DM, Thompson S, Bartley JA. X-linked progressive cone dystrophy. Clinical characteristics of affected males and female carriers. *Ophthalmology* 1989;96: 885–95.

Jacobson SG, Cideciyan AV, Bennett J, Kingsley RM, Sheffield VC, Stone EM. Novel mutation in the *TIMP3* gene causes Sorsby fundus dystrophy. *Arch Ophthalmol.* 2002;120:376-379.

Jacobson SG, Cideciyan AV, Regunath G, Rodriguez FJ, Vandeburgh K, Sheffield VC, Stone EM. Night blindness in Sorsby's fundus dystrophy reversed by vitamin A. *Nat Genet.* 1995;11:27-32.

Jacobson SG, Marmor MF, Kemp CM, Knighton RW. SWS (blue) cone hypersensitivity in a newly identified retinal degeneration. *Invest Ophthalmol Vis Sci.* 1990;31:827-838.

Jacobson SG, Roman AJ, Roman MI, Gass JD, Parker JA. Relatively enhanced S cone function in the Goldmann–Favre syndrome. *Am J Ophthalmol.* 1991;111: 446–53.

Jacobson SG, Voigt WJ, Parel JM, Apathy PP, Nghiem-Phu L, Myers SW, Patella VM. Automated light- and dark-adapted perimetry for evaluating retinitis pigmentosa. *Ophthalmology* 1986;93:1604-1611.

Jagla WM, Jagle H, Hayashi T, Sharpe LT, Deeb SS. The molecular basis of dichromatic color vision in males with multiple red and green visual pigment genes. *Hum Mol Genet.* 2002;11:23-32.

Jalkanen R, Demirci FY, Tynismaa H, Bech-Hansen T, Meindl A, Peippo M, Mantyjarvi M, Gorin MB, Alitalo T. A new genetic locus for X linked progressive cone-rod dystrophy. *J Med Genet.* 2003;40:418-423.

Jalili IK. Cone-rod congenital amaurosis associated with congenital hypertrichosis: an autosomal recessive condition. *J Med Genet.* 1989;26:504-510.

Jalili IK, Smith NJ. A progressive cone-rod dystrophy and amelogenesis imperfecta: a new syndrome. *J Med Genet.* 1988;25:738-740.

Johnson S, Halford S, Morris AG, Patel RJ, Wilkie SE, Hardcastle AJ, Moore AT, Zhang K, Hunt DM. Genomic organisation and alternative splicing of human *RIMI*, a gene implicated in autosomal dominant cone-rod dystrophy (CORD7). *Genomics* 2003;81:304-314.

Johnson S, Michaelides M, Aligianis IA, Ainsworth JR, Mollon JD, Maher ER, Moore AT, Hunt DM. Achromatopsia caused by novel mutations in both *CNGA3* and *CNGB3*. *J Med Genet.* 2004; (in press).

Kajiwara K, Hahn LB, Mukai S, Travis GH, Berson EL, Dryja TP. Mutations in the human retinal degeneration slow gene in autosomal dominant retinitis pigmentosa. *Nature* 1991;354:480-483.

Kaplan J, Gerber S, Larget-Piet D, Rozet JM, Dollfus H, Dufier JL, Odent S, Postel-Vinay A, Janin N, Briard ML. A gene for Stargardt's disease (fundus flavimaculatus) maps to the short arm of chromosome 1. *Nat Genet.* 1993;5:308-311.

Kaplan J, Pelet A, Martin C, Delrieu O, Ayme S, Bonneau D, Briard ML, Hanauer A, Larget-Piet L, Lefrancois P. Phenotype-genotype correlations in X linked retinitis pigmentosa. *J Med Genet.* 1992;29:615-623.

Karnik SS, Khorana HG. Assembly of functional rhodopsin requires a disulfide bond between cysteine residues 110 and 187. *J Biol Chem.* 1990;265:17520-17524.

Kato M, Kobayashi R, Watanabe I. Cone dysfunction and supernormal scotopic electroretinogram with a high-intensity stimulus. *Doc Ophthalmol.* 1993;84:71-81.

Katsanis N, Beales PL, Woods MO, Lewis RA, Green JS, Parfrey PS, Ansley SJ, Davidson WS, Lupski JR. Mutations in *MKKS* cause obesity, retinal dystrophy and renal malformations associated with Bardet-Biedl syndrome. *Nat Genet.* 2000;26:67-70.

Kaupp UB, Seifert R. Cyclic nucleotide-gated ion channels. *Physiol Rev.* 2002;82:769-824.

Kazmi MA, Sakmar TP, Ostrer H. Mutation of a conserved cysteine in the X-linked cone opsins causes color vision deficiencies by disrupting protein folding and stability. *Invest Ophthalmol Vis Sci.* 1997;38:1074-1081.

Kearns TP, Hollenhorst RW. Chloroquine retinopathy: evaluation by fluorescein angiography. *Arch Ophthalmol.* 1966;76:378-384.

Kefalov V, Fu Y, Marsh-Armstrong N, Yau KW. Role of visual pigment properties in rod and cone phototransduction. *Nature* 2003;425:526-531.

Kellner U, Sadowski B, Zrenner E, Foerster MH. Selective cone dystrophy with protan genotype. *Invest Ophthalmol Vis Sci.* 1995;36:2381-2387.

Kellsell RE, Godley BF, Evans K, Tiffin PA, Gregory CY, Plant C, Moore AT, Bird AC, Hunt DM. Localization of the gene for progressive bifocal chorioretinal atrophy (PBCRA) to chromosome 6q. *Hum Mol Genet.* 1995;4:1653-1656.

Kellsell RE, Gregory-Evans K, Gregory-Evans CY, Holder GE, Jay MR, Weber BH, Moore AT, Bird AC, Hunt DM. Localization of a gene (*CORD7*) for a dominant cone-rod dystrophy to chromosome 6q. *Am J Hum Genet.* 1998a;63:274-279.

Kellsell RE, Gregory-Evans K, Payne AM, Perrault I, Kaplan J, Yang RB, Garbers DL, Bird AC, Moore AT, Hunt DM. Mutations in the retinal guanylate cyclase (*RETGC-1*) gene in dominant cone-rod dystrophy. *Hum Mol Genet.* 1998b;7:1179-1184.

Kemp CM, Jacobson SG, Cideciyan AV, Kimura AE, Sheffield VC, Stone EM. *RDS* gene mutations causing retinitis pigmentosa or macular degeneration lead to the same abnormality in photoreceptor function. *Invest Ophthalmol Vis Sci.* 1994;35:3154-3162.

Keunen JEE, De Brabandere SRS, Liem ATA. Foveal densitometry and color matching in oligocone trichromacy. In: Drum B, ed. 12th IRGCVD Symposium, *Colour Vision Deficiencies XII* Kluwer Academic Publishers, 1995: 203-210.

Khaliq S, Hameed A, Ismail M, Anwar K, Leroy BP, Mehdi SQ, Payne AM, Bhattacharya SS. Novel locus for autosomal recessive cone-rod dystrophy *CORD8* mapping to chromosome 1q12-q24. *Invest Ophthalmol Vis Sci.* 2000;41:3709-3712.

Klaver CC, Kliffen M, van Duijn CM, Hofman A, Cruts M, Grobbee DE, van Broeckhoven C, de Jong PT. Genetic association of apolipoprotein E with age-related macular degeneration. *Am J Hum Genet.* 1998;63:200-206.

Klein ML, Schultz DW, Edwards A, Matise TC, Rust K, Berselli CB, Trzuppek K, Weleber RG, Ott J, Wirtz MK, Acott TS. Age-related macular degeneration. Clinical features in a large family and linkage to chromosome 1q. *Arch Ophthalmol.* 1998;116:1082-1088.

Klenchin VA, Calvert PD, Bownds MD. Inhibition of rhodopsin kinase by recoverin. Further evidence for a negative feedback system in phototransduction. *J Biol Chem.* 1995;270:16147-16152.

Kniazeva M, Chiang MF, Morgan B, Anduze AL, Zack DJ, Han M, Zhang K. A new locus for autosomal dominant Stargardt-like disease maps to chromosome 4. *Am J Hum Genet.* 1999;64:1394-1399.

Kniazeva M, Traboulsi EI, Yu Z, Stefko ST, Gorin MB, Shugart YY, O'Connell JR, Blaschak CJ, Cutting G, Han M, Zhang K. A new locus for dominant drusen and macular degeneration maps to chromosome 6q14. *Am J Ophthalmol.* 2000;130:197-202.

Kobayashi A, Higashide T, Hamasaki D, Kubota S, Sakuma H, An W, Fujimaki T, McLaren MJ, Weleber RG, Inana G. HRG4 (UNC119) mutation found in cone-rod dystrophy causes retinal degeneration in a transgenic model. *Invest Ophthalmol Vis Sci.* 2000;41:3268-3277.

Kobayashi M, Takezawa S, Hara K, Yu RT, Umesono Y, Agata K, Taniwaki M, Yasuda K, Umesono K. Identification of a photoreceptor cell-specific nuclear receptor. *Proc Natl Acad Sci U S A.* 1999;96:4814-4819.

Kohl S, Baumann B, Broghammer M, Jagle H, Sieving P, Kellner U, Spegal R, Anastasi M, Zrenner E, Sharpe LT, Wissinger B. Mutations in the *CNGB3* gene encoding the beta-subunit of the cone photoreceptor cGMP-gated channel are responsible for achromatopsia (*ACHM3*) linked to chromosome 8q21. *Hum Mol Genet.* 2000; 9:2107-2116.

Kohl S, Baumann B, Rosenberg T, Kellner U, Lorenz B, Vadala M, Jacobson SG, Wissinger B. Mutations in the cone photoreceptor G-protein alpha-subunit gene *GNAT2* in patients with achromatopsia. *Am J Hum Genet.* 2002;71:422-425.

Kohl S, Jäggle H, Zrenner E, Sharpe LT, Wissinger B. The genetics of achromatopsia. *Invest Ophthalmol Vis Sci* 2001;42:S324 (Abstract #1745).

Kohl S, Marx T, Giddings I, Jagle H, Jacobson SG, Apfelstedt-Sylla E, Zrenner E, Sharpe LT, Wissinger B. Total colour-blindness is caused by mutations in the gene encoding the alpha-subunit of the cone photoreceptor cGMP-gated cation channel. *Nat Genet.* 1998;19:257-259.

Kolb H, Goede P, Roberts S, McDermott R, Gouras P. Uniqueness of the S-cone pedicle in the human retina and consequences for color processing. *J Comp Neurol.* 1997;386:443-460.

Kools P, Vanhalst K, Van den Eynde E, van Roy F. The human cadherin-10 gene: complete coding sequence, predominant expression in the brain, and mapping on chromosome 5p13-14. *FEBS Lett.* 1999;452:328-334.

Koushika SP, Richmond JE, Hadwiger G, Weimer RM, Jorgensen EM, Nonet ML. A post-docking role for active zone protein Rim. *Nat Neurosci.* 2001;4:997-1005.

Kremer H, Pinckers A, van den Heim B, Deutman AF, Ropers HH, Mariman ECM. Localization of the gene for dominant cystoid macular dystrophy on chromosome 7p. *Hum Molec Genet.* 1994;3: 299-302.

Kremers J, Scholl HP, Knau H, Berendschot TT, Usui T, Sharpe LT. L/M cone ratios in human trichromats assessed by psychophysics, electroretinography, and retinal densitometry. *J Opt Soc Am A Opt Image Sci Vis.* 2000;17:517-526.

Krill AE, Deutman AF, Fishman M. The cone degenerations. *Doc Ophthalmol.* 1973;35:1-80.

Krill AE, Schneiderman A. Retinal function studies, including the electroretinogram, in an atypical monochromat. *Clinical Electroretinography, Supplement to Vision Research*, New York, Oxford Press, 1966, 351-361.

Kurz-Levin M, Halfyard AS, Bunce C, Bird AC, Holder GE. Clinical variations in assessment of Bull's Eye Maculopathy. *Arch Ophthalmol.* 2002;120:567-575.

Kylstra JA, Aylsworth AS. Cone-rod retinal dystrophy in a patient with neurofibromatosis type 1. *Can J Ophthalmol.* 1993;28:79-80.

Ladekjaer-Mikkelsen AS, Rosenberg T, Jorgensen AL. A new mechanism in blue cone monochromatism. *Hum Genet.* 1996;98:403-408.

Lamb TD. Ida Mann Lecture. Transduction in human photoreceptors. *Aust N Z J Ophthalmol.* 1996;24:105-110.

Lerea CL, Bunt-Milam AH, Hurley JB. Alpha transducin is present in blue-, green-, and red-sensitive cone photoreceptors in the human retina. *Neuron* 1989;3:367-376.

Lipton SA. cGMP and EGTA increase the light-sensitive current of retinal rods. *Brain Res.* 1983;265:41-48.

Liu Y, Arshavsky VY, Ruoho AE. Interaction sites of the COOH-terminal region of the gamma subunit of cGMP phosphodiesterase with the GTP-bound alpha subunit of transducin. *J Biol Chem*. 1996 271:26900-26907.

Lloyd TE, Bellen HJ. pRIMing synaptic vesicles for fusion. *Nat Neurosci*. 2001;4:965-966.

Lois N, Holder GE, Bunce C, Fitzke FW, Bird AC. Phenotypic subtypes of Stargardt macular dystrophy-fundus flavimaculatus. *Arch Ophthalmol*. 2001;119:359-369.

Lois N, Holder GE, Fitzke FW, Plant C, Bird AC. Intrafamilial variation of phenotype in Stargardt macular dystrophy-Fundus flavimaculatus. *Invest Ophthalmol Vis Sci*. 1999;40:2668-2675.

Lois N, Owens SL, Coco R, Hopkins J, Fitzke FW, Bird AC. Fundus autofluorescence in patients with age-related macular degeneration and high risk of visual loss. *Am J Ophthalmol*. 2002;133:341-349.

Lonart G. RIM1: an edge for presynaptic plasticity. *Trends Neurosci*. 2002;25:329-332.

Lotery AJ, Ennis KT, Silvestri G, Nicholl S, McGibbon D, Collins AD, Hughes AE. Localisation of a gene for central areolar choroidal dystrophy to chromosome 17p. *Hum Mol Genet*. 1996;5:705-708.

Lotery AJ, Munier FL, Fishman GA, Weleber RG, Jacobson SG, Affatigato LM, Nichols BE, Schorderet DF, Sheffield VC, Stone EM. Allelic variation in the VMD2 gene in best disease and age-related macular degeneration. *Invest Ophthalmol Vis Sci*. 2000;41:1291-1296.

Majewski J, Schultz DW, Weleber RG, Schain MB, Edwards AO, Matisse TC, Acott TS, Ott J, Klein ML. Age-related macular degeneration--a genome scan in extended families. *Am J Hum Genet*. 2003;73:540-550.

Marmor MF, Jacobson SG, Foerster MH, Kellner U, Weleber RG. Diagnostic clinical findings of a new syndrome with night blindness, maculopathy, and enhanced S cone sensitivity. *Am J Ophthalmol*. 1990;110:124-134.

Marmor MF, Tan F, Sutter EE, Bearse MA Jr. Topography of cone electrophysiology in the enhanced S cone syndrome. *Invest Ophthalmol Vis Sci*. 1999;40:1866-1873.

Marmor MF, Zrenner E. Standard for clinical electro-oculography. International Society for Clinical Electrophysiology of Vision. *Arch Ophthalmol*. 1993;111:601-604.

Marmor MF, Zrenner E. Standard for clinical electroretinography (1999 update). *Doc Ophthalmol*. 1998;97:143-156.

Marmorstein AD, Marmorstein LY, Rayborn M, Wang X, Hollyfield JG, Petrukhin K. Bestrophin, the product of the Best vitelliform macular dystrophy gene (VMD2), localizes to the basolateral plasma membrane of the retinal pigment epithelium. *Proc Natl Acad Sci U S A*. 2000;97:12758-12763.

Marmorstein LY, Munier FL, Arsenijevic Y, Schorderet DF, McLaughlin PJ, Chung D, Traboulsi E, Marmorstein AD. Aberrant accumulation of EFEMP1 underlies drusen formation in Malattia Leventinese and age-related macular degeneration. *Proc Natl Acad Sci U S A*. 2002;99:13067-13072.

Marré M, Marré E, Zenker HJ, Fulle D. Color vision in a family with autosomal dominant cone dystrophy. In: Drum B, Verriest G, ed. *Color vision deficiencies IX*. Dordrecht: Kluwer Academic Press, 1989: 181-186.

Martin TF. Prime movers of synaptic vesicle exocytosis. *Neuron* 2002;34:9-12.

Martinez-Mir A, Vilela C, Bayes M, Valverde D, Dain L, Beneyto M, Marco M, Baiget M, Grinberg D, Balcells S, Gonzalez-Duarte R, Vilageliu L. Putative association of a mutant ROM1 allele with retinitis pigmentosa. *Hum Genet*. 1997;99:827-830.

Massin P, Guillausseau PJ, Vialettes B, Paques M, Gin H, Porokhov B, Caillat-Zucman S, Froguel P, Paquis-Fluckinger V, Gaudric A, Guillausseau PJ. Macular pattern dystrophy associated with a mutation of mitochondrial DNA. *Am J Ophthalmol*. 1995;120:247-248.

Massin P, Virally-Monod M, Vialettes B, Paques M, Gin H, Porokhov B, Caillat-Zucman S, Froguel P, Paquis-Fluckinger V, Gaudric A, Guillausseau PJ. Prevalence of macular pattern dystrophy in maternally inherited diabetes and deafness. GEDIAM Group. *Ophthalmology* 1999;106:1821-1827.

Mata NL, Radu RA, Clemmons RC, Travis GH. Isomerization and oxidation of vitamin A in cone-dominant retinas: a novel pathway for visual-pigment regeneration in daylight. *Neuron* 2002;36:69-80.

Mata NL, Tzekov RT, Liu X, Weng J, Birch DG, Travis GH. Delayed dark-adaptation and lipofuscin accumulation in *abcr*^{+/-} mice: implications for involvement of *ABCR* in age-related macular degeneration. *Invest Ophthalmol Vis Sci*. 2001;42:1685-1690.

Mata NL, Weng J, Travis GH. Biosynthesis of a major lipofuscin fluorophore in mice and humans with *ABCR*-mediated retinal and macular degeneration. *Proc Natl Acad Sci U S A*. 2000;97:7154-7159.

Matulef K, Zagotta WN. Cyclic nucleotide-gated ion channels. *Annu Rev Cell Dev Biol*. 2003;19:23-44.

Maugeri A, Klevering BJ, Rohrschneider K, Blankenagel A, Brunner HG, Deutman AF, Hoyng CB, Cremers FP. Mutations in the *ABCA4* (*ABCR*) gene are the major cause of autosomal recessive cone-rod dystrophy. *Am J Hum Genet*. 2000;67:960-966.

Maw MA, Corbeil D, Koch J, Hellwig A, Wilson-Wheeler JC, Bridges RJ, Kumaramanickavel G, John S, Nancarrow D, Roper K, Weigmann A, Huttner WB, Denton MJ. A frameshift mutation in prominin (mouse)-like 1 causes human retinal degeneration. *Hum Mol Genet*. 2000;9:27-34.

Mears AJ, Hirianna S, Vervoort R, Yashar B, Gieser L, Fahrner S, Daiger SP, Heckenlively JR, Sieving PA, Wright AF, Swaroop A. Remapping of the RP15 locus for X-linked cone-rod degeneration to Xp11.4-p21.1, and identification of a de novo insertion in the *RPGR* exon ORF15. *Am J Hum Genet.* 2000;67:1000-1003.

Mears AJ, Kondo M, Swain PK, Takada Y, Bush RA, Saunders TL, Sieving PA, Swaroop A. Nrl is required for rod photoreceptor development. *Nat Genet.* 2001;29:447-452.

Meire FM, Bergen AAB, De Rouck A, Leys M, Delleman JW. X-linked progressive cone dystrophy. Localisation of the gene locus to Xp21-p11.1 by linkage analysis. *Br J Ophthalmol.* 1994;78:103-108.

Merbs SL, Nathans J. Role of hydroxyl-bearing amino acids in differentially tuning the absorption spectra of the human red and green cone pigments. *Photochem Photobiol.* 1993;58:706-710.

Michaelides M, Aligianis IA, Ainsworth JR, Good P, Mollon JD, Maher ER, Moore AT, Hunt DM. Progressive cone dystrophy associated with mutation in *CNGB3*. *Invest Ophthalmol Vis Sci.* 2004a; (in press).

Michaelides M, Aligianis IA, Holder GE, Simunovic MP, Mollon JD, Maher ER, Hunt DM, Moore AT. Cone dystrophy phenotype associated with a frameshift mutation (M280fsX291) in the alpha-subunit of cone specific transducin (*GNAT2*). *Br J Ophthalmol.* 2003a;87:1317-1320.

Michaelides M, Bloch-Zupan A, Holder GE, Hunt DM, Moore AT. An Autosomal Recessive Cone-Rod Dystrophy associated with Amelogenesis Imperfecta. *J Med Genet.* 2004b; (in press).

Michaelides M, Holder GE, Bradshaw K, Hunt DM, Mollon JD, Moore AT. Oligocone Trichromacy – a rare and unusual cone dysfunction syndrome. *Br J Ophthalmol.* 2004c; (in press).

Michaelides M, Hunt DM, Moore AT. The genetics of inherited macular dystrophies. *J Med Genet.* 2003b;40:641-650.

Michaelides M, Hunt DM, Moore AT. The cone dysfunction syndromes. *Br J Ophthalmol.* 2004d;88:291-297.

Michaelides M, Johnson S, Poulson A, Bradshaw K, Bellmann C, Hunt DM, Moore AT. An Autosomal Dominant Bull's-Eye Macular Dystrophy (MCDR2) that maps to the short arm of chromosome 4. *Invest Ophthalmol Vis Sci.* 2003c;44:1657-1662.

Michaelides M, Johnson S, Simunovic MP, Bradshaw K, Holder GE, Mollon JD, Moore AT, Hunt DM. Blue cone monochromatism: a phenotype and genotype assessment with evidence of progressive loss of cone function in older individuals. *Eye* 2004e; (in press).

Michaelides M, Johnson S, Tekriwal AK, Holder GE, Bellmann C, Kinning E, Woodruff G, Trembath RC, Hunt DM, Moore AT. An early-onset autosomal dominant macular dystrophy (MCDR3) resembling North Carolina macular dystrophy maps to chromosome 5. *Invest Ophthalmol Vis Sci.* 2003d;44:2178-2183.

Milam AH, Rose L, Cideciyan AV, Barakat MR, Tang WX, Gupta N, Aleman TS, Wright AF, Stone EM, Sheffield VC, Jacobson SG. The nuclear receptor NR2E3 plays a role in human retinal photoreceptor differentiation and degeneration. *Proc Natl Acad Sci U S A.* 2002;99:473-478.

Mohler CW, Fine SL. Long-term evaluation of patients with Best's vitelliform dystrophy. *Ophthalmology* 1981;88:688-692.

Molday LL, Rabin AR, Molday RS. ABCR expression in foveal cone photoreceptors and its role in stargardt macular dystrophy. *Nat Genet.* 2000;25:257-258.

Mollon JD. Neurobiology. The club-sandwich mystery. *Nature* 1990;343:16-17.

Mollon JD, Astell S, Reffin JP. A Minimalist test of colour vision. In: Drun B, Moreland JD, Serra A, ed. *Colour Vision Deficiencies*. Kluwer Academic Publishers, 1991:59-67.

Mollon JD, Reffin JP. A computer-controlled colour vision test that combines the principles of Chibret and of Stilling. *J Physiol.* 1989;414:5P.

Moore AT. Cone and cone-rod dystrophies. *J Med Genet.* 1992;29:289-290.

Morris TA, Fong SL. Characterisation of the gene encoding human cone transducin alpha-subunit (GNAT2). *Genomics* 1993;17:442-448.

Murakami A, Yajima T, Sakuma H, McLaren MJ, Inana G. X-arrestin: a new retinal arrestin mapping to the X chromosome. *FEBS Lett.* 1993;334:203-209.

Musarella M. Molecular genetics of macular degeneration. *Doc Ophthalmol.* 2001;102:165-177.

Musarella MA, Weleber RG, Murphy WH, Young RS, Anson-Cartwright L, Mets M, Kraft SP, Polemeno R, Litt M, Worton RG. Assignment of the gene for complete X-linked congenital stationary night blindness (CSNB1) to Xp11.3. *Genomics* 1989;5:727-737.

Myktyyn K, Braun T, Carmi R, Haider NB, Searby CC, Shastri M, Beck G, Wright AF, Iannaccone A, Elbedour K, Riise R, Baldi A, Raas-Rothschild A, Gorman SW, Duhl DM, Jacobson SG, Casavant T, Stone EM, Sheffield VC. Identification of the gene that, when mutated, causes the human obesity syndrome BBS4. *Nat Genet.* 2001;28:188-191.

Myktyyn K, Nishimura DY, Searby CC, Shastri M, Yen HJ, Beck JS, Braun T, Streb LM, Cornier AS, Cox GF, Fulton AB, Carmi R, Luleci G, Chandrasekharappa SC, Collins FS, Jacobson SG, Heckenlively JR, Weleber RG, Stone EM, Sheffield VC. Identification of the gene (*BBS1*) most commonly involved in Bardet-Biedl syndrome, a complex human obesity syndrome. *Nat Genet.* 2002;31:435-438.

Nakazawa M, Kikawa E, Chida Y, Wada Y, Shiono T, Tamai M. Autosomal dominant cone-rod dystrophy associated with mutations in codon 244 (Asn244His) and codon 184 (Tyr184Ser) of the *peripherin/RDS* gene. *Arch Ophthalmol*. 1996;114:72-78.

Nathans J, Davenport CM, Maumenee IH, Lewis RA, Hejtmancik JF, Litt M, Lovrien E, Weleber R, Bachynski B, Zwas F, Klingaman R, Fishman G. Molecular genetics of human blue cone monochromacy. *Science* 1989;245:831-838.

Nathans J, Hogness DS. Isolation and nucleotide sequence of the gene encoding human rhodopsin. *Proc Natl Acad Sci USA*. 1984;81:4851-4855.

Nathans J, Maumenee IH, Zrenner E, Sadowski B, Sharpe LT, Lewis RA, Hansen E, Rosenberg T, Schwartz M, Heckenlively JR, Traboulsi E, Klingaman R, Bech-Hansen NT, LaRoche GR, Pagon RA, Murphey WH, Weleber RG. Genetic heterogeneity among blue-cone monochromats. *Am J Hum Genet*. 1993;53:987-1000.

Nathans J, Piantanida TP, Eddy RL, Shows TB, Hogness DS. Molecular genetics of inherited variation in human color vision. *Science* 1986a;232:203-210.

Nathans J, Thomas D, Hogness DS. Molecular genetics of human colour vision: the genes encoding blue, green, and red pigments. *Science* 1986b;232:193-202.

Neitz M, Neitz J. Molecular genetics of color vision and color vision defects. *Arch Ophthalmol*. 2000;118:691-700.

Neitz M, Neitz J, Jacobs GH. Genetic basis of photopigment variations in human dichromats. *Vision Res*. 1995;35:2095-2103.

Neuhann T, Krastel H, Jaeger W. Differential diagnosis of typical and atypical congenital achromatopsia. Analysis of a progressive foveal dystrophy and a nonprogressive oligo-cone trichromacy (general cone dysfunction without achromatopsia), both of which at first had been diagnosed as achromatopsia. *Albrecht Von Graefes Arch Klin Exp Ophthalmol*. 1978;209:19-28.

Newbold RJ, Deery EC, Walker CE, Wilkie SE, Srinivasan N, Hunt DM, Bhattacharya SS, Warren MJ. The destabilization of human GCAP1 by a proline to leucine mutation might cause cone-rod dystrophy. *Hum Mol Genet*. 2001;10:47-54.

Ng L, Hurley JB, Dierks B, Srinivas M, Salto C, Vennstrom B, Reh TA, Forrest D. A thyroid hormone receptor that is required for the development of green cone photoreceptors. *Nat Genet*. 2001;27:94-98.

Ngo JT, Bateman JB, Klisak I, Mohandas T, Van Dop C, Sparkes RS. Regional mapping of a human rod alpha-transducin (GNAT1) gene to chromosome 3p22. *Genomics* 1993;18:724-725.

Ngo JT, Klisak I, Sparkes RS, Mohandas T, Yamaki K, Shinohara T, Bateman JB. Assignment of the S-antigen gene (SAG) to human chromosome 2q24-q37. *Genomics* 1990;7:84-87.

Nichols BE, Drack AV, Vandenberg K, Kimura AE, Sheffield VC, Stone EM. A 2 base pair deletion in the *RDS* gene associated with butterfly-shaped pigment dystrophy of the fovea. *Hum Mol Genet.* 1993;2:601-603.

Nicol GD, Miller WH. Cyclic GMP injected into retinal rod outer segments increases latency and amplitude of response to illumination. *Proc Natl Acad Sci U S A.* 1978;75:5217-5220.

Nishimura DY, Searby CC, Carmi R, Elbedour K, Van Maldergem L, Fulton AB, Lam BL, Powell BR, Swiderski RE, Bugge KE, Haider NB, Kwitek-Black AE, Ying L, Duhl DM, Gorman SW, Heon E, Iannaccone A, Bonneau D, Biesecker LG, Jacobson SG, Stone EM, Sheffield VC. Positional cloning of a novel gene on chromosome 16q causing Bardet-Biedl syndrome (BBS2). *Hum Mol Genet.* 2001;10:865-874.

Nystuen A, Legare ME, Shultz LD, Frankel WN. A null mutation in inositol polyphosphate 4-phosphatase type I causes selective neuronal loss in weeble mutant mice. *Neuron* 2001;32:203-212.

O'Donnell FE, Welch RB. Fenestrated sheen macular dystrophy. A new autosomal dominant maculopathy. *Arch Ophthalmol.* 1979;97:1292-1296.

Ong OC, Hu K, Rong H, Lee RH, Fung BK. Gene structure and chromosome localization of the G gamma c subunit of human cone G-protein (GNGT2). *Genomics* 1997;44:101-109.

Ong OC, Yamane HK, Phan KB, Fong HK, Bok D, Lee RH, Fung BK. Molecular cloning and characterization of the G protein gamma subunit of cone photoreceptors. *J Biol Chem.* 1995;270:8495-8500.

Palczewski K, Subbaraya I, Gorczyca WA, Helekar BS, Ruiz CC, Ohguro H, Huang J, Zhao X, Crabb JW, Johnson RS. Molecular cloning and characterization of retinal photoreceptor guanylyl cyclase-activating protein. *Neuron* 1994;13:395-404.

Paloma E, Coco R, Martinez-Mir A, Vilageliu L, Balcells S, Gonzalez-Duarte R. Analysis of *ABCA4* in mixed Spanish families segregating different retinal dystrophies. *Hum Mutat.* 2002;20:476-483.

Park CS, MacKinnon R. Divalent cation selectivity in a cyclic nucleotide-gated ion channel. *Biochemistry* 1995;34:13328-33.

Payne AM, Downes SM, Bessant DA, Taylor R, Holder GE, Warren MJ, Bird AC, Bhattacharya SS. A mutation in guanylate cyclase activator 1A (*GUCA1A*) in autosomal dominant cone dystrophy mapping to a new locus on chromosome 6p21.1. *Hum Mol Genet.* 1998;7:273-277.

Pawlyk BS, Sandberg MA, Berson EL. Effects of IBMX on the rod ERG of the isolated perfused cat eye: antagonism with light, calcium or L-cis-diltiazem. *Vision Res.* 1991;31:1093-1097.

Peng C, Rich ED, Thor CA, Varnum MD. Functionally important calmodulin-binding sites in both NH₂- and COOH-terminal regions of the cone photoreceptor cyclic nucleotide-gated channel CNGB3 subunit. *J Biol Chem*. 2003a;278:24617-24623.

Peng C, Rich ED, Varnum MD. Achromatopsia-associated mutation in the human cone photoreceptor cyclic nucleotide-gated channel CNGB3 subunit alters the ligand sensitivity and pore properties of heteromeric channels. *J Biol Chem*. 2003b;278:34533-34540.

Peng YW, Robishaw JD, Levine MA, Yau KW. Retinal rods and cones have distinct G protein beta and gamma subunits. *Proc Natl Acad Sci U S A*. 1992;89:10882-10886.

Pentao L, Lewis RA, Ledbetter DH, Patel PI, Lupski JR. Maternal uniparental isodisomy of chromosome 14: association with autosomal recessive rod monochromacy. *Am J Hum Genet*. 1992;50:690-699.

Petrukhin K, Koisti MJ, Bakall B, Li W, Xie G, Marknell T, Sandgren O, Forsman K, Holmgren G, Andreasson S, Vujic M, Bergen AA, McGarty-Dugan V, Figueroa D, Austin CP, Metzker ML, Caskey CT, Wadelius C. Identification of the gene responsible for Best macular dystrophy. *Nat Genet*. 1998;19:241-247.

Pianta MJ, Aleman TS, Cideciyan AV, Sunness JS, Li Y, Campochiaro BA, Campochiaro PA, Zack DJ, Stone EM, Jacobson SG. In vivo micropathology of Best macular dystrophy with optical coherence tomography. *Exp Eye Res*. 2003;76:203-211.

Piriev NI, Viczian AS, Ye J, Kerner B, Korenberg JR, Farber DB. Gene structure and amino acid sequence of the human cone photoreceptor cGMP-phosphodiesterase alpha' subunit (PDEA2) and its chromosomal localization to 10q24. *Genomics* 1995;28:429-435.

Pitt FHG. Monochromatism. *Nature* 1944;154:466-468.

Pittler SJ, Baehr W, Wasmuth JJ, McConnell DG, Champagne MS, vanTuinen P, Ledbetter D, Davis RL. Molecular characterization of human and bovine rod photoreceptor cGMP phosphodiesterase alpha-subunit and chromosomal localization of the human gene. *Genomics* 1990;6:272-283.

Poetsch A, Molday LL, Molday RS. The cGMP-gated channel and related glutamic acid-rich proteins interact with peripherin-2 at the rim region of rod photoreceptor disc membranes. *J Biol Chem*. 2001;276:48009-48016.

Pokorny J, Smith VC, Pinckers AJ, Cozijnsen M. Classification of complete and incomplete autosomal recessive achromatopsia. *Graefes Arch Clin Exp Ophthalmol*. 1982;219:121-130.

Pokorny J, Smith VC, Verriest G. Congenital color defects. In: Pokorny J, Smith VC, Verriest G, Pinckers AJ, eds. *Congenital and acquired color vision defects*. Grune & Stratton, New York, 1979:183.

Polymeropoulos MH, Ide S, Soares MB, Lennon GG. Sequence characterization and genetic mapping of the human VSNL1 gene, a homologue of the rat visinin-like peptide RNVP1. *Genomics* 1995;29:273-275.

Qi JH, Ebrahim Q, Moore N, Murphy G, Claesson-Welsh L, Bond M, Baker A, Anand-Apte B. A novel function for tissue inhibitor of metalloproteinases-3 (TIMP3): inhibition of angiogenesis by blockage of VEGF binding to VEGF receptor-2. *Nat Med.* 2003;9:407-415.

Rabb MF, Mullen L, Yelchits S, Udar N, Small KW. A North Carolina macular dystrophy phenotype in a Belizean family maps to the MCDR1 locus. *Am J Ophthalmol.* 1998;125:502-508.

Radu RA, Mata NL, Nusinowitz S, Liu X, Sieving PA, Travis GH. Treatment with isotretinoin inhibits lipofuscin accumulation in a mouse model of recessive Stargardt's macular degeneration. *Proc Natl Acad Sci U S A.* 2003;100:4742-4747.

Reardon W, Ross RJ, Sweeney MG, Luxon LM, Pembrey ME, Harding AE, Trembath RC. Diabetes mellitus associated with a pathogenic point mutation in mitochondrial DNA. *Lancet* 1992;340:1376-1379.

Regan BC, Reffin JP, Mollon JD. Luminance noise and the rapid determination of discrimination ellipses in colour deficiency. *Vision Res.* 1994;34:1279-1299.

Reichel E, Bruce AM, Sandberg MA, Berson EL. An electroretinographic and molecular genetic study of X-linked cone degeneration. *Am J Ophthalmol.* 1989;108:540-547.

Reichel MB, Kelsell RE, Fan J, Gregory CY, Evans K, Moore AT, Hunt DM, Fitzke FW, Bird AC. Phenotype of a British North Carolina macular dystrophy family linked to chromosome 6q. *Br J Ophthalmol.* 1998;82:1162-1168.

Reitner A, Sharpe LT, Zrenner E. Is colour vision possible with only rods and blue-sensitive cones? *Nature* 1991;352:798-800.

Reyniers E, Van Thienen MN, Meire F, De Boule K, Devries K, Kestelijn P, Willems PJ. Gene conversion between red and defective green opsin gene in blue cone monochromacy. *Genomics* 1995;29:323-328.

Robson AG, El-Amir A, Bailey C, Egan CA, Fitzke FW, Webster AR, Bird AC, Holder GE. Pattern ERG correlates of abnormal fundus autofluorescence in patients with retinitis pigmentosa and normal visual acuity. *Invest Ophthalmol Vis Sci.* 2003;44:3544-3550.

Rojas CV, Maria LS, Santos JL, Cortes F, Alliende MA. A frameshift insertion in the cone cyclic nucleotide gated cation channel causes complete achromatopsia in a consanguineous family from a rural isolate. *Eur J Hum Genet.* 2002;10:638-642.

Root MJ, MacKinnon R. Identification of an external divalent cation-binding site in the pore of a cGMP-activated channel. *Neuron* 1993;11:459-66.

- Roper K, Corbeil D, Huttner WB. Retention of prominin in microvilli reveals distinct cholesterol-based lipid micro-domains in the apical plasma membrane. *Nat Cell Biol.* 2000;2:582-592.
- Rosenberg T, Simonsen SE. Retinal cone dysfunction of supernormal rod ERG type. *Acta Ophthalmol.* 1993;71:246-255.
- Sakuma H, Inana G, Murakami A, Yajima T, Weleber RG, Murphey WH, Gass JD, Hotta Y, Hayakawa M, Fujiki K. A heterozygous putative null mutation in ROM1 without a mutation in peripherin/RDS in a family with retinitis pigmentosa. *Genomics* 1995;27:384-386.
- Sandberg MA, Miller S, Berson EL. Rod electroretinograms in an elevated cyclic guanosine monophosphate-type human retinal degeneration. Comparison with retinitis pigmentosa. *Invest Ophthalmol Vis Sci.* 1990;31:2283-2287.
- Sarra GM, Stephens C, de Alwis M, Bainbridge JW, Smith AJ, Thrasher AJ, Ali RR. Gene replacement therapy in the retinal degeneration slow (rds) mouse: the effect on retinal degeneration following partial transduction of the retina. *Hum Molec Genet.* 2001;10: 2353-2361.
- Sauer CG, Gehrig A, Warneke-Wittstock R, Marquardt A, Ewing CC, Gibson A, Lorenz B, Jurklies B, Weber BH. Positional cloning of the gene associated with X-linked juvenile retinoschisis. *Nat Genet.* 1997;17:164-170.
- Scherer SW, Feinstein DS, Oliveira L, Tsui LC, Pittler SJ. Gene structure and chromosome localization to 7q21.3 of the human rod photoreceptor transducin gamma-subunit gene (GNGT1). *Genomics* 1996;35:241-243.
- Schwartz M, Haim M, Skarsholm D. X-linked myopia: Bornholm Eye Disease. Linkage to DNA markers on the distal part of Xq. *Clin Genet.* 1990;38:281-286.
- Scullica L, Falsini B. Diagnosis and classification of macular degenerations: an approach based on retinal function testing. *Doc Ophthalmol.* 2001;102:237-250.
- Seifert R, Eismann E, Ludwig J, Baumann A, Kaupp UB. Molecular determinants of a Ca²⁺-binding site in the pore of cyclic nucleotide-gated channels: S5/S6 segments control affinity of intrapore glutamates. *EMBO J.* 1999;18:119-30.
- Sharon D, Sandberg MA, Caruso RC, Berson EL, Dryja TP. Shared mutations in NR2E3 in enhanced S-cone syndrome, Goldmann-Favre syndrome, and many cases of clumped pigmentary retinal degeneration. *Arch Ophthalmol.* 2003;121:1316-1323.
- Sharpe LT, Nordby K. Total colour-blindness: an introduction. In: Hess RF, Sharpe LT, Nordby K, eds. *Night Vision: basic, clinical and applied aspects*. Cambridge: Cambridge University Press, 1990:253-289.
- Sharpe LT, Stockman A, Jagle H, Nathans J. Opsin genes, cone photopigments and colourblindness. In: Gegenfurtner K, Sharpe LT eds. *Color vision: from genes to perception*. Cambridge: Cambridge University Press, 1999:3-52.

Sheffield VC, Carmi R, Kwitek-Black A, Rokhlina T, Nishimura D, Duyk GM, Elbedour K, Sunden SL, Stone EM. Identification of a Bardet-Biedl syndrome locus on chromosome 3 and evaluation of an efficient approach to homozygosity mapping. *Hum Mol Genet.* 1994;3:1331-1335.

Shimizu-Matsumoto A, Itoh K, Inazawa J, Nishida K, Matsumoto Y, Kinoshita S, Matsubara K, Okubo K. Isolation and chromosomal localization of the human cone cGMP phosphodiesterase gamma cDNA (PDE6H). *Genomics* 1996;32:121-124.

Sidjanin DJ, Lowe JK, McElwee JL, Milne BS, Phippen TM, Sargan DR, Aguirre GD, Acland GM, Ostrander EA. Canine *CNGB3* mutations establish cone degeneration as orthologous to the human achromatopsia locus ACHM3. *Hum Mol Genet.* 2002;11:1823-1833.

Simunovic MP. The cone dystrophies [PhD]. Cambridge University, 1999.

Simunovic MP, Moore AT. The cone dystrophies. *Eye* 1998;12:553-565.

Simunovic MP, Votruba M, Regan BC, Mollon JD. Colour discrimination ellipses in patients with dominant optic atrophy. *Vision Res.* 1998;38:3413-3420.

Small KW. North Carolina macular dystrophy: clinical features, genealogy, and genetic linkage analysis. *Trans Am Ophthalmol Soc.* 1998;96:925-961.

Small KW, Puech B, Mullen L, Yelchits S. North Carolina macular dystrophy phenotype in France maps to the MCDR1 locus. *Mol Vis.* 1997;3:1.

Small KW, Udar N, Yelchits S, Klein R, Garcia C, Gallardo G, Puech B, Puech V, Saperstein D, Lim J, Haller J, Flaxel C, Kelsell R, Hunt D, Evans K, Lennon F, Pericak-Vance M. North Carolina macular dystrophy (MCDR1) locus: A fine resolution genetic map and haplotype analysis. *Mol Vis.* 1999;5:38-42.

Small KW, Voo I, Flannery J, Udar N, Glasgow BJ. North Carolina macular dystrophy: Clinicopathologic correlation. *Tr Am Ophth Soc.* 2001;99:233-237.

Smallwood PM, Wang Y, Nathans J. Role of a locus control region in the mutually exclusive expression of human red and green cone pigment genes. *Proc Natl Acad Sci U S A.* 2002;99:1008-1011

Smith VC, Pokorny J, Newell FW. Autosomal recessive incomplete achromatopsia with protan luminosity function. *Ophthalmologica* 1978;177:197-207.

Smith VC, Pokorny J, Newell FW. Autosomal recessive incomplete achromatopsia with deutan luminosity. *Am J Ophthalmol.* 1979;87:393-402.

Sohocki MM, Perrault I, Leroy BP, Payne AM, Dharmaraj S, Bhattacharya SS, Kaplan J, Maumenee IH, Koenekoop R, Meire FM, Birch DG, Heckenlively JR, Daiger SP. Prevalence of *AIPL1* mutations in inherited retinal degenerative disease. *Mol Genet Metab.* 2000;70:142-150.

Sparrow JR, Nakanishi K, Parish CA. The lipofuscin fluorophore A2E mediates blue light-induced damage to retinal pigmented epithelial cells. *Invest Ophthalmol Vis Sci*. 2000;41:1981-1989.

Sparrow JR, Vollmer-Snarr HR, Zhou J, Jang YP, Jockusch S, Itagaki Y, Nakanishi K. A2E-epoxides damage DNA in retinal pigment epithelial cells. Vitamin E and other antioxidants inhibit A2E-epoxide formation. *J Biol Chem*. 2003;278:18207-18213.

Sparrow JR, Zhou J, Ben-Shabat S, Vollmer H, Itagaki Y, Nakanishi K. Involvement of oxidative mechanisms in blue-light-induced damage to A2E-laden RPE. *Invest Ophthalmol Vis Sci*. 2002;43:1222-1227.

Sprecher E, Bergman R, Richard G, Lurie R, Shalev S, Petronius D, Shalata A, Anbinder Y, Leibur R, Perlman I, Cohen N, Szargel R. Hypotrichosis with juvenile macular dystrophy is caused by a mutation in CDH3, encoding P-cadherin. *Nat Genet*. 2001;29:134-136.

Stefko ST, Zhang K, Gorin MB, Traboulsi EI. Clinical spectrum of chromosome 6-linked autosomal dominant drusen and macular degeneration. *Am J Ophthalmol*. 2000;130:203-208.

Steinmetz RL, Haimovici R, Jubb C, Fitzke FW, Bird AC. Symptomatic abnormalities of dark adaptation in patients with age-related Bruch's membrane change. *Br J Ophthalmol*. 1993;77:549-554.

Stone EM, Lotery AJ, Munier FL, Heon E, Piguet B, Guymer RH, Vandenberg K, Cousin P, Nishimura D, Swiderski RE, Silvestri G, Mackey DA, Hageman GS, Bird AC, Sheffield VC, Schorderet DF. A single *EFEMP1* mutation associated with both malattia Leventinese and Doyme honeycomb retinal dystrophy. *Nature Genet*. 1999;22:199-202.

Stone EM, Nichols BE, Kimura AE, Weingeist TA, Drack A, Sheffield VC. Clinical features of a Stargardt-like dominant progressive macular dystrophy with genetic linkage to chromosome 6q. *Arch. Ophthalmol*. 1994;112: 765-772.

Stone EM, Sheffield VC, Hageman GS. Molecular genetics of age-related macular degeneration. *Hum Mol Genet*. 2001;10:2285-2292.

Stone EM, Webster AR, Vandenberg K, Streb LM, Hockey RR, Lotery AJ, Sheffield VC. Allelic variation in *ABCR* associated with Stargardt disease but not age-related macular degeneration. *Nat Genet*. 1998;20:328-329.

Stryer L. Visual excitation and recovery. *J Biol Chem*. 1991;266:10711-10714.

Sun H, Nathans J. Stargardt's ABCR is localized to the disc membrane of retinal rod outer segments. *Nat Genet*. 1997;17:15-16.

Sun H, Smallwood PM, Nathans J. Biochemical defects in ABCR protein variants associated with human retinopathies. *Nat Genet*. 2000;26:242-246.

Sun H, Tsunenari T, Yau KW, Nathans J. The vitelliform macular dystrophy protein defines a new family of chloride channels. *Proc Natl Acad Sci U S A*. 2002;99:4008-4013.

Sun L, Bittner MA, Holz RW. RIM, a component of the presynaptic active zone and modulator of exocytosis, binds 14-3-3 through its N-terminus. *J Biol Chem*. 2003;278:38301-38309.

Sundin OH, Yang JM, Li Y, Zhu D, Hurd JN, Mitchell TN, Silva ED, Maumenee IH. Genetic basis of total colourblindness among the Pingelapese islanders. *Nat Genet*. 2000;25:289-293.

Suzuki S, Sano K, Tanihara H. Diversity of the cadherin family: evidence for eight new cadherins in nervous tissue. *Cell Regul*. 1991;2:261-270.

Szel A, Juliusson B, Bergstrom A, Wilke K, Ehinger B, van Veen T. Reversed ratio of color-specific cones in rabbit retinal cell transplants. *Brain Res Dev Brain Res*. 1994a;81:1-9.

Szel A, van Veen T, Rohlich P. Retinal cone differentiation. *Nature* 1994b;370:336.

Tarttelin EE, Gregory-Evans CY, Bird AC, Weleber RG, Klein ML, Blackburn J, Gregory-Evans K. Molecular genetic heterogeneity in autosomal dominant drusen. *J Med Genet*. 2001;38:381-384.

The Retinoschisis Consortium. Functional implications of the spectrum of mutations found in 234 cases with X-linked juvenile retinoschisis. *Hum Mol Genet*. 1998;7:1185-1192.

To KW, Adamian M, Jakobiec FA, Berson EL. Clinical and histopathologic findings in clumped pigmentary retinal degeneration. *Arch Ophthalmol*. 1996;114:950-955.

Travis GH, Sutcliffe JG, Bok D. The retinal degeneration slow (rds) gene product is a photoreceptor disc membrane-associated glycoprotein. *Neuron* 1991;6:61-70.

Trudeau MC, Zagotta WN. Mechanism of calcium/calmodulin inhibition of rod cyclic nucleotide-gated channels. *Proc Natl Acad Sci U S A*. 2002a;99:8424-8429.

Trudeau MC, Zagotta WN. An intersubunit interaction regulates trafficking of rod cyclic nucleotide-gated channels and is disrupted in an inherited form of blindness. *Neuron* 2002b;34:197-207.

Udar N, Yelchits S, Chalukya M, Yellore V, Nusinowitz S, Silva-Garcia R, Vrabec T, Hussles Maumenee I, Donoso L, Small KW. Identification of *GUCY2D* gene mutations in *CORD5* families and evidence of incomplete penetrance. *Hum Mutat*. 2003;21:170-171.

Ueyama H, Kuwayama S, Imai H, Tanabe S, Oda S, Nishida Y, Wada A, Shichida Y, Yamada S. Novel missense mutations in red/green opsin genes in congenital color-vision deficiencies. *Biochem Biophys Res Commun*. 2002;294:205-209.

Uliss A, Moore AT, Bird AC. The dark choroid in posterior retinal dystrophies. *Ophthalmology* 1987; 94: 1423-8.

van den Ouweland JM, Lemkes HH, Ruitenbeek W, Sandkuijl LA, de Vijlder MF, Struyvenberg PA, van de Kamp JJ, Maassen JA. Mutation in mitochondrial tRNA(Leu)(UUR) gene in a large pedigree with maternally transmitted type II diabetes mellitus and deafness. *Nat Genet.* 1992;1:368-371.

van Driel MA, Maugeri A, Klevering BJ, Hoyng CB, Cremers FP. ABCR unites what ophthalmologists divide(s). *Ophthalmic Genet.* 1998;19:117-122.

van Everdingen JA, Went LN, Keunen JE, Oosterhuis JA. X linked progressive cone dystrophy with specific attention to carrier detection. *J Med Genet.* 1992;29:291-294.

van Lith GHM. General cone dysfunction without achromatopsia. In: Pearlman JT, ed. 10th ISCERG Symposium, *Doc Ophthalmol Proc Ser.* 1973;2:175-180.

van Norren D, de Vries-de Mol EC. A case of incomplete achromatopsia of the deutan type. *Doc Ophthalmol.* 1981;51:365-372.

von Brederlow B, Bolz H, Janecke A, La O Cabrera A, Rudolph G, Lorenz B, Schwinger E, Gal A. Identification and In vitro expression of novel *CDH23* mutations of patients with Usher syndrome type 1D. *Human Mutation* 2002;19:268-273.

von Rückmann A, Fitzke FW, Bird AC. Distribution of fundus autofluorescence with a scanning laser ophthalmoscope. *Br J Ophthalmol.* 1995;79:407-412.

von Rückmann A, Fitzke FW, Bird AC. In vivo fundus autofluorescence in macular dystrophies. *Arch Ophthalmol.* 1997a;115:609-615.

von Rückmann A, Fitzke FW, Bird AC. Fundus autofluorescence in age related macular disease imaged with a scanning laser ophthalmoscope. *Invest Ophthalmol Vis Sci.* 1997b;38:478-486.

von Rückmann A, Fitzke FW, Bird AC. Distribution of pigment epithelium autofluorescence in retinal disease state recorded in vivo and its change over time. *Graefe's Arch Clin Exp Ophthalmol.* 1999;237:1-9.

Wang Y, Macke JP, Merbs SL, Zack DJ, Klaunberg B, Bennett J, Gearhart J, Nathans J. A locus control region adjacent to the human red and green visual pigment genes. *Neuron* 1992;9:429-440.

Wang Y, Okamoto M, Schmitz F, Hofmann K, Sudhof TC. Rim is a putative Rab3 effector in regulating synaptic-vesicle fusion. *Nature* 1997;388:593-598.

Wang Y, Smallwood PM, Cowan M, Blesh D, Lawler A, Nathans J. Mutually exclusive expression of human red and green visual pigment-reporter transgenes occurs at high frequency in murine cone photoreceptors. *Proc Natl Acad Sci U S A.* 1999;96:5251-5256.

Warburg M, Sjo O, Tranebjaerg L, Fledelius HC. Deletion mapping of a retinal cone-rod dystrophy: assignment to 18q211. *Am J Med Genet.* 1991;39:288-293.

Weale RA. Cone monochromatism. *J Physiol.* 1953;121:548-569.

Weale RA. Photosensitive reactions in foveae of normal and cone-monochromatic observers. *Opt Acta.* 1959;6:158-174.

Weber BH, Lin B, White K, Kohler K, Soboleva G, Herterich S, Seeliger MW, Jaissle GB, Grimm C, Reme C, Wenzel A, Asan E, Schrewe H. A mouse model for Sorsby fundus dystrophy. *Invest Ophthalmol Vis Sci.* 2002;43:2732-2740.

Weber BH, Vogt G, Pruett RC, Stohr H, Felbor U. Mutations in the tissue inhibitor of metalloproteinases-3 (TIMP3) in patients with Sorsby's fundus dystrophy. *Nat Genet.* 1994a;8:352-356.

Weber BH, Walker D, Muller B. Molecular evidence for non-penetrance in Best's disease. *J Med Genet.* 1994b;31:388-392.

Webster AR, Heon E, Lotery AJ, Vandeburgh K, Casavant TL, Oh KT, Beck G, Fishman GA, Lam BL, Levin A, Heckenlively JR, Jacobson SG, Weleber RG, Sheffield VC, Stone EM. An analysis of allelic variation in the ABCA4 gene. *Invest Ophthalmol Vis Sci.* 2001;42:1179-1189.

Weeks DE, Conley YP, Mah TS, Paul TO, Morse L, Ngo-Chang J, Dailey JP, Ferrell RE, Gorin MB. A full genome scan for age-related maculopathy. *Hum Mol Genet.* 2000;9:1329-1349.

Weeks DE, Conley YP, Tsai HJ, Mah TS, Rosenfeld PJ, Paul TO, Eller AW, Morse LS, Dailey JP, Ferrell RE, Gorin MB. Age-related maculopathy: an expanded genome-wide scan with evidence of susceptibility loci within the 1q31 and 17q25 regions. *Am J Ophthalmol.* 2001;132:682-692.

Weingeist TA, Kobrin JL, Watzke RC. Histopathology of Best's macular dystrophy. *Arch Ophthalmol.* 1982;100:1108-1114.

Weis AH, Biersdorf WR. Blue cone monochromatism. *J Pediatr Ophthalmol Strabismus* 1989;26:218-223.

Weissenbach J, Gyapay G, Dib C, Vignal A, Morissette J, Millasseau P, Vaysseix G, Lathrop M. A second-generation linkage map of the human genome. *Nature* 1992;359:794-801.

Weleber RG. Infantile and childhood retinal blindness: a molecular perspective (The Franceschetti Lecture). *Ophthalmic Genet.* 2002;23:71-97.

Weleber RG, Carr RE, Murphey WH, Sheffield VC, Stone EM. Phenotypic variation including retinitis pigmentosa, pattern dystrophy, and fundus flavimaculatus in a single family with a deletion of codon 153 or 154 of the *peripherin/RDS* gene. *Arch Ophthalmol.* 1993;111:1531-1542.

Weleber RG, Eisner A. Cone degeneration ('Bull's eye dystrophies') and colour vision defects. In: Newsome DA, ed. *Retinal dystrophies and degenerations*. New York: Raven Press, 1988: 233-256.

Weng J, Mata NL, Azarian SM, Tzekov RT, Birch DG, Travis GH. Insights into the function of Rim protein in photoreceptors and etiology of Stargardt's disease from the phenotype in abcr knockout mice. *Cell* 1999;98:13-23.

Went LN, van Schooneveld MJ, Oosterhuis JA. Late onset dominant cone dystrophy with early blue cone involvement. *J Med Genet*. 1992;29:295-298.

Wilkie SE, Li Y, Deery EC, Newbold RJ, Garibaldi D, Bateman JB, Zhang H, Lin W, Zack DJ, Bhattacharya SS, Warren MJ, Hunt DM, Zhang K. Identification and functional consequences of a new mutation (E155G) in the gene for GCAP1 that causes autosomal dominant cone dystrophy. *Am J Hum Genet*. 2001;69:471-480.

Wilkie SE, Newbold RJ, Deery E, Walker CE, Stinton I, Ramamurthy V, Hurley JB, Bhattacharya SS, Warren MJ, Hunt DM. Functional characterization of missense mutations at codon 838 in retinal guanylate cyclase correlates with disease severity in patients with autosomal dominant cone-rod dystrophy. *Hum Mol Genet*. 2000;9:3065-3073.

Winderickx J, Battisti L, Motulsky AG, Deeb SS. Selective expression of human X chromosome-linked green opsin genes. *Proc Natl Acad Sci U S A*. 1992;89:9710-9714.

Wing GL, Blanchard GC, Weiter JJ. The topography and age relationship of lipofuscin concentration in the retinal pigment epithelium. *Invest Ophthalmol Vis Sci*. 1978;17:601-607.

Winick JD, Blundell ML, Galke BL, Salam AA, Leal SM, Karayiorgou M. Homozygosity mapping of the achromatopsia locus in the Pingelapese. *Am J Hum Genet*. 1999;64:1679-1685.

Wissinger B, Gamer D, Jägle H, Giorda R, Marx T, Mayer S, Tippmann S, Broghammer M, Jurklics B, Rosenberg T, Jacobson SG, Sener EC, Tatlipinar S, Hoyng CB, Castellan C, Bitoun P, Andreasson S, Rudolph G, Kellner U, Lorenz B, Wolff G, Verellen-Dumoulin C, Schwartz M, Cremers FP, Apfelstedt-Sylla E, Zrenner E, Salati R, Sharpe LT, Kohl S. *CNGA3* mutations in hereditary cone photoreceptor disorders. *Am J Hum Genet*. 2001;69:722-737.

Wissinger B, Jagle H, Kohl S, Broghammer M, Baumann B, Hanna DB, Hedels C, Apfelstedt-Sylla E, Randazzo G, Jacobson SG, Zrenner E, Sharpe LT. Human rod monochromacy: linkage analysis and mapping of a cone photoreceptor expressed candidate gene on chromosome 2q11. *Genomics* 1998;51:325-331.

Wissinger B, Muller F, Weyand I, Schuffenhauer S, Thanos S, Kaupp UB, Zrenner E. Cloning, chromosomal localization and functional expression of the gene encoding the alpha-subunit of the cGMP-gated channel in human cone photoreceptors. *Eur J Neurosci*. 1997;9:2512-2521.

Yang Z, Peachey NS, Moshfeghi DM, Thirumalaichary S, Chorich L, Shugart YY, Fan K, Zhang K. Mutations in the RPGR gene cause X-linked cone dystrophy. *Hum Mol Genet.* 2002;11:605-611.

Yau KW. Phototransduction mechanism in retinal rods and cones. The Friedenwald Lecture. *Invest Ophthalmol Vis Sci.* 1994;35:9-32.

Young RS, Price J. Wavelength discrimination deteriorates with illumination in blue cone monochromats. *Invest Ophthalmol Vis Sci.* 1985;26:1543-1549.

Young TL, Penney L, Woods MO, Parfrey PS, Green JS, Hefferton D, Davidson WS. A fifth locus for Bardet-Biedl syndrome maps to chromosome 2q31. *Am J Hum Genet.* 1999;64:900-904.

Zhang K, Kniazeva M, Han M, Li W, Yu Z, Yang Z, Li Y, Metzker ML, Allikmets R, Zack DJ, Kakuk LE, Lagali PS, Wong PW, MacDonald IM, Sieving PA, Figueroa DJ, Austin CP, Gould RJ, Ayyagari R, Petrukhin K. A 5-bp deletion in *ELOVL4* is associated with two related forms of autosomal dominant macular dystrophy. *Nat Genet.* 2001;27:89-93.

Zheng J, Trudeau MC, Zagotta WN. Rod cyclic nucleotide-gated channels have a stoichiometry of three CNGA1 subunits and one CNGB1 subunit. *Neuron* 2002;36:891-896.

Zrenner E, Gouras P. Blue-sensitive cones of the cat produce a rod-like electroretinogram. *Invest Ophthalmol Vis Sci.* 1979;18:1076-1081.

CHAPTER 17

PUBLICATIONS

SHORT REPORT

Mapping of a novel locus for achromatopsia (*ACHM4*) to 1p and identification of a germline mutation in the α subunit of cone transducin (*GNAT2*)

I A Aligianis, T Forshew, S Johnson, M Michaelides, C A Johnson, R C Trembath, D M Hunt, A T Moore, E R Maher

J Med Genet 2002;**39**:656–660

Objective: To determine the molecular basis for achromatopsia using autozygosity mapping and positional candidate gene analysis.

Design and methods: A large consanguineous Pakistani family containing six subjects with autosomal recessive complete achromatopsia was ascertained. After excluding linkage to the two known achromatopsia genes (*CNGA3* and *CNGB3*), a genome wide linkage screen was undertaken.

Results: Significant linkage was detected to a 12 cM autozygous segment between markers D1S485 and D1S2881 on chromosome 1p13. Direct sequence analysis of the candidate gene *GNAT2* located within this interval identified a frameshift mutation in exon 7 (c842_843insTCAG; M280fsX291) that segregated with the disease.

Conclusions: The *GNAT2* gene codes for cone α -transducin, the G protein that couples the cone pigments to cGMP-phosphodiesterase in phototransduction. Although cone α -transducin has a fundamental role in cone phototransduction, mutations in *GNAT2* have not been described previously. Since mutations in the *CNGA3* gene may cause a variety of retinal dystrophies (complete and incomplete achromatopsia and progressive cone dystrophy), *GNAT2* mutations may also prove to be implicated in other forms of retinal dystrophy with cone dysfunction.

The photoreceptor dystrophies are an important cause of childhood blindness and represent a broad spectrum of diseases. Cone and cone-rod dystrophies are characterised by early involvement of the cone receptors and usually result in profound visual loss with abnormal colour vision and sensitivity to light. Various subtypes have been identified on the basis of natural history, psychophysical, and electrophysiological testing, a notable distinction being between stationary and progressive types.^{1,2} Cone and cone-rod dystrophies are genetically heterogeneous and may be inherited as autosomal dominant, recessive, or X linked traits. There is marked clinical and locus heterogeneity even within these subgroups. Furthermore, mutations in a single gene may cause a variety of phenotypes (Retnet database, <http://www.sph.uth.tmc.edu/Retnet/home.htm>).

Complete achromatopsia or rod monochromatism (MIM 216900, 262300, 603096) is a stationary cone dystrophy with an incidence of ~1 in 30 000.^{3,4} The condition is characterised by an absence of functional cone photoreceptors in the retina. Affected subjects usually present in infancy with nystagmus, poor visual acuity (20/200–20/400), photophobia, and complete colour blindness. Fundal examination is normal, but electroretinography shows absent photopic (light adapted or

cone) responses and normal scotopic (rod) responses. Subjects with incomplete achromatopsia retain some colour vision and have better visual acuity.⁵

Achromatopsia is recessively inherited and genetically heterogeneous. To date, two achromatopsia genes, *CNGA3*^{3–7} and *CNGB3*,^{8–10} have been characterised. *CNGA3* and *CNGB3* code for the alpha and beta subunits of the cGMP gated channel in cone cells, respectively. Germline *CNGA3* mutations have been detected in ~20% of achromatopsia kindreds and although *CNGB3* mutations are thought to account for more cases, it is likely that there is further genetic heterogeneity.⁷ A third achromatopsia locus (*ACHM1*) on chromosome 14 was suggested by the report of a patient with achromatopsia and isodisomy for chromosome 14.¹¹ In addition to causing complete achromatopsia, *CNGA3* mutations may also be associated with incomplete achromatopsia or severe progressive cone dystrophy.⁷

Autozygosity mapping in consanguineous families is a powerful strategy for localising recessive genes even in the presence of locus heterogeneity.^{12–17} To elucidate the molecular basis of achromatopsia further, we investigated a large consanguineous family originating from the Indian subcontinent. After excluding linkage to *CNGA3* and *CNGB3*, we performed a genome wide scan using an autozygosity mapping strategy, localised a novel achromatopsia locus (*ACHM4*) at 1p13, and identified a germline mutation in a candidate gene, *GNAT2*, that segregated with the disease.

PATIENTS AND METHODS

Patients

The pedigree of the three generation consanguineous Pakistani family containing six subjects with achromatopsia (and 10 unaffected relatives) is shown in fig 1. All patients had a history of nystagmus from infancy, marked photophobia, defective colour vision, and poor visual acuity. Fundus examination showed mild foveal atrophic changes. The visual impairment was non-progressive. One affected subject had electroretinography which showed normal rod responses but absent cone function, consistent with a diagnosis of achromatopsia. DNA was available as indicated (numbered subjects). Informed consent was obtained from the participants and the study was approved by the relevant local research ethics committees.

Molecular genetic studies

DNA was isolated from blood samples by standard techniques.¹⁸ Linkage to *CNGA3* and *CNGB3* was excluded by typing microsatellite markers flanking each gene (*CNGA3*: D2S133, D2S2175, D2S2311, D2S2187, and *CNGB3*: D8S167, D8S1119, D8S467). In addition, mutation analysis of *CNGA3* and *CNGB3* was performed by direct sequencing of exons and flanking intronic sequences (primer sequences are available on request). A 10 cM genome wide linkage screen was then

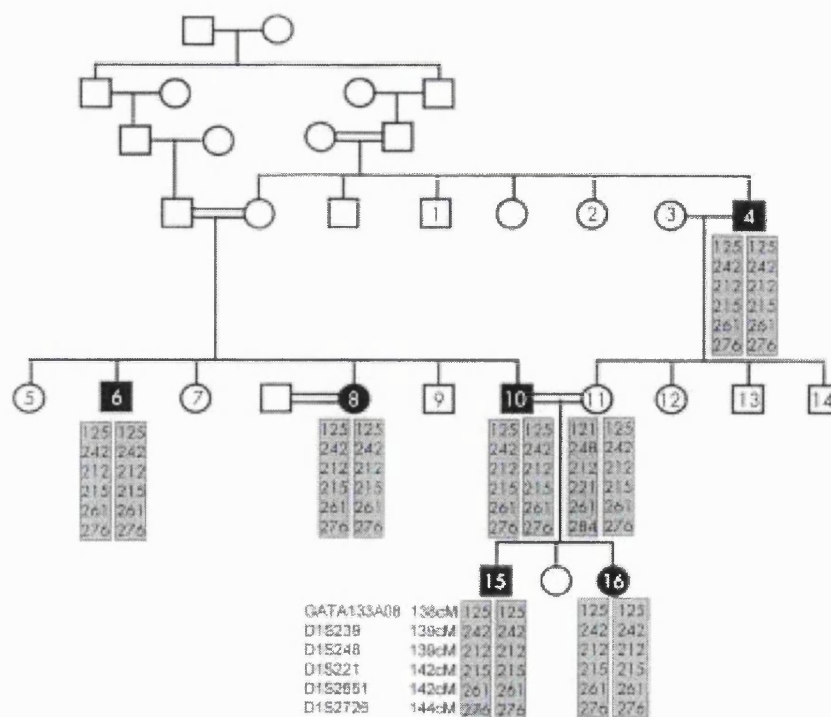


Figure 1 Family pedigree. Solid symbols indicate clinically affected subjects and open symbols represent unaffected subjects. DNA was available from subjects 1-16. Haplotype results for selected subjects are also illustrated.

undertaken using fluorescently labelled microsatellite markers from the Research Genetics version 10 mapping panel. PCR amplifications were performed in 10 μ l reactions with 20 ng of genomic DNA using standard conditions and "Thermoprime plus" *Taq* polymerase. The PCR products were then pooled into panels, diluted, and analysed on an ABI 377 DNA analyser. PCR product sizes were determined by reference to an internal standard (TAMRA GeneScan-500 size standard) using Genescan v 3.1.2 and Genotyper v 2.5.2 software (Applied Biosystems Ltd, Warrington, UK).

Mutation analysis of candidate gene

GNAT2 mutation analysis was undertaken with primers described by Magovcevic *et al*¹⁹ (table 1). Each of the eight

coding exons (and the exon-intron boundaries) were amplified separately. PCR products from both affected and unaffected subjects were sequenced with a BigDye (version 3) Terminator Cycle Sequencing Kit on both the forward and reverse strands using an ABI 377 DNA analyser (Applied Biosystems). The mutation was numbered according to the nucleotide sequence GenBank Accession number Z18859.

Statistical methods

Two point lod scores were calculated using the MLINK program of the LINKAGE (version 5.1) package²⁰ (<http://www.hgmp.mrc.ac.uk>), assuming a fully penetrant autosomal recessive gene with a disease allele frequency of 0.001. Alleles for the marker loci were assumed to be codominant and to

Table 1 Primers for PCR amplification of exons in the human cone α -transducin gene, *GNAT2*²²

Exon	Primer pairs (sense/antisense) 5'-3' direction	Amplified fragment length (bp)	Annealing temperature (°C)	(MgCl ₂) (mmol/l)
1	AGTTGAAGTAGGGAGTCTCA TCTCTGGCTCATCTCCCAT	350	55	1.50
2	GTGGAAATCGAAAGCATAAG TCTTACCCTATCTGTCTT	120	52	1.50
3	AGCTAAAGACAGAGTGTCTG CTGCTTCCACCCTTAACCCAC	210	55	1.50
4	TGTGAAGTCTTAACCAGGT CTAGAAGATTGCTTAAGCAT	240	55	1.00
5	GTCTTAGCCTGTCTGTG TGTATCCGAGATGCCCTAGG	220	55	1.50
6	GTATGTTGGCATAACCTATG TGTCTACCAAAGCTGCTTG	210	55	1.50
7	ATTCTATAAGCCAAATCTGA AGTCTCTACTAAAAGGCATT	250	55	1.50
8	TCAGCAACTACAAGGGTTC ATACCTGAGGAATGGTGAGG	270	55	1.50

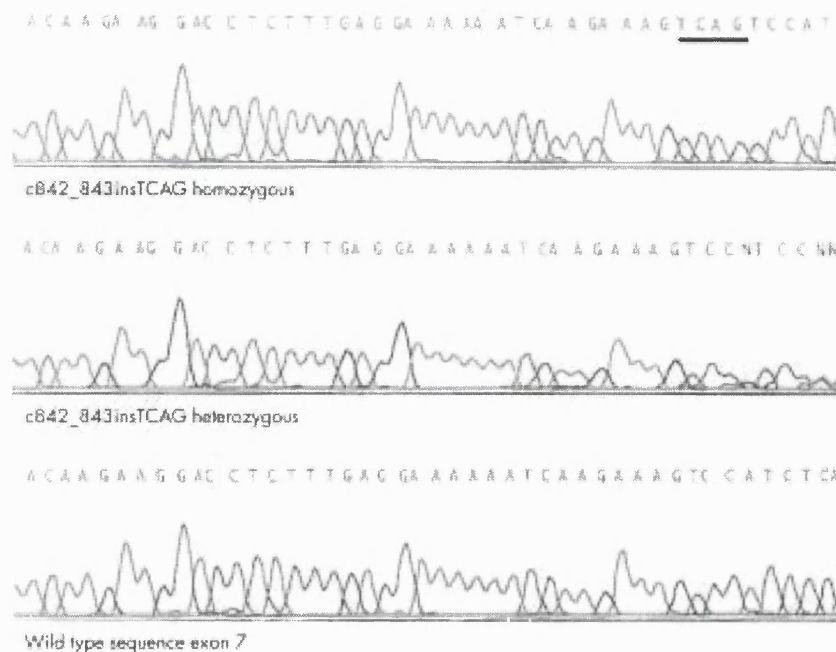


Figure 2 c842_843insTCAG GNAT2 mutation in achromatopsia: electropherograms for a homozygote, heterozygote, and wild type sequences.

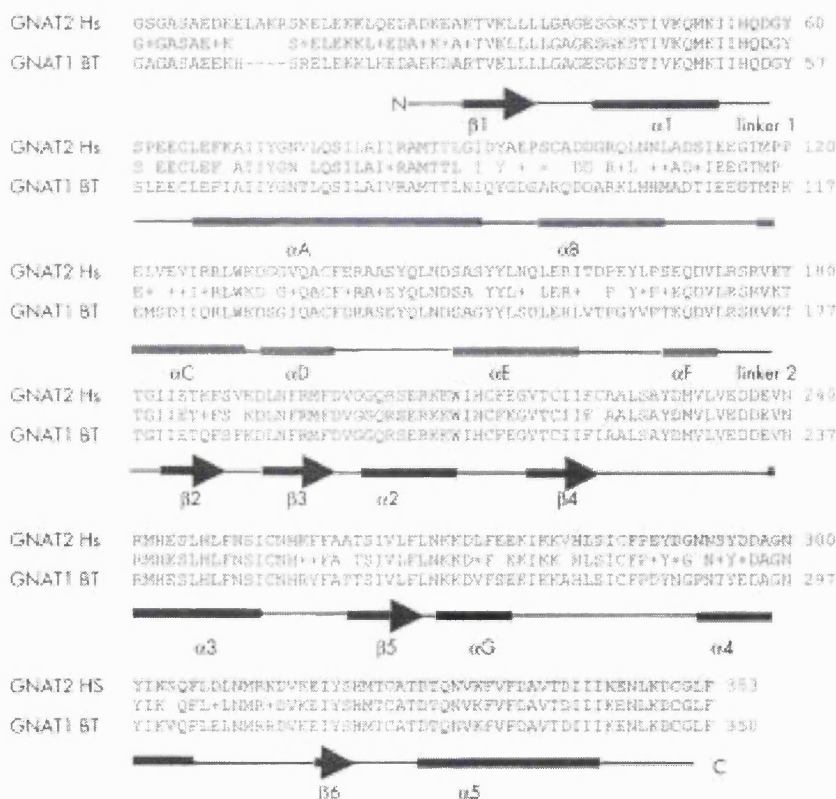


Figure 3 Comparison of amino acid sequences of bovine rod α -transducin (GNAT1 BT) and human cone α -transducin (GNAT2 Hs) showing 81% homology. Amino acids predicted to be absent from the mutant protein are shown in red. Structural domains as described by Lambright *et al*² are indicated. Two major functional domains have been defined (a) GTPase domain (in blue), which is common to the members of the GTPase family, consisting of five helices (α 1- α 5) surrounding a six stranded β sheet (β 1- β 6) and (b) an α -helical domain (in green) consisting of one long central α A helix surrounded by five shorter helices (α B- α F). These domains are linked by two extended linker strands (1 and 2). Between the 2 domains lies a deep cleft where the nucleotide is bound. Diagram derived from a blastp search (<http://www.ncbi.nih.gov/BLAST/>) of bovine α -transducin-gi 121031 and human α -transducin-gi 232151.

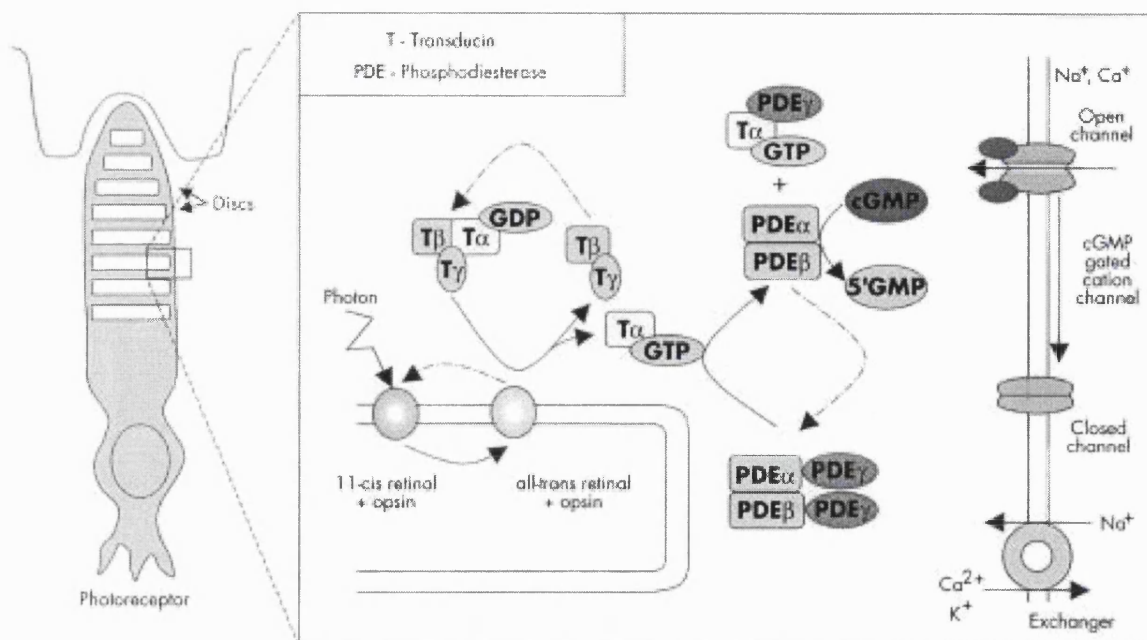


Figure 4 The phototransduction pathway. In cone photoreceptors, light activated photopigment interacts with transducin, a three subunit guanine nucleotide binding protein (G protein), stimulating the exchange of bound GDP for GTP. The cone specific α -transducin subunit which is bound to GTP is then released from its β and γ subunits and activates cGMP-phosphodiesterase by removing the inhibitory γ subunits from the active site of this enzyme. cGMP-phosphodiesterase lowers the concentration of cGMP in the photoreceptor, which results in the cGMP gated channel closing and hyperpolarisation of the photoreceptor.²¹⁻²⁴

occur at equal frequencies, because population allele frequencies were not available.

RESULTS

Analysis of *CNGA3* and *CNGB3*

Genotyping of 16 subjects (six affected and 10 unaffected) for microsatellite markers flanking *CNGA3* (D2S133, D2S2175, D2S2311, D2S2187) and *CNGB3* (D8S167, D8S1119, D8S467) showed no evidence of linkage and no evidence of homozygosity by descent in affected subjects. Furthermore, direct sequencing of all the *CNGA3* and *CNGB3* coding exons in three affected subjects did not show a germline mutation.

Autozygosity mapping

In order to map a novel achromatopsia locus, a genome wide linkage screen was performed with DNA from four affected family members. Thus, 404 highly polymorphic tri- and tetranucleotide markers from the Research Genetics v10 marker set (which covers the whole genome at an average density of 10 cM) were analysed. Initial inspection of the results showed seven homozygous regions and the whole kindred was then typed for the markers in each of these intervals. Following genotyping of additional family members, linkage was excluded in six of the seven candidate regions, but genotyping results for a 20 cM autozygous region on chromosome 1 were consistent with linkage. Typing of an additional 10 markers (D1S495, D1S485, D1S429, D1S239, D1S2688, D1S248, D1S2651, D1S221, D1S2726, and D1S2881) narrowed the homozygous segment to a 12 cM region between markers D1S485 and D1S2881. A maximum two point lod score was obtained at GATA133A08 ($Z_{\max}=3.10$ at $\theta=0$) assuming equal allele frequencies of 0.2.

Mutation analysis of *GNAT2*

Inspection of the Human Genome Draft sequence (Ensembl at the Sanger Centre, <http://www.ensembl.org> and the Human Genome Browser at University of California, Santa Cruz,

<http://genome.ucsc.edu/>) showed that the *GNAT2* gene was contained within the critical interval for our novel achromatopsia locus (*ACHM4*). *GNAT2* encodes the cone specific α -transducin protein and therefore represented an excellent candidate gene. Direct sequencing of each of the eight exons of *GNAT2* showed wild type sequence, except for a 4 bp insertion (c842_843insTCAG) in exon 7 (fig 2) that results in a frameshift mutation (M280fsX291). A stop codon is present 10 codons downstream of the insertion. The mutant allele therefore encodes a mutant protein 290 amino acids in length, the first 280 residues of which are wild type sequence, with 63 residues of the wild type protein being truncated at the carboxy-terminal (fig 3). All affected subjects within the family were homozygous for the c842_843insTCAG mutation, all obligate carriers were heterozygous, and unaffected at risk subjects were heterozygotes or homozygous wild type.

DISCUSSION

We have established homozygous *GNAT2* mutations as a novel cause for achromatopsia. *CNGA3* and *CNGB3* encode the alpha and beta subunits of the cone photoreceptor cGMP-gated channel, which is a critical component of the cone phototransduction cascade.⁵⁻¹⁰ In cone photoreceptors, light activated photopigment interacts with transducin, a three subunit guanine nucleotide binding protein (G protein), stimulating the exchange of bound GDP for GTP. The cone specific α -transducin subunit which is bound to GTP is then released from its β and γ subunits and activates cGMP-phosphodiesterase by removing the inhibitory γ subunits from the active site of this enzyme. cGMP-phosphodiesterase lowers the concentration of cGMP in the photoreceptor which results in the cGMP gated channel closing and hyperpolarisation of the photoreceptor²¹⁻²⁴ (fig 4). *GNAT2* encodes the cone specific α -transducin subunit.²⁵ Thus, the finding of a germline *GNAT2* mutation in achromatopsia is consistent with the known function of the *GNAT2* gene product. Furthermore, mutations in human rod specific α -transducin protein, *GNAT1*,

which is 83% homologous to cone α -transducin,^{25,26} cause congenital stationary night blindness, a stationary retinal dystrophy affecting the rod cells.²⁷ The frameshift mutation in the reported family would, if translated, result in a truncated protein that lacks 63 amino acids from the carboxy-terminus. This region of *GNAT2* contains important functional domains of α -transducin. Specifically, amino acid sequences 310-313 and 342-345 of α -transducin have been shown to interact with rhodopsin²⁸ and phosphodiesterase- γ interacts with multiple sites ($\alpha 3$, $\alpha 4$, and $\beta 6$ of the GTPase domain) on the carboxy-terminal of activated α -transducin²⁹ (fig 3). Further studies are required to determine if there are any phenotypic (clinical, electrodiagnostic, or psychophysical) differences between *GNAT2* associated achromatopsia and that associated with *CNGA3* and *CNGB3* mutations. Although the cone specific α -transducin was first described in 1986,²⁴ no disease phenotypes have previously been associated with mutations in *GNAT2*. Mutation analysis of 526 patients with retinitis pigmentosa³⁰ and 66 patients with Stargardt's disease¹⁹ were all negative. As *GNAT2* transcripts have also been detected in human fetal cochlea, mutation analysis was performed in 140 Usher syndrome type I and II patients; this was also negative.³¹ Further analysis is required to define the contribution of *GNAT2* mutations to achromatopsia in different ethnic groups. In view of the multiple phenotypes associated with *CNGA3* mutations⁷, further analysis of *GNAT2* is also indicated in incomplete achromatopsia and in other candidate diseases, such as the progressive cone dystrophies.

ACKNOWLEDGEMENTS

We thank the patients and their family members who contributed to this study. We acknowledge financial support from the Wellcome Trust (RCHX08477), the British Retinitis Pigmentosa Society, the Guide Dogs for the Blind Association, and Birmingham United Hospitals Endowment Fund. We are grateful to Andrew Jackson for helpful discussions.

NOTE ADDED IN PROOF

Kohl *et al* (*Am J Hum Genet*, in press) have also described *GNAT2* mutations in achromatopsia.

Authors' affiliations

I A Aligianis, T Forshew, C A Johnson, E R Maher, Section of Medical and Molecular Genetics, Department of Paediatrics and Child Health, University of Birmingham, Edgbaston, Birmingham B15 2TT, UK
I A Aligianis, E R Maher, West Midlands Regional Genetics Service, Birmingham Women's Hospital, Birmingham B15 2TG, UK
S Johnson, M Michaelides, D M Hunt, A T Moore, Institute of Ophthalmology, University College London, 11-43 Bath Street, London EC1V 9EW, UK
R C Trembath, Division of Medical Genetics, Departments of Medicine and Genetics, University of Leicester, Leicester LE1 7RH, UK

Correspondence to: Professor E R Maher, Section of Medical and Molecular Genetics, Department of Paediatrics and Child Health, University of Birmingham, The Medical School, Birmingham B15 2TT, UK; ermaher@hgmrc.ac.uk

Revised version received 3 July 2002
 Accepted for publication 4 July 2002

REFERENCES

- 1 Traboulsi EI. Cone dystrophies. In: Traboulsi EI, ed. *Genetic diseases of the eye*. Oxford: Oxford University Press, 1998:356-67.
- 2 Simunovic MP, Moore AT. The cone dystrophies. *Eye* 1998;12:553-65.
- 3 Sharpe LT, Nordby K. Total colourblindness: an introduction. In: Hess RF, Sharpe LT, Nordby K, eds. *Night vision: basic, clinical and applied aspects*. Cambridge: Cambridge University Press, 1990:253-89.
- 4 Sharpe LT, Stockman A, Jagle H, Nathans J. Opsin genes, cone photopigments and colourblindness. In: Gegenfurtner K, Sharpe LT, eds. *Color vision: from genes to perception*. Cambridge: Cambridge University Press, 1999:3-52.
- 5 Wissinger B, Jägle H, Kohl S, Broghammer M, Baumann B, Hanna DB, Hedels C, Apfelstedt-Sylla E, Randazzo G, Jacobson SG, Zrenner E, Sharpe LT. Human rod monochromacy: linkage analysis and mapping of a cone photoreceptor expressed candidate gene on chromosome 2q11. *Genomics* 1998;51:325-31.
- 6 Kohl S, Marx T, Giddings I, Jägle H, Jacobson SG, Apfelstedt-Sylla E, Zrenner E, Sharpe LT, Wissinger B. Total colourblindness is caused by mutations in the gene encoding the alpha-subunit of the cone photoreceptor cGMP-gated cation channel. *Nat Genet* 1998;19:257-9.
- 7 Wissinger B, Gamer D, Jägle H, Giorda R, Marx T, Mayer S, Tippmann S, Broghammer M, Jurklics B, Rosenberg T, Jacobson SG, Sener EC, Tatlipinar S, Hoyng CB, Castellon C, Bitoun P, Andreasson S, Rudolph G, Kellner U, Lorenz B, Wolff G, Verellen-Dumoulin C, Schwartz M, Cremers FPM, Apfelstedt-Sylla E, Zrenner E, Salati R, Sharpe L, Kohl S. *CNGA3* mutations in hereditary cone photoreceptor disorders. *Am J Hum Genet* 2001;69:722-37.
- 8 Winick JD, Blundell ML, Galke BL, Salam AA, Leal SM, Karayiorgou M. Homozygosity mapping of the achromatopsia locus in the Pingelapese. *Am J Hum Genet* 1999;64:1679-85.
- 9 Kohl S, Baumann B, Broghammer M, Jägle H, Sieving P, Kellner U, Spegal R, Anastasi M, Zrenner E, Sharpe LT, Wissinger B. Mutations in the *CNGB3* gene encoding the beta-subunit of the cone photoreceptor cGMP-gated channel are responsible for achromatopsia (*ACHM3*) linked to chromosome 8q21. *Hum Mol Genet* 2000;9:2107-16.
- 10 Sundin OH, Yang JM, Li Y, Zhu D, Hurd JN, Mitchell TN, Silva ED, Maumenee IH. Genetic basis of total colourblindness among the Pingelapese islanders. *Nat Genet* 2000;25:289-93.
- 11 Pentao L, Lewis RA, Leadbetter DH, Patel PI, Lupski JR. Maternal uniparental isodisomy of chromosome 14: association with recessive rod monochromacy. *Am J Hum Genet* 1992;50:690-9.
- 12 Lander ES, Botstein S. Homozygosity mapping: a way to map human recessive traits with the DNA of inbred children. *Science* 1987;236:1567-70.
- 13 Brown KA, Janjua AH, Karbani G, Parry G, Noble A, Crockford G, Bishop DT, Newton VE, Markham AF, Mueller RF. Linkage studies of non-syndromic recessive deafness (NSRD) in a family originating from the Mirpur region of Pakistan maps DFNB1 centromeric to D3S175. *Hum Mol Genet* 1996;5:169-73.
- 14 Mueller RF, Bishop DT. Autozygosity mapping, complex consanguinity and autosomal recessive disorders. *J Med Genet* 1993;30:798-9.
- 15 Sheffield VC, Nishimura DY, Stone EM. Novel approaches to linkage mapping. *Curr Opin in Genet Dev* 1995;5:335-41.
- 16 Sheffield VC, Piermont ME, Nishimura D, Beck JS, Burns TL, Berg MA, Stone EM, Patil SR, Luer RM. Identification of complex congenital heart defect susceptibility locus by using DNA pooling and shared segment analysis. *Hum Mol Genet* 1997;6:117-21.
- 17 Gswend M, Levan O, Kruglyak L, Ranade K, Verlander PC, Shen S, Faure S, Weissenbach J, Allay C, Lander ES, Auerbach AD, Botstein D. A locus for Fanconi-anaemia on 16q determined by homozygosity mapping. *Am J Hum Genet* 1996;59:377-84.
- 18 Mullenbach R, Lagoda PJ, Walter C. An efficient salt-chloroform extraction of DNA from blood and tissues. *Trends Genet* 1989;12:391.
- 19 Magovcevic I, Weremowicz S, Morton CC, Fong SL, Berson EL, Dryja TP. Mapping of the human cone transducin alpha-subunit (*GNAT2*) gene to 1p13 and negative mutation analysis in patients with Stargardt disease. *Genomics* 1995;25:288-90.
- 20 Cottingham RW, Idury RM, Schaffer AA. Faster sequential genetic linkage computations. *Am J Med Genet* 1993;53:252-63.
- 21 Stryer L. Cyclic GMP cascade of vision. *Annu Rev Neurosci* 1986;9:87-119.
- 22 Stryer L. Visual excitation and recovery. *J Biol Chem* 1991;266:10711-14.
- 23 Lerea CL, Somers DE, Hurley JB, Klock IB, Bunt-Milam AH. Identification of specific transducin alpha subunits in retinal rod and cone photoreceptors. *Science* 1986;234:77-80.
- 24 Lerea CL, Bunt-Milam AH, Hurley JB. Alpha transducin is present in blue-, green-, and red sensitive cone photoreceptor in the human retina. *Neuron* 1989;3:367-76.
- 25 Morris TA, Fong SL. Characterization of the gene encoding human cone transducin alpha-subunit (*GNAT2*). *Genomics* 1993;17:442-8.
- 26 Fong SL. Characterization of the human rod transducin alpha-subunit gene. *Nucleic Acids Res* 1992;20:2865-70.
- 27 Dryja TP, Hahn LB, Rebol T, Arnaud B. Missense mutation in the gene encoding the alpha subunit of rod transducin in the Nougaret form of congenital stationary night blindness. *Nat Genet* 1996;13:358-65.
- 28 Cai K, Itoh Y, Khorana HG. Mapping of contact sites in complex formation between transducin and light-activated rhodopsin by covalent crosslinking: use of a photoactivatable reagent. *Proc Natl Acad Sci USA* 2001;98:4877-82.
- 29 Liu Y, Arshavsky VY, Ruoho AE. Interaction sites of the COOH-terminal region of the gamma subunit of cGMP phosphodiesterase with the GTP-bound alpha subunit of transducin. *J Biol Chem* 1996;271:26900-7.
- 30 Ringens PJ, Fang M, Shinohara T, Bridges CD, Lerea CL, Berson EL, Dryja TP. Analysis of genes coding for S-antigen, interstitial retinol binding protein, and the alpha-subunit of cone transducin in patients with retinitis pigmentosa. *Invest Ophthalmol Vis Sci* 1990;8:1421-6.
- 31 Magovcevic I, Berson EL, Morton CC. Detection of cone alpha transducin mRNA in human fetal cochlea: negative mutation analysis in Usher syndrome. *Hear Res* 1996;99:7-12.
- 32 Lambright DG, Noel JP, Hamm HE, Sigler PB. Structural determinants for activation of the alpha-subunit of a heterotrimeric G protein. *Nature* 1994;369:621-8.

An Autosomal Dominant Bull's-Eye Macular Dystrophy (MCDR2) that Maps to the Short Arm of Chromosome 4

Michel Michaelides,¹ Samantha Johnson,¹ Arabella Poulson,² Keith Bradshaw,² Caren Bellmann,¹ David M. Hunt,¹ and Anthony T. Moore¹

PURPOSE. To describe the phenotype of an autosomal dominant macular dystrophy and identify the chromosomal locus.

METHODS. Eleven members of a five-generation, nonconsanguineous British family were examined clinically and also underwent automated perimetry, electrodiagnostic testing, fundus fluorescein angiography, and fundus autofluorescence imaging. Blood samples were taken for DNA extraction and linkage analysis was performed.

RESULTS. The phenotype is characterized by bull's-eye macular dystrophy first evident in the first or second decade of life. There is mild visual impairment, central scotomata, and electrophysiological testing indicates that most affected individuals have disease confined to the central retina but older subjects have more widespread rod and cone abnormalities, demonstrated by flash ERG. Genetic linkage analysis established linkage to chromosome 4 at p15.2-16.3 with a maximum lod score of 3.03 at a recombination fraction of 0.00 for marker *D4S391*. The locus for this autosomal dominant macular dystrophy lies between flanking markers *D4S3023* and *D4S3022*, and overlaps the Stargardt 4 locus.

CONCLUSIONS. A new locus was identified for a bull's-eye macular dystrophy on the short arm of chromosome 4. (*Invest Ophthalmol Vis Sci.* 2003;44:1657-1662) DOI:10.1167/iovs.02-0941

The hereditary central receptor dystrophies are characterized by bilateral visual loss and the finding of generally symmetrical macular abnormalities on ophthalmoscopy. The age of onset is variable, but it appears in most affected individuals in the first two decades of life. There is considerable clinical and genetic heterogeneity. Macular dystrophies showing autosomal dominant, autosomal recessive, X-linked recessive, and mitochondrial inheritance have all been reported, and there is considerable heterogeneity even within these subtypes.^{1,2} Several causative genes have now been identified (Table 1), but more remain to be discovered.

Age-related macular degeneration (ARMD) may also have a significant genetic component in its etiology. Approximately 20% of patients have a positive family history,¹⁷ and twin

studies support a strong genetic component.¹⁸ Putative susceptibility loci have been identified on 1q25-31¹⁹ and 17q25,²⁰ and it has been recently suggested that the *e4* allele of the apolipoprotein E gene may have a protective effect on risk of ARMD.²¹ Genes implicated in monogenic macular dystrophies are potential candidates for genes conferring risk for ARMD, although to date, with the possible exception of *ABCA4*, none of these genes has been shown to confer increased risk of ARMD.

In the present study we identified a locus on the short arm of chromosome 4 (4p) in a family with a dominantly inherited macular dystrophy in which there is a relatively mild phenotype.

PATIENTS AND METHODS

A five-generation family with an autosomal dominant macular dystrophy was ascertained. The protocol of the study adhered to the provisions of the Declaration of Helsinki. After informed consent was obtained, a full ophthalmic examination was performed, blood samples were collected for DNA extraction, and linkage analysis was performed.

Clinical Assessment

Eleven members of a five-generation, nonconsanguineous British family were examined (Fig. 1). Although there was no male-to-male transmission, males and females were equally affected, and autosomal dominant inheritance is thought to be most likely. A full medical and ophthalmic history was obtained and an ophthalmic examination performed. Color vision testing was performed with Hardy, Rand, Rittler (HRR) plates (American Optical Company, New York, NY). Affected subjects also underwent automated visual field perimetry (Humphrey Perimeter; Humphrey Systems, Dublin, CA), color fundus photography, and fundus autofluorescence imaging with a confocal scanning laser ophthalmoscope (cSLO) (Zeiss prototype; Carl Zeiss Inc., Oberkochen, Germany). Electrodiagnostic assessment included an electro-oculogram (EOG), a flash electroretinogram (ERG), and pattern ERG (PERG), according to the protocols recommended by the International Society for Clinical Electrophysiology of Vision.²²⁻²⁴ Patients IV:2 and V:1 underwent fundus fluorescein angiography (FFA).

The disease was diagnosed in individuals on the basis of the presence of macular abnormality and in most cases decreased visual acuity of variable severity.

Linkage Analysis Method

Genotyping. Genotyping was performed using markers from commercial linkage mapping sets (ABI MD-10 and HD-5, ver. 2.0; Linkage Mapping Sets; Applied Biosystems, Foster City, CA). These sets allow approximately 10- and 5-cM resolution of the human genome, respectively, and consist of fluorescence-labeled PCR primer pairs for 800 highly polymorphic dinucleotide repeat microsatellite markers chosen from a human linkage map provided by Gènèthon (www.genethon.fr; provided in the public domain by the French Association against Myopathies, Evry, France).²⁵⁻²⁷

PCR reactions were performed for each marker individually in a 5- μ L reaction volume, containing 25 ng DNA, 15 mM Tris-HCl (pH 8.0),

From the ¹Institute of Ophthalmology, University College London, London, United Kingdom; and the ²Department of Ophthalmology, Addenbrooke's Hospital, Cambridge, United Kingdom.

Supported by grants from the British Retinitis Pigmentosa Society and the Guide Dogs for the Blind Association.

Submitted for publication July 16, 2002; revised October 8, 2002; accepted November 7, 2002.

Disclosure: M. Michaelides, None; S. Johnson, None; A. Poulson, None; K. Bradshaw, None; C. Bellmann, None; D.M. Hunt, None; A.T. Moore, None

The publication costs of this article were defrayed in part by page charge payment. This article must therefore be marked "advertisement" in accordance with 18 U.S.C. §1734 solely to indicate this fact.

Corresponding author: Anthony T. Moore, Institute of Ophthalmology, University College London, 11-43 Bath Street, London, EC1V 9EL, UK; tony.moore@ucl.ac.uk.

TABLE 1. Chromosomal Loci and Causative Genes in Macular Dystrophies

Macular Dystrophy: OMIM Number	Mode of Inheritance	Chromosome Locus	Mutated Gene
Stargardt disease/fundus flavimaculatus; 248200 ³	Autosomal recessive	1p21-p22 (STGD1)	<i>ABCA4</i>
Stargardt-like macular dystrophy; 600110 ⁴	Autosomal dominant	6q14 (STGD3)	<i>ELOVL4</i>
Stargardt-like macular dystrophy; 603786 ⁵	Autosomal dominant	4p (STGD4)	Not identified
Adult vitelliform dystrophy; 179605 ⁶	Autosomal dominant	6p21.2-cen	<i>Peripherin/RDS</i>
Pattern dystrophy; 169150 ⁷	Autosomal dominant	6p21.2-cen	<i>Peripherin/RDS</i>
Best macular dystrophy; 153700 ⁸	Autosomal dominant	11q13	<i>VMD2</i>
Sorsby's fundus dystrophy; 136900 ⁹	Autosomal dominant	22q12.1-q13.2	<i>TIMP3</i>
Juvenile retinoschisis; 312700 ¹⁰	X-linked	Xp22.2	<i>XLRN1</i>
North Carolina macular dystrophy; 136550 ¹¹	Autosomal dominant	6q14-q16.2 (MCDR1)	Not identified
Central areolar choroidal dystrophy; 215500 ^{12,13}	Autosomal dominant	6p21.2-cen	<i>Peripherin/RDS</i>
Progressive bifocal chorioretinal atrophy; 600790 ¹⁴	Autosomal dominant	17p13	Not identified
Doyne honeycomb retinal dystrophy; 126600 ¹⁵	Autosomal dominant	6q14-q16.2	Not identified
Dominant cystoid macular dystrophy; 153880 ¹⁶	Autosomal dominant	2p16	<i>EFEMP1</i>
		7p15-p21	Not identified

50 mM KCl, 2.5 mM MgCl₂, 250 μM each dNTP, 1.25 pmol each primer and 0.25 U *Taq* polymerase (*AmpliTaq* Gold; Applied Biosystems). Reactions were performed on a thermocycler (model 9600; Perkin Elmer, Wellesley, MA) with a standard thermocycling profile for all markers. This consisted of an initial denaturation of 12 minutes immediately followed by 10 cycles of 95°C for 15 seconds, 55°C for 15 seconds, and 72°C for 30 seconds and then by 20 cycles of 89°C for 15

seconds, 55°C for 15 seconds, and 72°C for 30 seconds, with a single final extension step of 72°C for 10 minutes.

PCR products for selected sets of markers were pooled, diluted, and denatured in formamide and size fractionated using a gene analyzer (ABI 3100; Applied Biosystems). PCR products were automatically sized by the accompanying software (3100 Data Collection Software, ver. 1.0.1; Applied Biosystems), with ROX used as the size

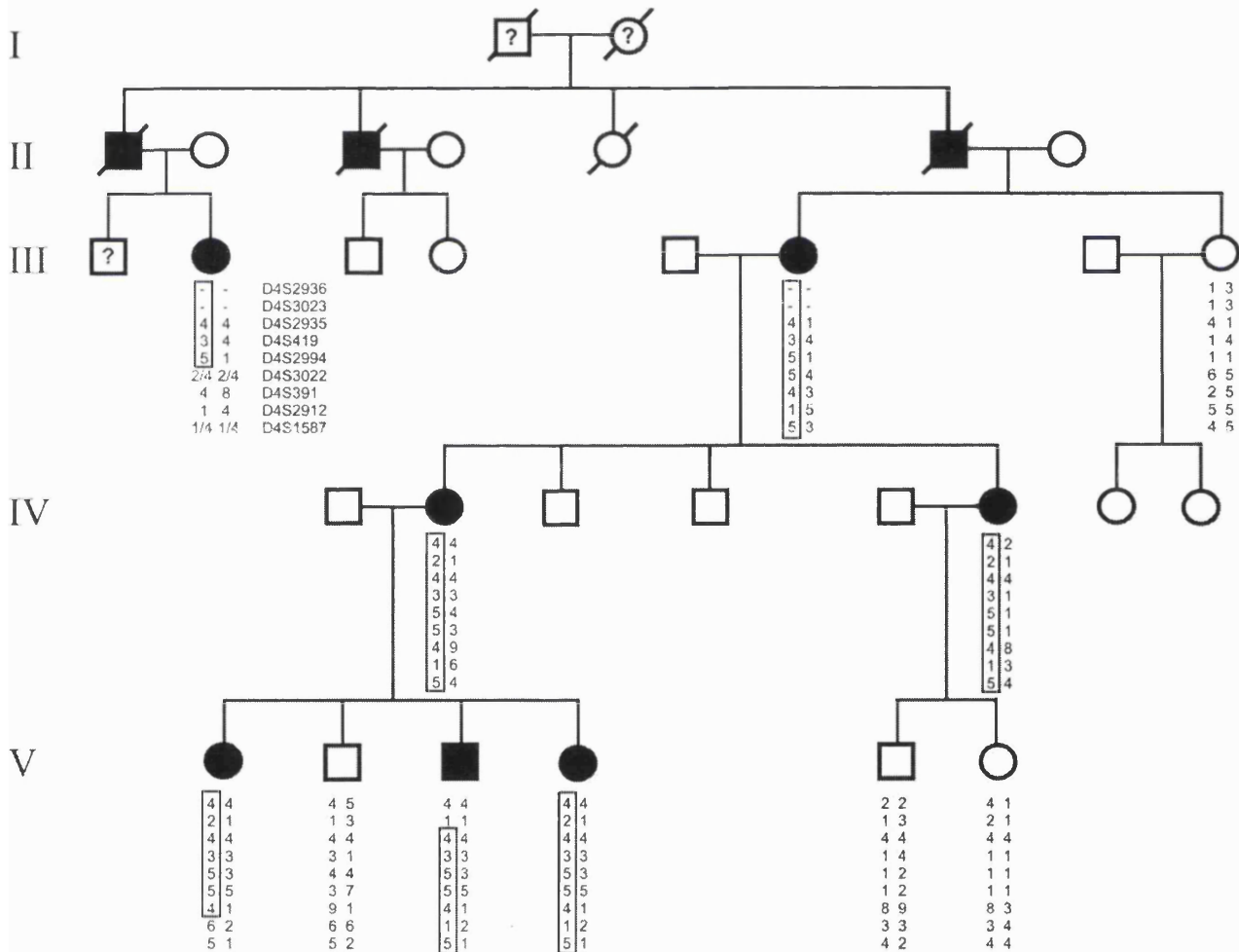


FIGURE 1. Five-generation pedigree of a family with autosomal dominant macular dystrophy. The alleles present for each of the nine chromosome 4p microsatellite markers used are shown. The minimal disease region for each affected individual is boxed.

standard, and scored by using GeneMapper (version 2.0; Applied Biosystems). Data were checked for genotyping errors using PedCheck (developed by Jeff O'Connell, University of Pittsburgh, Pittsburgh, PA).²⁸

Linkage Analysis. Subjects were classified as affected, unaffected, or status unknown according to their clinical status. Linkage analysis was performed by using standard lod score methods. Two point lod scores were calculated using the MLINK program of the LINKAGE (ver. 5.1) package (<http://www.hgmp.mrc.ac.uk/>; provided in the public domain by the Human Genome Mapping Project Resources Center, Cambridge, UK).²⁹ A fully penetrant dominant model with a disease allele frequency of 0.0001 was assumed. Marker allele frequencies were assumed to occur at equal frequencies, because population allele frequencies were not available.

RESULTS

The disorder was identified in a five-generation British family as shown in Figure 1.

Patient V:1

A 17-year-old woman (the proband) was first examined at age 13 having noticed blurred vision when reading and metamorphopsia. This difficulty with reading had gradually worsened. There were no reported problems with night vision. Visual acuity was 6/9 bilaterally. HRR testing revealed a mild red-green defect and medium tritan defect bilaterally. Dilated funduscopy revealed bilateral macular retinal pigment epithelium (RPE) mottling and atrophy with fine perifoveal red granular patches. Visual fields demonstrated mildly reduced central sensitivity. Fundus autofluorescence revealed a ring of moderately increased perifoveal autofluorescence bilaterally. Fluorescein angiography showed localized masking of the choroidal fluorescence in the perifoveal area. The PERG P50 component was mildly subnormal. EOG and flash ERG were normal.

Patient V:3

This 9-year-old boy had occasional difficulty with reading small print. Visual acuity was 6/6 bilaterally. HRR revealed mild red-green defect bilaterally. Fundoscopy revealed a bilateral prominent foveal reflex and a red-speckled appearance at the level of the RPE. Fundus autofluorescence revealed a mild perifoveal ring of increased autofluorescence. The ERG was normal. PERG and EOG were not performed because of poor cooperation.

Patient V:4

This 14-year-old girl was asymptomatic, except for noticing some difficulty with color vision, especially the color blue. Visual acuity was found to be 6/5 bilaterally. Color testing with HRR plates revealed a mild tritan and red-green defect in the left eye and normal color vision on the right. Fundus examination revealed a mild abnormality of the macula with bilateral red-speckled appearance at the level of the RPE, more prominent in the left than the right eye. There was once again a prominent foveal reflex bilaterally. Fundus autofluorescence was unremarkable. PERG, ERG, and EOG were normal.

Patient IV:2

This 41-year-old woman reported glare at night but was otherwise asymptomatic. Visual acuity was 6/5 bilaterally. Color vision assessment with the HRR plates revealed generalized dyschromatopsia affecting protan, deutan, and tritan axes. Fundoscopy revealed bilateral macular RPE mottling with a dark red perifoveal region (Fig. 2A). Visual field testing revealed bilateral central scotomata. Fundus autofluorescence imaging

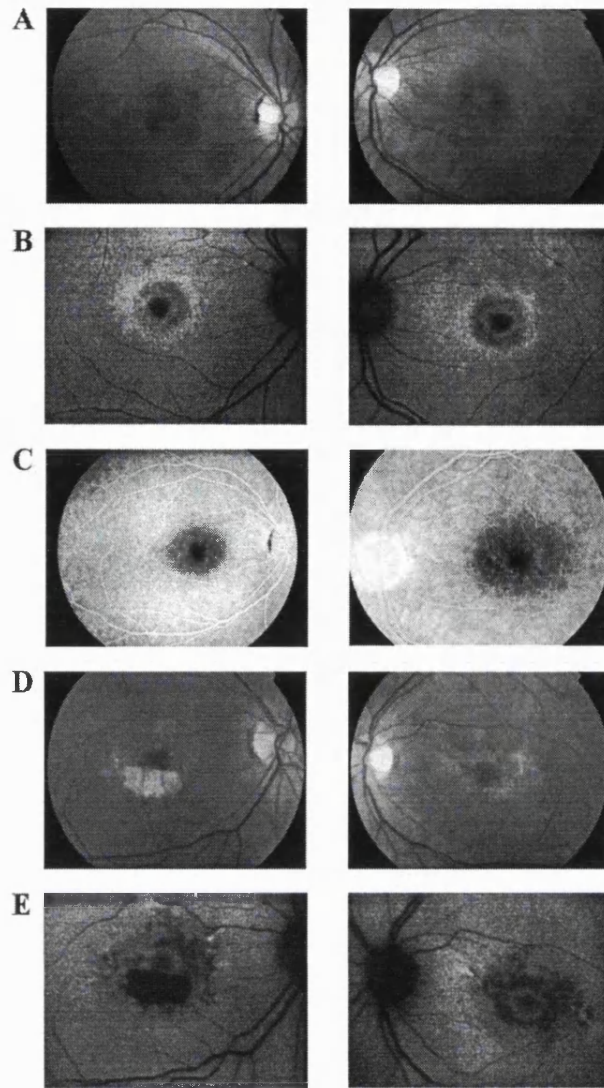


FIGURE 2. (A) Patient IV:2: fundus photograph showing bilateral RPE mottling and temporal optic disc pallor. (B) Patient IV:2: fundus autofluorescence imaging revealed bilateral bull's-eye-type lesions, comprising a ring of decreased perifoveal autofluorescence bordered peripherally and centrally by increased autofluorescence. (C) Patient IV:2: fluorescein angiography showing bilateral localized masking of the choroidal fluorescence in the perifoveal area. (D) Patient III:6: fundus photograph showing bilateral bull's-eye maculopathy, with a well-demarcated area of RPE atrophy at the right macula, and bilateral temporal optic disc pallor. (E) Patient III:6: fundus autofluorescence imaging revealed bilateral bull's-eye type lesions, more prominent in the left than the right.

revealed bilateral bull's-eye lesions, comprising a ring of decreased perifoveal autofluorescence bordered peripherally and centrally (to a lesser extent) by increased autofluorescence (Fig. 2B). Fluorescein angiography revealed masking of the choroidal fluorescence in the perifoveal area (Fig. 2C). There was no recordable PERG, but EOG and ERG were normal.

Patient IV:6

This 37-year-old woman had light sensitivity and reported glare at night. She had a visual acuity of 6/5 bilaterally and color vision was normal. Fundoscopy revealed subtle bilateral foveal abnormalities, with central pallor and surrounding mottling of

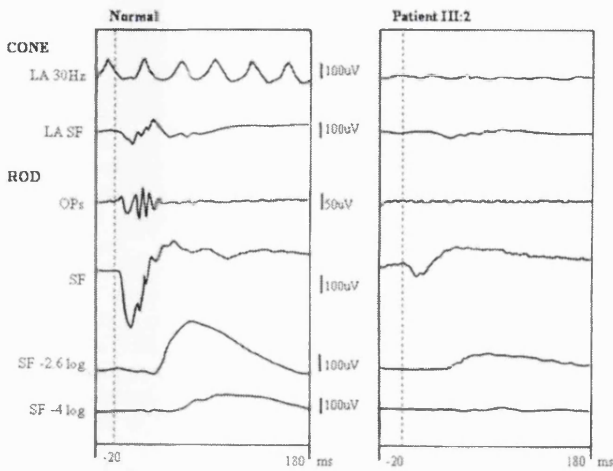


FIGURE 3. The flash ERG of Patient III:2, compared to normal control (*left*), showed reduced scotopic and photopic responses. LA, light adapted; SF, standard flash (ISCEV Clinical ERG Standard); OPs, oscillatory potentials. *Broken line*: time of stimulus flash.

the RPE. Fundus autofluorescence showed an increased signal in the perifoveal region. Visual field testing was within normal limits. The PERG P50 component revealed low-amplitude responses on the right and borderline abnormality on the left. EOG and flash ERG were normal.

Patient III:2

This 63-year-old woman was first seen at age 24, reporting difficulty with reading and bilateral central visual field defects. Visual field testing at first presentation with Bjerrum's tangent screen revealed bilateral central scotomata. Visual acuity at that time was 6/4 bilaterally. Granular pigmentation was noted at both maculae. Over a period of 35 years, visual acuity had gradually deteriorated to 6/24 in the right eye and 6/36 in the left. Fundoscopy revealed a bull's-eye maculopathy. The PERG was unrecordable from either eye. Rod and cone flash ERG responses were subnormal, suggesting a more widespread retinal dysfunction with disease progression (Fig. 3). EOG was not possible because of lack of cooperation.

Patient III:6

This 61-year-old woman was first seen at age 12 after having some difficulty with reading vision and light sensitivity. She thought that her vision was slow to adapt to dim illumination. Visual acuity was 6/6 in her right eye and 6/9 in her left. Color vision testing yielded normal results. Dilated funduscopy revealed bilateral RPE mottling, with a well-demarcated area of RPE atrophy at the right macula (Fig. 2D). She had bilateral central scotomata on visual field testing. Fundus autofluorescence imaging revealed bilateral bull's-eye lesions, which consisted of a ring of decreased perifoveal autofluorescence bordered peripherally (to a lesser extent) and centrally by increased autofluorescence (Fig. 2E). The PERG was unrecordable. EOG was normal, but the rod and cone flash ERG responses were subnormal.

Patients V:2, V:5, V:6, IV:3, and III:8

These patients were also assessed and were found to be asymptomatic, with clinical examination producing entirely normal findings.

Linkage Studies

Markers previously known to be linked to Stargardt disease (STGD) and cone-rod dystrophy (CORD) were examined in the first instance. No significant linkage was found in the following chromosome regions: *CORD6* on 17p,³⁰ *CORD7* on 6q,³¹ *CORD8* on 1q,³² *GCAP* on 6p,³³ *STGD1* on 1p,³ and *STGD3* on 6q.⁴ In total approximately 50% of the genome was screened involving genotyping of 195 markers before significant linkage was established to 4p15.2-16.3 with a maximum lod score of 3.03 at a recombination fraction of 0.00 for marker *D4S391* (Table 2).

Recombination in patients III:2 and V:3 (Fig. 1) identifies the flanking markers for this dominant macular dystrophy as *D4S3022* and *D4S3023*, a genetic distance of 32 cM.

DISCUSSION

We have mapped an autosomal dominant macular dystrophy to 4p15.2-16.3. According to the convention established by the nomenclature used for North Carolina macular dystrophy phenotype (MCDR1), we have termed this disorder MCDR2 (MC, macular; D, dystrophy; R, retinal). The macular dystrophy in this family is of early onset, and in most affected individuals the disease is confined to the macular region. The early macular abnormalities include an increased foveal reflex and a red-speckled macular appearance, progressing to a more classic bull's-eye maculopathy. Fluorescein angiography performed in two subjects with early disease showed hypofluorescence in the perifoveal area suggestive of accumulation in the RPE of an abnormal material that masks choroidal fluorescence. Older individuals have electrophysiological evidence of more widespread retinal dysfunction.

The term bull's-eye maculopathy (BEM) was first introduced to describe the characteristic appearance of chloroquine retinopathy.³⁴ Bull's-eye lesions have since been reported in cone dystrophy and CORD,³⁵ rod-cone dystrophy,³⁶ and in some forms of macular dystrophy.³⁷⁻³⁹ The pathogenesis of BEM is poorly understood. The characteristic appearance in which there is annular RPE atrophy, and central sparing may correspond to the pattern of lipofuscin accumulation in the RPE, which in healthy individuals is highest at the posterior pole and shows a depression at the fovea.^{40,41} The initially spared center usually becomes involved as the disease progresses.

Advances in ocular imaging have resulted in a new technique to visualize the RPE, taking advantage of its intrinsic fluorescence derived from lipofuscin.⁴²⁻⁴⁴ Autofluorescence imaging with a cSLO can provide useful information about the distribution of lipofuscin in the RPE and give indirect information on the level of metabolic activity of the RPE which is largely determined by the rate of turnover of photoreceptor

TABLE 2. Lod scores between Autosomal Dominant Macular Dystrophy and Microsatellite Markers on 4p

Marker	Lod Score at θ					
	0.00	0.05	0.10	0.20	0.30	0.40
<i>D4S2936</i>	−∞	−0.03	0.14	0.18	0.11	0.03
<i>D4S3023</i>	−∞	−0.4	−0.22	−0.05	−0.02	−0.01
<i>D4S2935</i>	0.45	0.41	0.36	0.27	0.17	0.08
<i>D4S419</i>	1.44	1.27	1.09	0.76	0.44	0.18
<i>D4S2994</i>	2.30	2.05	1.79	1.28	0.79	0.36
<i>D4S3022</i>	−2.25	1.07	1.21	1.12	0.83	0.45
<i>D4S391</i>	3.03	2.76	2.47	1.87	1.24	0.61
<i>D4S2912</i>	−∞	1.35	1.39	1.16	0.79	0.39
<i>D4S1587</i>	−∞	0.46	0.24	0.31	0.25	0.14

outer segments.⁴⁴ There is evidence of continuous degradation of autofluorescent material in the RPE.⁴⁴ Progressive loss of lipofuscin occurs when there is reduced metabolic demand because of photoreceptor cell loss, and this may explain the decreased autofluorescence (AF) seen in areas of photoreceptor cell loss in eyes with retinitis pigmentosa and rod-cone dystrophies.⁴⁴ Areas of increased AF correspond to a group of RPE cells containing higher quantities of lipofuscin than their neighbors and may represent areas at high risk for photoreceptor cell loss.⁴⁰ It has been demonstrated histologically that the number of photoreceptor cells is reduced in the presence of increased quantities of lipofuscin in the RPE, leading to the proposal that autofluorescent material may accumulate before cell death.⁴⁵ Increased lipofuscin may reflect either increased outer segment turnover or the inability of the RPE to process outer segment debris. In our family concentric areas of increased AF at the macula were evident in some individuals before there was ophthalmoscopic evidence of retinal atrophy. This may suggest that the primary site of dysfunction is in the RPE, but the findings of a normal EOG indicate that there is no widespread RPE abnormality. Alternatively, the increased AF could occur as a result of primary disease of the photoreceptors, which in the early stages of the disease is confined to the macular region but becomes more widespread in the late stages.

In our family we established linkage to 4p15.2-16.3. This region contains the candidate gene *PROML1*, encoding human prominin (mouse)-like-1 which belongs to the prominin family of 5-transmembrane domain proteins. *PROML1* is expressed in retinoblastoma cell lines and adult retina, and the product of the mouse orthologue (prom) is concentrated in membrane evaginations at the base of the outer segments of rod photoreceptors. A homozygous mutation in *PROML1* has been identified in an Indian pedigree with autosomal recessive retinal dystrophy. The mutation results in the production of a truncated protein, and functional studies in transfected CHO cells have demonstrated that the truncated prominin protein fails to reach the cell surface, indicating that the loss of prominin may lead to retinal degeneration through impaired generation of evaginations or conversion to outer segment disks.⁴⁶

A locus for an autosomal dominant Stargardt-like disease has also been mapped to the short arm of chromosome 4 (STGD4) in a Caribbean family.⁵ Analysis of extended haplotypes localized the disease gene to a 12-cM interval between loci *D4S1582* and *D4S2397*. This interval overlaps with our defined MCDR2 region. However our pedigree differs considerably from that of the Caribbean family, in that neither of our patients who underwent FFA demonstrated the characteristic dark choroid pattern that was seen in the Caribbean patients and our patients did not have the retinal flecks that were prominent in the Stargardt-like pedigree. The macular dystrophy we report appears to be clinically distinct from the STGD4 disorder. Therefore, even if both disorders are allelic, it is likely that different mutations are involved in their etiology. An alternative explanation is that the two disorders are caused by mutations in two different adjacent genes on 4p. The true situation will be resolved only by the identification of the underlying genetic mutations.

Acknowledgments

The authors thank the patients who kindly agreed to take part in this study.

References

1. Moore AT, Evans K. Molecular genetics of central retinal dystrophies. *Aust NZ J Ophthalmol.* 1996;24:189-198.

2. Musarella M. Molecular genetics of macular degeneration. *Doc Ophthalmol.* 2001;102:165-177.
3. Allikmets R, Singh N, Sun H, et al. A photoreceptor cell-specific ATP-binding transporter gene (ABCR) is mutated in recessive Stargardt macular dystrophy. *Nat Genet.* 1997;15:236-246.
4. Zhang K, Kniazeva M, Han M, et al. A 5-bp deletion in *ELOVL4* is associated with two related forms of autosomal dominant macular dystrophy. *Nat Genet.* 2001;27:89-93.
5. Kniazeva M, Chiang MF, Morgan B, et al. A new locus for autosomal dominant Stargardt-like disease maps to chromosome 4. *Am J Hum Genet.* 1999;64:1394-1399.
6. Felber U, Schilling H, Weber BHF. Adult vitelliform macular dystrophy is frequently associated with mutation in the peripherin/RDS gene. *Hum Mutat.* 1997;10:301-309.
7. Nichols BE, Drack AV, Vandenberg K, et al. A 2 base pair deletion in the RDS gene associated with butterfly-shaped pigment dystrophy of the fovea. *Hum Mol Genet.* 1993;2:601-603.
8. Petrukhin K, Koisti MJ, Bakall B, et al. Identification of the gene responsible for Best macular dystrophy. *Nat Genet.* 1998;19:241-247.
9. Weber BH, Vogt G, Pruett RC, Stohr H, Felber U. Mutations in the tissue inhibitor of metalloproteinases-3 (TIMP3) in patients with Sorsby's fundus dystrophy. *Nat Genet.* 1994;8:352-356.
10. Sauer CG, Gehrig A, Warneke-Wittstock R, et al. Positional cloning of the gene associated with X-linked juvenile retinoschisis. *Nat Genet.* 1997;17:164-170.
11. Small KW. North Carolina macular dystrophy: clinical features, genealogy, and genetic linkage analysis. *Trans Am Ophthalmol Soc.* 1998;96:925-961.
12. Reig C, Serra A, Gean E, et al. A point mutation in the RDS-peripherin gene in a Spanish family with central areolar choroidal dystrophy. *Ophthalmol Genet.* 1995;16:39-44.
13. Hughes AE, Lotery AJ, Silvestri G. Fine localisation of the gene for central areolar choroidal dystrophy on chromosome 17p. *J Med Genet.* 1998;35:770-772.
14. Kelsell RE, Godley BF, Evans K, et al. Localization of the gene for progressive bifocal chorioretinal atrophy (PBCRA) to chromosome 6q. *Hum Mol Genet.* 1995;4:1653-1656.
15. Stone EM, Lotery AJ, Munier FL, et al. A single EFEMP1 mutation associated with both Malattia Leventinese and Doyme honeycomb retinal dystrophy. *Nat Genet.* 1999;22:199-202.
16. Kremer H, Pinckers A, van den Helm B, et al. Localization of the gene for dominant cystoid macular dystrophy on chromosome 7p. *Hum Mol Genet.* 1994;3:299-302.
17. Klaver CC, Wolfs RC, Assink JJ, van Duijn CM, Hofman A, de Jong PT. Genetic risk of age-related maculopathy: population-based familial aggregation study. *Arch Ophthalmol.* 1998;116:1646-1651.
18. Meyers SM, Zachary AA. Monozygotic twins with age-related macular degeneration. *Arch Ophthalmol.* 1988;106:651-653.
19. Klein ML, Schultz DW, Edwards A, et al. Age-related macular degeneration: clinical features in a large family and linkage to chromosome 1q. *Arch Ophthalmol.* 1998;116:1082-1088.
20. Weeks DE, Conley YP, Tsai HJ, et al. Age-related maculopathy: an expanded genome-wide scan with evidence of susceptibility loci within the 1q31 and 17q25 regions. *Am J Ophthalmol.* 2001;132:682-692.
21. Klaver CC, Kliffen M, van Duijn CM, et al. Genetic association of apolipoprotein E with age-related macular degeneration. *Am J Hum Genet.* 1998;63:200-206.
22. Marmor MF, Zrenner E. Standard for clinical electroretinography (1994 update). *Doc Ophthalmol.* 1995;89:199-210.
23. Bach M, Hawlina M, Holder GE, et al. Standard for pattern electroretinography. International Society for Clinical Electrophysiology of Vision. *Doc Ophthalmol.* 2000;101:11-18.
24. Marmor MF, Zrenner E. Standard for clinical electro-oculography. International Society for Clinical Electrophysiology of Vision. *Arch Ophthalmol.* 1993;111:601-604.
25. Weissenbach J, Gyapay G, Dib C, et al. A second-generation linkage map of the human genome. *Nature* 1992;359:794-801.
26. Gyapay G, Morissette J, Vignal A, et al. The 1993-94 Génethon human genetic linkage map. *Nat Genet.* 1994;7:246-339.

27. Dib C, Faure S, Fizames C, et al. A comprehensive genetic map of the human genome based on 5,264 microsatellites. *Nature*. 1996;380:152-154.
28. O'Connell JR, Weeks DE. PedCheck: a program for identification of genotype incompatibilities in linkage analysis. *Am J Hum Genet*. 1998;63:259-266.
29. Cottingham RW, Idury RM, Schaffer AA. Faster sequential genetic linkage computations. *Am J Hum Genet*. 1993;53:252-263.
30. Kelsell RE, Evans K, Gregory CY, et al. Localisation of a gene for dominant cone-rod dystrophy (CORD6) to chromosome 17p. *Hum Mol Genet*. 1997;6:597-600.
31. Kelsell RE, Gregory-Evans K, Gregory-Evans CY, et al. Localization of a gene (CORD7) for a dominant cone-rod dystrophy to chromosome 6q. *Am J Hum Genet*. 1998;63:274-279.
32. Khaliq S, Hameed A, Ismail M, et al. Novel locus for autosomal recessive cone-rod dystrophy CORD8 mapping to chromosome 1q12-q24. *Invest Ophthalmol Vis Sci*. 2000;41:3709-3712.
33. Payne AM, Downes SM, Bessant D, et al. A mutation in guanylate cyclase activator 1A (GUCA1A) in an autosomal dominant cone dystrophy pedigree mapping to a new locus on chromosome 6p21.1. *Hum Molec Genet*. 1998;7:273-277.
34. Kearns TP, Hollenhorst RW. Chloroquine retinopathy: evaluation by fluorescein angiography. *Arch Ophthalmol*. 1966;76:378-384.
35. Krill AE, Deutman AF, Fishman M. The cone degenerations. *Doc Ophthalmol*. 1973;35:1-80.
36. Fishman GA, Fishman M, Maggiano J. Macular lesions associated with retinitis pigmentosa. *Arch Ophthalmol*. 1977;95:798-803.
37. Deutman AF. Benign concentric annular macular dystrophy. *Am J Ophthalmol*. 1974;78:384-396.
38. O'Donnell FE, Welch RB. Fenestrated sheen macular dystrophy: a new autosomal dominant maculopathy. *Arch Ophthalmol*. 1979;97:1292-1296.
39. Slagsvold JE. Fenestrated sheen macular dystrophy: a new autosomal dominant maculopathy. *Acta Ophthalmol (Copenb)*. 1981;59:683-688.
40. von Rückmann A, Fitzke FW, Bird AC. Fundus autofluorescence in age related macular disease imaged with a scanning laser ophthalmoscope. *Invest Ophthalmol Vis Sci*. 1997;38:478-486.
41. Wing GL, Blanchard GC, Weiter JJ. The topography and age relationship of lipofuscin concentration in the retinal pigment epithelium. *Invest Ophthalmol Vis Sci*. 1978;17:601-607.
42. von Rückmann A, Fitzke FW, Bird AC. Distribution of fundus autofluorescence with a scanning laser ophthalmoscope. *Br J Ophthalmol*. 1995;79:407-412.
43. von Rückmann A, Fitzke FW, Bird AC. In vivo fundus autofluorescence in macular dystrophies. *Arch Ophthalmol*. 1997;115:609-615.
44. von Rückmann A, Fitzke FW, Bird AC. Distribution of pigment epithelium autofluorescence in retinal disease state recorded in vivo and its change over time. *Graefes Arch Clin Exp Ophthalmol*. 1999;237:1-9.
45. Dorey CK, Wu G, Ebenstein D, Garsd A, Weiter JJ. Cell loss in the ageing retina: relationship to lipofuscin accumulation and macular degeneration. *Invest Ophthalmol Vis Sci*. 1989;30:1691-1699.
46. Maw MA, Corbeil D, Koch J, et al. A frameshift mutation in prominin (mouse)-like 1 causes human retinal degeneration. *Hum Mol Genet*. 2000;9:27-34.

An Early-Onset Autosomal Dominant Macular Dystrophy (MCDR3) Resembling North Carolina Macular Dystrophy Maps to Chromosome 5

Michel Michaelides,^{1,2} Samantha Johnson,^{1,2} Alok K. Tekriwal,³ Graham E. Holder,⁴ Caren Bellmann,¹ Esther Kinning,^{5,6} Geoffrey Woodruff,³ Richard C. Trembath,^{5,6} David M. Hunt,¹ and Anthony T. Moore¹

PURPOSE. To characterize the phenotype of an autosomal dominant macular dystrophy and identify the chromosomal locus.

METHODS. Thirteen members of a four-generation, nonconsanguineous British family were examined clinically and also underwent automated perimetry, fundus fluorescein angiography, and fundus autofluorescence imaging. After informed consent was obtained, blood samples were taken for DNA extraction, and genetic linkage analysis was performed.

RESULTS. The retinal changes have an early age of onset and are confined to the macular region. The macular abnormalities vary from mild retinal pigment epithelium (RPE) pigmentary change to atrophy. Drusen-like deposits are present to various degrees and are characteristic of the phenotype. Subretinal neovascular membrane (SRNVM) is an established complication. Genetic linkage analysis established linkage to chromosome 5, region p13.1-p15.33 with a maximum LOD score of 3.61 at a recombination fraction of 0.00 for marker *D5S630*. The locus for this autosomal dominant macular dystrophy lies between flanking markers *D5S1981* and *D5S2031*.

CONCLUSIONS. A novel locus has been identified for early-onset autosomal dominant macular dystrophy on chromosome 5. (*Invest Ophthalmol Vis Sci.* 2003;44:2178-2183) DOI: 10.1167/iovs.02-1094

The central receptor or macular dystrophies comprise a heterogeneous group of disorders in which there is variable visual loss associated with bilateral symmetrical macular abnormalities. Autosomal dominant, autosomal recessive, X-linked recessive, and mitochondrial inheritance have all been reported, and there is considerable heterogeneity even within these subtypes.^{1,2} A number of different genes that cause

macular dystrophy have been identified, including *ABCA4*,³ *ELOVL4*,⁴ *peripherin/RDS*,⁵⁻⁷ *VMD2*,⁸ *TIMP3*,⁹ *XLRS1*,¹⁰ and *EFEMP1*,¹¹ and the study of gene expression and function of the encoded proteins has improved our understanding of disease pathogenesis.

Although in most macular dystrophies the abnormal fundoscopic appearance is confined to the macular region, there is usually electrophysiological, psychophysical, or histological evidence of widespread photoreceptor and retinal pigment epithelial dysfunction.^{1,2} This is consistent with the fact that most genes identified as causing macular dystrophy are expressed throughout the retina, rather than solely in the macular region.² There are, however, a few disorders in which the disease appears to be confined to the macular region. For example, in North Carolina macular dystrophy, results of psychophysical and electrophysiological tests demonstrate that normal peripheral retinal function is retained.¹²

In the present study we report the clinical and electrophysiological findings in a family with a dominantly inherited macular dystrophy, resembling North Carolina macular dystrophy (MCDR1). We have excluded the *MCDR1* locus on chromosome 6 and have demonstrated linkage in this family to a novel locus on chromosome 5.

PATIENTS AND METHODS

Thirteen members of a four-generation, nonconsanguineous British family with an autosomal dominant macular dystrophy were assessed (Fig. 1). We were also able to review the clinical notes of three additional affected family members who were not available for examination. After informed consent was obtained, a medical history was taken and a full ophthalmic examination performed. Blood samples were taken for DNA extraction and linkage analysis was performed. The protocol of the study adhered to the provisions of the Declaration of Helsinki.

Clinical Assessment

Color vision testing was performed using Hardy, Rand, Rittler (HRR) plates (American Optical Company, New York, NY). Affected subjects also underwent Humphrey automated perimetry (Zeiss-Humphrey Systems; Dublin, CA), color fundus photography, and fundus autofluorescence (AF) imaging, using a confocal scanning laser ophthalmoscope (cSLO; Heidelberg Retina Angiograph; Heidelberg Engineering, Heidelberg, Germany). Electrodiagnostic assessment included an electro-oculogram (EOG) and a flash electroretinogram (ERG) according to the protocols recommended by the International Society for Clinical Electrophysiology of Vision.^{13,14} Two subjects underwent fundus fluorescein angiography (FFA).

Individuals were diagnosed as affected on the basis of the presence of macular abnormality and, in most cases, associated decreased visual acuity.

From the ¹Institute of Ophthalmology, University College London, London, United Kingdom; the ²Department of Ophthalmology, Leicester Royal Infirmary, Leicester, United Kingdom; ³Department of Electrophysiology, Moorfields Eye Hospital, London, United Kingdom; and the Departments of ⁵Medicine and ⁶Genetics, Division of Medical Genetics, University of Leicester, Leicester, United Kingdom.

²Contributed equally to the work and therefore should be considered equivalent authors.

Supported by grants from the British Retinitis Pigmentosa Society and the Guide Dogs for the Blind Association.

Submitted for publication October 25, 2002; revised December 4, 2002; accepted December 16, 2002.

Disclosure: M. Michaelides, None; S. Johnson, None; A.K. Tekriwal, None; G.E. Holder, None; C. Bellmann, None; E. Kinning, None; G. Woodruff, None; R.C. Trembath, None; D.M. Hunt, None; A.T. Moore, None

The publication costs of this article were defrayed in part by page charge payment. This article must therefore be marked "advertisement" in accordance with 18 U.S.C. §1734 solely to indicate this fact.

Corresponding author: Anthony T. Moore, Institute of Ophthalmology, University College London, 11-43 Bath Street, London EC1V 9EL, UK; tony.moore@ucl.ac.uk.

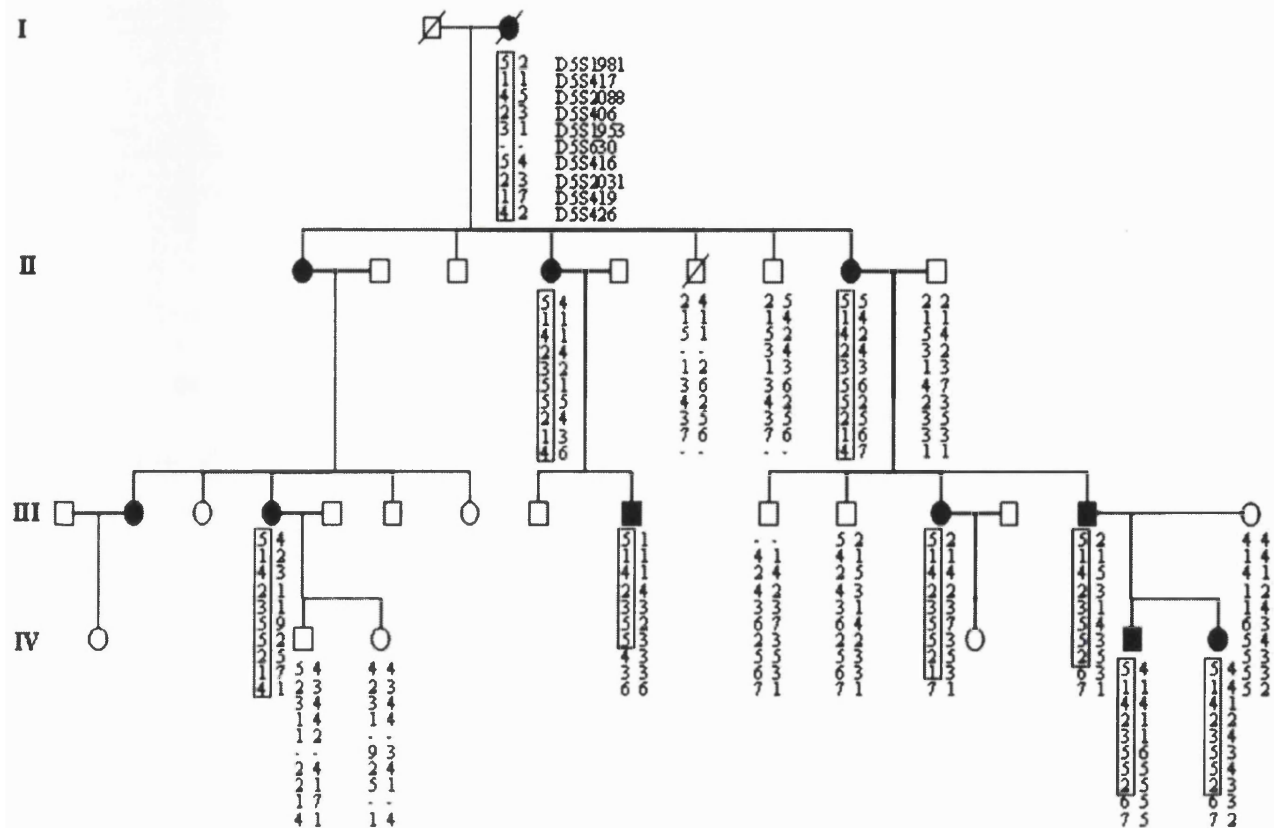


FIGURE 1. Four-generation pedigree of a family with autosomal dominant macular dystrophy. Individuals are numbered according to generation (indicated) and position in each generation, numbering from *left* to *right*. The alleles present for each of the 10 microsatellite markers on 5p are shown. The minimal disease region for each affected individual is boxed. Disease haplotype is defined by recombination events in individuals III:9 and IV:2. Unaffected individual IV:2 has two recombination events in the chromosome inherited from his affected mother which, along with the haplotype information for individual III:9 establishes *D5S1981* and *D5S2031* as the markers flanking the disease region.

Linkage Analysis Method

Genotyping. Genotyping was achieved by using markers from a commercial mapping set (ABI MD-10 and HD-5 Linkage Mapping Sets, ver. 2.0; Applied Biosystems, Foster City, CA). These sets allow approximately 10- and 5-cM resolution of the human genome, respectively, and consist of fluorescently labeled PCR primer pairs for 800 highly polymorphic dinucleotide-repeat microsatellite markers chosen from the Genethon human linkage map (<http://www.genethon.fr>; provided in the public domain by the French Association against Myopathies, Evry, France).¹⁵⁻¹⁷

PCR reactions were performed for each marker individually in a 5- μ L reaction volume, containing 25 ng DNA, 15 mM Tris-HCl (pH 8.0), 50 mM KCl, 2.5 mM MgCl₂, 250 μ M each dNTP, 1.25 pmol each primer, and 0.25 U *Taq* polymerase (Ampli Taq Gold; Applied Biosystems). Reactions were performed on a thermocycler (model 9600; Perkin Elmer, Wellesley, MA) with a standard thermocycling profile for all markers. This consisted of an initial denaturation of 12 minutes immediately followed by 10 cycles of 95°C for 15 seconds, 55°C for 15 seconds, and 72°C for 30 seconds, and then by 20 cycles of 89°C for 15 seconds, 55°C for 15 seconds, and 72°C for 30 seconds, with a single final extension step of 72°C for 10 minutes.

PCR products for selected sets of markers were pooled, diluted, and denatured in formamide and size-fractionated with an automated gene analyzer (model 3100; Applied Biosystems). PCR products were automatically sized by the accompanying software (3100 Data Collection Software, ver. 1.0.1; Applied Biosystems), using ROX as the size standard and scored using a commercial mapping program (GeneMapper, ver. 2.0; Applied Biosystems). Data were checked for genotyping

errors with PedCheck (<http://watson.hgen.pitt.edu/register/docs/ped-check.html>; developed by Jeff O'Connell, University of Pittsburgh, Pittsburgh, PA).¹⁸

Linkage Analysis. Subjects were classified as affected, unaffected or of unknown status according to their clinical status. Linkage analysis was performed with standard lod score methods. Two-point lod scores were calculated using the MLINK program of the LINKAGE (version 5.1) package (<http://www.hgmp.mrc.ac.uk>; provided in the public domain by the Human Genome Mapping Project Resources Center, Cambridge, UK).¹⁹ A fully penetrant dominant model with a disease allele frequency of 0.0001 was assumed. Marker allele frequencies were assumed to occur at equal frequencies, because population allele frequencies were not available.

RESULTS

The disorder is present in a four-generation British family, as shown in Figure 1. Patients III:10, III:11, III:15, IV:2, IV:3, and IV:4, were assessed and were found to be asymptomatic, with normal findings in a clinical examination and were designated as unaffected. The affected individuals showed a range of macular appearances varying from multiple drusen-like deposits to focal atrophy and pigmentation (Table 1, Fig. 2). EOG and flash ERG was normal in all affected individuals.

Markers known to demonstrate linkage to cone-rod dystrophies (CORD) and to *MCDR1* were examined in the first instance. No significant linkage was found at the following chromosome regions: *CORD6* on 17p,²⁰ *CORD7* on 6q,²¹

TABLE 1. Clinical Findings

Patient	Sex	Age	Visual Acuity		Fundus	AF Imaging	EOG	ERG	Visual Fields	Color Vision
			OD	OS						
I:2*	F	80	—	—	Bilateral SRNVM	—	—	—	—	—
II:1*	F	63	—	—	Bilateral SRNVM	—	—	—	—	—
II:4	F	50	6/18	6/60	Bilateral macular scarring associated with subretinal fibrosis and surrounding fine drusen-like deposits. FFA was consistent with previous bilateral SRNVM	—	N	N	Bilateral central scotomata	Bilateral protan, deutan and tritan defects
II:8	F	60	6/9	6/9	Bilateral fine macular drusen-like deposits with areas of RPE atrophy and pigmentation	Increased AF at both maculae, corresponding to the drusen-like deposits	N	N	N	Bilateral protan, deutan and tritan defects
III:2*	F	37	6/60	6/12	Right: SRNVM Left: Macular drusen-like deposits with areas of RPE atrophy and pigmentation (Fig. 2C)	—	—	—	—	—
III:4	F	36	6/5	6/5	Bilateral fine macular drusen-like deposits with areas of RPE atrophy and pigmentation	—	N	N	N	Bilateral protan and deutan defects
III:9	M	16	6/60	6/60	Bilateral extensive macular atrophy and pigmentation	—	N	N	Bilateral central scotomata	N
III:12	F	27	6/6	6/6	Bilateral fine macular drusen-like deposits with areas of RPE atrophy and pigmentation	—	N	N	N	N
III:14	M	37	6/6	6/6	Bilateral fine macular drusen-like deposits with associated RPE atrophy and pigmentation (Fig. 2D)	Increased AF at both maculae, corresponding to the drusen-like deposits (Fig. 2E)	N	N	N	N
IV:5	M	11	6/18	6/12	Bilateral macular RPE atrophy and pigment clumping, with surrounding drusen-like deposits (Fig. 2A)	Bilateral decreased AF centrally with a surrounding ring of relative increased AF (Fig. 2B)	N	N	—	Bilateral protan, deutan and tritan defects
IV:6	F	9	6/4	6/4	Bilateral macular atrophy and pigmentation	—	N	N	N	N

N, Normal.

* Patients I:2, II:1, and III:2 were not available for study, but examination of clinical records, retinal photography, and fluorescein angiography was performed. III:2 had SRNVM before the age of 17 years in her right eye. II:1 had bilateral disciform maculopathy before the age of 20 years.

TABLE 2. Lod Scores between Autosomal Dominant Macular Dystrophy and Microsatellite Markers on 5p

Marker	Lod Score at θ						Distance from Telomere (Mb)
	0.00	0.05	0.10	0.20	0.30	0.40	
D5S1981	1.69	1.58	1.44	1.19	0.73	0.32	1.3
D5S417	1.93	1.79	1.63	1.30	0.93	0.50	3.2
D5S2088	3.55	3.24	2.93	2.25	1.51	0.72	4.4
D5S406	3.52	3.23	2.92	2.27	1.54	0.75	5.1
D5S1953	2.23	2.02	1.81	1.35	0.87	0.39	7.8
D5S630	3.61	3.30	2.97	2.26	1.45	0.59	9.7
D5S416	3.44	3.14	2.82	2.15	1.41	0.65	16.7
D5S2031	— ∞	1.03	1.34	1.32	0.98	0.49	20.8
D5S419	— ∞	-0.79	-0.10	0.34	0.39	0.20	26.3
D5S426	— ∞	-0.86	-0.18	0.25	0.29	0.17	34.7

CORD8 on 1q,²² *GCAP* on 6p,²³ *STGD1* on 1p,⁵ *STGD3* on 6q,²⁴ *STGD4* on 4p,²⁵ and *MCDRI* on 6q.^{12,26} In total approximately 50% of the genome was screened involving genotyping of 195 markers before significant linkage was established to chromosome 5p13.1-15.33, with a maximum lod score of 3.61 at a recombination fraction of 0.00, for marker *D5S630* (Table 2, Fig. 1) in a family in which the maximum two-point lod

score would be 4.21. Critical recombination events observed in individuals III:9 and IV:2 define the locus for this autosomal dominant macular dystrophy as between flanking markers *D5S1981* and *D5S2031*. This represents a genetic distance of 35 cM and a physical distance of 19.5 Mb. The distance between the flanking markers *D5S1981* and *D5S2031* and their nearest nonrecombinant markers (*D5S417* and *D5S416*) is 1.9

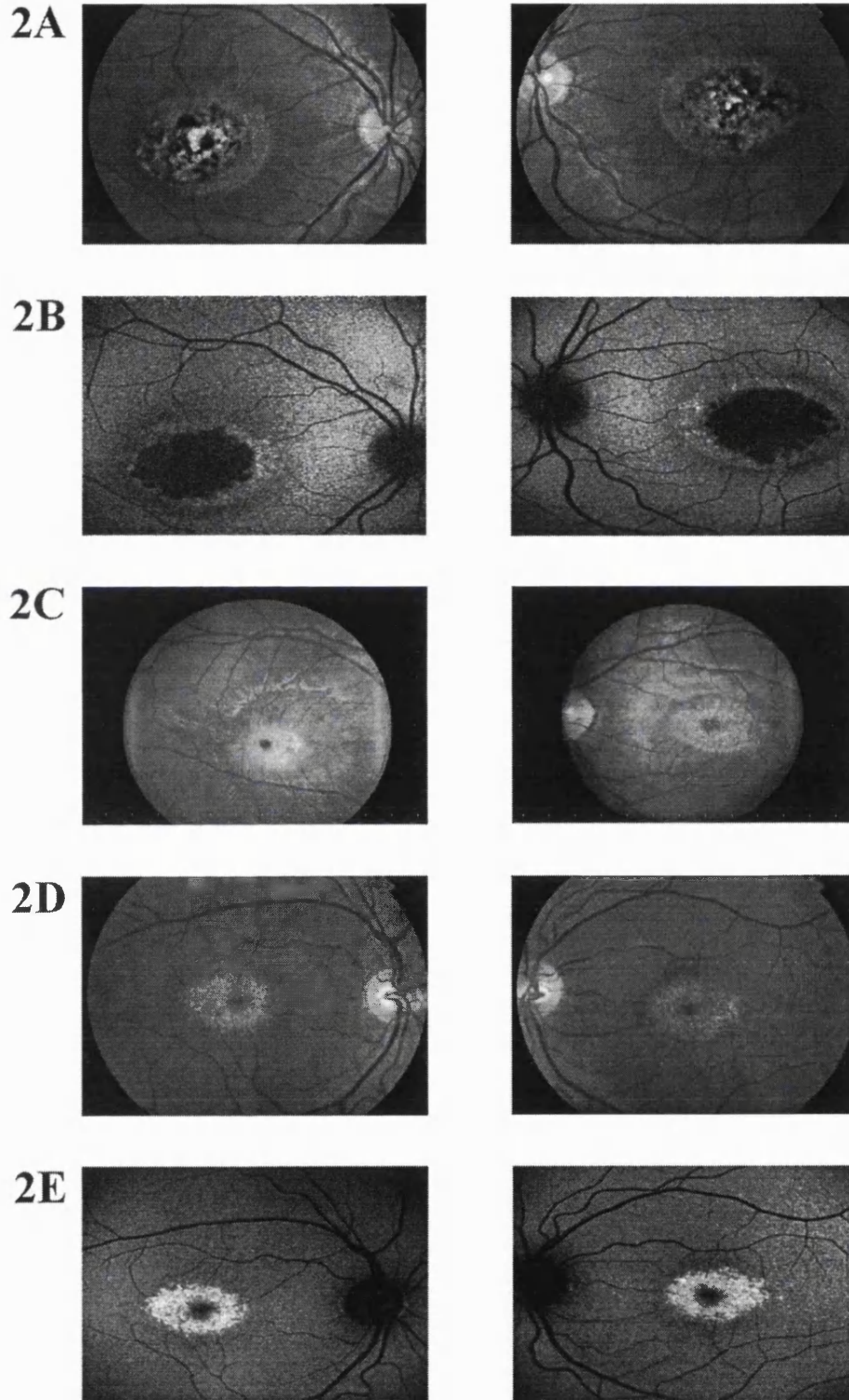


FIGURE 2. (A) Patient IV:5: fundus photograph showing bilateral macular RPE atrophy and pigment clumping, with surrounding drusen-like deposits and (B) fundus AF imaging showing bilateral decreased AF centrally with a surrounding ring of relative increased AF. (C) Patient III:2: fundus photograph showing acute SRNVM at the right macula and RPE atrophy with fine drusen-like deposits at the left macula. (D) Patient III:14: fundus photograph showing bilateral typical fine macular drusen-like deposits with associated RPE atrophy and pigmentation and (E) fundus AF imaging showing increased AF at both maculae, which corresponds to the drusen-like deposits. In addition, slight decreased AF is seen centrally in both eyes.

and 4.1 Mb, respectively. The chromosome inherited from the affected parent of individual IV:2 has two recombination events separated by 35 cM and enables exclusion of the region telomeric to *D5S1981* from the disease interval.

In view of the phenotypic similarity of this disorder to the North Carolina macular dystrophy (MCDR1) that maps to 6q16, we have examined this region in our family in greater detail. Multipoint linkage analysis has previously indicated that the *MCDR1* gene is in the interval between *D6S249* and *D6S1671*.²⁶ The lod scores for these markers in our family were both $-\infty$ at $\theta = 0.0$. In addition, haplotype analyses of these and additional markers adjacent to the *MCDR1* region confirm that the disease in our family does not map to this region of the genome.

DISCUSSION

The autosomal dominant macular dystrophy in this family has an unusual phenotype. It is characterized by an early age of onset and is generally associated with relatively good vision, despite significant macular abnormalities evident on ophthalmoscopy. Mild color vision abnormalities are variably present in affected individuals. The macular appearance varies from multiple drusen-like deposits to focal atrophy and pigmentation. With the exception of one young individual (IV:5) who showed an increase in retinal pigmentation and drusen-like deposits over a 5-year period, there was no evidence of change in macular appearance over time. Furthermore, although the retinal phenotype varied widely within the family, the severity of the changes was unrelated to age. Two individuals had angiographic evidence of SRNVM, and in an additional two, the macular appearances were consistent with this diagnosis. In accordance with the convention established by the nomenclature used for North Carolina macular dystrophy phenotype (MCDR1), we have termed this disorder MCDR3 (MC, macular; D, dystrophy; R, retinal).

Visual field loss in family members was demonstrated only over the central macular lesions. The normal EOG and ERG in all affected individuals suggests that the dystrophy is localized to the macula and that there is no widespread involvement of retinal photoreceptors.

Autofluorescence (AF) imaging is a relatively new technique to visualize the RPE, taking advantage of its intrinsic fluorescence derived from lipofuscin.²⁷⁻²⁹ Affected subjects showed decreased AF corresponding to areas of atrophy seen ophthalmoscopically (Fig. 2). In addition, concentric perifoveal areas of increased AF were evident and were found to correspond to the drusen-like deposits. This finding is in direct contrast to drusen in age-related macular degeneration (ARMD), in which there is generally little correspondence between the distribution of drusen and AF, although large, soft foveal drusen may be associated with increased AF.²⁹⁻³¹ However, the drusen-like deposits in the phenotype we describe are small and fine, are present from a young age, and are likely to have a different pathogenesis than the hard drusen in the aging eye. There are currently no published data on either the autofluorescence associated with MCDR1 drusen-like deposits, or on their chemical composition. However, it has been recently proposed that misfolding and aberrant accumulation of EFEMP1 within RPE cells and between the RPE and Bruch's membrane may underlie drusen formation in Doyme honeycomb retinal dystrophy and ARMD, although EFEMP1 itself does not appear to be a major component of the drusen.³² Histopathology is available of the eye of one patient with MCDR1 which showed accumulation of lipofuscin in the RPE within the atrophic macular lesion.³³ The mechanism of drusen formation in MCDR1 and MCDR3 is uncertain, however, our understanding will be improved by identification of the causative genetic mutations.

MCDR3 has many phenotypic similarities to MCDR1, an autosomal dominant macular dystrophy that is characterized by a variable macular phenotype. Bilaterally symmetrical fundus appearances in MCDR1 range from a few small ($<50 \mu\text{m}$) yellow drusen-like lesions in the central macula (grade 1) to larger confluent lesions (grade 2) and macular colobomatous lesions (grade 3).¹² All three grades of lesion were seen in our pedigree. The electrophysiological changes detected in our family are also consistent with those reported in MCDR1.¹² The only significant differences in the two phenotypes is that, in our family, color vision testing was abnormal in the majority of affected individuals, and there was evidence of disease progression, albeit in a single case.

Linkage studies have mapped MCDR1 to a locus on chromosome 6, region q16. To date, MCDR1 has been described in various countries and no evidence of genetic heterogeneity has been reported.^{26,34-36} In the family reported herein we have excluded linkage to the MCDR1 locus and have obtained significant linkage to the short arm of chromosome 5. This region contains three members of the cadherin gene family, cadherin-6, -10, and -12, which are all highly expressed in the brain.^{37,38} Retinal expression has yet to be examined. These represent potential candidates, especially in light of the recent identification of mutations in cadherin-23 in patients with Usher syndrome type 1D, a condition that includes retinitis pigmentosa.³⁹ However, the region is large, and many more potential candidate genes within the disease interval remain to be characterized. Identification of the genes responsible for these disorders will help to improve our understanding of the mechanisms underlying macular development and may shed light on the pathogenesis of drusen and SRNVM.

Acknowledgments

The authors thank the patients who kindly agreed to take part in this study and Peter Francis for help in ascertaining the family.

References

1. Scullica L, Falsini B. Diagnosis and classification of macular degenerations: an approach based on retinal function testing. *Doc Ophthalmol.* 2001;102:237-250.
2. Musarella M. Molecular genetics of macular degeneration. *Doc Ophthalmol.* 2001;102:165-177.
3. Allikmets R, Singh N, Sun H, et al. A photoreceptor cell-specific ATP-binding transporter gene (ABCR) is mutated in recessive Stargardt macular dystrophy. *Nat Genet.* 1997;15:236-246.
4. Zhang K, Kniazeva M, Han M, et al. A 5-bp deletion in *ELOVL4* is associated with two related forms of autosomal dominant macular dystrophy. *Nat Genet.* 2001;27:89-93.
5. Felbor U, Schilling H, Weber BHF. Adult vitelliform macular dystrophy is frequently associated with mutation in the peripherin/RDS gene. *Hum Mutat.* 1997;10:301-309.
6. Nichols BE, Drack AV, Vandenberg K, et al. A 2 base pair deletion in the RDS gene associated with butterfly-shaped pigment dystrophy of the fovea. *Hum Mol Genet.* 1993;2:601-603.
7. Reig C, Serra A, Gean E, et al. A point mutation in the RDS-peripherin gene in a Spanish family with central areolar choroidal dystrophy. *Ophthalmic Genet.* 1995;16:39-44.
8. Petrukhin K, Koisti MJ, Bakall B, et al. Identification of the gene responsible for Best macular dystrophy. *Nat Genet.* 1998;19:241-247.
9. Weber BH, Vogt G, Pruett RC, Stohr H, Felbor U. Mutations in the tissue inhibitor of metalloproteinases-3 (TIMP3) in patients with Sorsby's fundus dystrophy. *Nat Genet.* 1994;8:352-356.
10. Sauer CG, Gehrig A, Warneke-Wittstock R, et al. Positional cloning of the gene associated with X-linked juvenile retinoschisis. *Nat Genet.* 1997;17:164-170.
11. Stone EM, Lotery AJ, Munier FL, et al. A single EFEMP1 mutation associated with both Malattia Leventinese and Doyme honeycomb retinal dystrophy. *Nat Genet.* 1999;22:199-202.

12. Small KW. North Carolina macular dystrophy: clinical features, genealogy, and genetic linkage analysis. *Trans Am Ophthalmol Soc.* 1998;96:925-961.
13. Marmor MF, Zrenner E. Standard for clinical electroretinography (1994 update). *Doc Ophthalmol.* 1995;89:199-210.
14. Marmor MF, Zrenner E. Standard for clinical electro-oculography. International Society for Clinical Electrophysiology of Vision. *Arch Ophthalmol.* 1993;111:601-604.
15. Weissenbach J, Gyapay G, Dib C, et al. A second-generation linkage map of the human genome. *Nature.* 1992;359:794-801.
16. Gyapay G, Morissette J, Vignal A, et al. The 1993-94 Gènèthon human genetic linkage map. *Nat Genet.* 1994;7:246-339.
17. Dib C, Faure S, Fizames C, et al. A comprehensive genetic map of the human genome based on 5,264 microsatellites. *Nature.* 1996;380:152-154.
18. O'Connell JR, Weeks DE. PedCheck: a program for identification of genotype incompatibilities in linkage analysis. *Am J Hum Genet.* 1998;63:259-266.
19. Cottingham RW, Idury RM, Schaffer AA. Faster sequential genetic linkage computations. *Am J Hum Genet.* 1993;53:252-263.
20. Kelsell RE, Evans K, Gregory CY, et al. Localisation of a gene for dominant cone-rod dystrophy (CORD6) to chromosome 17p. *Hum Mol Genet.* 1997;6:597-600.
21. Kelsell RE, Gregory-Evans K, Gregory-Evans CY, et al. Localization of a gene (CORD7) for a dominant cone-rod dystrophy to chromosome 6q. *Am J Hum Genet.* 1998;63:274-279.
22. Khaliq S, Hameed A, Ismail M, et al. Novel locus for autosomal recessive cone-rod dystrophy CORD8 mapping to chromosome 1q12-q24. *Invest Ophthalmol Vis Sci.* 2000;41:3709-3712.
23. Payne AM, Downes SM, Bessant DAR, et al. A mutation in guanylate cyclase activator 1A (GUCA1A) in an autosomal dominant cone dystrophy pedigree mapping to a new locus on chromosome 6p21.1. *Hum Mol Genet.* 1998;7:273-277.
24. Stone EM, Nichols BE, Kimura AE, et al. Clinical features of a Stargardt-like dominant progressive macular dystrophy with genetic linkage to chromosome 6q. *Arch Ophthalmol.* 1994;112:765-772.
25. Kniazeva M, Chiang MF, Morgan B, et al. A new locus for autosomal dominant Stargardt-like disease maps to chromosome 4. *Am J Hum Genet.* 1999;64:1394-1399.
26. Small KW, Udari N, Yelchits S, et al. North Carolina macular dystrophy (MCDR1) locus: A fine resolution genetic map and haplotype analysis. *Mol Vis.* 1999;5:38-42.
27. von Rückmann A, Fitzke FW, Bird AC. Distribution of fundus autofluorescence with a scanning laser ophthalmoscope. *Br J Ophthalmol.* 1995;79:407-412.
28. von Rückmann A, Fitzke FW, Bird AC. In vivo fundus autofluorescence in macular dystrophies. *Arch Ophthalmol.* 1997;115:609-615.
29. von Rückmann A, Fitzke FW, Bird AC. Distribution of pigment epithelium autofluorescence in retinal disease state recorded in vivo and its change over time. *Graefes Arch Clin Exp Ophthalmol.* 1999;237:1-9.
30. von Rückmann A, Fitzke FW, Bird AC. Fundus autofluorescence in age related macular disease imaged with a scanning laser ophthalmoscope. *Invest Ophthalmol Vis Sci.* 1997;38:478-486.
31. Lois N, Owens SL, Coco R, et al. Fundus autofluorescence in patients with are-related macular degeneration and high risk of visual loss. *Am J Ophthalmol.* 2002;133:341-349.
32. Marmorstein LY, Munier FL, Arsenijevic Y, et al. Aberrant accumulation of EFEMP1 underlies drusen formation in Malattia Leventinese and age-related macular degeneration. *Proc Natl Acad Sci USA.* 2002;99:13067-13072.
33. Small KW, Voo I, Flannery J, Udari N, Glasgow BJ. North Carolina macular dystrophy: clinicopathologic correlation. *Trans Am Ophthalmol Soc.* 2001;99:233-237.
34. Reichel MB, Kelsell RE, Fan J, et al. Phenotype of a British North Carolina macular dystrophy family linked to chromosome 6q. *Br J Ophthalmol.* 1998;82:1162-1168.
35. Small KW, Puech B, Mullen L, Yelchits S. North Carolina macular dystrophy phenotype in France maps to the MCDR1 locus. *Mol Vis.* 1997;3:1.
36. Rabb MF, Mullen L, Yelchits S, et al. A North Carolina macular dystrophy phenotype in a Belizean family maps to the MCDR1 locus. *Am J Ophthalmol.* 1998;125:502-508.
37. Suzuki S, Sano K, Tanihara H. Diversity of the cadherin family: evidence for eight new cadherins in nervous tissue. *Cell Regul.* 1991;2:261-270.
38. Kools P, Vanhalst K, Van den Eynde E, et al. The human cadherin-10 gene: complete coding sequence, predominant expression in the brain, and mapping on chromosome 5p13-14. *FEBS Lett.* 1999;452:328-334.
39. von Brederlow B, Bolz H, Janecke A, et al. Identification and in vitro expression of novel *CDH23* mutations of patients with Usher syndrome type 1D. *Hum Mutat.* 2002;19:268-273.

REVIEW

The genetics of inherited macular dystrophies

M Michaelides, D M Hunt, A T Moore

The inherited macular dystrophies comprise a heterogeneous group of disorders characterised by central visual loss and atrophy of the macula and underlying retinal pigment epithelium (RPE). The different forms of macular degeneration encompass a wide range of clinical, psychophysical and histological findings. The complexity of the molecular basis of monogenic macular disease is now beginning to be elucidated with the identification of many of the disease-causing genes. Age related macular degeneration (ARMD), the leading cause of blind registration in the developed world, may also have a significant genetic component to its aetiology. Genes implicated in monogenic macular dystrophies are good candidate susceptibility genes for ARMD, although to date, with the possible exception of *ABCA4*, none of these genes have been shown to confer increased risk of ARMD. The aim of this paper is to review current knowledge relating to the monogenic macular dystrophies, with discussion of currently mapped genes, chromosomal loci and genotype-phenotype relationships. Inherited systemic disorders with a macular dystrophy component will not be discussed.

The inherited macular dystrophies are characterised by bilateral visual loss and the finding of generally symmetrical macular abnormalities on ophthalmoscopy. The age of onset is variable, but most present in the first two decades of life. There is considerable clinical and genetic heterogeneity; macular dystrophies showing autosomal dominant, autosomal recessive, X linked recessive and mitochondrial inheritance have all been reported. Most of the disorders are uncommon and have been incompletely characterised, and thus classification based on phenotypic characteristics is at present unsatisfactory.

A classification based upon molecular pathology would be more satisfactory but research into the molecular genetic basis of this group of disorders is still at an early stage. Seven disease-causing genes have been identified to date (table 1) and their identification has provided new insights into the pathogenesis of macular degeneration. Age related macular degeneration (ARMD) also has a genetic contribution to its aetiology. Approximately 20% of patients have a positive family history¹ and twin studies support a strong genetic component.² Genes

implicated in monogenic macular dystrophies are potential candidates for genes conferring risk for ARMD.

AUTOSOMAL RECESSIVE INHERITANCE Stargardt disease and fundus flavimaculatus

Stargardt macular dystrophy (STGD) is the most common inherited macular dystrophy with a prevalence of 1 in 10 000 and an autosomal recessive mode of inheritance. It shows a very variable phenotype with a variable age of onset and severity. Most cases present with central visual loss in early teens and there is typically macular atrophy with white flecks at the level of the RPE at the posterior pole on ophthalmoscopy (fig 1). Fluorescein angiography classically reveals a dark or masked choroid.³⁻⁴ The reduced visualisation of the choroidal circulation in the early phase of fundus fluorescein angiography (FFA) is believed to be secondary to excess lipofuscin accumulation in the RPE, thereby obscuring fluorescence emanating from choroidal capillaries.³⁻⁴ The retinal flecks appear hypofluorescent on FFA early in their evolution but at a later stage they appear hyperfluorescent due to RPE atrophy. Recently a new method has been developed to visualise the RPE, autofluorescence imaging, which takes advantage of its intrinsic fluorescence derived from lipofuscin.⁵⁻⁷ Autofluorescence imaging with a confocal scanning laser ophthalmoscope can provide useful information about the distribution of lipofuscin in the RPE, and give indirect information on the level of metabolic activity of the RPE which is largely determined by the rate of turnover of photoreceptor outer segments.⁷ There is evidence of continuous degradation of autofluorescent material in the RPE.⁷ Progressive loss of lipofuscin occurs when there is reduced metabolic demand due to photoreceptor cell loss, which appear as areas of decreased autofluorescence (AF).⁷ Areas of increased AF correspond to a group of RPE cells containing higher quantities of lipofuscin than their neighbours and may represent areas at high risk for photoreceptor cell

See end of article for authors' affiliations

Correspondence to: Professor Moore, Institute of Ophthalmology, University College London, 11-43 Bath Street, London EC1V 9EL, UK; tony.moore@ucl.ac.uk

Abbreviations: adMD, autosomal dominant atrophic macular degeneration; AF, autofluorescence; ARMD, age related macular degeneration; AVMD, adult vitelliform macular dystrophy; CACD, central areolar choroidal dystrophy; CODR, cone-rod dystrophy; EOG, electro-oculography; ERG, electroretinography; FFA, fundus fluorescein angiography; PBCRA, progressive bifocal chorioretinal atrophy; RP, retinitis pigmentosa; RPE, retinal pigment epithelium; SFD, Sorsby fundus dystrophy; SRNVM, subretinal neovascular membrane; VEGF, vascular endothelial growth factor

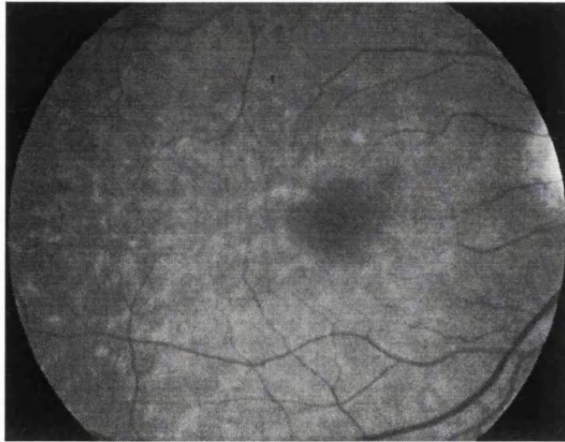


Figure 1 Stargardt disease. Fundus photograph of a right eye showing white flecks at the level of the RPE at the posterior pole. There is early macular atrophy.

loss.⁸ It has been demonstrated histologically that the number of photoreceptor cells is reduced in the presence of increased quantities of lipofuscin in the RPE, leading to the proposal that autofluorescent material may accumulate prior to cell death.⁹ The abnormal accumulation of lipofuscin, the presence of active and resorbed flecks, and RPE atrophy all

contribute to a characteristic appearance on fundus autofluorescence imaging in STGD.¹⁰

Histopathology of donated eyes has revealed that changes in the RPE begin near the equatorial peripheral retina and include increasingly excessive lipofuscin content and cell loss towards the macula. The changes in the retina parallel those in the RPE, including accumulation of lipofuscin in photoreceptor inner segments, loss of photoreceptors, and reactive Muller cell hypertrophy. Scanning electron microscopy shows a progressively marked heterogeneity in the size of RPE cells.^{11, 12}

Stargardt disease may also present in adult life when the visual loss may be milder. When the retinal flecks are seen without atrophy the term fundus flavimaculatus (FFM) is often used to describe the phenotype but it appears that Stargardt disease and FFM are caused by mutations in the same gene and both patterns may be seen within the same family. In a recent detailed phenotypic study, based on electroretinography (ERG) findings, patients with STGD/FFM could be classified into 3 groups.¹⁰ In group 1, there was severe pattern ERG abnormality with normal scotopic and full-field ERGs. In group 2, there was additional loss of photopic function, and in group 3, there was loss of both photopic and scotopic function. Differences among groups were not explained on the basis of differences in age of onset or duration of disease, suggesting that these electrophysiological groups may represent different phenotypic subtypes, and thereby be useful in helping to provide an accurate prognosis.¹⁰ Patients in group 1 generally had better visual

Table 1 Chromosomal loci and causative genes in inherited macular dystrophies

Macular dystrophy; OMIM number	Mode of inheritance	Chromosome locus	Mutated gene	References
Stargardt disease/fundus flavimaculatus; 248200	Autosomal recessive	1p21-p22 (STGD1)	ABCA4	13, 14
Stargardt-like macular dystrophy; 600110	Autosomal dominant	6q14 (STGD3)	ELOVL4	42, 44
Stargardt-like macular dystrophy; 603786	Autosomal dominant	4p (STGD4)	PROML1*	43
Autosomal dominant "bull's-eye" macular dystrophy	Autosomal dominant	4p (MCDR2)	PROML1*	47
Best macular dystrophy; 153700	Autosomal dominant	11q13	VMD2	51-53
Adult vitelliform dystrophy; 179605	Autosomal dominant	6p21.2-cen	Peripherin/RDS	62
Pattern dystrophy; 169150	Autosomal dominant	6p21.2-cen	Peripherin/RDS	64-66
Dayne honeycomb retinal dystrophy; 126600	Autosomal dominant	2p16	EFEMP1	74
North Carolina macular dystrophy; 136550	Autosomal dominant	6q14-q16.2 (MCDR1)	Not identified	81-83
Autosomal dominant macular dystrophy resembling MCDR1	Autosomal dominant	5p15.33-p13.1 (MCDR3)	Not identified	84
North Carolina-like macular dystrophy associated with deafness	Autosomal dominant	14p (MCDR4)	Not identified	85
Progressive bifocal chorioretinal atrophy; 600790	Autosomal dominant	6q14-q16.2	Not identified	88
Sorsby's fundus dystrophy; 136900	Autosomal dominant	22q12.1-q13.2	TIMP3	90-92
Central areolar choroidal dystrophy; 215500	Autosomal dominant	6p21.2-cen 17p13	Peripherin/RDS Not identified	100 101-102
Dominant cystoid macular dystrophy; 153880	Autosomal dominant	7p15-p21	Not identified	105
Juvenile retinoschisis; 312700	X linked	Xp22.2	XLRS1	110

*Unpublished data, see text.

acuity, more restricted distribution of flecks and macular atrophy, whereas those in group 3 had the worst visual acuity, more widespread flecks and macular atrophy was universal.¹⁰

The locus for STGD/FFM was mapped to chromosome 1p using homozygosity mapping in inbred families,¹³ and the causative gene characterised, *ABCA4* (previously denoted *ABCR*).¹⁴ Subsequently mutations in *ABCA4* have been implicated in other disorders, including retinitis pigmentosa (RP)^{15–16} and cone-rod dystrophy (CORD).¹⁷ *ABCA4* encodes a transmembrane rim protein located in the discs of rod and foveal cone outer segments, that is involved in ATP dependent transport of retinoids from photoreceptor to RPE.^{19–21} Failure of this transport results in deposition of a major lipofuscin fluorophore, A2E (N-retinylidene-N-retinylethanolamine), in the RPE.²¹ It is proposed that this accumulation may be deleterious to the RPE, with consequent secondary photoreceptor degeneration.

Mutation screening of patients with STGD/FFM has been performed by several groups in recent years.^{22–25} The high allelic heterogeneity of *ABCA4* is clearly demonstrated by the fact that approximately 400 sequence variations in this gene have been reported. This highlights the potential difficulties in confidently assigning disease-causing status to sequence variants detected when screening such a large (50 exons) and polymorphic gene. Nonsense mutations that can be predicted to have a major effect on the encoded protein can be confidently predicted to be disease-causing. However a major problem occurs with missense mutations since sequence variants are common in controls and therefore establishing pathogenicity may be problematic. Hence large studies assessing whether particular sequence variants are statistically more frequently seen in STGD patients than controls are likely to be helpful.²⁶ Direct evidence of pathogenicity can be established by functional analysis of the encoded mutant protein,²⁷ although such studies are very time consuming and labour intensive. The availability of multiple independent families with the same mutation may also provide evidence in support of disease causation.

It is currently believed that: (1) homozygous null mutations cause the most severe phenotype of autosomal recessive RP; (2) combinations of a null mutation with a moderate missense mutation result in autosomal recessive CORD, and (3) combinations of null/mild missense or two moderate missense mutations cause STGD/FFM.²⁸

Assessment of functional activity of mutant *ABCA4* transporter has been performed by Sun *et al.*²⁷ For example the missense mutations, L541P and G1961E, are associated with severely reduced but not abolished ATPase activity, whereas nonsense mutations would be predicted to have a more severe effect on protein function. Such predictions and functional assay results²⁷ have been used to establish whether genotype-phenotype correlations can be reliably made. Gerth *et al.*²⁹ have recently reported a detailed assessment of the phenotype of sixteen patients with STGD/FFM with known *ABCA4* mutations. Correlation between the type and combination of *ABCA4* mutations with the severity of the phenotype in terms of age of onset and level of photoreceptor dysfunction was possible in many cases. However in some siblings there were unexplained differences in phenotype. It has been proposed that in these instances other genes may have a modifying effect or environmental factors may have a role to play.³⁰ This is a recurring theme in the inherited macular dystrophies, in that the underlying “genetic context” within which mutations associated with disease are expressed can influence the eventual phenotype observed. In addition, variable retinal phenotype within families may be explained by different combinations of *ABCA4* mutations segregating within a single family.³¹

The ocular phenotype in *ABCA4* knockout mice has been determined. Knockout mice (*abca4*^{-/-}) show delayed dark adaptation, increased all-*trans*-retinaldehyde (all-*trans*-RAL) following light exposure, and striking deposition of the major lipofuscin fluorophore, A2E, in the RPE. Delayed dark adaptation is likely to be due to the accumulation in outer segment discs of the non-covalent complex between opsin and all-*trans*-RAL.²¹ Delayed recovery of rod sensitivity after light exposure is also a clinical feature of human subjects with both STGD and ARMD.^{32–33} Heterozygous loss of the *ABCA4* protein has also been shown to be sufficient to cause a phenotype in mice similar to STGD and ARMD in humans.³⁴ These data are consistent with the suggestion that the STGD carrier-state may predispose to the development of ARMD.

Light-exposed A2E-laden RPE exhibits a propensity for apoptosis especially with light in the blue part of the spectrum.³⁵ During RPE irradiation (430 nm), A2E self-generates singlet oxygen with the latter in turn reacting with A2E to generate epoxides.³⁶ It has been recently demonstrated that these A2E epoxides exhibit damaging reactivity towards DNA.³⁷ Moreover, mass spectrometry revealed that the antioxidants vitamins E and C reduce A2E epoxidation, with a corresponding reduction in the incidence of DNA damage and cell death. Vitamin E produced a more pronounced decrease in A2E epoxidation than vitamin C. Studies in which singlet oxygen was generated by endoperoxide in the presence of A2E, revealed that vitamin E reduced A2E epoxidation by quenching singlet oxygen.³⁷ This study raises the exciting possibility of a simple therapy. The potential for pharmacological manipulation of *ABCA4* activity has also been demonstrated by *in vitro* studies.³⁸ For example, amiodarone has been found to enhance ATPase activity *in vitro*.³⁸ Therefore such compounds which act to augment *ABCA4*-related retinoid transport may prove to be beneficial *in vivo* in patients with STGD or in a subset of individuals at risk for ARMD.

A different strategy of reducing A2E related toxicity, by inhibiting the formation of such lipofuscin pigments has also been reported.^{39–40} It has been shown that A2E synthesis can be virtually blocked by raising *abca4*^{-/-} mice in total darkness.³⁹ Recently it has been demonstrated in the *abca4*^{-/-} mouse model that isotretinoin blocked the formation of A2E and the accumulation of lipofuscin pigments in the RPE.⁴⁰ Isotretinoin (13-*cis*-retinoic acid) is known to slow the synthesis of 11-*cis*-retinaldehyde and regeneration of rhodopsin by inhibiting 11-*cis*-retinol dehydrogenase in the visual cycle. Light activation of rhodopsin results in the release of all-*trans*-RAL, which constitutes the first reactant in A2E biosynthesis. Treatment with isotretinoin, an established treatment for acne, may inhibit lipofuscin accumulation and thus delay the onset of visual loss in STGD.⁴⁰ It remains to be assessed whether isotretinoin is a potential treatment for other forms of macular degeneration associated with lipofuscin accumulation.

AUTOSOMAL DOMINANT INHERITANCE

Autosomal dominant Stargardt-like macular dystrophy

The clinical appearance of autosomal dominant (AD) Stargardt-like macular dystrophy is so similar to the common autosomal recessive form of the disorder that it is difficult to differentiate between them by fundus examination alone.⁴¹ However individuals reported with features of AD STGD-like dystrophy have a milder phenotype with relatively good functional vision, minimal colour vision defects and no significant electro-oculography (EOG) or ERG abnormalities.⁴¹ The “dark choroid” sign on fluorescein angiography which is typical in the recessive form, but not diagnostic, is uncommon in the dominant form of the disorder.

Two chromosomal loci have been identified, 6q14 (STGD3) and 4p (STGD4).⁴²⁻⁴³ Two mutations, a 5-bp deletion and two 1-bp deletions separated by four nucleotides, in the gene *ELOVL4* have been associated with STGD3 and other macular dystrophy phenotypes including pattern dystrophy.⁴⁴⁻⁴⁵ *ELOVL4* is expressed in the rod and cone photoreceptor inner segments. The protein product is believed to be involved in retinal fatty acid metabolism since it has significant homology to a family of proteins involved in fatty acid elongation. A missense mutation in *PROML1* has recently been found to co-segregate with disease in the STGD4 pedigree (personal communication, K Zhang). The gene *PROML1* encodes human prominin (mouse)-like 1, which belongs to the prominin family of five-transmembrane domain proteins. *PROML1* is expressed in retinoblastoma cell lines and adult retina, and the product of the mouse orthologue (prom) is concentrated in membrane evaginations at the base of the outer segments of rod photoreceptors.⁴⁶ A homozygous mutation in *PROML1* has been identified in an Indian pedigree with an autosomal recessive retinal dystrophy. The mutation results in the production of a truncated protein and functional studies in transfected CHO cells has demonstrated that the truncated prominin protein fails to reach the cell surface, indicating that the loss of prominin may lead to retinal degeneration via the impaired generation of evaginations or conversion to outer segment disks.⁴⁶

We have recently reported a British family with an autosomal dominant "Bull's-Eye" macular dystrophy (MCDR2) also mapping to chromosome 4p,⁴⁷ and overlapping the STGD4 disease interval reported by Kniazeva *et al.*⁴³ The MCDR2 phenotype that we have described is clinically distinct from that of STGD4 in that retinal flecks are absent and there is also no evidence of a dark choroid on fluorescein angiography, both of which are prominent features of the STGD4 family. We have however identified the same missense mutation in *PROML1* as has been found in the STGD4 pedigree (unpublished data). This therefore represents another example where the eventual macular dystrophy phenotype observed would appear to be dependent on the genetic context/background within which a mutation in a particular gene is expressed.

Best disease (vitelliform macular dystrophy)

Best disease is a dominantly inherited macular dystrophy which is characterised clinically by the classical feature of a round or oval yellow subretinal macular deposit. The yellow material is gradually resorbed over time, leaving an area of

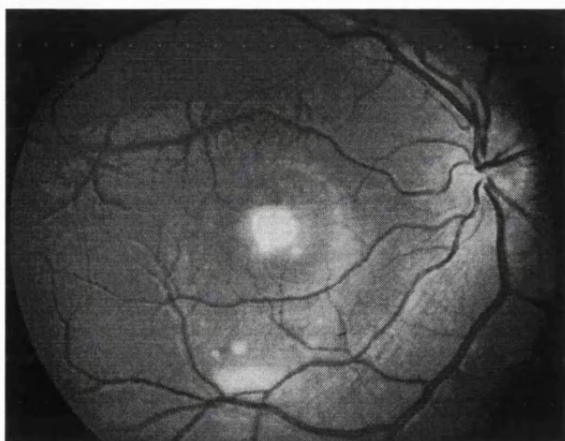


Figure 2 Best disease. Fundus photograph of a right eye showing a partially resorbed yellow subretinal macular deposit.

RPE atrophy and often subretinal fibrosis (fig 2). The flash ERG is normal but the EOG shows a very reduced or absent light rise indicating that there is widespread dysfunction of the RPE.⁴⁸ In common with STGD, histopathology of donated eyes from patients with Best disease has shown accumulation of lipofuscin throughout the RPE.⁴⁹⁻⁵⁰ Although the ophthalmoscopic abnormality is usually confined to the macular region, this evidence of more widespread retinal involvement is in common with the majority of inherited macular dystrophies described to date. The disease shows very variable expressivity. Most individuals carrying mutations in the *VMD2* gene on chromosome 11q13⁵¹⁻⁵³ have an abnormal EOG, but the macular appearance may be normal in some.⁵⁴ There is only one individual reported with evidence of non-penetrance, in that he is a mutant *VMD2* gene carrier with a normal fundus examination and normal EOG.⁵⁵ The visual prognosis in Best disease is surprisingly good, with most patients retaining reading vision into the fifth decade of life or beyond. Family members who carry a mutation in the *VMD2* gene and who have minimal macular abnormality or a normal fundus appearance (but abnormal EOG) in early adult life, usually retain near normal visual acuity long term.

The protein product of *VMD2*, bestrophin, has been localised to the basolateral plasma membrane of the RPE where it forms a component of a chloride channel responsible for maintaining chloride conductance across the basolateral membrane of the RPE.⁵⁶⁻⁵⁷ This chloride current regulates fluid transport across the RPE, and it has been suggested following optical coherence tomography of patients with Best's, that impaired fluid transport in the RPE secondary to abnormal chloride conductance may lead to accumulation of fluid and/or debris between RPE and photoreceptors and between RPE and Bruch's membrane, leading to detachment and secondary photoreceptor degeneration.⁵⁶⁻⁶⁰

The variable expression of Best disease remains unexplained, and here once again, other genes in addition to *VMD2*, and/or environmental influences may play a role in the wide range of clinical expression seen.

Adult vitelliform macular dystrophy

Adult vitelliform macular dystrophy (AVMD) is often confused with Best disease, although as the name suggests it has a later onset, lacks the typical course through different stages of macular disease seen in classical Best's, and the electro-oculogram (EOG) is usually normal.⁶¹ The typical clinical appearance is of bilateral, round or oval, yellow, symmetrical, sub-retinal lesions, typically one third to one half optic disc diameter in size.

Mutations in the *peripherin/RDS* gene on chromosome 6p have been identified in AVMD.⁶² It has been proposed that mutations in *peripherin/RDS* are present in approximately 20% of patients with AVMD,⁶² which implies further genetic heterogeneity.

Pattern dystrophy

The pattern dystrophies are a group of inherited disorders of the RPE which are characterised by bilateral symmetrical yellow-orange deposits at the macula in various distributions, including butterfly or reticular-like patterns. These dystrophies are often associated with a relatively good visual prognosis, although in some cases a slowly progressive loss of central vision can occur. There is usually psychophysical or electrophysiological evidence of widespread photoreceptor dysfunction.⁶³ Electrophysiological findings usually reveal abnormal pattern ERG, normal flash ERG, but abnormal EOG.

Mutations in the *peripherin/RDS* gene on chromosome 6p have been identified in patients with pattern dystrophies,⁶⁴⁻⁶⁶ and have also been implicated in autosomal dominant RP.⁶⁷⁻⁶⁸ The *RDS* gene was originally identified in a strain of mice

with a photoreceptor degeneration known as "retinal degeneration, slow" (rds). Subsequently, the orthologous human *peripherin/RDS* gene was shown to cause autosomal dominant RP.⁶⁷⁻⁶⁹ Mutation in codon 172 of *peripherin/RDS* has also been implicated in autosomal dominant macular dystrophy.⁶⁹ The *peripherin/RDS* protein is a membrane associated glycoprotein restricted to photoreceptor outer segment discs in a complex with ROM1. It may function as an adhesion molecule involved in the stabilisation and maintenance of a compact arrangement of outer segment discs.⁷⁰ *Peripherin* has also been shown to interact with the GARP domain (glutamic acid- and proline-rich region) of the beta-subunit of rod cGMP-gated channels, in a complex including the Na/Ca-K exchanger.⁷¹ This interaction may have a role in anchoring the channel-exchanger complex in the rod outer segment plasma membrane. Weleber *et al* described a single family in which a 3-bp deletion in *peripherin/RDS* resulted in retinitis pigmentosa, pattern dystrophy and FFM in different individuals.⁶⁶ This represents a further example of the likely modifying effects of genetic background or environment.

The rds mouse, which is homozygous for a null mutation in *peripherin/RDS*, is characterised by a complete failure to develop photoreceptor discs and outer segments, down-regulation of red opsin expression, and apoptotic loss of photoreceptor cells. Ali *et al*⁷² have demonstrated that subretinal injection in these mice of recombinant adeno-associated virus encoding a *peripherin/RDS* transgene, resulted in the generation of outer segment structures and formation of new stacks of discs containing both *peripherin/RDS* and rhodopsin. Moreover, electrophysiological function was also preserved. This study demonstrates in an animal model the efficacy of *in vivo* gene transfer to restore structure and more importantly function.⁷² Further assessment of this model has shown that the potential for ultrastructural improvement is dependent upon the age at treatment, but the effect of a single injection on photoreceptor ultrastructure may be long lasting.⁷³ These findings suggest that successful gene therapy in patients with photoreceptor defects may ultimately depend upon intervention in early stages of disease and upon accurate control of transgene expression.

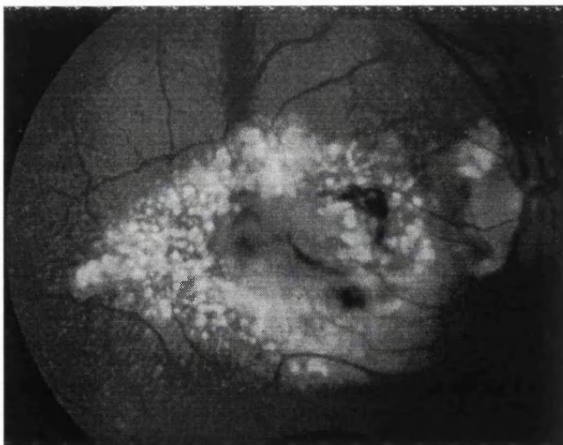


Figure 3 Doyme honeycomb retinal dystrophy. Fundus photograph of a right eye showing multiple drusen-like deposits at the macula and around the optic disc. Small drusen-like deposits can also be seen to radiate from the periphery of the main drusen mass. The established complication of subretinal neovascular membrane (SRNVM) is present centrally.

Doyme honeycomb retinal dystrophy (malattia leventinese; autosomal dominant drusen)

In this disorder small round yellow-white deposits under the RPE are characteristically distributed at the macula and around the optic disc, and begin to appear in early adult life (fig 3). Visual acuity is maintained through the fifth decade, but patients usually become legally blind by the seventh decade. Visual loss is usually due to macular atrophy, but less commonly may follow subretinal neovascular membrane (SRNVM). The presence of drusen-like deposits makes this dystrophy potentially very relevant to ARMD.

A single mutation, Arg-345-to-Trp (R345W) in the gene *EFEMP1* on chromosome 2p has been identified in the majority of patients with dominant drusen.⁷⁴ *EFEMP1* is a widely expressed gene of unknown function. Based on its sequence homology to the fibulin and fibrillin gene families, *EFEMP1* is predicted to be an extracellular matrix glycoprotein, but otherwise is uncharacterised. However, it has been recently proposed that misfolding and aberrant accumulation of *EFEMP1* within RPE cells and between the RPE and Bruch's membrane may underlie drusen formation in Doyme Honeycomb retinal dystrophy and ARMD. *EFEMP1* itself does not appear to be a major component of the drusen.⁷⁵

Genetic heterogeneity in autosomal dominant drusen has been suggested by Tarttelin *et al*⁷⁶, since they found that only seven of the 10 families (70%) and one of the 17 sporadic patients (6%) investigated had the R345W mutation. No other *EFEMP1* mutation was detected in these patients. Other families showing linkage to chromosome 2p16 raise the possibility of an upstream *EFEMP1* promoter mutation or a second dominant drusen gene at this locus.

Autosomal dominant drusen and macular degeneration (DD)

Stefko *et al*⁷⁷ have described a highly variable clinical phenotype in a North American family with an autosomal dominant drusen disorder with macular degeneration (DD). Most young adults had fine macular drusen and good vision. Affected infants and children may have congenital atrophic maculopathy and drusen. There was also evidence of progression in late adulthood with moderate visual loss.

The gene for the disease has been mapped to chromosome 6q14 and appears to be adjacent to but distinct from the locus for North Carolina macular dystrophy (MCDR1).⁷⁸ The disease interval overlaps with that of STGD3 and an autosomal dominant atrophic macular degeneration (adMD),⁷⁹ raising the possibility that they may be allelic disorders. However the phenotype of DD differs from that of STGD3 and adMD. Macular drusen are a hallmark of DD, whilst RPE atrophy and subretinal flecks are prominent features of STGD3 and adMD. The true situation will only be resolved by the identification of the underlying genetic mutations.

North Carolina macular dystrophy

North Carolina macular dystrophy (MCDR1) is an autosomal dominant disorder which is characterised by a variable macular phenotype and a non-progressive natural history. Bilaterally symmetrical fundus appearances in MCDR1 range from a few small (less than 50 µm) yellow drusen-like lesions in the central macula (grade 1) to larger confluent lesions (grade 2) and macular colobomatous lesions (grade 3) (fig 4).⁸⁰ Occasionally MCDR1 is complicated by SRNVM formation at the macula. EOG and ERG are normal indicating that there is no generalised retinal dysfunction.

Linkage studies have mapped MCDR1 to a locus on chromosome 6q16. To date, MCDR1 has been described in various countries and no evidence of genetic heterogeneity has been reported.⁸¹⁻⁸³ The identification of the gene

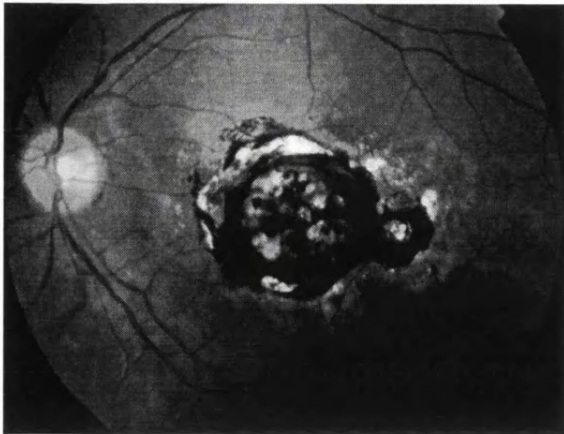


Figure 4 North Carolina macular dystrophy. Fundus photograph of a left eye showing macular atrophy and hyperpigmentation with surrounding drusen-like deposits.

responsible for this disorder is keenly awaited as it will help to improve our understanding of the pathogenesis of drusen and SRNVM.

An early onset autosomal dominant macular dystrophy (MCDR3) resembling MCDR1 has been recently mapped to chromosome 5p.⁸⁴ Linkage to the MCDR1 locus was excluded. The only significant differences in the two phenotypes is that in MCDR3 colour vision is abnormal in the majority of affected individuals and there was evidence of disease progression, albeit in a single case. A further MCDR1-like macular dystrophy associated with deafness has also been described recently.⁸⁵

Progressive bifocal chorioretinal atrophy (PBCRA)

PBCRA is an autosomal dominant disorder characterised by nystagmus, myopia and progressive macular and nasal retinal atrophic lesions.⁸⁶ Marked photopsia in early/middle age and retinal detachment extending from the posterior pole are recognised complications.⁸⁷ Both ERG and EOG are abnormal, reflecting widespread abnormality of photoreceptors and RPE.

PBCRA has been linked to 6q14-q16.2.⁸⁸ The PBCRA disease interval overlaps with the established MCDR1 interval. These two autosomal dominant dystrophies have many phenotypic similarities. However PBCRA differs significantly from MCDR1 in several important ways, including slow progression, abnormal colour vision, extensive nasal as well as macular atrophy and abnormal ERG and EOG. Therefore, if allelic, it is likely that different mutations are involved in their aetiology. An alternative explanation is that PBCRA and MCDR1 are caused by mutations in two different adjacent genes.

Sorsby fundus dystrophy

Sorsby fundus dystrophy (SFD) is a rare, autosomal dominant macular dystrophy, with onset of night blindness in the third decade and loss of central vision from macular atrophy or SRNVM by the fifth decade (fig 5). A tritan colour vision defect has been previously suggested as an early sign in SFD.⁸⁹

The tissue inhibitor of metalloproteinase-3 (*TIMP3*) gene on chromosome 22q) is implicated in SFD.⁹⁰⁻⁹² Most of the known mutations in *TIMP3*, including Ser181Cys,⁹⁰ Ser156Cys,⁹¹ and Tyr172Cys,⁹² introduce potentially unpaired cysteine residues in the C-terminus of the protein, thereby resulting in inappropriate disulfide bond formation and an abnormal tertiary protein structure. This may alter *TIMP3* mediated extracellular matrix turnover leading to the



Figure 5 Sorsby fundus dystrophy. Fundus photograph of a right eye showing subretinal haemorrhage as a complication of choroidal neovascularisation, in a 45 year old woman carrying the Ser156Cys mutation in *TIMP3*.

thickening of Bruch's membrane and the widespread accumulation of abnormal material beneath the RPE that is seen histologically.⁹³⁻⁹⁴ The finding that treatment with high doses of oral vitamin A reverses night blindness in this disorder,⁹⁵ suggests that retinal dysfunction may be due to a reduction in the permeability of Bruch's membrane, resulting in the hindrance of transport of vitamin A from the choriocapillaris to the photoreceptors by accumulated extracellular debris beneath the RPE. In addition, Majid *et al*⁹⁶ have demonstrated that mutant *TIMP3* can induce apoptosis of RPE cells suggesting that apoptosis may be the final pathway for cell death in this disorder. Furthermore, *TIMP3* has been recently shown to be a potent inhibitor of angiogenesis, which may account for the recognised complication of choroidal neovascularisation seen in SFD.⁹⁷ *TIMP3* inhibits vascular endothelial growth factor (VEGF)-mediated angiogenesis, most probably by blockade of VEGF-2 receptors.⁹⁷

Further insights into the pathophysiology of SFD may follow the development of a knock-in mouse carrying a disease-related Ser156Cys mutation in the orthologous murine *TIMP3* gene.⁹⁸ Immunolabeling studies and biochemical data from these mice suggested that site specific excess rather than absence or deficiency of functional *TIMP3* may be the primary consequence of the known *TIMP3* mutations.

Central areolar choroidal dystrophy (CACD)

CACD is characterised by bilateral, symmetrical, subtle mottling of the RPE at the macula in the early stages. The mottling then progresses to atrophy of the RPE and choriocapillaris.⁹⁹

An Arg142Trp mutation in *peripherin/RDS* has been implicated as one cause of this rare autosomal dominant macular dystrophy.¹⁰⁰ Sporadic cases of CACD have also been described but no mutations were found in *peripherin/RDS*.¹⁰⁰ A second locus at chromosome 17p13 has also been identified by a genome wide linkage search in a large Northern Irish family.¹⁰¹⁻¹⁰²

Dominant cystoid macular dystrophy (dominant cystoid macular oedema)

This rare autosomal dominantly inherited macular dystrophy was first described by Deutman *et al*.¹⁰³ Cystoid macular oedema with leaking perifoveal capillaries on fluorescein angiography is seen in all affected patients. Other features include onset usually in the fourth decade, typically a

moderate to high hypermetropic refractive error, and a normal ERG.¹⁰³⁻¹⁰⁴ Genetic linkage has been established to 7p15-p21.¹⁰⁵ The causative gene remains to be identified.

In addition to those described above there are several other autosomal dominant macular dystrophies whose phenotypes are not well described.

X LINKED INHERITANCE

X linked juvenile retinoschisis (XLRS)

XLRS is a vitreoretinal degeneration which presents either in an infant with nystagmus, or more commonly in childhood with mild loss of central vision.¹⁰⁶ The characteristic fundus abnormality is a cystic spokewheel-like maculopathy (foveal schisis) in virtually all affected males (fig 6). Peripheral retinal abnormalities including bilateral schisis cavities, vascular closure, inner retinal sheen, and pigmentary retinopathy are seen in approximately 50% of cases.¹⁰⁷ Flash ERG typically reveals a negative waveform, in that the a-wave is larger in amplitude than the b-wave. Prognosis is good in most affected males as long as retinal detachment or vitreous haemorrhage does not occur. The histopathological findings in XLRS include splitting within the superficial layers of the retina, degeneration of photoreceptors, thinning of the ganglion cell layer, and a focally absent or proliferative RPE.¹⁰⁸⁻¹⁰⁹

XLRS has been linked to Xp22.2 and mutations in the gene *XLRS1* (also recently referred to as *RS1*) have been identified.¹¹⁰ Juvenile retinoschisis shows a wide variability in the phenotype between, as well as within, families with different genotypes.¹¹¹ *XLRS1* encodes a 224 amino acid protein, retinoschisin (RS1), which contains a highly conserved discoidin domain implicated in cell-cell adhesion and cell-matrix interactions, functions which correlate well with the observed splitting of the retina in XLRS.

Many missense and protein truncating mutations of *XLRS1* have now been identified and are thought to be inactivating.¹¹² It has been demonstrated that although *XLRS1* is expressed predominantly in photoreceptors,¹¹³⁻¹¹⁴ it is also expressed in bipolar cells.¹¹⁴ RS1 is assembled in photoreceptors of the outer retina and bipolar cells of the inner retina as a disulfide-linked oligomeric protein complex. The secreted complex associates with the surface of these cells, where it may function as a cell adhesion protein to maintain the integrity of the central and peripheral retina.¹¹⁴ To gain further insight into the function of the retinoschisin protein, knockout mice have been generated, deficient in *Rs1h*, the

murine orthologue of the human *XLRS1* gene.¹¹⁵ The hemizygous *Rs1h*^{-/-} male mouse was shown to share several diagnostic features with human XLRS, including the typical "negative ERG" response and the development of cystic structures within the inner retina, followed by a dramatic loss of photoreceptor cells. Whilst the major pathology in the retina of the retinoschisin deficient mouse seemed to be a generalised disruption of cell layer architecture, atypical ribbon synapse formation at the photoreceptor terminals was also noted. This suggests a direct or indirect role of RS1 in the assembly and stabilisation of this synaptic region of the cell.¹¹⁵ Failure to establish or maintain these synaptic connections could lead to subsequent photoreceptor cell death.

MITOCHONDRIAL INHERITANCE

Maternally inherited diabetes and deafness (MIDD)

MIDD is a recently described subtype of diabetes mellitus that co-segregates with an adenine-to-guanine transition at position 3243 of mitochondrial DNA (A3243G), in a transfer RNA leucine (tRNA^{Leu} (UUR)) encoding region.¹¹⁶⁻¹¹⁷ This mitochondrial DNA mutation can also be associated with a severe encephalopathy with death at a young age (MELAS: mitochondrial encephalomyopathy with lactic acidosis and stroke-like episodes).¹¹⁸

Macular pattern dystrophy (MPD) has been found in association with MIDD.¹¹⁹ In a multicentre study, 86% of MIDD patients were found to have bilateral MPD, characterised by RPE hyperpigmentation that can surround the macula or be more extensive and also encompass the optic disc.¹²⁰ In advanced cases areas of RPE atrophy encircling the macula can be seen, which may coalesce and involve the fovea at a late stage (fig 7). However prognosis is generally good, with 80% of patients in the multicentre study having visual acuity of 6/7.5 or better in both eyes.¹²⁰ As the prevalence of MPD in MIDD is high, the association of a MPD with diabetes should raise the possibility of screening for a mutation of mitochondrial DNA.

AGE RELATED MACULAR DEGENERATION

ARMD is by far the most common form of macular degeneration. ARMD is the leading cause of blindness in patients over the age of 65 years in the western world. Despite its prevalence, its aetiology and pathogenesis are still poorly understood, and, currently, effective treatment options are limited for the majority of patients.



Figure 6 X linked juvenile retinoschisis. Fundus photograph of a right eye showing the characteristic fundus abnormality of a cystic spokewheel-like maculopathy (foveal schisis).

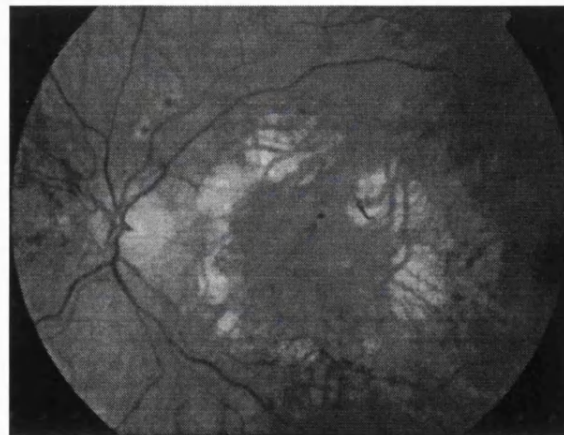


Figure 7 Maternally inherited diabetes and deafness. Fundus photograph of a left eye showing areas of macular atrophy surrounding the macula, through which underlying choroidal vessels are visible. This patient was found to be carrying the adenine-to-guanine transition at position 3243 of mitochondrial DNA (A3243G).

ARMD has a genetic contribution to its aetiology. Putative susceptibility loci have been identified on chromosome 1q25-q31,¹²¹ chromosome 17q25¹²² and on chromosomes 5, 9, and 10,¹²³ whereas it has been suggested that the e4 allele of the apolipoprotein E gene and an Alu polymorphism in the angiotensin-converting enzyme gene may have a protective effect on ARMD risk.¹²⁴¹²⁵

Inherited monogenic macular dystrophies share many important features with ARMD and have the advantage that they are more readily studied. One of the major difficulties in studies of ARMD is its late onset. Parents of affected individuals are often deceased and their children have yet to manifest the disease. In contrast, there are several forms of macular dystrophy, such as STGD/FFM, Best disease and MCDRI, which manifest signs and symptoms at an early age. These dystrophies and others have been characterised in large numbers of family members, spanning several generations, thereby making them far more amenable to genetic analysis. Furthermore, several of these macular dystrophies share many important clinical and histopathological similarities with ARMD, including an abnormal accumulation of lipofuscin in the RPE and a concomitant loss of function of overlying photoreceptors and central vision.¹²⁶¹²⁷

However to date, with the possible exception of *ABCA4*, none of these genes have been shown to confer increased risk of ARMD.⁴⁴⁷⁴¹²³¹²⁸⁻¹³² However, all new macular dystrophy genes represent good candidates for ARMD.

CONCLUSIONS

Although in some inherited macular dystrophies, the disease is confined to the macular region, in other disorders, perhaps the majority, there is electrophysiological, psychophysical, or histological evidence of widespread retinal dysfunction. This may partly account for the fact that to date, genes implicated in monogenic macular dystrophies have not been found to have a significant role in the genetic predisposition to ARMD.

Another possible reason for the lack of significant ARMD association with variation in the monogenic macular dystrophy genes so far identified is the hypothesis that the co-occurrence of subclinical mutations in a number of genes involved in the formation and function of the macula could be responsible in a polygenic fashion for cases of ARMD. However, it also remains a possibility that the susceptibility genes are neither specifically retinal nor macular.

Improved knowledge of the mechanisms of inherited macular dystrophy and the underlying molecular genetics, has not only raised the potential for future development of rational therapeutic regimens, but has helped to refine diagnosis, disease classification and prognosis, and improved genetic counselling.

ACKNOWLEDGEMENTS

We thank Professor A Bird for permission to reproduce the fundal photo used as an example of North Carolina macular dystrophy.

Authors' affiliations

M Michaelides, D M Hunt, A T Moore, Institute of Ophthalmology, University College London, London, UK

REFERENCES

- Klaver CC, Wolfs RC, Assink JJ, et al. Genetic risk of age-related maculopathy. Population-based familial aggregation study. *Arch Ophthalmol* 1998;116:1646-51.
- Meyers SM, Zachary AA. Monozygotic twins with age-related macular degeneration. *Arch Ophthalmol* 1988;106:651-3.
- Fish G, Grey R, Sehmi KS, et al. The dark choroid in posterior retinal dystrophies. *Br J Ophthalmol* 1981;65:359-63.
- Fishman GA, Farber M, Patel BS, et al. Visual acuity loss in patients with Stargardt's macular dystrophy. *Ophthalmology* 1987;94:809-14.
- von Rückmann A, Fitzke FW, Bird AC. Distribution of fundus autofluorescence with a scanning laser ophthalmoscope. *Br J Ophthalmol* 1995;79:407-12.
- von Rückmann A, Fitzke FW, Bird AC. In vivo fundus autofluorescence in macular dystrophies. *Arch Ophthalmol* 1997;115:609-15.
- von Rückmann A, Fitzke FW, Bird AC. Distribution of pigment epithelium autofluorescence in retinal disease state recorded in vivo and its change over time. *Graefes Arch Clin Exp Ophthalmol* 1999;237:1-9.
- von Rückmann A, Fitzke FW, Bird AC. Fundus autofluorescence in age related macular disease imaged with a scanning laser ophthalmoscope. *Invest Ophthalmol Vis Sci* 1997;38:478-86.
- Dorey CK, Wu G, Ebenstein D, et al. Cell loss in the ageing retina: relationship to lipofuscin accumulation and macular degeneration. *Invest Ophthalmol Vis Sci* 1989;30:1691-9.
- Lois N, Holder GE, Bunce C, et al. Phenotypic subtypes of Stargardt macular dystrophy-fundus flavimaculatus. *Arch Ophthalmol* 2001;119:359-69.
- Eagle RC, Lucier AC, Bernardino VB, et al. Retinal pigment epithelial abnormalities in fundus flavimaculatus: a light and electron microscopic study. *Ophthalmology* 1980;87:1189-200.
- Birbaich CD, Jarvelainen M, Possin DE, et al. Histopathology and immunocytochemistry of the neurosensory retina in fundus flavimaculatus. *Ophthalmology* 1994;101:1211-19.
- Kaplan J, Gerber S, Larget-Piet D, et al. A gene for Stargardt's disease (fundus flavimaculatus) maps to the short arm of chromosome 1. *Nat Genet* 1993;5:308-11.
- Allikmets R, Singh N, Sun H, et al. A photoreceptor cell-specific ATP-binding transporter gene (*ABCR*) is mutated in recessive Stargardt macular dystrophy. *Nat Genet* 1997;15:236-46.
- Martinez-Mir A, Bayes M, Vilageliu L, et al. A new locus for autosomal recessive retinitis pigmentosa (*RP19*) maps to 1p13-1p21. *Genomics* 1997;40:142-6.
- Martinez-Mir A, Paloma E, Allikmets R, et al. Retinitis pigmentosa caused by a homozygous mutation in the Stargardt disease gene *ABCR*. *Nat Genet* 1998;18:11-12.
- Cremeris FP, van de Pol DJ, van Driel M, et al. Autosomal recessive retinitis pigmentosa and cone-rod dystrophy caused by splice site mutations in the Stargardt's disease gene *ABCR*. *Hum Mol Genet* 1998;7:355-62.
- Maugeri A, Klevering BJ, Rohrschneider K, et al. Mutations in the *ABCA4* (*ABCR*) gene are the major cause of autosomal recessive cone-rod dystrophy. *Am J Hum Genet* 2000;67:960-6.
- Sun H, Nathans J. Stargardt's *ABCR* is localized to the disc membrane of retinal rod outer segments. *Nat Genet* 1997;17:15-16.
- Molday LL, Robin AR, Molday RS. *ABCR* expression in foveal cone photoreceptors and its role in stargardt macular dystrophy. *Nat Genet* 2000;25:257-8.
- Weng J, Mata NL, Azarian SM, et al. Insights into the function of Rim protein in photoreceptors and etiology of Stargardt's disease from the phenotype in *abcr* knockout mice. *Cell* 1999;98:13-23.
- Rozet JM, Gerber S, Souied E, et al. Spectrum of *ABCR* gene mutations in autosomal recessive macular dystrophies. *Eur J Hum Genet* 1998;6:291-5.
- Maugeri A, van Driel MA, van de Pol DJ, et al. The 2588G→C mutation in the *ABCR* gene is a mild frequent founder mutation in the Western European population and allows the classification of *ABCR* mutations in patients with Stargardt disease. *Am J Hum Genet* 1999;64:1024-35.
- Rivera A, White K, Stohr H, et al. A comprehensive survey of sequence variation in the *ABCA4* (*ABCR*) gene in Stargardt disease and age-related macular degeneration. *Am J Hum Genet* 2000;67:800-13.
- Simonelli F, Testa F, de Crecchio G, et al. New *ABCR* mutations and clinical phenotype in Italian patients with Stargardt disease. *Invest Ophthalmol Vis Sci* 2000;41:892-7.
- Webster AR, Heon E, Lotery AJ, et al. An analysis of allelic variation in the *ABCA4* gene. *Invest Ophthalmol Vis Sci* 2001;42:1179-89.
- Sun H, Smallwood PM, Nathans J, et al. Biochemical defects in *ABCR* protein variants associated with human retinopathies. *Nat Genet* 2000;26:242-6.
- van Driel MA, Maugeri A, Klevering BJ, et al. *ABCR* unites what ophthalmologists divide(s). *Ophthalmic Genet* 1998;19:117-22.
- Gerth C, Andrassi-Darida M, Bock M, et al. Phenotypes of 16 Stargardt macular dystrophy/fundus flavimaculatus patients with known *ABCA4* mutations and evaluation of genotype-phenotype correlation. *Graefes Arch Clin Exp Ophthalmol* 2002;240:628-38.
- Lois N, Holder GE, Fitzke FW, et al. Intrafamilial variation of phenotype in Stargardt macular dystrophy-Fundus flavimaculatus. *Invest Ophthalmol Vis Sci* 1999;40:2668-75.
- Paloma E, Coco R, Martinez-Mir A, et al. Analysis of *ABCA4* in mixed Spanish families segregating different retinal dystrophies. *Hum Mutat* 2002;20:476-83.
- Fishman GA, Farbman JS, Alexander KR. Delayed rod dark adaptation in patients with Stargardt's disease. *Ophthalmology* 1991;98:957-62.
- Steinmetz RL, Haimovici R, Jubb C, et al. Symptomatic abnormalities of dark adaptation in patients with age-related Bruch's membrane change. *Br J Ophthalmol* 1993;77:549-54.
- Mata NL, Tzekov RT, Liu X, et al. Delayed dark-adaptation and lipofuscin accumulation in *abcr*^{+/-} mice: implications for involvement of *ABCR* in age-related macular degeneration. *Invest Ophthalmol Vis Sci* 2001;42:1685-90.
- Sparrow JR, Nakanishi K, Parish CA. The lipofuscin fluorophore A2E mediates blue light-induced damage to retinal pigmented epithelial cells. *Invest Ophthalmol Vis Sci* 2000;41:1981-9.
- Sparrow JR, Zhou J, Ben-Shabat S, et al. Involvement of oxidative mechanisms in blue-light-induced damage to A2E-laden RPE. *Invest Ophthalmol Vis Sci* 2002;43:1222-7.

- 37 Sparrow JR, Vollmer-Snarr HR, Zhou J, et al. A2E-epoxides damage DNA in retinal pigment epithelial cells. Vitamin E and other antioxidants inhibit A2E-epoxide formation. *J Biol Chem* 2003;(in press).
- 38 Sun H, Molday RS, Nathans J. Retinal stimulates ATP hydrolysis by purified and reconstituted ABCR, the photoreceptor-specific ATP-binding cassette transporter responsible for Stargardt disease. *J Biol Chem* 1999;274:8269-81.
- 39 Mata NL, Weng J, Travis GH. Biosynthesis of a major lipofuscin fluorophore in mice and humans with ABCR-mediated retinal and macular degeneration. *Proc Natl Acad Sci U S A* 2000;97:7154-9.
- 40 Radu RA, Mata NL, Nusinowitz S, et al. Treatment with isotretinoin inhibits lipofuscin accumulation in a mouse model of recessive Stargardt's macular degeneration. *Proc Natl Acad Sci U S A* 2003;100:4742-7.
- 41 Donoso LA, Edwards AO, Frost A, et al. Autosomal dominant Stargardt-like macular dystrophy. *Surv Ophthalmol* 2001;46:149-63.
- 42 Stone EM, Nichols BE, Kimura AE, et al. Clinical features of a Stargardt-like dominant progressive macular dystrophy with genetic linkage to chromosome 6q. *Arch Ophthalmol* 1994;112:765-72.
- 43 Kniazeva M, Chiang MF, Morgan B, et al. A new locus for autosomal dominant Stargardt-like disease maps to chromosome 4. *Am J Hum Genet* 1999;64:1394-9.
- 44 Zhang K, Kniazeva M, Han M, et al. A 5-bp deletion in *ELOVL4* is associated with two related forms of autosomal dominant macular dystrophy. *Nat Genet* 2001;27:89-93.
- 45 Bernstein PS, Tammur J, Singh N, et al. Diverse macular dystrophy phenotype caused by a novel complex mutation in the *ELOVL4* gene. *Invest Ophthalmol Vis Sci* 2001;42:3331-6.
- 46 Maw MA, Corbeil D, Koch J, et al. A frameshift mutation in proaminin (mouse)-like 1 causes human retinal degeneration. *Hum Mol Genet* 2000;9:27-34.
- 47 Michaelides M, Johnson S, Poulson A, et al. An Autosomal Dominant Bull's-Eye Macular Dystrophy (MCDR2) that maps to the short arm of chromosome 4. *Invest Ophthalmol Vis Sci* 2003;44:1657-62.
- 48 Deutman AF. Electro-oculography in families with vitelliform dystrophy of the fovea. Detection of the carrier state. *Arch Ophthalmol* 1969;81:305-16.
- 49 Weingeist TA, Kobrin JL, Watzke RC. Histopathology of Best's macular dystrophy. *Arch Ophthalmol* 1982;100:1108-14.
- 50 Frangieh GT, Green WR, Fine SL. A histopathologic study of Best's macular dystrophy. *Arch Ophthalmol* 1982;100:1115-21.
- 51 Forsman K, Graff C, Nordstrom S, et al. The gene for Best's macular dystrophy is located at 11q13 in a Swedish family. *Clin Genet* 1992;42:156-9.
- 52 Petrukhin K, Koisti MJ, Bakall B, et al. Identification of the gene responsible for Best macular dystrophy. *Nat Genet* 1998;19:241-7.
- 53 Caldwell GM, Kakuk LE, Griesinger TB, et al. Bestrophin gene mutations in patients with Best vitelliform macular dystrophy. *Genomics* 1999;58:98-101.
- 54 Mohler CW, Fine SL. Long-term evaluation of patients with Best's vitelliform dystrophy. *Ophthalmology* 1981;88:688-92.
- 55 Weber BH, Walker D, Muller B. Molecular evidence for non-penetrance in Best's disease. *J Med Genet* 1994;31:388-92.
- 56 Marmorstein AD, Marmorstein LY, Rayborn M, et al. Bestrophin, the product of the Best vitelliform macular dystrophy gene (VMD2), localizes to the basolateral plasma membrane of the retinal pigment epithelium. *Proc Natl Acad Sci U S A* 2000;97:12758-63.
- 57 Sun H, Tsunenari T, Yau KW, et al. The vitelliform macular dystrophy protein defines a new family of chloride channels. *Proc Natl Acad Sci U S A* 2002;99:4008-13.
- 58 Pianta MJ, Aleman TS, Cideciyan AV, et al. In vivo micropathology of Best macular dystrophy with optical coherence tomography. *Exp Eye Res* 2003;76:203-11.
- 59 Bird AC. Pathogenesis of serous detachment of the retina and pigment epithelium. In: Ryan SJ, eds. *Retina*. 2. St. Louis: Mosby, 1994:1019-26.
- 60 Fisher SK, Stone J, Rex TS, et al. Experimental retinal detachment: a paradigm for understanding the effects of induced photoreceptor degeneration. *Prog Brain Res* 2001;131:679-98.
- 61 Brecher R, Bird AC. Adult vitelliform macular dystrophy. *Eye* 1990;4:210-15.
- 62 Felber U, Schilling H, Weber BHF. Adult vitelliform macular dystrophy is frequently associated with mutation in the *peripherin/RDS* gene. *Hum Mutat* 1997;10:301-9.
- 63 Kemp CM, Jacobson SG, Cideciyan AV, et al. *RDS* gene mutations causing retinitis pigmentosa or macular degeneration lead to the same abnormality in photoreceptor function. *Invest Ophthalmol Vis Sci* 1994;35:3154-62.
- 64 Nichols BE, Sheffield VC, Vandenburgh K, et al. Butterfly-shaped pigment dystrophy of the fovea caused by a point mutation in codon 167 of the *RDS* gene. *Nat Genet* 1993;3:202-7.
- 65 Nichols BE, Drack AV, Vandenburgh K, et al. A 2 base pair deletion in the *RDS* gene associated with butterfly-shaped pigment dystrophy of the fovea. *Hum Mol Genet* 1993;2:601-3.
- 66 Weleber RG, Carr RE, Murphy WH, et al. Phenotypic variation including retinitis pigmentosa, pattern dystrophy, and fundus flavimaculatus in a single family with a deletion of codon 153 or 154 of the *peripherin/RDS* gene. *Arch Ophthalmol* 1993;111:1531-42.
- 67 Farrar GJ, Kenna P, Jordan SA, et al. A three-base-pair deletion in the *peripherin-RDS* gene in one form of retinitis pigmentosa. *Nature* 1991;354:478-80.
- 68 Kajiwara K, Hahn LB, Mukai S, et al. Mutations in the human retinal degeneration slow gene in autosomal dominant retinitis pigmentosa. *Nature* 1991;354:480-3.
- 69 Downes SM, Fitzke FW, Holder GE, et al. Clinical features of codon 172 *RDS* macular dystrophy: similar phenotype in 12 families. *Arch Ophthalmol* 1999;117:1373-83.
- 70 Travis GH, Sutcliffe JG, Bok D. The retinal degeneration slow (rds) gene product is a photoreceptor disc membrane-associated glycoprotein. *Neuron* 1991;6:61-70.
- 71 Poetsch A, Molday LL, Molday RS. The cGMP-gated channel and related glutamic acid-rich proteins interact with peripherin-2 at the rim region of rod photoreceptor disc membranes. *J Biol Chem* 2001;276:48009-16.
- 72 Ali RR, Sarra GM, Stephens C, et al. Restoration of photoreceptor ultrastructure and function in retinal degeneration slow mice by gene therapy. *Nature Genet* 2000;25:306-10.
- 73 Sarra GM, Stephens C, de Alwis M, et al. Gene replacement therapy in the retinal degeneration slow (rds) mouse: the effect on retinal degeneration following partial transduction of the retina. *Hum Molec Genet* 2001;10:2353-61.
- 74 Stone EM, Lotery AJ, Munier FL, et al. A single *EFEMP1* mutation associated with both malattia Leventinese and Doyme honeycomb retinal dystrophy. *Nature Genet* 1999;22:199-202.
- 75 Marmorstein LY, Munier FL, Arsenijevic Y, et al. Aberrant accumulation of *EFEMP1* underlies drusen formation in Malattia Leventinese and age-related macular degeneration. *Proc Natl Acad Sci U S A* 2002;99:13067-72.
- 76 Tartelin EE, Gregory-Evans CY, Bird AC, et al. Molecular genetic heterogeneity in autosomal dominant drusen. *J Med Genet* 2001;38:381-4.
- 77 Stefko ST, Zhang K, Gorin MB, et al. Clinical spectrum of chromosome 6-linked autosomal dominant drusen and macular degeneration. *Am J Ophthalmol* 2000;130:203-8.
- 78 Kniazeva M, Traboulsi EI, Yu Z, et al. A new locus for dominant drusen and macular degeneration maps to chromosome 6q14. *Am J Ophthalmol* 2000;130:197-202.
- 79 Griesinger IB, Sieving PA, Ayyagari R. Autosomal dominant macular atrophy at 6q14 excludes *CORD7* and *MCDR1/PBCRA* loci. *Invest Ophthalmol Vis Sci* 2000;41:248-55.
- 80 Small KW. North Carolina macular dystrophy: clinical features, genealogy, and genetic linkage analysis. *Trans Am Ophthalmol Soc* 1998;96:925-61.
- 81 Small KW, Udar N, Yelchits S, et al. North Carolina macular dystrophy (*MCDR1*) locus: A fine resolution genetic map and haplotype analysis. *Mol Vis* 1999;5:38-42.
- 82 Reichel MB, Kelsell RE, Fan J, et al. Phenotype of a British North Carolina macular dystrophy family linked to chromosome 6q. *Br J Ophthalmol* 1998;82:1162-8.
- 83 Rabb MF, Mullen L, Yelchits S, et al. A North Carolina macular dystrophy phenotype in a Belizean family maps to the *MCDR1* locus. *Am J Ophthalmol* 1998;125:502-8.
- 84 Michaelides M, Johnson S, Tekriwal AK, et al. An early-onset autosomal dominant macular dystrophy (*MCDR3*) resembling North Carolina macular dystrophy maps to chromosome 5. *Invest Ophthalmol Vis Sci* 2003;44:2178-83.
- 85 Francis PJ, Johnson S, Edmunds B, et al. Genetic linkage analysis of a novel syndrome comprising North Carolina-like macular dystrophy and progressive sensorineural hearing loss. *Br J Ophthalmol* 2003;87:893-8.
- 86 Douglas AA, Waheed I, Wyse CT. Progressive bifocal chorio-retinal atrophy. A rare familial disease of the eyes. *Br J Ophthalmol* 1968;52:742-51.
- 87 Godley BF, Tiffin PA, Evans K, et al. Clinical features of progressive bifocal chorioretinal atrophy: a retinal dystrophy linked to chromosome 6q. *Ophthalmology* 1996;103:893-8.
- 88 Kelsell RE, Godley BF, Evans K, et al. Localization of the gene for progressive bifocal chorioretinal atrophy (*PBCRA*) to chromosome 6q. *Hum Mol Genet* 1995;4:1653-6.
- 89 Beminger TA, Polkinghorne PJ, Capon MR, et al. Color vision defect. A early sign of Sorsby retinal dystrophy? *Ophthalmology* 1993;90:515-18.
- 90 Weber BH, Vogt G, Pruet RC, et al. Mutations in the tissue inhibitor of metalloproteinases-3 (*TIMP3*) in patients with Sorsby's fundus dystrophy. *Nat Genet* 1994;8:352-6.
- 91 Felber U, Stohr H, Amann T, et al. A novel Ser156Cys mutation in the tissue inhibitor of metalloproteinases-3 (*TIMP3*) in Sorsby's fundus dystrophy with unusual clinical features. *Hum Mol Genet* 1995;4:2415-16.
- 92 Jacobson SG, Cideciyan AV, Bennett J, et al. Novel mutation in the *TIMP3* gene causes Sorsby fundus dystrophy. *Arch Ophthalmol* 2002;120:376-9.
- 93 Chong NH, Alexander RA, Gin T, et al. *TIMP-3*, collagen, and elastin immunohistochemistry and histopathology of Sorsby's fundus dystrophy. *Invest Ophthalmol Vis Sci* 2000;41:898-902.
- 94 Capon MR, Marshall J, Krafft JI, et al. Sorsby's fundus dystrophy. A light and electron microscopic study. *Ophthalmology* 1989;96:1769-77.
- 95 Jacobson SG, Cideciyan AV, Regunath G, et al. Night blindness in Sorsby's fundus dystrophy reversed by vitamin A. *Nat Genet* 1995;11:27-32.
- 96 Majid MA, Smith VA, Easty DL, et al. Sorsby's fundus dystrophy mutant tissue inhibitors of metalloproteinase-3 induce apoptosis of retinal pigment epithelial and MCF-7 cells. *FEBS Lett* 2002;529:281-5.
- 97 Qi JH, Ebrohem Q, Moore N, et al. A novel function for tissue inhibitor of metalloproteinases-3 (*TIMP3*): inhibition of angiogenesis by blockage of VEGF binding to VEGF receptor-2. *Nat Med* 2003;9:407-15.
- 98 Weber BH, Lin B, White K, et al. A mouse model for Sorsby fundus dystrophy. *Invest Ophthalmol Vis Sci* 2002;43:2732-40.
- 99 Hoyng CB, Deutman AF. The development of central areolar choroidal dystrophy. *Graefes Arch Clin Exp Ophthalmol* 1996;234:87-93.
- 100 Hoyng CB, Heutink P, Testers L, et al. Autosomal dominant central areolar choroidal dystrophy caused by a mutation in codon 142 in the *peripherin/RDS* gene. *Am J Ophthalmol* 1996;121:623-9.

- 101 **Lotery AJ**, Ennis KT, Silvestri G, *et al.* Localisation of a gene for central areolar choroidal dystrophy to chromosome 17p. *Hum Mol Genet* 1996;**5**:705-8.
- 102 **Hughes AE**, Lotery AJ, Silvestri G. Fine localisation of the gene for central areolar choroidal dystrophy on chromosome 17p. *J Med Genet* 1998;**35**:770-2.
- 103 **Deutman AF**, Pinckers ALL, Aan de Kerk AL. Dominantly inherited cystoid macular oedema. *Am J Ophthalmol* 1976;**82**:540-8.
- 104 **Pinckers A**, Deutman AF, Lion F, *et al.* Dominant cystoid macular dystrophy (DCMD). *Ophthalmol Paediat Genet* 1983;**3**:157-67.
- 105 **Kremer H**, Pinckers A, van den Heim B, *et al.* Localization of the gene for dominant cystoid macular dystrophy on chromosome 7p. *Hum Molec Genet* 1994;**3**:299-302.
- 106 **George ND**, Yates JR, Bradshaw K, *et al.* Infantile presentation of X linked retinoschisis. *Br J Ophthalmol* 1995;**79**:653-657.
- 107 **George ND**, Yates JR, Moore AT. X linked retinoschisis. *Br J Ophthalmol* 1995;**79**:697-702.
- 108 **Yanoff M**, Rahn EK, Zimmerman LE. Histopathology of juvenile retinoschisis. *Arch Ophthalmol* 1968;**79**:49-53.
- 109 **Manschot WA**. Pathology of hereditary juvenile retinoschisis. *Arch Ophthalmol* 1972;**88**:131-8.
- 110 **Sauer CG**, Gehrig A, Warneke-Wittstock R, *et al.* Positional cloning of the gene associated with X-linked juvenile retinoschisis. *Nat Genet* 1997;**17**:164-70.
- 111 **Eksandh LC**, Ponjavic V, Ayyagari R, *et al.* Phenotypic expression of juvenile X-linked retinoschisis in Swedish families with different mutations in the *XLR51* gene. *Arch Ophthalmol* 2000;**118**:1098-104.
- 112 **The Retinoschisis Consortium**. Functional implications of the spectrum of mutations found in 234 cases with X-linked juvenile retinoschisis. *Hum Mol Genet* 1998;**7**:1185-92.
- 113 **Grayson C**, Reid SN, Ellis JA, *et al.* Retinoschisin, the X-linked retinoschisis protein, is a secreted photoreceptor protein, and is expressed and released by Weri-Rb1 cells. *Hum Mol Genet* 2000;**9**:1873-9.
- 114 **Molday LL**, Hicks D, Sauer CG, *et al.* Expression of X-linked retinoschisis protein R51 in photoreceptor and bipolar cells. *Invest Ophthalmol Vis Sci* 2001;**42**:816-25.
- 115 **Weber BH**, Schrewe H, Molday LL, *et al.* Inactivation of the murine X-linked juvenile retinoschisis gene, *Rs1h*, suggests a role of retinoschisin in retinal cell layer organization and synaptic structure. *Proc Natl Acad Sci U S A* 2002;**99**:6222-7.
- 116 **van den Ouweland JM**, Lemkes HH, Ruitenbeek W, *et al.* Mutation in mitochondrial tRNA(Leu)(UUR) gene in a large pedigree with maternally transmitted type II diabetes mellitus and deafness. *Nat Genet* 1992;**1**:368-71.
- 117 **Reardon W**, Ross RJ, Sweeney MG, *et al.* Diabetes mellitus associated with a pathogenic point mutation in mitochondrial DNA. *Lancet* 1992;**340**:1376-9.
- 118 **Goto Y**, Nonaka I, Horai S. A mutation in the tRNA(Leu)(UUR) gene associated with the MELAS subgroup of mitochondrial encephalomyopathies. *Nature* 1990;**348**:651-3.
- 119 **Massin P**, Guillausseau PJ, Violette B, *et al.* Macular pattern dystrophy associated with a mutation of mitochondrial DNA. *Am J Ophthalmol* 1995;**120**:247-8.
- 120 **Massin P**, Virally-Monod M, Violette B, *et al.* Prevalence of macular pattern dystrophy in maternally inherited diabetes and deafness. GEDIAM Group. *Ophthalmology* 1999;**106**:1821-7.
- 121 **Klein ML**, Schultz DW, Edwards A, *et al.* Age-related macular degeneration. Clinical features in a large family and linkage to chromosome 1q. *Arch Ophthalmol* 1998;**116**:1082-8.
- 122 **Weeks DE**, Conley YP, Tsai HJ, *et al.* Age-related maculopathy: an expanded genome-wide scan with evidence of susceptibility loci within the 1q31 and 17q25 regions. *Am J Ophthalmol* 2001;**132**:682-92.
- 123 **Weeks DE**, Conley YP, Mah TS, *et al.* A full genome scan for age-related maculopathy. *Hum Mol Genet* 2000;**9**:1329-49.
- 124 **Klaver CC**, Kliffen M, van Duijn CM, *et al.* Genetic association of apolipoprotein E with age-related macular degeneration. *Am J Hum Genet* 1998;**63**:200-6.
- 125 **Hamdi HK**, Reznik J, Castellon R, *et al.* Alu DNA polymorphism in ACE gene is protective for age-related macular degeneration. *Biochem Biophys Res Commun* 2002;**295**:668-72.
- 126 **Swann PG**, Lovie-Kitchin. Age-related maculopathy. A review of its morphology and effects on visual function. *Ophthalmol Physiol Opt* 1990;**10**:149-58.
- 127 **Young RW**. Pathophysiology of age-related macular degeneration. *Surv Ophthalmol* 1987;**31**:291-306.
- 128 **Allikmets R**, Shroyer NF, Singh N, *et al.* Mutation of the Stargardt disease gene (*ABCR*) in age-related macular degeneration. *Science* 1997;**277**:1805-7.
- 129 **Stone EM**, Webster AR, Vandenburgh K, *et al.* Allelic variation in *ABCR* associated with Stargardt disease but not age-related macular degeneration. *Nat Genet* 1998;**20**:328-9.
- 130 **De La Paz MA**, Guy VK, Abou-Donia S, *et al.* Analysis of the Stargardt disease gene (*ABCR*) in age-related macular degeneration. *Ophthalmology* 1999;**106**:1531-6.
- 131 **Lotery AJ**, Munier FL, Fishman GA, *et al.* Allelic variation in the *VMD2* gene in best disease and age-related macular degeneration. *Invest Ophthalmol Vis Sci* 2000;**41**:1291-6.
- 132 **Stone EM**, Sheffield VC, Hageman GS. Molecular genetics of age-related macular degeneration. *Hum Mol Genet* 2001;**10**:2285-92.

Want full text but don't have
a subscription?

Pay per view

For just \$8 you can purchase the full text of individual articles using our secure online ordering service. You will have access to the full text of the relevant article for 48 hours during which time you may download and print the pdf file for personal use.

www.jmedgenet.com

SCIENTIFIC REPORT

Cone dystrophy phenotype associated with a frameshift mutation (M280fsX291) in the α -subunit of cone specific transducin (*GNAT2*)

M Michaelides, I A Aligianis, G E Holder, M P Simunovic, J D Mollon, E R Maher, D M Hunt, A T Moore

Br J Ophthalmol 2003;87:1317-1320

Aim: To describe the phenotype of a three generation consanguineous Pakistani family containing six individuals with autosomal recessive cone dystrophy caused by mutation in *GNAT2*.

Methods: Five of the six affected individuals underwent an ophthalmological examination, electrodiagnostic testing, fundus photography, autofluorescence imaging, and detailed psychophysical testing.

Results: All five examined patients had a history of nystagmus from infancy, photophobia, defective colour vision, and poor visual acuity. The nystagmus in three of the individuals had lessened with time. Fundus examination revealed an abnormal foveal appearance, without frank atrophy or pigmentation. Electroretinography (ERG) revealed absent ISCEV cone flicker ERGs with some preservation of responses to short wavelength stimulation. Rod ERGs showed no definite abnormality, but maximal (mixed rod-cone) response a-wave amplitudes were mildly subnormal. Rudimentary residual colour vision was detected in three individuals. There is clinical evidence of progressive visual acuity reduction in two older individuals.

Conclusion: Mutation in the α -subunit of cone specific transducin (*GNAT2*) is characterised by an infantile onset cone dystrophy. Some affected individuals may show deterioration of visual acuity with time.

Fundus examination is usually normal, but electroretinography reveals absent photopic (cone) responses and normal scotopic (rod) responses. Individuals with incomplete achromatopsia retain some colour vision.

Achromatopsia is recessively inherited and genetically heterogeneous. To date, three achromatopsia genes have been characterised, the first two described being *CNGA3*⁸⁻¹⁰ and *CNGB3*,¹¹⁻¹³ located at 2q11 and 8q21 respectively. *CNGA3* and *CNGB3* code for the α and β subunits of the cGMP gated cation channel in cone cells, respectively. The gene coding for the α -subunit of cone specific transducin (*GNAT2*) was proposed as a candidate gene for achromatopsia by Mollon in 1997,¹⁴ and mutations in this gene have recently been described in patients with achromatopsia.^{15,16} However, a detailed description of the phenotype associated with *GNAT2* inactivation has not been presented. In this report we have reviewed the phenotype of the large consanguineous Pakistani family in whom we identified a novel frameshift mutation in *GNAT2* (c842_843insTCAG; M280fsX291).¹⁶

PATIENTS AND METHODS

Five affected members of a three generation, consanguineous Pakistani family with cone dystrophy were assessed after informed consent was obtained (Fig 1).

A full medical history was taken and an ophthalmological examination performed. Examined subjects also underwent colour fundus photography and fundus autofluorescence imaging using the confocal scanning laser ophthalmoscope (cSLO) (Zeiss Prototype; Carl Zeiss Inc, Oberkochen, Germany). Electrodiagnostic assessment included electro-oculography (EOG), full field electroretinography (ERG) and pattern ERG (PERG), incorporating the protocols recommended by the International Society for Clinical Electrophysiology of Vision.¹⁷⁻¹⁹ S-cone ERGs were also recorded using a previously described protocol.²⁰

Colour vision testing included the use of the Hardy, Rand, Rittler (HRR) plates (American Optical Company, New York, NY, USA), Sloan achromatopsia plates, enlarged Farnsworth D-15 (PV-16), the enlarged Mollon-Reffin (M-R) minimal test,²¹ and the Nagel anomaloscope. The PV-16, Sloan achromatopsia plates, and the M-R test were all performed under CIE Standard Illuminant C from a MacBeth Easel lamp.

The PV-16 and the enlarged M-R test were used in order to detect any residual colour discrimination that might be present in patients with low vision: the coloured discs of the PV-16 were 33 mm in diameter and those of the enlarged M-R test were 26 mm in diameter (corresponding to visual angles of 3.8 and 3.3 deg at a viewing distance of 500 mm). With the same purpose in mind, we also used a modification of the Cambridge colour test, a computerised test that allows the measurement of colour discrimination along different

The cone and cone-rod dystrophies form part of a clinically heterogeneous group of retinal dystrophies that are a major cause of childhood blindness. The major clinical features of cone dystrophies are reduced visual acuity, abnormal colour vision, photophobia, central scotomata, and often nystagmus. Cone dystrophies have been described with autosomal dominant, autosomal recessive, or X linked patterns of inheritance.^{1,2}

Cone and cone-rod dystrophies are also phenotypically heterogeneous.² Various subtypes have been identified on the basis of natural history and psychophysical and electrophysiological testing.¹⁻⁵ These disorders may be stationary or progressive. The two well characterised stationary cone dystrophies are blue cone monochromatism, an X linked disorder in which there are only two functional classes of photoreceptor (rods and S-cones), and rod monochromatism.

Rod monochromatism or complete achromatopsia is a stationary cone dystrophy, with an incidence of approximately 1 in 30 000, in which there is an absence of functioning cone photoreceptors.^{6,7} Affected individuals usually present in infancy with nystagmus, poor visual acuity, photophobia, and complete colour blindness.

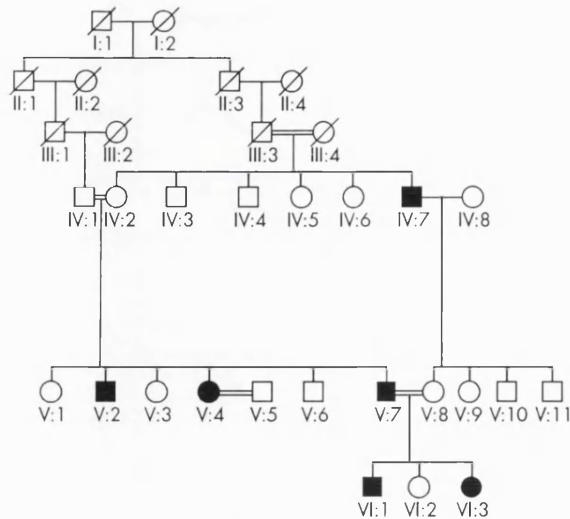


Figure 1 Family pedigree. Solid symbols indicate clinically affected individuals and open symbols represent unaffected individuals.

directions in colour space.^{22, 23} In the modified test, the stimulus array consisted of only four large discs, organised in a diamond pattern. Each disc subtended 4 degrees of visual angle at the viewing distance of 1 metre. On any presentation, one of the discs differed in chromaticity from the remaining three, and the patient's task was to identify this disc by pressing one of four buttons within 4 seconds. To ensure that the discrimination was on the basis of chromaticity, the luminance of each disc was given a random value chosen from six levels between 4 cd/m² and 24 cd/m². To establish the patient's threshold for a given direction in colour space, the chromatic difference between the target and distractor discs was adjusted by a double staircase procedure.²⁴

RESULTS

All five patients had a history of nystagmus from infancy, mild photophobia, defective colour vision, and poor visual acuity (6/60 to CF). They all described improved vision in mesopic conditions. Examination of the anterior segment was unremarkable, except for one individual (VI:3) who had a unilateral congenital cataract. Fundus examination revealed a mildly abnormal foveal appearance but without frank atrophy or pigmentation (Fig 2). Peripheral retinal examination was normal in all subjects. ERG showed absent cone responses to 30 Hz flicker, small responses to short wavelength stimulation, and normal rod specific ERGs, but mildly subnormal maximal response a-wave amplitudes (Fig 3). Autofluorescence imaging was normal in all individuals. Clinical findings are summarised in Table 1.

Two older individuals (V:2 and V:7) described a gradual deterioration of vision. Visual acuity in V:7 was 6/36 in both eyes when he first presented 30 years ago, while his current best corrected acuity is counting fingers. His brother V:2, also showed evidence of deterioration of visual acuity from 6/60 in both eyes documented 10 years ago, to counting fingers at present. Both subjects have more prominent horizontal pendular nystagmus than other affected family members.

All five patients had abnormal colour vision. At the Nagel anomaloscope all five patients exhibited a scotopic spectral sensitivity. Four patients displayed a scotopic pattern of arrangement on PV-16. One patient, V:7, unlike a typical patient with complete achromatopsia, produced only one major transposition on the PV-16. Rudimentary colour

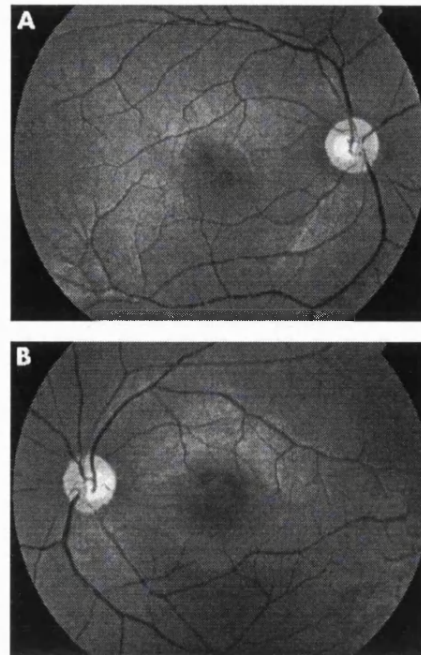


Figure 2 Fundus photographs. Mildly abnormal foveal appearance, but without frank atrophy or pigmentation.

discrimination was also detected in three individuals on testing with the M-R minimal test, with variable ability to identify the most saturated chip along the deutan and/or tritan axes. Further evidence of residual colour vision was provided by the colour discrimination ellipses produced on computerised colour vision testing. The other two individuals, V:2 and V:4, displayed no residual colour vision and showed typical achromatopic matches on Sloan plates.

DISCUSSION

The phenotype in this family with a novel homozygous frameshift mutation in the cone α -transducin gene, *GNAT2*, is characterised by mild photophobia, nystagmus, abnormal colour vision, and poor visual acuity (6/36 to CF). Electroretinography using the ISCEV protocol revealed absent cone responses, with normal rod specific ERGs, but mild reduction in maximal response a-wave amplitudes. Small photopic responses to short wavelength stimulation were detectable. On detailed colour vision testing, residual colour discrimination was detected in three individuals.

This phenotype is similar therefore to the incomplete form of achromatopsia arising from certain mutations in *CNGA3*, the gene encoding the α -subunit of the cGMP gated cation channel in cones.¹⁰ Unlike complete achromatopsia, we have been able to record S-cone ERG responses in our patients and, in two older subjects, a worsening of visual acuity with age has been documented, although we have no definite evidence of progressive deterioration in retinal function. In achromatopsia we have found only one case report of progressive retinal degeneration in the form of mid-peripheral retinal pigmentation and concentric constriction of the peripheral visual fields.²⁵ It was also reported that a few of the younger subjects in that achromatopsia series had small residual cone responses on ERG. Taken together, therefore, these findings may represent evidence that progression in retinal dysfunction may be present in at least some individuals with achromatopsia, but no natural history studies are available to corroborate this.²⁵

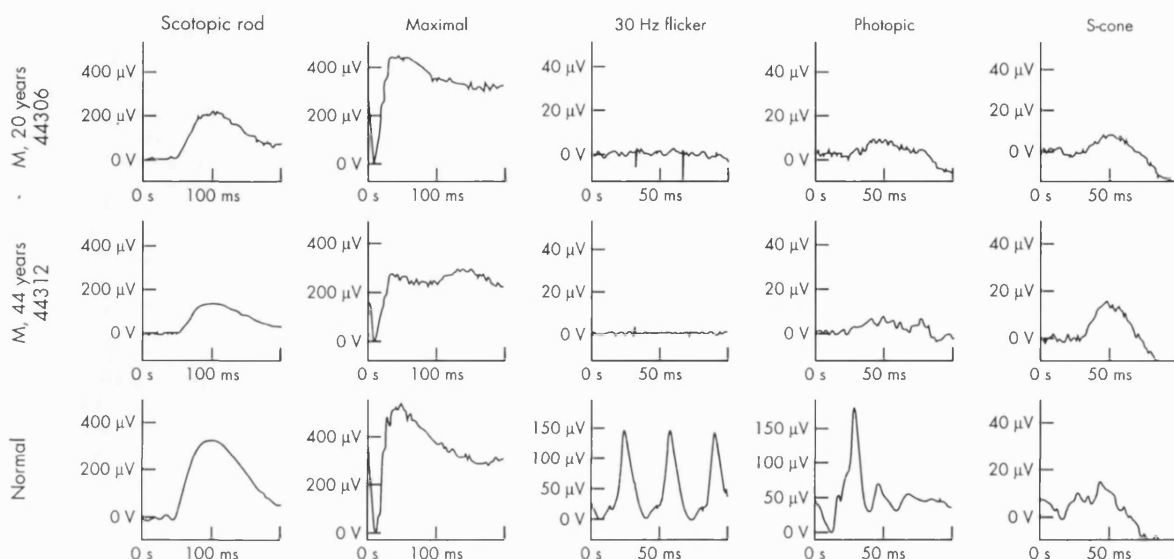


Figure 3 Electrophysiological data from two patients, a father (V:7) and son (VI:1). A normal control is shown for comparison. Note the differences in calibration between the normal and the two patients for the cone derived ERGs. Both patients have normal rod specific ERGs, with borderline subnormal a-wave in the maximal response of the son, mildly subnormal in the father. Flicker ERG is undetectable in both patients, but there is some very low amplitude activity with photopic single flash stimulation. S-cone specific stimulation, using a blue light superimposed on an orange background,²⁰ suggests some preservation of mechanisms sensitive to short wavelengths. Note the presence of an earlier peak at ~30 ms in the normal, absent in the two patients, which reflects activity from L/M cone systems.

Retinal dysfunction in our family is predominantly confined to cone photoreceptors. In cone cells, light activated photopigment interacts with transducin, a three subunit guanine nucleotide binding protein, stimulating the exchange of bound GDP for GTP. The cone α -transducin subunit (encoded by *GNAT2*), which is bound to GTP, is then released from its β and γ subunits and activates cGMP phosphodiesterase by removing the inhibitory γ subunits from the active site of this enzyme. cGMP phosphodiesterase lowers the concentration of cGMP in the photoreceptor which results in closure of cGMP gated cation channels and consequent hyperpolarisation of the photoreceptor.²⁶ Thus, the finding of a germline *GNAT2* mutation in a family with cone dystrophy is consistent with the known function of the

GNAT2 product. Furthermore, mutations in human rod specific α -transducin, which is 83% homologous to cone α -transducin,^{27,28} have been shown to be associated with the Nougaret form of congenital stationary night blindness.²⁹

The frameshift mutation identified in our family results in a truncated protein that lacks 63 amino acids from the carboxy terminal.¹⁶ All the *GNAT2* mutations identified by Kohl *et al* would also result in premature translation termination and in protein truncation at the carboxy terminal.¹⁵ This region contains important functional domains of α -transducin which have been shown to interact with the rhodopsin³⁰ and phosphodiesterase γ -subunits.³¹ However, if this mutation were to lead to a complete lack of α -transducin function, it is difficult to explain the residual

Table 1 Summary of clinical findings

Patient	Age	VA	Refraction	Horizontal pendular nystagmus	ERG	Fundus	M-R colour vision test
V:2	35	R CF	-3.5/+3.0x30	Prominent	Absent 30 Hz cone responses; Normal rod specific responses	Abnormal foveal appearance	P(no)D(no)T(no)
		L CF	-4.0/+3.0x160				P(no)D(no)T(no)
V:4	41	R 6/60	-2.0/+2.0x110	Absent	Absent 30 Hz cone responses; Normal rod specific responses	Abnormal foveal appearance	P(no)D(no)T(no)
		L 6/60	-2.5/+1.5x70				P(no)D(no)T(no)
V:7	44	R CF	-2.0/+2.0x135	Prominent	Absent 30 Hz cone responses; Normal rod specific responses	Abnormal foveal appearance	P(no)D(7)T(5)
		L CF	-1.5/+1.5x45				P(no)D(6)T(5)
VI:1	20	R 6/60	+1.5/+1.5x110	Absent	Absent 30 Hz cone responses; Normal rod specific responses	Abnormal foveal appearance	P(no)D(7)T(4)
		L 6/60	+1.0/+2.0x80				P(no)D(no)T(5)
VI:3	19	R CF	Balance	Minimal	Absent 30 Hz cone responses; Normal rod specific responses	Abnormal foveal appearance	NA
		L 6/60	-2.0/+3.0x75				P(no)D(6)T(5)

ERG = counting fingers; M-R = Mollon-Reffin test. The letters give the axis P = protan, D = deutan, and T = tritan. The number in parentheses gives the least saturated chip that could be discriminated from the greys; VI:3 has a right sided congenital cataract.

colour vision along deutan and tritan axes in these individuals, if these are entirely cone mediated mechanisms. It is possible that the mutation results in a protein that, although severely reduced in efficacy, may still show some residual α -transducin function. Alternatively, there may be some redundancy within the cone phototransduction pathway that allows a level of continued function despite suboptimal or absent function of one of the components of the cascade.

The human cone transducin α -subunit (*GNAT2*) gene was completely characterised by Morris and Fong in 1993²⁷ and the evidence that this gene is expressed in all three cone types comes from the immunohistochemical demonstration that an antibody raised against cone α -transducin peptides cross-reacts with all three classes of cone photoreceptor in the human retina.³² This does not however definitively rule out the possibility that S-cones may express an alternative form of α -transducin since identical epitopes may be present on both forms. It may also be significant that Southern blot analysis of human genomic DNA indicated that there may be more than one cone α -transducin gene.³² Therefore, although there are no subsequent studies that provide any direct evidence for an S-cone specific cone α -transducin, it remains a possibility that *GNAT2* is not expressed in S-cones, and that the residual S-cone function detected in our family arises from the use of this other distinct form of α -transducin. In this case therefore, the residual tritan colour discrimination may be accounted for by a comparison of quantum catches in the remaining functional S-cones and rod photoreceptors, in the manner proposed to underlie colour discrimination detected in blue cone monochromatism.³³

A detailed description of the phenotype associated with mutation in the α -subunit of cone specific transducin has not been previously reported. It is characterised by a cone dystrophy with an infantile onset, a deterioration of visual acuity with time in older individuals, and residual S-cone function.

ACKNOWLEDGEMENTS

The work was supported by grants from the British Retinitis Pigmentosa Society, the Guide Dogs for the Blind Association, and the Wellcome Trust. We are also grateful to the patients who kindly agreed to take part in this study.

Authors' affiliations

M Michaelides, D M Hunt, A T Moore, Institute of Ophthalmology, University College London, 11–43 Bath Street, London EC1V 9EV, UK
I A Aligianis, E R Maher, Section of Medical and Molecular Genetics, Department of Paediatrics and Child Health, University of Birmingham, Edgbaston, Birmingham B15 2TT, and West Midlands Regional Genetics Service, Birmingham Women's Hospital, Birmingham B15 2TG, UK
G E Holder, Moorfields Eye Hospital, City Road, London EC1V 2PD, UK
M Simunovic, J D Mollon, Department of Experimental Psychology, University of Cambridge, Downing Street, Cambridge CB2 3EB, UK

Correspondence to: Professor A T Moore, Institute of Ophthalmology, University College London, 11–43 Bath Street, London, EC1V 9EL, UK; tony.moore@ucl.ac.uk

Accepted for publication 3 March 2003

REFERENCES

- 1 Goodman G, Ripps H, Siegel IM. Cone dysfunction syndromes. *Arch Ophthalmol* 1963;70:214–31.

- 2 Simunovic MP, Moore AT. The cone dystrophies. *Eye* 1998;12:553–65.
- 3 Pokorny J, Smith VC, Verriest G, et al. *Congenital and acquired colour vision defects*. New York: Grune and Stratton, 1979.
- 4 Szyk J, Fishman GA, Alexander KR, et al. Clinical subtypes of cone-rod dystrophy. *Arch Ophthalmol* 1993;111:781–8.
- 5 Sadowski B, Zrenner E. Cone and rod function in cone degenerations. *Vis Res* 1997;37:2303–2314.
- 6 Sharpe LT, Nordby K. Total colour-blindness: an introduction. In: Hess RF, Sharpe LT, Nordby K, ed. *Night vision: basic, clinical and applied aspects*. Cambridge: Cambridge University Press, 1990:253–89.
- 7 Sharpe LT, Stockman A, Jagle H, et al. Opsin genes, cone photopigments and colourblindness. In: Gegenfurtner K, Sharpe LT, ed. *Color vision: from genes to perception*. Cambridge: Cambridge University Press, 1999:3–52.
- 8 Wissinger B, Jägle H, Kohl S, et al. Human rod monochromacy: linkage analysis and mapping of a cone photoreceptor expressed candidate gene on chromosome 2q11. *Genomics* 1998;51:325–31.
- 9 Kohl S, Marx T, Giddings I, et al. Total colourblindness is caused by mutations in the gene encoding the alpha-subunit of the cone photoreceptor cGMP-gated cation channel. *Nat Genet* 1998;19:257–9.
- 10 Wissinger B, Gamer D, Jägle H, et al. *CNGA3* mutations in hereditary cone photoreceptor disorders. *Am J Hum Genet* 2001;69:722–37.
- 11 Winick JD, Blundell ML, Galke BL, et al. Homozygosity mapping of the achromatopsia locus in the Pingelapese. *Am J Hum Genet* 1999;64:1679–85.
- 12 Kohl S, Baumann B, Broghammer M, et al. Mutations in the *CNGB3* gene encoding the beta-subunit of the cone photoreceptor cGMP-gated channel are responsible for achromatopsia (*ACHM3*) linked to chromosome 8q21. *Hum Mol Genet* 2000;9:2107–16.
- 13 Sundin OH, Yang J-M, Li Y, et al. Genetic basis of total colourblindness among the Pingelapese islanders. *Nat Genet* 2000;25:289–93.
- 14 Mollon JD. '...aus dreierley Arten von Membranen oder Molekülen': George Palmer's legacy. In: Cavonius CR, ed. *Colour vision deficiencies XIII*. Kluwer Academic Publishers, 1997:3–20.
- 15 Kohl S, Baumann B, Rosenberg T, et al. Mutations in the cone photoreceptor G-protein alpha-subunit gene *GNAT2* in patients with achromatopsia. *Am J Hum Genet* 2002;71:422–5.
- 16 Aligianis IA, Forshew T, Johnson S, et al. Mapping of a novel locus for achromatopsia (*ACHM4*) to 1p and identification of a germline mutation in the α subunit of cone transducin (*GNAT2*). *J Med Genet* 2002;39:656–60.
- 17 Marmor MF, Zrenner E. Standard for clinical electroretinography (1994 update). *Doc Ophthalmol* 1995;89:199–210.
- 18 Bach M, Hawlina M, Holder GE, et al. Standard for pattern electroretinography. International Society for Clinical Electrophysiology of Vision. *Doc Ophthalmol* 2000;101:11–18.
- 19 Marmor MF, Zrenner E. Standard for clinical electro-oculography. International Society for Clinical Electrophysiology of Vision. *Arch Ophthalmol* 1993;111:601–4.
- 20 Arden G, Wolf J, Berninger T, et al. S-cone ERGs elicited by a simple technique in normals and in tritanopes. *Vis Res* 1999;39:641–50.
- 21 Mollon JD, Astell S, Reffin JP. A Minimalist test of colour vision. In: Drum B, Moreland JD, Serra A, ed. *Colour vision deficiencies XI* Kluwer Academic Publishers, 1991:59–67.
- 22 Mollon JD, Reffin JP. A computer-controlled colour vision test that combines the principles of Chibret and of Stilling. *J Physiol* 1989;414:5P.
- 23 Regan BC, Reffin JP, Mollon JD. Luminance noise and the rapid determination of discrimination ellipses in colour deficiency. *Vis Res* 1994;34:1279–99.
- 24 Simunovic MP, Votruba M, Regan BC, Mollon JD. Colour discrimination ellipses in patients with dominant optic atrophy. *Vis Res* 1998;38:3413–20.
- 25 Eksandh L, Kohl S, Wissinger B. Clinical features of achromatopsia in Swedish patients with defined genotypes. *Ophthalmic Genet* 2002;23:109–20.
- 26 Stryer L. Visual excitation and recovery. *J Biol Chem* 1991;266:10711–14.
- 27 Morris TA, Fong SL. Characterisation of the gene encoding human cone transducin alpha-subunit (*GNAT2*). *Genomics* 1993;17:442–8.
- 28 Fong SL. Characterisation of the human rod transducin alpha-subunit gene. *Nucleic Acids Res* 1992;20:2865–70.
- 29 Dryja TP, Hahn LB, Reiboul T, et al. Missense mutation in the gene encoding the alpha subunit of rod transducin in the Nougaret form of congenital stationary night blindness. *Nat Genet* 1996;13:358–60.
- 30 Cai K, Itoh Y, Khorana HG. Mapping of contact sites in complex formation between transducin and light-activated rhodopsin by covalent crosslinking: use of a photoactivatable reagent. *Proc Natl Acad Sci* 2001;98:4877–82.
- 31 Liu Y, Arshavsky VY, Ruoho AE. Interaction sites of the COOH-terminal region of the gamma subunit of cGMP phosphodiesterase with the GTP-bound alpha subunit of transducin. *J Biol Chem* 1996;271:26900–7.
- 32 Lerea CL, Bunt-Milam AH, Hurlley JB. Alpha transducin is present in blue-, green-, and red-sensitive cone photoreceptors in the human retina. *Neuron* 1989;3:367–376.
- 33 Reitner A, Sharpe LT, Zrenner E. Is colour vision possible with only rods and blue-sensitive cones? *Nature* 1991;352:798–800.

PERSPECTIVE

The cone dysfunction syndromes

M Michaelides, D M Hunt, A T Moore

Br J Ophthalmol 2004;**88**:291–297. doi: 10.1136/bjo.2003.027102

The cone dystrophies comprise a heterogeneous group of disorders characterised by visual loss, abnormalities of colour vision, central scotomata, and a variable degree of nystagmus and photophobia. They may be stationary or progressive. The stationary cone dystrophies are better described as cone dysfunction syndromes since a dystrophy often describes a progressive process. These different syndromes encompass a wide range of clinical and psychophysical findings. The aim is to review current knowledge relating to the cone dysfunction syndromes, with discussion of the various phenotypes, the currently mapped genes, and genotype-phenotype relations. The cone dysfunction syndromes that will be discussed are complete and incomplete achromatopsia, oligocone trichromacy, cone monochromatism, blue cone monochromatism, and Bornholm eye disease. Disorders with a progressive cone dystrophy phenotype will not be discussed.

Affected individuals usually present in infancy with pendular nystagmus, poor visual acuity, and photophobia. A hypermetropic refractive error is common and it is often found that the nystagmus wanes with time.³ Fundal examination is usually normal; however, infrequently, central or mid-peripheral retinal pigment epithelial abnormalities are present. Electroretinography (ERG) reveals absent cone responses and normal rod responses.⁶ Affected individuals usually achieve a visual acuity of 6/60, have absent colour vision, and have normal rod function but absent cone function on psychophysical testing.⁷

Achromatopsia is recessively inherited and genetically heterogeneous. To date, three achromatopsia genes have been identified, *CNGA3*, *CNGB3*, and *GNAT2*; all three genes will be described in detail in the discussion that follows. The first molecular genetic report of achromatopsia was a cytogenetic analysis of a 20 year old woman with achromatopsia and multiple developmental abnormalities.⁸ Maternal isodisomy of chromosome 14 was demonstrated (both copies of chromosome 14 were of maternal origin). However, there has been no subsequent confirmation of a locus on chromosome 14. In 1997 a genome-wide search for linkage was performed in a consanguineous Jewish kindred, establishing linkage to a 14 cM region on 2q11.⁹ This disease interval was further refined to a 3 cM region in 1998 in a study of eight families of different ethnic and racial origins, and *CNGA3* was identified as a candidate gene within this interval.¹⁰ *CNGA3* encodes the α -subunit of the cGMP gated (CNG) cation channel in human cone photoreceptors, the final critical effector in the phototransduction cascade. In the dark, cGMP levels are high in cone photoreceptors, therefore enabling cGMP to bind to the α and β -subunits of CNG channels, resulting in them adopting an open conformation and permitting an influx of cations, with consequent cone depolarisation. However, in light conditions, activated photopigment initiates a cascade culminating in increased cGMP phosphodiesterase activity, thereby lowering the concentration of cGMP in the photoreceptor which results in closure of CNG cation channels and consequent cone hyperpolarisation.¹¹

Missense mutations in highly conserved residues of *CNGA3* were initially described in five families with complete achromatopsia from Germany, Norway, and the United States.¹² Since then more recent studies have revealed more than 50 disease causing mutations in *CNGA3*.^{13,14} Mutations have been identified throughout the *CNGA3* protein, including the five transmembrane domains, the pore region,

The cone dystrophies are characterised by bilateral visual loss, colour vision abnormalities, central scotomata, variable degrees of nystagmus and photophobia, together with electrophysiological or psychophysical evidence of abnormal cone function. There is considerable clinical and genetic heterogeneity; cone dystrophies showing autosomal dominant, autosomal recessive, and X linked recessive inheritance have all been reported. These disorders may be stationary or progressive. The stationary subtypes are congenital with normal rod function, whereas in progressive cone dystrophies, onset is usually in childhood or early adult life and patients often develop rod photoreceptor dysfunction in later life. The stationary disorders are better described as cone dysfunction syndromes. In this review we will describe the various phenotypes and disease causing genes that have been recently identified in this group of disorders (table 1). We will not consider the various forms of colour vision deficiency; the molecular genetic basis of these disorders has now been well characterised and several reviews have been published on the subject.^{1,2}

COMPLETE ACHROMATOPSIA

Complete achromatopsia, typical achromatopsia or rod monochromatism, is a stationary disorder in which there is an absence of functioning cone photoreceptors in the retina.^{3,5} It is uncommon with an incidence of about 1 in 30 000.^{3,4}

See end of article for authors' affiliations

Correspondence to: Professor Anthony T Moore, Institute of Ophthalmology, University College London, 11-43 Bath Street, London EC1V 9EL, UK; tony.moore@ucl.ac.uk

Accepted for publication 21 July 2003

Table 1 Summary of the cone dysfunction syndromes

Cone dysfunction syndrome	Alternative names	Mode of inheritance	Visual acuity	Refractive error	Nystagmus	Colour vision	Fundi	Mutated gene(s) or chromosome locus
Complete achromatopsia	Rod monochromatism Typical achromatopsia	Autosomal recessive	6/36-6/60	Often hypermetropia	Present	Absent	Usually normal	CNGA3 CNGB3 GNAT2
Incomplete achromatopsia Oligocone trichromacy	Atypical achromatopsia Oligocone syndrome	Autosomal recessive Autosomal recessive	6/24-6/60 6/12-6/24	Often hypermetropia Equal incidence of myopia and hypermetropia	Present Usually absent	Residual Normal	Usually normal Normal	Chromosome 14 CNGA3
Cone monochromatism	-	Uncertain	6/6	-	Absent	Absent or markedly reduced	Normal	-
Blue cone monochromatism	X linked atypical achromatopsia X linked incomplete achromatopsia	X linked	6/24-6/60	Often myopia	Present	Residual tritan discrimination	Usually normal	(i) Deletion of the LCR (ii) Single inactivated L/M hybrid gene* Xq28
Bornholm eye disease	-	X linked	6/9-6/18	Moderate to high myopia with astigmatism	Absent	Deuteranopia	Myopic	-

LCR = locus control region; deletion in this region abolishes transcription of all L and M genes in the opsin pigment gene array and therefore inactivates both L and M cones.

*In the second class of mutations the LCR is preserved but changes within the L and M gene array lead to loss of functional pigment production. The most common genotype in this class consists of a single inactivated L/M hybrid gene. The most frequent inactivating mutation described results in a cysteine to arginine substitution, (Cys203Arg), a mutation known to disrupt the folding of cone opsin molecules.

and cGMP binding site. However, four mutations in particular (Arg277Cys, Arg283Trp, Arg436Trp and Phe547Leu) are found most commonly, accounting for approximately 40% of all mutant *CNGA3* alleles.¹³ Moreover, subsequent analysis of the homologous *CNGA3* knockout mouse model showed complete absence of physiologically measurable cone function, a decrease in the number of cones in the retina, and morphological abnormalities of the remaining cones.¹⁵

The second gene identified in patients with achromatopsia was aided by a population with an unusually high incidence of the disease; 5% to 10% of the Pingelapese people of the Eastern Caroline Islands in Micronesia in the western Pacific have achromatopsia.¹⁶ This is most probably related to the sharp reduction of the island's population to approximately 20 individuals following a typhoon in 1775, with the island being subsequently repopulated during two centuries of isolation. In 1999 linkage analysis excluded 2q but demonstrated linkage to 8q21-q22.¹⁷ Sundin *et al* narrowed the region to 1.4 cM and identified a missense mutation, Ser435Phe, in the Pingelapese achromats, at a highly conserved site in *CNGB3*, the gene coding for the β -subunit of cone photoreceptor CNG cation channels.¹⁸ They also identified two independent frameshift deletions in a different population, Pro273fs and Thr383fs, thereby establishing that achromatopsia is the null phenotype of *CNGB3*. A similar study by Kohl *et al* identified six mutations in *CNGB3*; three were novel—Arg203stop, Glu366stop, and a putative splice site defect.¹⁹ Rojas *et al* have since identified Asp149fs in a consanguineous Chilean family.²⁰ The most frequent mutation of *CNGB3* identified to date is the 1 base pair frameshift deletion, 1148delC (Thr383fs), which accounts for up to 84% of *CNGB3* mutant disease chromosomes.^{19, 21}

Currently there is far greater allelic heterogeneity of *CNGA3* mutants (over 50 mutations described) when compared to *CNGB3* (~7). It is known that *CNGA3* subunits can form functional homomeric channels when expressed alone, whereas *CNGB3* subunits alone do not appear to form functional channels.²² In our opinion it is therefore plausible that some *CNGB3* null mutations are not detected since sufficient channel function is possible solely with normal *CNGA3* subunits, leading to a relatively normal phenotype.

These studies of *CNGA3* and *CNGB3* have demonstrated that both the α and β -subunits of the CNG cation channel are essential for phototransduction in all three classes of cones. The majority of *CNGA3* mutations identified to date are missense mutations, indicating that there is little tolerance for substitutions with respect to functional and structural integrity of the channel polypeptide. This notion is supported by the high degree of evolutionary conservation among CNG channel α -subunits. In contrast, the majority of *CNGB3* alterations are nonsense mutations. It is currently proposed that approximately 25% of achromatopsia results from mutations of *CNGA3*¹³ and 40-50% from mutations of *CNGB3*.^{19, 21} Therefore, while mutations in the cone channel subunit genes, *CNGA3* and *CNGB3*, account for the majority of achromats, there is a significant proportion of patients for whom neither *CNGA3* nor *CNGB3* mutations can be found (~30%). The phenotype associated with mutations in these two channel protein genes appears to be in keeping with previous clinical descriptions of achromatopsia.^{12-14, 18-20}

It is of interest that missense mutations in *CNGA3* have also been reported in two individuals with cone-rod dystrophy and in a single individual with a progressive cone dystrophy phenotype.¹³ Possible reasons for a progressive phenotype in these individuals may include the particular combination of missense mutations present in these three subjects; some amino acid substitutions may be more deleterious to channel function than others. Other potential

phenotypic influences include the presence of other modifier genes or environmental effects.

Cone degeneration (cd) is an autosomal recessive canine disease that occurs naturally in the Alaskan Malamute and German shorthaired pointer breeds and is phenotypically similar to human achromatopsia.²³ Canine *CNGB3* mutations have recently been identified in both of these breeds, thereby establishing these cd affected dogs as the only naturally occurring large animal model of human achromatopsia, and therefore providing a valuable system for exploring disease mechanisms and evaluating potential genetic therapeutic intervention in human achromatopsia.²³

GNAT2, located at 1p13, is the third gene to be implicated in achromatopsia.^{24–25} *GNAT2* codes for the α -subunit of cone specific transducin. In cone cells, light activated photopigment interacts with transducin, a three subunit guanine nucleotide binding protein, stimulating the exchange of bound GDP for GTP. The cone α -transducin subunit, which is bound to GTP, is then released from its β and γ -subunits and activates cGMP phosphodiesterase by removing the inhibitory γ -subunits from the active site of this enzyme. cGMP phosphodiesterase lowers the concentration of cGMP in the photoreceptor which results in closure of cGMP gated cation channels.¹¹ All the *GNAT2* mutations identified to date result in premature translation termination and in protein truncation at the carboxy terminus.^{24–25} However, mutations in this gene are thought to be responsible for less than 2% of patients affected with this disorder,²⁴ suggesting the presence of further genetic heterogeneity in achromatopsia.

We have recently undertaken a detailed description of the phenotype associated with *GNAT2* inactivation in a large consanguineous Pakistani family.²⁶ The phenotype is characterised by mild photophobia, nystagmus, abnormal colour vision, and poor visual acuity (6/36 to counting fingers). On detailed colour vision testing, residual colour discrimination was detected in three individuals. ERGs revealed absent cone responses, with normal rod specific ERGs. We were able to record S cone ERG responses in all patients. In two older subjects, a worsening of visual acuity with age has been documented, although we have no definite evidence of progressive deterioration in retinal function. The residual S cone function detected in this *GNAT2* associated phenotype is intriguing. The evidence that *GNAT2* is expressed in all three cone types comes from the immunohistochemical demonstration that an antibody raised against cone α -transducin peptides cross reacts with all three classes of cone photoreceptor in the human retina.²⁷ This does not however definitively rule out the possibility that S cones may express an alternative form of α -transducin, since identical epitopes may be present on both forms. It may also be significant that Southern blot analysis of human genomic DNA indicated that there may be more than one cone α -transducin gene.²⁷ Therefore, it remains a possibility that *GNAT2* is not expressed in S cones, and that the residual S cone function detected in our family arises from the use of another distinct form of α -transducin. The residual tritan colour discrimination detected may be accounted for by a comparison between quantum catches in the remaining functional S cones and rod photoreceptors, in the manner proposed to underlie colour discrimination detected in blue cone monochromatism.²⁸

The three genes described to date associated with achromatopsia, *CNGA3*, *CNGB3* and *GNAT2*, encode proteins in the cone phototransduction cascade. It is therefore reasonable to propose that further cone specific intermediates involved in phototransduction represent good candidates. These include the genes encoding the cone specific β and γ -transducin subunits and cone phosphodiesterase. It is of note that immunological studies of the canine cd affected retina have demonstrated a specific absence or delocalisation of

β and γ cone specific transducin subunits from the outer segments of pre-degenerate cone photoreceptors. However, genes for both subunit proteins have been excluded as canine cd genes.^{29–30}

INCOMPLETE ACHROMATOPSIA

Previously, before the underlying pathogenesis of blue cone monochromatism (BCM) had been identified, BCM was known as X linked incomplete or atypical achromatopsia. However, the term incomplete/atypical achromatopsia is best reserved for the description of individuals with autosomal recessive disease where the phenotype is a variant of complete achromatopsia. Individuals with incomplete achromatopsia (atypical achromatopsia) retain residual colour vision and have mildly better visual acuity (6/24–6/60) than those with complete achromatopsia.^{5–31} In all other respects, the phenotype of these two conditions is indistinguishable. Three subtypes of incomplete achromatopsia have been demonstrated via colour matching experiments³¹:

- colour matches are governed by rods and M cones (incomplete achromatopsia with protan luminosity)³²;
- colour matches are governed by L and M cones;
- colour matches mediated by rods, L cones, and S cones (incomplete achromatopsia with deutan luminosity).^{33–34}

As in the complete form, mutations in *CNGA3*, the gene encoding the α -subunit of the cGMP gated cation channel in cones, have been identified in individuals with incomplete achromatopsia.¹³ The psychophysical data provided in this study¹³ are inadequate to be able to classify these individuals into the three colour matching subtypes described above.^{31–34} The 19 mutations identified were all missense mutations, located throughout the channel polypeptide including the transmembrane domains, ion pore, and cGMP binding region. However, only three of these missense mutations, Arg427Cys, Arg563His, and Thr565Met, were found exclusively in patients with incomplete achromatopsia.¹³ Therefore in the majority of cases of incomplete achromatopsia, factors other than the specific causative mutation, such as modifier genes, or environmental influences, may dictate the phenotype. The missense variants identified in incomplete achromatopsia must be compatible with residual channel function since the phenotype is milder than in complete achromatopsia.

Mutations in *CNGB3* or *GNAT2* have not been reported in association with incomplete achromatopsia, despite mutant *CNGB3* alleles being identified twice as commonly as *CNGA3* variants as the cause of complete achromatopsia. However all *GNAT2* mutations to date, and the vast majority of *CNGB3* mutants, result in premature termination of translation, and thereby truncated and most probably non-functional phototransduction proteins. Therefore an incomplete achromatopsia phenotype is unlikely to be compatible with these genotypes which are predicted to encode mutant products lacking any residual function.

OLIGOCONE TRICHROMACY

Oligocone trichromacy is a rare cone dysfunction syndrome, which is characterised by reduced visual acuity, mild photophobia, normal fundi, reduced amplitude of the cone electroretinogram but with colour vision within normal limits. The disorder was first described by Van Lith in 1973.³⁵ Since then Keunen *et al* have described a further four patients,³⁶ while Neuhann *et al*, and, more recently, Ehlich *et al* have each reported a single case.^{37–38} The two cases reported by Van Lith and Ehlich both had pendular nystagmus.

It has been proposed that these patients might have a reduced number of normal functioning cones (oligocone

syndrome) with preservation of the three cone types in the normal proportions, thereby permitting trichromacy.³⁵ Keunen *et al* tested this hypothesis by screening foveal cone photopigment density.³⁶ A reduced density difference of the foveal cone photopigment with a normal time constant of photopigment regeneration was found in all patients. Colour matching and increment threshold spectral sensitivity were normal. This provided evidence for the hypothesis of a reduced number of foveal cones (decreased density differences) with otherwise normal functioning residual cones.

We have recently detailed the phenotype of six patients with oligocone trichromacy.^{36a} All six affected patients had a history of reduced visual acuity from infancy (6/12 to 6/24). They complained of very mild photophobia, but were not aware of any colour vision deficiency. They had no nystagmus and fundi were normal. On examination, all patients were found to have good colour vision. The various colour vision tests either revealed completely normal colour vision or slightly elevated discrimination thresholds. Anomaloscopy revealed matching ranges within normal limits, indicating the presence of long and middle wave cones of normal spectral sensitivity at the macula, while the absence of pseudoprotanomaly suggests that photopigment is present at normal optical densities in individual cone photoreceptors. The slightly elevated discrimination thresholds that were detected are compatible with a reduction in cone numbers. The cone ERG findings in our patients were poorly concordant, but could broadly be divided into two classes. In the first group (five individuals) cone responses were absent or markedly reduced. In the second group (one individual), cone b-waves were more markedly reduced than a-waves, implying a predominantly inner retinal abnormality in the cone system. These electrophysiological data suggest that there may be more than one disease mechanism and therefore more than one disease causing gene.

Oligocone trichromacy is likely to be inherited as an autosomal recessive trait. The molecular genetic basis of the disorder is unknown. Genes involved in retinal photoreceptor differentiation, when cone numbers are being determined, may represent good candidate genes.

CONE MONOCHROMATISM

Monochromatic vision is diagnosed by a patient's ability to match any two colours merely by adjusting their radiance, when all other cues are absent. In rod monochromatism there is an absence of functioning cone photoreceptors with visual perception depending almost exclusively on rods. The rod monochromat therefore has markedly reduced visual acuity and total colour blindness.

Cone monochromatism is another rare form of congenital colour blindness, in which visual acuity is normal.³⁹⁻⁴⁰ The incidence of cone monochromatism is estimated at one in 100 million.⁴¹ Unlike rod monochromatism, cone monochromatism has never been noted in more than one family member.³⁹ The colour vision defect may be incomplete for certain colours and may vary both with the size of the field viewed and the level of luminance.³⁹⁻⁴⁰⁻⁴² A normal ERG is present in this disorder thereby supporting the notion of abnormal processing central to the retinal photoreceptors and bipolar cells.⁴³⁻⁴⁴ This notion was first proposed following the demonstration of red and green sensitive pigments at the fovea in cone monochromats⁴⁰ and the ability of such patients to use ocular chromatic aberration as a cue for altering accommodation.⁴⁵ In addition, Gibson has been able to demonstrate the presence of three mechanism sensitivity curves for the cone monochromat that are similar to those found in normal individuals, representing evidence of colour mediating mechanisms in the cone monochromat, and

thereby providing further evidence for a post-receptoral defect in this disorder.⁴⁶

BLUE CONE MONOCHROMATISM

Blue cone monochromatism (BCM), previously also known as X linked incomplete achromatopsia, affects fewer than 1 in 100 000 individuals, and is characterised by absence of L and M cone function.⁴⁷ Thus, the blue cone monochromat possesses rod vision and a normal short wavelength sensitive cone mechanism.

As in rod monochromacy, BCM typically presents in infancy with reduced visual acuity, pendular nystagmus, photophobia and normal fundi.⁴⁸ The nystagmus often wanes with time. Visual acuity is of the order of 6/24 to 6/60. Eccentric fixation may be present and myopia is a common finding.⁴⁸ BCM is distinguished from rod monochromatism (RM) via psychophysical and electrophysiological testing. The photopic ERG is profoundly reduced in both, although the S cone ERG is well preserved in BCM.⁴⁹ Classification can also be aided by family history, because BCM is inherited as an X linked recessive trait, whereas both subtypes of rod monochromacy show autosomal recessive inheritance.

Rod monochromats cannot make colour judgments, but rather will use brightness cues to differentiate between colours. This contrasts with blue cone monochromats who do have access to colour discrimination, though this does depend upon the luminance of the task: at mesopic levels, they have rudimentary dichromatic colour discrimination based upon a comparison of the quantum catches obtained by the rods and the S cones (blue cones).²⁸⁻³⁰ Colour discrimination is reported to deteriorate with increasing luminance.³¹ Therefore blue cone monochromats may be distinguished from rod monochromats by means of colour vision testing: blue cone monochromats are reported to display fewer errors along the vertical axis in the Farnsworth 100 Hue test (fewer tritan errors), and they may also display protan-like ordering patterns on the Farnsworth D-15.³² In addition, the Berson plates have been claimed to provide a good separation of blue cone monochromats from rod monochromats.³³⁻³⁴ Therefore, in order to clinically distinguish RM and BCM one needs to use colour vision tests that probe the tritan axis of colour as well as the deutan and protan, since the presence of residual tritan discrimination suggests BCM.³²⁻³⁴

In order to derive colour vision, the normal human visual system compares the rate of quantum catches in three classes of cone; the short (S) wavelength sensitive, middle (M) wavelength sensitive, and long (L) wavelength sensitive cones are maximally sensitive to light at 430 nm, 535 nm, and 565 nm, respectively. Whereas the L (red) and M (green) pigment genes are located on the X chromosome, the S cone (blue) pigment is encoded by a gene located on chromosome 7.³⁵⁻³⁶ The wild type arrangement of the L and M opsin genes consists of a head to tail tandem array of two or more repeat units of 39 kb on chromosome Xq28 that are 98% identical at the DNA level.³⁵⁻³⁶ The highly homologous L and M opsin genes are as a consequence predisposed to unequal intergenic and intragenic recombination. Transcriptional regulation of the L and M visual pigment genes is controlled by an upstream locus control region (LCR).³⁷ Mutations in the L and M pigment gene array that result in the lack of functional L and M pigments, and thus inactivate the corresponding cones, have been identified in the majority of BCM cases studied.³⁷⁻³⁸

Mutation analyses introduced by Nathans and collaborators have proved highly efficient at establishing the molecular basis for BCM.³⁷⁻³⁸ The mutations in the L and M pigment gene array causing BCM fall into two classes. In the first class, a normal L and M pigment gene array is inactivated by

a deletion in the LCR, located upstream of the L pigment gene. A deletion in this region abolishes transcription of all genes in the pigment gene array and therefore inactivates both L and M cones.⁵⁹ In the second class of mutations the LCR is preserved but changes within the L and M pigment gene array lead to loss of functional pigment production. The most common genotype in this class consists of a single inactivated L/M hybrid gene. The first step in this second mechanism is unequal crossing over reducing the number of genes in the array to one, followed in the second step by a mutation that inactivates the remaining gene. The most frequent inactivating mutation that has been described is a thymine to cytosine transition at nucleotide 648, which results in a cysteine to arginine substitution at codon 203 (Cys203Arg), a mutation known to disrupt the folding of cone opsin molecules.⁶⁰ Reyniers *et al* have also described a family where BCM is the result of Cys203Arg mutations in both L and M pigment genes in the array.⁶¹ A third molecular genetic mechanism has been described in a single family of BCM where exon 4 of an isolated red pigment gene had been deleted.⁶²

BCM is generally accepted to be a stationary disorder, although Fleischman and O'Donnell reported one BCM family with macular atrophy and noted a slight deterioration of visual acuity and colour vision during a 12 year follow up period, as well as foveal pigmentary changes.⁶³ There are two further reports of individuals with BCM displaying a progressive retinal degeneration.^{57 64} In two of the families that we have studied there has also been progression in the severity of the condition^{64a} in that visual acuity and residual colour vision have been seen to deteriorate.

Combined results of previous studies^{57 58 64 65} provide evidence for the general conclusion, first put forward by Nathans *et al*, that there are different mutational pathways to BCM. The data suggest that 40% of blue cone monochromat genotypes are a result of a one step mutational pathway that leads to deletion of the LCR. The remaining 60% of blue cone monochromat genotypes comprise a heterogeneous group of multistep pathways. The evidence thus far shows that many of these multistep pathways produce visual pigment genes that carry the inactivating Cys203Arg mutation, which eliminates a highly conserved disulphide bond.⁶⁶ This cysteine residue is located in the second extracellular loop of the opsin and, together with a conserved cysteine residue at position 126 in the first extracellular loop, forms a disulphide bond necessary for stabilisation of the tertiary structure of the protein.⁶⁰

These studies have failed to detect the genetic alteration that would explain the BCM phenotype in all assessed individuals.^{58 65} Indeed, Nathans *et al*⁵⁸ found that in nine out of 35 individuals with BCM (25%), the structure of the opsin array did not reveal the genetic mechanism for the disorder. This failure to identify disease causing variants in the opsin array may suggest that there is genetic heterogeneity yet to be identified in BCM.

BORNHOLM EYE DISEASE

Myopia can be inherited as an autosomal recessive, autosomal dominant, or as an X linked trait and, in the latter case, it is well known as a component of congenital stationary night blindness⁶⁷ and retinitis pigmentosa.⁶⁸ X linked myopia has been reported in a large five generation Danish family that had its origins on the Danish island of Bornholm. The syndrome has therefore been named Bornholm eye disease (BED).^{69 70} In that family, the syndrome manifests as moderate to high myopia combined with astigmatism and impaired visual acuity. Additional signs are moderate optic nerve head hypoplasia, thinning of the retinal pigment epithelium in the posterior pole with visible choroidal

vasculature, and abnormal photopic ERG flicker function as the most constant finding.⁶⁹ Affected members in this family are all deuteranopes, with a stationary natural history. This disorder is therefore best characterised as an X linked cone dysfunction syndrome with myopia and deuteranopia.

Linkage analysis performed in the original BED family has mapped the locus to Xq28, in the same chromosomal region therefore as the L/M opsin gene array.⁷⁰ It remains to be seen whether molecular genetic analysis of the opsin array will reveal mutations that account for both the cone dysfunction and the colour vision phenotype. However, it may also be possible that rearrangements within the opsin gene array will be found to account for the colour vision findings, while the cone dysfunction component of the disorder may be ascribed to mutation within an adjacent but separate locus. The cone dystrophy that has been mapped to Xq27 (COD2) however, displays a different phenotype which is progressive.⁷¹ Nevertheless, it is becoming increasingly common in retinal molecular genetics to find that disparate phenotypes can be caused either by different mutations in the same gene, or even the same mutation in the same gene. In the latter situation it is currently believed that other genetic factors—namely, the “genetic context” within which the primary disease causing mutation is expressed, and/or environmental factors may determine the final phenotype.

MANAGEMENT

There is currently no specific treatment for any of the cone dysfunction syndromes. Nevertheless, it is important that the correct diagnosis is made in order to provide accurate information on prognosis and to offer informed genetic counselling. Prenatal diagnosis is possible when the mutation(s) causing disease in the family is known.

Although there is no specific treatment available for this group of disorders, the provision of appropriate spectacle correction, low vision aids, and educational support is very important. Photophobia is often a prominent symptom in the cone dysfunction syndromes and therefore tinted spectacles or contact lenses may be beneficial to patients, in terms of both improved comfort and vision. In achromatopsia spectacle or contact lens tint aims to prevent rod saturation while maintaining residual cone function. In complete achromatopsia a deep red tint is most effective, allowing wavelengths of low luminous efficiency for rod photoreceptors to be transmitted to the retina, while those of a higher luminous efficiency (short wavelength light) are absorbed by the filter.^{54 72} Incomplete achromats are thought to benefit more from reddish brown lenses rather than deep red lenses, which on account of their narrow spectral transmission, would eliminate their residual colour discrimination.⁵⁴ In contrast, magenta tints which prevent rod saturation while allowing transmission of blue light are indicated in BCM.⁵⁴

CONCLUSIONS

The cone dysfunction syndromes comprise a group of disorders that are both clinically and genetically heterogeneous. Their phenotypes are now well characterised both clinically and psychophysically and many causative genes have been identified. Perhaps not surprisingly these genes mainly encode proteins involved in the cone phototransduction pathway. Other genes remain to be identified before the complete molecular pathology of this interesting group of disorders can be established.

Authors' affiliations

M Michaelides, D M Hunt, A T Moore, Institute of Ophthalmology, University College London, 11-43 Bath Street, London EC1V 9EL, UK

REFERENCES

- 1 Mallon JD. '...aus dreierley Arten von Membranen oder Molekülen': George Palmer's legacy. In: Cavonius CR, ed. *Colour vision deficiencies XIII*. Amsterdam: Kluwer Academic Publishers, 1997:3-20.
- 2 Neitz M, Neitz J. Molecular genetics of color vision and color vision defects. *Arch Ophthalmol* 2000;118:691-700.
- 3 Sharpe LT, Nordby K. Total colour-blindness: an introduction. In: Hess RF, Sharpe LT, Nordby K, eds. *Night vision: basic, clinical and applied aspects*. Cambridge: Cambridge University Press, 1990:253-89.
- 4 Sharpe LT, Stockman A, Jagle H, et al. Opsin genes, cone photopigments and colourblindness. In: Gegenfurtner K, Sharpe LT, eds. *Color vision: from genes to perception*. Cambridge: Cambridge University Press, 1999:3-52.
- 5 Simunovic MP, Moore AT. The cone dystrophies. *Eye* 1998;12:553-65.
- 6 Andreasson S, Tornqvist K. Electroretinograms in patients with achromatopsia. *Acta Ophthalmol (Copenh)* 1991;69:711-16.
- 7 Hess RF, Nordby K. Spatial and temporal limits of vision in the achromat. *J Physiol* 1986;371:365-85.
- 8 Pentao L, Lewis RA, Ledbetter DH, et al. Maternal uniparental isodisomy of chromosome 14: association with autosomal recessive rod monochromacy. *Am J Hum Genet* 1992;50:690-9.
- 9 Arbour NC, Zlotogora J, Knowlton RG, et al. Homozygosity mapping of achromatopsia to chromosome 2 using DNA pooling. *Hum Mol Genet* 1997;6:689-94.
- 10 Wissinger B, Jagle H, Kohl S, et al. Human rod monochromacy: linkage analysis and mapping of a cone photoreceptor expressed candidate gene on chromosome 2q11. *Genomics* 1998;51:325-31.
- 11 Stryer L. Visual excitation and recovery. *J Biol Chem* 1991;266:10711-14.
- 12 Kohl S, Marx T, Giddings I, et al. Total colour-blindness is caused by mutations in the gene encoding the alpha-subunit of the cone photoreceptor cGMP-gated cation channel. *Nat Genet* 1998;19:257-9.
- 13 Wissinger B, Gomer D, Jäggle H, et al. CNGA3 mutations in hereditary cone photoreceptor disorders. *Am J Hum Genet* 2001;69:722-37.
- 14 Eksandh L, Kohl S, Wissinger B. Clinical features of achromatopsia in Swedish patients with defined genotypes. *Ophthalmic Genet* 2002;23:109-20.
- 15 Biel M, Seeliger M, Pfeifer A, et al. Selective loss of cone function in mice lacking the cyclic nucleotide-gated channel CNG3. *Proc Natl Acad Sci USA* 1999;96:7553-7.
- 16 Brody JA, Hussels I, Brink E, et al. Hereditary blindness among Pingelapese people of Eastern Caroline Islands. *Lancet* 1970;1:1253-7.
- 17 Winick JD, Blundell ML, Galke BL, et al. Homozygosity mapping of the achromatopsia locus in the Pingelapese. *Am J Hum Genet* 1999;64:1679-85.
- 18 Sundin OH, Yang J-M, Li Y, et al. Genetic basis of total colour-blindness among the Pingelapese islanders. *Nat Genet* 2000;25:289-93.
- 19 Kohl S, Baumann B, Broghammer M, et al. Mutations in the CNGB3 gene encoding the beta-subunit of the cone photoreceptor cGMP-gated channel are responsible for achromatopsia (ACHM3) linked to chromosome 8q21. *Hum Mol Genet* 2000;9:2107-16.
- 20 Rojas CV, Maria LS, Santos JL, et al. A frameshift insertion in the cone cyclic nucleotide-gated cation channel causes complete achromatopsia in a consanguineous family from a rural isolate. *Eur J Hum Genet* 2002;10:638-42.
- 21 Kohl S, Jäggle H, Zrenner E, et al. The genetics of achromatopsia. *Invest Ophthalmol Vis Sci* 2001;42:5324 (Abstract 1745).
- 22 Finn JT, Krautwurst D, Schroeder JE, et al. Functional co-assembly among subunits of cyclic-nucleotide-activated, nonselective cation channels, and across species from nematode to human. *Biophys J* 1998;74:1333-45.
- 23 Sidjanin DJ, Lowe JK, McElwae JL, et al. Canine CNGB3 mutations establish cone degeneration as orthologous to the human achromatopsia locus ACHM3. *Hum Mol Genet* 2002;11:1823-33.
- 24 Kohl S, Baumann B, Rosenberg T, et al. Mutations in the cone photoreceptor G-protein alpha-subunit gene GNAT2 in patients with achromatopsia. *Am J Hum Genet* 2002;71:422-5.
- 25 Aligianis IA, Forshew T, Johnson S, et al. Mapping of a novel locus for achromatopsia (ACHM4) to 1p and identification of a germline mutation in the alpha subunit of cone transducin (GNAT2). *J Med Genet* 2002;39:656-60.
- 26 Michaelides M, Aligianis IA, Holder GE, et al. Cone dystrophy phenotype associated with a frameshift mutation (M280fsX291) in the alpha-subunit of cone specific transducin (GNAT2). *Br J Ophthalmol* 2003;87:1317-20.
- 27 Lerea CL, Bunt-Milam AH, Hurley JB. Alpha transducin is present in blue-, green-, and red-sensitive cone photoreceptors in the human retina. *Neuron* 1989;3:367-76.
- 28 Reitner A, Sharpe LT, Zrenner E. Is colour vision possible with only rods and blue-sensitive cones? *Nature* 1991;352:798-800.
- 29 Akhmedov NB, Piriev NI, Pearce-Kelling S, et al. Canine cone transducin-gamma gene and cone degeneration in the cd dog. *Invest Ophthalmol Vis Sci* 1998;39:1775-81.
- 30 Akhmedov NB, Piriev NI, Ray K, et al. Structure and analysis of the transducin beta3-subunit gene, a candidate for inherited cone degeneration (cd) in the dog. *Gene* 1997;194:47-56.
- 31 Pokorny J, Smith VC, Pinckers AJ, et al. Classification of complete and incomplete autosomal recessive achromatopsia. *Graefes Arch Clin Exp Ophthalmol* 1982;219:121-30.
- 32 Smith VC, Pokorny J, Newell FW. Autosomal recessive incomplete achromatopsia with protan luminosity function. *Ophthalmologica* 1978;177:197-207.
- 33 Smith VC, Pokorny J, Newell FW. Autosomal recessive incomplete achromatopsia with deutan luminosity. *Am J Ophthalmol* 1979;87:393-402.
- 34 van Norren D, de Vries-de Mol EC. A case of incomplete achromatopsia of the deutan type. *Doc Ophthalmol* 1981;51:365-72.
- 35 van Lith GHM. General cone dysfunction without achromatopsia. In: Pearlman JT, ed. *10th ISCERG Symposium, Doc Ophthalmol Proc Ser* 1973;2:175-80.
- 36 Keunen JEE, De Brabandere SRS, Liem ATA. Foveal densitometry and color matching in oligocone trichromacy. In: Drum B, ed. *12th IRGCV D Symposium—Colour vision deficiencies XII*. Amsterdam: Kluwer Academic Publishers, 1995:203-10.
- 36a Michaelides M, Holder GE, Bradshaw K, et al. Oligocone trichromacy—a rare and unusual cone dysfunction syndrome. *Br J Ophthalmol* 2004;[in press].
- 37 Neuhann T, Krastel H, Jaeger W. Differential diagnosis of typical and atypical congenital achromatopsia. Analysis of a progressive foveal dystrophy and a nonprogressive oligo-cone trichromacy (general cone dysfunction without achromatopsia), both of which at first had been diagnosed as achromatopsia. *Albrecht Von Graefes Arch Klin Exp Ophthalmol* 1978;209:19-28.
- 38 Ehlich P, Sadowski B, Zrenner E. Oligocone trichromacy, a rare form of incomplete achromatopsia. *Ophthalmologie* 1997;94:801-6.
- 39 Weale RA. Cone monochromatism. *J Physiol* 1953;121:548-69.
- 40 Weale RA. Photosensitive reactions in foveae of normal and cone-monochromatic observers. *Opt Acta* 1959;6:158-174.
- 41 Pitt FHG. Monochromatism. *Nature* 1944;154:466-8.
- 42 Crone RA. Combined forms of congenital colour defects: a pedigree with atypical total colour blindness. *Br J Ophthalmol* 1956;40:462-72.
- 43 Ikeda H, Ripps H. The electroretinogram of a cone-monochromat. *Arch Ophthalmol* 1966;75:513-17.
- 44 Krill AE, Schneiderman A. Retinal function studies, including the electroretinogram, in an atypical monochromat. *Clinical Electrophysiology, Supplement to Vision Research*. New York: Oxford Press, 1966:351-61.
- 45 Fincham E. Defects of the colour-sense mechanism as indicated by the accommodation reflex. *J Physiol* 1953;121:570-80.
- 46 Gibson IM. Visual mechanisms in a cone-monochromat. *J Physiol* 1962;161:P10-11.
- 47 Pokorny J, Smith VC, Verriest G. Congenital color defects. In: Pokorny J, Smith VC, Verriest G, Pinckers AJ, eds. *Congenital and acquired color vision defects*. New York: Grune & Stratton, 1979:183.
- 48 Weleber RG, Eisner A. Cone degeneration ('bull's eye dystrophies') and colour vision defects. In: Newsome DA, ed. *Retinal dystrophies and degenerations*. New York: Raven Press, 1988:233-56.
- 49 Gouras P, MacKay CJ. Electroretinographic responses of the short-wavelength-sensitive cones. *Invest Ophthalmol Vis Sci* 1990;31:1203-9.
- 50 Alpern M, Lee GB, Maaseidvaag F, et al. Colour vision in blue cone monochromacy. *J Physiol* 1971;212:211-33.
- 51 Young RS, Price J. Wavelength discrimination deteriorates with illumination in blue cone monochromats. *Invest Ophthalmol Vis Sci* 1985;26:1543-9.
- 52 Weis AH, Biersdorf WR. Blue cone monochromatism. *J Pediatr Ophthalmol Strabismus* 1989;26:218-23.
- 53 Berson EL, Sandberg MA, Rosner B, et al. Color plates to help identify patients with blue cone monochromatism. *Am J Ophthalmol* 1983;95:741-7.
- 54 Haegerstrom-Portnoy G, Schneck ME, Verdon WA, et al. Clinical vision characteristics of the congenital achromatopsias. II. Color vision. *Optom Vis Sci* 1996;73:457-65.
- 55 Nathans J, Thomas D, Hogness DS. Molecular genetics of human colour vision: the genes encoding blue, green, and red pigments. *Science* 1986;232:193-202.
- 56 Nathans J, Piantanida TP, Eddy RL, et al. Molecular genetics of inherited variation in human color vision. *Science* 1986;232:203-10.
- 57 Nathans J, Davenport CM, Maumenee IH, et al. Molecular genetics of human blue cone monochromacy. *Science* 1989;245:831-8.
- 58 Nathans J, Maumenee IH, Zrenner E, et al. Genetic heterogeneity among blue-cone monochromats. *Am J Hum Genet* 1993;53:987-1000.
- 59 Wang Y, Macke JP, Merbs SL, et al. A locus control region adjacent to the human red and green visual pigment genes. *Neuron* 1992;9:429-40.
- 60 Kazmi MA, Sakmar TP, Ostrer H. Mutation of a conserved cysteine in the X-linked cone opsin causes color vision deficiencies by disrupting protein folding and stability. *Invest Ophthalmol Vis Sci* 1997;38:1074-81.
- 61 Reyniers E, Van Thienen MN, Meire F, et al. Gene conversion between red and defective green opsin gene in blue cone monochromacy. *Genomics* 1995;29:323-8.
- 62 Ladekjaer-Mikkelsen AS, Rosenberg T, Jorgensen AL. A new mechanism in blue cone monochromatism. *Hum Genet* 1996;98:403-8.
- 63 Fleischman JA, O'Donnell FE. Congenital X-linked incomplete achromatopsia. Evidence for slow progression, carrier fundus findings, and possible genetic linkage with glucose-6-phosphate dehydrogenase locus. *Arch Ophthalmol* 1981;99:468-72.
- 64 Ayyagari R, Kakuk LE, Coats EL, et al. Bilateral macular atrophy in blue cone monochromacy (BCM) with loss of the locus control region (LCR) and part of the red pigment gene. *Mol Vis* 1999;5:13-18.
- 64a Michaelides M, Johnson S, Simunovic M, et al. Blue cone monochromatism: a phenotype and genotype assessment with evidence of progressive loss of cone function in older individuals. *Eye* 2004;[in press].
- 65 Ayyagari R, Kakuk LE, Bingham EL, et al. Spectrum of color gene deletions and phenotype in patients with blue cone monochromacy. *Hum Genet* 2000;107:75-82.
- 66 Karmik SS, Khorana HG. Assembly of functional rhodopsin requires a disulfide bond between cysteine residues 110 and 187. *J Biol Chem* 1990;265:17520-4.
- 67 Musarella MA, Weleber RG, Murphy WH, et al. Assignment of the gene for complete X-linked congenital stationary night blindness (CSNB1) to Xp11.3. *Genomics* 1989;5:727-37.
- 68 Kaplan J, Pelet A, Martin C, et al. Phenotype-genotype correlations in X linked retinitis pigmentosa. *J Med Genet* 1992;29:615-23.

- 69 Haim M, Fledelius HC, Skarsholm D. X-linked myopia in a Danish family. *Acta Ophthalmol (Copenh)* 1988;**66**:450-6.
- 70 Schwartz M, Haim M, Skarsholm D. X-linked myopia: Bornholm Eye Disease. Linkage to DNA markers on the distal part of Xq. *Clin Genet* 1990;**38**:281-6.
- 71 Bergen AA, Pinckers AJ. Localization of a novel X-linked progressive cone dystrophy gene to Xq27: evidence for genetic heterogeneity. *Am J Hum Genet* 1997;**60**:1468-73.
- 72 Terry RL. The use of tinted contact lenses in a case of congenital rod monochromatism. *Clin Exp Optom* 1988;**71**:188-90.

Video reports

To view the video reports in full visit our website www.bjophthalmol.com and click on the link to video reports.

- Feeder vessel treatment with high speed ICG angiography. *D Stanescu-Segall, G Coscas, F Coscas, G Soubrane*
- Endoscopy to aid anterior segment surgery. *J E Moore, A Sharma*
- Penetrating ocular injury due to a fish hook: surgical removal. *S D M Chen, D Chiu, C K Patel*
- Retinal ganglion cell axon response to guidance molecules *S F Oster, D W Sretavan*
- Marin-Amat syndrome *A Jogiya, C Sandy*
- Excision of subcutaneous dirofilariasis of the eyelid *D Mallick, T P Ittyerah*
- Thixotropy: a novel explanation for the cause of lagophthalmos after peripheral facial nerve palsy. *M Aramideh, J H T M Koelman, P P Devriese, F VanderWerf, J D Speelman*
- Surgical revision of leaking filtering blebs with an autologous conjunctival graft. *K Taherian, A Azuara-Blanco*
- *Dipetalonema reconditum* in the human eye. *T Huynh, J Thean, R Maini*
- Evaluation of leucocyte dynamics in mouse retinal circulation with scanning laser ophthalmoscopy. *H Xu, A Manivannan, G Daniels, J Liversidge, P F Sharp, J V Forrester, I J Crane*
- An intraocular steroid delivery system for cataract surgery. *D F Chang*
- Pearls for implanting the Staar toric IOL. *D F Chang*
- Capsule staining and mature cataracts: a comparison of indocyanine green and trypan blue dyes. *D F Chang*